

A University of Sussex PhD thesis

Available online via Sussex Research Online:

http://sro.sussex.ac.uk/

This thesis is protected by copyright which belongs to the author.

This thesis cannot be reproduced or quoted extensively from without first obtaining permission in writing from the Author

The content must not be changed in any way or sold commercially in any format or medium without the formal permission of the Author

When referring to this work, full bibliographic details including the author, title, awarding institution and date of the thesis must be given

Please visit Sussex Research Online for more information and further details

THE UNIVERSITY OF SUSSEX

Anita Brožková

PhD Thesis in Genome Stability

Thesis title:

The Role of the Human SMC5/6 Complex in Genome Stability

January 2020

Declaration

I hereby declare that this thesis has not been and will not be, submitted in whole or in part to another University for the award of any other degree.

Signature:.....

Acknowledgements

Firstly, I would like to thank my supervisor Jo Murray for providing me with the opportunity to undertake a PhD, and for her support and guidance during the project. I would also like to thank Owen Wells for his patience and research advice, and for the technical support during the early months in the lab. I also have to acknowledge Nadia Hegarat, who kindly helped me with human tissue culture and Marek Adamowicz for sharing his ScanR expertise, and for his support during the toughest times in the lab. A big thank you belongs to Alice Copsey and Zuza Kozik, who both helped me with the proteomics part of the project, and Murat Eravci who helped me with the mass spec data analysis. I would also like to express my gratitude to Katka Zabrady for stimulating Smc5/6 conversations, and to Cong Liu for sharing his science passion and ideas.

Secondly, I want to acknowledge the lab members of both the Murray and Carr lab, who made the PhD journey much less difficult.

A special thanks belongs to Adam Watson, who influenced me greatly and made my time in Brighton genuinely special. I will miss you.

I would also like to acknowledge the guys from our GDSC running club, especially Will, Owen and David – we covered some great miles together around the South Downs. I cannot forget to thank Vicky, who bravely suffered with me through all the up hills.

Finally, thanks to Kate, Jon, Arthur and Novia for your love and support. You were the best housemates I could have ever wished for.

Úplně nazávěr bych chtěla poděkovat svým rodičům, kteří mne podporovali po celý čas mých studií a ve kterých jsem vždy měla velkou oporu. Bez Vás bych se až sem nedostala.

Summary

The Smc5/6 complex is a member of the SMC family of protein complexes, comprising cohesin, condensin and Smc5/6. However, in comparison to cohesin and condensin, the cellular role of the Smc5/6 complex is much less understood. Smc5/6 in essential in yeasts and its absence in mice is embryonically lethal. Studies in fission and budding yeast have reported roles for Smc5/6 in homologous recombination repair, and the maintenance of replication fork stability. Recent studies in human cells identified two different syndromes resulting from mutations in distinct SMC5/6 subunits, NSMCE2 and NSMCE3. Both syndromes are characterised by chromosomal instability and failure to recover from replication stress. To further examine the requirements for human SMC5/6, we took advantage of a T-REx Flp-In cell line, which allowed for an inducible downregulation of a specific gene of interest. The endogenous SMC5/6 subunit, NSMCE4a, was first complemented with a regulatable NSMCE4a-Strep-6xHis cDNA, and subsequently knocked out. Additional removal of the ectopic NSMCE4a in the knock out cell line demonstrated that NSMCE4a is essential in human cells.

We took advantage of a bottom up proteomics approach to purify the SMC5/6 complex using NSMCE4a-Strep-6xHis and search for its interactors during an unperturbed cell cycle, upon replication fork stalling and after fork collapse.

In parallel, we found that downregulation of ectopic NSMCE4a destabilises the SMC5/6 complex in T-REx Flp-In 293 cells, similarly to the NSMCE3 patient cells. SMC5/6 destabilisation results in aneuploidy, genome instability, an increase in DNA damage markers and replication stress. The cells are capable of homologous recombination as evidenced by Rad51 foci and display elevated non-allelic homologous recombination. Interestingly, we found that the depletion of SMC5/6 by NSMCE4a shut off leads to strong sensitivity to PARP inhibition. Our data suggest that this is due to a failure to protect replication fork and/or misregulation of homologous recombination.

Table of contents

Abbreviations ..... *VIII*
List of figures ..... *XI*
List of tables ..... *XV*
List of appendices ..... *XI*
1 Chapter 1 Introduction *1*
1.1 DNA damage **2**
1.1.1 Sources of DNA damage 3
1.1.2 DNA damage signalling – cellular response to DNA damage 4
1.1.3 DNA double strand break repair pathways 9
1.2 The SMC complexes **16**
1.2.2 Cohesin 20
1.2.3 Condensin 21
1.2.4 The SMC5/6 complex 22
1.3 The role of Smc5/6 in DNA repair **30**
1.3.1 Smc5/6 in homologous recombination repair 30
1.3.2 Smc5/6 in replication fork stability maintenance 31
1.3.3 Smc5/6 and ribosomal DNA stability 33
1.3.4 The role of Smc5/6 in meiosis 34
1.4 Other functions of the Smc5/6 complex **37**
1.4.1 Timing and spatial localisation of Smc5/6 37
1.4.2 Cell cycle specific functions of Smc5/6 38
1.4.3 Interplay between Smc5/6 and cohesin 38
1.4.4 Smc5/6 and topological stress 40
1.4.5 The role of Smc5/6 in viral genome transcription 42
1.5 Human SMC5/6 ..... **44**
1.5.1 Human syndromes associated with mutation in the SMC5/6 complex 45
Aims of the project *50*
2 Chapter 2 Materials and Methods *51*
2.1 Cell biology techniques **51**
2.1.1 Human tissue culture 51
2.1.2 Transfections 52
2.1.3 Flow cytometry 52
2.1.4 Clonogenics survival 53
2.1.5 Metaphase spreads 53

2.1.6 Growth curve 54
2.1.7 Micronuclei scoring 54
2.1.8 EdU incorporation assay 54
2.2 DNA cloning and molecular techniques 55
2.2.1 Polymerase chain reaction (PCR) 55
2.2.2 DNA gel electrophoresis 56
2.2.3 Digestion and Ligation 56
2.2.4 Transformation of E.coli 56
2.2.5 Guide RNA insertion into the Cas9 vector 57
2.2.6 Topo cloning 57
2.2.7 Surveyor assay 58
2.2.8 Immunofluorescence 62
2.2.9 Western blot 62
2.2.10 SDS-PAGE 63
2.2.11 Silver stain 64
2.2.12 Coomassie stain 64
2.3 Affinity Purification and Mass Spectrometry 64
2.3.1 Purification of the 6xHis-Nse4a NSMCE4a antigen 64
2.3.2 Purification of the NSMCE4a antibody on nitrocellulose strips 65
2.3.3 Ni^{2+}-NTA and TALON affinity purification 66
2.3.4 Strep-tag affinity purification 67
2.3.5 Chromatin enrichment for proteomics (ChEP) 67
2.3.6 Sample preparation for MS analysis 69
2.3.7 Mass spectrometry 69
2.3.8 Mass spectrometry analysis 70
3 Chapter 3 Results I: Establishing a system to study components of the SMC5/6 complex in mammalian cells 71
3.1 Introduction 71
3.1.1 The Flp-In T-REx system 72
3.2 Aims 74
3.3 Results 75
3.3.1 NSMCE3 p.Leu264Phe leads to destabilisation of the SMC5/6 complex and increased genome instability 75
3.3.2 Construction of stable T-Rex Flp-In 293 cell lines 77
3.3.3 CRISPR/Cas9 knock out of the endogenous NSMCE3 gene 83
3.3.4 CRISPR/Cas9 knock out of the endogenous NSMCE4a gene 86

3.3.5 Characterisation of the constructed T-REx Flp-In cell lines 89
3.3.6 Validation of the NSMCE4a knock out cell line by Flp back- transfection . 92
3.4 Discussion 94
4 Chapter 4 Results II: Affinity purification of NSMCE4a and mass spectrometry analysis of SMC5/6 protein interactors 96
4.1 Introduction 96
4.2 Aims 97
4.3 Results 98
4.3.1 Affinity purification of NSMCE4a coupled with mass spectrometry identifies all the SMC5/6 complex subunits 98
4.3.2 Optimisation of the NSMCE4a purification using 6xHis tag 102
4.3.3 Two step purification of SMC5/6 coupled with nano-LC/MS did not increase the SMC5/6 yield over background 106
4.3.4 Mass spectrometry analysis of protein-protein interactors of SMC5/6 complex 111
4.3.5 Purification of SMC5/6 from chromatin fraction 124
4.3.6 SILAC 133
4.4 Discussion 136
5 Chapter 5 Results III: Characterisation of the NSMCE4a shut off and its effects on genome stability 138
5.1 Introduction 138
5.2 Aims 139
5.3 Results 140
5.3.1 Identification of NSMCE4a shut off conditions 140
5.3.2 Timely regulation of NSMCE4a shut off 144
5.3.3 Characterisation of a long term NSMCE4a shut off 146
5.3.4 Long term depletion of NSMCE4a leads to the accumulation of DNA damage and genomic instability 153
5.4 Discussion 163
6 Chapter 6 Results IV: Investigation of the response of NSMCE4a shut off cells to DNA damage 165
6.1 Introduction 165
6.2 Aims 166
6.3 Results 167
6.3.1 NSMCE4a shut off and replication stress 167
6.3.2 DNA double strand breaks repair kinetics in SMC5/6 deficient cell line .. 170

6.3.3 The role of SMC5/6 in DNA double strand break repair of ectopic template 177

6.3.4 Viability of NSMCE4a shut off cells upon different DNA damaging agents 179

6.3.5 PARP inhibition in NSMCE4a shut off cell line decreases the number of replicating cells and leads to increase in G2/M population..... 186

6.4 Discussion 190

7 Chapter 7 Discussion 192

7.1 Usage of the Flp-In T-REx 293 system to generate regulatable SMC5/6 cell lines 192

7.1.1 Regulation of the NSMCE4a levels using the Flp-In T-Rex system 193

7.2 Search for interactors of the SMC5/6 complex using AP-MS 195

7.3 SMC5/6 and regulation of homologous recombination..... 196

7.3.1 Interplay between the SMC5/6 complex and PARP 197

7.4 Conclusion 200

Bibliography..... 201

Appendix.....224

Abbreviations

ACN	Acetonitrile
AID	Auxin-inducible degron
AP-MS	Affinity-purification mass spectrometry
ATM	Ataxia-telangiectasia mutated
ATR	Ataxia-telangiectasia and Rad3 related
BIR	Break-induced replication
BLM	Bloom syndrome
BSA	Bovine serum albumin
BSR	Blasticidine
cccDNA	Covalently-closed circular DNA
CDK	Cyclin dependent kinase
ChIP-Seq	Chromatin immunoprecipitation coupled with sequencing
CK2	Casein kinase 2
c-NHEJ	canonical NHEJ
CPT	Camptothecin
dd H2O	double-distilled water
DDR	DNA damage response
dHJ	double Holliday junction
D-loop	Displacement loop
DNA-PKcs	DNA-dependent protein kinase catalytic subunit
dNTP	Deoxyribonucleoside tri-phosphate
DOX	Doxycycline
DSB	Double strand break
dsDNA	double stranded DNA
DTT	Dithiotreitol
EDTA	Ethylenediaminetetraacetic acid
EdU	5-Ethynyl-2´-deoxyuridine
FCS	Foetal calf serum
FDR	False discovery rate

Gy	Gray (unit)
Hawk	HEAT repeat proteins associated with kleisins
HBS	HBS-buffered saline
HBV	Hepatitis B virus
HDR	Homology directed repair
HR	Homologous recombination
HRR	Homologous recombination repair
IMAC	Immobilized metal-affinity chromatography
IR	Ionizing radiation
JMs	Joint molecules
Kite	Kleisin interacting winged-helix tandem elements
LC	Liquid chromatography
LFQ	Label-free quantification
LIG4	DNA ligase IV
MHD	MAGE-homology domain
MS	Mass spectrometry
NAD^+	Nicotinamide adenine dinucleotide
NAHR	Non-allelic homologous recombination
Nano-LC	Nano flow liquid chromatography
NBS1	Nijmegen breakage syndrome protein-1
NHEJ	Non-homologous end-joining
$Ni2^+$-NTA	Nickel-nitrilotriacetic acid
Nse	Non-SMC element (yeast)
NSMCE	Non-Structural Maintenance of Chromosomes Element (human)
PARP	Poly (ADP-ribose) polymerase
PARPi	PARP inhibitor
PBS	Phosphate-buffered saline
PFA	Paraformaldehyde
PIKK	phosphatidylinositol 3-kinase-related kinase
PLK1	Polo-like kinase-1

PP2A	Protein phosphatase 2A
RFB	Replication fork barrier
RNAi	RNA interference
rNTP	Ribonucleoside tri-phosphate
ROS	Reactive oxygen species
RPA	Replication protein A
RT	Room temperature
SDSA	Synthesis-dependent strand annealing
SDS-PAGE	Sodium dodecyl sulphate–polyacrylamide gel electrophoresis
SEI	single-end invasion
SILAC	Stable-isotope labelling with amino acids in tissue culture
siRNA	Small interfering RNA
SMASh	Small molecule-assisted shutoff
SMC	Structural Maintenance of Chromosomes
spSmc5/6	*S. pombe* Smc5/6
SSB	Single strand break
ssDNA	single stranded DNA
TFA	Trifluoracetic acid
Top1	DNA topoisomerase 1
Top1-cc	Topoisomerase 1 cleavage complex
Top2	DNA topoisomerase 2
TOPBP1	Topoisomerase-binding protein-1
UV	Ultra-violet
V(D)J	Variable Diversity Joining
WCE	Whole cell extract
WH	Winged-helix
γ-H2AX	H2AX phosphorylated on serine 139

List of figures

Figure 1.1: Scheme of DNA lesions recognised by activators of the sensor PIKK and the DNA damage response cascade after ATR activation……...6

Figure 1.2: Pathways of double strand break repair in mammalian cells……..10

Figure 1.3: Contribution of various DSB repair pathways during mammalian cells 12

Figure 1.4: Architecture of the eukaryotic SMC complexes……..17

Figure 1.5: Model of formation of chromatin loops by SMC complexes, cohesin and condensin……19

Figure 1.6: Architecture of the Smc5/6 complexes in different organisms……23

Figure 1.7: Models of the Smc5/6 hinge and the Nse1/Nse3 binding to dsDNA……25

Figure 1.8: Release of replication-induced superhelical tension by topoisomerases or fork rotation……...……41

Figure 1.9: Model of SMC5/6 function during Hepatitis B virus infection……..43

Figure 1.10: Schematic illustration of NSMCE2 and NSMCE3 mutations……..46

Figure 1.11: Phenotype comparison of mutations in NSMCE2 and NSMCE3……49

Figure 3.1: Scheme of the human T-REx Flp-In system in the 293 host cell line….73

Figure 3.2: Destabilisation of the SMC5/6 complex and increased genome instability in NSMCE3 patient fibroblasts……76

Figure 3.3: NSMCE4a antibody purification from crude serum……78

Figure 3.4: Generation and initial characterisation of stable NSMCE4a and NSMCE3 Flp-In T-REx 293 cell lines……..81

Figure 3.5: Generation of NSMCE3 T-REx Flp-In 293 knock out cell line.……85

Figure 3.6: Generation of NSMCE4a T-REx Flp-In 293 knock out cell line……..88

Figure 3.7: Characterisation of created NSMCE4a T-REx Flp-In 293 cell lines…...90

Figure 3.8: Overexpression of ectopic NSMCE4a does not decrease cell viability…91

Figure 3.9: FRT-NSMCE4a-Strep-6xHis is the only functional copy in the T-REx Flp-In 293 knock out cell line and is essential for cell survival…….93

Figure 4.1: C-terminal His tag of NSMCE4a-Strep-6xHis can be used to recover the SMC5/6 complex……99

Figure 4.2: Improvement of elution purity using gradually increasing imidazole concentration……...103

Figure 4.3: Optimisation of NSMCE4a-Strep-6xHis pull down using different IMAC columns and conditions……..105

Figure 4.4: Two-step affinity purification of NSMCE4a-Strep-6xHis using TALON resin and StepTactin magnetic beads…….108

Figure 4.5: One-step pull down using TALON resin results in higher yield of the SMC5/6 complex than two-step pull down using TALON/StrepTactin…….110

Figure 4.6: Workflow scheme of label free approach to purify the SMC5/6 complex coupled with mass spectrometry…….112

Figure 4.7: AP-MS of NSMCE4a-Strep-6xHis coupled with MaxQuant search and Perseus analysis of protein interactors upon non-treated conditions…….114

Figure 4.8: AP-MS of NSMCE4a-Strep-6xHis coupled with MaxQuant search and Perseus analysis of protein interactors upon non-treated conditions…….116

Figure 4.9: Affinity purification of NSMCE4a-Strep-6xHis after 2 and 24 hours of 2mM hydroxyurea treatment…….…..119

Figure 4.10: Analysis of NSMCE4a interactors after 2 hrs of HU treatment……121

Figure 4.11: Analysis of NSMCE4a interactors after 24 hrs of HU treatment……123

Figure 4.12: Chromatin fractionation for purification of chromatin bound SMC5/6.....127

Figure 4.13: Purification of SMC5/6 from chromatin fraction by NSMCE4a-Strep-6xHis using IMAC……129

Figure 4.14: Pull down of SMC5/6 using StrepTactin beads and purification of SMC5/6 from chromatin fraction using cross-linking (ChEP) protocol……131

Figure 4.15: Affinity purification of NSMCE4a using TALON after SILAC…….135

Figure 5.1: Shut off of the ectopic NSMCE4a requires active selection for the Tet repressor protein……..141

Figure 5.2: Phenotype of T-REx Flp-In 293 created cell lines after one week of Blasticidin selection……..142

Figure 5.3: Kinetics of the decrease in protein levels of NSMCE4a and SMC5 after NSMCE4a shut off……...145

Figure 5.4: NSMCE4a shut off decreases cell viability……147

Figure 5.5: Long term NSMCE4a shut off leads to moderate slow growth defect..149

Figure 5.6: Protein levels of the ectopic NSMCE4a and SMC5 under different conditions……..150

Figure 5.7: Long term NSMCE4a shut off does not influence distribution of cells throughout the cell cycle……..152

Figure 5.8: Long term NSMCE4a shut off increases chromosome instability……154

Figure 5.9: Long term NSMCE4a shut off leads to chromosome loss……158

Figure 5.10: Long term NSMCE4a shut off leads to an increase in endogenous γ-H2AX foci……..160

Figure 5.11: Long term NSMCE4a shut off leads to increase in endogenous γ-H2AX signalling and phosphorylation RPA2 by ATR……...162

Figure 6.1: NSMCE4a shut off confers sensitivity to replication fork stalling and collapse……..169

Figure 6.2: NSMCE4a shut off does not result in replication defects after short-time exposure to replication stress……..171

Figure 6.3: Dynamics of γ-H2AX foci after ionizing radiation treatment……173

Figure 6.4: NSMCE4a shut off cell line is proficient in Rad51 foci formation…….175

Figure 6.5: Moderate decrease in Rad51 foci formation in NSMCE4a shut off cell line…….176

Figure 6.6: NSMCE4a shut off leads to increase in ectopic homologous recombination……..178

Figure 6.7: NSMCE4a shut off does not sensitise cells to ionizing radiation……..181

Figure 6.8: NSMCE4a shut off sensitises cells to Camptothecin……..183

Figure 6.9: NSMCE4a shut off confers hypersensitivity to PARP inhibitor……185

Figure 6.10: Replication recovery defect in NSMCE4a shut off cell line upon PARPi treatment……..187

Figure 6.11: PARP inhibition leads to decrease in S-phase population and increase of in G2/M population in NSMCE4a shut off cells…….189

Figure 7.1: Model of SMC5/6 function during replication fork stabilisation and repair…….198

List of tables

Table 2.1 Drug concentrations for the Flp-In T-REx 293 cell line……51

Table 2.2: DNA oligos used in this study……..59

Table 2.3: Primary antibodies for immunofluorescence…….....61

Table 2.4: Primary antibodies for western blot……61

Table 2.5: Secondary antibodies used in this study……..62

Table 2.6: SDS-PAGE gel composition…….64

Table 2.7: Volumes for affinity purification reactions ……66

List of appendices

Figure A.1: Illustration of multi-step gradient method for peptide elution

Table A.2: MaxQuant search parameters and identified proteins for initial NSMCE4a affinity purification using IMAC (Figure 4.1 C)

Table A.3: Proteins identified in MASCOT search using one-step TALON or two-step TALON/StrepTactin NSMCE4a affinity purification (Figure 4.5)

Table A.4: MaxQuant search parameters and identified protein interactors of NSMCE4a upon non-treated conditions (Figure 4.7)

Table A.5: Perseus statistical analysis of protein hits identified by MaxQuant search for non-treated conditions (Figure 4.7)

Table A.6: MaxQuant search parameters and identified protein interactors of NSMCE4a after 2h and 24h of hydroxyurea treatment (Figure 4.10 and 4.11)

Table A.7: Perseus statistical analysis of protein hits identified by MaxQuant search for 2h HU treatment (Figure 4.10)

Table A.8: Perseus statistical analysis of protein hits identified by MaxQuant search for 24h HU treatment (Figure 4.11)

Table A.9: MaxQuant search results for initial SILAC experiment (Figure 4.15)

1 Chapter 1

Introduction

In this thesis, a characterisation of a human cell line, with an inducible SMC5/6 shut off, is presented. Smc5/6, related to cohesin and condensin, has been shown to be required for regulation of homologous recombination and response to replication stress. The introduction will put in broader context the role of the human SMC5/6 complex in DNA repair and genome stability maintenance. Initially, the common endogenous sources of DNA damage will be discussed, with the main focus on DNA double strand breaks. Next, the main DNA double strand break repair pathways, homologous recombination and non-homologous end-joining, will be described. The emphasis will be put on homologous recombination, since the Smc5/6 complex is associated with this particular repair pathway. The next section will cover a general introduction to the SMC complexes and their well established, as well as recently emerging roles in genome structure and organisation. Finally, an overview of the current knowledge on Smc5/6 in different cellular processes will be given. The last section will introduce the human SMC5/6 complex, the main subject of the project.

1.1 DNA damage

Genetic information of each living system from unicellular bacteria to complex organisms, such as humans, has to be passed on the next generation in a high-fidelity fashion. The genetic information encoded by the DNA molecule is inherently exposed to a wide range of factors that disrupt its integrity, or interfere with DNA metabolic processes, such as replication and transcription. In order to maintain genome stability, living systems have evolved multiple mechanisms to protect and repair their DNA. The sources of DNA damage are endogenous, arising from metabolic processes in the cells, as well as exogenous, such as ultra-violet (UV) light and ionizing radiation (IR). UV is one of the most pervasive environmental DNA-damaging agent. Strong sunlight can induce as many as 100 000 DNA lesions per cells within an hour. Even though normal cells are able to cope with physiological amount of DNA damage, each lesion has a potential to be converted into a mutation. DNA damage has different character and specific DNA repair machineries dealing with particular type of damage. The most common type of DNA damage, representing about 75% of all DNA lesions, are DNA single strand breaks (SSBs). Repair enzymes, such as photolyases and nucleotide excision repair machineries, deal with UV-induced pyrimidine dimers or mis-incorporated nucleotides. On the other hand, IR can directly induce DNA double strand breaks (DSBs), which possess the biggest threat for the cell. Compared to pyrimidine dimers or DNA single-strand breaks, DNA DSBs are relatively rare, but extremely toxic DNA lesions. Unrepaired DNA DSB leads to cell death, incorrectly repaired DSBs can cause chromosome abnormalities and gene mutations. Even though normal level of mutagenicity is a source of genetic diversity and can be evolutionarily beneficial, increased rate of mutations is a source of genome instability. Genome instability and increased mutation rate often leads to malignancies, which in humans are associated with cancer development (reviewed in: Jackson and Bartek, 2009 and Tubbs and Nussenzweig, 2017). Therefore, the ways in which organisms deal with different DNA damage have been the scope of many biological studies. In the next section, the sources of DNA damage, as well as the mechanisms of its repair on cellular level, will be discussed.

1.1.1 Sources of DNA damage

Even during the normal cell cycle, the integrity of DNA can be jeopardised by metabolic products, such as reactive oxygen species (ROS). A common by-product of a mitochondrial respiration is hydrogen peroxide, which can in turn generate ROS in a Fenton reaction catalysed by transition metals, such as copper or iron. ROS can than cross-react with DNA backbone and create variety of lesions, such as altered bases or abasic sites, these are usually repaired by the base-excision repair machinery (reviewed in: Maynard et al., 2009). Another potential source or DNA damage is the replication process itself. Despite the replication machinery being highly accurate due to their proofreading activity, the eukaryotic DNA polymerases responsible for the majority of DNA replication, pol δ and pol ε, have strikingly high rate of mis-incorporation of ribonucleoside tri-phosphate (rNTPs) instead of deoxyribonucleoside tri-phosphate (dNTPs). The mis-incorporated rNTPs must be recognised and removed by the essential enzyme RNAse H2 (Sparks et al., 2012). Another potential thread to DNA replication are DNA sequences that are intrinsically challenging to replicate. These can be abnormal DNA structures, such as G-quadruplexes arising by alternative base-pairing in CG-rich regions. If these structures are not correctly unwound by specific DNA helicases, they create an obstacle for the replication machinery (reviewed in: Zeman and Cimprich, 2014).

Proteins that covalently bind DNA represent another source of endogenous DNA damage. One such proteins are topoisomerases, abundant nuclear enzymes that alleviate topological stress. In order to do so, topoisomerases bind to DNA and generate transient DNA breaks. Topoisomerase 1 creates DNA SSB by covalent binding of its tyrosine residue to the sugar-phosphate backbone of DNA. When replication machinery encounters this covalently bound Top1-DNA complex, it might be converted into one-ended DSB. In order to repair this one-ended DSB, cells have to utilise homologous recombination repair (HRR) pathway called break-induced replication (BIR) for its repair (reviewed in: Zeman and Cimprich, 2014).

Moreover, essential DNA metabolic processes, such as transcription, can also represent an obstacle for DNA replication. During transcription, the newly transcribed RNA can re-hybridise with the DNA template forming a structure called the R-loop. This RNA-DNA hybrid structure is more stable than double stranded DNA, thus, must be enzymatically resolved to restore the original DNA double helix. R-loops also have

biological relevance in regulation of gene expression or rearrangement events. However, misregulation of R-loop resolution can promote genome instability implicated with human neurodegenerative diseases and cancer (reviewed in: Allison and Wang, 2019). Uncontrolled collision between replication and transcription machinery can also have fatal consequences. Transcription of very long genes during S-phase is associated with DSB hotspots, known as common fragile sites (Helmrich et al., 2011). Head-on collisions between transcription and replication machinery has been shown to lead to R-loop formation and potential genome instability (Hamperl et al., 2017). Therefore, under normal conditions, all these processes have to be tightly regulated to protect the genome integrity.

Deregulation of any of the processes controlling replication fork progression, or different sources of replication fork impediments discussed above, collectively result in a situation called replication stress. Replication stress can be defined as slowing down or stalling of replication fork/DNA replication process (reviewed in: Zeman and Cimprich, 2014). Replication stress is usually connected with accumulation of single stranded DNA (ssDNA), which becomes rapidly bound by replication protein A (RPA). RPA is a trimeric protein ssDNA binding protein, which plays an essential role in many aspects of DNA metabolism (reviewed in: Zou et al., 2006). During replication stress, the slowing replisome becomes uncoupled from the replicative helicase complex, which continues in DNA unwinding and thus, results in generation of excessive amount of ssDNA. Excessive amount of RPA coated ssDNA triggers a cellular surveillance mechanisms called the S-phase checkpoint (Byun et al., 2005). In the presence of a functional S-phase checkpoint the checkpoint kinases prevent replication fork collapse by maintaining the stability of arrested replication forks and allowing time for appropriate repair by delaying mitotic entry (Cobb et al., 2003; Lopes et al., 2001). If the replication checkpoint mechanism is compromised, replication fork stalling results in replication fork collapse. Replication fork collapse can be defined here, as a loss of potential to resume replication. In this scenario, collapsed forks need to undergo active repair usually relying on recombination-mediated fork restart (reviewed in: Cortez, 2015).

1.1.2 DNA damage signalling – cellular response to DNA damage

DNA damage signalling is a general term for coordinated cellular response to DNA damage, which involves activation of DNA damage checkpoint, transcriptional response,

chromatin remodelling, DNA repair and DNA-damage induced apoptosis. The DNA damage response is coordinated by three major sensors belonging to the family of phosphatidylinositol 3-kinase-related kinase (PIKK): ATR, ATM and DNA-PKcs. Early response to DNA damage involves mechanisms which sense DNA lesions. The PIKK kinases can detect DNA lesions, this triggers their activation, which leads to phosphorylation of dozens of substrates, this way they orchestrate the cellular response to DNA damage. Activation of ATR and ATM can trigger DNA damage checkpoint, a signalling cascade which promotes cell cycle arrest. Checkpoint activation provides time to repair DNA damage and prevent mitotic entry with unresolved DNA lesions. Since the cells are constantly exposed to a certain level of DNA lesions, the activity of the checkpoint kinases must be tightly regulated to prevent constant checkpoint activation. Therefore, activation of the PIKK kinases can be regarded as a threshold mechanism, which requires specific DNA substrates, as well as certain amount of DNA damage to initiate the DNA damage signalling pathway. Each of the DNA damage sensor kinases senses DNA lesions via interaction with their specific binding partner: ATRIP for ATR, NBS1 for ATM and Ku70/Ku80 heterodimer for DNA-PKcs (Figure 1.1 A).

The first sensor kinase identified was DNA-dependent protein kinase, catalytic subunit (DNA-PKcs); DNA-PKcs senses DNA double strand breaks bound by Ku heterodimer (Ku70/Ku80) and is mainly involved in DNA double strand break repair by non-homologous end-joining (NHEJ). It does so by DSB end tethering and recruitment of NHEJ repair factors to the site of double strand break. The second sensor kinase is named after patients carrying mutation in its gene, ataxia-telangiectasia mutated (ATM). ATM is an apical kinase, which orchestrates global response to DNA damage by phosphorylation of hundreds of substrate proteins and effector kinases. ATM is recruited to DNA DSBs and activated via interaction with the Nijmegen breakage syndrome protein-1 (NBS1), a subunit of the MRN complex (Falck et al., 2005). The last of the three kinases is ataxia-telangiectasia and Rad3 related (ATR). In comparison to DNA-PKcs and ATM, ATR is an essential protein in proliferating cells and it responds to larger variety of DNA lesions. ATR primarily senses RPA-bound single stranded DNA, which is often a hallmark of endogenous replication stress. ATR, ATM and DNA-PKcs have partially overlapping, as well as unique roles in DNA damage response. They phosphorylate many common substrates, such as histone variant H2AX but they also have unique substrates (reviewed in: Blackford and Jackson, 2017).

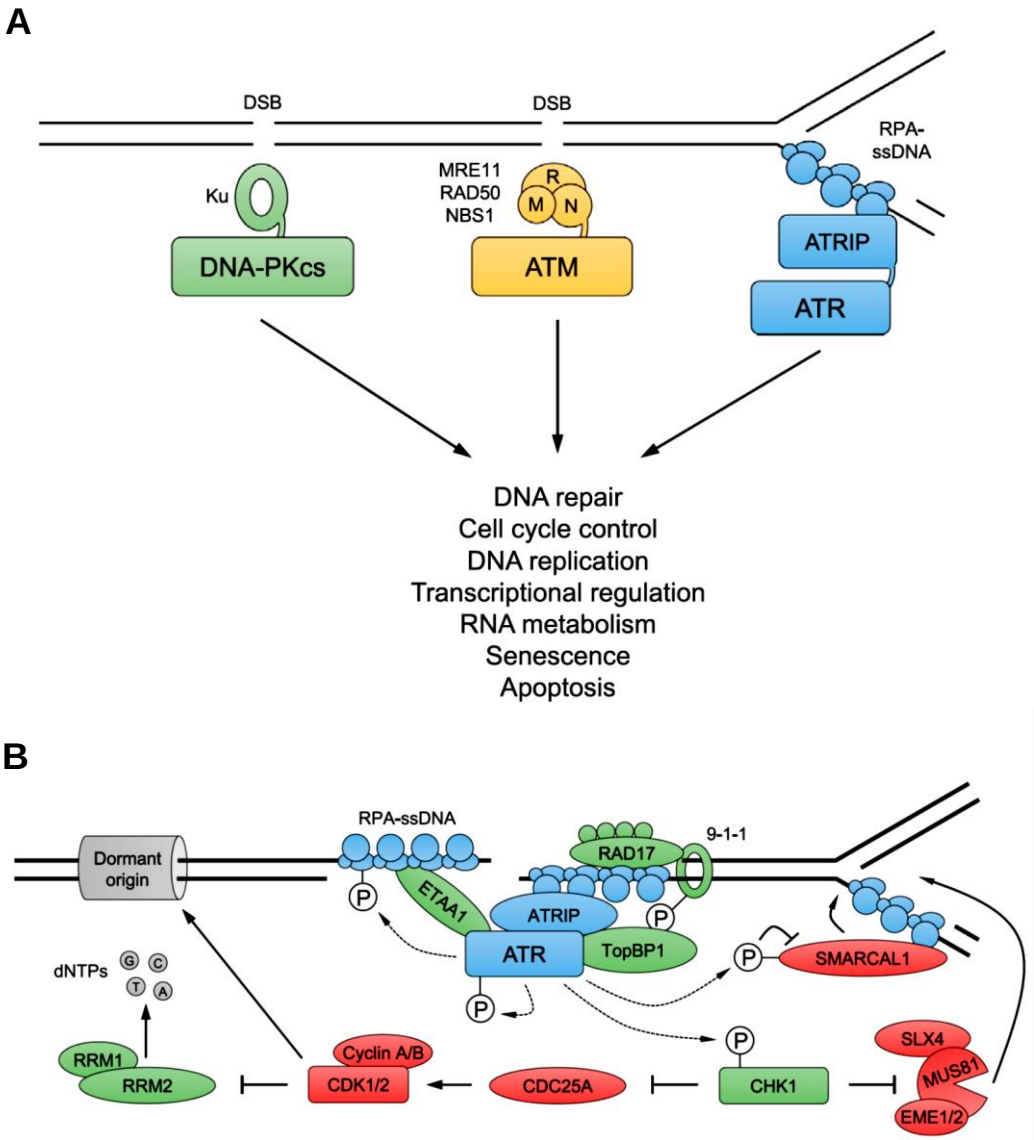


Figure 1.1: Scheme of DNA lesions recognised by activators of the sensor PIKK and the DNA damage response cascade after ATR activation
A. Each of the PIKK kinases have their obligatory sensor partner, for DNA-PKcs it is the Ku80 protein, binding to DNA double strand breaks, for ATM it is the NBS1 (subunit of the MRN complex), involved in DNA DSB resection and for ATR it is ATRIP, which binds to the RPA coated ssDNA. After sensing the DNA lesions, the PIKK orchestrate a multiple-level DNA damage response. **B.** Detection of DNA lesion causes activation of ATR which orchestrates the cellular response, ssDNA bound by RPA are sensed by ATRIP which brings ATR to the lesion, ATR is activated by TOPBP1/9-1-1 complex, ATR undergoes auto-phosphorylation and phosphorylates its downstream substrates and directly restrains fork remodeling helicases (SMARCAL1), CHK1 phosphorylation leads to degradation of CDC25A, which inhibits cell cycle progression by deactivating the CDK kinases and inhibits firing of new origins, inactivation of CDKs increases the dNTP pool by stabilisation of RRM2, CHK1 also inhibits structure-specific nucleases that can cleave the replication fork (Mus81/Eme1/2, SLX4); adapted from: Blackford and Jackson, 2017.

1.1.2.1 ATR mediated response to replication stress

ATR was firstly described in *S. pombe* as a rad3 gene, mutation of which prevented normal G2 arrest after exposure to DNA damage (al-Khodairy and Carr, 1992; Jimenez et al., 1992). Shortly after, ATR was characterised in budding yeast as the Mitotic entry checkpoint (MEC1) gene, which was essential for cell cycle arrest in S and G2 and viability (Weinert et al., 1994). The human ATR gene was identified after, based on homology to the rad3 gene in *S.pombe* and MEC1 in *S. cerevisiae* (Bentley et al., 1996). In vertebrates, ATR together with its obligatory binding partner ATRIP recognises the extensive patches of ssDNA bound RPA and phosphorylates multiple substrates to facilitate processes such as stalled replication fork stabilisation, inhibition of new origin firing and phosphorylation of DNA damage response proteins to alleviate the replication obstacles (Zou and Elledge, 2003, reviewed in: Blackford and Jackson, 2017). For optimal activation, ATR requires its specific activators; the first one is Topoisomerase-binding protein-1 (TOPBP1) containing the ATR-activating domain, which enhances ATR kinase activity *in vitro* (Kumagai et al., 2006). The second ATR activator is RAD9–RAD1–HUS1, so called the 9-1-1 complex. The 9-1-1 complex is a clamp protein which is loaded to the sites of DNA damage by the clamp-loader Rad17/RFC complex and facilitates ATR activation. Interaction of the 9-1-1 complex with TOPBP1 is necessary for ATR/ATRIP binding and activation (Lee et al., 2007, reviewed in: Parrilla-Castellar et al., 2004).

One of the primary role of ATR is to phosphorylate a key effector kinase CHK1. Phosphorylation of CHK1 leads to its activation and DNA damage signalling cascade, as well as proteasomal degradation of CDC25A, a protein phosphatase that removes the inhibitory phosphorylation of cyclin dependent kinases (CDKs) (Figure 1.1 B). This results in reduction of CDK activity and extension of the cell cycle providing time for resolution of DNA damage (reviewed in: Shen and Huang, 2012). Moreover, ATR signalling inhibits new origin firing, which prevents more replication initiation events in the presence of DNA damage (Costanzo et al., 2003; Tercero and Diffley, 2001). Initiation of new origin firing during replication stress will eventually lead to RPA pool exhaustion, a situation, which inevitably leads to replication catastrophe (Toledo et al., 2013). Further, ATR protects replication forks by stabilising them in a conformation, which is not prone to cleavage by structure specific nucleases such as SLX4/MUS81.

It does so by directly targeting helicases, such as SMARCAL1, which would normally lead to fork remodelling and cleavage (Forment et al., 2011). Lastly, ATR-mediated phosphorylation of CHK1 also regulates the dNTP pool by stabilising the RRM2 subunit on transcriptional and post-translational level (Buisson et al., 2015). Other ATR targets at the stalled replication fork are RPA and MCM helicase complex. ATR-dependent phosphorylation of the 32 kDa subunit of RPA (RPA2) on Serine 33 and Threonine 21 limits ssDNA accumulation during replication fork stalling and promotes recovery from replication stress (Olson et al., 2006; Vassin et al., 2009). ATR dependent phosphorylation of MCM complex subunit, MCM2, leads to recruitment of polo-like kinase-1 (PLK1). PLK1 promotes replication in the vicinity of stalled fork, this mechanism is presumably important for completing replication upon DNA damage (Trenz et al., 2008, reviewed in: Blackford and Jackson, 2017).

1.1.2.2 Role of H2AX phosphorylation in DNA damage response

Another important ATR substrate, which is common for ATM and DNA-PKcs, is H2AX. H2AX is a highly conserved histone variant, which constitutes approximately 10% of total H2A protein and it plays an important role during DNA damage signalling. H2AX becomes phosphorylated on serine 139 (Ser139) in response to large variety of DNA lesions (Rogakou et al., 1998; Ward and Chen, 2001). Phosphorylated H2AX (γ-H2AX) creates nuclear foci at the sites of DNA damage. Since γ-H2AX foci are created rapidly and correlate with DNA damage foci, they can be used as a sensitive biological marker of DNA damage and to track the repair kinetics (reviewed in: Sharma et al., 2012). During S-phase DNA DSBs occur when replication fork encounters DNA lesion, or after prolonged stalling, which can lead to replication fork collapse. In this scenario, γ-H2AX is important for recruitment of DNA repair factors and prompt repair. Even though γ-H2AX is not essential for viability in mice and for checkpoint signalling *per se*, it creates a platform for assembly of DNA repair machinery around the DNA lesion (Celeste et al., 2002; Paull et al., 2000). γ-H2AX directly recruits MDC1 protein, which in turn recruits and activates the ATM kinase, this process leads to further amplification of the checkpoint signal (Stucki and Jackson, 2006). MDC1 is phosphorylated by Casein kinase 2 (CK2), which promotes chromatin retention of the MRN complex to the sites of DNA damage (Chapman and Jackson, 2008). The γ-H2AX signal spreads rapidly from the site of original DSB up to several mega base pairs (Mbp), which creates a platform to enhance

local protein interactions and the DNA repair process (reviewed in: Kinner et al., 2008). In human cells, rapid H2AX phosphorylation occurs 20 minutes after exposure to IR and reaches its peaks around 2 hours after DSB induction by IR. In normal cells the γ-H2AX signal gradually decreases close to its normal levels within 24 hours (Sharma et al., 2015). To stop the DNA damage signalling, γ-H2AX has to becomes dephosphorylated by protein phosphatase 2A (PP2A). De-phosphorylation of γ-H2AX occurs independently on PIKKs and allows appropriate completion of DNA repair and cell cycle progression (Chowdhury et al., 2005).

1.1.3 DNA double strand break repair pathways

As aforementioned, DNA double strand breaks are one of the most toxic DNA lesions. Unrepaired DSBs in most cases lead to cell death or senescence, whereas incorrectly repaired DSBs can lead to chromosome rearrangements and potentiate carcinogenesis. There are two major repair pathways of DNA double strand break repair: non-homologous end-joining (NHEJ) and homologous recombination (HR) (Figure 1.2). The repair pathway choice can be regarded, as a combination of competing mechanisms favouring one or the other pathway and circumstances, each of them influencing whether the DSB will undergo NHEJ or HR mediated repair. As its name suggests, NHEJ does not require, or requires just minimal, exposure of homologous DNA sequence to repair the two-ended DNA DSBs, Hence, it can be simplistically described as a direct ligation of two broken DNA ends. In mammalian systems, NHEJ is the predominant DNA DSB repair pathway operating throughout the cell cycle (Figure 1.3 A). Completion of DSB repair by canonical NHEJ (c-NHEJ) in human cells takes approximately 30 minutes, with much faster kinetics in comparison to DNA repair by HR, which usually requires at least 7 hours to complete (Mao et al., 2008). Thus, DSBs experimentally generated by IR are mostly repaired by NHEJ with fast kinetics within the first 2 – 4 hours after exposure (Figure 1.3 B). However, due to the absence of homologous template, NHEJ, in comparison to HR, is more likely to generate chromosome rearrangements or mutations. On the other hand, HR is largely restricted to S/G2 phase of the cell cycle, when the emergence of sister chromatid can serve as a repair template (Figure 1.3 A). HR is considered to be an error-free DSB repair pathway during the normal cell cycle and is primarily involved in rescue of stalled or collapsed replication forks. DSB repair by HR

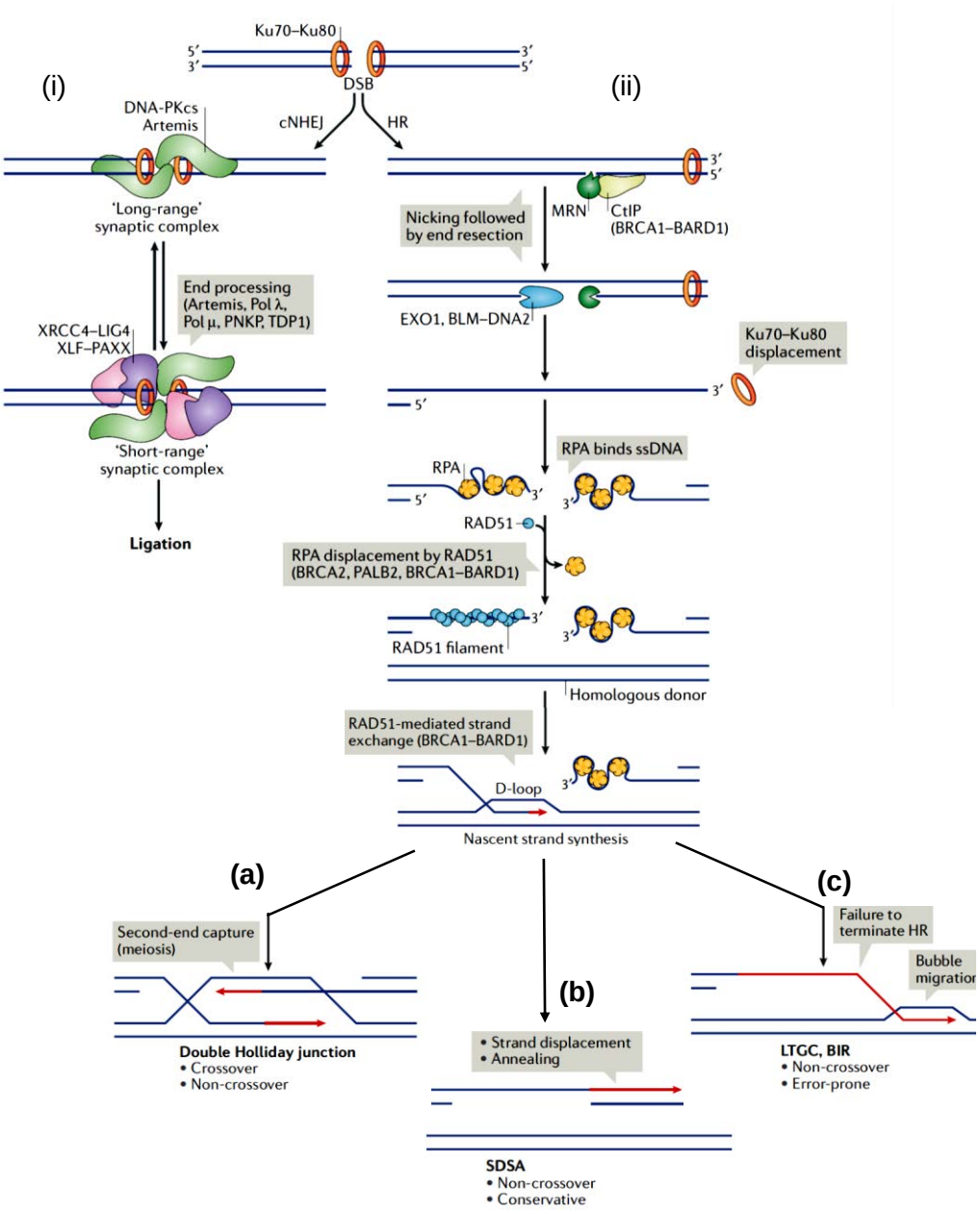


Figure 1.2: Pathways of double strand break repair in mammalian cells
DNA double strand break is bound by the Ku70/80 heterodimer which directs the repair pathway towards canonical NHEJ (cNHEJ) (i): DNA-PKcs is recruited by physical interaction with Ku70/80 heterodimer which leads to formation of a long-range synapse, additional NHEJ factors, XRCC4, LIG4 and XLF, PAXX are essential for formation of a short-range synapse prior to DNA end ligation by LIG4, damaged and non-ligatable DNA ends can be processed by additional factors, such as Artemis, Pol μ and λ or PNKP; when the DNA DSB cannot be repaired by NHEJ, HR is initiated (ii): MRN complex mediates short range resection, long range resection is mediated by the EXO1 and DNA2/BLM to expose homologous 3' end, RPA coated ssDNA overhangs are displaced by Rad51, which catalyses the strand invasion of the homologous donor template, D-loop formation precedes different HR sub-pathways: (a) during meiosis, double Holliday junction forms between homologs resolved either by crossover or non-crossover (b) in somatic cells synthesis-dependent strand annealing is the predominant pathway, where only one end of DSB is extended before template switching (c) failure to properly terminate HR leads to mutagenic break induced replication, which can lead to loss of heterozygosity; adapted from: Scully et al., 2019.

occurs with much slower kinetics than repair by NHEJ (Figure 1.3 B). Compromising the HR-repair pathway is associated with increased risk of malignancies and cancer incidence (reviewed in: Rothkamm et al., 2003 and Löbrich and Jeggo, 2017).

1.1.3.1 Non-homologous end joining

In mammalian cells, the majority of DNA DSBs are repaired by canonical or alternative NHEJ pathway. c-NHEJ is typically initiated by binding of Ku70/Ku80 to a double-ended DSB, the Ku70/80 heterodimer can encircle and slide alongside the DNA double helix (Walker et al., 2001). Ku70/80 bound DNA DSB serves as a scaffold for recruitment of other NHEJ repair factors: DNA-PKcs, DNA ligase IV (LIG4) and associated scaffolding proteins, XRCC4 and XLF and PAXX (Ahnesorg et al., 2006; Gottlieb and Jackson, 1993; Ochi et al., 2015; Yano et al., 2008, reviewed in: Davis and Chen, 2013). NHEJ often involves DNA DSB-end trimming prior to the ligation step and the Artemis nuclease, another NHEJ factor, can be involved in additional processing of Ku70/80 bound DSB breaks prior to ligation (Figure 1.3) (reviewed in: Scully et al., 2019). Artemis has a nuclease activity involved in processing of a range of DNA intermediates during DSB repair using both NHEJ and HR. Artemis forms a complex with and is phosphorylated by DNA-PKcs, which allows it to open and process DNA hairpins, a common intermediates during V(D)J recombination (Ma et al., 2002). c-NHEJ can be Artemis dependent or independent, Artemis dependent c-NHEJ occurs with slower kinetics than Artemis independent c-NHEJ (reviewed in: Löbrich and Jeggo, 2017).

In vertebrates, NHEJ plays a key role in the adaptive immune system response. During T and B lymphocytes development, NHEJ is essential for generation of variable receptors to generate diverse immunoglobulins/antibodies and T-cell receptors in a process called V(D)J recombination. During V(D)J recombination, immunoglobulin and the T-cell receptor gene segments randomly assemble by recombination between Variable (V) Diversity (D) Joining (J) gene segments. After introduction of DSBs by the RAG nuclease complex, the DNA is repaired by the NHEJ machinery. This results in generation of novel amino acid sequence in the antigen receptors and sustains the plasticity of the adaptive immune system (reviewed in: Malu et al., 2012).

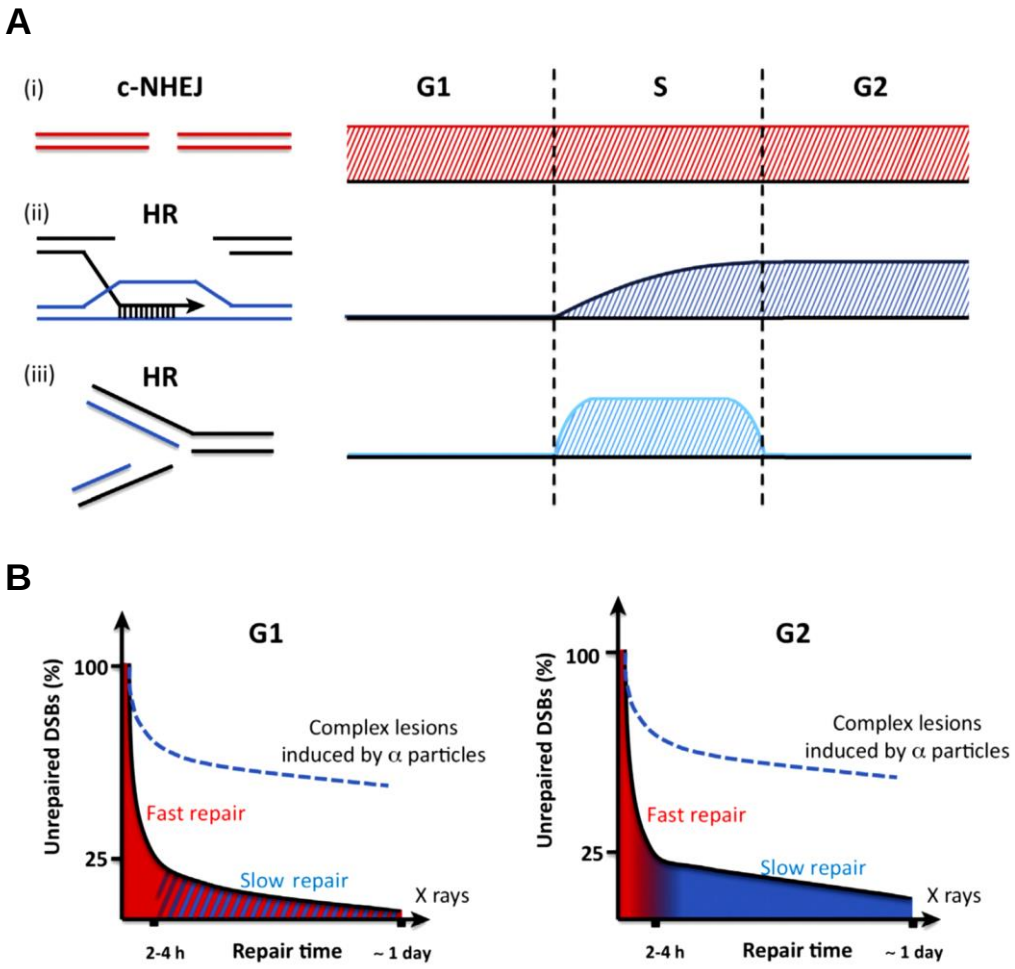


Figure 1.3: Contribution of various DSB repair pathways during mammalian cells **A.** Schematic illustration of DNA repair pathways operating throughout the cell cycle, (i) canonical NHEJ (c-NHEJ) is a predominant DSB repair pathway operating throughout all phases of the cell cycle, (ii) a subset of two-ended DNA DSB generated for example by IR, usually in heterochromatic regions, can be repaired during S and G2 phase of cell cycle using the sister chromatid as a repair template, (iii) replication dependent one-ended DNA breaks are repaired in a HR-dependent mechanism called break induced-replication, which leads to loss of heterozygosity (LOH). **B.** Graph of repair kinetics of IR induced DNA double strand breaks; in G1 phase of the cell cycle, majority of DSBs are repaired by c-NHEJ with fast kinetics within the first 2 – 4 hours (in red), the slow repair fraction is usually connected with ATM signalling activation, the repair usually involves Artemis dependent c-NHEJ, which share similarities between HR and NHEJ (red with blue stripes); in G2 the fast repair fraction involves the c-NHEJ mechanism, whereas the slow repair fraction is repaired by HR (blue); adapted from: Löbrich and Jeggo, 2017.

1.1.3.2 Homologous recombination

In comparison to NHEJ, which repairs the vast majority of DNA DSB in mammalian systems, HR is a process restricted to relatively small subset of DNA lesions in S/G2 phase of the cell cycle. In S-phase, HR is thought to play primarily role during replication fork stalling and collapse (reviewed in: Löbrich and Jeggo, 2017). However, homologous recombination is also critical for repair of DNA inter-strand crosslinks. Canonical HR favours recombination between sister chromatids, which are spatially aligned and held in a close proximity by cohesin during and after DNA replication. This ensures that in mitotic cells, recombination between sister chromatids is preferred over recombination between homologous chromosomes (Gerlich et al., 2006; reviewed in: Scully et al., 2019). In contrast, during meiotic division, HR between homologous chromosomes is the preferred pathway. The preference for inter-homologue HR during meiosis is driven by specialised proteins. There is a programmed generation of DNA DSBs by Spo11 endonuclease and instead of canonical Rad51 recombinase, a meiotic recombinase Dmc1 is utilised (reviewed in: Krejci et al., 2012).

One of the determining step for HR pathway is a nucleolytic processing of the 5' ends of the DSB (Figure 1.2). Upon conditions, which do not favour the DSBs repair by c-NHEJ, the DSB can undergo nucleolytic processing termed DNA end resection. This process is initiated by the MRN (MRE11-RAD50-NBS1) complex, in particularly by the MRE11 subunit, which possess both endo and exonuclease activity. Facilitated by interaction with CtIP, MRE11 endonuclease activity generates a nick downstream of the DSB and processes the DNA end by its 3' – 5' exonuclease activity to generate 3' ssDNA overhang (Limbo et al., 2007). Equally, MRE11 DNA nicking generates an entry point for a long range resection carried out by EXO1 and DNA2 with Bloom syndrome (BLM) helicase. The long range resection has 5' – 3' polarity and can span up to thousands of nucleotide. During long range resection, the nucleolytic DNA degradation is mediated by the exonuclease activity of EXO1. The whole resection is facilitated by DNA unwinding mediated by the BLM helicase. Long range resection is essential to expose the homologous ssDNA overhangs in order to allow the homology search (Mimitou and Symington, 2008). RPA bound to the ssDNA overhangs is then exchanged for the Rad51 recombinase in a process mediated by BRCA2 with PALB2 (Jensen et al., 2010; Yang et al., 2005). Rad51 is a key homologous recombination factor, which forms pre-synaptic

filament and catalyses the strand invasion step into the homologous DNA template. Human Rad51 protein is essential for most types of homologous recombination and forms distinct nuclear foci during S-phase at the sites of double-strand breaks (Tashiro et al., 1996, 2000; reviewed in: Krejci et al., 2012).

The assembled Rad51-ssDNA nucleofilament is a dynamic structure, which can invade the donor DNA template to perform a homology search. The process of homology search is regulated by multiple factors, such as BRCA1/BARD1, the Rad54 family of proteins and RecQ helicases (Tavares et al., 2019; Zhao et al., 2017; reviewed in: Wu, 2008). The homology search is a tightly controlled process influenced by organisation, spatial proximity and chromosome landscape around the DSB. Rad51 nucleofilament is known to sample the donor DNA, until a suitable homologous template is found (reviewed in: Greene, 2016). Sufficient base pairing between the homologous template and the invading ssDNA nucleofilament drives stabilisation of the synapse, and initiates the formation of a displacement loop (D-loop). D-loop formation is driven by Rad51 ATP hydrolysis and disassembly. The invading strand is then extended by DNA polymerase δ (Maloisel et al., 2008; reviewed in: McVey et al., 2016). Rad51-mediated synapse can then lead to different HR sub-pathways (Figure 1.2): (a) Second end capture dictates the formation of double Holiday junction (dHJ), which can be either dissolved by the BLM–TOP3–RMI1 complex, or be resolved in a crossover or non-crossover manner. (b) Synthesis-dependent strand annealing (SDSA) is the most prominent HR sub-pathway in somatic cells. During SDSA only one side of the DSB engages in the D-loop extension, typically using sister chromatid as a homologous donor. SDSA does not lead to dHJ formation, hence, does not lead to crossovers. (c) Failure to engage the second end in SDSA or repair of one-ended DSB can lead to alternative and more error prone HR sub-pathways, such as long-tract gene conversion or break-induced replication (BIR). During long-tract gene conversion the invading strand synthesis spans over kilobases prior to termination. BIR often occurs at replication dependent one-ended DSBs, when the homologous template (sister chromatid) has not been synthesised. Due to the absence of the second DSB, BIR can span over hundreds of kilobases and generates extensive ssDNA that are prone to mutations, template switching and genome rearrangements (Saini et al., 2013; Smith et al., 2007). However, the mutagenicity of BIR has been shown to be alleviated *in vivo* by Mus81 and a converging fork coming from the opposite direction (Mayle et al., 2015).

1.1.3.3 Repair at stalled or collapsed replication fork

Homologous recombination has been shown to play a key role in genome stability maintenance during S-phase, namely in re-establishing collapsed fork. Stalled replication forks differ in many aspects from a conventional DSB in that they contain branched DNA intermediates, ssDNA gaps and replisome components. Stalled forks trigger a specific DNA damage response pathway primarily coordinated by ATR. The stalled fork undergoes active remodelling, which involves fork reversal (reviewed in: Scully et al., 2019). Replication fork reversal has recently been recognised as a regulated response to replication fork stalling ensuring replication completion and protecting genome integrity. During replication fork reversal, the two parental strands undergo reannealing and simultaneously, the newly synthesised strands anneal together. This leads to formation of a four-way junction at the original three-way replication fork, which enables transmission of the DNA lesion ahead of the fork. Fork reversal appears to be a common response to naturally occurring replication stress, as well as a range of genotoxic treatments (Amunugama et al., 2018; reviewed in: Neelsen and Lopes, 2015). Rad51 recombinase is essential to convert the stalled replication fork into a reversed fork (Zellweger et al., 2015). Recently, BRCA2 has been shown to play a role in maintenance of reversed fork stability by protecting the Rad51 filament at reversed fork from nucleolytic degradation by MRE11 (Kolinjivadi et al., 2017).

Another factor playing an important role in replication and replication fork protection in mammalian cells is Poly (ADP-ribose) polymerase (PARP). PARP is an abundant nuclear protein activated by DNA strand breaks, as well as stalled replication forks (Bryant et al., 2009; Satoh and Lindahl, 1992). Its activity is associated with active DNA replication; PARP physically interacts and PARylates several replication proteins, such as DNA polymerase α, PCNA, or Topoisomerase I (Simbulan-Rosenthal et al., 1996). PARP is activated by stalled replication forks, to which it recruits the MRN complex to mediate nucleolytic processing and replication fork restart (Bryant et al., 2009). Moreover, PARP1 activity has been shown to be a key mediator of replication fork by reversal during Top1 inhibition (Ray Chaudhuri et al., 2012). PARP1 stabilises the replication fork in a regressed state (four-way junction) by antagonising the RECQ1 helicase, which is, on the other hand, important for replication fork restoration after reversal (Berti et al., 2013; reviewed in: Liao et al., 2018).

1.2 The SMC complexes

In order to successfully divide, each eukaryotic cell has to undergo highly organised process of chromosome duplication and segregation. Structural Maintenance of Chromosomes (SMC) proteins play pivotal roles in maintaining of genomic stability by organisation of higher-order chromosome structure and dynamics throughout the cell cycle. The SMC family of proteins is well-conserved from bacteria to human. Bacterial genomes usually encodes only a single SMC, which forms a homodimer, whereas there are at least six Smc paralogs (Smc1 – 6) in eukaryotes (Soppa, 2001; reviewed in: Hirano, 2002). In eukaryotes, Smc proteins are the core parts of three SMC complexes: Cohesin, condensin and the Smc5/6 complex. Eukaryotic Smc proteins form heterodimers that share a similar architecture: an N- and C-terminal globular heads with ATPase domains, interconnecting coiled-coiled arms, and hinge domains important for complex dimerisation. The length of the Smc coiled coil arms is approximately 50 nm. Smc proteins associate with each other at the hinge and ATP binding and hydrolysis occurs in two active sites formed by association between the dimer globular heads (Figure 1.4 A). They associate with other non-structural elements to form a functional holocomplex (Haering et al., 2002; reviewed in: Losada and Hirano, 2005). Kleisins, which bridge the globular domains of the Smc proteins, are common elements for all eukaryotic SMC complexes (Figure 1.4 B). There are other regulatory subunits associated with kleisins. In case of the Smc5/6 complex, these are termed Kites (Kleisin interacting winged-helix tandem elements) and in case of cohesin and condensin Hawks (HEAT proteins associated with kleisins). The Kite proteins of the Smc5/6 complex are structurally related to the bacterial Smc proteins. The Hawk proteins form an evolutionary related cluster, which seems to have displaced Kites in cohesin and condensin (Figure 1.4 B). The appearance of Hawk – kleisin – Smc architecture seems to be uniquely eukaryotic (reviewed in: Palecek and Gruber, 2015). Due to the common presence of Hawk proteins, cohesin and condensin seem to be closer related, whereas the Smc5/6 complex resemble the prokaryotic Smc complexes (reviewed in: Wells et al., 2017). Condensin, consists of Smc2/Smc4 heterodimer and three non-SMC elements, is important for sister chromatid condensation and proper chromosome segregation in meiosis mitosis (Hirano and Mitchison, 1994). Cohesin, comprising Smc1/Smc3 and four non-SMC elements, mediates sister chromatid cohesion (Haering et al., 2008), transcriptional regulation

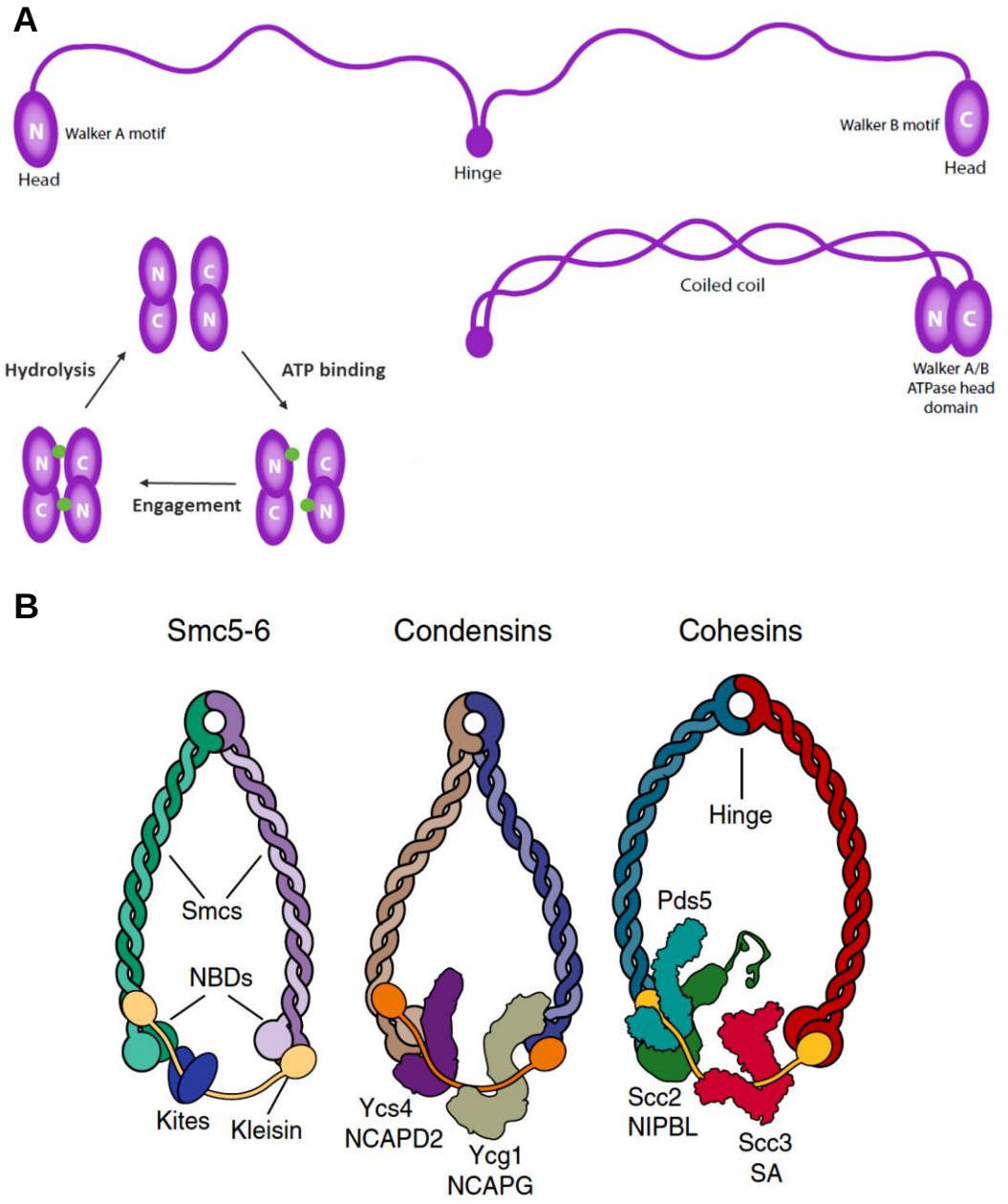


Figure 1.4: Architecture of the eukaryotic SMC complexes
A. SMC proteis contain globular C- and N-terminal ATPase domains (Walker boxes) linked through two α-helices that form a coiled coil domain and are attached together at a hinge domain; ATPase cycle of SMC proteins: binding of two ATP molecules (green) between the head domains inducing their engagement, subsequent ATP hydrolysis induces their disengagement; adjusted from: Verver et al., 2016 and Shintomi and Hirano, 2007. **B.** Schematic illustration of the eukaryotic SMC complexes: Smc5/6, condensin and cohesin; the Smc heterodimers associate together at the hinge regions, the N and C terminal domains of the SMC proteins form the globular nucleotide-binding domain (NBD), kleisins (yellow), a common subunits for all SMC complexes, bridge the globular head domains of the Smcs allowing topological entrapment of DNA; In Smc5/6, Kite (Kleisin interacting winged-helix tandem elements) proteins interact with kleisins, in cohesin and condensin, Hawk (HEAT proteins associated with kleisins) proteins interact with kleisins; in cohesin, Scc2 competes with Pds5 for its binding site on the kleisin; adapted from: Wells et al., 2017.

(Remeseiro et al., 2012) and DNA double strand break (DSB) repair (Strom et al., 2007; Ström et al., 2004). The Smc5/6 complex remains functionally unnamed, as its function is not yet clear. Smc5/6 is an essential complex, which function is required for the DNA damage response and genome stability (Murray and Carr, 2008).

1.2.1.1 Loop extrusion as an emerging mechanism of genome organisation

The eukaryotic SMC proteins are key genome organisers. It has been found that both cohesin and condensin are capable of chromosome organisation into loop structures. Recent studies have suggested a new concept for how the SMC complexes could organise the genome. In about 2015 the hypothesis of 'loop extrusion' as a central process of chromosome organisation was developed by Leonid Mirny and John Marko; Leonid Mirny's lab used polymer simulations of chromosome dynamics to propose 'loop extrusion' as a model of rapid chromosome compaction by condensin (Goloborodko et al., 2016). Loop extrusion models are also consistent with experimental evidence for the formation of topological domains. Hi-C experiments in mammalian cells revealed that interphase chromosomes are organised into topologically associated domains (TADs), within which certain DNA regions interact more frequently. The boundaries of TADs are enriched of the insulator factor CTCF and housekeeping genes (Dixon et al., 2012). Recent polymer simulation experiments led to a model, where cohesin mediated loop extrusion is responsible for organisation of interphase chromatin into TADs (de Wit et al., 2015; Fudenberg et al., 2016; Goloborodko et al., 2016; Nuebler et al., 2018). In the current model of TAD organisation, CTCF serves as a boundary element that blocks the loop extrusion by cohesin (Figure 1.5 A). The fact that CTCF serves as a boundary element for loop extrusion is supported by studies showing that depletion of CTCF leads to defects at TAD boundaries and abrogation of chromatin loops formed between CTCF elements (Nora et al., 2017). Similarly to cohesin, loop extrusion by condensin has recently been proposed to mediate chromatin compaction prior to mitosis or meiosis. A recent *in vitro* study revealed that condensin is a mechanochemical motor, which uses its ATPase activity to translocate along the DNA curtains (Terakawa et al., 2017). Further evidence for condensin being capable of loop extrusion is based on a study showing that purified budding yeast condensin can progressively enlarge DNA loops in an ATP dependent manner (Ganji et al., 2018). The results further support the role of condensin in 3D genome organisations via loop extrusion and represent an important step in

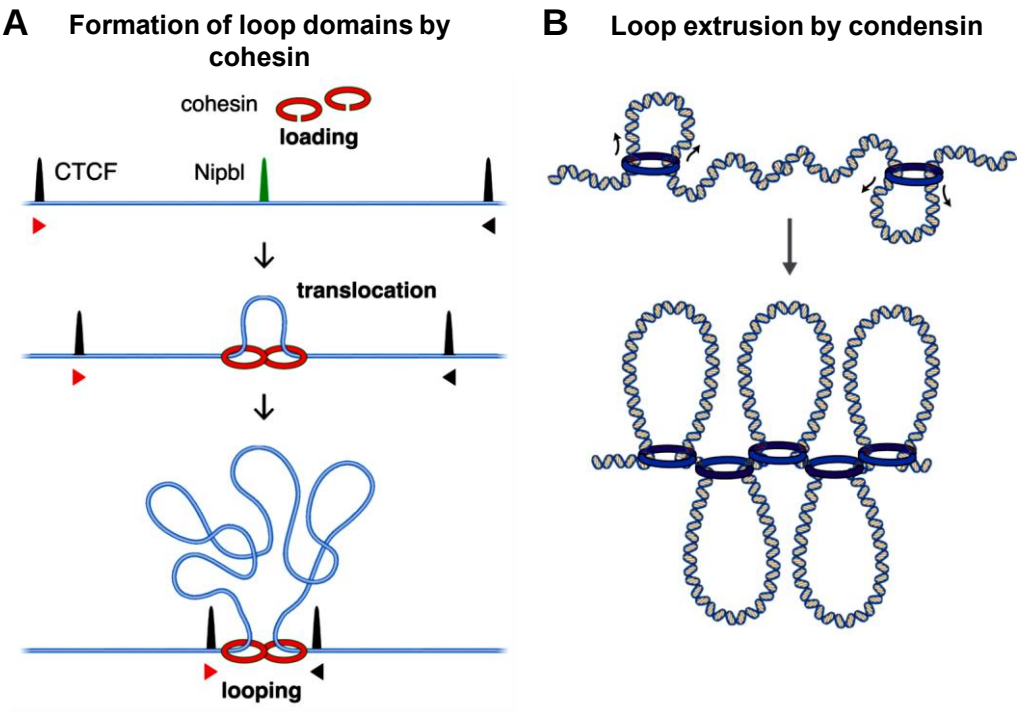


Figure 1.5: Model of formation of chromatin loops by SMC complexes, cohesin and condensin

A. Model of topological domain formation by cohesin mediated loop-extrusion; cohesin is loaded by a loader complex (Nipbl), single or physically tethered cohesin complexes work as motors, which extrude DNA to form loops, in order to extrude loops, cohesin does not bind DNA topologically; adapted from: Vian et al., 2018. **B.** Model of condensin mediated organisation of mitotic chromosome around axial core; condensin mediated loop extrusion facilitates the formation of individual compacted chromatids during cell division; adapted from: Yatskevich et al., 2019.

understanding of how condensins might compact the chromosomes prior to cell division (Figure 1.5 B). The loop extrusion model is a relatively new hypothesis explaining the genome organisation by the SMC complexes. To date, there are different models of the mechanism, by which the SMC complexes extrude loops. However, a satisfactory explanation of how the SMC complexes translocate on DNA and extrude loops is still awaiting more detailed experimental validation.

1.2.2 Cohesin

The cohesin complex is widely known for tethering sister chromatids during S-phase, an essential prerequisite for chromosome segregation during cell division. Cohesin is loaded onto chromosomes immediately after chromosome segregation in G1 phase, the loading process depends on the Scc2/Scc4 cohesin loader complex (Ciosk et al., 2000; Watrin et al., 2006). The establishment of sister chromatid cohesion requires acetylation of cohesin subunit Smc3 by acetyltransferase Eco1 and is coupled to DNA replication (Ben-Shahar et al., 2008; Song et al., 2012; reviewed in: Makrantoni and Marston, 2018). In most organisms studied, including human cells, cohesin is removed from chromosomes during mitosis in a two-step fashion; during prophase cohesin is stripped from chromosome arms in Wapl dependent manner and requires phosphorylation of SA2 subunit (Hauf et al., 2005). This process is regulated by Plk1 and Aurora B dependent manner (Kueng et al., 2006; Losada et al., 2002). At the metaphase to anaphase transition, the residual centromeric cohesin is removed from the centromeres in by cleavage of its kleisin subunit (SCC1) by separase and this process is regulated by the APC complex (Nakajima et al., 2007; Waizenegger et al., 2000; reviewed in: Tapia-Alveal et al., 2014). Cohesin does not have a fixed pattern of localisation on chromosomes, it is loaded onto and can slide alongside DNA. Cohesin localises to sites of convergent transcription and it has been suggested that cohesin can be pushed to slide along DNA by transcription machinery (Lengronne et al., 2004; Ocampo-Hafalla et al., 2016). However, cohesin localisation on chromosomes in mammalian systems does not seem to be driven by transcription. Instead, cohesin has been shown to localise at the CTCF binding sites and its localisation is dependent on the presence of CTCF (Parelho et al., 2008).

Cohesin also plays a key role during DNA repair; in budding yeast, cohesin localises in a replication independent manner to the vicinity of double strand breaks and this is important to allow correct DSB repair (Ström et al., 2004). Although sister chromatid

cohesion is typically limited to S-phase, post-replicative cohesion establishment also occurs in a replication-independent manner during G2/M. Post-replicative cohesion is triggered by DNA double strand break and depends on DNA damage response factors and cohesin regulators (Strom et al., 2007; Ünal et al., 2007). As mentioned above, cohesin has been found to be a key element mediating the formation of topologically associated domains (TADs), likely by gradual enlargement of DNA loops (Nuebler et al., 2018). Equally, cohesin mediated loop extrusion has also been implicated in regulation of transcription and homologous recombination (Vian et al., 2018).

1.2.3 Condensin

The SMC subunits of the condensin complex, were first identified as a heterodimeric coiled coil proteins important for assembly of mitotic chromosomes in *X. laevis* egg extract (Hirano and Mitchison, 1994). Since then many studies have been performed on condensins. Due to the presence of Hawk proteins, condensins seem to be evolutionary closer to cohesin (reviewed in: Wells et al., 2017) . Eukaryotic condensins can be divided into two types, condensin I and condensin II, both sharing the Smc2 and Smc4 heterodimer and differ in kleisin and Hawk subunits (Ono et al., 2004). In a hermaphrodite worm, *C. elegans*, a condensin I-like complex has been identified. The complex differs from condensin I in the Smc4 subunit and is known to regulate dosage compensation, i.e. reduces the sex chromosome gene expression (Chuang et al., 1994; Csankovszki et al., 2009). While condensin I is conserved from yeasts to human, condensin II has is absent in yeast and studied excavates and ciliates. However, the absence of condensin II seem to be due to its loss in evolution rather than its appearance in higher eukaryotes (reviewed in: Hirano, 2012). Both condensin complexes have non-redundant roles in chromosome metabolism, however their roles largely vary between species. In mammalian cells, condensin I is sequestered in cytoplasm during interphase, whereas condensin II is in the nucleus (Ono et al., 2004). Work in *X. laevis* egg extract showed that the ratio between cohesin, condensin I and condensin II seems to dictate the chromosome shape. While condensin II contributes to axial shortening of chromosomes, condensin I, together with cohesin, drive the juxtaposition of sister chromatid arms (Shintomi and Hirano, 2011). The kleisin subunit of mammalian condensin II (*kleisin-β*) has been shown to be important for the normal immune response in mice. Mice with a point mutation in the *kleisin-β* gene showed defect in T-cell development and diminished T-cell dependent antibody response

but no defects in B-cell function (Gosling et al., 2008). Condensin II has also been shown to regulate erythroid cell differentiation by transcriptional regulation (Xu et al., 2006). In *S. cerevisiae*, condensin has been shown to function together with the Fob1 protein at the replication barrier site (RFB) to prevent contraction of the rDNA repeats (Johzuka et al., 2006). The recruitment of condensin to the RFB site requires Fob1, as well as two subunits of the fork protection complex, Csm1 and Tof1 and a nucleolar protein Lrs4, and is important for appropriate rDNA segregation (Johzuka and Horiuchi, 2009). Condensin is also responsible for generation of positive supercoils on sister DNA molecules in Top2 depleted yeast cells. During normal cell cycle, the generation of positive supercoils drives Top2 mediated decatenation of sister chromatids before segregation (Baxter et al., 2011; reviewed in: Hirano, 2012). Similarly to cohesin, loop extrusion by condensin has recently been proposed to mediate chromatin compaction prior to mitosis or meiosis; organisation of mitotic DNA into chromatids can be explained by a processive loop expansion around the axial core created by condensins (Figure 1.5 B) (reviewed in: Yatskevich et al., 2019).

1.2.4 The SMC5/6 complex

The Smc5/6 complex was originally discovered through the analysis of a radiation sensitive mutant (*rad18-X*) in fission yeast (*Schizosaccharomyces pombe*) (Lehmann et al., 1995; Nasim and Smith, 1975). Rad18 was later shown to be part of a novel SMC complex associated with DNA repair (Fousteri and Lehmann, 2000). Nomenclature of the complex was standardised and the mutant renamed *smc6-X* to avoid confusion with the unrelated budding yeast Rad18, required for post replication repair. The Smc5/6 complex consists of two Smc proteins and four to six non-SMC elements (denoted Nse in yeast and NSMCE in mammals). Similarly to cohesin and condensin, the Smc5/6 complex also exhibits ATPase activity, which has been shown to be stimulated by double stranded DNA (Fousteri and Lehmann, 2000). Despite the Smc5/6 complex being highly conserved, its architecture varies slightly between species. In fission yeast the Nse5 and Nse6 subunits interact with the globular head domains of Smc5 and Smc6. In contrast, in budding yeast, both Nse5 and Nse6 seem to interact with the hinge domains of Smc5 and Smc6. The mammalian Smc5/6 complex contains the SMC5/SMC6 heterodimer and four non-SMC elements (reviewed in: Verver et al., 2016a). There are homologs of Nse5 and Nse6 in human, termed SLF2 and SLF1 respectively (Räschle et al., 2015) (Figure 1.6).

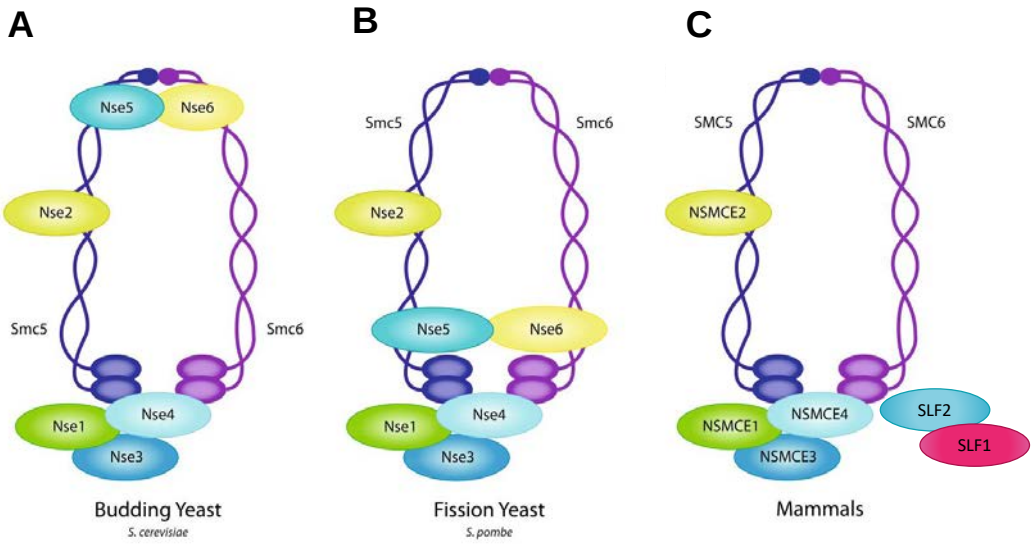


Figure 1.6: Architecture of the Smc5/6 complexes in different organisms
A – B. Yeast Smc5/6 contains the Smc5/6 coiled coil arms and six non-SMC elements, the Nse2 SUMO ligase interacts with the coiled-coil arm of Smc5, in budding yeast essential Nse5, Nse6 components interact with the hinge domains of Smc5/6 heterodimer (A), in fission yeast, non-essential Nse5 and Nse6 interact with the globular head domains of Smc5/Smc6 (B). **C.** Mammalian Smc5/6 complex contains the SMC5/SMC6 heterodimer and four non-SMC elements, there are homologs of Nse5 and Nse6 in vertebrates, termed SLF1 and SLF2 respectively; adjusted from: Verver et al., 2016.

Smc5/6 complex can be divided to three sub-complexes: The first one is Smc5 and Smc6 heterodimer and a SUMO-ligase Nse2 which associated with Smc5 (Duan et al., 2009a; Zhao and Blobel, 2005). The second sub-complex comprises tightly bound Nse1-Nse3-Nse4 heterotrimer bridging the globular domains of Smc5 and Smc6 (Palecek et al., 2006). The third sub-complex comprises Nse5 and Nse6, which are involved in the recruitment of Smc5/6 to DNA lesions (Bustard et al., 2012; Oravcová et al., 2019; Pebernard et al., 2006).

1.2.4.1 The Smc5/Smc6 and Nse2 sub-complex

Smc5 and Smc6 are coiled coil proteins forming approximately 50 nm long heterodimer connected via their hinge domains (Alt et al., 2017). The globular domains of Smc5 and Smc6 are bridged together by the Nse1-Nse3-Nse4 heterotrimer (Palecek et al., 2006). Heterodimerisation of Smc5 and Smc6 increases their affinity to DNA substrates, which resemble Holliday junctions and replication forks (Roy et al., 2015). The hinge domain of the Smc5/6 complex shares similar architecture with cohesin and condensin hinge, which form a 'donut-like' toroidal structure (Figure 1.7 A) (Alt et al., 2017; Griese et al., 2010; Kurze et al., 2011). However, unlike the other SMC proteins, the Smc5/6 hinge has a unique interface stabilised by a molecular 'latch' and 'hub' features. The latch is formed by a conserved Smc5-C loop, whereas the hub is formed by Smc6. Both features are important for the Smc5/6 function in yeast and human cells and they are likely to contribute to the more dynamic loading/unloading of the Smc5/6 complex in comparison to cohesin and condensin (Alt et al., 2017). Similarly to the mouse condensin hinge (Griese et al., 2010), the Smc5/6 hinge has been shown to preferentially bind to single stranded DNA (Alt et al., 2017; Roy et al., 2015).

Nse2 (also known as Mms21) physically interacts with coiled-coil domain of Smc5 arm (Duan et al., 2009a) and contains a variant of a RING motif called SP-RING (reviewed in: Hochstrasser, 2001). Nse2 exhibits SUMO (Small Ubiquitin-like Modifier) E3 ligase activity, it is autosumoylated and among other substrates sumoylates Smc6 in fission yeast and humans, and Smc5 in budding yeast (*Saccharomyces cerevisiae*) (Andrews et al., 2005; Potts and Yu, 2005; Zhao and Blobel, 2005). Abolishment of its SUMO ligase activity confers cell sensitivity to DNA damage in S phase and thus, it is important for the S-phase DNA repair function of Smc5/6 (Andrews et al., 2005; Potts and Yu, 2005; Zhao and Blobel, 2005; reviewed in: Kegel and Sjögren, 2010). The SUMO-ligase

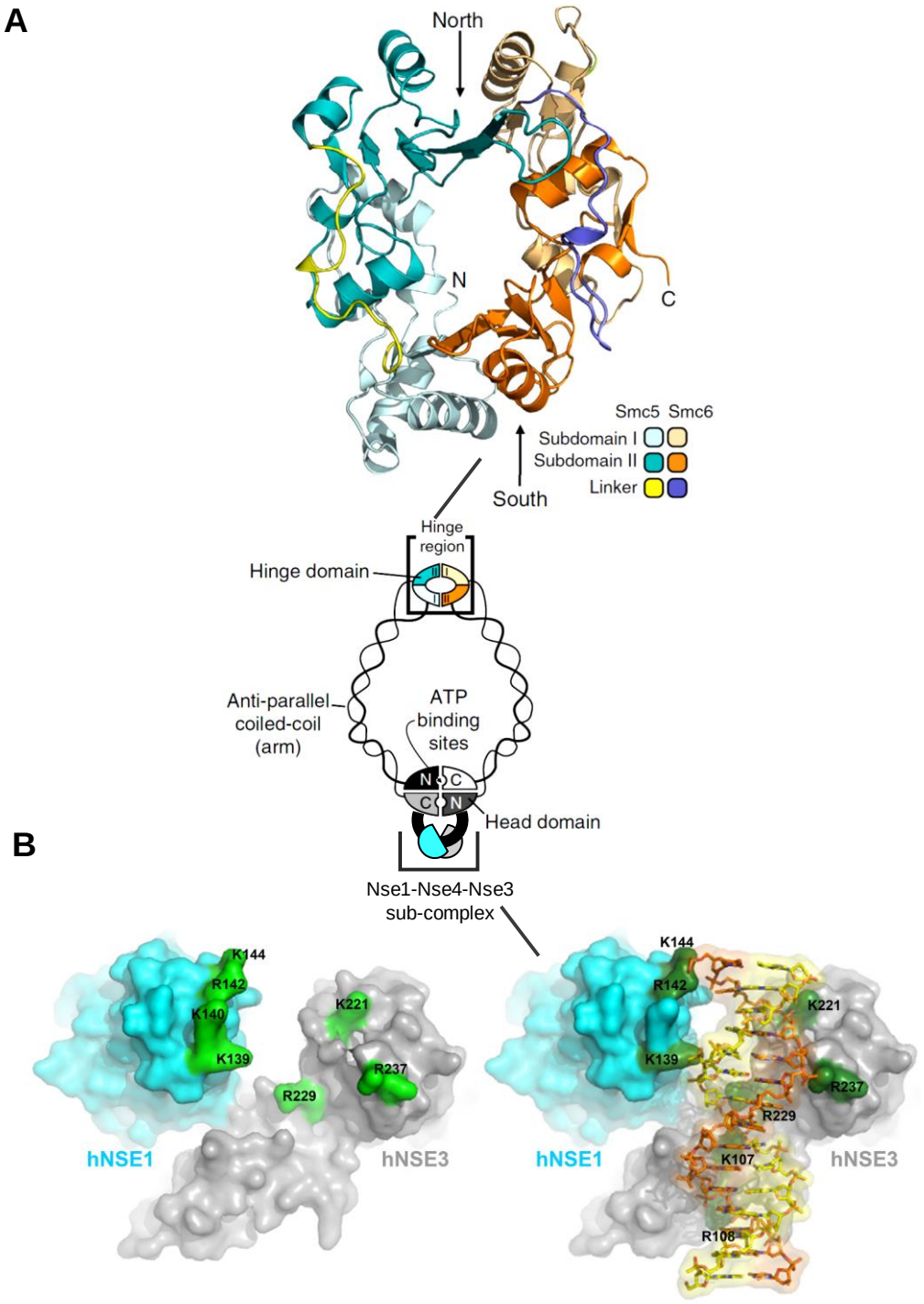


Figure 1.7: Models of the Smc5/6 hinge and the Nse1/Nse3 binding to dsDNA
A. Molecular model of an X-ray crystal structure of the *S. pombe* Smc5/6 heterodimeric hinge; the Smc5/6 hinge forms a toroidal structure (donut), individual Smc5 and Smc6 hinges interact together via two interfaces termed the North and South; adjusted from: Alt et al., 2017. **B.** Model of human Nse1 and Nse3 structure and binding to DNA, representation of human Nse1-Nse3 heterodimer unbound and DNA bound. Highlighted in green are basic residues of a putative DNA binding cleft formed by WH-B domain of NSMCE3 (hNse3) in gray and NSMCE1 (hNse1) loop in cyan; adapted from: Zabrady et al., 2016.

activity of Nse2 has been also shown to be important for chromosomal localisation of Smc5/6 to telomeres in response to MMS treatment (Pebernard et al., 2008a). The human ortholog of Nse2, NSMCE2, also stimulates sumoylation of a cohesin subunit Scc1 and this sumoylation has also been shown to be important for an appropriate repair of DSB (Wu et al., 2012).

1.2.4.2 The Nse1-Nse3-Nse4 sub-complex

The Nse1-Nse3-Nse4 sub-complex bridges the globular head domains of Smc5/6 (Palecek et al., 2006; Sergeant et al., 2005) and is capable of binding dsDNA *in vitro* (Zabrady et al., 2016). Nse3 and Nse1 are Kite proteins that interact with Nse4, the kleisin subunit of the Smc5/6 complex (reviewed in: Palecek and Gruber, 2015; Palecek et al., 2006). Nse1 contains a RING-like motif characteristic for ubiquitin E3 ligases (McDonald et al., 2003). The E3-ubiquitin ligase activity of Nse1 has been shown to be stimulated by the MAGE domain of Nse3 *in vitro* (Doyle et al., 2010). Further, the RING-like motif of Nse1 is essential for the DNA repair function of the Smc5/6 complex *in vivo*, as well as for stable formation of Nse1-Nse3-Nse4 heterotrimer (Pebernard et al., 2008b). Nse4 is the kleisin subunit bridging the head domains of Smc5 and Smc6. The C-terminal part of Nse4 forms a winged-helix (WH) domain which binds to Smc5 head and the N-terminal part forms helix-turn-helix motif (Palecek et al., 2006). The N-terminal part of Nse4 binds a hydrophobic pocket of Nse3 and the C-terminus of Nse1. These interactions are important for the stability of the Nse1-Nse3-Nse4 trimer (Guerineau et al., 2012; Hudson et al., 2011). Nse4 has also been reported to be phosphorylated on Thr^{58} but the study was carried out in a high-throughput setup and the biological relevance of its phosphorylation has to be elucidated (Hegemann et al., 2011).

Nse3 is a member of MAGE (melanoma-associated antigens) superfamily of proteins. Mammalian ortholog of Nse3 is MAGEG1 (NSMCE3 in human). MAGE proteins have a conserved MAGE-homology domain (MHD) which is composed of two winged-helix motifs (WH-A and WH-B). MAGE proteins apparently diversified relatively recently, as most eukaryotes, excepting placental mammals, have only one MAGE protein which is an Nse3 ortholog (Chomez et al., 2001; Doyle et al., 2010). MAGE proteins bind RING E3 ubiquitin ligases via their MHD and stimulate their activity, this has been shown for Nse3, which binds to Nse1 and stimulates its E3 ubiquitin ligase activity (Doyle et al., 2010; Kozakova et al., 2015). Nse3 has also been shown to mediate DNA binding of the

Smc5/6 complex. The C-terminal WH-B domain of Nse3 is essential for DNA binding, however efficient DNA binding is further stimulated by Nse1, whose loop together with WH-B domain of Nse3 forms a DNA binding cleft (Figure 1.7 B). WH-A domain of Nse3, as well as Nse4, which stabilise the whole sub-complex, also contribute to DNA binding. Interestingly, despite the importance of Smc5/6 in DNA intermediates processing, the Nse1-Nse3-Nse4 sub-complex does not preferentially bind to aberrant DNA structures such as HR or replication intermediates (Zabrady et al., 2016).

1.2.4.3 The Nse5/Nse6 subunits in yeast and mammals

Two additional subunits of Smc5/6, Nse5 and Nse6, are present in both fission and budding yeast (reviewed in: Verver et al., 2016a). Nse5 and Nse6 associate with the Smc5/6 complex more loosely and play a role in recruitment of the Smc5/6 to chromatin during replication stress and promote its DNA repair role (Bustard et al., 2012; Oravcová et al., 2019). Nse5 and Nse6 are essential proteins in budding yeast where they are proposed to interact with the hinge region of Smc5/6 (Duan et al., 2009b). In contrast, Nse5 and Nse6 are not essential in fission yeast and nse5 and nse6 null mutants exhibit slow growth phenotype coupled with sensitivity to DNA damage and deficiency in HR (Pebernard et al., 2006). Smc5/6 also non-stoichiometrically interacts with Rad60 (budding yeast Esc2), which possess C-terminal SUMO-like domains and is important for restoration of stalled or collapsed replication fork and the DNA repair function of Smc5/6 (Boddy et al., 2003; Miyabe et al., 2006; Sollier et al., 2009).

The human Nse6 homologue, termed SMC5/6 localisation 2 (SLF2), have recently been identified (Räschle et al., 2015). SLF2 together with a BRCT-domain containing protein SLF1, are not part of the core SMC5/6 complex (Taylor et al., 2008). However, they physically link the E3 Ubiquitin ligase protein RAD18 to SMC5/6 and are required to recruit SMC5/6 to DNA lesions (Räschle et al., 2015).

1.2.4.4 Smc5/6 deficiency phenotype and genetic interactions

The fact that the core components of the Smc5/6 complex are essential in fission and budding yeast and both Smc6 and Nse2 are embryonic lethal in mouse reflects its crucial function *in vivo* (Jacome et al., 2015; Ju et al., 2013; Zhao and Blobel, 2005). Experiments with temperature sensitive mutants in budding yeast revealed that the Smc5/6 deficient

cells activate the DNA damage checkpoint, but only after passage through mitosis. This suggests that the DNA damage is generated during aberrant mitosis, likely caused by aberrant chromosome segregation (Torres-Rosell et al., 2005a). Similarly, observations in fission yeast indicate that Smc6 thermo-sensitive mutants are able to undergo a couple of aberrant mitotic divisions, after shift to non-permissive conditions, during each division the viability is gradually lost (Sergeant et al., 2005). In fission yeast hypomorphic *smc6, nse1, nse2, nse3* and *nse4* alleles are defective in homologous recombination repair (HRR) and exhibit increased DNA damage sensitivity (Ampatzidou et al., 2006; Harvey et al., 2004; Lehmann et al., 1995; McDonald et al., 2003; Morikawa et al., 2004; Pebernard et al., 2004). In budding yeast, the Smc5/6 complex has been shown to promote HR between sister chromatids, thus, supress the error prone non-sister chromatid recombination events (De Piccoli et al., 2006). The sensitivity of *smc5/6* hypomorphs at low levels of damage is alleviated by deletion of homologous recombination genes (Ampatzidou et al., 2006; Lehmann et al., 1995). The same phenomenon was observed in budding yeast where removal of the central recombination protein Rad52 results in synthetic viability with a *smc5* temperature sensitive allele at restrictive temperature (Cost and Cozzarelli, 2006).

Hypomorphic *smc6* mutants in fission yeast are capable of normal DNA damage checkpoint activation, however fail to maintain stable G2 checkpoint arrest resulting in "cut" phenotype (septation despite abnormal chromosome segregation) and mitotic catastrophe. Two mutant alleles of *smc6* have been well characterised: *smc6-74* and *smc6-X*. *smc6-74* is a mutation in the arginine finger motif (A151T) in the ATP-binding pocket of the N-terminal globular domain, whereas *smc6-X* maps to the hinge domain (R706C) (Alt et al., 2017; Verkade et al., 1999). Both mutants are sensitive to DNA damage and defective in homologous recombination repair (HRR) but sufficient to maintain Smc5/6 essential functions (Lehmann et al., 1995; Verkade et al., 1999). Interestingly, the sensitivity to DNA damage of *smc6-74* but not *smc6-X* can be suppressed by overexpression of Brc1 (Verkade et al., 1999). Brc1 is a six-BRCT-domain protein which has been shown to be important during S-phase for replication fork (RF) stabilisation and recovery (Lee et al., 2007b, 2013). The suppression of *smc6-74* sensitivity is dependent on structure-specific nucleases, Mus81 and Slx1, which are known to be involved in processing of recombination intermediates (Sheedy et al., 2005). One interpretation of these observations is that Brc1 can, dependent on Slx1, generate alternative structures that

can be repaired by an Smc5/6-independent mechanisms. However, this bypass is not possible in *smc6-X* suggesting that the repair defect caused by this mutation is different.

The *smc6-X* (R706C) and *nse2-SA* (SUMO-ligase dead) hypomorphic mutants show increased sensitivity to DNA damaging agents, such as MMS. The *smc6-X* mutation shows stronger sensitivity to DNA damage than the SUMO-ligase mutant *nse2-SA*, which is only sensitive to damage in S phase (Andrews et al., 2005). Smc5 mutations in a conserved loop of the hinge region (Y612G and R609E/R615E) lead to severe growth defect after camptothecin, hydroxyurea and UV (Alt et al., 2017). On the other hand, Smc5 deficient chicken cells show sensitivity to IR which is, however, less severe than deficiency in homologous recombination gene Rad54 (Stephan et al., 2011).

Survival of Smc5/6 hypomorphs is generally dependent on Mus81 and the RecQ helicase (*S. pombe* Rqh1; *S. cerevisiae* Sgs1; human BLM), both known to be important for HR intermediates processing (Pebernard et al., 2006). This phenomenon of synthetic lethality with HR is also observed between *rqh1-d* and *mus81* (Laursen et al., 2003). The synthetic lethality has been suggested to be due the trapping of toxic intermediates, when more than one HR regulatory step is compromised (reviewed in: Heyer, 2015). In the context of HR, the RecQ helicase and Smc5/6 act as anti-recombinases but are also required together with Mus81 for resolution of recombination intermediates (reviewed in: Murray and Carr, 2008).

Another characteristic of *smc6, nse2* and *rad60* hypomorphic mutants in fission yeast is a strong synthetic lethality with the temperature-sensitive mutant of topoisomerase II, *top2-191*, at a semipermissive temperature (Outwin et al., 2009; Verkade et al., 1999). Even without exogenous DNA damage, *top2-191 smc6-74* double mutants exhibit cut phenotypes, entering mitosis with normal kinetics but failing to segregate the chromosomes, which results in mitotic catastrophe. Overexpression of catalytic dead mutant of Top2 (Top2-Y835F) rescues the synthetic lethality of *top2-191 smc6-74* double mutant, hence the observed synthetic lethality is not caused by the absence of Top2 catalytic activity (Outwin et al., 2009). These genetic data point towards the role of Smc5/6 in maintenance of chromosome structure and segregation.

1.3 The role of Smc5/6 in DNA repair

The implication of the Smc5/6 complex in DNA repair and genome integrity maintenance was initially based on the fact that hypomorphic yeast Smc5/6 mutants are sensitive to various sources of DNA damage (reviewed in: De Piccoli et al., 2009). Studies in plants also emphasise the importance of the Smc5/6 complex in the DNA damage response. *smc5/6* hypomorphic mutants in plants exhibit increased sensitivity to DNA damage. In addition, Smc5 is essential for seed development, which implies a function during plant meiosis (Díaz et al., 2019; Watanabe et al., 2009).

Human NSMCE2 knock out U2OS cells showed only mild sensitivity to IR in comparison to wild type cells (Verver et al., 2016a). NSMCE2 mutant (SUMO-ligase dead) patient lymphoblastoid cells do not display hypersensitivity to Camptothecin or alkylating agent Mechlorethamine in comparison to BLM-deficient lymphoblastoid cells (Payne et al., 2014). Similarly, destabilisation of the SMC5/6 complex in the NSMCE3 patient fibroblasts results only in moderate sensitivity to IR, UV and Camptothecin (van der Crabben et al., 2016). However, in human cells DSB repair using NHEJ predominates, which might explain the phenotypic difference of Smc5/6 deficiency between yeast and human.

Even though the molecular mechanism by which Smc5/6 promotes DNA repair is enigmatic, numerous studies argue that Smc5/6 is crucial for faithful HR, replication fork progression and maintenance of replication fork stability (Ampatzidou et al., 2006; Harvey et al., 2004; Irmisch et al., 2009; De Piccoli et al., 2006; Bustard et al., 2012; Meng et al., 2019; Zapatka et al., 2019).

1.3.1 Smc5/6 in homologous recombination repair

Work in yeast clarified the Smc5/6 role in homologous recombination; Smc5/6 deficiency is associated with HR defects, particularly failure to choose appropriate homologous template, as well as compromised ability to resolve HR intermediates, which persist and lead to chromosome missegregation, the terminal phenotype of which is a mitotic or meiotic catastrophe (Ampatzidou et al., 2006; Copsey et al., 2013; Miyabe et al., 2006). *S. pombe* Smc5/6 is not essential for recruitment of HR factors to sites of DNA lesions created by hydroxyurea treatment, but is required during late stages for correct resolution

of HR intermediates (Ampatzidou et al., 2006). The role of SMC5/6 in HR is further supported by analysis in vertebrate cells (Stephan et al., 2011)

In both fission and budding yeast, the majority of DNA DSBs is repaired by homologous recombination, which utilises a homologous DNA template. During the response to DNA double strand breaks, one of the first proteins recruited to the site of DSB, is a DNA-break sensor protein, Mre11 (Lisby et al., 2004). Smc5/6 has been shown to localise at the sites of DNA DSBs in yeasts (Lindroos et al., 2006; De Piccoli et al., 2006b) and its recruitment to DSB has been shown to be dependent on Mre11 (Lindroos et al., 2006). The first evidence for the role of Smc5/6 in homologous recombination repair (HRR) was based on the observations that hypomorphic Smc5/6 mutants were epistatic with HRR genes (Cost and Cozzarelli, 2006; Lehmann et al., 1995; McDonald et al., 2003; Pebernard et al., 2004, 2006). Furthermore, cells with deficient Smc5/6 complex exhibit misregulation of HRR and accumulate unresolved HR-dependent DNA intermediates (Ampatzidou et al., 2006; Bermúdez-López et al., 2010; Branzei et al., 2006; reviewed in: Murray and Carr, 2008a). Functional Smc5/6 is also important in meiosis, where multiple programmed DNA DSBs are generated and repaired by homologous recombination, which further support the importance of Smc5/6 in HRR (Copsey et al., 2013; Lilienthal et al., 2013).

However, chicken SMC5 deficient cells were proficient in homologous recombination, as demonstrated by increase in gene targeting and sister-chromatid exchange (Stephan et al., 2011). After siRNA knockdown of NSMCE2, human cells were also proficient in HR, but the siRNA was later shown to have off target effects (Potts et al., 2006; Wu et al, 2012). Based on the available data (Ampatzidou et al., 2006; Chavez et al., 2011; Irmisch et al., 2009; Stephan et al., 2011), a more accurate interpretation of the Smc5/6 deficiency phenotype in connection to HR, is that Smc5/6 regulates the outcomes of HR and its function is essential to prevent toxic HR.

1.3.2 Smc5/6 in replication fork stability maintenance

To study replication stress responses in cellular systems, replication stalling can be specifically induced by certain drugs, such as hydroxyurea or aphidicolin. Hydroxyurea is an inhibitor of ribonucleotide reductase (RNR), an enzyme that synthesises dNTPs from rNTPs. RNR is essential for maintain steady levels of dNTPs, which are the building

blocks for newly replicated DNA (Nordlund and Reichard, 2006). Replication inhibition by hydroxyurea is reversible and the capability of replication forks to resume after hydroxyurea-induced block depends on the time of the arrest and hydroxyurea dosage. Short term exposure to hydroxyurea renders most replication forks capable of replication resumption. On the other hand, prolonged exposure to hydroxyurea eventually leads to replication fork collapse. A collapsed replication fork can generally be defined as a fork, which is not capable of replication resumption. In order to complete DNA replication, the collapsed replication fork has to be rescued by an active replication fork emanating from an adjacent origin, or actively restarted by homology-directed repair (reviwed in: Cortez, 2015).

It has been shown that Smc6 hypomorphic mutants are proficient in recruitment of HR proteins to collapsed replication forks (Ampatzidou et al., 2006). In the presence of an active checkpoint, Smc6 deficient mutants can maintain normal replication fork arrest upon replication fork stalling induced by hydroxyurea. However, they accumulate unresolved HR-dependent DNA intermediates when replication forks collapses (Ampatzidou et al., 2006; Bustard et al., 2012). Analysis of two fission yeast Smc6 mutants, *smc6-74* and *smc6-X,* identified two separate functions of Smc5/6 at replication forks. The "early" function is required to maintain stalled replication forks in a recombination competent conformation. Evidence for this comes from the observations that *smc6-74* cells fail to properly recruit RPA, and the recombination protein Rad52 to stalled replication forks. This correlates with a decrease in recombination in the rDNA (Irmisch et al., 2009). The second "late" function of Smc5/6 is essential for the resolution of HR-dependent intermediates; *smc6-74*, *smc6-X* and other hypomorphic Smc5/6 mutants accumulate unresolved recombination intermediates upon fork collapse, resulting in chromosome missegregation in mitosis (Bustard et al., 2012; Irmisch et al., 2009; reviewed in: Murray and Carr, 2008a).

The question is, what is the mechanism by which the Smc5/6 complex prevents accumulation of these aberrant DNA structures? One possible explanation could be a functional interaction between Smc5/6 and the Mph1 helicase. Budding yeast Mph1 is homologous to human FANCM and fission yeast Fml and regulates the recombination subpathway that is involved in error-free bypass of DNA lesions (Osman et al., 2016; Prakash et al., 2005; Schurer et al., 2004). It has been shown that Mph1 co-

immunoprecipitates with Smc5 and that deletion of *MPH1* suppresses the phenotype of Smc5/6 deficient mutants (Chavez et al., 2011; Chen et al., 2009). Xue et al., 2014 demonstrated the ability of Mph1 to catalyse replication fork regression; they used *in vitro* assays to show that Smc5/6 acted to restrain branch migration and replication fork regression catalysed by Mph1. Interestingly, binding of Smc5/6 to DNA is dispensable to exert this function (Xue et al., 2014). Thus, one possible interpretation of these data is that Smc5/6 deficient mutants accumulate HR-dependent intermediates due to misregulation of Mph1-catalyzed replication fork regression.

Recently, budding yeast Smc5 has been shown to be sumoylated in response to replication fork damage and abrogation of Smc5 sumoylation increases the rate of spontaneous mutagenesis. This study implicates the Smc5/6 complex in regulation of the Mph1 helicase; the authors propose that sumoylation of Smc5 activates Mph1, which in turn promotes replication fork regression. Mph1 mediated replication fork regression prevents excessive engagement of a mutagenic trans-lesion synthesis, which in turn protects genome integrity (Zapatka et al., 2019).

Recent studies in budding yeast revealed the importance of the Smc5/6 complex in replication progression by sumoylation of polymerase ε (Meng et al., 2019; Winczura et al., 2019). Sumoylation of polymerase ε positively regulates replication fork progression (Meng et al., 2019). During replication fork stalling, sumoylation of polymerase ε by the Smc5/6 complex is dependent of the S-phase checkpoint (Winczura et al., 2019).

1.3.3 Smc5/6 and ribosomal DNA stability

The nucleolus is a nuclear sub-compartment containing multiple ribosomal DNA (rDNA) repeats (around 150 – 200 repeats in yeast genome). This highly repetitive and actively transcribed sequence inherently represents a challenge for DNA replication. In order to prevent collision between replication and transcription machinery, each rDNA repeat contains a specific replication fork barrier (RFB) site, this facilitates unidirectional replication and transcription (reviewed in: Rothstein et al., 2000). In this case, replication fork arrest may have severe consequences, since replication cannot be rescued by second replication fork coming from an adjacent origin. Hence, HR-mediated restart is extremely important for replication forks arrested within the rDNA repeats.

Numerous studies suggest Smc5/6 to play a role in nucleolar integrity; a significant fraction of Smc5/6 localises to the nucleolus and mutants lacking functional Smc5/6 complex display defects in rDNA segregation (Ampatzidou et al., 2006; Torres-Rosell et al., 2005b, 2005a). rDNA repeats in budding yeast Smc5/6 thermo-sensitive mutants are not resolved during anaphase, demonstrated by accumulation of Holliday junctions at the rDNA (Torres-Rosell et al., 2005b). Further, depletion of Smc5/6 causes defective replication of rDNA after the first cell cycle, which is alleviated by additional deletion of Mph1 helicase or Fob1 (Peng et al., 2018). These phenotypes suggest that Smc5/6 has a role in DNA replication and appropriate sister chromatid segregation and this is the most apparent at the rDNA repeat array (Torres-Rosell et al., 2005b, 2005a). The Smc5/6 complex also negatively regulates hyper-recombination at the rDNA locus (Irmisch et al., 2009; Torres-Rosell et al., 2007). Despite the important role of Smc5/6 in the nucleolus, the replication and recombination functions of Smc5/6 are not confined to rDNA; rDNA rather provides a sensitive readout for defects in replication and recombination. Hence, the rDNA instability of Smc5/6 mutants likely reflects a general role of the Smc5/6 complex in HR and replication fork maintenance than an rDNA-specific function (Murray and Carr, 2008a; Peng et al., 2018).

1.3.4 The role of Smc5/6 in meiosis

Meiosis is the cell division in which a diploid cell divides into four haploid cells. Meiosis begins with replication of each parental chromosome followed by two rounds of DNA segregation (meiosis I and meiosis II). During prophase I a protein structure called synaptonemal complex forms between homologous chromosomes and enables appropriate meiotic recombination and subsequent exchange of whole chromosome fragments in process called crossing over. In order to facilitate homolog exchange, programmed DNA double-strand breaks have to be generated by topoisomerase-like enzyme Spo11. DNA DSBs are then resected to expose the 3’ overhangs, which invade the complementary sequence of the homologous chromosome. This single-end invasion (SEI) is characteristic for all recombinational pathways during meiosis. SEI results in formation of joint molecules (JMs) which have to be resolved to subsequently give rise to two products: cross-overs, resulting from mutual exchange of whole parts of homologous chromosomes and/or non-cross overs that arise by homologous recombination repair without mutual exchange. Formation of JMs is imperative to

meiosis but is usually down-regulated during the mitotic cell cycle as JMs represent potentially dangerous intermediates if not properly resolved (reviewed in: Martinez-Perez and Colaiacovo, 2009 and Verver et al., 2016). The whole process of meiosis is highly coordinated and involves substantial structural changes to chromosomes. The SMC complexes are some of the main actors facilitating this process. Cohesin and condensin have both well-established roles during meiosis, mediating chromosome compaction, sister chromatid cohesion and formation of synaptonemal complex (reviewed in: Revenkova and Jessberger, 2005; Yu and Koshland, 2003). Given the role of Smc5/6 in HR, multiple studies focused on exploring the role of Smc5/6 in meiosis, which is summarised in this section.

The first implication of a role for Smc5/6 in meiosis was an up-regulated expression of human SMC5 and SMC6 in testis (cca 30-fold in comparison to somatic cells) and association of the SMC5 and SMC6 proteins with chromosomes during late phase of meiosis (Taylor et al., 2001). In addition, a testis-specific allele of the kleisin subunit Nse4, NSMCE4b, was identified in human (Taylor et al., 2008). This may be analogous to the cohesin meiosis-specific kleisin, Rec8 (Stoop-Myer and Amon, 1999). Studies in mice showed that the Smc5/6 complex localised to a central region of synaptonemal complex, chromocenters and sex body during first meiotic prophase (Gómez et al., 2013).

In worms (*C. elegans*) Smc5/6 mutants accumulate HR-dependent intermediates during meiotic DSB repair. Smc5/6 was dispensable for cross over formation between homologs, but essential for homolog-independent HR (Bickel et al., 2010).

Similarly, multiple studies in budding yeast reported that Smc5/6 was crucial for appropriate chromosome segregation in meiosis; Smc5/6 localised to centromeres, cohesin binding sites and sites of meiotic DSBs. Meiosis specific depletion of Smc5 and Nse4 results in formation of micronuclei, aberrant chromosomal morphology and the accumulation of JMs. However, Smc5 or Nse4 depleted cells still progress through meiosis which results in meiotic catastrophe (failure to separate DNA at meiosis I and II) (Copsey et al., 2013; Farmer et al., 2011). Importantly, meiotic defects observed in Smc5/6 mutants are not solely dependent on meiotic recombination; failure to complete meiotic division in Smc5/6 mutants is not rescued by additional deletion of Spo11 (Farmer et al., 2011). Independent studies showed that Smc5/6 does not play a roles in meiotic DSB formation and does not alter the number of crossing overs between

homologs (Farmer et al., 2011; Lilienthal et al., 2013). However, it plays a critical role in meiosis by antagonizing the formation of aberrant joint molecules by: (i) engagement of Nse2/Mms21 E3 SUMO ligase function to antagonise JMs formation by destabilisation of SEI intermediates (Xaver et al., 2013) and (ii) promotion of JMs resolution by structure-specific resolvases (Mus81-Mms4and Slx1-Slx4) (Copsey et al., 2013; Lilienthal et al., 2013; Xaver et al., 2013). Smc5/6 meiotic shut off mutants also exhibit misregulation of cohesin establishment and retention on chromosomes during meiosis, which presumably also contributes to the failure in chromosome separation during meiosis (Copsey et al., 2013). Fission yeast Nse5 and Nse6, non-essential components of the Smc5/6 complex, have been shown to be important for resolution of JMs during meiosis. Both *nse5Δ* and *nse6Δ* deletion mutants show sporulation defects and accumulation of JMs which can be partially suppressed by overexpression of bacterial resolvase RusA (Wehrkamp-Richter et al., 2012). These observations are in line with previous studies on Smc5/6 during mitotic cycle, and emphasise its role in faithful recombinational repair and cohesin regulation.

1.4 Other functions of the Smc5/6 complex

The first hints that Smc5/6 has other essential functions outside HRR came from genetic analyses. Deletion of HR genes does not result in lethality during normal cell cycle in yeast, whereas deletion of most Smc5/6 components does (Verkade et al., 1999; reviewed in: Kegel and Sjögren, 2010). As a member of the SMC family, the Smc5/6 complex is likely to be involved in different aspects of DNA metabolism and chromatin organisation. Hence, the cell cycle regulation, sub-nuclear localisation and the involvement of Smc5/6 in diverse nuclear processes has been extensively studied. The section will focus on different functions of Smc5/6, its cell cycle specific functions and connection to various aspects of DNA metabolism, such as transcription and DNA topology.

1.4.1 Timing and spatial localisation of Smc5/6

Lindroos et al., 2006 used ChIP-on-chip technique in budding yeast to show that the Smc5/6 complex was the most abundant at telomeres, centromeres and rDNA repeats (Lindroos et al., 2006). In fission yeast Smc5/6 localisation to centromeres is stimulated by replication fork stalling caused by HU treatment (Pebernard et al., 2008a). The centromere localisation was dependent on heterochromatin establishment, as it was not seen at centromeres in the absence of the HP1 homologue, Swi6. However, this may be due to an alteration in replication timing as early replication of centromeres is dependent on Swi6 (Hayashi et al., 2009). Mouse SMC5/6 complex localises to centromeres and chromatid axes during both mitotic and meiotic division (Gómez et al., 2013).

The chromosomal localisation of the Smc5/6 complex changes during the cell cycle. In budding yeast Smc5/6 localises to chromosomes mainly during late stages of DNA replication and G2/M phase when chromosomes are fully replicated (Lindroos et al., 2006). In frogs (*Xenopus laevis*), Smc5/6 is associates with chromatin in replication dependent manner and dissociates during mitosis (Tsuyama et al., 2006). A recent study in humans showed that Smc5/6 was bound to chromatin throughout interphase and rapidly removed during mitosis (Gallego-Paez et al., 2014). This reflects a slight difference in Smc5/6 binding pattern compared to frog and budding yeast, where only a small amount of Smc5/6 is bound to chromatin during G1. In contrast, a substantial fraction of Smc5/6 associates with chromatin already in early G1 in humans. This indicates that the SMC5/6

complex in humans might have additional role before DNA replication (Gallego-Paez et al., 2014).

1.4.2 Cell cycle specific functions of Smc5/6

The protein levels of Smc5/6 subunits have been shown to be constant throughout the cell cycle (Palecek et al., 2006; Taylor et al., 2001). An elegant study performed in *S. cerevisiae* characterised the essential role of Smc5/6 during the cell cycle; using cell cycle regulated alleles, they restricted expression of Smc5/6 subunits only to S or G2 phase. In agreement with previous studies, they reported that essential functions of Smc5/6 were performed during G2/M phase. Mutants in which subunits of the Smc5/6 complex are restricted to G2/M phase are viable and display normal origin firing and replication fork progression. In contrast, restriction of Smc5/6 subunits only to S-phase was lethal (Menolfi et al., 2015). Two separate functions of Smc5/6 were identified in a genetic screen: the first involved Smc5/6 dependent resolution of recombination DNA structures arising during endogenous replication stress. This function is well supported by previous studies showing accumulation of HR-dependent DNA structures and chromosome missegregation resulting in catastrophic mitosis (Ampatzidou et al., 2006; Harvey et al., 2004; Irmisch et al., 2009; Torres-Rosell et al., 2005a). The second function was the protection of the replication fork during stalling at natural pausing sites. This was hypothesised is based on the observations that Smc5/6 functionally cooperated with Rrm3 helicase/sweepase. Rrm3 is known to facilitate replication through natural replication pausing sites and facilitate fork progression through non-covalently bound protein-DNA complexes (Ivessa et al., 2003). *rrm3Δ* mutants are synthetically sick with Smc6 restricted to S-phase (hereafter S-SMC6), but not with those where Smc6 is restricted to G2/M phase. Further, Rrm3, like Smc5/6, has been shown to be significantly enriched at natural RF pausing site and the phenotype of S-SMC6 *rrm3Δ* double mutant was rescued by removal of factors enforcing replication fork pausing (Menolfi et al., 2015). This second function is not essential, as long as Smc5/6 is present in G2 to deal with the consequences of the loss of replication fork stability.

1.4.3 Interplay between Smc5/6 and cohesin

Studies in different organisms have implicated a functional cross-talk between cohesin and the Smc5/6 complex (Jeppsson et al., 2014; Lindroos et al., 2006; Outwin et al., 2009;

reviewed in: Tapia-Alveal et al., 2014). Localisation of cohesin and Smc5/6 on chromosomes are significantly overlapping. Furthermore, both complexes are enriched at sites of DNA double strand breaks and replication stress (Lindroos et al., 2006; De Piccoli et al., 2006; Ström et al., 2004; Ünal et al., 2004, 2007). In budding yeast the recruitment of Smc5/6 to undamaged chromosomes was initially shown to require Scc2, but Smc5/6 recruitment to rDNA was Scc2 independent (Lindroos et al., 2006). However, a more recent study by the same group using ChIP-seq (Chromatin immunoprecipitation coupled with sequencing), suggests that Smc5/6 chromatin association is not directly dependent on Scc2, or physical interaction with cohesin, but rather on cohesin-mediated sister chromatid cohesion (Jeppsson et al., 2014).

Post-replicative localisation of cohesin to DSBs was independent of Smc5/6 in budding yeast (Strom et al., 2007). In contrast, siRNA studies in human cells led to the proposal that Smc5/6 facilitates DNA repair by recruitment of cohesin to the site of DNA DSBs, which would provide a plausible explanation for recombination defects of Smc5/6 mutants (Potts et al., 2006). However, this result turned out to be an artefact caused by an off-target effects of siRNA and the same group later showed that Smc5/6 is dispensable for cohesin loading at DNA damage sites in human cells (Wu et al., 2012). Thus, Smc5/6 is not required for cohesin localisation to DSBs in yeast and mammalian cells.

In fission yeast overexpression of separase (*cut1*) was shown to suppress the mitotic catastrophe of *smc6* mutants after exposure to replication stress (Outwin et al., 2009). Since cohesin was retained on chromosome arms in mitosis this suggests that the Smc5/6 complex is required for cohesin removal after replication stress. In addition, overexpression of separase also suppressed the mitotic defects of *smc6-74 top2-191* double mutants. As these were not dependent on Rad51, it suggests that the role of Smc5/6 in cohesin removal is independent of its function in HR. These observations led to the hypothesis that the segregation block in Smc5/6 hypomorphic mutants, was caused by DNA bound proteins rather than unresolved DNA intermediates (Outwin et al., 2009). Since overexpression of separase could not suppress the chromosome segregation defects after DNA damage, mitotic failure in Smc5/6 mutants is presumably due to a combination of defective cohesin removal from sister chromatid arms and unresolved DNA intermediates (Outwin et al., 2009).

1.4.4 Smc5/6 and topological stress

Processes of DNA metabolism, such as replication, transcription or DNA repair inherently generate topological problems such as supercoiling (overwinding or underwinding) or entanglements between chromosomal regions. If left unresolved, these structures can become cytotoxic. Therefore, there are specialised enzymes, called topoisomerases, to handle topological problems. There are two main classes of topoisomerases, type I and type II. The class I topoisomerases (TopIA, TopIB) include Top1 and Top3 and the class II includes Top2. The class I topoisomerases relax superhelical tension by generating DNA nicks, whereas the class II enzymes facilitate passage of a double stranded DNA (dsDNA) molecule though another dsDNA molecule. Both Top1 and Top2 are important during DNA strand synthesis; Top1 relaxes positive supercoils ahead of the replication forks, whereas Top2 is essential for removal of sister chromatid intertwinings (SCIs) in order to facilitate chromosome segregation (Bermejo et al., 2007; reviewed in: Vos et al., 2011). Positive supercoils ahead of the fork can alternatively be relaxed by fork rotation creating DNA precatenates behind the fork that are consequently resolved by Top2 (Figure 1.8). Replication-induced superhelical stress increases with increasing chromosome length (Kegel et al., 2011). Interestingly, Smc5/6 association with chromosomes also increases with chromosome length. Kegel et al., 2011 showed that longer chromosomes in budding yeast have a marked delay in replication in the absence of functional Smc5/6. Smc5/6 association with chromosomes significantly increases during S-phase after depletion of Top2 (Kanno et al., 2015; Kegel et al., 2011). Furthermore, Smc5/6 amasses on circularised chromosomes and this observed enrichment is not due to its DNA repair function, since this association is not dependent on Mre11, which has been shown to be required for Smc5/6 recruitment to DNA DSBs (Kanno et al., 2015; Lindroos et al., 2006). These observations imply that the Smc5/6 complex may play a role in handling topological stress, alternatively, topological stress increases replication stress, which recruits Smc5/6. The authors of the topological studies interpret their results as follows: loss of Top2 function leads to accumulation of sister chromatid interwinings during DNA replication and this induces chromatin binding of Smc5/6. These SCI are bound and sequestered by Smc5/6, which drives fork rotation and relaxes DNA topological stress. Hence, Smc5/6 might play a vital role in chromosome topology by facilitation of fork rotation and relief of topological stress, which together allows normal DNA replication (Kanno et al., 2015; Kegel et al., 2011).

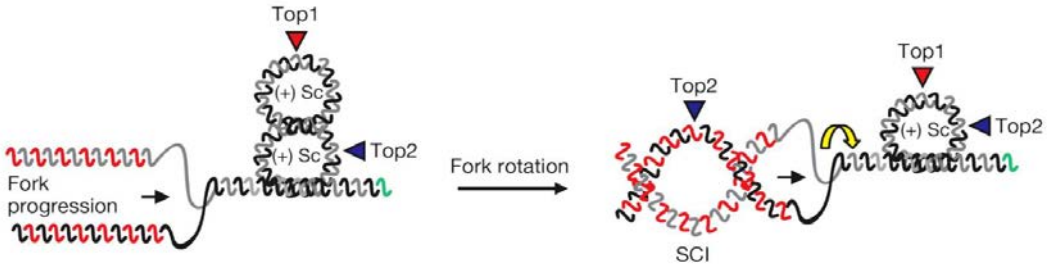


Figure 1.8: Release of replication-induced superhelical tension by topo-isomerases or fork rotation
Top1 has a central function in the release of supercoils ahead of the replication fork. Top2 is crucial for removal of sister chromatid intertwinings, which is a prerequisite for correct chromosome segregation. Under normal circumstance, fork rotation is restricted; within hard-to-replicate sites fork rotation can occur, this relaxes topological stress ahead of the fork and generates sister chromatid intertwines behind the fork instead; (+) SC: positive supercoils, SCI: sister chromatid intertwines, yellow arrow indicates fork rotation; adapted from: Kegel et al., 2011.

However, fork rotation has been recently shown to be restricted *in vivo* only to certain hard-to-replicate fragile sites and excessive fork rotation to result in increased DNA damage (Schalbetter et al., 2015). Hence, more detailed studies are essential to clarify the role of Smc5/6 in topological stress.

1.4.5 The role of Smc5/6 in viral genome transcription

In 2016, Strubin's lab first reported that the SMC5/6 complex was a restriction factor for Hepatitis B virus (HBV). The study described a mechanism, by which the HBV hijacks the cellular ubiquitin-proteasome system to target the SMC5/6 complex for degradation (Decorsière et al., 2016); the regulatory viral protein HBx, has been shown to interact with the cellular DDB1 protein, a subunit of an CUL4 E3 ubiquitin ligase complex (Leupin et al., 2003). The HBx-bound DDB1-E3 ligase targets the SMC5/6 for proteasomal degradation and this promotes transcription of extrachromosomal viral DNA. Moreover, SMC5/6 has been shown to associate with the HBV episomal DNA genome. Further, destabilisation of the SMC5/6 complex stimulates expression from episomal HBV constructs, but has no effect on chromosomal reporters (Figure 1.9) (Decorsière et al., 2016). Similar findings about the SMC5/6 being a target of HBV, were reported shortly after by a different group (Murphy et al., 2016); this study identified the components of the SMC5/6 complex by mass spectrometry, in a search for interaction partners of the viral HBx protein. The authors found that the HBx mediated degradation of SMC5/6 enhances the HBV genome replication and that the proteasomal targeting is specific for SMC5/6 and not for the other SMC complexes, cohesin and condensin (Murphy et al., 2016). A possible explanations for the SMC5/6 function during HBV cycle are: (i) by binding to the viral genome, SMC5/6 sterically blocks transcription of viral proteins, or (ii) SMC5/6 influences the topology of the viral genome, which blocks the transcription of viral genes, alternatively (iii) SMC5/6 stimulates catenation of viral genome in a Top2-dependent mechanism, which interferes with transcription of viral proteins. Since the yeast Smc5/6 has been shown to stimulate Top2-mediated catenation of plasmid substrates (Kanno et al., 2015), the last scenario is likely to be part of the SMC5/6 mediated mechanism of blocking viral transcription. The SMC5/6 complex has also been shown to interact with human papillomavirus protein E2 (Bentley et al., 2018; Jang et al., 2015; Wu et al., 2006). However, in contrast to HBV virus, SMC5/6 does not influence transcription or replication of the human papilloma virus, but instead seems to

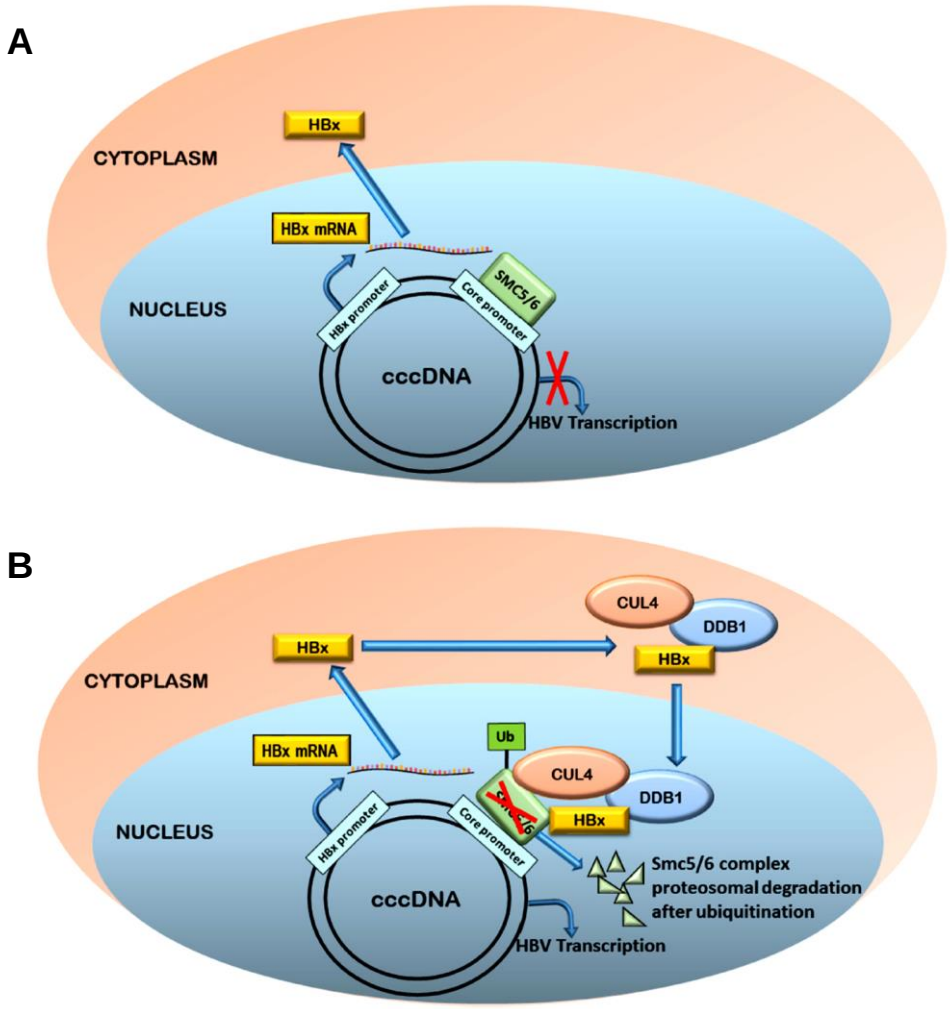


Figure 1.9: Model of SMC5/6 function during Hepatitis B virus infection
A. In the absence of the viral HBx protein, SMC5/6 binds to viral genome (cccDNA) and inhibits the transcription of viral genes by a yet unknown mechanism. **B.** Once translated, the Hepatitis B viral protein HBx binds to the CUL4 E3 ubiquitin ligase complex and brings it to close proximity of SMC5/6, this results in Ubiqutilation of SMC5/6, which targets is for proteasomal degradation, this mechanism enhances transcription of viral genome; cccDNA: covalently-closed circular DNA; adapted from: Mitra and Guo, 2017.

play a role in viral genome maintenance (Bentley et al., 2018). Unfortunately, a mechanistic insight into the SMC5/6 function in viral genome metabolism is lacking. Therefore, more research is needed to elucidate the function of SMC5/6 in context of episomal DNA maintenance.

1.5 Human SMC5/6

In comparison to the numerous studies on Smc5/6 in yeast, much less is known about human SMC5/6 and its functions *in vivo*. The human SMC5/6 complex was described in 2001 by Taylor et al., as a homologous complex to the Smc5/6 in fission yeast. In this first report it was shown that human Smc6 (SMC6) was phosphorylated *in vivo* and the phosphorylated form of SMC6 co-localised with nuclear speckles. Furthermore, the expression of SMC5 and SMC6 was greatly up-regulated in testis (cca 30-fold). SMC6 gene has was shown to encode two transcripts: a major one of 4.2 kb and a minor one of 5.6 kb (Taylor et al., 2001). Human SMC5/6 has been shown to associate with chromatin during interphase and most of it dissociates during mitosis (Gallego-Paez et al., 2014; Taylor et al., 2001). Depletion of SMC5 or SMC6 by siRNA caused abnormal chromosome morphology ('curly' chromosomes) and mislocalisation of condensin and Top2 along mitotic chromosome axis. SMC5/6 depleted cells also displayed delayed cell cycle progression and increase in replication-related DNA damage markers (BLM and γ-H2AX foci). Further, these cells showed delayed replication at centromeric and telomeric regions and defective chromosome segregation (Gallego-Paez et al., 2014).

The E3-SUMO ligase activity of human NSMCE2 (Nse2) was shown to be important for the normal response to DNA damage (Payne et al., 2014; Pond et al., 2019). NSMCE2 was found to be autosumoylated both *in vitro* and *in vivo* and SMC6 and TRAX were identified as other sumoylation substrates (Potts and Yu, 2005). In an early study, Potts et al., 2006 showed SMC5/6 to be recruited to DNA double strand breaks and they further employed reporter assays to demonstrate the particular importance of SMC5/6 for homologous recombination between sister chromatids (Potts et al., 2006). They used a long tract sister chromatid recombination (LTGC/SCR) reporter (Johnson and Jasin, 2000; Puget et al., 2005) and sister chromatid exchange (SCE) assays to show that depletion of SMC5/6 by siRNA knock down led to a decrease in sister-chromatid dependent HR and an increase of episomal HR and intra-chromatid HR (Potts et al., 2006). However, it

should be noted that the siRNAs used in this study were later shown to have off target effects (Wu et al., 2012). Hence, the interpretation of these data has to be treated with caution and the experimental outcomes have to be validated. A recent study in human HEK293 and U2OS cells revealed that NSMCE2 depleted cells are defective in processing of collapsed replication forks and accumulate mitotic DNA damage caused by replication stress. The cells were shown to accumulate excessive Rad51 at collapsed replication forks and exhibited decrease in hydroxyurea-induced sister chromatid exchanges (Pond et al., 2019).

1.5.1 Human syndromes associated with mutation in the SMC5/6 complex

Despite the lack of studies on the human SMC5/6 complex, recently the discovery of novel human syndromes has triggered intensive studies on human SMC5/6 and emphasised its importance in clinical context. These human syndromes are caused by mutations in different subunits of the SMC5/6 complex, which result in strikingly different phenotypes. Patients carrying SUMO-ligase dead mutation in NSMCE2 are viable, but have a distinct clinical phenotype. In contrast, mutation in the NSMCE3, which leads to destabilisation of the SMC5/6 complex, is lethal in infancy, in spite of the normal appearance of patients (van der Crabben et al., 2016; Payne et al., 2014) (Figure 1.11). The next sections describe in more detail cellular and global phenotypes of patients carrying mutations in SMC5/6 subunits and their implications to understanding the function of human SMC5/6.

1.5.1.1 Mutation in NSMCE2 leads to primordial dwarfism and insulin resistance

The first study, published in 2014, reported that a heterozygous frameshift mutation in E3 SUMO-ligase NSMCE2 led to primordial dwarfism, extreme insulin resistance and primary gonadal failure. The whole genome sequencing identified compound heterozygozity for two rare mutations: p.Ser116Leufs*18, which removes the whole SP-RING domain of NSMCE2 and thus abrogates its sumoylation activity and p.Ala234Glufs*4 removing only 14 amino acids of SP-RING (Figure 1.10 A). Patients had normal karyotypes, however exhibit chromosomal instability manifested by increased micronuclei and nucleoplasmic bridges formation, as well as problems with DNA segregation (Payne et al., 2014). Similar phenotypes were recently observed in hypomorphic NSMCE2 mutants in mice (Jacome et al., 2015). The protein level of

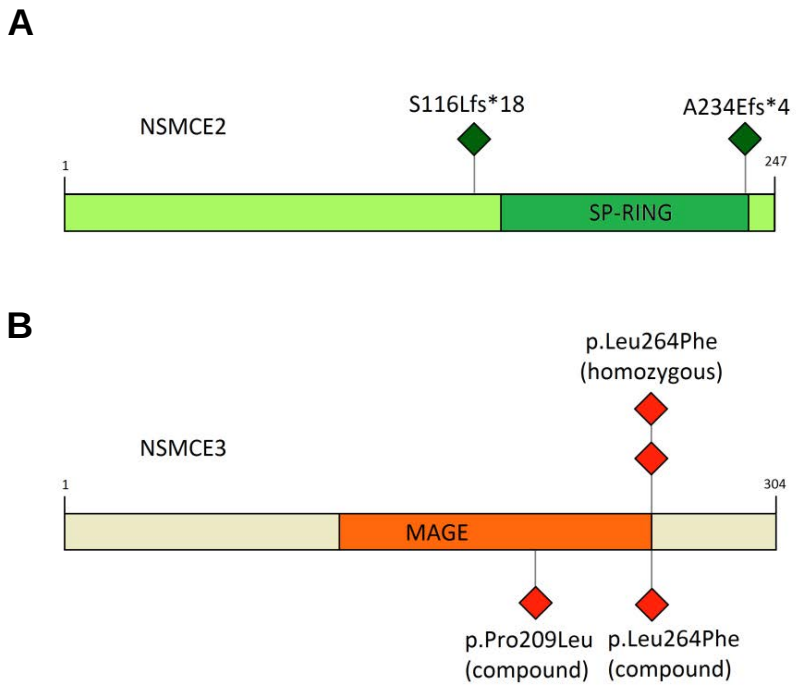


Figure 1.10: Schematic illustration of NSMCE2 and NSMCE3 mutations
A. Frameshift mutations in NSMCE2, p.Ser116Leufs*18 removes the whole SP-RING domain and p.Ala234Glufs*4 removes only 14 amino acids of the SP-RING domain
B. Missense compound heterozygous and homozygous mutations in the MAGE domain of NSMCE3; adjusted from: Payne et al., 2014 and van der Crabben et al., 2016

NSMCE2 in patient cells was significantly decreased but there was only a slight decrease in SMC5 and SMC6 protein levels. Thus, consistent with findings in yeast (Andrews et al., 2005; Zhao and Blobel, 2005) and humans (Taylor et al., 2008), mutations in the NSMCE2 RING domain do not significantly destabilise the whole complex. Lymphoblastoid cells of NSMCE2 patients showed wild type replication kinetics, however, recovery of replication after hydroxyurea-induced replication stress was impaired. Further, the NSMCE2 patient cells displayed increased sister chromatid exchanges (SCEs), but no significant sensitivity to replication-dependent DSBs (Camptothecin) and only very mild sensitivity to DNA crosslinking agent (HN2) (Payne et al., 2014). These observations implicate the function of SUMO ligase activity of NSMCE2 during replication stress. Importantly, the NSMCE2 patients exhibited similar phenotypes to patients with Seckel or Bloom syndromes, which are characterised by defective replication stress response (reviewed in: Kaseb and Hozayen, 2019).

1.5.1.2 Mutation in NSMCE3 leads to chromosome breakage syndrome

In contrast, mutations in NSMCE3 (human homolog to yeast Nse3) lead to destabilisation of the SMC5/6 complex and manifest as a very different syndrome (van der Crabben et al., 2016). This study, carried out in our laboratory in collaboration with Dutch and American clinicians, described a novel chromosome breakage syndrome associated with mutations in NSMCE3 gene; four patients from two independent families died at the age of 12 – 14 months due to severe lung disease following pneumonia. Whole genome sequencing identified two mutations in NSMCE3 gene: a homozygous p.Leu264Phe and a compound heterozygous p.Leu264Phe, p.Pro209Leu (Figure 1.10 B). *In vitro* analysis suggests that Pro209Leu leads to destabilisation of the C-terminus of NSMCE3. The Leu264Phe mutation allows formation of complex with NSMCE1, but reduces interaction with NSMCE4 and SMC6. The phenotype of NSMCE3 patients was weight loss, mild psychomotor retardation and increased infection susceptibility. Another hallmark of the NSMCE3 patients was decreased number of T-lymphocytes and failure to respond to recall antigens. NSMCE3 patient lymphocytes exhibited multiple chromosome rearrangements and, similarly to the NSMCE2 patients, fibroblasts had high levels of micronuclei, indicating increased genome instability. Primary fibroblasts of NSMCE3 patients showed mild sensitivity to DNA damaging agents and a repair defect in G2, consistent with a defect in HRR. Similarly to NSMCE2 patient cells, they showed a

failure to recover from replication stress (van der Crabben et al., 2016). Thus, the requirements for Smc5/6 in response to replication stress and for HRR are likely conserved from yeast to man. It is particularly interesting that mutations in different subunits of the same complex result in strikingly different phenotypes (Figure 1.11). Destabilisation of the whole complex was much more pronounced in case of NSMCE3 patients than in NSMCE2 patients (van der Crabben et al., 2016; Payne et al., 2014). It is surprising that this level of SMC5/6 destabilisation does not lead to abnormal embryo development, as the SMC6 and NSMCE2 knock out in mice is early embryonic lethal (Jacome et al., 2015; Ju et al., 2013).

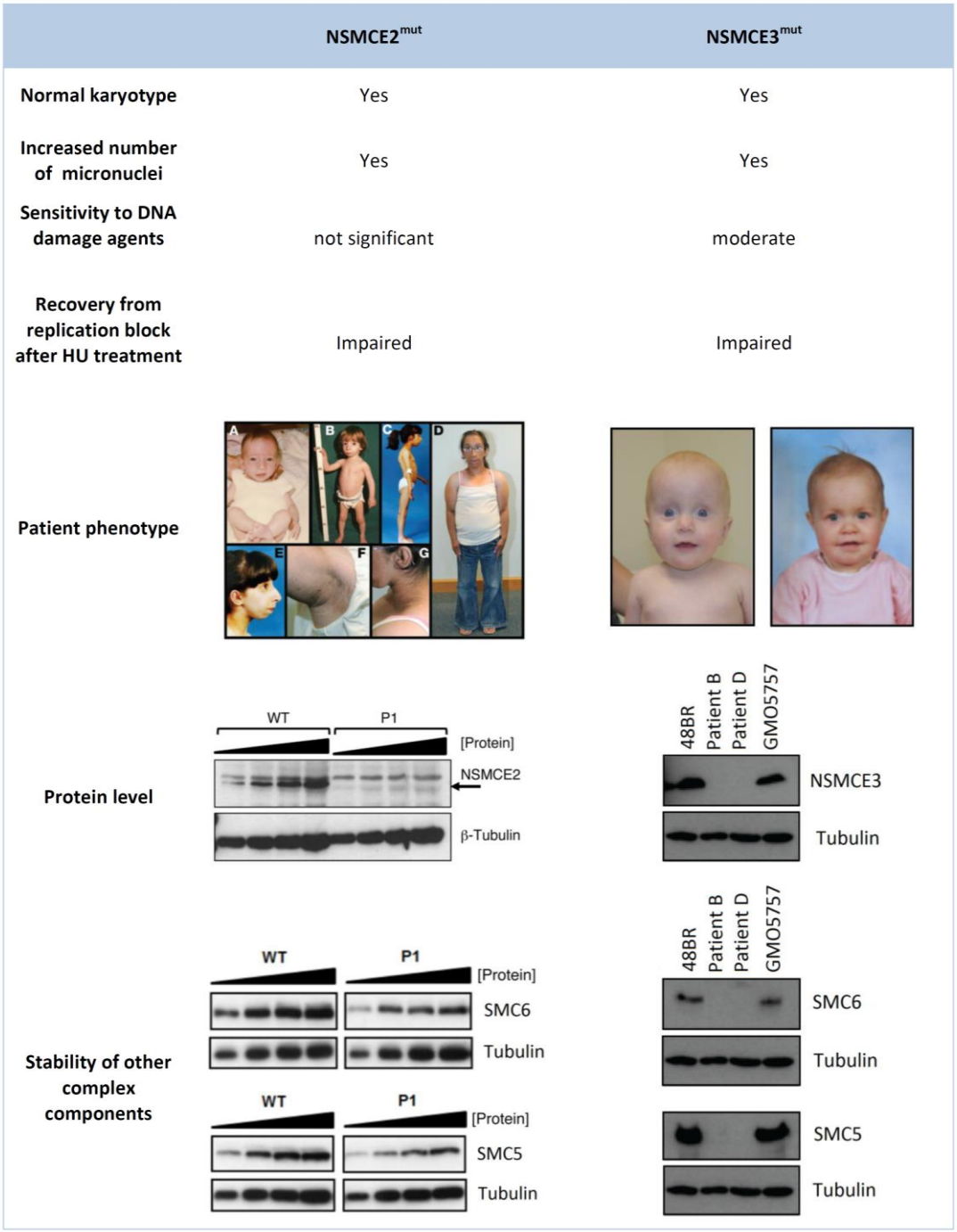


Figure 1.11: Phenotype comparison of mutations in NSMCE2 and NSMCE3 NSMCE2 patient bears compound heterozygous frameshift mutations in p.Ser116Leufs*18 and p.Ala234Glufs*4 (P1); NSMCE3 patient bears either homozygous missense mutation p.Leu264Phe (Patient B) or compound heterozygous missense mutation p.Leu264Phe, p.Pro209Leu (Patient D), 48BR and GMO5757 are control primary fibroblast cell lines; source: Payne et al., 2014 and van der Crabben et al., 2016.

Aims of the project

Despite the importance of the Smc5/6 functions all organisms studied, there was a paucity of knowledge examining the molecular functions of the complex in human cells. In order to investigate the role of and expand the knowledge on human SMC5/6 the aims of the project were to:

i) Generate a human system, which allows controllable expression of SMC5/6
ii) Use the created system to study the SMC5/6 complex during normal cell cycle and upon DNA damage
iii) Use the created system coupled with proteomic approach to purify the SMC5/6 complex and search for its interacting partners

2 Chapter 2

Materials and Methods

2.1 Cell biology techniques

2.1.1 Human tissue culture

Flp-In T-REx 293 cell lines were grown at 37°C, 5% CO_2 in Dulbecco's Modified Eagle Medium (Gibco) supplemented with 2mM L-Glutamine (Gibco), 100 U/ml Penicillin-Streptomycin (Sigma) and 10% Fetal Calf Serum (FCS). For NSMCE4a shut off experiments, cells were grown in media described above supplemented with 10% Tetracycline free Fetal Bovine Serum (PAN Biotech) instead of normal FCS. Primary patient cells were grown at 37°C, 5% CO_2 in Minimum Essential Media (Gibco) supplemented with 2mM L-Glutamine (Gibco), 100 U/ml Penicillin-Streptomycin (Sigma) and 15% FCS. Routine passaging was performed to sustain exponential cell growth: media was removed, cells were washed in PBS trypsinised using Trypsin-EDTA solution (0.1% w/v trypsin, 0.1% v/v EDTA pH 7.5, PBS), spun in sterile universal tube 1200 rpm/2 minutes and desired fraction of cells was re-plated in fresh media. For NSMCE4a shut off experiments, cells were grown for 15 – 20 days in media containing 10 µg/ml of Blasticidin at the day of experiment.

Table 2.1 Drug concentrations for the Flp-In T-REx 293 cell line

Drug	Final concentration (µg/ml)
Blasticidin	10
Doxycycline	0.01
G418	800
Hygromycin	200
Puromycin	1
Zeocin	100

2.1.2 Transfections

The calcium phosphate method was used for tranfections of Flp-In T-REx 293 cell lines. A day before transfection 2 x 10^5 cells was plated into each well of a 6-well plate and incubated overnight, so that at the day of transfection cells were about 40 – 60% confluent. The DNA mixture was prepared in a fresh 1.5 ml tube; for each 6-well the transfection mixture consisted of 2 µg of plasmid DNA, 12 µg of 2M $CaCl_2$ and dd H_2O up to final volume of 100 µl. The DNA mixture was then drop-wise added onto 100 µl of freshly thawed 2 x HBS buffer (273mM NaCl, 1.5 mM Na_2HPO_4 x 7·H_2O, 55mM HEPES, pH 7.0) while mixing the 2 x HBS by bubbling. The final mixture was then added drop-wise onto the cells. Cells were incubated at 37°C, 5% CO_2 with transfection mixture for minimum 8 hours. After that, media was removed, cells were washed in PBS and fresh media added.

2.1.3 Flow cytometry

Cells were grown in 6-well plates, in order to harvest all cells for analysis. Media in each well was carefully removed and kept in a universal tube, cells were washed in PBS and this was added to the same universal tube. After that, trypsin was added to cells for 5 minutes, then neutralised using the previously collected media. Cells were spun 1200 rpm for 2 minutes and the supernatant was removed. The pellet was washed once in 1 ml PBS, spun 1200 rpm for 2 minutes and the supernatant was removed. Cells were resuspended in 50 µl of PBS and fixed by adding drop-wise 1 ml of 70% ice-cold ethanol while being mixed by vortexing. Fixed cells were stored in -20°C until the sample preparation step. Cells in 70% ethanol were spun (400 x g for 2 minutes) and the supernatant was removed. The cell pellet was washed in 1 ml PBS and spun (400 x g for 2 minutes). The pellet was gently resuspended in 50 µl of RNAse solution (100µg/ml RNAseA in PBS) and incubated for 30 minutes at RT. Cells were resuspended in 200 µl of PI solution (PBS, 0.1% NP40, RNAseA 200µg/ml, propidium iodide 12.5µg/ml) was added and the cell mixture was filtered through 40um Sterile Cell Strainer (Fisher Scientific) into a new tube. Cells were subjected to flow cytometry using BD Accurri C6 flow cytometer. Samples were analysed and gated using BD CS Sampler software.

For DNA repair GFP reporter assays, trypsinised cells were washed in PBS and resuspended in 300 µl of cold PBS before being directly subjected to flow cytometry analysis. Samples were analysed and gated using BD CS Sampler software.

2.1.4 Clonogenics survival

Flp-In T-REx 293 cell lines were either grown in Tetracycline free media without Blasticidin (BSR) (ON), or media containing 10µg/ml BSR media for 15 – 20 days (OFF, WT) before performing experiment. Exponentially growing cells were plated in 10 cm dishes in triplicates minimum 2 hours before exposure to various doses of following DNA damaging agents; IR (X-Ray): 2Gy, 4Gy, 6Gy; Camptothecin (Selleckchem): 5nM, 10nM, 20nM; PARPi (KU0058948, Axon Medchem): 0.5uM, 1uM, 2uM; Hydroxyurea (Sigma): 2mM. Cells were exposed to Camptothecin and PARPi for 24 hours after that media was removed and replaced with fresh media and cells were grown for 12 – 15 days to form macroscopic colonies. For hydroxyurea experiments, cells were exposed to 2mM HU for 2 or 24 hours before being plated into 10 cm dishes. When macroscopic colonies were formed, cells were fixed in 100% ethanol, washed in PBS and stained in crystal violet solution (1% formaldehyde, 1% methanol, 0.07% crystal violet in PSB). Number of colonies of more than 50 cells were scored. Plating efficiency (PE) was calculated as number of colonies counted divided by number of colonies plated:

$$PE\ (\%) = (\text{Colonies Counted} / \text{Cells Inoculated}) \times 100$$

Survival factor was calculated as a plating efficiency of treated cells divided by plating efficiency of non-treated cells:

$$SF\ (\%) = (PE_{(treated)} / PE_{(non\text{-}treated)}) \times 100$$

2.1.5 Metaphase spreads

Cells in 10 cm dishes containing 10 ml of media were cultured to reach approximately 80% confluency. The day of metaphase spread preparation, cells were treated with 100 ng/ml Colcemide (Roche) and incubated for 1.5 hours at 37°C, 5% CO_2. After incubation, media was transferred into 15 ml conical tube and cells were washed with 2 ml of PBS which was then transferred into the same conical tube. 2 ml of Trypsin-EDTA solution was added to dish, cells were incubated 5 minutes at 37°C, transferred to the conical tube and spun 1000 rpm for 5 minutes. The supernatant was removed leaving 500µl of media

to resuspend the cell pellet by gentle mixing. 7 ml of pre-warmed (37°C) hypotonic solution (75mM KCl) was drop-wise added onto the cell pellet while gently tapping the tube to mix. Cells were incubated at 37°C for 5 minutes to swell and centrifuged 1000 rpm for 5 minutes. The supernatant was removed and the pellet was gently resuspended. Cells were fixed by adding 7 ml of Carnoy's fixative (75% v/v methanol, 25% v/v glacial acetic acid) in a drop-wise fashion while tapping the tube to mix.

2.1.6 Growth curve

Flp-In T-REx 293 cell lines were grown until exponential phase before performing the experiment. Cells were passaged and plated in triplicates into 6-well plates in a 1:1 dilution row fashion for each time point counted. Every 24 hours cells were trypsinised and re-suspended in similar amount of media before being counted. Each triplicate was averaged and plotted as a number of cells/ml.

2.1.7 Micronuclei scoring

Exponentially growing cells were plated on coverslips in 6-well plates containing one day before experiment to rich approximately 60 – 80% confluency. The next day, the cells were washed once in PBS and fixed for 10 minutes in 3.7% paraformaldehyde (PFA) at room temperature (RT). Coverslips were gently washed in PBS and permeabilised in 0.2% Triton-X for 10 minutes. Coverslips were washed in PBS, stained with DAPI (1µg/ml DAPI in PBS) for 6 minutes. After DAPI staining, coverslips were quickly rinsed in double distilled water and air-dried on Whatman paper. Coverslips were mounted onto glass slides with 4.5 µl of mounting media (Vectashield). Pictures of cells were taken under a wide-field fluorescence microscope (Nikon E400) using 100 x objective. Number of micronuclei for each cell line was scored manually.

2.1.8 EdU incorporation assay

5-Ethynyl-2′-deoxyuridine (EdU) incorporation assay was performed both for microscopy and flow cytometry analysis. For microscopy applications, 2 x 10^5 cells per well were plated into a 6-well plate one day before experiment. Next day, cells were treated with 1µM PARP inhibitor (KU0058948) for 24 hours. Cells were washed once in media and released for 60 minutes into fresh media containing 10µM EdU. Next, cells were washed once in PBS, fixed for 10 minutes in 3.7% PFA, permeabilised in 0.2%

Triton-X for 10 minutes and blocked for 45 minutes in 0.5% BSA in PBS. Click chemistry was performed using home prepared cocktail (100mM Tris pH 8.5, 1mM $CuSO_4$, 1µM Alexa Fluor 488, 100mM ascorbate). Coverslips were washed twice in 0.5% BSA in PBS, stained DAPI in PBS (1µg/ml), rinsed in double distilled water and air-dried before being mounted on glass slides using 4.5 µl of mounting media (Vectashield). Pictures of cells were taken using wide-field fluorescence microscope (Nikon E400) and cells were manually scored. For each experiment minimum of 150 cells were scored.

For flow cytometry applications 5 x 10^5 cells per well were plated into a 6-well plate one day before experiment. Next day, cells were treated with 1mM KU0058948 for 24 hours. Cells were washed once in media and released for 60 minutes into fresh media containing 10µM EdU. Next, media was removed, cells were washed once in PBS and harvested using trypsin-EDTA. Cells were collected in a universal tube, spun 1200 rpm for 2 minutes, washed once in PBS and fixed in 70% ice-cold ethanol, while being mixed using vortex. Fixed cells were stored at -20°C. Before click chemistry was performed, cells were washed twice in 500µl of 3% BSA in PBS and incubated for 45 minutes in reaction cocktail (100mM Tris pH 8.5, 1mM $CuSO_4$, 1µM Alexa Fluor 488, 100mM ascorbate). Cells were washed twice in 500µl of 3% BSA in PBS and re-suspended in propidium iodide solution (1µg/ml propidium iodide, 250 µg/ml RNAseA in PBS). Flow cytometry analysis was performed using BD Accurri C6 flow cytometer instrument.

2.2 DNA cloning and molecular techniques

2.2.1 Polymerase chain reaction (PCR)

KOD Hot Start DNA polymerase (Millipore) was used for amplification of DNA inserts from plasmids according to manufacturer's guidelines. Typically, 10 ng of plasmid DNA was used as a template. Initial denaturation was carried out at 94°C for 2 minutes followed by 25 cycles: 94°C for 30 seconds, primer annealing at 55°C for 30 seconds, followed by extension step of 72°C for 1 minute, final extension step was 72°C for 7 minutes. Phusion DNA polymerase (NEB) was used for Topo-TA cloning and amplifications from genomic DNA in High-Fidelity buffer (NEB), PCR was performed according to manufacturer's guidelines. Typically, 100 ng of genomic DNA was used for each reaction. Initial denaturation denaturation step was carried out at 95°C for 5 minutes followed by 31 cycles of: 95°C for 20 seconds, primer annealing at 65°C for 20 seconds, followed by extension step of 72°C for 30 seconds, final extension step was 72°C for 5 minutes.

Before further downstream applications, PCR products were separated on 1% w/v agarose gel in and purified using QIAquick Gel Extraction Kit (QIAGEN) according to manufacturer's guidelines.

2.2.2 DNA gel electrophoresis

All DNA electrophoresis were performed in 1 x TBE buffer (89mM Tris base, 89mM Boric acid, 2 mM EDTA). Typically, 6 cm gel was separated at 100V for 33 minutes, GeneRuler 1 kb (Thermo Fisher) ladder was used as a size reference. PCR or restriction digest products were separated on 1% agarose gels (1% w/v agarose, 0.5 µl/ml ethidium bromide in 1 x TBE). Gels were visualised and captured under UV light using Syngene Bio Imaging UV box and Gene-Snap (Syngene) software.

2.2.3 Digestion and Ligation

Restriction digests were carried out using enzymes from NEB. Typically, purified vector and insert DNA was digested in an appropriate buffer for 2 hours at 37°C and ligated using T4 DNA ligase in 1:3 vector to insert ration. Ligation was performed in 1 x T4 ligase ligation buffer at 16°C overnight before being transformed into chemically competent DH5α *E. Coli* cells.

2.2.4 Transformation of E.coli

Typically, 5 µl of ligation reaction or 10 ng of vector DNA was transformed into competent bacterial cells. First, DNA was mixed with 25 µl of thawed competent DH5α *E. Coli* cells and incubated 10 minutes on ice. After, cells were heat-shocked at 42°C for 60 seconds and immediately put on ice for 10 minutes. 200 µl of S.O.C media (0.5% Yeast Extract, 2% w/v Tryptone, 10 mM NaCl, 2.5 mM KCl, 10 mM $MgCl_2$, 10 mM $MgSO_4$, 20 mM Glucose) was added and cells were incubated at 37°C and 200 rpm agitation for 1.5 hours. Transformed bacterial culture was then spread on LA (lysogeny broth media with agar) plates containing appropriate antibiotic selection. Ampicillin was used in 100 µg/ml and kanamycin in 50 µg/ml final concentration.

2.2.5 Guide RNA insertion into the Cas9 vector

To create the guide RNA (gRNA) containing Cas9 vector, the gRNA sequence-containing oligonucleotide was inserted into sgRNA scaffold within the Cas9 vector. For the first round of NSMCE3 CRISPR/Cas9 gene knock out, the px330nse3fwd and px330nse3rev oligonucleotides were inserted into the pX459 vector. For the second round of CRISPR/Cas9 gene knock out, the Nse3 crRNA1 oligo1 and Nse3 crRNA1 oligo2 oligonucleotides were inserted into the pX459 vector. For NSMCE4a gene knock out, px330nse4fwd and px330nse4rev oligonucleotides were inserted into the pX330 vector, as described in the Target Sequence Cloning Protocol from Zhang lab (available online).

Briefly, the gRNA sequence containing oligonucleotides were synthesised to carry 5' overhangs complementary to the overhangs created by BbsI enzyme digestion. Next, the pX459/pX330 vector was digested by the BbsI enzyme for 30 minutes at 37ºC. Digested vector was then gel purified using QIAquick Gel Extraction Kit according to manufacturer's guidelines. Meanwhile, the guide RNA sequence containing oligonucleotides were phosphorylated in 10 µl reaction containing each oligonucleotide in 10µM concentration, 1 x T4 ligation buffer and 5 Units of T4 PNK (NEB). Oligonucleotides were annealed in thermocycler using following program: 37 ºC 30 min 95 ºC 5 min and then ramp down to 25 ºC at 5 ºC per minute. Annealed and phosphorylated oligonucleotides were inserted into the pX459/pX330 vector using T4 DNA ligase. Created pX330/pX459 vector was transformed into competent DH5-alpha *E.Coli* cells and purified using plasmid purification kit (QIAGEN) according to manufacturer's guidelines. The correct insertion was validated by sequencing.

2.2.6 Topo cloning

Topo-TA cloning was performed in order to validate CRISPR/Cas9 mediated gene knock out. . Briefly, PCR on genomic DNA was performed to amplify DNA sequence in vicinity of the guide RNA target site. Purified PCR product was then cloned into linearised activated pC2.1-TOPO vector using TOPO-TA Cloning Kit (Invitrogen) according to manufacturer's guidelines.

2.2.7 Surveyor assay

Surveyor assay was utilised to screen for CRISPR/Cas9 knock out clones. Briefly, genomic DNA from selected CRISPR knock out clones was isolated using DNeasy Blood & Tissue Kit (QIAGEN). 100 ng of genomic DNA was amplified using Phusion DNA polymerase (NEB) in 20 µl PCR reaction. The reaction product was annealed to form heteroduplex product with a control genomic DNA using the following program: 95°C for 10 minute, 95 to 85°C by 2 °C per second, 85°C for 1 minute, 85 to 75 °C by 0.3°C per second, 75 °C for 1 min, 75 to 65°C by 0.3°C per second, 65 °C for 1 minute, 65 to 55 °C, by 0.3°C per second, 55°C for 1 minute, 55 to 45 °C, by 0.3°C per second, 45°C for 1 minute, 45 to 35°C by 0.3°C per second, 35 °C for 1 minute, 35 to 25°C by 0.3°C per second, 25°C for 1 minute, 25 to 4°C by 0.3°C per second. Annealed DNA was subjected to T7 endonuclease I (NEB) digestion: 15 µl of annealed reaction in NEB2 buffer was incubated with 2.5 units of T7 endonuclease I for 30 minutes. Final product was separated on 1% agarose gel and imaged under UV light.

Plasmid name	Description	Source
DR-GFP	GFP reporter to measure HDR after I-SceI double strand break induction	Dr. Owen Wells
SA-GFP	GFP reporter to measure SSA after I-SceI double strand break induction	Dr. Owen Wells
pCBASceI	I-SceI expression vector	Dr. Owen Wells
Tdp1-GFP	GFP expression vector to check transfection efficiency	Dr. Owen Wells
pXPSN2	Empty vector control for GFP reporter assays	Dr. Owen Wells
H2B-GFP	GFP expression vector to check transfection efficiency	Dr. Nadia Hegarat
pOGG44	Flp-Recombinase expression vector	Prof. Mark O'Driscoll
pcDNA5/FRT/TO	FRT expression vector for Flp-In T-REx system	Prof. Mark O'Driscoll

Table 2.2: DNA oligos used in this study

Oligo name	creator	Sequence 5' - 3'	Purpose
ntermnse4fwd	Owen Wells	gcaggtaccATGAGTGGTGATTCGTCGGGCCGTGGTCCGG	forward primer to generate NSMCE4a mutant or wt insert into T-rex vector
ntermnse4rev	Owen Wells	aagcggccgctgaaccaccgcccccCGCACTCGGTTTCTGC	reverse primer to generate NSMCE4a mutant or wt insert with potential C-terminal tag
nse4fwd.v2	Owen Wells	caagcaggtaccATGAGTGGTGATTC	Forward primer to clone NSMCE4a into pcDNA5tetO using KpnI and EcoRV enzymes
nse4rev.v2	Owen Wells	caatgcgatatcccgccgccCGCACTCGGTTTC	Reverse primer to clone NSMCE4a into pcDNA5tetO using KpnI and EcoRV enzymes
Rev NeoR/KanR	Anita Brozkova	TTCAGTGACAACGTCGAGCACA	Revrese primern to Fwd Surveyor; to test the presence of Neomycin (G418) resistance cassette
Rev BsdR_2	Anita Brozkova	TCAAGATGCCCCTGTTCTCATT	Revrese primern to Fwd Surveyor; to test the presence of Blasticidin (BSR) resistance cassette
px330nse3fwd	Owen Wells	caccgGTAGTCGACGGGGTCGGTG	to clone in gRNA into px330 for NSMCE3 CRISPR KO
px330nse3rev	Owen Wells	aaacCACCGACCCCGTCGACTACc	to clone in gRNA into px330 for NSMCE3 CRISPR KO

Oligo name	creator	Sequence 5' - 3'	Purpose
px330nse4fwd	Owen Wells	caccgGCCGGTGACAAATTAACAG	to clone in gRNA into px330 for NSMCE4a CRISPR KO
px330nse4rev	Owen Wells	aaacCTGTTAATTTGTCACCGGCc	to clone in gRNA into px330 for NSMCE4a CRISPR KO
SurFwd1_Nse3	Anita Brozkova	CACGTCATCGGGGACTACAA	To check Cas9 mediated knock-out in NSMCE3 exon1
SurRev1_Nse3	Anita Brozkova	AGCAATATGCTCCCTGGGTT	To check Cas9 mediated knock-out in NSMCE3 exon1
Nse4_2nd_fwd ab1	Anita Brozkova	GGGTTAAGGTTAGAGGGAGCTA	To sequence Cas9 mediated knock-out in NSMCE4 exon2
Nse4_2nd_rev ab1	Anita Brozkova	TTAACACAGACTGCGGAACC	To sequence Cas9 mediated knock-out in NSMCE4 exon2
Nse3 crRNA1 oligo1	Anita Brozkova	CACCGGCTTATACCCGAAGACGT AC	to clone in gRNA1 from genscript into px459 for NSMCE3 Cas9 mediated knock-out
Nse3 crRNA1 oligo2	Anita Brozkova	AAACGTACGTCTTCGGGTATAAGC C	to clone in gRNA1 from genscript into px459 for NSMCE3 Cas9 mediated knock-out
gU6-F	Anita Brozkova	GAGGGCCTATTTCCCATGATT	sequencing primer for pX459 crRNA cloning product
Hyg_fwd1	Anita Brozkova	CTCTCGGAGGGCGAAGAATC	To check insertion of HygromycinR cassette (pcDNA5/FRT/5TO)
Hyg_rev1	Anita Brozkova	ATTTGTGTACGCCCGACAGT	To check insertion of HygromycinR cassette (pcDNA5/FRT/5TO)

Table 2.3: Primary antibodies for immunofluorescence

Primary antibody	Organism	Catalogue number	Dilution	Source
6 x His	rabbit	ab9108	1:300	Abcam
BLM	rabbit	ab2179	1:250	Abcam
Rad51	rabbit	sc-8349	1:250	Santa Cruz
Rad51	rabbit	PC130	1:250	Calbiochem
phospho-H2A.X (Ser139)	mouse	05-636	1:1500	Millipore
phospho-H2A.X (phospho S139)	rabbit	ab11174	1:1500	Abcam
RPA2	rabbit	NB100-544	1:1000	Novus Biologicals

Table 2.4: Primary antibodies for western blot

Primary antibody	Organism	Catalogue number/serum	Dilution	Source
NSMCE4a	rabbit	#SK3616	1:500	Elaine Taylor
SMC5	rabbit	EQ Big Bertha #2	1:100	Elaine Taylor
Strep	mouse	34850	1:5000	QIAGEN
Ku80	rabbit	ab80592	1:1000	Abcam
RPA2	rabbit	NB100-544	1:1000	Novus Biologicals
phospho-H2A.X (phospho S139)	rabbit	ab11174	1:5000	Abcam
tubulin	rat	ab6160	1:5000	Abcam
Histone 1.2	rabbit	ab17677	1:1000	Abcam
Flag	mouse	F3165	1:3000	Sigma
Tdp1	rabbit	Serum purified	1:500	Eurogentec
GFP	rabbit	ab290	1:1000	Abcam

Table 2.5: Secondary antibodies used in this study

Secondary antibody	Source
Polyclonal Rabbit anti-Mouse immunoglobulins/HRP	Dako
Polyclonal Swine anti-Rabbit immunoglobulins/HRP	Dako
Polyclonal Rabbit anti-Rat IgG/HRP ab6734	Abcam
Goat Anti-Mouse IgG H&L (Alexa Fluor 647)	Abcam
Donkey Anti-Rabbit IgG H&L (Alexa Fluor 488)	Abcam

2.2.8 Immunofluorescence

When performing immunofluorescence with Flp-In T-REx 293 cells, coverslips were coated in poly-D-lysine (Millipore), washed twice in dd H_2O and left to dry before plating cells. Exponentially growing cells were plated one day before experiment in 6 or 12-well plates to rich approximately 60 – 80% confluency on the day of experiment. If pre-extraction step was included in order to visualise foci when using antibody for unmodified nuclear protein, cells were treated with 0.1% Triton-X for 2 minutes prior to fixation in 3.7% paraformaldehyde (PFA) and then treated with ice-cold methanol/acetone (1:1). When using normal protocol without pre-extraction, media was removed, coverslips were gently washed in PBS and fixed in 3.7% PFA for 10 minutes, then directly permeabilised in 0.2% Triton-X for 10 minutes and blocked for 45 minutes in 0.5% BSA in PBS. After blocking coverslips were incubated with 0.5% BSA containing primary antibody for 1 hour in a wet chamber to prevent evaporation of antibody solution. After this, coverslips were gently washed 3 x 5 minutes in PBS and incubated with secondary antibody conjugated to Alexa Fluor dye (1:1000) in 0.5% BSA for 1 hour protected from light. Next, coverslips were washed 2 x 5 minutes in PBS and nuclei were stained using DAPI in PBS (1µg/ml) for 6 minutes. Coverslips were washed once more in PBS, rinsed in dd H_2O and let air dry on slices of Whatman filter paper. When dry, coverslips were mounted on glass slides using Vectashied (4.5 µl per coverslip).

2.2.9 Western blot

Western blot analysis was performed as follows unless indicated otherwise; cells were trypsinised and washed once in PBS before lysis in Urea lysis buffer (9M Urea, 50mM

Tris base, 1% 2-mercaptoethanol, pH 7.5). After lysis cells were sonicated using probe sonicator (Sonics & Materials inc. Vibra Cell) 20% amplitude for 3.5 seconds, spun for 10 minutes at 16000 x g at RT using table centrifuge (Eppnedorf). Supernatant was subjected to Bradford protein assay (Bio-Rad) to determine the protein concentration in the whole cell extract. Same amount of protein was loaded on appropriate sized SDS-PAGE gel and SDS-PAGE electrophoresis was performed. After resolving, proteins were transferred onto nitrocellulose blotting membrane (Amersham, Protran 0.2 μM NC, GE Healthcare) in 1 x Tris-glycine buffer (25mM Tris, 192mM glycine, 10% methanol) at 30V for 1.5 hours, 4°C. Membrane was subjected to Ponceau staining in order to visualise the proteins after transfer, scanned, cut to appropriate size and washed 5 minutes in PBST buffer (PBS + 0.1% Tween20) before blocking in 3% non-fat dry milk (Marvel) in PBST for 30 minutes. Membrane was further incubated with primary antibody overnight at 4°C on roller. Next day membrane was washed 3 x 10 minutes in PBST before incubation with secondary antibody conjugated to horseradish peroxidase (HRP) in PBST + 3% milk for 1 hours at RT. After, the membrane was washed 3 x 10 minutes in PBST and developed using Pierce ECL Western Blotting Substrate (#32106) emitted chemiluminescence was captured on CL-Xposure film (Thermo Scientific) which was developed using X-ray film processor Photon Imaging Systems Ecomax. Developed films were scanned, quantification of western blots was performed using FiJi (ImageJ) software.

Primary antibody was used in concentrations specified in Table 2.3 Secondary antibody was used in concentration 1:2500 in 3% milk with PBST. For phosphor-antibodies, PBST was replaced by TBST (20mM Tris, 150mM NaCl, 0.1% Tween20).

2.2.10 SDS-PAGE

Generally, proteins were separated on hand-casted 12% SDS-PAGE separation gel using Bio-Rad apparatus. For each mini-gel, 5 ml of separation gel was used (gel composition described in Table 2.5) ammonium persulfate (APS) and TEMED was added last before gel polymerization. Stacking gel was added (1 ml per one mini-gel) after the separation gel has fully polymerised. Whole cell extract in urea buffer was mixed with 4 x sample buffer (200mM Tris-HCl pH 6.8, 50mM EDTA, 8% SDS, 40% glycerol, 0.08% bromophenol blue, 4 % v/v 2-mercaptoethanol) in 3 : 1 ratio and boiled at 90°C for 10 minutes before being loaded on the gel. Proteins were separated in 1 x SDS running buffer (2.5mM Tris-HCl, 20mM glycine, 0.01% w/v SDS) first 15 minutes at 70 V, after which

voltage was increased up to 120 V until the sample was fully separated. For NSMCE4a pull down experiments, 10% SDS-PAGE gels were used in order to better separate SMC5 from NSMCE4a.

Table 2.6: SDS-PAGE gel composition

10 ml Separation gel %	ddH_2O (ml)	30% acrylamide (ml)	1.5 M Tris-HCl, pH 8.8 (ml)	10% SDS (µl)	10% APS (µl)	TEMED (µl)
10%	3.8	3.4	2.6	100	100	10
12%	3.2	4.0	2.6	100	100	10
10 ml Stacking gel %	**ddH_2O (ml)**	**30% acrylamide (ml)**	**0.5 M Tris-HCl, pH 6.8 (ml)**	**10% SDS (µl)**	**10% APS (µl)**	**TEMED (µl)**
5%	5.86	1.34	2.6	100	100	10

2.2.11 Silver stain

Silver staining was carried out using the Bio-Rad Silver Stain Plus kit according to manufacturer's instructions.

2.2.12 Coomassie stain

SDS-gels were incubated with the Coomassie solution (Coomassie R250, 0.1% w/v, 10% acetic acid, 40% methanol) with gentle agitation for 1 – 2 hours. After that the gels were rinsed twice in ddH_2O and incubated overnight in the destain solution (20% methanol, 10% acetic acid).

2.3 Affinity Purification and Mass Spectrometry

2.3.1 Purification of the 6xHis-Nse4a NSMCE4a antigen

The 6xHis-Nse4a (php96) antigen in

the pQE32 vector was transformed and expressed in the M15 *E.Coli* expression cells (QIAGEN), where the expression of gene of interest is induced by addition of isopropyl-β-D-thiogalactoside (IPTG). Before addition of 1mM IPTG for 3-5 hours, 50 µl of the culture was kept for SDS-PAGE analysis. After induction by IPTG, the cells were pelleted by centrifugation (5000 x g, 4°C for 10 minutes). The pellet was washed in PBS and

resuspended in 25ml/500 µl of cell pellet sonication buffer (500mM NaCl, 20mM MOPS pH 7.9) supplemented with EDTA-free protease inhibitors (Roche). Cells were sonicated 5 x 30 seconds 30% amplitude, chilled on ice between cycles. Sonicates were split between tubes and spun 10 minutes 10 000 x g at RT. Soluble fraction was discarded, 50 µl was kept for SDS-PAGE. The pellet was resuspended in 5 ml binding buffer (500mM NaCl, 8M Urea, 5mM imidazole, 20mM MOPS pH 7.9) and sonicated again 20% amplitude 30 seconds per cycle and vortexing in between for 1 hour. After, the mixture was spun for 10 minutes 10 000 x g at RT and supernatant was removed. 50 µl of the supernatant was kept for SDS-PAGE analysis. Solubilised proteins was added to the equilibrated Ni-NTA beads. For 1 litre of bacterial culture, 1 ml of Ni-NTA agarose was used to bind the antigen. To equilibrate 1 ml Ni-NTA agarose beads, the beads were washed in 3 x 5 ml of binding buffer (spun 1000 rpm/1 minute between washes). In soluble fraction was added to the equilibrated beads and incubated with end-to-end rotation at RT for 1 hour. After incubation the whole agarose bead and protein mixture was transferred to a 10 ml empty gravity column (Bio-Rad). 50 µl of the flow through fraction was kept for SDS-PAGE analysis. Wash was performed first in 25 ml of binding buffer and then in 10 ml wash buffer (500mM NaCl, 8M Urea, 40mM imidazole, 20mM MOPS pH 7.9). Elution was performed by addition of 10 x 500 µl of elution buffer (500mM NaCl, 8M Urea, 150mM imidazole, 20mM MOPS pH 7.9). 50 µl of each elution was kept for SDS-PAGE analysis. The elution fractions were pooled and concentrated on concentration columns Vivaspin 500 10,000 Daltons MWCO PES (Satorius). Concentrated antigen was snap frozen in liquid nitrogen and stored at -80°C.

2.3.2 Purification of the NSMCE4a antibody on nitrocellulose strips

Maximum amount of the purified 6xHis-Nse4a antigen was loaded and onto SDS-PAGE gel (12%) using single well comb and separated. After, the antigen was transferred onto nitrocellulose membrane (Amersham, Protran 0.2 µM NC, GE Healthcare). Membrane was subjected to Ponceau staining in order to visualise the antigen, the band in the antigen size was cut. The cut stripe of membrane was blocked in 5% milk in PBST for 1 hour. After, the membrane was rinsed in PBS and incubated with 10 ml of crude serum (SK3616) containing the NSMCE4a antibody overnight at 4°C. Membrane was washed 5 x in PBST, cut into small pieces to fit into 1.5 ml Eppendorf tube. Membrane was pre-eluted in 500 µl of 10mM phosphate buffer pH6.8. Antibody was eluted by 200mM

glycine, pH 2.5 in 4 x 300 µl elutions. Each elution was performed for 30 seconds and immediately transferred to an Eppendorf tube containing 30 µl of 1.5mM Tris pH8.8. The antibody concentration was determined by BSA/Bradford assay. The purified antibody was stored in 10% glycerol in -20°C.

2.3.3 Ni^{2+}-NTA and TALON affinity purification

All affinity purifications were performed under native conditions unless stated otherwise. All purifications steps from cell lysis onwards were performed in lo-bind 1.5 ml tubes (Eppendorf) tubes to minimalize sample loss. Cells were harvested from 15 cm dishes and lysed in lyses buffer (40mM NaCl, 0.5% NP40, 20mM Hepes pH 7.4, 2mM $MgCl_2$) supplemented with 1 x EDTA-free Protease Inhibitor Cocktail (Roche), 1 x PhosSTOP (Roche) and 1µl/ml benzonase for 1 hour on ice. After benzonase digestion, the cell lysate was spun for 15 mins at 16 000 x g, 4°C and the supernatant was collected (soluble fraction). The pellet was re-suspended in the same volume, as was the elution volume, of urea buffer. Protein concentration in the soluble fraction was determined by Bradford Assay using Bradford Reagent (Bio-Rad) according to manufacturer's instructions. The NaCl concentration of soluble fraction was increased to 150mM. The volume of charged agarose beads for each reaction was approximately 100 µl of 50% slurry for 3 – 5 mg of whole cell extract; Table 2.6 shows estimated volumes of reagents for different experiments. The same amount of protein extract for each cell line/condition, was added to equilibrated agarose beads.

Table 2.7: Volumes for affinity purification reactions

15 cm plate (number)	Lysis buffer (ml)	Benzonase (µl)	Agarose beads (µl)	Elution volume (µl)
1	0.5	0.5	60	100
2	1	1	80	100
5	2	2	120	150
12	4	4	300	500

Standard protocol for nickel affinity purification using nickel charged Ni-NTA agarose beads (QIAGEN): beads were equilibrated 3 times in 5 column volume of wash buffer (150mM NaCl, 20mM Hepes pH7.4) containing 30mM imidazole. Imidazole was added to the whole cell extract to final concentration of 30mM. Sample was added to the equilibrated beads in a 1.5ml tube and incubated at 4°C with end-to-end rotation for 1

hour. After that, samples were spun for 1 minute at 800 x g 4°C, supernatant was removed and kept as a flow through fraction for Western Blot analysis. Beads were washed 5 times in 5 column volumes of wash buffer supplemented with 30mM imidazole. After each wash, beads were spun for 1 minute at 800 x g and supernatant was carefully removed. First elution was performed using wash buffer supplemented with 60mM imidazole. Beads were incubated with end-to end-rotation at 4°C for 15 minutes, spun for 1 minute at 800 x g, 4°C and supernatant was kept in a new tube (elution 1). Second elution was performed using wash buffer supplemented with 150mM imidazole in a similar manner as the first elution, supernatant was kept in a new tube (elution 2). The beads were re-suspended in 1 x SDS running buffer (1: 3 SDS running buffer: wash buffer) and boiled at 90°C for 10 minutes. Supernatant was kept as a "beads" fraction for Western Blot analysis. All fractions were snap-frozen in liquid nitrogen and stored at -80°C before any further applications.

Standard protocol for TALON Metal Affinity Resin (Clontech) was similar to Ni-NTA protocol with different imidazole concentrations; for equilibration and binding step, wash buffer supplemented with 10mM imidazole was used.

2.3.4 Strep-tag affinity purification

Strep-tag affinity purification was performed using MagStrep "type3" XT Beads (iba). Typically, 30 µl of XT magnetic beads was used for 150 µl of elution 2 (150mM imidazole in wash buffer) from Nickel/TALON pull down. Elution was directly used for the second affinity purification, which was performed according to manufacturer's guidelines.

2.3.5 Chromatin enrichment for proteomics (ChEP)

The method was performed as previously described in (Kustatscher et al., 2014). All steps were carried out in lo-binding tubes and using lo-binding tips (Eppendorf). The input material was approximately 3 x 10^7 cells (2 x 15 cm dishes) for each cell line was used (bait, control). Briefly, cells were exposed to 1% (w/v) formaldehyde for 10 minutes at 37°C, cross-linking reaction was terminated by addition of glycine up to 250 mM. Cells were harvested by scraping off the 15 mm dishes, snap frozen and stored in -80°C until chromatin enrichment. Each cell pellet was thawed and re-suspended in 1 ml of ice-cold cell lysis buffer (25 mM Tris pH 7.4, 0.1% (v/v) Triton X-100, 85 mM KCl, 1 tablet of

Roche protease inhibitors/ 10 ml buffer) and homogenised by cut 200 µl tip. The cell suspension was centrifuged at 2300 x g for 5 min at 4 °C, the pellet was the nuclei fraction. Each nuclei pellet was re-suspended in 500 µl of cell lysis buffer containing 200 µg/ml RNase A and incubated for 15 min at 37 °C. The pooled nuclei suspension was centrifuged at 2300 x g for 10 min at 4 °C and subjected to the chromatin enrichment step; nuclei were re-suspended in 500 µl of SDS buffer (50 mM Tris pH 7.4, 4% w/v SDS, 1 tablet of Roche protease inhibitors per 10 ml buffer) and incubated for 10 min at room temperature. Next, 1.5 ml of urea buffer (10 mM Tris pH 7.4, 8 M urea) was added and the sample was mixed thoroughly by inverting the tube several times; the sample was centrifuged at 16100 x g for 30 minutes at 25 °C, the supernatant was discarded. To wash the contaminants, the pellet was re-suspended in 0.5 ml 500 µl of SDS using lo-bind tip with a cut end, 1.5 ml of urea buffer was added. Sample was mixed by inverting the tube several times and spun at 16100 x g for 25 minutes at 25 °C. To wash away urea, 500 µl of SDS buffer was added and the chromatin pellet was re-suspended carefully by lo-bind tip with a cut end; another 1.5 ml of SDS buffer was added and the sample was mixed by inverting the tube several times. Residual SDS that could interfere with binding to TALON column, was removed by washing the pellet with 350 µl storage buffer (10 mM Tris pH 7.4, 25 mM NaCl, 10% (v/v) glycerol, 1 tablet of Roche protease inhibitors per 10 ml buffer) by flicking to dislodge the pellet, which was spun at 16100 x g for 5 minutes. Pellet was covered with 350 µl of fresh storage buffer and subjected to 15 minutes of sonication using Q800R2 sonicator (Qsonica) at 70% amplitude (cycle: 30 second ON, 30 seconds OFF, total time 30 minutes). Sonicated pellet was spun at 16100 x g for 30 minutes at 4 °C. The supernatant containing sheared, cross-linked chromatin, was transferred into a new tube. BSA-Bradford assay was performed to determine the protein amount in each sample. Similar amount of material was used for pull down using TALON IMAC column, as described in methods section 2.3.3 (Ni^{2+}NTA and TALON affinity purification). Two consecutive elutions using 60mM and 150nM imidazole were performed. After, the TALON beads, as well as both elutions were boiled for 30 min at 98 °C to reverse the formation of cross-links. The de-crosslinked sample was stored at -20°C until the western blot and silver stain analysis was performed.

2.3.6 Sample preparation for MS analysis

Elutions from TALON/Nickel columns were digested by trypsin, desalted, dried and resuspended in 0.1% TFA (trifluoracetic acid) before mass spectrometry analysis. All steps were performed in lo-bind 1.5 ml tubes (Eppendorf). Thawed elutions from TALON/Nickel were first pH adjusted to pH 7.8 by adding ammonium bicarbonate up to 50mM. Cysteines were reduced by adding dithiotreitol (DTT) to final concentration of 1mM and incubated for 30 minutes at RT. Sample was alkylated using 55 mM chloroacetamide for 30 minute at RT, protected from the light. Tryptic digest was performed using Trypsin Gold (Promega); trypsin was added to the sample in 1: 20 – 1: 50 (trypsin: protein) mass to mass ratio, samples were incubated at 37°C overnight. Digested peptides were subjected to a desalting step using Pierce C18 Spin Columns according to manufacturer's guidelines. Peptides were eluted from C18 column in 40 µl of 70% ACN (acetonitrile), sample volume was reduces to final volume of cca 4 µl using SpeedVac Concentrator (Thermo Scientific). Concentrated peptides were re-suspended in 20 µl of 0.1% TFA before being subjected to mass spectrometry analysis or stored at -20°C. For the Strep-tag affinity purification, on-bead digest was performed. Samples were treated the same way as described for TALON/Nickel affinity purification.

2.3.7 Mass spectrometry

Mass spectrometry analysis was carried out using LTQ OrbitrapXL instrument (Thermo Fisher) paired with ultra-high-performance liquid chromatography (UHPLC) UltiMate 3000 system (Thermo Fisher). Peptides in 0.1% TFA were loaded on a PepMap100 C18 LC trap cartridge (Thermo Fisher), and separated on a PepMap100 analytical column (Thermo Fisher) at a flow rate of in 300 nl/min. Peptides were eluted with 90 minute gradient increasing from 1% - 43.3% solution B (90% acetonitrile) in 0.1% FA. Detailed description and illustration of the method is listed in Appendix Figure A.1. Eluted peptides were ionised using electro-spray and measured after transfer using LTQ Orpitrap XL instrument. When running different conditions, between every 2 samples (bait-control) 2 µl of blank solution (0.1% TFA) was injected to minimalize the carryover.

2.3.8 Mass spectrometry analysis

Peptide search was performed using MASCOT (Matrix Science, version 2.3.02) database. For analysis of multiple biological repeats or fractions of the same sample, the data search was performed by MaxQuant (version 1.6.3.3) quantitative proteomics software (Cox and Mann, 2008). For statistical analysis, Max Quant search results were further analysed using Perseus (version 1.6.2.1) framework (Tyanova et al., 2016).

3 Chapter 3

Results I

Establishing a system to study components of the SMC5/6 complex in mammalian cells

3.1 Introduction

Mutant screens in *S.pombe* identified two separation of function mutants in the *smc6* gene, *smc6-X* and *smc6-74* (Nasim and Smith, 1975; Verkade et al., 1999). Analysis of these mutants has established different functions of the Smc5/6 complex in homologous recombination. The first is the 'early' function, which maintains stalled replication forks in recombination-competent manner. The second 'late' function is the resolution of recombination intermediates after homologous recombination. Since the SMC5/6 complex is conserved from yeast to human, these functions are likely to be conserved in higher eukaryotes (Ampatzidou et al., 2006; Irmisch et al., 2009). The results in yeast demonstrate that different mutations in one subunit of the Smc5/6 complex can result in different phenotypes, which in humans, may result in different clinical presentations. Studies on SMC5/6 patient cell lines, which contain mutations in different components of the complex, emphasise its role in homologous recombination and replication stress (van der Crabben et al., 2016; Payne et al., 2014). Mutation in the SUMO-ligase NSMCE2 result in destabilisation of the NSMCE2 subunit, but only mild decrease in the protein levels of the other complex components. Patients carrying the mutation in NSMCE2 displayed primordial dwarfism and primary gonadal failure coupled with extreme insulin resistance, but were viable until adulthood (Payne et al., 2014). Patient cells with mutations in the NSMCE3 subunits show destabilisation of the SMC5/6 complex, and the patients develop a chromosome breakage syndrome with terminal lung disease. The patients die during infancy and display genome instability and a DNA repair defect in G2 phase of the cell cycle. These studies demonstrate how mutations in different subunits of the SMC5/6 complex result in strikingly different phenotypes.

However, the patient cells are not an ideal model to dissect the function of the SMC5/6 complex and studying the effect of SMC5/6 mutations in isogenic cell lines has not yet

been possible. Knock down experiments performed in Yu lab on the human SMC5/6 complex have failed to clarify mechanisms of action due to off target effects of the siRNA (Wu et al., 2012). Therefore, there is a need to develop a model human system, which would enable the elucidation of the SMC5/6 complex function in more detail.

Since SMC5/6 components are likely to be essential in human cells, we took the approach of integrating a functional cDNA encoding an SMC5/6 subunit before using CRISPR/Cas9 to knock out the endogenous copies. To do so, we used a commercially available Flp-In T-REx 293 cell line, which allows generation of stable and regulatable isogenic cell lines with ectopically inserted gene of interest. The principals of the T-REx Flp-In system is described in the next section; this system will be used throughout the thesis to gain further insights into the cellular function of the SMC5/6 complex.

3.1.1 The Flp-In T-REx system

This system allows the generation of a stable human cell lines expressing a gene of interest in an inducible manner. The Flp-In T-REx system consists of three core components:

i) The host Flp-In T-REx-293 cell line
ii) The FRT expression vector with a gene of interest (pcDNA5/FRT/TO)
iii) The Flp expression vector (pOGG44)

The Flp-In T-REx-293 host cell line is a commercially available cell line derived from HEK293 (ATCC accession number CRL-1573) cell line. It contains two stably inserted plasmids in its genome; first plasmid contains a single Flp Recombination Target (FRT) site and a Zeocin resistance cassette, second plasmid contains Tetracycline regulatable repressor (TetR) gene and a Blasticidin resistance cassette (Figure 3.1 A). The gene of interest is expressed from the FRT expression vector, which contains a single FRT site, a hybrid cytomegalovirus (CMV) promoter, and a Hygromycin resistance cassette. The expression of the gene of interest is controlled by the tetracycline-regulated CMV promoter. The promoter contains two Tet operator ($TetO_2$) elements, each of them binds two molecules of Tet repressor protein.

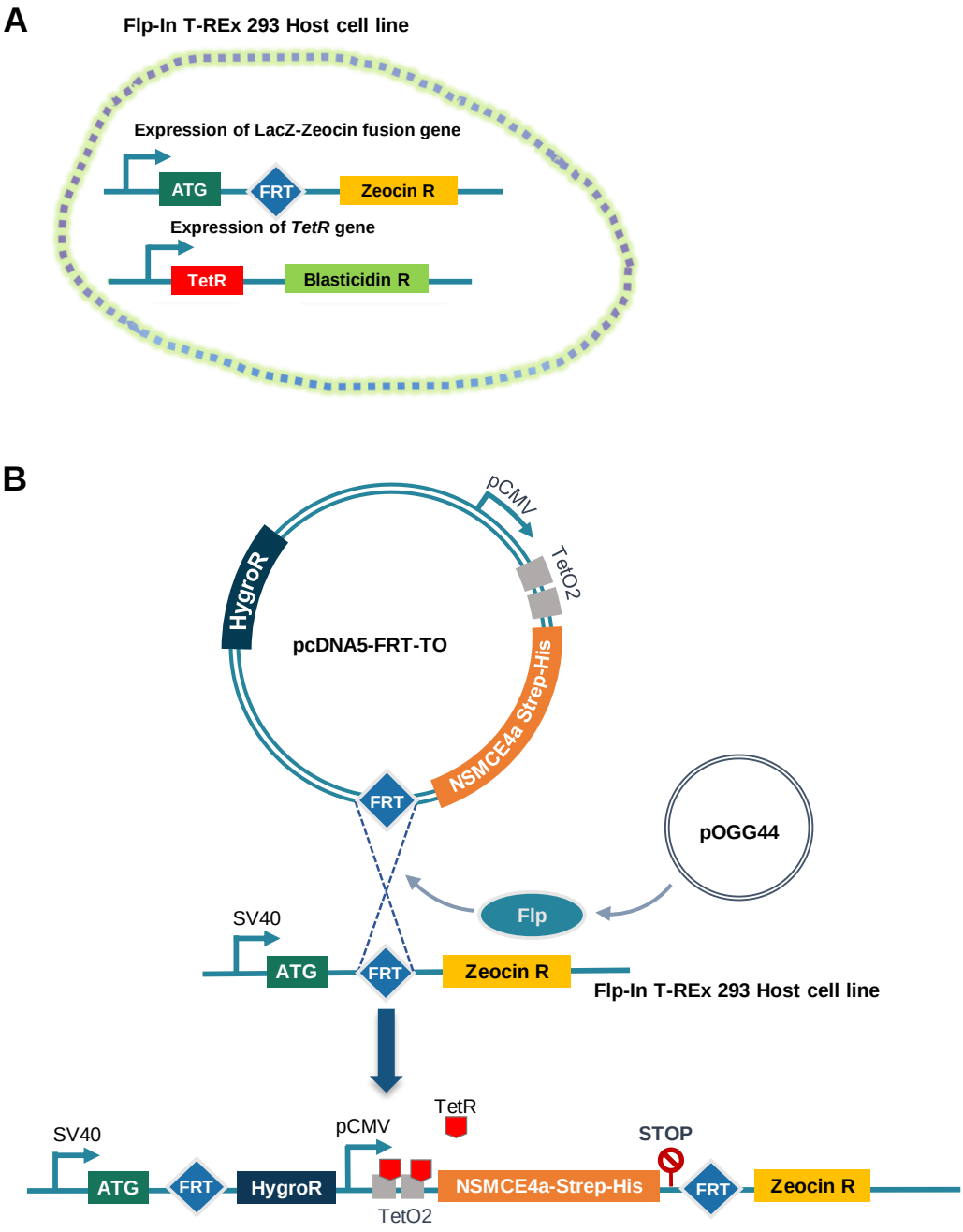


Figure 3.1: Scheme of the human T-REx Flp-In system in the 293 host cell line
A. Flp-In T-REx 293 cell line containing two stable inserted constructs: (i) single copy of the FRT site and Zeocin resistance gene generated by insertion of pFRT/lacZeo plasmid and (ii) Tet repressor (TetR) and Blasticidin resistance gene generated by insertion of pcDNA6/TR plasmid. **B.** Flp-In T-REx 293 cell line is co-transfected with pcDNA5-FRT-TO containing gene of interest and pOGG44, the Flippase (Flp) expression vector. Flp catalysed site-specific recombination between the FRT sites results in stable integration of the whole pcDNA5-FRT-TO into the genome. The successful insertion confers resistance to Hygromycin and generates a stop codon preventing expression of the Zeocin resistance gene. Screening for positive clones is performed by selection on Hygromycin.

The Flp expression vector, which constitutively expressed Flp recombinase under the control of the human CMV promoter. The Flp recombinase, originally isolated from *Saccharomyces cerevisiae*, is a site-specific recombinase, which recognises the Flp Recombination Target (FRT) site. The FRT is a specific 34 bp DNA sequence, the Flp recombinase cleaves and catalyses a site-specific recombination between the FRT sites (Gronostajski and Sadowski, 1985; Sauer, 1994).

In order to generate a stable cell line, the gene of interest is first inserted into the FRT-expression vector. This vector is then co-transfected into the cells together with the Flp-expression vector (pOGG44). Constitutively expressed Flp recombinase then catalyses a site specific recombination between the FRT site in the genome of the host cell line, and the FRT site of the expression vector (pcDNA5/FRT/TO) (O'Gorman et al., 1991). This leads to genome integration of the whole FRT-expression vector specifically at the FRT site (Figure 3.1 B). The FRT-expression vector contains a stop codon, so the newly created cell line will lose its original Zeocin resistance and gain the Hygromycin resistance instead. Importantly, the Hygromycin resistance cassette lacks its own promoter, thus, is expressed only if correctly inserted at the FRT site of the host cell line. Successfully created stable cell line can be selected on Hygromycin. The resulting system is a Tet-ON system, which means that expression of gene of interest is activated in the presence of Tetracycline, or its analogue, Doxycycline. In the absence of Tetracycline the Tet Repressor (TetR) binds the $TetO_2$ and represses the expression of the gene of interest.

3.2 Aims

i) To generate stable isogenic cell lines to validate the phenotype of the NSMCE3 mutation

ii) To create regulatable system to investigate the effect of human SMC5/6 complex destabilisation

3.3 Results

3.3.1 NSMCE3 p.Leu264Phe leads to destabilisation of the SMC5/6 complex and increased genome instability

After the first study on NSMCE3 patients was published by van der Crabben et al., 2016, our laboratory received a new NSMCE3 patient cell line (svdc01), from a new family but carrying the same homozygous mutation (p.Leu264Phe) in the NSMCE3 gene, as previously described. To test if the mutation in NSMCE3 in this second patient cell line resulted in the same phenotype the protein levels of the SMC5/6 complex were assessed by western blot and compared to the previously published patient cell line (GVH02) and a wild type primary cell line (1BR).

As expected, both patient cell lines show destabilisation of the whole SMC5/6 complex, which is reflected in low protein levels of different complex components when compared to the wild type control (Figure 3.2 A). This is not due to differences in loading, as shown by the tubulin loading control. Destabilisation of the SMC5/6 complex also led to a significant increase in micronuclei formation, a hallmark of genome instability (Figure 3.2 B and C).

The primary patient fibroblast were not an ideal model system due to various constraints, such as difficult transfection, slow growth and the ability to be grown only for a limited passage number, due to replicative senescence. In order to overcome some of these limitations, we attempted to immortalise the patient fibroblasts by transfection with human telomerase reverse transcriptase (hTERT). However, two independent attempts to immortalise the patient svdc01 fibroblast cell line failed. Similar attempts with the GVH02 patient cell line also repeatedly failed. This could be related to the role of the SMC5/6 complex in telomere maintenance. SMC5/6 was shown to play a role in telomere maintenance in human cells with activated alternative lengthening of telomeres (ALT) pathway (Potts and Yu, 2007). However, as the siRNA used have been reported to have an off target effects, this data have to be treated with caution. In addition, the budding yeast homolog of NSMCE3 (Nse3) is important for Smc5/6 binding to telomeres and maintenance of telomere length in budding yeast (Moradi-Fard et al., 2016). We can therefore speculate whether the repeated failure immortalise the patient cells was due to an altered telomere metabolism caused by destabilisation of the SMC5/6 complex.

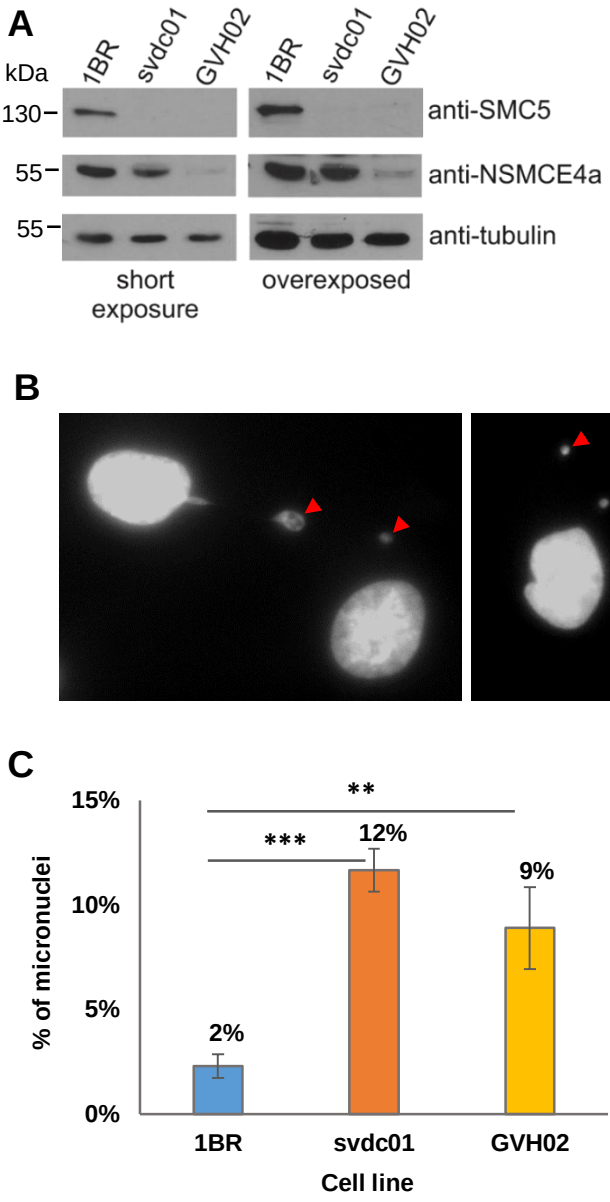


Figure 3.2: Destabilisation of the SMC5/6 complex and increased genome instability in NSMCE3 patient fibroblasts

A. Western blot showing decreased levels of SMC5/6 complex components in two patient cell lines (svdc01 and GVH02) in comparison to wild type cells (1BR). **B.** Example of micronuclei, indicated by red arrows, cells were imaged using 400 x magnification, **C.** Quantification of micronuclei percentage in NSMCE3 patient cell lines; error bars represent +/- standard deviation of three independent repeats, two-tailed Student t-test was used to calculate statistical significance ** $p \leq 0.01$, *** $p \leq 0.001$.

3.3.2 Construction of stable T-Rex Flp-In 293 cell lines

The results with the patient cell lines led us to develop systems in an independent human cell line, to investigate:

i) The effect of point mutations in NSMCE3
ii) The effect of destabilisation of the SMC5/6 complex

The NSMCE3 patient mutation leads to the destabilisation of the whole SMC5/6 complex. As previously described above, the T-REx Flp-In system allows generation of a stable cell line expressing the gene of interest from a regulatable promoter. In parallel with creation of the stable NSMCE3 cell line to mimic the SMC5/6 complex destabilisation, a stable and regulatable NSMCE4a cell line was developed. NSMCE4a was chosen because it directly interacts with NSMCE3 and this protein interaction is abolished by the NSMCE3 p.Leu264Phe mutation (van der Crabben et al., 2016). The yeast homolog of human NSMCE4a, was shown to be regulatable and could be C-terminally tagged without disrupting the protein function. Furthermore, Nse4 shut off in budding yeast leads to decrease in protein levels of the whole Smc5/6 complex (Copsey et al., 2013). This is also supported by observations in human cells, where siRNA depletion of the NSMCE4a, leads to destabilisation of the whole SMC5/6 complex (Taylor et al., 2008).

3.3.2.1 Purification of the NSMCE4a antibody

In order to monitor the protein levels and easily screen for the CRISPR/Cas9 knock out of the SMC5/6 subunits, it was important to have an antibody specific to endogenous NSMCE3 and NSMCE4a. In the laboratory, we only had a crude serum for the NSMCE4a antibody, which needed to be purified and validated. To purify the NSMCE4a antibody we first expressed and purified the antigen that was used to raise the original antibody. The 6xHis-Nse4a (php96) antigen in pQE32 vector was transformed and expressed in the M15 *E.Coli* expression cells (QIAGEN), where the expression of gene of interest is induced by addition of isopropyl-β-D-thiogalactoside (IPTG). The 6xHis-Nse4a antigen was purified from the insoluble fraction using Ni-NTA agarose column, ten elutions were pooled and concentrated (Figure 3.3 A). Final concentration of the purified 6xHis-Nse4a was determined from a BSA/Bradford calibration curve. Purified antigen was then separated by SDS-PAGE, transferred to a nitrocellulose membrane and used to affinity

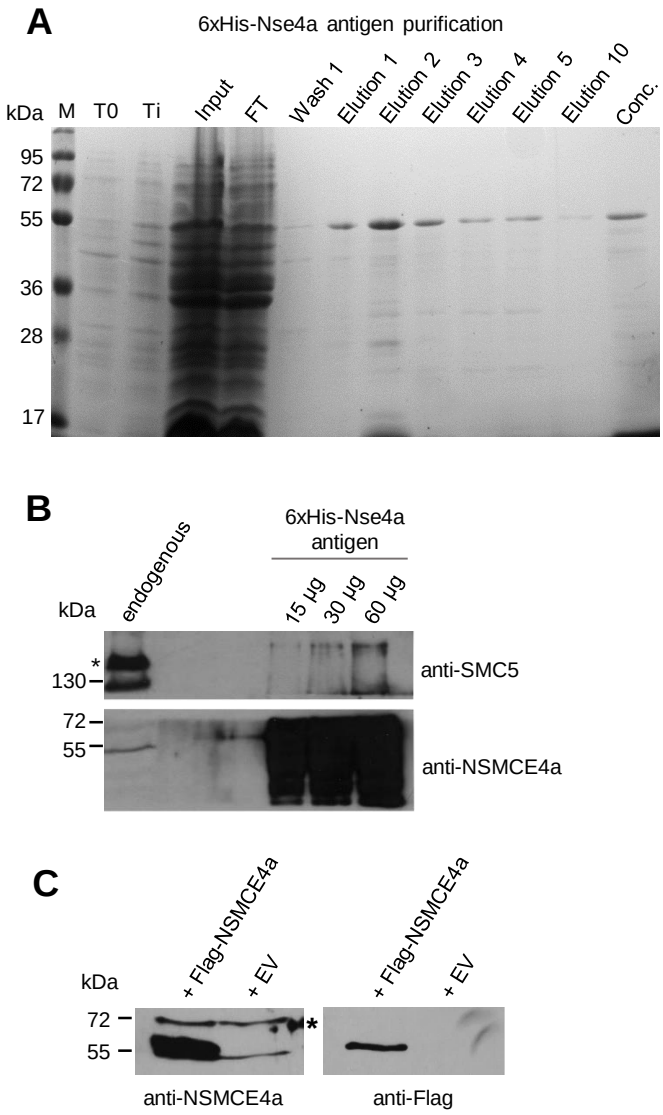


Figure 3.3: NSMCE4a antibody purification from crude serum

A. 6xHis Nse4 antigen purification, Coomassie stained SDS-PAGE gel showing different fractions of purification procedure: the bacterial lysate before induction with IPTG (T0), 3 hours after induction with 1mM IPTG (Ti), the concentrated insoluble fraction (Input), first wash (wash 1), elutions (Elution 1 – 10) and the purified concentrated antigen (conc.). **B.** Initial testing of NSMCE4a antibody, first lane contains whole cell extract from U2OS cell line (endogenous), other lanes contain different concentrations of purified NSMCE4a antigen (6xHis-Nse4a), membrane was probed with SMC5 antibody to test it on the whole cell extract, band above 130 kDa is a non specific band recognised by the SMC5 antibody (*). **C.** Flp-In T-REx 293 cell line was transfected with either Flag-NSMCE4a containing vector (Flag-NSMCE4a) or an empty vector (EV) and probed with anti-Flag or purified NSMCE4a antibody, the band at 55 kDa corresponds to the endogenous NSMCE4a, the band around 72 kDa is a non-specific band recognised by the NSMCE4a antibody (*).

purify the NSMCE4a antibody from a crude serum, as described in Materials and Methods.

To validate the functionality of the purified antibody, we initially performed a western blot using increasing concentrations (15 - 60 µg) of the purified 6xHis-Nse4a antigen, as well as 30 µg of the whole cell extract. Probing the western blot membrane with the purified NSMCE4a antibody in a 1:1000 concentration gave a strong signal ranging from 35 and 72 kDa in the lanes containing the purified antigen (Figure 3.3 B, lane 2-4). Another band around approximately 55 kDa was present in the lane containing the whole cell extract, which corresponds to the size of the endogenous NSMCE4a protein (Figure 3.3 B, lane 1). This confirms that the purified antibody is able to detect the antigen against which it was raised, as well as the endogenous NSMCE4a in a whole cell extract. To further validate that the band detected in the whole cell extract is indeed NSMCE4a, U2OS cells were transfected with a construct carrying Flag tagged NSMCE4a and an empty vector. Whole cell extract was prepared and subjected to the Western blot using the NSMCE4a antibody and anti-Flag antibody. The Flag-NSMCE4a transfected cells display a strong band around 55 kDa (Figure 3.3 C, lane 1), the empty vector transfected cells display a weaker band at a similar size, when probed with the NSMCE4a antibody. Probing with an anti-Flag antibody confirmed that this observed 55kDa band is the transfected Flag-NSMCE4a (Figure 3.3 C, lane 3). Thus, confirming that the purified antibody recognised both NSMCE4a-Flag and the endogenous NSMCE4a protein. We could also observe a band around 72 kDa, which is most likely an unspecific band recognised by the NSMCE4a antibody.

3.3.2.2 Genome insertion of the NSMCE3 and NSMCE4a using the Flp-In system

To create a regulatable NSMCE3 and NSMCE4a, the approach was as follows:

i) To integrate a spare allele of a wild type, epitope tagged subunit of the SMC5/6 complex into the T-Rex Flp-In host cell line
ii) To knock out the endogenous subunit using CRISPR/Cas9

The rationale is that the spare wild type SMC5/6 subunit would cover the loss of the endogenous copies and at the same time, enable us to validate the viability of the epitope tagged alleles. This step-wise approach was taken because all the components of the

Smc5/6 complex are essential in budding yeast (Zhao and Blobel, 2005) and the absence of Smc5/6 is embryonic lethal in mice (Jacome et al., 2015).

The first step to construct the NSMCE3 T-REx Flp-In 293 cell line was to insert a wild-type NSMCE3 gene with an N-terminal 10xHis-Flag tag into the FRT expression vector. An NSMCE3 gene was commercially synthesised by GenScript in pUC57 vector. The gene was codon optimised in order to be resistant to the CRISPR guide RNA cleavage. The pUC57 vector carrying 10xHis-Flag NSMCE3 was digested with HindIII and XhoI and the insert cloned into the pcDNA5/FRT/TO vector, the product was validated by sequencing.

For insertion of NSMCE4a gene, the codon optimised NSMCE4a was amplified from the pre-synthesised vector using ntermnse4fwd and ntermnse4rev primers (Table 2.2). An additional EcoRV restriction site was introduced to the C-terminus of NSMCE4a by PCR with nse4fwd.v2 nse4rev.v2 primers. PCR product was digested with KpnI and EcoRV and inserted into the pcDNA5/FRT/TO. The final product was validated by sequencing.

The codon optimised NSMCE3 and NSMCE4a FRT-expression vectors were co-transfected with the Flp-expression vector into the T-REx Flp-In 293 cells in 1:3 ratio using a total of 2 µg of DNA. Transfected cells were grown in normal media without any selection for 48 hours in order to allow the Flp-mediated recombination to take place. After 48 hours, cells were washed and normal media replaced with media containing 200 µg/ml of Hygromycin. Cells were grown for another 10 – 14 days to form macroscopic colonies. Single cells were selected and then grown to confluency in 6 well plates. Positive clones were further validated for the correct insertion of the pcDNA5/FRT/TO vector by selection on Zeocin in parallel with Hygromycin. Cells were grown in 6-well plates in duplicates containing media with either Zeocin (100 µg/ml) or Hygromycin (200 µg/ml). Clones that did not display Zeocin resistance were selected and tested for the presence of tagged NSMCE3 and NSMCE4a protein by western blotting (Figure 3.4 A). The FRT-inserted NSMCE4a and NSMCE3 respectively, can be distinguished from the endogenous gene due to the presence of the tag, which results in a slower migrating band. The endogenous NSMCE3 runs around 35 kDa, whereas the 10xHis-Flag can be seen at a slightly higher molecular weight (Figure 3.4 A, lower panel, red arrow). Similarly, the endogenous NSMCE4a runs at 55 kDa and the Strep-6xHis NSMCE4a is above (Figure 3.4 A, upper panel, red arrow). To further confirm that the observed upshift is indeed the

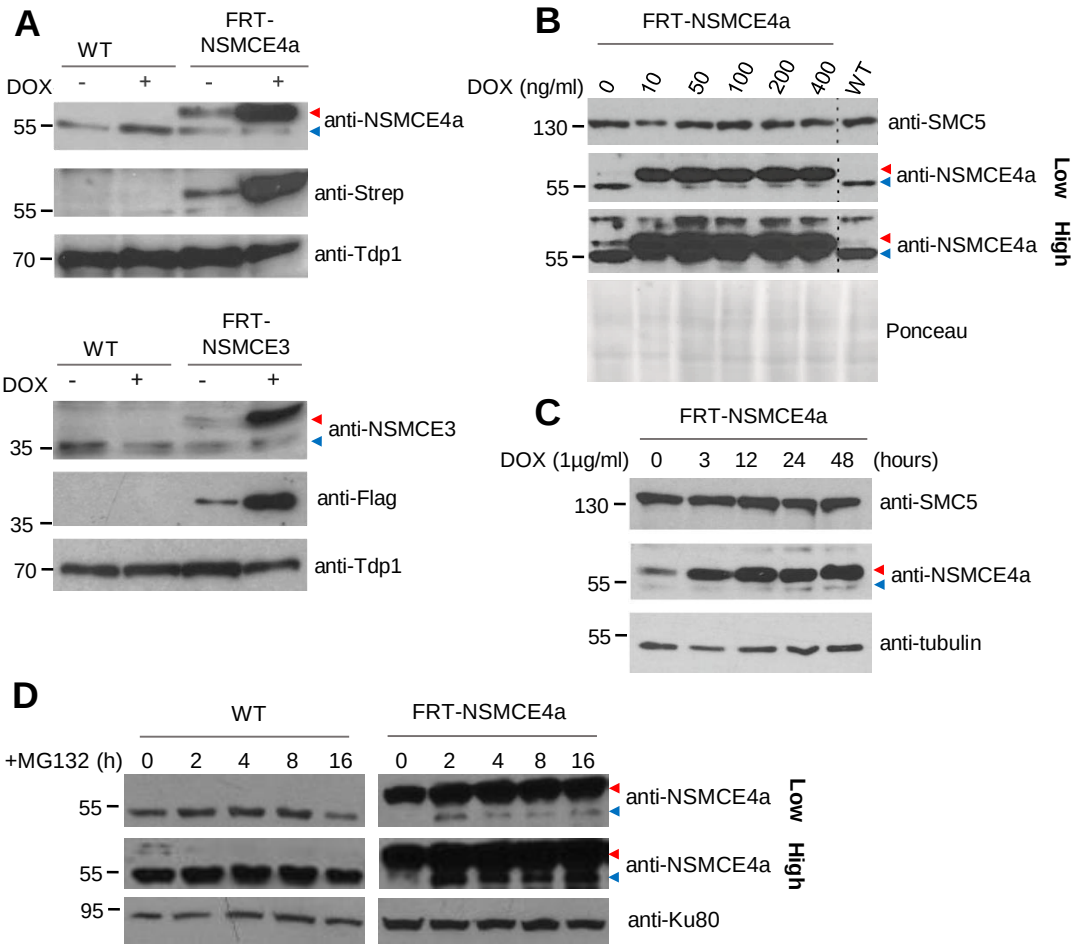


Figure 3.4: Generation and initial characterisation of stable NSMCE4a and NSMCE3 Flp-In T-REx 293 cell lines

A. Western blot showing stable integration of Strep-His tagged NSMCE4a (FRT-NSMCE4a) and his-Flag tagged NSMCE3 (FRT-NSMCE3) in pcDNA5/FRT/TO vector via the Flp-FRT recombination, DOX +: cells grown for 24 hours with media containing 1 µg/ml Doxycycline, anti-Tdp1 is a loading control; western blot performed by Owen Wells. **B.** Titration of Doxycycline in FRT-NSMCE4a cell line does not result in proportional increase in protein levels of NSMCE4a and does not lead to increase in protein levels of SMC5, cells were grown in media containing 10 µl/ml Blasticidin, indicated concentrations of Doxycycline were added 24 hours before cells were harvested for western blot. **C.** Kinetics of the ectopic NSMCE4a induction by Doxycycline, 1 µg/ml Doxycycline was added to cell culture, cells were collected for western blot analysis at 0, 3, 12, 24 and 48 hours after Doxycycline addition. **D.** Proteasome inhibition (+MG132) restores protein levels of endogenous NSMCE4a, cells were grown for 2 days in the presence of 10 ng/ml Doxycycline before addition of 10µM MG132, time point 0 represents DMSO treated control. **A – D.** Flp-In T-REx 293 host cell line (WT) is a control with no regulatable FRT-inserted gene, red arrow indicates the FRT-inserted tagged subunit, blue arrow indicates the endogenous subunit, High indicates higher exposure time, Low indicates shorter exposure time, tubulin and Ku80 are loading controls.

FRT-inserted gene, the membrane was probed with antibody recognizing Flag (Sigma, F3165, 1:3000) in case of NSMCE3, and Strep (QIAGEN, 34850, 1:5000) in case of NSMCE4a (Figure 3.4 A). The band observed after probing the membrane with anti-Strep has the same size as the band on a membrane probed with anti-NSMCE4a (Figure 3.4 A, upper panel). Similarly, the band size after probing with anti-Flag corresponds the size of endogenous NSMCE3 (Figure 3.4 A, lower panel). This confirms that we have successfully created the cell lines stably expressing FRT-inserted NSMCE4a and NSMCE3 ectopic genes.

3.3.2.3 Characterisation of inducibility of the T-REx Flp-In system

As both NSMCE3 and NSMCE4a are likely to be essential in human cells, we selected the clones that displayed similar-to-endogenous levels of the FRT-inserted subunits (Figure 3.4 A, lane 3). This would prevent the potential non-viability of the cells after the CRISPR/Cas9 mediated knock out of the endogenous subunit. The observed levels of the inserted subunits in the absence of Tetracycline might be caused leakiness of the Tet inducible promoter, or due to the presence of residual Tetracycline in normal foetal calf serum. Inducibility of the system was tested by addition of Doxycycline (1 µg/ml) to the media for 24 hours. The increase in protein levels of FRT-inserted subunits demonstrates that the expression of FRT-integrated NSMCE4a and NSMCE3 can be induced by addition of Doxycycline (Figure 3.4 A, lane 4). Together, the western blot data demonstrate the successful generation of stable and inducible T-Rex Flp-In NSMCE3 (FRT-NSMCE3) and T-Rex Flp-In NSMCE4a (FRT-NSMCE4a) cell lines.

Next, we tested whether the protein level of FRT-integrated subunits could be regulated by Doxycycline titration; the expression of the NSMCE4a was induced using a range of Doxycycline concentrations for 24 hours (Figure 3.4 B). However, the protein levels of the FRT-integrated NSMCE4a tested range 10 – 400 ng/ml, were approximately similar. These results suggest that the Tetracycline regulatable promoter can only be used as an ON/OFF system, but does not allow fine regulation of the protein levels. Our observations are similar to the results of a recent study by Szczesny et al., 2018, using the same Flp-In T-REx system. The induction of a gene expression by different concentration of Doxycycline ranging from 5 – 50 ng/ml, did not result in different protein levels of genes of interest in Flp-In T-REx 293 cell lines (Szczesny et al., 2018). Furthermore, overexpression of NSMCE4a did not lead to a proportional increase in protein levels of

the other components of the SMC5/6 complex, demonstrated by probing with anti-SMC5 antibody (Figure 3.4 B, top panel).

Next, we wanted to assess the kinetics of the ectopic NSMCE4a expression. Therefore, expression of the ectopic NSMCE4a in the FRT-NSMCE4a cell line was induced by addition of 1 µg/ml of Doxycycline to the growth media. Cells were collected for western blot analysis 3, 12, 24 and 48 hours after Doxycycline addition. Whole cell extracts were probed for NSMCE4a and SMC5 (Figure 3.4 C). Rapid induction of the ectopic NSMCE4a was observed already 3 hours after Doxycycline addition and reached its maximum level by 12 hours (Figure 3.4 C, lane 2, 3). No further increase in protein levels of the ectopic NSMCE4a was observed after time point 12 hours (Figure 3.4 C, lane 4, 5) and similarly to our previous observations (Figure 3.4 B), did not lead to proportional increase in protein levels of SMC5 (Figure 3.4 C, upper panel).

Interestingly, overexpression of NSMCE4a by Doxycycline induction in the FRT-NSMCE4a cell line, led to a decrease of protein levels of the endogenous NSMCE4a (Figure 3.4 B, blue arrow). To determine whether this downregulation of endogenous NSMCE4a is at the protein or mRNA level, NSMCE4a overexpression was induced with 1 µg/ml of Doxycycline for 24 hours and degradation by the proteasome was inhibited by addition of 10µM MG132. 2 hours after proteasome inhibition, a restoration of protein levels of the endogenous NSMCE4a was observed (Figure 3.4 D). This suggests that the decrease in endogenous NSMCE4a is caused by proteasomal degradation. Upon induction (+ Doxycycline), both the endogenous and the ectopic NSMCE4a are being targeted for proteasomal degradation. However, the levels of endogenous NSMCE4a are much lower in comparison to the induced ectopic NSMCE4a. Therefore, the decrease in protein levels is only apparent for the endogenous NSMCE4a. Together, our results indicate that the observed regulation of NSMCE4a happens at the protein level and that the NSMCE4a is likely targeted for degradation unless stably incorporated into the SMC5/6 complex.

3.3.3 CRISPR/Cas9 knock out of the endogenous NSMCE3 gene

After having successfully created the stable and inducible T-REx Flp-In NSMCE3 cell line, the next step was to generate a functional knock out of the endogenous NSMCE3 gene. Firstly, the Cas9 vector carrying the guide RNA targeting the endogenous NSMCE3

gene was constructed. The guide RNA sequence for NSMCE3 was chosen from the GenScript guide RNA database. The NSMCE3 gene has only one exon and one splice variant that encodes a 304 amino acid protein. The chosen guide RNA (GenScript, crRNA2) targets the 719 to 738 nucleotide of the translated sequence of the NSMCE3 exon. The guide RNA was inserted into the pX459 Cas9 vector as described in Materials and Methods.

T-REx Flp-In NSMCE3 cells were transfected with 1 µg pX459 containing NSMCE3 single guide RNA (sgRNA). After 48 hours the transfected cells were selected for the presence of pX459 plasmid using 1 µg/ml Puromycin for four days. Media containing Puromycin was removed and replaced with fresh media without Puromycin to lower the probability of the pX459 vector randomly integrating into the genome. Cells were grown until macroscopic colonies were formed. From each round of CRISPR/Cas9 transfection, approximately 50 single clones were screened using the surveyor assay, the principal of which is illustrated in Figure 3.5 A. Briefly, the DNA region targeted by the sgRNA is amplified by PCR on genomic DNA. The PCR product of a suspected CRISPR/Cas9 clone is annealed together with a PCR product of a non-transfected isogenic cell line. If the screened clone contains CRISPR/Cas9 mediated insertion/deletion in the target DNA fragment, it will result in a mismatch in the heteroduplex of the wild type and the CRISPR/Cas9 modified DNA. The mismatch can be recognised and cleaved by a structure specific endonuclease, and visualised by separation on an agarose gel.

In order to check the efficiency of the guide RNA, the surveyor assay was performed on the genomic DNA isolated from the population of CRISPR/Cas9 transfected cells. The DNA fragment amplified by SurFwd1_Nse3 and SurRev1_Nse3 primers has expected size of 676 bp, which is observed in the empty vector transfected control (Figure 3.5 B, lane 1, +EV). There are two bands between 300 and 500 bp in the lane containing genomic DNA from population transfected with the sgRNA-Cas9 vector (Figure 3.5 B, lane 2, +pX459). This indicates the cut by the T7-endonuclease validating the efficiency of the CRISPR/Cas9 together with designed guide RNA and confirms that the sgRNA correctly recognised the NSMCE3 exon.

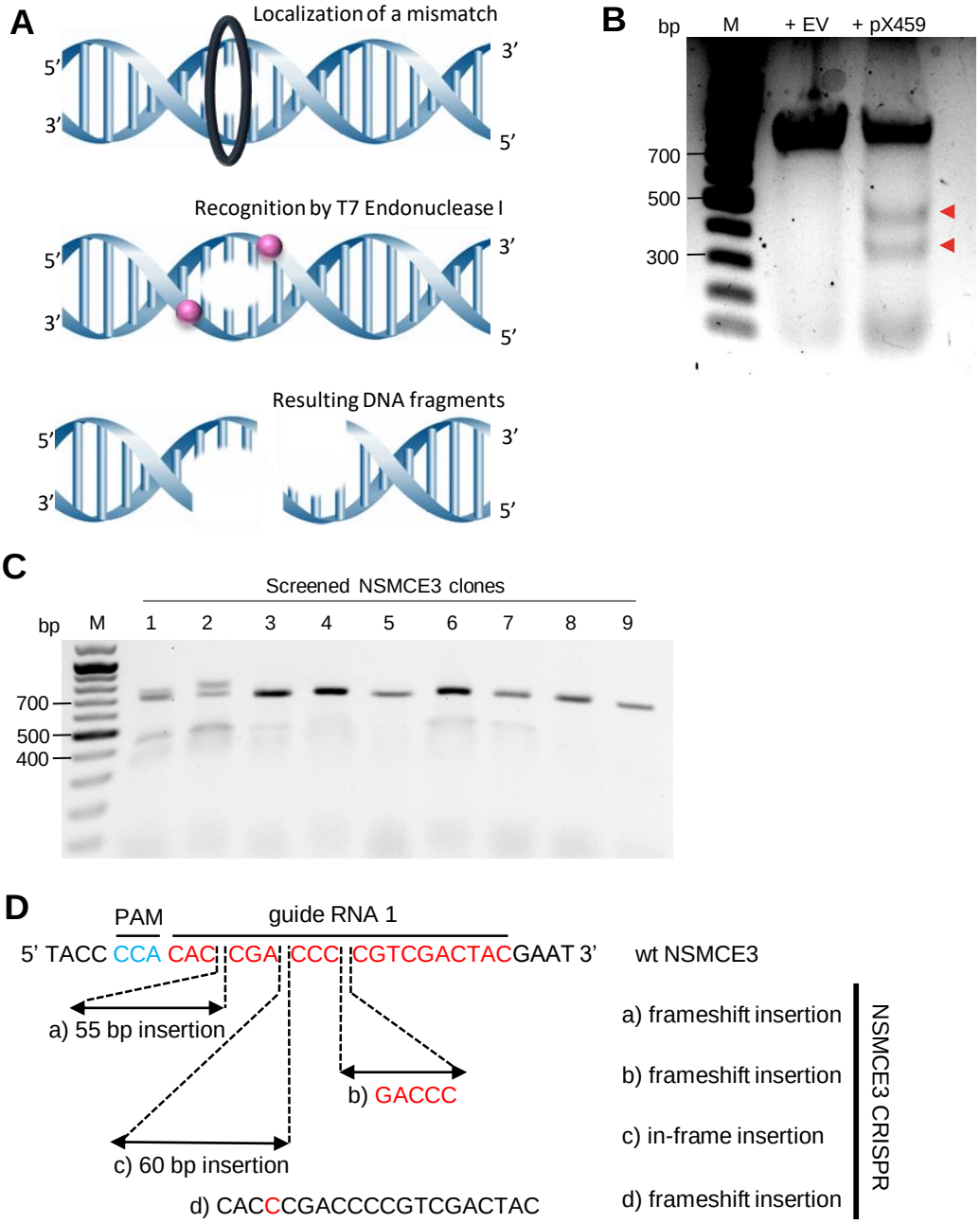


Figure 3.5: Generation of NSMCE3 T-REx Flp-In 293 knock out cell line
A. Illustration of the principle of surveyor assay; CRISPR/Cas9 mediated cut results in a mismatch between the heteroduplex of a control DNA and the CRISPR/Cas9 modified DNA, the mismatch is detected and cleaved at both sites by of the mismatch by T7 Endonuclease I; cleaved DNA fragments can be visualised on agarose gels. **B.** Surveyor assay on DNA isolated from cell population transfected either with empty vector (+EV) or Cas9 vector containing guide RNA sequence targeting endogenous NSMCE3 (+pX459). PCR products on genomic DNA using Nse3_sur_fwd together with Nse3_sur_rev primers separated on 1% agarose gel, the resulting cuts (red arrows) confirm the efficiency of the used guide RNA. **C.** Example of Surveyor assay on screened NSMCE3 clones after transfection with the guide RNA containing Cas9 vector. **D**. Schematic illustration of different mutations generated after first round of CRISPR, sequence targeted by the guide RNA is in red, PAM sequence is in blue, red italics indicated base insertions.

After validating the efficiency of the sgRNA, each viable CRISPR/Cas9 single clone was screened using the surveyor assay on genomic DNA. Figure 3.5 C shows an example of NSMCE3 CRISPR/Cas9 clones screening. The clones with the presence of two lower bands around 400 bp were further characterised (Figure 3.5 C, lane 1 and 2).

Since the outcome of the Cas9 cut might result in different mutations in each allele of the targeted gene, TOPO-TA cloning was performed prior to sequencing. In principal, TOPO-TA cloning is an insertion of single PCR fragment with poly A-overhangs directly into a sequencing vector. Sequencing results of selected knock out clones showed different frame-shift and in-frame insertions in the proximity of the PAM sequence (Figure 3.5 C), however, the wild-type NSMCE3 allele was still present. To rule out that a functional part of the pX459 vector was inserted around the PAM sequence, we performed an alignment of the inserted sequences to the pX459 vector. No significant similarity was found. Together, the results show that the first round of CRISPR/Cas9 transfection resulted in generation of a heterozygous NSMCE3 knock out.

In order to get the full NSMCE3 knock out, the heterozygous NSMCE3 knock out cell line (N3KO1) was subjected to a second round of CRISPR/Cas9 using a new guide RNA. The second guide RNA sequence was chosen from the GenScript guide RNA database and inserted into the pX459 vector similarly to the first CRISPR/Cas9 round (described above). The second CRISPR guide RNA (GenScript, crRNA1) targets nucleotides 404 to 424 of the only NSMCE3 exon. Transfection of the second guide into the N3KO1 cell line led to generation of cell lines that, after TOPO-TA cloning and sequencing, did not show any wild type allele. However, when these suspected knock out clones were further tested, they were not viable. Since these clones contain the stably expressed FRT-10xHis-Flag-NSMCE3, the most likely explanation for the non-viability is that the 10xHis-Flag N-terminal tag on ectopic NSMCE3 compromises its function. Hence, upon the full knock out of the endogenous NSMCE3, the cells have no functional of NSMCE3, and this is lethal.

3.3.4 CRISPR/Cas9 knock out of the endogenous NSMCE4a gene

NSMCE4a knock out was also performed; the NSMCE4a gene has eleven exons and eleven splice variants, only two of them being protein coding. The first isoform encodes a 385 amino acid protein (NSMCE4A-202) is the canonical isoform, the second one is

only 316 amino acids long protein (NSMCE4A-201). The guide RNA sequence for NSMCE4a was chosen from the GenScript guide RNA database and targets exon 2 of both NSMCE4a isoforms. Guide RNA was inserted into the pX330 Cas9 vector as described in Materials and Methods. 2 µg of the created pX330 vector containing the NSMCE4a gRNA was co-transfected with a pCD2E selection vector, containing G418 resistance cassette, in 3:1 ratio into the FRT-NSMCE4a cell line. Two days after transfection, the cells were washed in PBS and split into 150 mm dishes (Corning) containing media with G418 (800 µg/ml) until macroscopic colonies had formed. To estimate the transfection efficiency, a GFP containing vector (Tdp1-GFP) was transfected into the FRT-NSMCE4a cell line in parallel with the sgRNA-NSMCE4a containing Cas9 plasmid. Western blot analysis showed the Tdp1-GFP to be expressed (Figure 3.6 A), confirming the efficiency of the transfection. In order to check the efficiency of the guide RNA and Cas9 cleavage, western blot on the whole population of CRISPR/Cas9 transfected cells was performed. Probing with the NSMCE4a antibody showed a decrease in protein levels of the endogenous NSMCE4a in the population transfected with the Cas9 plasmid containing sgRNA-NSMCE4a (Figure 3.6 A, lane 1, blue arrow). In contrast, no decrease of the endogenous NSMCE4a was observed in the Tdp1-GFP transfected cells. The result confirms that the guide RNA successfully targets the endogenous NSMCE4a gene. In each round of CRISPR/Cas9 transfection approximately 50 single clones were screened by western blotting. During the first round of screening, a single clone was identified, where band corresponding to the endogenous NSMCE4a size was absent (Figure 3.6 B, lane 2). The clone was picked to be further characterised to confirm full NSMCE4a knock out.

Genomic DNA was isolated from the suspected NSMCE4a knock out clone and PCR was performed using Nse4 2nd fwd ab1 and Nse4 2nd rev ab1 primer (Table 2.2). This resulted in a 532 bp fragment flanking the guide RNA target sequence. The amplified fragment was cloned into a TOPO-TA vector and sequenced. The sequencing results of selected TOPO-clones showed two insertions in proximity of the PAM sequence (Figure 3.6 C). In order to trace the origin of the insertions, both of them were blasted against the human genome using *Homo sapiens* (human) BLASTN 2.9.0 + program (Zhang et al., 2000) and aligned to pX330 Cas9 expression plasmid. First 135 bp insertion fragment was aligned to the pX330 and no significant similarity was found.

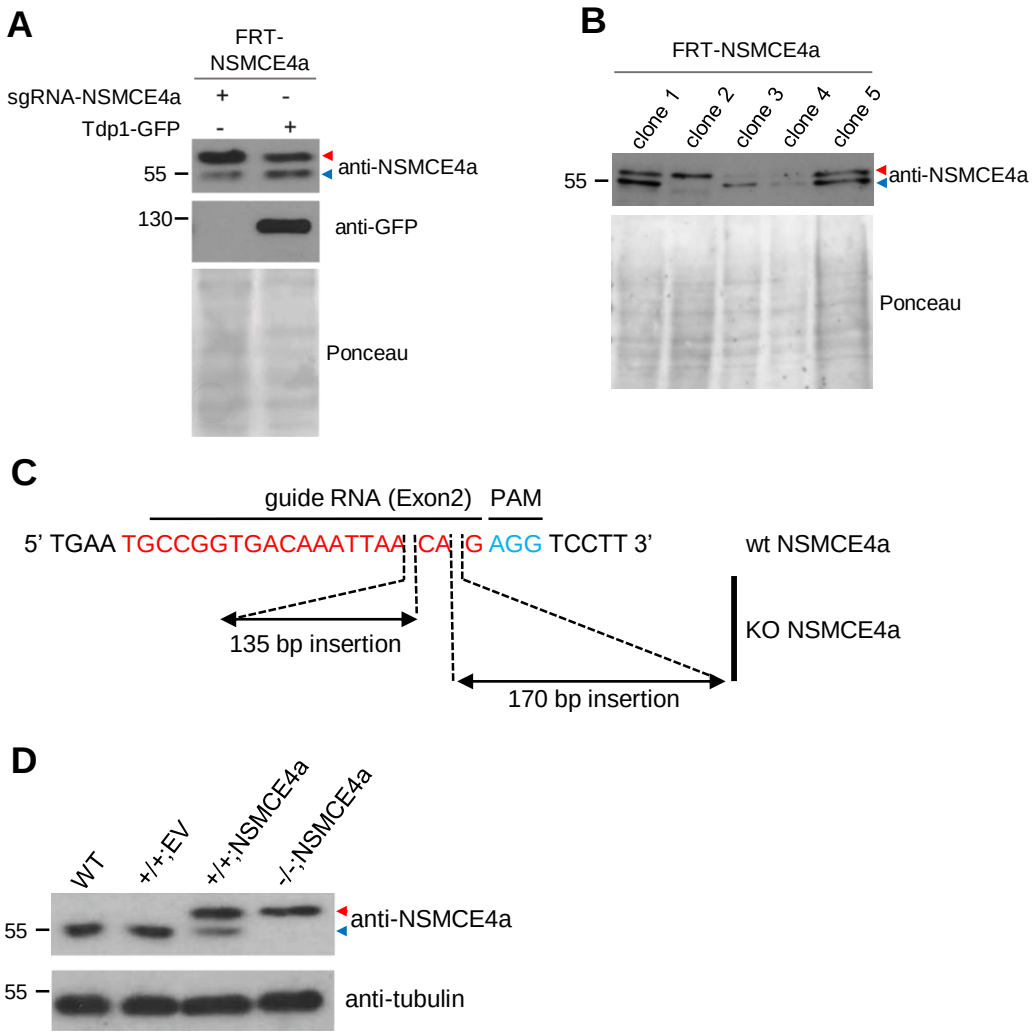


Figure 3.6: Generation of NSMCE4a T-REx Flp-In 293 knock out cell line
A. Western blot on whole cell extract from population transfected by either pX330 containing NSMCE4a guide RNA (sgRNA-NSMCE4a) or control vector containing GFP (Tdp1-GFP), Ponceau stain serves as a loading control. **B.** Example of western blot of initial screening for NSMCE4a knock out, clone 2 lacks the band in the size of endogenous NSMCE4a, blue arrow indicates the endogenous protein, red arrow the FRT-inserted NSMCE4a-Strep-6xHis. **C.** Illustration of NSMCE4a CRISPR/Cas9 mediated knock out cell line after guide RNA transfection; sequencing results showed two insertions, a 135 bp insertion generating frameshift and stop codon resulting in 14.5 kDa NSMCE4a truncation and a 170 bp insertion generating frameshift and 15 kDa NSMCE4a truncation and no wild type allele. **D.** Western blot showing generated cell lines; legend: WT: T-REx Flp-In 293, +/+;EV: FRT-inserted empty vector in T-REx Flp-In 293, +/+;NSMCE4a: FRT-inserted NSMCE4a-Strep-6xHis in T-REx Flp-In 293, -/-;NSMCE4a: +/+;NSMCE4a cell line with endogenous NSMCE4a knock out.

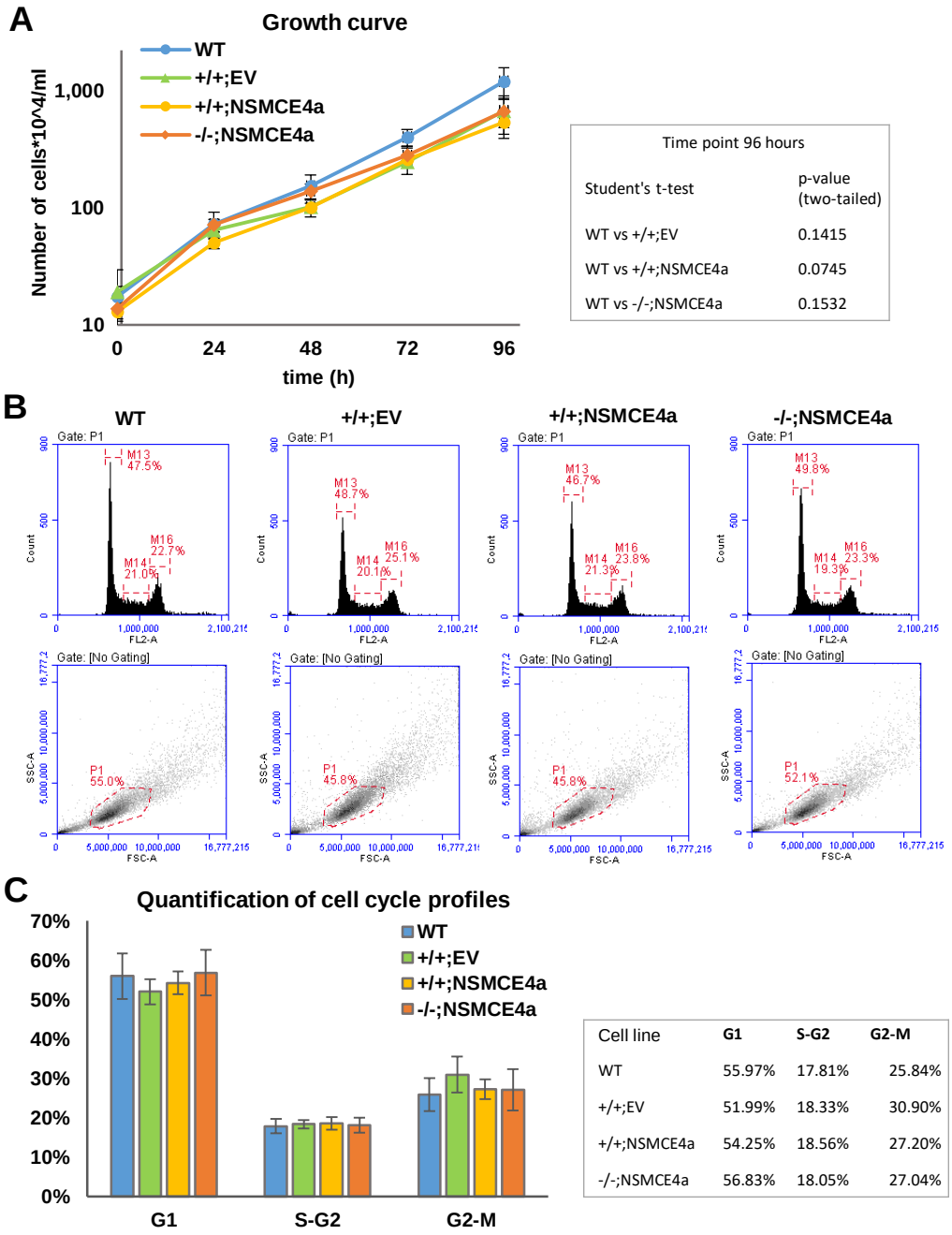
When the same 135 bp sequence was blasted against the human genome, a 41 bp insertion matched a sequence found on chromosome 19. The second insertion was a 170 bp insertion. The first 122 bp matches a fragment of the Cas9 gene, thus most likely originates from the pX330 vector. The last 50 bp aligns to a sequence on chromosome 12. The first 135 bp insertion creates frameshift generating 14.5 kDa NSMCE4a truncation. The second 170 bp insertion generates a 15 kDa truncation of NSMCE4a. Together, the western blot screening and sequencing results indicate no presence of a wild type NSMCE4a allele. The created knock out cell line was designated -/-;NSMCE4a.

3.3.5 Characterisation of the constructed T-REx Flp-In 293 cell lines

To assess the functionality of the tagged NSMCE4a (NSMCE4a-Strep-6xHis), as well as the overall viability of the created Flp-In T-REx-293 cell lines, we monitored the cell growth over 4 days. The growth curve shows that insertion of both empty and NSMCE4a containing pcDNA5/FRT/TO results in moderate slow growth phenotype (Figure 3.7 A). To check whether the insertion of either empty vector/tagged NSMCE4a at the FRT site influences the overall cell cycle distribution in the created cell lines, the cell cycle profiles analysis was performed. The DNA was stained using propidium iodide and cells were manually gated at G1, S and G2-M (Figure 3.7 B). The percentage of cells in different phases of the cell cycle for each cell line separately was calculated from the flow cytometry profiles and quantified (Figure 3.7 C). Our data does not show any significant difference in cell cycle phase distributions within the created cell lines. Importantly, the -/-;NSMCE4a cell line does not show any growth defect in comparison to +/+;NSMCE4a cell line, which indicates that the ectopic NSMCE4a-Strep-6xHis is functional.

3.3.5.1 Doxycycline mediated induction of the ectopic NSMCE4a does not decrease viability of FRT-NSMCE4a cell lines

Previous studies in yeast showed that overexpression of wild type or mutant Smc6 gene leads to cell cycle arrest and gross structural changes in the nucleus (Harvey et al., 2004). To explore the possibility that overexpression of NSMCE4a can be toxic to the human Flp-In T-REx 293 cells, clonogenics viability after NSMCE4a overexpression was performed. The overexpression of NSMCE4a-Step-6xHis was induced for 3 days before plating the cells for viability assay.



Cell line	G1	S-G2	G2-M
WT	55.97%	17.81%	25.84%
+/+;EV	51.99%	18.33%	30.90%
+/+;NSMCE4a	54.25%	18.56%	27.20%
-/-;NSMCE4a	56.83%	18.05%	27.04%

Figure 3.7: Characterisation of created NSMCE4a T-REx Flp-In 293 cell lines
A. Insertion of NSMCE4a or empty pcDNA5/FRT/TO vector, or NSMCE4a knock out does not result in significant growth defect. Growth curve shows number of cells counted at indicated time points, error bars represent standard deviation of three independent experiments. For time point 96 hours, two-tailed Student's t-test was performed to calculate statistical significance, p-values are displayed in the table. **B.** Example of flow cytometry profiles of created cell lines, graphs show gated population for cells with normal circularity and granularity, quantification of each cell cycle phase was done by manual gating. **C.** Quantification of percentage of cells in different phases of the cell cycle, WT: T-REx Flp-In 293, +/+;EV: FRT-inserted empty vector in T-REx Flp-In 293, +/+;NSMCE4a: FRT-inserted NSMCE4a-Strep-6xHis in T-REx Flp-In 293, -/-;NSMCE4a: +/+;NSMCE4a cell line with endogenous NSMCE4a knock out, error bars show +/- standard deviation of 6 independent experiments, the averaged value are displayed in the table.

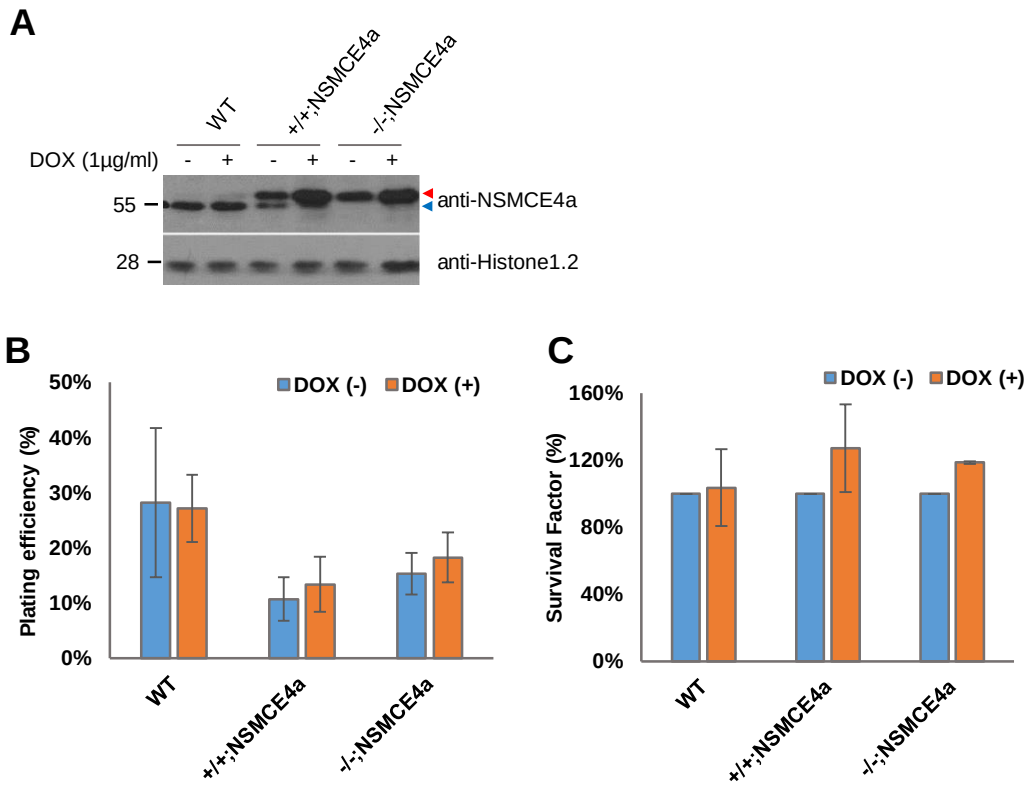


Figure 3.8: Overexpression of ectopic NSMCE4a does not decrease cell viability
A. Example of a western blot showing protein levels of NSMCE4a in different cell lines after (1 µg/ml) Doxycycline induction, blue arrow indicates the endogenous NSMCE4a, red arrow the FRT-inserted NSMCE4a-Strep-6xHis, Histone 1.2 is a loading control. **B.** Plating efficiency of cells grown for 3 days before experiment in media without Doxycycline (DOX (-)) or media containing 1 µg/ml Doxycycline (DOX (+)), plating efficiency was calculated as (number of cells counted)/(number of cells plated), error bars represent +/- standard deviation of three independent experiments. **C.** Doxycycline triggered overexpression of NSMCE4a-Strep-6xHis does not decrease cell survival, cells were grown for 3 days in media containing 1 µg/ml Doxycycline before being plated in 10 cm dishes, error bars represent +/- standard deviation of three independent experiments. **A - C.** WT: T-REx Flp-In 293 cell line, +/+;NSMCE4a: FRT-inserted NSMCE4a-Strep-6xHis in T-REx Flp-In 293, -/-;NSMCE4a: +/+;NSMCE4a cell line with endogenous NSMCE4a knock out.

Protein levels of NSMCE4a on the day of experiment showed that the inducible NSMCE4a-Strep-6xHis transgene was successfully overexpressed (Figure 3.8 A). Plating efficiency showed that both created FRT-NSMCE4a cell lines have slightly decreased viability than the parental T-REx Flp-In 293 cell line (Figure 3.8 B). Surprisingly, the survival of both +/+;NSMCE4a and -/-;NSMCE4a cell line increased after Doxycycline induced overexpression. Our results argue that overexpression of NSMCE4a-Strep-6xHis in the Flp-In T-REx 293 cell line does not lead to lethality.

3.3.6 Validation of the NSMCE4a knock out cell line by Flp back- transfection

The -/-;NSMCE4a cell line was further validated for full NSMCE4a knock out by back transfection of the Flp expression vector (pOGG44). The rationale for this experiment is the Flp mediated recombination between the two FRT sites, flanking the pcDNA5/FRT/TO vector insert, will lead to its loss. Cells that have lost the whole insert will lose Hygromycin resistance and gain Zeocin resistance (Figure 3.9 A). Viable Zeocin resistant cells would indicate that the NSMCE4a truncation formed by the frameshift mutations in the -/-;NSMCE4a knock out cell line is viable. If cells are not viable, it indicates that the NSMCE4a is an essential gene.

The Flp expression plasmid (pOG44) was transfected into cell lines containing either empty pcDNA5/FRT/TO (+/+;EV) or pcDNA5/FRT/TO with NSMCE4a (+/+;NSMCE4a). Two days after transfection, 10 000 cells were plated in triplicates into 10 cm plates with media containing Zeocin. Cells were allowed to form macroscopic colonies for 10 – 12 days, after which the number of colonies per plate was scored. The results of the Flp back-transfection assay showed that 16 to 19% of the +/+;EV and the +/+;NSMCE4a cells successfully lost the pcDNA5/FRT/TO and gained Zeocin resistance (Figure 3.9 B). In contrast, the loss of FRT-inserted NSMCE4a gene in the -/-;NSMCE4a cell line, led to complete lethality. These results show that i) FRT-inserted NSMCE4a gene is the only functional NSMCE4a copy in the knock out cell line and ii) NSMCE4a is an essential gene in human Flp-In T-REx-293 cell line.

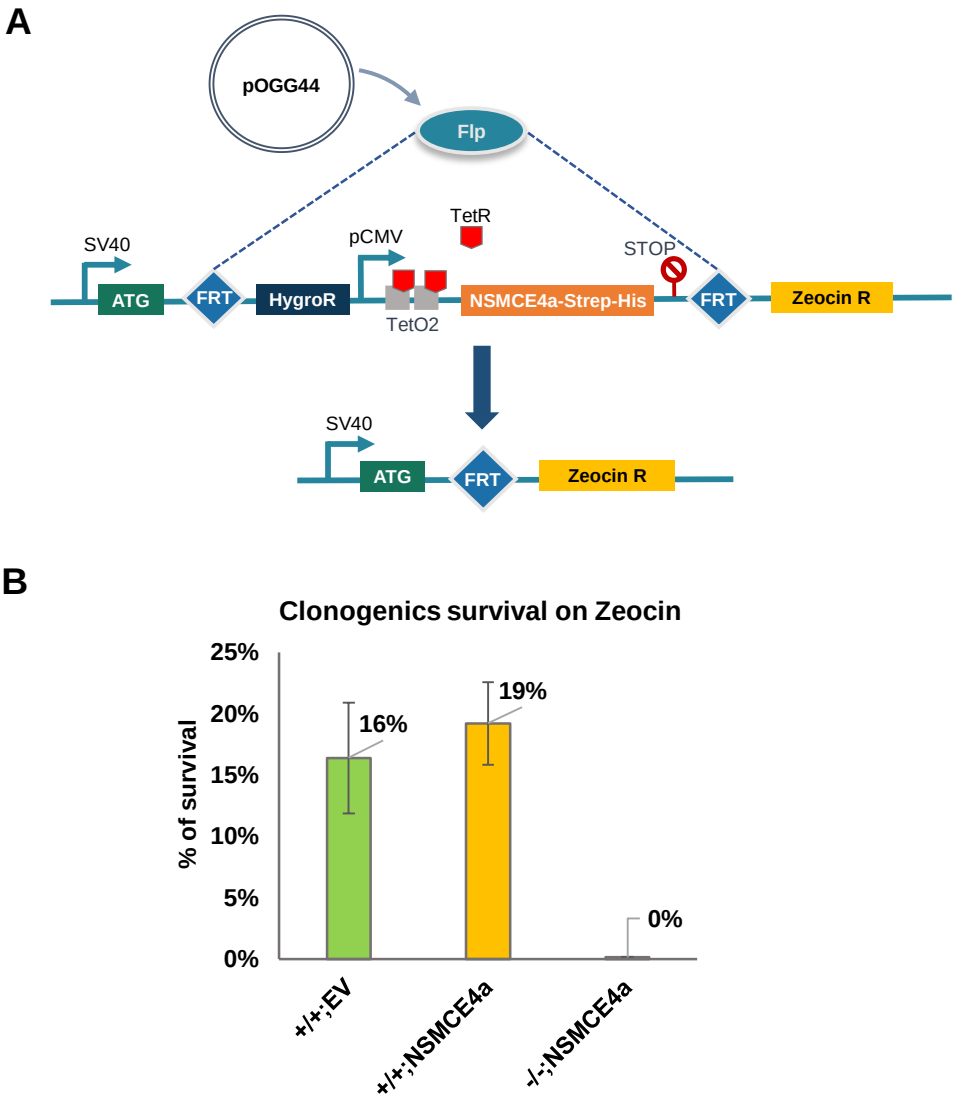


Figure 3.9: FRT-NSMCE4a-Strep-6xHis is the only functional copy in the T-REx Flp-In 293 knock out cell line and is essential for cell survival
A. Diagram of Flp-out experiment; Flp expressed from pOGG44 vector catalyses recombination between the FRT sites, which leads to loss of the inserted FRT vector and gain of Zeocin resistance **B.** Flip out of the last functional NSMCE4a copy is lethal. Clonogenics viability assay after back-transfection of Flp expression vector and selection on Zeocin; cell lines key: +/+;EV: FRT-inserted empty vector in T-REx Flp-In 293, +/+;NSMCE4a: FRT-inserted NSMCE4a-Strep-6xHis in T-REx Flp-In 293, -/-;NSMCE4a: +/+;NSMCE4a cell line with endogenous NSMCE4a knock out, error bars represent +/- standard deviation of three independent experiments.

3.4 Discussion

In this chapter, stable integration and regulation of the NSMCE4a and NSMCE3 genes using the Flp-In T-REx host cell line has been described. The NSMCE4a cell lines created by insertion of FRT-expression vector showed mild slow growth phenotype. However, the slow growth phenotype did not depend on the presence of gene of interest in the FRT-expression vector. During the generation of the Flp-In T-REx host cell line, the target site vector (pFRT/lacZeo) was randomly inserted into the genome at a single site. Hence, Flp mediated insertion of the FRT-expression vector could affect expression or regulation of a housekeeping gene, causing the mild growth defect. Whilst there is a mild slow growth phenotype of the created cell lines, there is no significant difference in the cell cycle distribution within the tested cell lines. The created Flp-In T-REx cell lines are inducible by Doxycycline, but the levels of induction cannot be regulated by Doxycycline titration. Hence, the Flp-In T-REx system is not well suited to study the effect of differential levels of a protein of interest.

Upon overexpression of the inducible NSMCE4a, we observed a downregulation of the endogenous NSMCE4a. Inhibition of proteasomal degradation lead to restoration of protein levels of the endogenous NSMCE4a, which indicates that this regulation of expression occurs at the protein level. This points towards a cellular mechanism, which dynamically and strictly regulates the protein levels in the cell. Our findings are in accordance with the recent study utilizing high-throughput proteomics, which revealed that subunits of protein complexes tightly maintain their abundance post-transcriptionally (Roumeliotis et al., 2017).

Our attempts to generate the NSMCE3 knock out cell line repeatedly failed; despite the fact that the guide RNA was shown to be efficient. More than two clones generated in two independent CRISPR screens, in which no endogenous NSMCE3 allele was detected by TOPO-TA/sequencing, were not viable. The reason why the NSMCE3 knock out failed, could be that the FRT-inserted NSMCE3 gene had an N-terminal 10xHis-Flag tag, which could compromise the protein function or folding. To test this theory creating an untagged NSMCE3 stable cell line could have been an option. If the endogenous NSMCE3 could then be targeted, the study of different mutations within the NSMCE3 gene would have been attainable. However, due to time constraints, and the fact that an

NSMCE4 knock out cell line had been established, it was decided to focus on the NSMCE4a project.

Successful knock out of the endogenous NSMCE4a in the FRT-NSMCE4a cell line was achieved. TOPO-TA cloning and sequencing, together with back transfection of the Flp-recombinase confirmed that FRT-inserted NSMCE4a is the only functional NSMCE4a gene in the knock out cell line. Therefore the ectopic, epitope tagged NSMCE4a likely integrates within and forms a functional SMC5/6 complex. Furthermore, this chapter shows that the loss of FRT-inserted NSMCE4a in the NSMCE4a knock out cell line is lethal. These results confirm that NSMCE4a is an essential gene in human cells.

The Flp-In T-REx 293 cell lines can be utilised for versatile insertions of gene of interest. Once the wild type subunit of the SMC5/6 complex is inserted, the stably inserted gene can be simply exchanged for a new mutated or tagged version. This can be simply done by changing the resistance cassette in the FRT-expression vector, cloning in the mutated gene of interest and co-transfection with the Flp-recombinase plasmid. The system can be used to create cell lines carrying known or predicted mutations in the SMC5/6, such as the patient mutation in the NSMCE3 gene, or predicted mutations in the NSMCE4a gene, or the SMC6 separation of function mutations.

4 Chapter 4

Results II

Affinity purification of NSMCE4a and mass spectrometry analysis of SMC5/6 protein interactors

4.1 Introduction

Previous chapter described the successful creation of a T-REx Flp-In 293 cell line, with the only functional NSMCE4a being the FRT-inserted NSMCE4a-Strep-6xHis. We aimed to take advantage of the affinity tags to map the interactors of the SMC5/6 complex using affinity purification coupled with mass spectrometry (AP-MS) analysis. Identification of the SMC5/6 interactors could add to our understanding of its enigmatic role in the cell and involvement in different cellular pathways. However, purification of the SMC5/6 complex is challenging due to its large size and relatively low abundance. The advantage of the created -/-;NSMCE4a cell line for interaction studies is that the protein levels of the ectopic NSMCE4a-Strep-6xHis are close to the endogenous NSMCE4a even in the absence of Doxycycline (Chapter 3). Thus, the system should not be biased by overexpression of the bait protein, which might bring artificial interactors. Another advantage of the system is the presence of the double tag on the NSMCE4a, which allows one-step or two-step affinity purification. In comparison to immunoprecipitation (IP) using a specific antibody to that recognised an epitope on the protein of interest, affinity purification provide a cheaper, less biased and more efficient way of purifying the protein of interest. The affinity tag could impact the NSMCE4a protein functionality. However, the growth curve, flow cytometry analysis and Flp-back transfection experiments (Chapter 3, Figure 3.6 and 3.7) suggest that the Strep-6xHis tag on the ectopic NSMCE4a does not interfere with its function. Since the ectopic NSMCE4a has two affinity tags, 6xHis and Strep, the aim was to optimise the protocol for affinity purification of the SMC5/6 complex using either one or both tags. Previous attempts to purify and search for SMC5/6 interactors were limited by the availability of the SMC5/6 antibodies used for immunoprecipitation, as well as much less available algorithms and platforms for analysis of mass spectrometry data (Taylor et al., 2008).

4.2 Aims

i. Use created isogenic T-REx Flp-In cell lines to affinity purify the human SMC5/6 complex
ii. Use affinity purification coupled with mass spectrometry to identify interactors of the human SMC5/6 complex

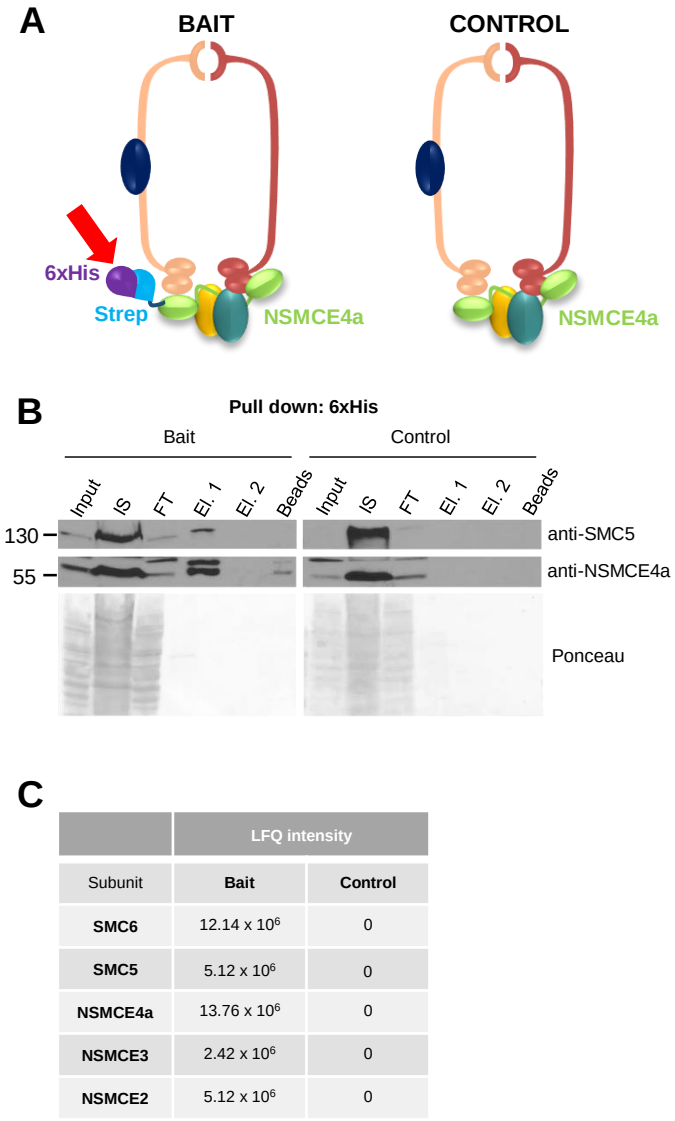
4.3 Results

4.3.1 Affinity purification of NSMCE4a coupled with mass spectrometry identifies all the SMC5/6 complex subunits

Results in Chapter 3 showed that the -/-;NSMCE4a cell line, where the only functional NSMCE4a is the FRT-inserted C-terminally tagged NSMCE4a, is viable and loses its viability after additional loss of the ectopic NSMCE4a copy (Figure 3.9 B). Therefore, ectopic NSMCE4a-Strep-6xHis is likely to form a functional part of the SMC5/6 complex. Initially, we wanted to test whether we are able to purify the whole SMC5/6 complex using the C-terminal tag on the NSMCE4a subunit. The experimental setup was to use the NSMCE4a knock out cell line containing ectopic FRT-inserted NSMCE4a-Strep-6xHis, as a bait and the isogenic T-REx Flp-In 293 cell line as a control for unspecific binding of the SMC5/6 to the beads (Figure 4.1 A). The bait cell line contains only the ectopic NSMCE4a-Strep-6xHis gene copy, which is expressed from the tetracycline inducible CMV promoter. The protein levels of the ectopic NSMCE4a in the created -/-;NSMCE4a cell line were close to endogenous NSMCE4a, even without Doxycycline addition (Figure 3.6 D, lane 1 and 4). Therefore, for affinity purification experiments, the NSMCE4a expression was not induced by Doxycycline. Throughout this chapter the cell line is going to be annotated as the bait and the T-REx Flp-In 293 cell line as the control.

4.3.1.1 Recovery of SMC5 by affinity purification of NSMCE4a-Strep-6xHis by immobilised metal affinity chromatography (IMAC).

Previous experiments performed in the lab reported that recovery of the yeast Smc5/6 complex using Strep tag by elution off the StrepTactin affinity column under native conditions by biotin/desthiobiotin was not successful (Owen Wells, personal communication). Therefore, we decided to initially test affinity purification of the SMC5/6 using the 6xHis tag on NAMCE4a. His tag is a small tag consisting of a polyhistidine chain, with usually six (6xHis), or ten histidine residues (10xHis). Purification using the His tag is performed by immobilised metal-affinity chromatography (IMAC). Histidine contains an aromatic imidazole ring, which forms coordination bond with the immobilised metal ions. Proteins containing consecutive histidine residues engage stably in the coordination bond and are retained on the IMAC column. The IMAC column consists of a support resin, a chelating ligand and metal ions,



C

	LFQ intensity	
Subunit	**Bait**	**Control**
SMC6	12.14 x 10^6	0
SMC5	5.12 x 10^6	0
NSMCE4a	13.76 x 10^6	0
NSMCE3	2.42 x 10^6	0
NSMCE2	5.12 x 10^6	0

Figure 4.1: C-terminal His tag of NSMCE4a-Strep-6xHis can be used to recover the SMC5/6 complex
A. Illustration of the C-terminally tagged NSMCE4a. **B.** Western blot showing different fractions of NSMCE4a pull down using Ni-NTA agarose (QIAGEN); Input - cell lysate before addition to the beads, IS: insoluble pellet fraction after benzonase digest, FT: flow through (lysate after incubation with Ni-NTA agarose beads), El.1: first elution with 300mM imidazole, El.2: second elution with 300mM imidazole, Beads: Ni-NTA beads boiled for 5 minutes in 1xSDS loading buffer; for Input and Flow through, 1% of the whole fraction was used for western blot, for Elutions, Insoluble and Beads fractions, 5.5% of the whole fraction was used for western blot. Bait: -/-;NSMCE4a-Strep-6xHis cell line, Control: T-REx Flp-In 293 cell line. **C.** MaxQuant search of the raw mass spectrometry data from Elution 1 fraction shown in (B), subunits of the SMC5/6 complex identified in the bait cell line, LFQ intensity – a quantitative measure of proteins present in the sample for label-free approach.

such as nickel (Ni^{2+}) or cobalt (Co^{2+}) (reviewed in: Bornhorst and Falke, 2000). Affinity purification using Ni^{2+}-NTA resin enables about 100-fold enrichment of His-tagged protein in a single purification step and can be performed both under denaturing or native conditions. Elution using increasing concentration of imidazole allows the recovery of the protein of interest in its native conformation. This preserves protein-protein interactions, which makes it a convenient method for interaction studies (reviewed in: Schmitt et al., 1993).

For the initial pull down experiment, we used 1 x T-75 flask (Corning) of confluent T-REx Flp-In 293 cells, which equals to approximately 10 x 10^6 cells. Harvested cells were lysed under native conditions in a lysis buffer containing 0.5% NP-40 and the DNA was digested using 250 units/ml of lysate benzonase. Benzonase is an endonuclease from *Serratia marcescens*, which efficiently degrades both DNA and RNA. After the benzonase digestion the insoluble and soluble fractions were separated by centrifugation. The protein amount in the soluble fraction after benzonase digest was determined by Bradford assay. The same protein amount (cca 1 mg) of the soluble fraction from the bait cell line and the control cell line was used as the input in the affinity pull down. The pull down was performed using Ni^{2+}-NTA agarose beads under native conditions with the bait and control cell line in parallel using the same conditions. The imidazole concentration in the lysate before the binding step was adjusted to 30mM to eliminate binding of non-specific proteins to the beads. After binding and washing steps, the proteins were eluted from the Ni^{2+}-NTA beads using 300mM imidazole. Figure 4.1 B shows western blot analysis of different fractions of each purification step. The results indicate that the tagged NSMCE4a specifically binds to the Ni^{2+}-NTA column, as we can observe less NSMCE4a-Strep-His in the flow through fraction (Figure 4.1 B, left panel, lane 3). In the bait cell line, most of the NSMCE4a-Strep-His was recovered in the first elution using 300mM imidazole (Figure 4.1 B, left panel, lane 4). Importantly, we were able to recover SMC5 together with the NSMCE4a in the first elution, which indicates, that the tagged NSMCE4a can be used to purify the SMC5/6 complex. There was a small amount of NSMCE4a-Strep-6xHis in the bait cell line stuck to the agarose beads, which was released from the boiled agarose beads upon denaturing conditions (Figure 4.1 B, lane 6). No subunits of the SMC5/6 complex were detected in elution fractions and beads by western blot in the control cell line (Figure 4.1 B right panel, lane 4 – 6). This confirms that both the NSMCE4a and SMC5 in the bait cell line were specifically recovered by affinity

binding to the Ni^{2+}-NTA column. Together, the data showed that we were able to recover the NSMCE4a and SMC5 by elution under native conditions by affinity purification on Ni^{2+}-NTA column.

4.3.1.2 Mass spectrometry analysis after elution of NSMCE4a-Strep-6xHis from Ni-NTA identifies all SMC5/6 subunits

The western blot results showed in Figure 4.1 B confirmed that we are able to recover SMC5 together with NSMCE4a by imidazole elution. This indicates that the NSMCE4a properly incorporates into the SMC5/6 complex and the whole complex can be recovered by affinity purification of tagged NSMCE4a. In order to validate this hypothesis, we subjected the first elution fraction (El.1) to high performance nano flow liquid chromatography coupled with mass spectrometry (nano-LC/MS). Elution fractions from both bait and control cell line were subjected to reduction and alkylation before tryptic digest. Reduced and alkylated peptides were then subjected to desalting step on Pierce C18 spin columns. Desalted peptides were dried and re-suspended in 0.1% TFA. Over 50% of the elution fraction was subjected to the high performance liquid chromatography coupled with mass spectrometry using an LTQ Orbitrap XL instrument. Raw data were analysed by MaxQuant software (version 1.6.3.3) and a search was performed against the human database (Human Swiss-Prot 20200, June 2017). The search parameters are listed in Appendix (Table A.2 A). Protein groups identified by the MaxQuant search are listed in Appendix (Table A.2 B). The MaxQuant search identified five of the six SMC5/6 complex components in the bait cell line and none in the control cell line (Table A.2 B). The advantage of MaxQuant software is that it uses the MaxLFQ algorithm to calculate label-free quantification (LFQ) intensities for each identified protein. LFQ intensities can be used as a quantitative measurement for label-free methods (Cox et al., 2014). The LFQ intensities for each identified SMC5/6 subunit are listed in a table (Figure 4.1 C). The MaxQuant search failed to identify the NSMCE1 subunit. This can, however, be due to the relatively low yield of the SMC5/6 complex by the affinity purification or NSMCE1 degradation during sample preparation. Together, our data suggest that we can recover the SMC5/6 by affinity purification of NSMCE4a-Strep-6xHis using IMAC.

4.3.2 Optimisation of the NSMCE4a purification using 6xHis tag

4.3.2.1 Improvement of elution purity by gradual increase in imidazole concentration

From the initial mass spectrometry data, it is obvious that despite the SMC5/6 complex being detected in elution fractions, the protein coverage of the bait (NSMCE4a-Strep-His) was quite low in comparison to the background. Therefore, we aimed to optimise the purification method to enrich for the SMC5/6 complex components and its potential interactors and simultaneously decrease the number of unspecific proteins in the elutions. To do so, at first more elution steps using increasing concentrations of imidazole were included. Introduction of elutions by increasing imidazole concentration should remove weakly bound proteins non-specifically binding to the Ni-NTA column. This step should increase the purity of the eluate containing NSMCE4a-Strep-His and its interactors. Therefore, we included three consecutive elutions using 60, 150 and 250mM imidazole (Figure 4.2 A, lane 4 - 6). Comparable amount of the NSMCE4a and SMC5 eluted with both 60mM and 150mM imidazole (Figure 4.2 A, lane 4 and 5). However, elution with 150mM imidazole contained less unspecific proteins then elution with 60mM imidazole, as visualised by silver staining (Figure 4.2 B). Importantly, substantial amount of SMC5 and NSMCE4a was stuck to the beads even after the elution with 250mM imidazole (Figure 4.2 A, lane 7). This phenomenon could be explained by unspecific binding of the complex to the agarose beads, either directly or through unspecific binding to proteins that stick to the agarose beads. Despite the successful detection of SMC5 in NSMCE4a pull down by western blot, we were not able to detect any significant band of the size of NSMCE4a or SMC5 using silver stain (Figure 4.2 C). This indicates that enrichment of the SMC5/6 complex by IMAC purification is still too low to distinguish the complex subunits.

Even though including the 60mM imidazole elution improved the purity of the 150mM elution fraction, both fractions still contained a significant amount of contaminants (Figure 4.2 C). Therefore, we continued to optimise the NSMCE4a affinity purification using 6xHis tag. To do so, we compared two different protocols for the Ni-NTA column, as well as the standard Ni-NTA purification protocol and different IMAC column, TALON.

First, we tried to pre-incubate the Ni-NTA agarose beads with a mock cell lysate before incubating the beads with the lysate containing the tagged protein. This step could

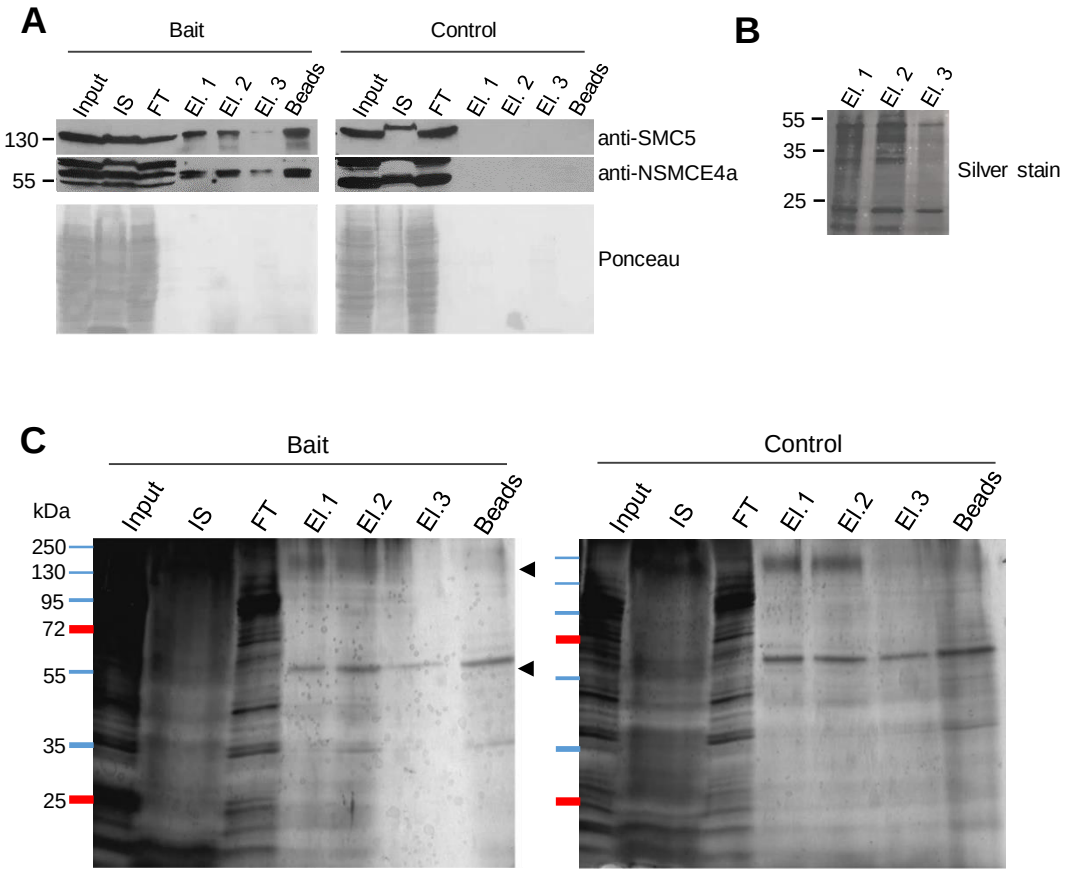


Figure 4.2: Improvement of elution purity using gradually increasing imidazole concentration

A. Western blot showing NSMCE4a pull down using Ni-NTA agarose beads under different elution conditions to improve purity of SMC5/6 complex, **B.** Example of a silver stain gel to demonstrate elimination of non-specific proteins bound to Ni-NTA resin by including 60mM elution. **C.** Silver stain of fractions from IMAC purification of NSMCE4a-Strep-6xHis; cell lysate was prepared from approximately 2 x 10^7 cells, affinity purification was performed using Ni-NTA agarose beads, black arrows indicate the estimated size of SMC5 (around 130 kDa) and NSMCE4a (around 55 kDa). No apparent band is detected by silver staining in size of NSMCE4a or the other complex subunits in the Bait cell line in comparison to Control cell line. **A - C.** Input: soluble fraction of whole cell lysate after benzonase digestion, IS: insoluble fraction pelleted after benzonase digestion, FT: flow through, El.1: elution with 60mM imidazole, El.2: elution with 150mM imidazole, El.3: elution with 250mM imidazole, Beads: Ni-NTA agarose beads boiled in 1 x SDS sample buffer; Bait: -/-;NSMCE4a-Strep-6xHis cell line, Control: T-REx Flp-In 293.

improve the yield of the SMC5/6 complex by blocking its unspecific binding to the agarose beads. The western blot results indicate that pre-coating the Ni-NTA beads results in decreased unspecific binding of the SMC5/6 complex to the agarose beads (Figure 4.3 C, lanes 4 - 7) in comparison to the standard Ni-NTA protocol (Figure 4.3 A). The amount of unspecific proteins in all three elution fractions (60, 150 and 250mM imidazole) was analysed using silver staining. Pre-coating the beads with mock lysate lowered the amount of unspecific proteins in the second elution (150mM imidazole) (Figure 4.2 C, left panel, lane 2) and did not affect the ability of NSMCE4a-Strep-6xHis to bind the Ni-NTA column (Figure 4.2 C, right panel, lane 5).

Next, we striped the Ni-NTA column by addition of 50mM EDTA, pre-incubated the stripped matrix with a mock cell lysate and re-charge the column with Nickel. The rationale for this step was to prevent histidine rich proteins from occupying the binding sites for the 6xHis tag of NSMCE4a. Stripping the Ni-NTA beads prior to pre-coating with a mock lysate resulted slight decrease in unspecific binding. However, silver staining revealed that most of the contaminants were eluted with the second elution fraction, which contains most of the NSMCE4a and SMC5 (Figure 4.3 D, left panel).

We also compared the affinity purification using Ni-NTA and TALON column. Another option to optimise the purity of the pull downs was to test the TALON IMAC column. TALON matrix utilised a solid resin containing carboxyl-methyl-aspartate charged with Cobalt ions (Co^{2+}-CMA). In comparison to Ni-NTA, the Co^{2+}-CMA column displays slightly lower affinity, but has higher selectivity for the 6xHis tag. It also exhibits lower affinity to unspecific proteins and thus, is likely to give a lower background signal. Due to the lower affinity of cobalt ions to the 6xHis tag, the binding and washing steps were performed using 10mM, instead of 30mM imidazole. Purification using the TALON matrix resulted in the highest yield of NSMCE4a in elution using 150mM imidazole in comparison to the other fractions (Figure 4.3 B). Even though some of the NSMCE4a was lost in the first elution (60mM imidazole), silver stain analysis showed that most of the contaminant proteins also eluted with the 60mM imidazole elution (Figure 4.2 B, left panel). No NSMCE4a was detected in the third elution (250mM imidazole) (Figure 4.2 B, lane 6). Despite the loss of some of the NSMCE4a in the first elution the maximum of the NSMCE4a was eluted in the second elution (150mM imidazole), which was also shown to purest elution. Even though pre-coating of the Ni-NTA beads gave comparable

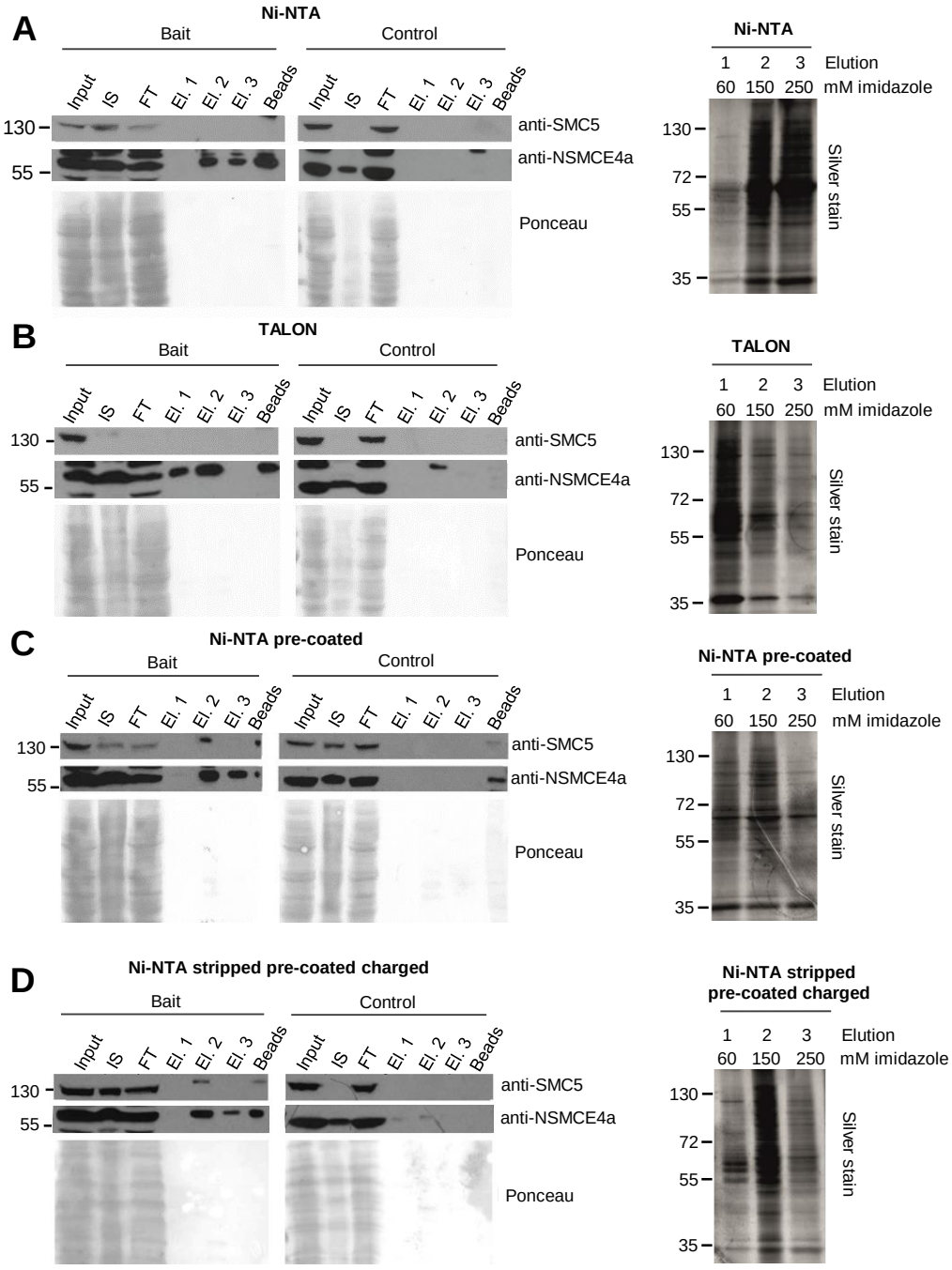


Figure 4.3: Optimization of NSMCE4a-Strep-6xHis pull down using different IMAC columns and conditions

A. Ni-NTA: IMAC column using nickel ions, binding in 30mM imidazole, left panel: silver stain showing amount of proteins in different elution fractions from bait cell line. **B.** TALON: IMAC column using cobalt ions, binding step was performed in 10mM imidazole. **C.** Pre-coated: Ni-NTA agarose was incubated for 1 hours with a mock cell lysate from T-REx cell line prior binding step. **D.** Stripped pre-coated charged: Ni-NTA column was stripped by addition of 2 x 500 ul of 50mM EDTA and pre-incubated with 1 hours with a mock cell lysate from Control cell line prior binding step, Silver stain comparing different elution fractions from **A – D**: 2% of Input and 10% of Insoluble and Elution fractions were used for western blot, 10% of elution volume was used for the Silver stain gel, Bait: FRT-inserted NSMCE4a-Strep-6xHis, endogenous NSMCE4a KO cell line, Control: T-REx Flp-In 293 cell line.

yield and purity of NSMCE4a as the TALON column, for simplicity and efficiency, we decided to use the TALON column for further experiments.

4.3.3 Two step purification of SMC5/6 coupled with nano-LC/MS did not increase the SMC5/6 yield over background

Despite optimisation of the SMC5/6 purification conditions using IMAC, the abundance of the SMC5/6 complex in elution fractions still remained relatively low in comparison to background. To further increase the yield of the SMC5/6 complex and lower the amount of non-specific interactors, we aimed to purify of the SMC5/6 using both affinity tags. During the two step affinity purification using His and Strep tag, purification using IMAC is usually performed as the first step. Firstly, it allows easy elution of proteins of interest upon native conditions, which does not disturb protein-protein interactions. Secondly, there is no need for buffer exchange before the next purification step, so the elution from IMAC column, can be directly loaded onto the StrepTactin matrix for the second purification step.

4.3.3.1 First step purification of SMC5 using TALON IMAC column

Since the SMC5/6 complex can be recovered from the IMAC column under native conditions by imidazole elution (Figure 4.2 A and 4.3 A – D), we decided to use the His tag pull down as an initial purification step. To have enough input material for the Strep tag purification step, the number of cells used for the initial IMAC pull down was up-scaled. Approximately 25 x 10^7 cells was used for the first step purification using the TALON column. IMAC purification was performed in parallel with bait and control cell line; cells were lysed and the DNA was digested by benzonase for 50 minutes, NaCl concentration was increased to 150mM and cells were incubated for another 20 minutes. Imidazole concentration in the buffer was adjusted to 10mM before binding to the TALON column. After binding step, additional pre-elution (El.1) with 30mM imidazole was introduced in order to further increase the purity of the elution containing the SMC5/6 complex. The efficiency of the purification was assessed by analysing each fraction by western blotting (Figure 4.4 A). In order to determine the purity of elutions in comparison to the other fractions, silver staining was performed in parallel with western blot (Figure 4.4 B). The western blot results showed successful recovery of NSMCE4a and SMC5 in the bait cell line, however the SMC5/6 complex subunits in the bait cell line were not

detectable by silver staining (Figure 4.4 B, black arrows). The 150mM elution fraction (El.3) of the bait cell line contained the highest yield of SMC5 and NSMCE4a (Figure 4.4 A) and lowest amount of background signal (Figure 4.4 B). Therefore, the elution 3 fraction used for the second purification step; 20% of the total volume of elution 3, from both cell lines, was subjected to the second purification step using magnetic StrepTactin beads (iba). The other 50% of the elution from TALON column was used for preparation of samples for MS analysis.

4.3.3.2 Second step purification of SMC5/6 by using StrepTactin magnetic beads

Strep tag is a small eight amino acid fusion tag (WSHPQFEK), its development was originally based on the strongest naturally occurring non-covalent interaction between streptavidin protein and biotin molecule. The binding specificity of the Strep tag to bind streptavidin is comparable to biotin. However, Strep tag binds nearly 100 times tighter to specifically engineered protein called StrepTactin, off which it can be reversibly eluted. Elution can be performed by desthiobiotin, which displaces the Strep tagged proteins by competitive binding to StrepTactin. This results in a mild elution, which can be used under native conditions. Therefore, purification of Strep tagged fusion proteins using StrepTactin affinity column allows rapid recovery and high purity of the protein of interest (reviewed in: Skerra and Schmidt, 2000 and Schmidt and Skerra, 2007). 100 µl of the 150mM elution from the TALON column was directly loaded onto equilibrated StrepTactin XT magnetic beads (iba) and binding was performed following manufacturer's instructions. The ability of the human SMC5/6 complex to be recovered by desthiobiotin elution was tested; two consecutive elutions using 2.5 mM desthiobiotin were performed. After elution steps, 25% of the StrepTactin beads were boiled for 5 minutes in 1 x SDS loading buffer and 75% of the beads was subjected to tryptic on-bead digest for further mass spectrometry analysis. Each of the fractions from Strep tag purification was analysed by western blotting for the presence of SMC5 and NSMCE4a. NSMCE4a-Strep-6xHis was able to bind the StrepTactin matrix, as in the bait cell line most of the NSMCE4a was not observed in the flow through in comparison to the input fraction (Figure 4.4 C, bait, lane 1, 2). No detectable NSMCE4a or SMC5 was recovered by 2.5mM desthiobiotin elution under native conditions (Figure 4.4 C, bait, lane 3, 4). However, elution under denaturing conditions (boiling the Beads fraction in 1 x SDS buffer) resulted in recovery of both SMC5 and NSMCE4a in the bait cell line (Figure 4.4

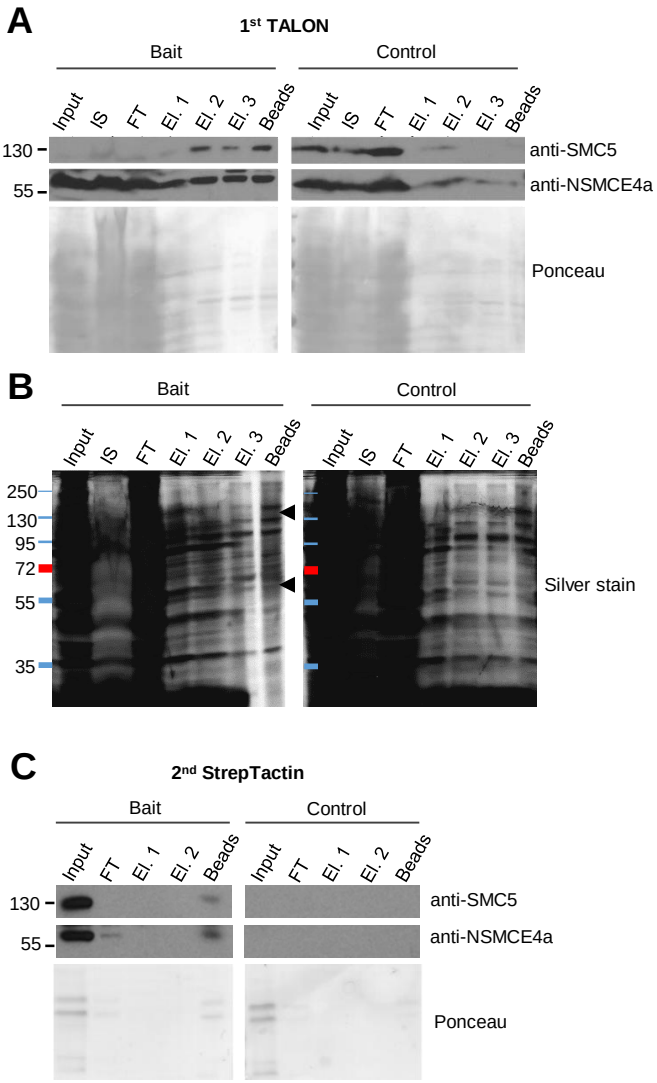


Figure 4.4: Two-step affinity purification of NSMCE4a-Strep-6xHis using TALON resin and StepTactin magnetic beads

A. Western blot showing the IMAC affinity purification of NSMCE4a-Strep-6xHis using TALON resin, 0.5% of Input, 2% of the Insoluble and 2% of the total elution volume was used for western blot, elution volume was 500 µl (3.33 column volumes); 20% of Elution 3 was subjected to the second step affinity purification using StrepTactin magnetic beads (iba). 50% of the El.3 was subjected to nano-LC/MS. **B.** Silver stain showing the IMAC purification of NSMCE4a-Strep-6xHis using TALON resin, 0.5% of Input, 2% of the Insoluble and 2% of the total elution volume and boiled beads was used for silver stained gel, black arrows indicate the approximate size of expected NSMCE4a (55 kDa) and SMC5 (130 kDa) bands. **A – B.** El.1: pre-elution with 30mM imidazole, El.2: elution with 60mM imidazole, El.3: elution with 150mM, Beads: boiled TALON resin. **C.** Western blot showing the second step of affinity purification using StrepTactin magnetic beads, Input: 20% of 150mM imidazole elution (El.3) from TALON resin, El.1 and El.2: elutions by 40 ul of 2.5mM desthiobiotin, Beads: StrepTactin magnetic beads boiled 5 minutes in 1 x SDS loading buffer; 10% of the Input and Flow through volume and 25% of the El.1, El.2 and Beads fraction was used for western blot, 75% of the StrepTactin magnetic beads were directly digested by trypsin, desalted and subjected to nano-LC/MS.

C, lane 5, Beads). Together, our data suggest that despite the ability of the SMC5/6 complex to bind to the StrepTactin XT magnetic beads, we were able to recover the SMC5/6 only under denaturing conditions.

4.3.3.3 Comparison of nano-LC/MS results of both purification steps

After validation of the two-step purification of the SMC5/6 complex by western blot, it had to be established whether introduction of the second purification step indeed improves the purity and yield of the SMC5/6 complex. Therefore, both the 3rd elution fraction (150mM imidazole) from the TALON column, and the on-bead digest from the StrepTactin column were subjected to nano-LC/MS analysis. Peptides were reduced and alkylated before performing the tryptic digestion. Digested proteins were desalted using Pierce C18 Spin Columns and re-suspended in 0.1% TFA. Approximately 50% of the peptide sample was subjected to nano-LC/MS analysis. The initial search was performed by MASCOT (Matrix Science) search engine. Search parameters and results for both bait and control cell line and condition are listed in Appendix (Table A.3). As a measure of the SMC5/6 yield in each pull down, the number of unique peptides of the SMC5/6 subunits in control and bait cell line was scored. The number of proteins identified for each sample is listed in Figure 4.5 B and D. The MASCOT search identified all the subunits of the SMC5/6 complex in the elution 3 (150mM imidazole) from the TALON column in the bait cell line (Figure 4.5 A and Table A.3 B). None of the SMC5/6 components was present in the control cell line. In contrast, only five SMC5/6 subunits were identified in the on-bead digest from the two-step pull down using TALON/StrepTactin of the bait cell line (Figure 4.5 C and Table A.3 D). No peptides of the SMC5/6 subunits were present in the control cell line (Figure 4.5 C and Table A.3 D). The total number of identified proteins using the one-step TALON purification was higher (644 bait, 598 control) than the two-step purification using TALON/StrepTactin (496 bait, 459 control) (Figure 4.5 B and D). This indicates that the amount of background is lower for the two-step purification. However, the amount of the peptide sample subjected to the nano-LC/MS was proportionally higher in case of the TALON elution (approximately 50% of the total input), in comparison to the on-bead digest from the two-step TALON/StrepTactin purification (approximately 15% of the total input). Therefore, the direct comparison of the two approaches can only be used only as an estimation. The number of unique peptides identified for the SMC5/6 subunit was, nevertheless, higher

A

TALON

	Unique peptides	
Subunit	Bait	Control
SMC6	10	0
SMC5	13	0
NSMCE4a	3	0
NSMCE3	7	0
NSMCE2	3	0
NSMCE1	3	0

B

TALON

Total number of hits	
Bait	Control
644	598

C

TALON/StrepTactin

	Unique peptides	
Subunit	Bait	Control
SMC6	5	0
SMC5	5	0
NSMCE4a	2	0
NSMCE3	3	0
NSMCE2	2	0
NSMCE1	0	0

D

TALON/StrepTactin

Total number of hits	
Bait	Control
496	459

Figure 4.5: One-step pull down using TALON resin results in higher yield of the SMC5/6 complex than two-step pull down using TALON/StrepTactin

A. 50% of the elution 150mM imidazole from TALON pull down was digested by trypsin and prepared peptides were subjected to nano-LC/MS, number of unique peptides of the SMC5/6 complex components identified by MASCOT (version 2.3.02) search against human Swiss prot database. **B.** Total number of unique proteins identified by MASCOT search in the peptide sample prepared from the 150mM elution fraction of the TALON pull down in the bait and control cell line. **C.** 15% of the two-step TALON/StrepTactin pull down was subjected to an on-bead digest by trypsin and prepared peptides were subjected to nano-LC/MS, number of unique peptides of the SMC5/6 complex components identified by MASCOT (version 2.3.02) search against human Swiss prot database. **D.** Total number of unique proteins identified by MASCOT search in the peptide sample from two-step affinity purification using TALON/StrepTactin in the bait and control cell line.

in the sample from the single-step TALON pull down than in the sample from the two-step purification using TALON/StrepTactin. These preliminary observations imply that introduction of the second step pull down on StrepTactin column rather increases the loss of SMC5/6 and potential interactors and does not substantially decrease the background. Since the main objective was to search for interactors of the SMC5/6 complex, we decided to compromise the purity and use the single step purification using IMAC on TALON column.

4.3.4 Mass spectrometry analysis of protein-protein interactors of SMC5/6 complex

After the optimisation of affinity purification of the SMC5/6 complex using either 6xHis or both 6xHis and Strep tag described in previous section, we searched for interaction partners of SMC5/6 using nano-LC/MS. The single-step affinity purification by His tag pull down of NSMCE4a-Strep-6xHis on TALON column was chosen. This was the optimal method of SMC5/6 affinity purification, since it minimised the loss of potential SMC5/6 interactors and allowed elution of SMC5/6 under native conditions. We aimed at identifying SMC5/6 interactors during normal cell cycle and test whether these interactors change, (increase or decrease) upon treatment with DNA damaging agent. As the SMC5/6 complex has been shown to play a role during replication fork stalling and/or collapse (Ampatzidou et al., 2006; Bustard et al., 2012; Irmisch et al., 2009), we aimed at searching for interactors during replication fork stalling and replication fork collapse. The experimental workflow is described in Figure 4.6; isogenic cells lines with tagged NSMCE4a (Bait) and untagged NSMCE4a (Control) were grown in parallel. Cells were harvested and pull down of NSMCE4a using TALON column was performed. Elution containing the best yield of SMC5/6 subunits in the bait cell line and the lowest amount of background proteins, was subjected to bottom up proteomics analysis. Proteins in the elution fraction were subjected to in-solution tryptic digest. Digested peptides were further desalted and prepared for nano-LC/MS analysis. Peptide mixture was separated using nanoscale liquid chromatography and eluted off the chromatographic column in an acetonitrile gradient. Electrospray ionised peptides entered the LTQ-Orbitrap XL instrument and were subjected to first MS scan (Orbitrap) and second MS/MS scans (ion trap). For sample identification, ten scan events were performed for each MS/MS scan. Raw files were analysed using MaxQuant software with Andromeda search engine (Cox and Mann, 2008). Peptide identification is achieved by comparing the tandem mass

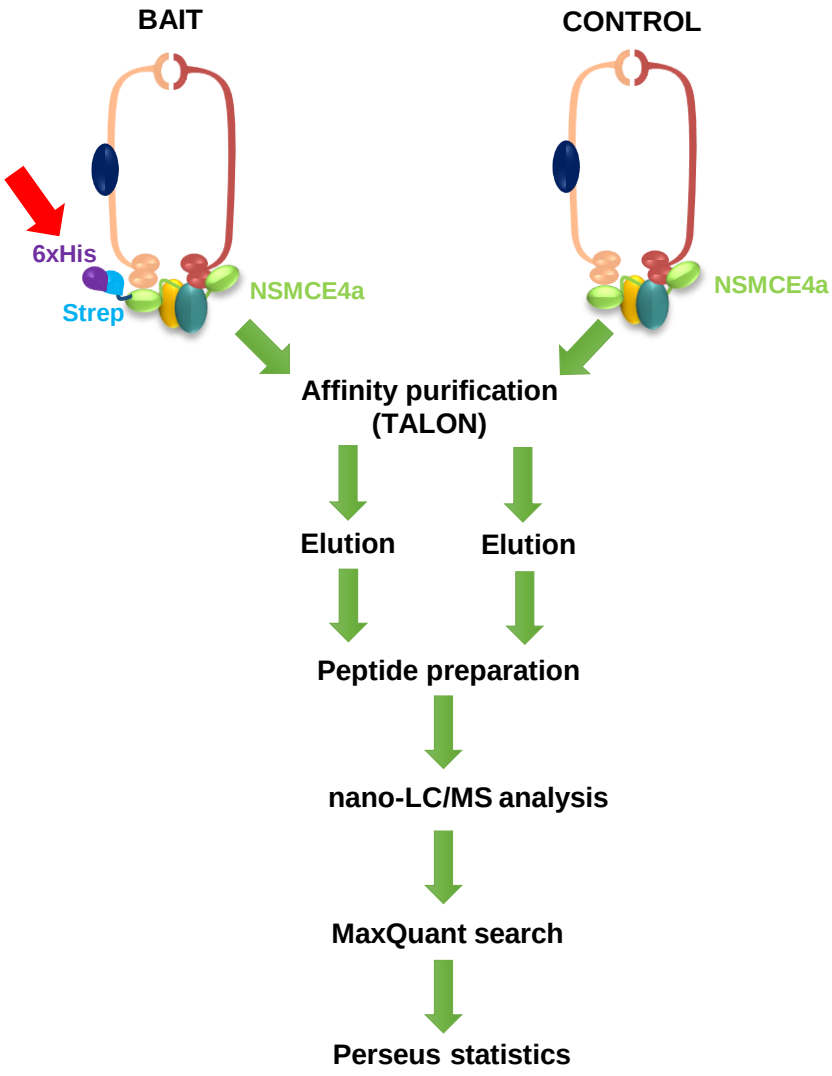
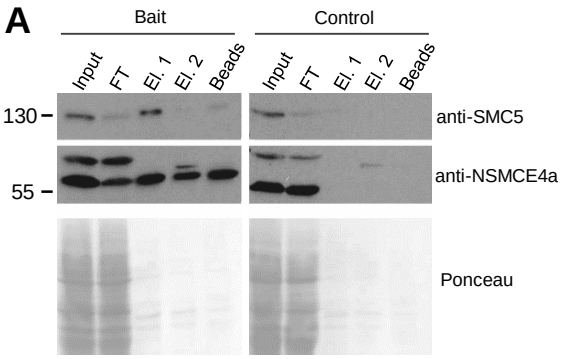


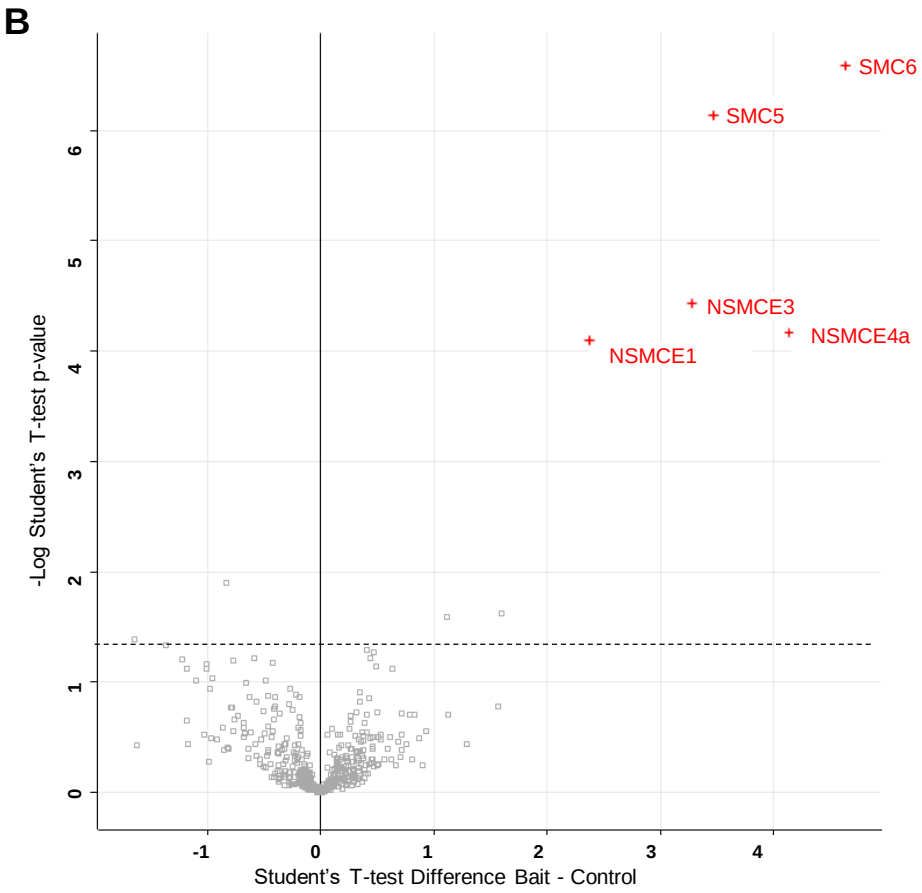
Figure 4.6: Workflow scheme of label free approach to purify the SMC5/6 complex coupled with mass spectrometry
For affinity purification of the SMC5/6 complex using the label-free approach, the Bait cell line, which has an affinity tagged NSMCE4a and a control cell line with untagged NSMCE4a was used; both cell lines were subjected to affinity purification using TALON matrix; the elution fractions from TALON column were subjected to bottom-up proteomics; eluted proteins were subjected to tryptic digest, desalting and concentrated before mass spectrometry analysis; peptide mixture was subjected to Liquid chromatography coupled with mass spectrometry (LC-MS) using LTQ Orbitrap XL instrument; raw data was analysed using MaxQuant software; Further data processing and statistical analysis was performed using Perseus platform.

spectra derived from peptide fragmentation with theoretical tandem mass spectra generated from *in silico* digestion of a protein database (reviewed in: Zhang et al., 2013). Search results of three or more replicates were subjected to statistical analysis using Perseus platform ver. 1.6.1.1 (Tyanova et al., 2016).

4.3.4.1 During unperturbed cell cycle the SMC5/6 complex does not have a stable interaction partners

To search for protein interactors of the SMC5/6 complex during unperturbed cell cycle, we performed affinity purification of SMC5/6 using the 6xHis tag on NSMCE4a. In order to get reproducible and statistically significant results using the label free quantification (LFQ) approach, we performed four independent biological affinity purification experiments. An example of western blot analysis of different fractions of the NSMCE4a pull down is shown in Figure 4.7 A. Optimisation of the affinity purification using the TALON column showed that the second elution (150mM imidazole) gives the optimal yield and purity (Figure 4.3 B). The starting material for each pull down experiment was 4.5 x 10^7 cells (3 x 15 cm dishes) for each cell line. The average input amount of whole cell extract determined by BSA/Bradford assay was 7 mg. Each fraction of affinity purification was subjected to western blot analysis to validate successful recovery of tagged NSMCE4a and SMC5 (Figure 4.7 A). 75% of the second elution fractions of control and bait cell line (Figure 4.7 A, lane 4) were subjected to a tryptic digest, peptide desalting and to nano-LC/MS analysis. The raw mass spectrometry from four biological replicates were subjected to a MaxQuant search with the matching between runs feature enabled. This is an algorithm that enables quantification of a mass spectra features in the whole data set for each measurement. In other words, if in one sample a peptide X is not identified due to the absence of MS/MS, its MS1 quantitative information can be used by matching to its corresponding identified peptide from another sample. Thus, the matching between runs feature leads to increase in number of quantified proteins in the sample. For quantification and statistical evaluation of the hits, the label free quantification (LFQ) intensities were used as a quantitative measure of identified peptides. The MaxQuant search parameters and results are listed in Appendix (Table A.4 A and B). LFQ intensities obtained by MaxQuant search were than analysed in Perseus framework, the statistical values for each identified protein in the sample are listed in Appendix (Table A.5). The protein hits identified by MaxQuant search were filtered from potential contaminants, hits





C

Gene	Student's T-test (Bait - Control) (Benjamini-Hochberg FDR correction) Significant	-Log p	Difference	q-value
SMC6	+	6.56	4.65	0.000
SMC5	+	6.16	3.48	0.000
NSMCE3	+	4.44	3.27	0.005
NSMCE4a	+	4.15	4.17	0.008
NSMCE1	+	4.09	2.36	0.007

D

Gene	Student's T-test (Bait - Control) Significant	-Log p	Difference
SMC6	+	6.56	4.65
SMC5	+	6.16	3.48
NSMCE3	+	4.44	3.27
NSMCE4a	+	4.15	4.17
NSMCE1	+	4.09	2.36
CRTC2	+	1.62	1.60
NSMCE2	+	1.60	1.12

Figure 4.7: AP-MS of NSMCE4a-Strep-6xHis coupled with MaxQuant search and Perseus analysis of protein interactors upon non-treated conditions
A. Example of a western blot showing different fractions of affinity purification of NSMCE4a-Strep-6xHis using TALON column, 100 µl (75%) of the second elution (El.2) from bait and control cell line was digested by trypsin, desalted and subjected mass spectrometry analysis; Input: soluble fraction after 1 hour benzonase digest, FT: flow through, El.1: elution with 60mM imidazole, El.2: elution with 150mM imidazole, Beads: TALON beads boiled in 1 x SDS sample buffer, each lane contains 1.5% of total 650 µl Input and flow FT and 6.7% of elutions and Beads. **B.** Volcano plot of statistical significance versus fold change of protein hits identified by MaxQuant search in control and bait cell lines, all identified hits are represented by squares, statistically significant hits are represented by red cross, x axis shows Student's t-test difference of bait/control, hits > 0 are enriched in bait over control, hits < 0 are enriched in control compared to bait, y axis shows –log p-value for each hit, dashed line indicates p-value = 0.05 (without FDR correction), for analysis Perseus (ver. 1.6.1.1) platform was used. **C.** Table of statistically significant hits analyzed by Perseus (B), statistical significance of four independent repeats was calculated using two-tailed Student's T-test, Benjamini-Hochberg FDR correction (FDR = 0.05) was used to exclude false positive hits, + : statistically significant hit, q-value: FDR adjusted p-value. **D.** Table of statistically significant hits analyzed by Perseus (B) without FDR adjustment, statistical significance of four independent repeats was calculated using two-tailed Student's T-test.

only identified by site and reverse. The four replicates containing eight samples in total (4 bait + 4 control) were divided into two sample groups named Bait and Control. The rows were filtered to keep for further analysis only rows containing minimum of 3 valid LFQ intensity values in at least one group, i.e. minimum of three valid values had to be present in either control or bait cell line. In order not to exclude hits with certain missing values from the downstream analysis, the missing LFQ intensities were replaced with values from normal distribution by imputation (Imputation parameters: Width: 0.3, Downshift:1.8). To calculate the statistical significance of identified hits, two-sample Student's T-test was used. To correct for false discovered interactors, the p-value of the analysed data set was adjusted by Benjamini-Hochberg false discovery rate (FDR) correction (Benjamini and Hochberg, 1995). Statistically significant hits are graphically depicted in a volcano plot (Figure 4.7 B), protein names, corresponding q-value, -Log p-value and Student's T-test difference are listed in table below (Figure 4.7 C). Using the Benjamini-Hochberg FDR correction, statistical analysis showed all the SMC5/6 components, excepting NSMCE2, as significant interactors of NSMCE4a. This is in line with previous study by Taylor et al. and, hence, validate our experimental setup (Taylor et al., 2008). However, using the FDR correction, no more statistically significant interactors of the SMC5/6 complex were discovered by the label-free approach combined with our experimental setup. However, as the pull down experiments performed to identify SMC5/6 interactors were not hypothesis driven, the potential interactors identified by p-value without the FDR correction could be used to generate a hypothesis. Therefore, we compared the list of significant hits after Perseus analysis, which was only based on the Student's T-test p-value (Figure 4.7 D). Two additional proteins were identified as statistically significant, one of them being NSMCE2, which is known to be a core component of the SMC5/6 complex, and CRCT2; CRCT2 is a CREB Regulated Transcription Coactivator 2, which localises both to the nucleus and cytoplasm, it acts as a co-activator of the SIK/TORC signalling pathway. To compare out experiment with the predicted interactors of the NSMCE4a protein, we used the STRING (Search Tool for the Retrieval of Interacting Genes/Proteins) database (Figure 4.8). Based on the STRING database, the biochemically validated NSMCE4a interactors are SMC5, SMC6, NSMCE1 and NSMCE3. These are the same proteins identified as significant hits by out label-free AP-MS approach. The database predicted NSMCE4a interactor partners are subunits of the cohesin complex: SMC3, SMC1A and RAD21, the SUMO-conjugating enzyme UBC9 (UBE21 gene), as well as SUMO1, a common post-translation modifier protein.

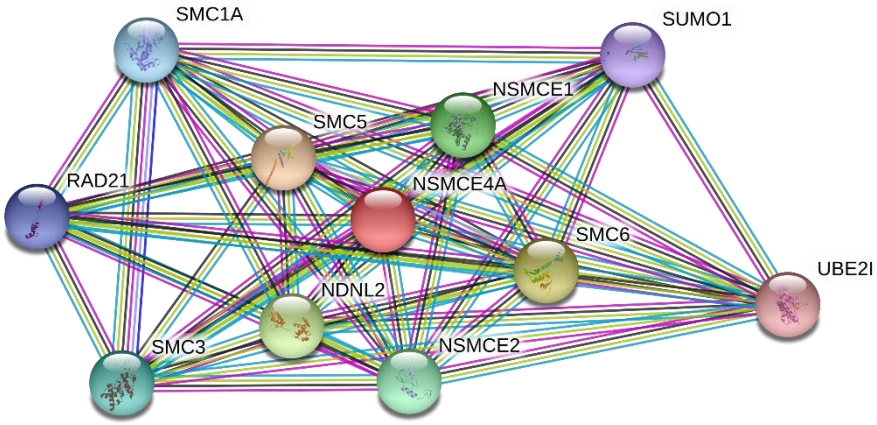


Figure 4.8: AP-MS of NSMCE4a-Strep-6xHis coupled with MaxQuant search and Perseus analysis of protein interactors upon non-treated conditions
Diagram of the known and predicted interactors of the NSMCE4a protein, biochemical evidence exists for interaction between NSMCE4a and NSMCE3, NSMCE1, SMC5 and SMC6, other proteins displayed are predicted based on databases prediction; source: STRING database (https://string-db.org).

Despite having identified the biochemically validated SMC5/6 components as interactors of the NSMCE4a, none of the database predicted interactors were identified by the MaxQuant search in the NSMCE4a pull down elutions (Table A.4 B). To date, the label-free quantification methods are very robust only with high enough number (typically > 5) of biological, as well as technical replicates. The caveats of our experimental setup were: (i) not enough biological replicates (ii) relatively high variability among the replicates caused by the mass spectrometry step being performed at different days and (iii) low yield of SMC5/6 in the elution fraction of the TALON column. An alternative interpretation of the results is that the SMC5/6 in the soluble fraction and DNA fraction solubilised by benzonase treatment, does not have any stable interactors, which can be detected by the label-free approach using the described protocol.

4.3.4.2 Searching for SMC5/6 interactors under replication stress conditions

The label-free quantification identified only the other SMC5/6 components as statistically significant interactors of the NSMCE4a-Strep-6xHis. Single molecule tracking data from our lab on *S.pombe* Smc5/6 (spSmc5/6) show that the majority of the complex during unperturbed cell cycle is mobile (Etheridge et al., manuscript in preparation). Hence, this Smc5/6 fraction is likely not to be chromatin bound. Previous studies reported the role of spSmc5/6 during replication stress; the spSmc5/6 has been shown to maintain replication forks in a recombination competent conformation and to allow appropriate repair of collapsed replication forks (Ampatzidou et al., 2006; Irmisch et al., 2009). Chromatin immunoprecipitation and immunofluorescence experiments indicate that hydroxyurea induced replication stress leads to increase in DNA bound fraction of spSmc5/6 (Ampatzidou et al., 2006; Oravcová et al., 2019). Thus, most of the less transient protein-protein interactions of SMC5/6 are likely to occur when the complex is bound to chromatin. We hypothesised that after replication stress, induced by hydroxyurea, the SMC5/6 complex will become chromatin bound and we will be able to detect more of its protein interactors by affinity-purification mass spectrometry. In human cells, the majority of replication forks are capable of resuming a replication after short time exposure, to replication inhibitor, hydroxyurea. Prolonged exposure to hydroxyurea leads to replication collapse, when the collapsed fork relies on rescue by homologous recombination repair, alternatively on replication completion by an adjacent functional fork (reviewed in: Cortez, 2015). Therefore, we aimed to search for SMC5/6 interactors

upon (i) replication fork stalling and (ii) replication fork collapse. Treatment of human cells with 2 mM hydroxyurea for 2 hours has been shown to cause replication fork stalling, whereas, treatment with 2mM hydroxyurea for 24 hours causes replication fork collapse (Petermann et al., 2010).

A Similar experimental setup, as described in previous section, was used; approximately 4.5 x 10^7 cells (3 x 15 cm dishes) for each cell line (control and bait) were treated with 2mM hydroxyurea for (i) 2 hours and (ii) 24 hours. The efficiency of hydroxyurea treatment was monitored by flow cytometry analysis of cell cycle (Figure 4.9 B). Replication inhibition by 2mM hydroxyurea will lead to gradual accumulation of cells in G1 and S phase and decrease in G2/M population. The cell cycle profiles show the gradual decrease of the G2 population, which is apparent after 24 hours of hydroxyurea treatment. This confirms the functionality of hydroxyurea used in the experiment. For each condition, the average input amount of protein in the pull down reaction was 7 mg of WCE. Affinity purification using TALON IMAC column was performed as described previously in Figure 4.3. The efficiency of affinity purification using TALON column was validated by western blot analysis of each pull down fraction (Figure 4.9 A). Second elution (El.2) was subjected to a tryptic digest (Figure 4.9 A, lane 4), digested peptides were desalted using Pierce C18 spin columns. Desalted peptides were dried and re-suspended in 0.1% TFA. Three independent biological replicates were performed for control and each treatment condition (non-treated, 2h HU and 24h HU). 75% of the desalted peptides from bait and control cell lines was subjected to nano-LC mass spectrometry. Raw mass spectrometry data from all replicates and all conditions were subjected to MaxQuant search against human database. To gain maximum of identified peptides identification by matching between runs was allowed. The parameters and search results are listed in Appendix (Table A. 6A, B).

4.3.4.3 Searching for NSMCE4a interactors during replication fork stalling

To identify the interactors of the SMC5/6 complex upon replication fork stalling (2 hours treatment with 2mM hydroxyurea), the MaxQuant search results were statistically analysed in Perseus framework. The LFQ intensities were used as a quantitative measure of identified proteins. The triplicate dataset was initially filtered for potential contaminants, reverse proteins and the proteins that are only identified by site. Next, to allow statistical processing, the LFQ values were transformed into the logarithmic format

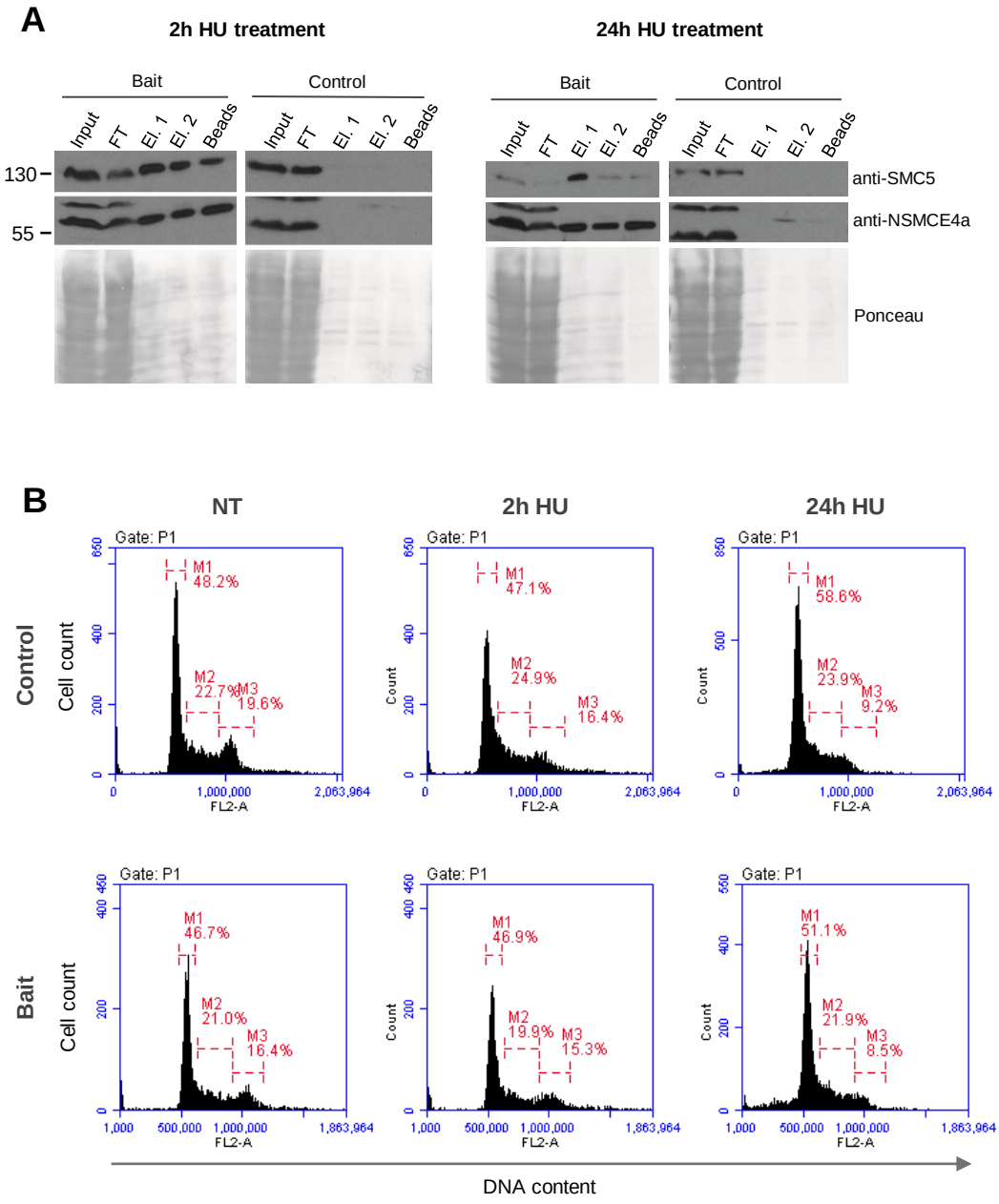
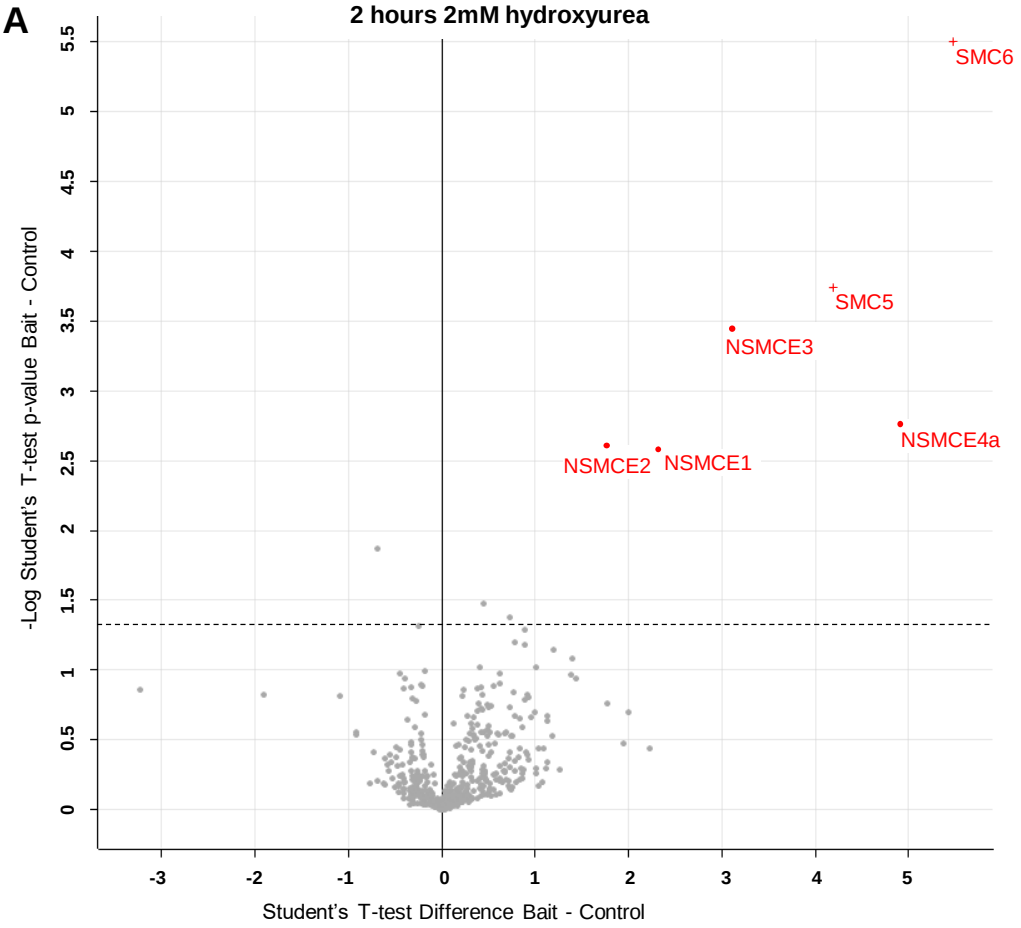


Figure 4.9: Affinity purification of NSMCE4a-Strep-6xHis after 2 and 24 hours of 2mM hydroxyurea treatment

A. Example of a western blot showing different fractions of affinity purification of NSMCE4a-Strep-6xHis using TALON column, 100 µl (75%) of the second elution (El.2) from bait and control cell line was digested by trypsin, desalted and subjected mass spectrometry analysis; Input: soluble fraction after 1 hour benzonase digest, FT: flow through, El.1: elution with 60mM imidazole, El.2: elution with 150mM imidazole, Beads: TALON beads boiled in 1 x SDS sample buffer, each lane contains 1.5% of total 650 µl Input and flow FT and 6.7% of elutions (El.1/El.2) and Beads. **B.** Flow cytometry profiles of cells used for AP-MS; example of flow cytometry profiles of control and bait cell line upon unperturbed cell cycle (NT), after 2 hours (2h HU) and 24 hours (24h HU) of 2mM hydroxyurea treatment; gating for cells with normal circularity was performed, gates M1 – M3 show estimated amount of cells in G1 (M1), S (M2) and G2/M (M3).

(log2). Data from three replicates were categorically annotated as ‘Bait’ and ‘Control’ categories; the data were further filtered to maintain only rows that contain minimum of two valid LFQ intensity values in at least one categorically annotated group. In order not to exclude the proteins only identified in either bait or control cell line, the LFQ intensities were imputed from normal distribution (Imputation parameters: Width: 0.3, Downshift: 1.8). To calculate the statistical significant quantitative difference between proteins identified in the bait over the control cell line, two-sample Student’s T-test was used. To get rid of false positive hits, the Benjamini-Hochberg FDR correction was applied. The results of the Perseus analysis are listed in the appendix (Table A.7) and graphically depicted in a volcano plot (Figure 4.10 A). The only statistically significant hits, enriched in the bait cell line after Benjamini-Hochberg FDR correction, were SMC6 and SMC5 (Figure 4.10 B). This indicates that the SMC5/6 complex was successfully recovered by NSMCE4a pull down, however, some of the previously identified hits were not significantly enriched in the bait cell line. The reason why the other complex components were not identified as significant is likely due to the overall low yield of the complex by affinity purification in comparison to the background; another factor is the lower molecular weight of the NSMCE proteins in comparison to the relatively large SMC5 and SMC6 proteins. A common bias of the mass spectrometry methods is that smaller proteins containing lower amounts of peptides are identified by MS with lower probability. When using the p-value without FDR correction, which is allowed in case we are looking for novel interactors, there were eight proteins identified after Perseus analysis (Figure 4.10 C). Without the FDR correction, all six SMC5/6 subunits and two novel proteins were identified as significantly enriched in the bait cell line (p-value < 0.05). One of the proteins identified as significantly enriched in the bait cell line, (p-value $= 0.033$) was a protein encoded by the BCSL1L gene (Figure 4.10 C). Based on the Uniprot database, this protein is a mitochondrial chaperone involved in the assembly of mitochondrial respiratory chain complex III, its localisation is exclusively mitochondrial. Considering that the SMC5/6 complex has entirely nuclear localisation, this hit is likely to be an artefact, or reflects the variability in proteomes of the bait and the control cell line. Another protein identified using p-value as a significant hit was G3BP2 (p-value $= 0.042$). This protein is a scaffold protein that plays an essential role in cytoplasmic stress granule formation. Since G3BP2 protein has cytoplasmic localisation, it is also likely to be a false positive hit. Furthermore, equally to the bait cell line, there were proteins significantly enriched in the control cell line over the bait cell line, such as WDR33 (p-value $= 0.048$)

A



B

Gene names	Student's T-test (Bait – Control 2h HU) Benjamini-Hochberg FDR correction			
	-Log p	q-value	Difference	Statistic
SMC6	5.50	0.002	5.48	37.12
SMC5	3.74	0.046	4.20	13.37

C

Gene names	Student's T-test (Bait – Control 2h HU)		
	-Log p	Difference	Statistic
SMC6	5.50	5.48	37.12
SMC5	3.74	4.20	13.37
NSMCE3	3.45	3.11	11.23
NSMCE4a	2.76	4.90	7.45
NSMCE2	2.58	1.77	6.68
NSMCE1	2.57	2.31	6.62
BCS1L	1.48	0.45	3.20
G3BP2	1.38	0.73	2.95

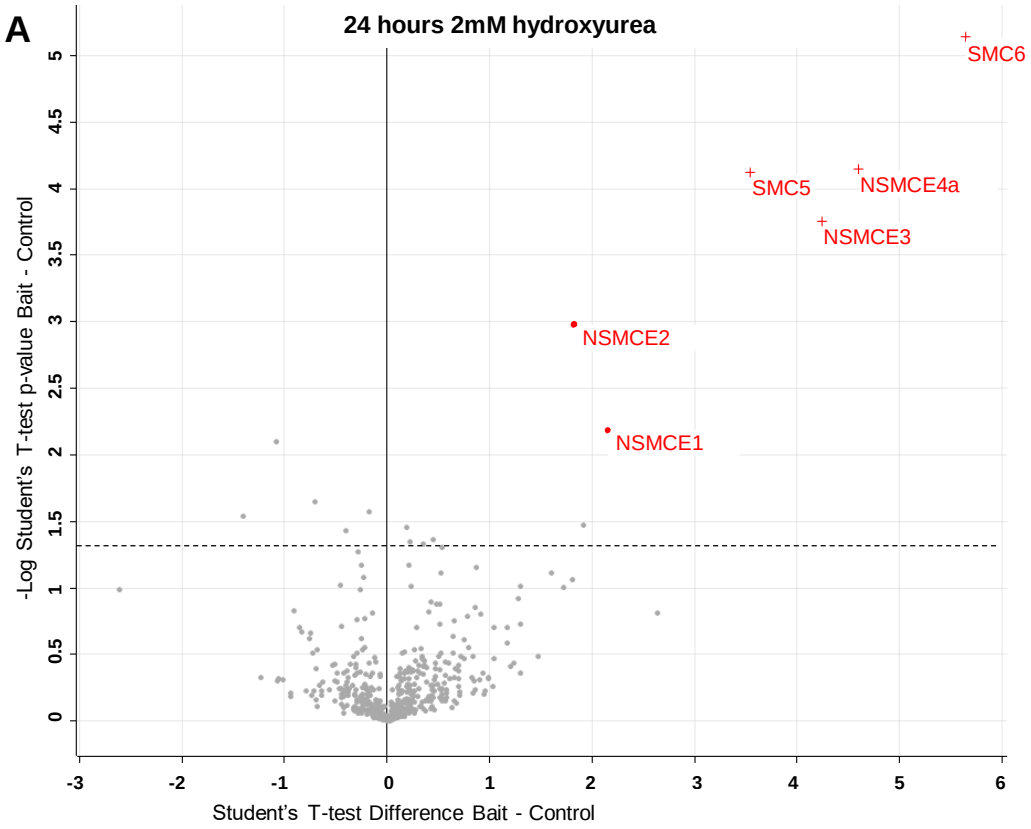
Figure 4.10: Analysis of NSMCE4a interactors after 2 hrs of HU treatment
A. Volcano plot of statistical significance versus fold change of protein hits identified by MaxQuant search against human database in control and bait cell lines, all identified hits are represented by filled dots, statistically significant hits (FDR correction) are represented by red cross, In red are SMC5/6 components; x axis shows Student's t-test difference of bait/control, dashed line: p-value = 0.05; Perseus (ver. 1.6.1.1) platform was used for statistical analysis. **B.** Statistically significant hits identified by Student's T-test after Benjamini-Hochberg FDR correction (FDR = 0.05). **C.** Statistically significant hits identified in the bait cell line by Student's T-test without FDR-correction. **B – C.** -Log p: $-\text{Log}_{10}$ of p-value, q-value: FDR adjusted p-value, Difference: value of Student's T-test difference of Bait/Control, Statistic: Student's T-test statistic value.

or LRPAP1 (p-value = 0.013) (Table A.7). Hence, it is likely that the label free approach experiment performed in only three biological replicates was not robust enough to identify any known or novel interactors of the SMC5/6 complex.

4.3.4.4 Searching for NSMCE4a interactors after replication fork collapse

To identify the interactors of the SMC5/6 complex upon replication fork collapse (24 hours treatment with 2mM Hydroxyurea), the MaxQuant search results were statistically analysed in Perseus in a fashion analogous to the one performed for replication fork stalling. Briefly, the triplicate data were filtered from potential contaminants, reverse proteins and the proteins that are only identified by site. Proteins with a minimum of two valid LFQ intensities in at least one categorically annotated group (Bait/Control) were kept for the downstream analysis. Statistically significant hits were identified by two-sample Student's T-test with Benjamini-Hochberg FDR, as well as by p-value without FDR corrections. The results of the statistical analysis are listed in the appendix (Table A. graphically depicted in a volcano plot (Figure 4.11 A). Statistically significant hits using Benjamini-Hochberg correction are listed in a table (Figure 4.11 B). After the FDR correction, the statistically significant interactors were SMC5, SMC6 and NSMCE3. Similarly to the non-treated and 2h hydroxyurea treated samples, there were no significant interactors other than the complex components when the FDR correction was applied. When only the p-value cut-off was used ($p < 0.05$), the other complex components, NSMCE1 and NSMCE2, as well as other potential hits, were identified (Figure 4.11 C). After the SMC5/6 components, the protein with the lowest p-value was a cytosolic protein FBXO21 (p-value = 0.034). This protein is a mostly uncharacterised substrate-recognition component of the SKP1-CUL1-F-box protein-type E3 ubiquitin ligase complex. Another protein within the p-value range was PABPC4 (p-value = 0.035), a cytoplasmic protein that binds the poly(A) tail of mRNA and might be involved in cytoplasmic regulatory processes of mRNA metabolism.

Next potential hit was CSNK2A2 (p-value = 0.044), which is a catalytic subunit of a casein kinase 2. Casein kinase 2 is a serine/threonine-protein kinase complex with both nuclear and cytoplasmic localisation. This protein kinase is involved in many processes, such as regulation of cell cycle progression, apoptosis (reviewed in: Litchfield, 2003). The activity of Casein kinase 2 holocomplex (CK2) is stimulated upon herpes simplex virus type-1 infection (Koffa et al., 2003). Furthermore, the CK2 holoenzyme might



B

Gene names	Student's T-test (Bait – Control 24hHU) Benjamini-Hochberg FDR correction			
	-Log p	q-value	Difference	Statistic
SMC6	5.14	0.003	5.64	30.18
NSMCE4a	4.15	0.017	4.6	16.93
SMC5	4.13	0.012	3.54	16.73
NSMCE3	3.76	0.021	4.24	13.48

C

Gene names	Student's T-test (Bait – Control 24hHU)		
	-Log p	Difference	Statistic
SMC6	5.14	30.18	30.18
NSMCE4a	4.15	16.93	16.93
SMC5	4.13	16.73	16.73
NSMCE3	3.76	13.48	13.48
NSMCE2	2.98	8.49	8.49
NSMCE1	2.19	5.2	5.2
FBXO21	1.47	3.18	3.18
PABPC4	1.45	3.13	3.13
CSNK2A2	1.36	2.92	2.92
SMARCA4	1.35	2.88	2.88
TUBG1;TUBG2	1.33	2.84	2.84
GIT1	1.30	2.78	2.78

Figure 4.11: Analysis of NSMCE4a interactors after 24 hrs of HU treatment
A. Volcano plot of statistical significance versus fold change of protein hits identified by MaxQuant search against human database in control and bait cell lines, all identified hits are represented by filled dots, statistically significant hits (FDR correction) are represented by red cross, x axis shows Student's t-test difference of bait/control, Perseus (ver. 1.6.1.1) platform was used for statistical analysis, dashed line: p-value = 0.05. **B.** Statistically significant hits identified by Student's T-test after Benjamini-Hochberg FDR correction (FDR = 0.05). **C.** Statistically significant hits identified in the bait cell line by Student's T-test without FDR-correction. **B – C.** -Log p: $-\text{Log}_{10}$ of p-value, q-value: FDR adjusted p-value, Difference: value of Student's T-test difference of Bait/Control, Statistic: Student's T-test statistic value.

stimulate viral replication by phosphorylation of viral proteins in hepatitis B virus (HBV) infected cells (Enomoto et al., 2006). The fact that the human SMC5/6 complex has recently been identified as a restriction factor of HBV (Abdul et al., 2018; Decorsière et al., 2016) might link the SMC5/6 and CK2 to the HBV pathway during infection. Another potential NSMCE4a interactor with a significant p-value was SMARCA4 (p = 0.045), an ATP-dependent DNA helicase, which is a part of the SWI/SNF chromatin remodelling complex (reviewed in: Hargreaves and Crabtree, 2011). It is a nuclear protein with chromatin remodelling activity involved in promotor activation and regulation of gene expression. SMARCA4 has also been shown to be mutated in different cancer cell lines, is therefore being identified as a tumor suppressor gene (Wong et al., 2000). These two potential interactors of the SMC5/6 seem plausible in order to exclude the possibility that they are false positive hits, they would have to be validated by other biochemical assays.

Two more proteins were identified within the range of p-value, GIT1 (p-value = 0.05) and TUB1/2 (p-value = 0.047). GIT1 is a mostly uncharacterised zinc-finger containing protein with a role in cell motility. TUBG1/2 is a gene encoding gamma tubulin, a main part of cytoskeleton, which is localised in the cytoplasm. Therefore, these two hits are likely to be false positives.

4.3.5 Purification of SMC5/6 from chromatin fraction

Mass spectrometry analysis of NSMCE4a pull down from solubilised fraction did not reveal any strong interactor of SMC5/6 (Figure 4.7). However, we noticed that almost the same amount of the SMC5/6 complex, still remains insoluble fraction after 1 hour of DNA digestion with benzonase, which was used in all the aforementioned protocols for SMC5/6 purification (Figure 4.7 A 4.9 A). Therefore, most of the chromatin bound SMC5/6 in the input fraction might have been excluded from the purification. Moreover, SMC5/6 is a DNA binding protein and its function is likely to be executed when bound to chromatin. It is therefore plausible that most of the protein interactions of the SMC5/6 complex occur while the SMC5/6 is bound to DNA. Hence, we aimed at specifically purifying chromatin bound SMC5/6 to search for its interactors. In order to preserve endogenously occurring interactions, we initially decided to perform chromatin fractionation upon native conditions. Eventually, a cross-linking protocol coupled with purification of SMC5/6 upon denaturing conditions was attempted.

4.3.5.1 Optimisation of chromatin fractionation

At first, a protocol for chromatin fractionation had to be optimised. For each of four different conditions (without fractionation (w/o) and fractionation A - B), approximately 2 x 10^7 cells were used. Chromatin fractionation was performed by lysis of cells on ice with a standard lysis buffer, supplemented with protease and phosphatase inhibitor cocktail, for 45 minutes on ice. Afterwards, the lysate was spun 45 minutes 16 000 x g at 4°C. The supernatant was removed and stored for western blot analysis (Soluble fraction). The pellet, which contained chromatin fraction, was subjected to 1:300 benzonase treatment upon various conditions; as a default condition to compare the optimisation steps with, the whole cell extract without chromatin fractionation was digested with 1:300 benzonase for 45 minutes on ice (w/o). Even though benzonase is effective under large temperature range (0 – 42°C), its optimal performance is at 37°C. However, high temperature leads to proteolytic degradation of proteins, including the purified protein of interest. Therefore, in condition A, the chromatin fraction was subjected to 10 minutes digestion at 37°C, followed by 45 minutes digestion on ice. In condition B, the isolated chromatin fraction was subjected to 45 minutes digestion on ice, similarly to the standard protocol. In condition C, the chromatin fraction was subjected to an overnight benzonase digest at 4°C on rotation wheel. The efficiency of benzonase digestion was assessed by analysis of the size of digested DNA fragments on an agarose gel (Figure 4.12 B). The results revealed that for condition A and B, the benzonase digest was the same efficient as for the non-fractionated sample (w/o), the majority of DNA fragments ranged from 200 to 1000 bp (Figure 4.12 B, lane 1 – 3). DNA digestion was not substantially improved by additional pre-incubation at 37°C (Figure 4.12 B, lane 2). However, overnight incubation with benzonase at 4°C improved the efficiency of the DNA digest. No DNA fragments were observed between 200 – 1000 bp, this implies that the DNA in the sample was degraded into nucleotides (Figure 4.12 B, lane 4). Chromatin fractionations prepared by different benzonase digests were analysed by western blotting (Figure 4.12 C). As a comparison to fractionation protocols, the non-fractionated sample was analysed in parallel (Figure 4.12 C, w/o). Histone H1.2 was used as a marker for the chromatin fraction, tubulin as a marker of the cytosolic (soluble) fraction. When using the whole cell extract is digested by benzonase (non-fractionation protocol), comparable amount of SMC5 and NSMCE4a are in the soluble and insoluble (pellet) fraction (Figure 4.12 C, lane 1, 2). After separation the chromatin fraction, substantial amount of NSMCE4a and

SMC5 was present in the cytosolic and soluble nuclear fraction (Figure 4.12 C, lane 3). In order to get rid of cytosolic and other non-specifically bound soluble proteins, the chromatin fraction was washed twice in 0.3 ml of lysis buffer and spun for 4 minutes 16 000 x g at 4°C. Each wash fraction was analysed by western blot (Figure 4.12 C, lane 4, 5). The washed chromatin fraction was digested by benzonase in lysis buffer (1:300) under the three different conditions described above for DNA digestion. The digested chromatin fraction was spun 15 minutes at 16 000 x g at 4°C, the supernatant fraction contained chromatin, which was solubilised (release) (Figure 4.12 C, right panel, lane 1 - 3). Western blot analysis revealed that the most SMC5 and NSMCE4a was released from chromatin after 45 minutes benzonase digestion on ice (condition B). However, in all three conditions, most chromatin remained insoluble after benzonase digestion, thus, most SMC5 and NSMCE4a remained insoluble (Figure 4.12 C, right panel, lane 4 – 6).

4.3.5.2 Pull down of chromatin released SMC5/6 using IMAC

Despite the fact that only a minor fraction of SMC5 and NSMCE4a was solubilised using the chromatin fractionation and benzonase digestion, affinity purification of NSMCE4a from the solubilised chromatin fraction was tested. The input amount of cells was up-scaled to approximately 3.5 x 107 for both bait and control cell line, to provide enough starting material for NSMCE4a pull down from solubilised chromatin. Cells from each cell line were lysed in 0.6 ml of lysis buffer for 45 minutes on ice. After the chromatin fraction was separated from the cytoplasmic and soluble nuclear fraction by centrifugation for 45 minutes at 16 000 x g, 4°C. Chromatin was washed twice in 300 µl of lysis buffer before being re-suspended in (1:300) benzonase in 300 µl lysis buffer, chromatin was digested for 45 minutes on ice. To check the efficiency of benzonase digest, isolated chromatin before and after benzonase digestion was collected and separated on 1% agarose gel. Figure 4.13 B shows that the average DNA fragments after benzonase digestion ranged from 100 – 1000 bp (lane 2). The solubilised fraction (release) was separated from the non-digested chromatin by centrifugation at 15 minutes at 16 000 x g, 4°C. Each fraction of the chromatin fractionation steps was analysed by western blotting (Figure 4.13 A).

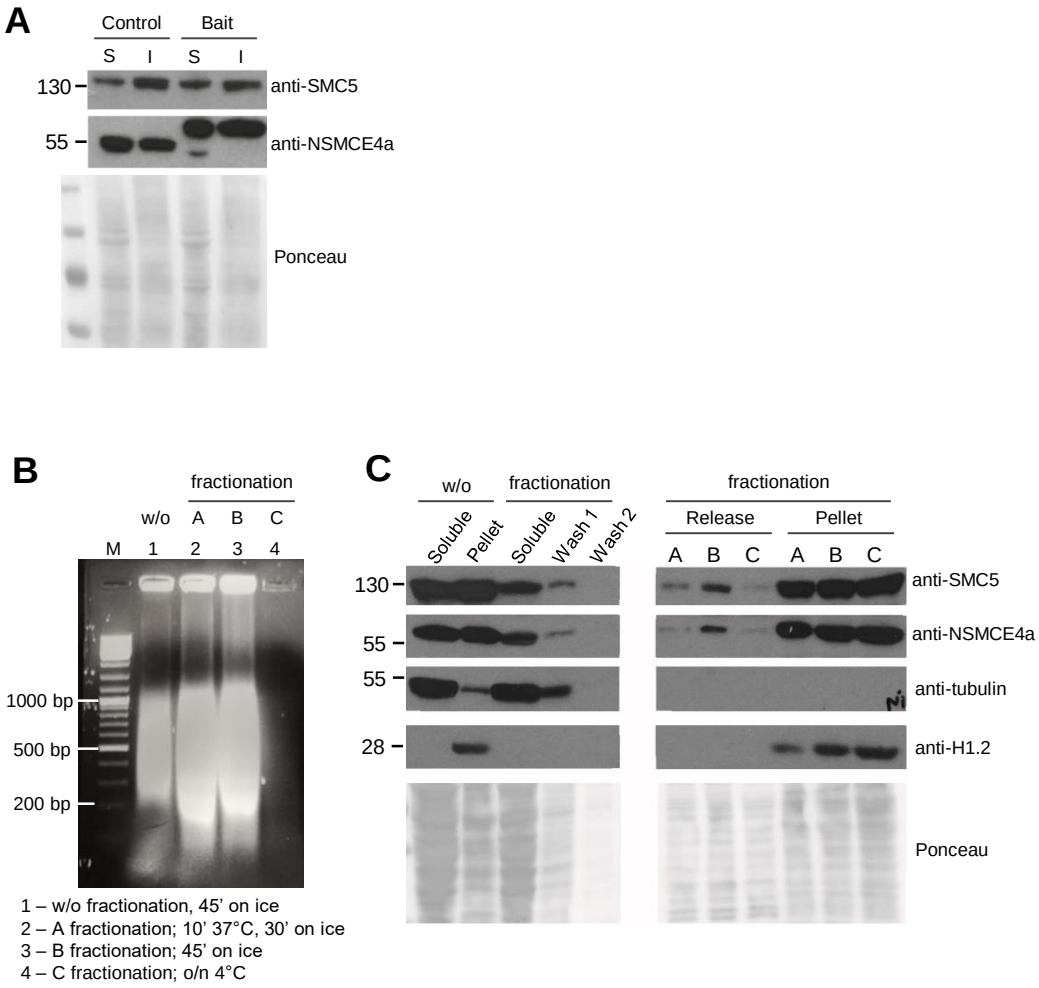


Figure 4.12: Chromatin fractionation for purification of chromatin bound SMC5/6 A. Example of western blot showing the amount of SMC5/6 subunits (NSMCE4a and SMC5) in a fraction solubilised after 45 minutes digestion with 1:300 benzonase in lysis buffer (S) and the pelleted insoluble fraction (I). **B.** DNA gel showing the efficiency of benzonase digest upon different conditions; w/o fractionation: standard protocol, cells were lysed the whole cell extract was digested for 45' with 1:300 benzonase in lysis buffer, A: chromatin fraction digested with 1:300 benzonase in lysis buffer for 10 minutes at 37°C, followed by 30 minutes on ice digestion, B: chromatin fraction digested with 1:300 benzonase in lysis buffer for 45 minutes on ice, C: chromatin fraction digested with 1:300 benzonase in lysis buffer overnight at 4°C with end-to-end rotation, 10% of the sample was loaded per lane. **C.** Western blot showing different fractions during chromatin fractionation protocol; left panel, lane 1 – 2 shows content of SMC5 and NSMCE4a in soluble fraction and pellet without fractionation (w/o), 4% of sample loaded per lane; left panel, lane 3 – 5 shows content of SMC5 and NSMCE4a in soluble fraction after separation of chromatin fraction (lane 3, soluble) and in two chromatin fraction washes (wash 1 and 2), 4% of soluble and 2% of the wash was loaded per lane; right panel, chromatin fraction digested by benzonase, western blot to show content of SMC5 and NSMCE4 in supernatant fraction (release A - C) and pellet fraction after benzonase digestion (pellet A – C), 8% of each fraction (release and pellet) was loaded per lane; for each well, tubulin marks soluble/cytosolic fraction, histone1.2 (H1.2) marks chromatin fraction.

Western blot results revealed that the developed fractionation protocol led to partial solubilisation of chromatin bound SMC5 and NSMCE4a in both bait and control cell line (Figure 4.13 A, Release). The protein amount in the solubilised chromatin fraction (release) was determined by Bradford assay. The input amount of protein used for IMAC pull down was approximately 980 µg. Before binding to the IMAC column, the imidazole concentration was adjusted to 10mM and the fraction was incubated with equilibrated TALON beads for 1 hour. After that, two consecutive elutions with 60 and 150mM imidazole were performed. To monitor the amount of non-specific binding of SMC5 and NSMCE4a to the IMAC column, the TALON beads were boiled in 1 x SDS sample buffer for 5 minutes. Figure 4.13 C shows that the NSMCE4a antibody failed to detect NSMCE4a in the input fraction of the bait cell line (Figure 4.13 C, lane1). This was presumable caused by the amount of NSMCE4a protein being below the antibody detection limit. This is further supported by the observation of a weak signal of NSMCE4a was observed in the Beads fraction (boiled TALON beads). Since the beads were boiled in half of the buffer volume of the input (release), this could explain why reduction of the buffer volume increases the protein concentration, allowing its detection by antibody (Figure 4.13 C, lane 4). However, no NSMCE4a was detected in any of the elution fractions of the bait cell line. On the other hand, the SMC5 was detected by antibody in the Release fraction of the bait cell line. However, as for the NSMCE4a, no SMC5 was observed in any of the imidazole elutions (Figure 4.13 C, lane 2, 3). However, SMC5 was detected in both cell lines after boiling the TALON beads in SDS sample buffer (Figure 4.13, lane 4, 8). These results indicate that: (i) the amount of NSMCE4a and SMC5 in imidazole elutions was below the antibody detection limit or (ii) most of the NSMCE4a and SMC5 released from chromatin fraction bound non-specifically to the TALON column and therefore we failed to recover the proteins by imidazole elution, alternatively (iii) DNA bound NSMCE4a-Strep-6xHis is not able to specifically bind the TALON column due to steric hindrance created by SMC5/6 interaction with DNA. We conclude that even though we were able to partly solubilise chromatin bound SMC5/6 (Figure 4.10 C, 4.11 A) the attempt to purify chromatin bound SMC5/6 by NSMCE4a-Strep-6xHis using IMAC was not successful. Assuming that NSMCE4a-Strep-6xHis in the chromatin bound SMC5/6 complex can bind the TALON column, an alternative would be to further upscale the number of cells to gain more solubilised chromatin fraction. Higher yield of solubilised SMC5/6 could improve the specific binding to TALON column. However, due to time constrains further optimisation steps were not performed.

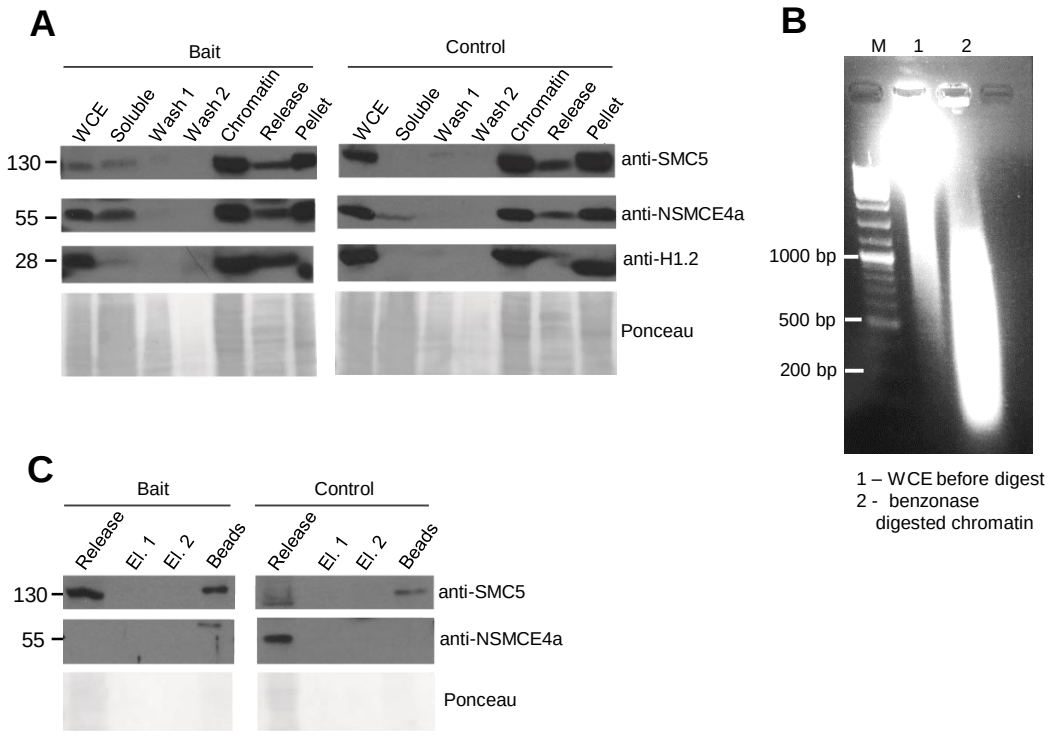


Figure 4.13: Purification of SMC5/6 from chromatin fraction by NSMCE4a-Strep-6xHis using IMAC

A. Western blot showing fractions of chromatin fractionation, WCE: whole cell extract before fractionation, Soluble: cytosolic and soluble nuclear fraction after cell lysis, Wash 1 and 2: supernatant after wash of chromatin fraction with lysis buffer, Chromatin: purified chromatin fraction, Release: soluble fraction after chromatin digestion by benzonase, Pellet: insoluble fraction after benzonase digest, WCE and Soluble: 1.7% of sample loaded per lane, for the rest of fractions, 3.3% of the sample was loaded per lane, histone H1.2 was used as a marker of chromatin fraction. **B.** DNA gel showing the size of DNA fragments after benzonase digestion of chromatin fraction, 2.5% of sample per lane was loaded onto 1% agarose. **C.** Affinity purification of NSMCE4a-Strep-6xHis released from chromatin fraction using TALON column, Release: solubilised chromatin fraction from (A), El.1: elution with 60mM imidazole, El.2: elution with 150mM imidazole, Beads: TALON beads boiled for 5 minutes in 1 x SDS sample buffer, 3.3% of Release fraction and 6.7% of El.1, El.2 and Beads was loaded per lane.

4.3.5.3 Pull down of chromatin bound SMC5/6 using StrepTactin magnetic beads

After the attempt to purify SMC5/6 from chromatin fraction by the His tag on IMAC column failed, purification of the SMC5/6 complex from chromatin fraction was attempted using the Strep tag. Chromatin fractionation was performed using the aforementioned optimised protocol (Figure 4.13 A). The input amount of cells was approximately 6 x 10^7 cells. The amount of protein in solubilised chromatin fraction was determined by Bradford assay and approximately 1.1 mg of solubilised proteins was added to 30 µl of equilibrated StrepTactin beads (1.5 µl bed volume) and bound for 30 minutes with end-to-end rotation at 4°C. Beads were washed in 5 x column volume of wash buffer and elution under denaturing conditions (boiling in 1 x SDS sample buffer) was performed. Each fraction was analysed by western blotting probing for NSMCE4a and SMC5 (Figure 4.14 A). Only minimal signal of SMC5 was detected in the solubilised chromatin fraction (release) in both control and bait cell line. This could, however, be caused by the SMC5 concentration being under the detection limit of the SMC5 antibody (Figure 4.14 A, upper panel, Release). On the other hand, NSMCE4a was detected in solubilised fraction in both bait and control cell line (Figure 4.14 A, middle panel, Release). However, the solubilised NSMCE4a-Strep-6xHis did not bind the StrepTactin beads, as all the NSMCE4a was detected in the flow through fraction (Figure 4.14 A, middle panel, FT). None of the NSMCE4a was detected in the boiled beads fraction (Figure 4.14 A, middle panel, Beads). The results imply that despite the fact that the solubilisation of chromatin bound SMC5 and NSMCE4a was successful, the Strep tagged NSMCE4a does not specifically bind the StrepTactin beads. Based on the observations that chromatin bound SMC5/6 binds neither the TALON, nor the StrepTactin column, we can speculate that chromatin bound SMC5/6 does not allow the C-terminally tagged NSMCE4a binding to the affinity columns.

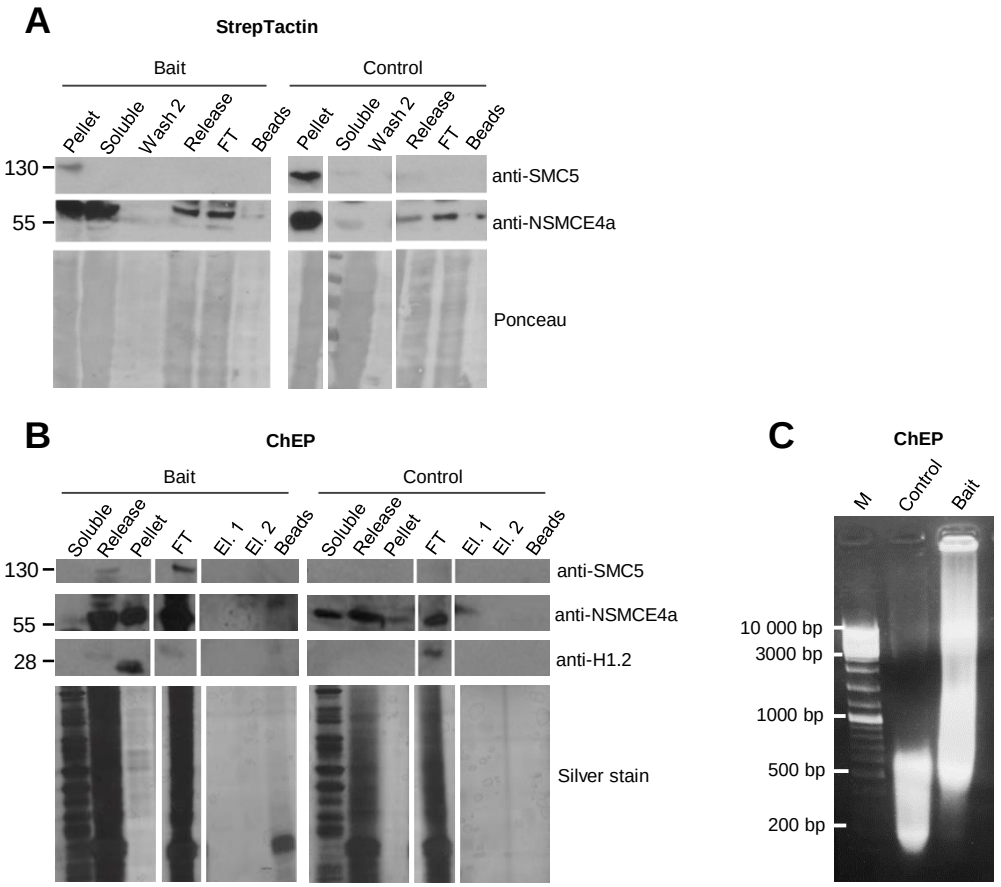


Figure 4.14: Pull down of SMC5/6 using StrepTactin beads and purification of SMC5/6 from chromatin fraction using cross-linking (ChEP) protocol

A. Western blot showing chromatin fractionation to solubilise SMC5/6 and affinity purification of SMC5/6 by NSMCE4a-Strep-6xHis using StrepTactin beads; Pellet: Chromatin fraction before benzonase digestion, Soluble: soluble nuclear and cytosolic fraction, Wash 2: second wash of chromatin fraction in lysis buffer before benzonase digestion, Release: solubilised chromatin fraction after benzonase digestion, FT: flow through after incubation of solubilised chromatin with StrepTactin beads, Beads: elution fraction, boiled StrepTactin beads in 1 x SDS buffer; 1.7% of pellet, soluble and wash fraction, 3.3% of release and flow through (FT) and 25% of elution (Beads) was loaded per lane. **B.** Chromatin enrichment for proteomics (ChEP) coupled with NSMCE4a-Strep-6xHis pull down using IMAC column, Soluble: supernatant fraction after nuclear isolation, Release: solubilised chromatin fraction after sonication, Pellet: insoluble chromatin fraction after sonication, FT: flow through, unbound proteins after incubation with IMAC TALON column, El.1: elution by 60mM imidazole, El.2: elution by 150mM imidazole, Beads: boiled TALON beads in 1 x SDS sample buffer. **C.** DNA gel showing fragmented DNA of control and bait cell line (B) after sonication, DNA was separated on 1% DNA gel.

4.3.5.4 Chromatin fractionation using chromatin enrichment for proteomics

After the unsuccessful attempts to purify chromatin bound SMC5/6 under native conditions, an attempt was made to purify chromatin bound SMC5/6 under denaturing conditions. For that reason, we decided to follow a recently developed protocol for chromatin enrichment for proteomics (ChEP) (Kustatscher et al., 2014). This method allows to take a 'snapshot' of chromatin and identify even transiently bound factors. In principal, it utilises *in vivo* cross-linking of chromatin bound proteins to DNA by formaldehyde. The purpose of cross-linking is to covalently link proteins that bind directly and indirectly to DNA. After cross-linking step, cells are lysed and digested nuclei are thoroughly washed under strong denaturing conditions, in order to remove all unbound proteins. This protocol has originally been developed for SILAC applications comparing two states of chromatin (treated/non-treated). Nevertheless, we attempted to use this protocol for affinity purification of SMC5/6 and its interactors. As a starting material, approximately 3 x 10^7 cells (2 x 15 cm dishes) for each cell line was used. Formaldehyde cross-linked cell pellets were subjected to cell lysis and RNAse A digestion, after which the nuclei were separated from the soluble cytosolic fraction. The isolated nuclei were then lysed and chromatin fraction was repeatedly washed in 8M Urea buffer, followed by second wash in Urea buffer mixed with 4% SDS buffer in order to remove non-specifically bound proteins. Additional wash in 4% SDS buffer was carried out, to remove the residual urea. In order to get rid of SDS prior to binding step, cross-linked chromatin was washed twice in storage buffer (for details see Materials and Methods section), afterwards, the chromatin was sonicated to fragment the DNA. The size of the DNA fragments after sonication was visualised by separation on a DNA gel (Figure 4.14 C). The size of DNA fragments in the control cell line was in relatively narrow range, from 100 – 600 bp, whereas the size of DNA fragments of the bait cell line varied from 500 - 10 000 bp with a substantial fraction of non-fragmented DNA. This huge variability within the samples was likely due to variability in the input cell amount; the amount of cells in the bait sample was higher and this could have lowered the sonication efficiency. The sonicated sample was spun and the supernatant, containing sheared, cross-linked DNA, was subjected to binding step using equilibrated TALON beads. Two elutions steps, using 60mM and 150mM imidazole were performed. 1 x SDS sample buffer was added to the TALON beads and all analysed fractions were boiled for 30 minutes to de-crosslink the formaldehyde-stabilised interactions. Each fraction was

subjected to a western blot analysis probing for NSMCE4a and SMC5, as well as to silver staining to assess the purity and protein yield (Figure 4.14 B). The western blot results revealed that the chromatin solubilisation was efficient; in the bait cell line, approximately equal amount of NSMCE4a and most of SMC5 was solubilised by sonication (Figure 4.14 B, lane 2, 3). In the bait cell line, most of the chromatin was not solubilised, indicated by the presence of histones (H1.2) in the pellet fraction (Figure 4.14 B, lane 3). In the control cell line, presumably due to less cells in the input, most of the chromatin-bound NSMCE4a was solubilised (Figure 4.14 B, lane 9). No SMC5 was detected in the control cell line by western blotting, likely due to the SMC5 amount being below the detection limit of the antibody. However, no NSMCE4a or SMC5 was detected in the imidazole or 1 x SDS sample buffer elutions (Figure 4.14 B, lane 5 – 7). High amount of NSMCE4a and SMC5 was present in the flow through fraction of the bait cell line (Figure 4.14 B, lane 4). This indicates that the NSMCE4a-Strep-6xHis was not binding to the TALON column under cross-linking conditions. Together, these experiments reveal that we are able to solubilise the chromatin bound NSMCE4a using the *in-vivo* cross-linking ChEP protocol. However, the cross-linking is likely to interfere with binding of NSMCE4a-Strep-6xHis to the TALON column. Therefore, the chromatin enrichment for proteomics (ChEP) protocol cannot be used for affinity purification of NSMCE4a-Strep-6xHis using IMAC TALON column.

4.3.6 SILAC

Another possibility to gain more quantitative and accurate identification of SMC5/6 protein interactors can be the usage of Stable-Isotope Labelling with Amino acids in tissue Culture (SILAC). This method provides more quantitative information about the identified proteins. Since SILAC utilises metabolic labelling, the potential error stemming from multiple-steps during the MS sample preparation is minimised. Therefore, we decided to use SILAC to get better quantitative resolution of SMC5/6 interactors. Due to time constrains only one biological repeat of the SILAC experiment was performed and analysed. Briefly, 5 x 15 cm dishes (7.5 x 10^7 cells) with either bait or control cells were grown over 5 generations in media containing either light (L, L-lysine ^{12}C/L-Arginine ^{12}C) or heavy (Heavy, L-lysine ^{13}C/L-Arginine ^{13}C) amino lysine and arginine. Cell culture was either non-treated (NT) or treated with 2mM Hydroxyurea for 2 or 24 hours. When being harvested, the cells were counted and similar amount of control and bait cells

was mixed together and snap frozen. Samples were stored in -80°C until the affinity purification was performed. The input amount of WCE in each reaction was 40 mg of protein for non-treated, 20 mg for 2h and 30 mg for 24h hydroxyurea treated cells. The pull down experiment was performed using TALON IMAC column, the bed volume of TALON beads was 150 µl. Each pull down fraction was analysed by western blotting (Figure 4.15). After the binding step, a pre-elution step was performed with 50mM imidazole (Elution 1). To maximise the yield of the SMC5/6 complex, additional third elution under denaturing conditions was included; after elution with 150mM imidazole, the SMC5/6 was eluted in 150mM imidazole buffer containing 2% of SDS. The highest amount of SMC5 and NSMCE4a was present in the second and third elution (Figure 4.15, El.2, El.3). This way the majority of SMC5/6 was recovered from the TALON beads. The elution fractions 2 and 3 were sent off to a mass spectrometry facility (University of Oxford) to be digested and subjected to mass spectrometry. The peptide search was performed using MaxQuant, The search parameters and list of search results are listed in the appendix (Table A.9). However, due to the lack of biological repeats, the SILAC search results can only be compared by difference in H and L intensities.

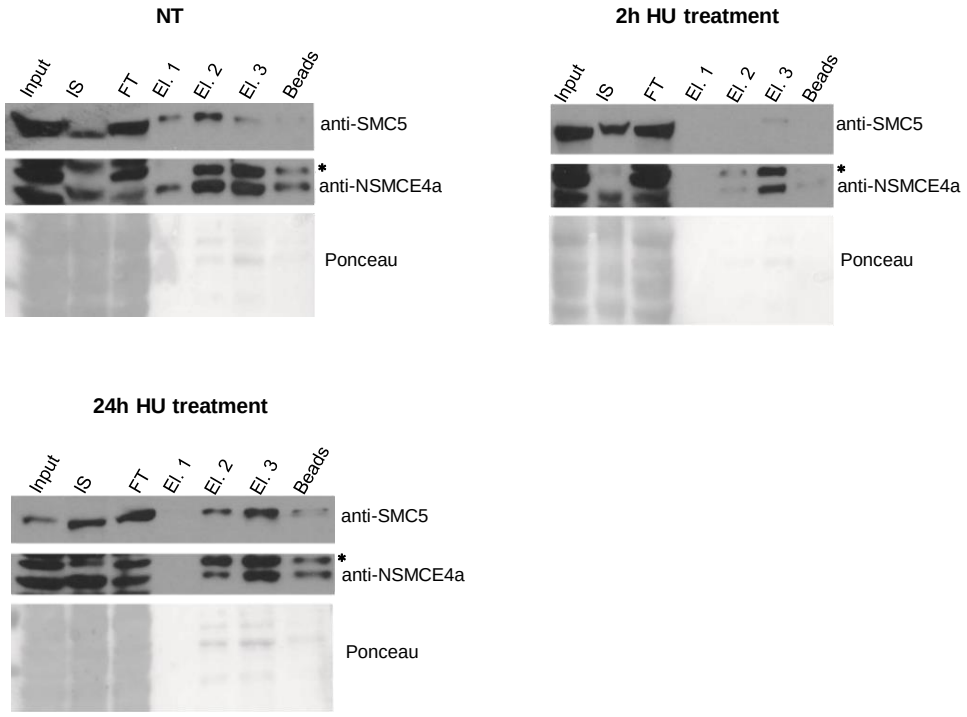


Figure 4.15: Affinity purification of NSMCE4a using TALON after SILAC
Western blot showing different fractions of affinity purification of NSMCE4a-Strep-6xHis after SILAC using TALON column, the second (El.2) and third elution (El.3) were send off for bottom-up proteomics and mass spectrometry analysis using Q Exactive Hybrid Quadrupole-Orbitrap (Thermo Scientific) instrument at TDI Mass Spectrometry Laboratory (University of Oxford); Input: soluble fraction after 1 hour benzonase digest, IS: insoluble fraction after benzonase digest, FT: flow through, El.1: elution with 50mM imidazole, El.2: elution with 150mM imidazole, El.3: Beads: elution with 150mM imidazole with 2% SDS, Beads: TALON beads boiled in 1 x SDS sample buffer, each lane contains 0.33% of total 3000 µl Input, IS and flow FT fraction and 3.3% of elutions (El.1/El.2/El.3) and Beads.

4.4 Discussion

The aim of this chapter was to use the created T-REx Flp-In 293 isogenic cell lines to affinity purify the tagged NSMCE4a subunit and couple the purification with mass spectrometry analysis to search for interactors of the SMC5/6 complex. The NSMCE4a protein was C-terminally tagged with Strep and 6 x Histidine tag. Western blot assays demonstrated successful recovery of SMC5 by IMAC affinity purification using 6 x His tag of NSMCE4a-Strep-6xHis. Initial mass spectrometry results revealed that the whole SMC5/6 complex is recovered by purification of NSMCE4a on IMAC column using 6 x His tag. However, affinity purification using 6xHis-tag in mammalian systems often results in high background, due to high abundance of histidine rich proteins in mammalian cells. Therefore, we aimed to use both purification by 6 x His tag as the first step and increase the purity of the SMC5/6 complex by introducing the second purification step on StrepTactin matrix. The mass spectrometry results of the on-bead digested purified fraction, did not lead to a substantial improvement in the SMC5/6 yield to purity ratio, in comparison to a single step purification using IMAC (Figure 4.5). Despite multiple attempts to optimise the SMC5/6 purification method, we failed to gain high yield and purity of the complex. Purification of the SMC5/6 complex has been reported to be challenging by different labs (O. Wells and K. Zabrady, personal communication). This is likely to be due to its relatively low abundance in cells, as well as the large size of the coiled coil SMC5 and SMC6 arms, which is likely to make them prone to non-specific binding. Another option to improve the SMC5/6 purification would be re-tagging of the NSMCE4a with a different affinity tag, such as Flag, and optimisation of the new purification protocol. Despite the low yield of the SMC5/6 complex and high amount of contaminant proteins, we were able to identify the complex and some of its potential interactors by the optimised purification protocol (Figure 4.7, 4.9 and 4.10). However, the potential interactors were identified only by the p-value cut-off, without an FDR correction. These hits should, therefore, be further validated by other biochemical, genetic or *in vitro* assays. Using the currently optimised label-free approach coupled with mass spectrometry analysis and MaxQuant search can be used to identification of potential interactors of the SMC5/6 complex; the statistical significance of potential interactors could be increased by introducing more biological replicates to enable more robust statistical analysis.

More quantitatively accurate approach to search for the SMC5/6 interactors is SILAC, however, due to time constrains, only one biological repeat of a SILAC experiment was carried out. This experiment provides a preliminary data set, where the potential SMC5/6 interactors can be the proteins with higher light than heavy intensity.

An alternative possibility to search for the SMC5/6 interactors would be the use of a BioID approach. This method involves a proximity ligation with a promiscuous biotin ligase enzyme fused to the bait protein. The ligation reaction can be specifically induced and enables identification of transient, as well as more stable protein interactors *in vivo* over a defined period (hours). Biotinylated proteins (potential interactors) are then selectively affinity purified by streptavidin capture and subjected to mass spectrometry. Exchange of the genome-inserted NSMCE4a-Strep-6xHis with BioID tagged NSMCE4a should be fast and simple by constructing a BioID tagged NSMCE4a cassette and exchange the Hygromycin resistance marker in the pcDNA5/TO with a different selection marker. A caveat of the BioID approach is to distinguish direct physical interactors from proteins that are only in the proximity of the bait protein. Therefore, it would be ideal to compare the BioID approach with a standard affinity purification method.

Based on the fission yeast data obtained by single-molecule microscopy (T. Etheridge, unpublished data), we hypothesised that during an unperturbed cell cycle, the majority of the SMC5/6 complex is not bound to DNA. Since the SMC5/6 is thought to execute its function when bound to DNA, most of the protein interactions are likely to occur when the complex is chromatin-bound. Therefore, we attempted to purify the SMC5/6 specifically from chromatin fraction, both under native conditions and upon denaturing conditions after cross-linking. Unfortunately, under native conditions we failed to solubilise enough SMC5/6 from chromatin fraction to be able to recover detectable amount by IMAC pull down (Figure 4.14 C). The alternative would be to upscale the input cellular material for chromatin fractionation, which would however increase the cost of the method. On the other hand, purification of chromatin bound NSMCE4a-Strep-6xHis upon denaturing conditions after cross-linking did not allow the binding of the 6 x His tag on C-terminus of NSMCE4a to the IMAC column, likely due to modification of the tag structure by the cross-linking reagent.

5 Chapter 5

Results III

Characterisation of the NSMCE4a shut off and its effects on genome stability

5.1 Introduction

The first results chapter described the construction and initial characterisation of a regulatable NSMCE4a knock out cell line (-/-;NSMCE4a), where the only functional NSMCE4a copy is the regulatable FRT-inserted NSMCE4a gene. The whole system operates as an inducible system (Tet-ON), where the expression of the FRT-inserted NSMCE4a is induced by Tetracycline, or by its more stable analogue Doxycycline (DOX). This chapter aims to further characterise the phenotypic effects of SMC5/6 complex depletion *in vivo*. This system directly aims at regulating the protein level of NSMCE4a, without the use of RNA interference (RNAi). Several studies carried out in mammalian systems have used RNAi to deplete specific components of the SMC5/6 complex. However, despite the importance of RNAi methods, there remains a high risk of off-target effects. Previous studies using RNAi against the human SMC5/6 complex have reported off-target effects (Wu et al., 2012). Therefore, the main objective of this study was to use the T-REx Flp-In system, which allows inducible shut off of the ectopic NSMCE4a[1] gene. This would enable us to use an isogenic cell line to study the effects of NSMCE4a depletion in human cells. Furthermore, depletion of any of the human SMC5/6 components, except NSMCE2, leads to a destabilisation of the whole SMC5/6 complex (Taylor et al., 2008). Thus, NSMCE4a shut off is expected to lead to the destabilisation of the whole SMC5/6 complex in the T-REx Flp-In 293 cell line, which would mimic the destabilisation of the SMC5/6 complex in the NSMCE3 patient cells. Therefore, the isogenic T-REx Flp-In 293 cell line could be used to support and validate the phenotypes of the NSMCE3 patient cell line.

[1] Ectopic NSMCE4a: genome inserted NSMCE4a cDNA at the FRT-site

The effects of the yeast Smc5/6 complex deficiency during an unperturbed cell cycle have been investigated in a number of studies. It has been indicated that the essential role of the Smc5/6 complex may be during chromosome segregation, and/or the resolution of recombinational intermediates; since the terminal phenotype of Smc5/6 deficient cells is mitotic catastrophe (Ampatzidou et al., 2006; Bermúdez-López et al., 2010; Outwin et al., 2009; Pryzhkova and Jordan, 2016). In fission yeast, chromosome segregation errors in *smc5/6* hypomorphic mutants correlate with a failure to remove cohesin from chromosome arms before anaphase onset (Outwin et al., 2009). In line with the yeast studies, experiments in human cells also reported aberrant mitotic chromosome phenotypes. These were described as so called 'curly chromosomes', which were also associated with segregation errors (Gallego-Paez et al., 2014). Thus, we wanted to utilise our shut off system to validate the effects of SMC5/6 depletion on chromosome stability.

This chapter demonstrates the usage of the Tet-ON system as a tool for protein depletion and gives a detailed description of the conditions required for NSMCE4a shut off. Timely regulation and effects of NSMCE4a shut off on the protein levels of other SMC5/6 components are also discussed. Finally, the phenotypic outcome of cells with long-term depletion of NSMCE4a is also characterised.

5.2 Aims

iii) To characterise the created stable isogenic cell lines upon NSMCE4a shut off

iv) To investigate the effects of a long term NSMCE4a shut off on genome stability

5.3 Results

5.3.1 Identification of NSMCE4a shut off conditions

Western blot analysis revealed that the created -/-;NSMCE4a[2] cell line contained similar-to-endogenous levels of the ectopic NSMCE4a protein, when grown in normal media (Chapter 3). However, under non-inducing conditions (no Doxycycline/Tetracycline), the expression of the ectopic NSMCE4a is expected to be repressed. One reason for the high levels of the ectopic NSMCE4a could be the 'leakiness' of the Tet-ON system, due to the presence of residual tetracycline in the foetal calf serum (FCS). Therefore, the protein level of endogenous NSMCE4a was assessed in the -/-;NSMCE4a cell line, grown in media containing different FCS. Cells were grown over two weeks in media containing either tetracycline free FCS (Tet free), or regular FCS (Normal). As a positive control, 1 µg/ml of Doxycycline was added to cells grown in normal media, 2 days prior to the whole cell extract preparation (+DOX). Western blot analysis revealed that cells grown in Tet free media did not display any decrease in the protein level of ectopic NSMCE4a, compared to cells grown in media containing regular FCS (Figure 5.1 A, lane 2). The results indicate that the observed protein levels of ectopic NSMCE4a are not caused by the leakiness of the Tet-ON promoter.

Another possibility why the ectopic NSMCE4a remained expressed could be the absence of the Tet repressor protein. The Blasticidin resistance gene is expressed from the same genome inserted construct as the Tet repressor gene, thus, in the presence of Blasticidin, only cells that actively express both genes are expected to survive. Initial growth of -/-;NSMCE4a cell line in the presence of 10 µg/ml Blasticidin resulted in dramatic cell death (Figure 5.2). This cell death occurred in both the -/-;NSMCE4a and +/+;NSMCE4a[3] cell lines, but not in the wild type (WT)[4] cells and a cell line containing an empty vector inserted at the FRT-site. This suggests that the cell lines containing FRT- NSMCE4a do not express the Blasticidin resistance gene and thus, it is likely that they neither express the TetR gene. The product of the TetR gene controls expression from the genome inserted FRT-vector, in our case the ectopic FRT-inserted NSMCE4a.

[2] Endogenous NSMCE4a knock out cell line with ectopic FRT-inserted NSMCE4a-Strep-6xHis
[3] Cell line containing both endogenous NSMCE4a and ectopic FRT-inserted NSMCE4a-Strep-6xHis
[4] Flp-In T-REx 293 cell line

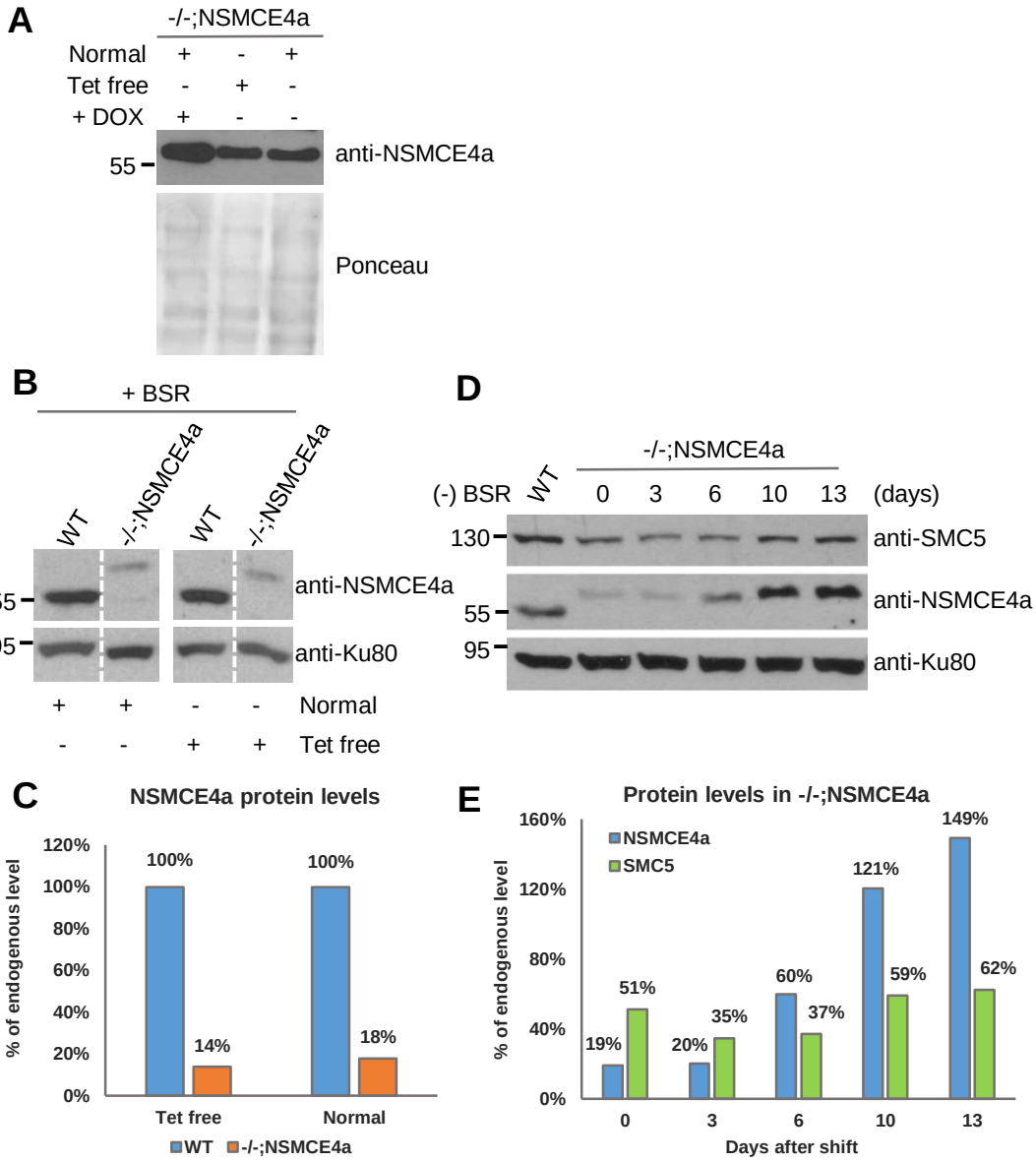


Figure 5.1: Shut off of the ectopic NSMCE4a requires active selection for the Tet repressor protein

A. Comparison of protein levels of NSMCE4a in -/-;NSMCE4a cells grown in different media; cells were grown in media containing either tetracycline free calf serum (Tet free) or normal foetal calf serum with (+DOX) or without (Normal) 1 µg/ml Doxycycline, 30 µg of whole cell extract was loaded in each well, Ponceau stain was used as a loading control. **B.** Example of western blot showing decrease of ectopic NSMCE4a in -/-;NSMCE4a cell line grown in media containing Tetracycline free foetal calf serum (Tet free) or normal foetal calf serum (Normal) in the presence of 10 µg/ml Blasticidin. **C.** Quantification of B; protein levels of NSMCE4a upon shut off were normalised on the endogenous NSMCE4a levels in the parental cell line (WT). **D.** Blasticidin selection is necessary for maintenance of NSMCE4a shut off; cells were grown in media containing Blasticidin for 14 days before shifted into media without Blasticidin, whole cell extract was prepared from cells at indicated time points after shift, Ku80 antibody was used as a loading control. **E.** Quantification of D; protein levels of NSMCE4a and SMC5 were normalised on the endogenous levels of NSMCE4a and SMC5 in the parental cell line (WT); WT: T-REx Flp-In 293, -/-;NSMCE4a: endogenous NSMCE4a KO, FRT-NSMCE4a-Strep-6xHis in T-REx Flp-In 293.

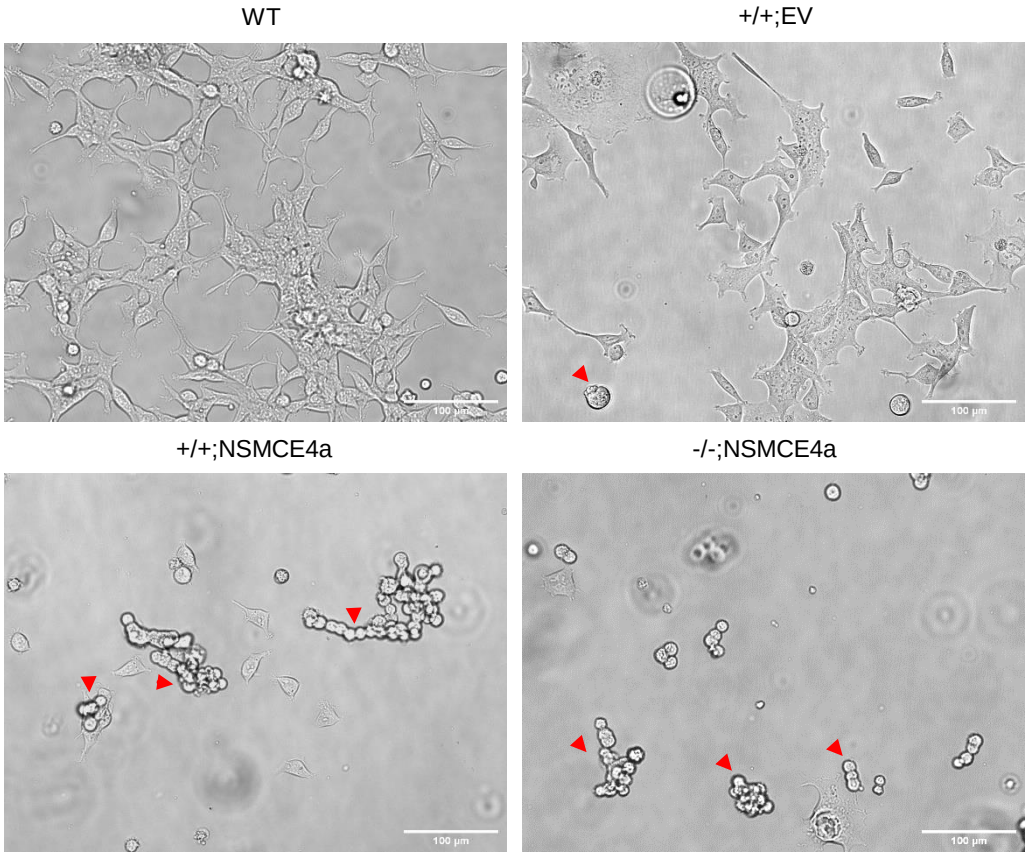


Figure 5.2: Phenotype of T-REx Flp-In 293 created cell lines after one week of Blasticidin selection

Cells were grown in Tetracycline free media supplemented with 10 µg/ml Blasticidin, pictures of cells were taken 1 week after Blasticidin addition to media, cells were imaged using 100 x magnification, scale bar represents 100 µm; red arrows indicate dead cells, high rate of cell death was observed in case of both +/+;NSMCE4a and -/-;NSMCE4a cell line; WT: T-REx Flp-In 293 cell line, +/+;EV: T-REx Flp-In 293 cell line with FRT-genome inserted empty vector (pcDNA5/FRT/TO), +/+;NSMCE4a: T-REx Flp-In 293 cell line with FRT-genome inserted NSMCE4a-Strep-6xHis, -/-;NSMCE4a: T-REx Flp-In 293 cell line with FRT-genome inserted NSMCE4a-Strep-6xHis and knock out of the endogenous NSMCE4a.

During construction of the NSMCE4a knock out cell lines, we actively selected for cells expressing similar-to-endogenous levels of ectopic NSMCE4a, so that they survive the consecutive NSMCE4a gene knock out. Hence, the created cells might have silenced the expression of the Blasticidin/TetR cassette, in order to allow the expression of the Tet regulatable ectopic NSMCE4a.

Continuous growth of -/-;NSMCE4a cells over two weeks, in media containing 10 µg/ml Blasticidin (+BSR), resulted in a dramatic decrease in protein level of the ectopic NSMCE4a (Figure 5.1. B). Western blot quantification revealed that the protein level of ectopic NSMCE4a in Tet free media dropped down to 14% and to 18% in normal media down, compared with endogenous NSMCE4a (Figure 5.1 C). This indicates that the growth of -/-;NSMCE4a cells in Tet free media results in a tighter shut off than in normal media. Importantly, these experiments explain the reason for the close-to-endogenous protein levels of ectopic NSMCE4a in the created NSMCE4a cell lines. The elevated protein levels of the ectopic NSMCE4a are presumably not caused by the Tet-regulatable promoter leakage. The more likely explanation is either silencing of the TetR gene, or alternatively, a polyclonal cell population with differential expression levels of ectopic NSMCE4a.

5.3.1.1 Continuous selection for TetR is necessary for NSMCE4a shut off

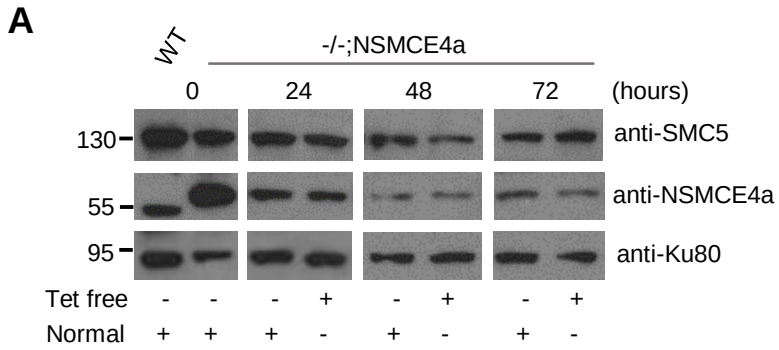
Next, we aimed to determine whether continuous Blasticidin selection is necessary to maintain the shut off levels of ectopic NSMCE4a. Cells were pre-selected in media containing 10 µg/ml Blasticidin for 14 days prior to shift into media non-containing Blasticidin (-BSR). The protein levels of NSMCE4a were monitored over 13 days in a time-course experiment (Figure 5.1 D). Protein levels of ectopic NSMCE4a started to increase 6 days after Blasticidin removal and exceeded endogenous levels of NSMCE4a 10 days after Blasticidin removal (Figure 5.1 E). Similarly to the previous study by Taylor et al., 2008, we observed a decrease in SMC5 protein levels after NSMCE4a shut off (Taylor et al., 2008). Interestingly, the protein levels of SMC5 appeared to further decrease 3 days after Blasticidin removal conditions, but increased back to around 60 % of endogenous levels 10 – 13 days after media change. This demonstrates that even though the stability of the SMC5 protein depends on the presence of NSMCE4a, the kinetics of SMC5 protein destabilisation is different to directly regulatable NSMCE4a. Together, these results show that, shut off of the ectopic NSMCE4a gene is possible only

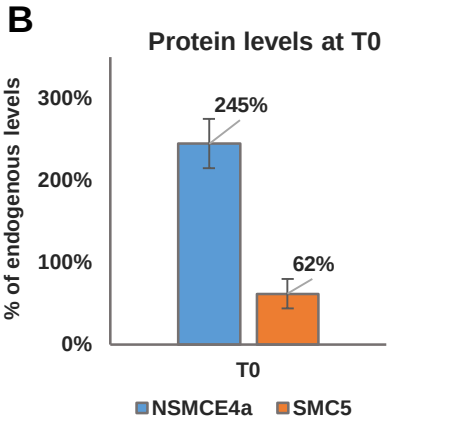
under selection in media containing Blasticidin. Further, these results demonstrated that the shut off of NSMCE4a leads to the destabilisation of other components of the SMC5/6 complex, supporting data from previous work.

5.3.2 Timely regulation of NSMCE4a shut off

Once the shut off conditions were identified, the kinetics of protein depletion of NSMCE4a and other SMC5/6 components was investigated. To measure the kinetics of the NSMCE4a shut off, -/-;NSMCE4a cells were grown for two weeks in media containing 10 µg/ml Blasticidin and 10 ng/ml Doxycycline. These conditions maintain the expression of both NSMCE4a and TetR. After two weeks cells were harvested and re-plated into either Tet free, or normal media containing 10 µg/ml Blasticidin and the protein levels of NSMCE4a were monitored over three days (Figure 5.3 A). The protein levels of NSMCE4a in the -/-;NSMCE4a cell line on the day of media change were around 250% of the endogenous NSMCE4a levels in the T-REx Flp-In 293 parental cell line (Figure 5.3 B). This is in accordance with the results in Chapter 3, showing that in the presence of Doxycycline, the expression of NSMCE4a is induced and exceeds the endogenous levels. In contrast, the protein levels of SMC5 were only around 60 % of the endogenous SMC5 (Figure 5.3 B). This indicates that overexpression of the ectopic NSMCE4a causes a decrease in protein levels of the SMC5 subunit. Alternatively, lower levels of SMC5 could be explained by variability in the cell population (explained in section 5.3.3.1).

Quantification of NSMCE4a and SMC5 protein levels over three days after media change to non-permissive conditions (-DOX, +BSR) is listed in tables (Figure 5.3 E). The protein levels of NSMCE4a in the -/-;NSMCE4a cell line dropped on average from 245% to 110% of the endogenous NSMCE4a within 24 hours (Figure 5.3 B, C). This implies that ectopic NSMCE4a is rapidly downregulated in the absence of Doxycycline. Three days after the shift into the non-permissive conditions, the protein levels of NSMCE4a reduced to 25% of endogenous levels. Importantly, a similar decrease in the protein levels of NSMCE4a was observed in both Tet free and normal media (Figure 5.3 C). However, the SMC5 protein levels did not decrease significantly within 3 days after NSMCE4a shut off (Figure 5.3 D). This is likely due to the fact that SMC5, in contrast to NSMCE4a, is not directly regulated at the mRNA level by shut off. Therefore, its turnover occurs mainly at the protein level. Higher stability of the SMC5 protein could also contribute to its slower





E

NSMCE4a (average % of WT)				
Time (hrs)	T0	24	48	72
Normal	245%	110%	57%	23%
Tet free	245%	110%	58%	26%

SMC5 (average % of WT)				
Time (hrs)	T0	24	48	72
Normal	62%	61%	42%	46%
Tet free	62%	48%	31%	56%

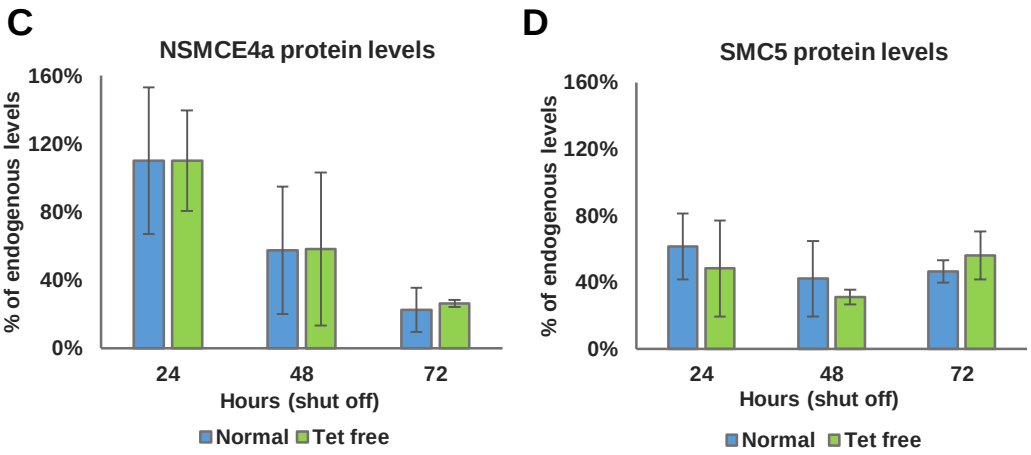


Figure 5.3: **Kinetics of the decrease in protein levels of NSMCE4a and SMC5 after NSMCE4a shut off**

A. Example of a western blot showing protein levels of NSMCE4a and SMC5 after shift from media + 10ng/ml Doxycycline to, cells were grown for 14 days in media + 10µg/ml Blasticidin and 10ng/ml Doxycycline before media shift; cells were collected at indicated time points for western blot analysis. **B.** Protein levels of NSMCE4a and SMC5 before shift to normal or Tet free media (0 hours) **C – D.** Quantification of NSMCE4a and SMC5 protein levels over three days after shift to media not containing Doxycycline. **E.** Table showing protein levels of NSMCE4a (C) and SMC5 (D) expressed as average % of wild type protein levels. **B – E** protein levels were normalised on endogenous levels of WT (T-REx Flp-In 293 parental cell line), western blot was quantified using FiJi software, error bars represent standard deviation of three independent experiments, Normal: media with normal foetal calf serum, Tet free: media with tetracycline free foetal calf serum.

turnover. Together, the results indicate, that within 3 days of non-permissive growth conditions, the protein level of ectopic NSMCE4a decreases to 25 %. Meanwhile, the protein level of SMC5 does not appear to decrease significantly within this time-frame.

5.3.2.1 Cell viability upon NSMCE4a shut off

To address whether the destabilisation of the SMC5/6 complex, induced by the NSMCE4a shut off, affects the cell viability, clonogenic survival assays were performed. WT, -/-;NSMCE4a and +/+;NSMCE4 cell lines were grown for 7 days in media containing 10 µg/ml Blasticidin and 10 ng/ml Doxycycline to induce NSMCE4a expression. After, cells were washed and plated into 10 cm dishes, containing either the same media (NSMCE4a induction), or Tet free media containing 10 µg/ml Blasticidin (NSMCE4a shut off). Cells were grown for 12 days to form macroscopic colonies. The number of colonies in each plate was scored in triplicate and survival factor was calculated as a plating efficiency of cells growing in non-permissive conditions (NSMCE4a shut off), divided by plating efficiency of cells growing in permissive conditions (NSMCE4a induction by 10 ng/ml of Doxycycline). In parallel to the viability assay, the whole cell extract was collected every two days to monitor the protein levels of the SMC5/6 complex upon the NSMCE4a shut off. The results show that after 12 days in non-permissive growth conditions, the viability of the -/-;NSMCE4a cells, in comparison to the WT and +/+;NSMCE4a cell lines, decreases to 52% (Figure 5.3 A). Western blot analysis of NSMCE4a and SMC5 also revealed that in both the -/-;NSMCE4a and +/+;NSMCE4a cell line, the protein levels of regulatable NSMCE4a gradually decreased until day 12 (Figure 5.4 B). Importantly, quantification of the western blot demonstrated that after a shift to Tet free media, the protein level of SMC5 in the -/-;NSMCE4a cell line, decreased to 6%, although with slower kinetics than NSMCE4a (Figure 5.3 C). These results demonstrate, that the NSMCE4a shut off leads to the destabilisation of other SMC5/6 complex components over time, notably SMC5, and this compromises cell viability. Further, the protein levels of both SMC5 and NSMCE4a gradually decrease after NSMCE4a shut off, reaching minimal levels at day 12.

5.3.3 Characterisation of a long term NSMCE4a shut off

Previous experiments showed that to sustain maximal shut off of endogenous NSMCE4a, the -/-;NSMCE4a cells need to be grown in the presence of Blasticidin for a minimum of

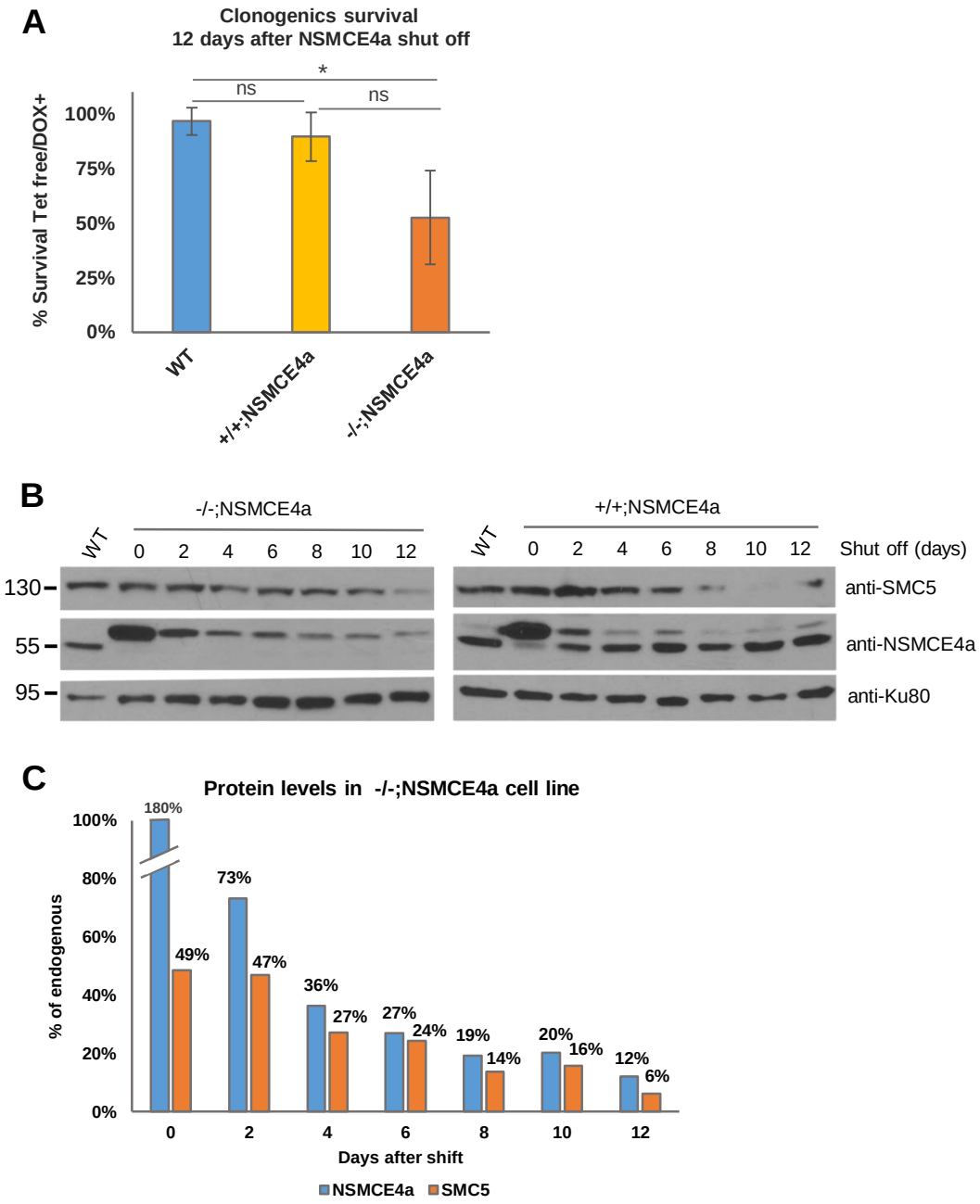


Figure 5.4: NSMCE4a shut off decreases cell viability

A. Clonogenics viability of cells 12 days after shift from 10ng/m Doxycycline containing media to Tet free media containing 10µg/ml Blasticidin, the number of colonies was scored and survival factor was counted as number of cells on Tet free (+Blasticidin)/ Tet free (+DOX), error bars represent standard deviation of three independent experiments, two-tailed Student t-test was used to calculate statistical significance * $p \leq 0.05$. **B.** Example of a western blot showing protein levels of NSMCE4a and SMC5 in different cell lines after shift from media containing 10ng/ml Doxycycline to Tet free media containing 10µg/ml Blasticidin, cells were collected for western blot every two days for 12 days after media shift, Ku80 is a loading control. Cells were grown for 14 days in media + 10µg/ml Blasticidin and 10ng/ml Doxycycline before media shift; cells were collected at indicated time points for western blot analysis. **C.** Quantification of (B) NSMCE4a and SMC5 protein levels over three days after shift to media not containing Doxycycline, western blot was quantified using FiJi software.

12 days (Figure 5.4 B and 5.5 B). To investigate the cell phenotype upon maximal NSMCE4a shut off, wild type and -/-;NSMCE4a cell lines were grown in the presence of Blasticidin for more than two weeks (condition hereafter referred as a long term shut off). As a control, the wild type (T-REx Flp-In 293) cell line, containing endogenous levels of NSMCE4a, was grown in the presence of Blasticidin. As another control, the -/-;NSMCE4a cell line, with an isogenic genetic background, was grown in the absence of Blasticidin selection (condition denoted as NSMCE4a ON).

5.3.3.1 Protein levels of NSMCE4a and SMC5 after a long term NSMCE4a shut off

To quantify the protein levels of NSMCE4a and SMC5 in the -/-;NSMCE4a cell line, after a long term shut off[5], the -/-;NSMCE4a cell line was grown for 15 – 17 days, either in media containing 10 µg/ml Blasticidin (NSMCE4a OFF), or in media not containing Blasticidin (NSMCE4a ON). As a control with endogenous NSMCE4a protein level, the T-REx Flp-In 293 cell line (WT) was grown in parallel. After, the cells were harvested and the whole cell extract was subjected to western blot analysis (Figure 5.4 A). Quantification of the NSMCE4a and SMC5 protein levels after the long term shut off, showed a decrease of NSMCE4a and SMC5 protein levels, down to 11% and 18%, respectively (Figure 5.5 B). Notably, the NSMCE4a protein level in the NSMCE4a ON[6] was elevated in comparison to endogenous levels (WT) (Figure 5.5 B). The increased NSMCE4a protein level in the NSMCE4a ON cell line (157% of endogenous), could be explained by a stronger promoter driving the expression of ectopic NSMCE4a in the absence of the TetR protein. We showed that some cells in the -/-;NSMCE4a cell line can maintain the expression of the ectopic NSMCE4a gene unless selected on Blasticidin. However, the expression of the ectopic NSMCE4a from the strong CMV promoter can exceed endogenous levels. Hence, the total protein level of NSMCE4a in a whole cell extract appears higher than the endogenous level. In contrast, the SMC5 protein level in the NSMCE4a ON cell line was lower than endogenous (WT) (Figure 5.5 C). An explanation for this phenomenon, is likely to be due to the heterogeneity in the -/-;NSMCE4a population (Figure 5.6); the -/-;NSMCE4a cell line without Blasticidin selection, contains a population of cells with different protein levels of the ectopic NSMCE4a (Figure 5.6 B, right panel); in some of the cells in the ON cell line, the protein

[5] Cells grown for minimum of 14 days in the presence of Blasticidin
[6] -/-;NSMCE4a cell line grown in the absence of Blasticidin selection

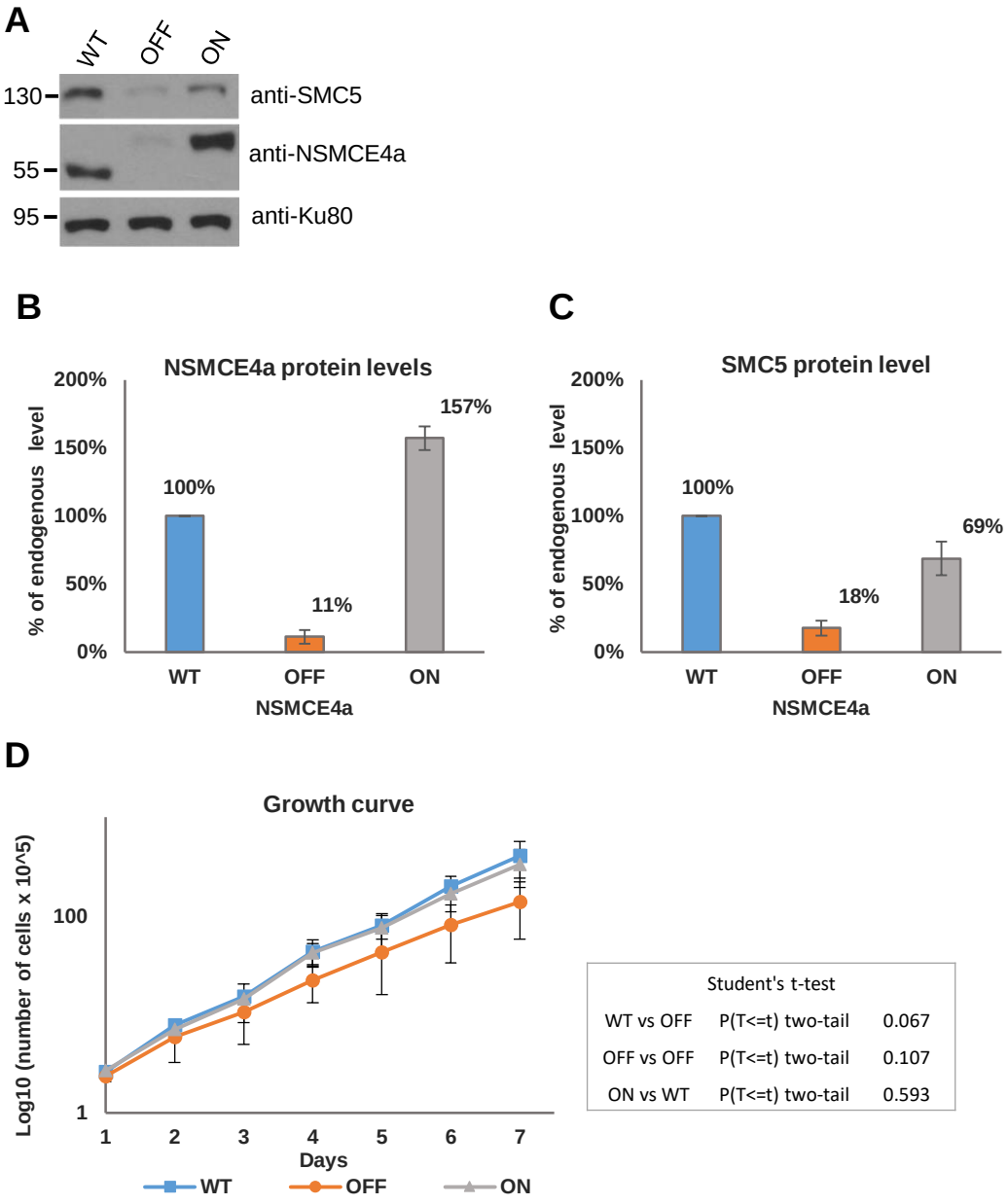


Figure 5.5: Long term NSMCE4a shut off leads to moderate slow growth defect
A. Example of a western blot showing the protein levels of NSMCE4a and SMC5 in the parental T-REx Flp-In 293 cell line (WT) and -/-;NSMCE4a cell line upon NSMCE4a shut off (OFF) or without Blasticidin selection (ON) . **B - C.** Quantification of NSMCE4a (**B**) and SMC5 (**C**) protein levels after 14 – 17 days of NSMCE4a shut off (Tet free media + 10 µg/ml Blasticidin), NSMCE4a and SMC5 protein levels were normalised on protein levels of the endogenous protein levels of NSMCE4a and SMC5 in the T-REx Flp-In cell line (WT), error bars show standard deviation of three independent experiments. **D.** Growth curve upon long term NSMCE4a shut off, exponentially growing cells were counted each 24 hours for 7 days and cell number per ml was plotted, error bars represent +/- standard deviation of three independent experiments, two-tailed Student t-test was used to calculate statistical significance.

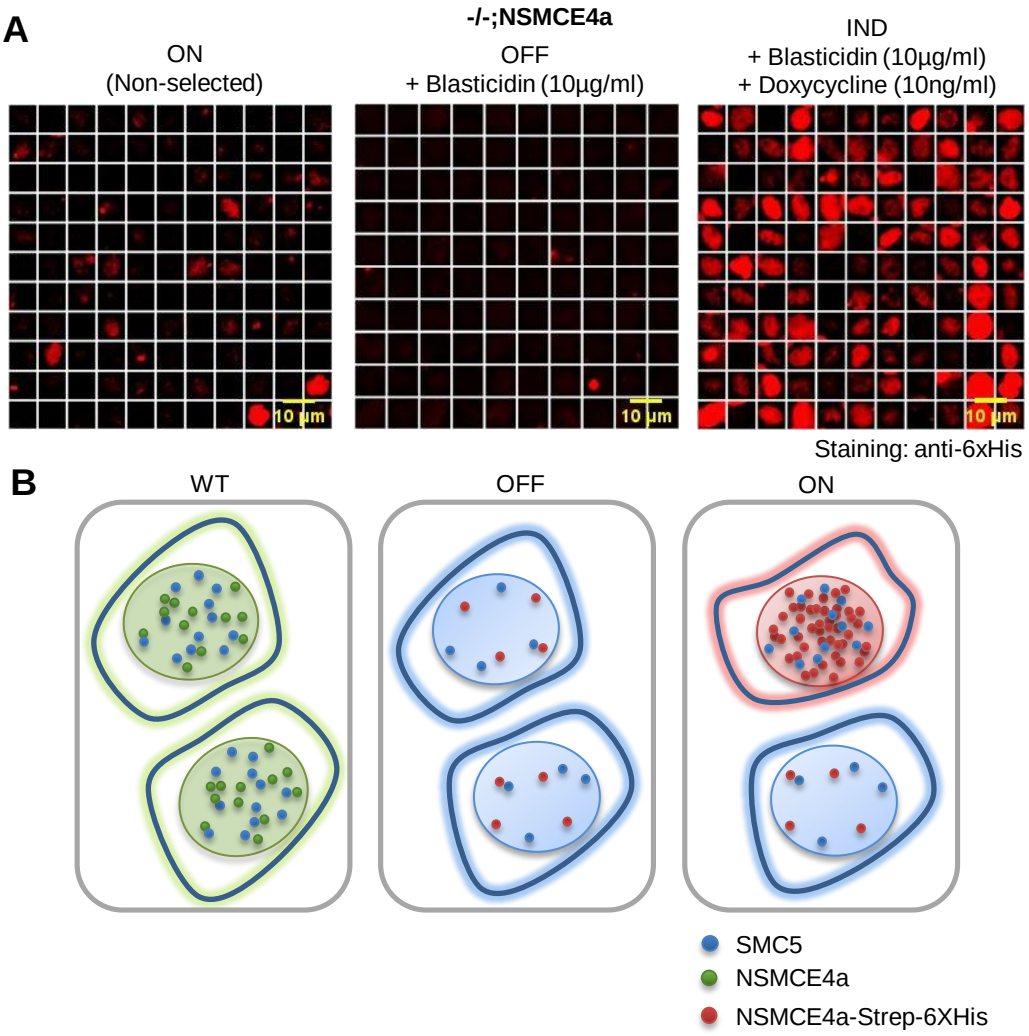


Figure 5.6: Protein levels of the ectopic NSMCE4a and SMC5 under different conditions

A. Immunofluorescence with anti-His antibody to visualise the protein levels of ectopic NSMCE4a-Strep-6xHis in the -/-;NSMCE4a cell line upon different induction states; ON: cells grown in Tet free media without Blasticidin or Doxycycline (non-selected), OFF: cells were grown for two weeks in media containing 10µg/ml Blasticidin (NSMCE4a shut off), IND: cells were grown for two weeks in media containing 10ng/ml Doxycycline and 10µg/ml Blasticidin (NSMCE4a induced), scale bar represents 10 µm. **B.** Schematic illustration of the protein levels of the ectopic (NSMCE4a-Strep-6xHis) and endogenous NSMCE4a and how these influence the levels of different SMC5/6 subunit (SMC5); WT: T-REx Flp-In 293 cell line with endogenous levels of NSMCE4a and SMC5, OFF: -/-;NSMCE4a cell line upon NSMCE4a shut off, levels of both ectopic NSMCE4a and endogenous SMC5 are decreased, ON: -/-;NSMCE4a cell line without selection is a heterogeneous cell population containing different levels of ectopic NSMCE4a, some cells have low levels of NSMCE4a leading to decrease in SMC5 (blue cell) , some cells have high levels of NSMCE4a (red cell) while the SMC5 levels stay the same, this model explains the difference in SMC5 and NSMCE4a protein levels observed by western blot (Figure 5.5 A).

levels of both NSMCE4a and SMC5 (and other components), will be decreased. In contrast, cells that maintain an active expression of the ectopic NSMCE4a, will contain high levels of NSMCE4a, which however does not result in a proportional increase of other SMC5/6 components (Figure 3.4 B). Western blot assay on the whole cell extract will only show an average protein levels in the whole population. Hence, the SMC5 protein level in NSMCE4a ON cells appears lower than endogenous, whereas the NSMCE4a protein level appear higher than endogenous (Figure 5.5 A).

5.3.3.2 Cellular growth and cell cycle analysis upon NSMCE4a shut off

To validate whether the long term NSMCE4a shut off influences the growth rate and cell cycle, growth curves and cell cycle profiles for each cell line were measured. The NSMCE4a shut off in the -/-;NSMCE4a cell line was induced for 14 – 17 days. The number of exponentially growing cells with three different levels of NSMCE4a (NSMCE4a WT, ON and OFF) was recorded at the same time over 7 days. The calculated growth curve shows that long term NSMCE4a shut off (OFF) results in a moderate slow growth phenotype (Figure 5.5 D).

Based on the observed slow growth of the NSMCE4a shut off cell line, it had to be determined, whether there is any difference in cell cycle distribution within the created cell lines. To check whether NSMCE4a shut off alters the cell cycle distribution, EdU incorporation assay, coupled with flow cytometry analysis was performed. Exponentially growing cells with long term NSMCE4a shut off were pulse labelled with 10μM EdU for 60 minutes to visualise actively replicating cells. Fixed cells were than stained with propidium iodide (2 μg/ml) to visualise DNA content. Forward and side scatter gating was performed prior to quantification of cell cycle phases in order to eliminate cell debris and fragments from the analysis (Figure 5.7 B). Flow cytometry of propidium iodide and EdU double labelled cells was performed and population of cells in G1, S and G2/M phase was gated (Figure 5.7 A). Quantification of cell cycle profiles revealed that the NSMCE4a shut off cell line had on average 35% of cells in G1, 46.3% in S and 18.7% in G2/M phase. Cell lines growing under permissive conditions (NSMCE4a ON) had on average 35.5% of cells in G1, 48.3% in S and 16.2% in G2/M phase. The parental cell line (WT) had an average cell cycle distribution of 35.7% cells in G1, 45% in S and 19.3% in G2/M phase. Descriptive statistics of the data did not show any significant difference in cell cycle distribution of cells with long term NSMCE4a shut off, in comparison to the

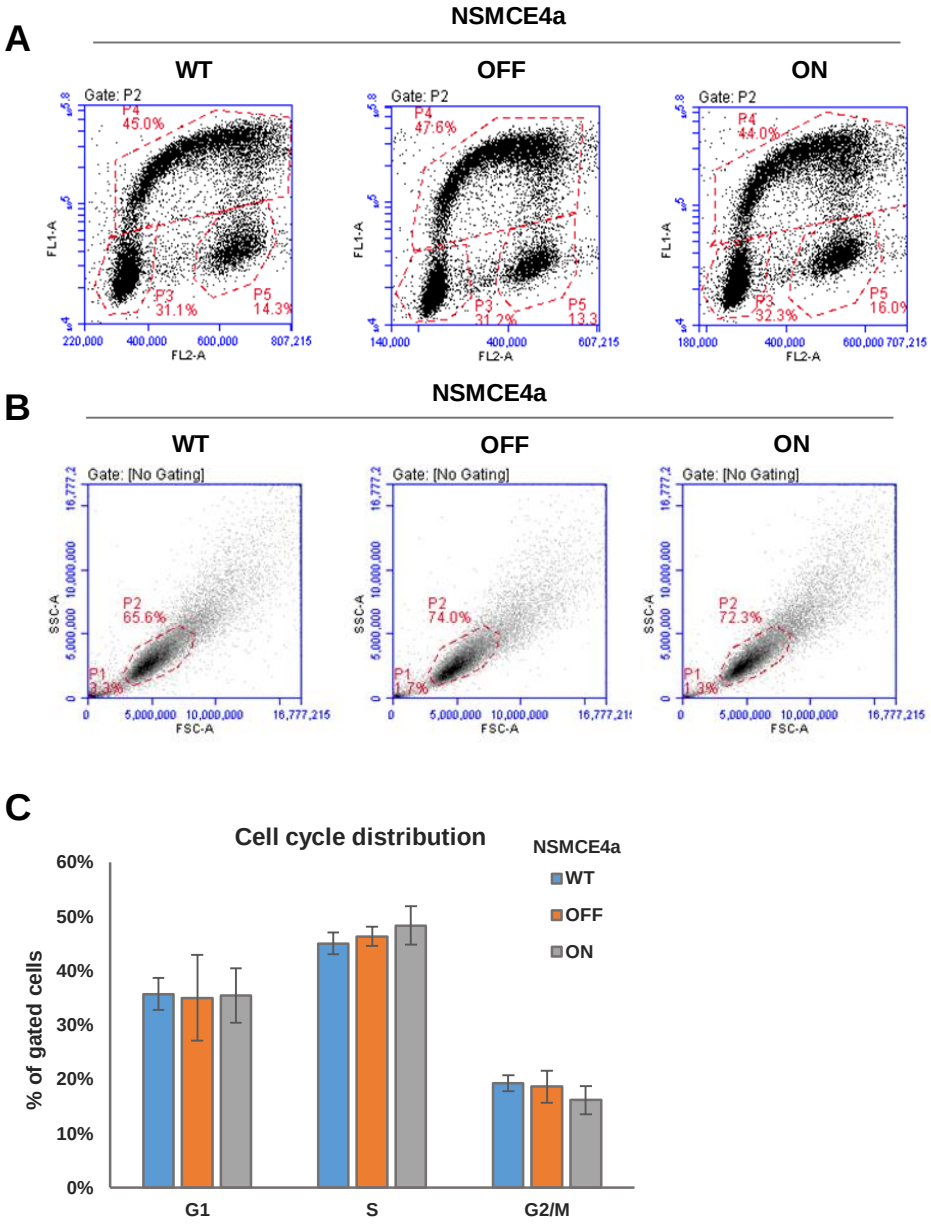


Figure 5.7: Long term NSMCE4a shut off does not influence distribution of cells throughout the cell cycle

A. Example of flow cytometry analysis to quantify percentage of cells in different cell cycle phases; exponentially growing cells were pulsed for 60 minutes with EdU before being harvested and fixed, Click chemistry was performed and cells were analysed by flow cytometry, cell populations in G1, S and G2/M were gated, FL2-A photodetector was used for propidium iodide and FL1-A for EdU. **B.** Forward and side scatter gating of (A). **C.** Quantification of percentage of cells in different cell cycle phases, gating was performed as shown in (A), error bars show standard deviation of three independent repeats; WT: T-REx Flp-In 293 parental cell line, OFF: -/-;NSMCE4a cell line after 15 - 20 days of BSR selection, ON: -/-;NSMCE4a cell line without Blasticidin selection.

control cell lines (Figure 5.5 C). Together, the results suggest that long term NSMCE4a shut off leads to a mild slow growth phenotype, but does not significantly influence the cell cycle distribution.

5.3.4 Long term depletion of NSMCE4a leads to the accumulation of DNA damage and genomic instability

5.3.4.1 Depletion of NSMCE4a leads to increased micronuclei formation

Micronuclei are aberrant cellular structures that contain chromatin encapsulated by a nuclear envelope. The chromatin in micronuclei usually originates from chromosome fragments or lagging chromosomes that underwent an abnormal anaphase. Micronuclei can also contain whole chromosomes, due to incorrect spindle attachment during chromosome segregation, and can thus lead to chromosome loss (Fenech and Morley, 1989; Ford et al., 1988; reviewed in: Terradas et al., 2010). Typically, micronuclei formation is associated with DNA damage repair deficiency, disturbed cell cycle checkpoint activation or chromosomal instability. Unrepaired DNA double-strand breaks, as well as persisting replication stress intermediates can also give rise to micronuclei. The SMC complexes are crucial for correct sister chromatid separation, therefore compromising the function of SMC complexes is likely to result in an increased formation of micronuclei (reviewed in: Fenech et al., 2011).

In order to investigate whether the NSMCE4a shut off in the -/-;NSMCE4a cell line leads to increased chromosome instability, quantification of micronuclei in cell lines containing different NSMCE4a levels were scored. Cells fixed on glass coverslips were stained with DAPI and imaged under 400x magnification (Figure 5.8 A). To monitor the protein levels of NSMCE4a and SMC5 a western blot analysis on the whole cell extract was performed in parallel (Figure 5.8 B). Micronuclei quantification revealed that cells with long term shut off of NSMCE4a display on average 23% nuclei containing micronuclei. In contrast, both the isogenic cell line, growing in non-permissive conditions (NSMCE4a ON), and the parental cell line (WT) displayed on average 14% of nuclei with micronuclei (Figure 5.8 C). Statistical analysis revealed a significant increase in micronuclei formation in comparison to both control cell lines (Figure 5.8 C). It is apparent that all the cell lines derived from T-REx Flp-In 293 cell lines have increased basal level of micronuclei when compared to primary cell lines. The primary fibroblasts show 2% of nuclei with micronuclei, in the case of the control cell line (1BR), and 12% (svdc01) and 9%

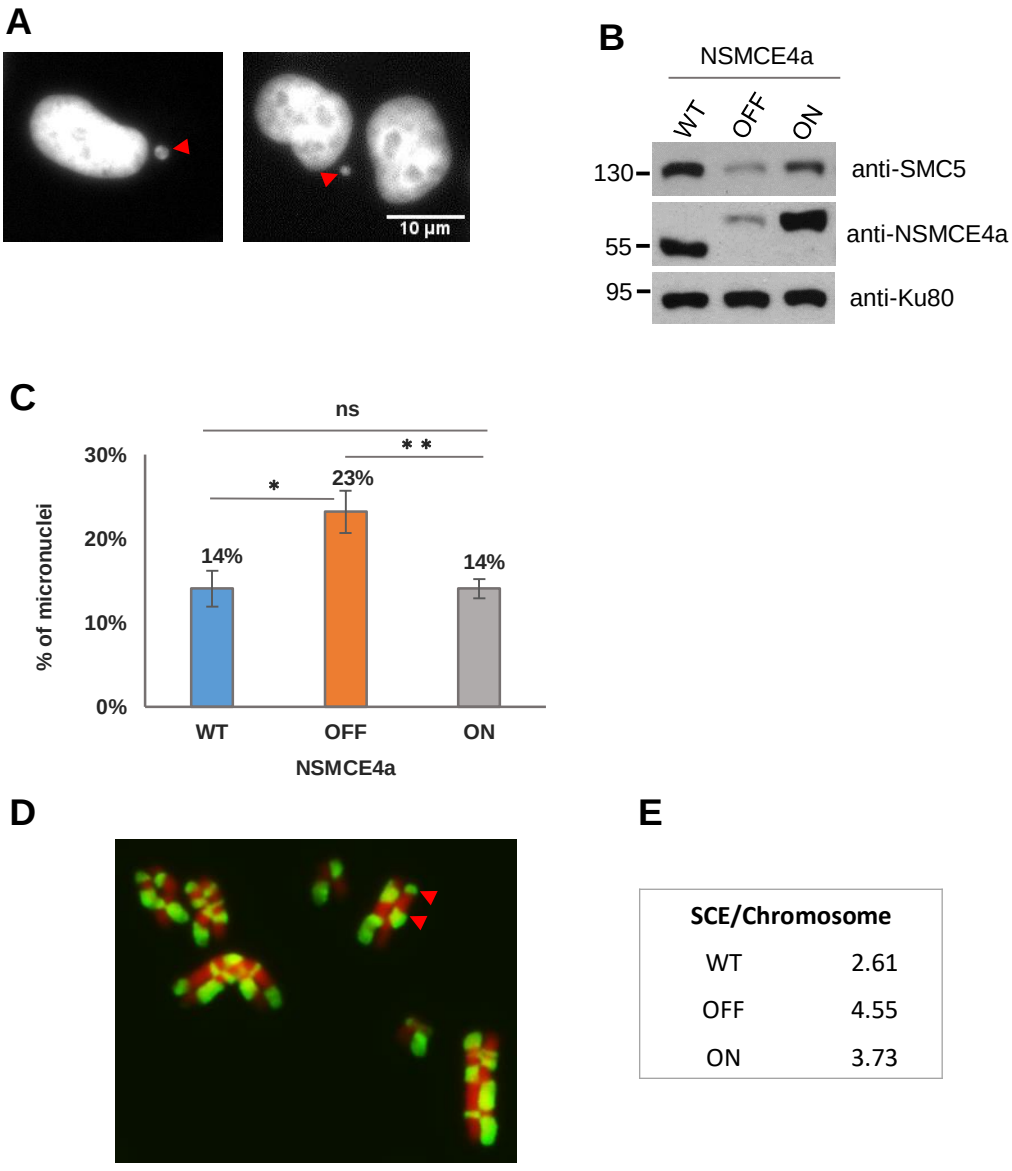


Figure 5.8: Long term NSMCE4a shut off increases chromosome instability
A. Example of micronuclei in cell line: -/-;NSMCE4a, micronuclei are indicated by red arrows, scale bar 10 µm. **B.** Western blot example to show the protein levels of NSMCE4a and SMC5 at the time of micronuclei scoring, WT: T-REx Flp-In parental cell line, OFF: -/-;NSMCE4a cell line after 15 -20 days of BSR selection, ON: -/-;NSMCE4a cell line without Blasticidin selection. **C.** Quantification of micronuclei, for each experiment minimum of 250 cells were scored, error bars represent +/- standard deviation of three independent experiments, two-tailed Student t-test was used to calculate statistical significance * $p \leq 0.05$, ** $p \leq 0.01$. **D.** Example of sister chromatid exchange in an untreated T-REx Flp-In 293 cells, chromosome were imaged under 1000 x magnification, red arrow indicate one sister chromatid exchange, scale bar represents 5 µm. **E.** Preliminary results of sister chromosome exchange quantification, minimum of 70 chromosomes from at least five different spreads for each cell line was scored.

(GVH02), in the case of the NSMCE3 patient cell line (Figure 3.1 C). The striking difference in the level of micronuclei between the primary and the T-REx Flp-In 293 cell lines is in line with increased genome and karyotype instability of transformed cell lines (T-REx Flp-In 293) in comparison to primary fibroblasts. The T-REx Flp-In 293 cell line is derived from the HEK293 cell line, a transformed cell line, which has been immortalised with the adenovirus and is known to express viral proteins that can deregulate the pRb and p53 tumor suppressor genes. Furthermore, the HEK293 cells also display an unstable karyotype, and a number of polymorphisms and copy number alterations in genes involved in cell cycle control and DNA damage repair (Bylund et al., 2004; Lin et al., 2014; reviewed in: Stepanenko and Dmitrenko, 2015). Despite the higher endogenous level of micronuclei in the T-REx Flp-In 293 cell line, the long term NSMCE4a shut off further increases the number of nuclei containing micronuclei. Together, this data implies that the stability of the SMC5/6 complex significantly contributes to genome stability maintenance in transformed cell lines.

5.3.4.2 Depletion of NSMCE4a leads to increase in SCEs

Another marker of increased genomic instability, or deficiency in HR-pathways, is increased sister chromatid exchange (SCE). The formation of SCEs in most cases relies on homologous recombination and indicates a cross over between sister chromatids (Sonoda et al., 1999). SCEs arise during DNA replication, typically as a result of replication fork collisions with transcription machinery or other DNA lesions. SCEs arise spontaneously during an unperturbed cell cycle, the normal level of SCEs is 3 – 4 per diploid cell (Kato, 1974). The origin of endogenous SCEs is often caused by DNA single strand breaks. Sister chromatid exchange is routinely used to detect alterations in cellular processes underlying homologous recombination pathways (reviewed in: Wilson and Thompson, 2007). The NSMCE2 patients lymphoblastoid cells did not show any significant difference in endogenous SCE formation, however, they did display a reproducible increase in SCE upon UV treatment (Payne et al., 2014). Furthermore, chicken DT40 Smc5 knock out cells displayed an increase in SCEs, both during an unperturbed cell cycle and upon Mitomycin C treatment (Stephan et al., 2011a). Lastly, a recent study in human cells showed that knock out of NSMCE2 in HEK293 cells does not result in a significant change in spontaneous SCEs, compared to the wild type cell line (Pond et al., 2019). To assess whether long term NSMCE4a shut off influences

spontaneous SCE formation in the T-REx Flp-In 293 cell line, the number of SCEs were scored. The NSMCE4a shut off (OFF) cell line, alongside the two control cell lines (ON and WT) were grown for 24 hours in the presence of 0.5 µM EdU, after which the cells were washed and allowed to undergo one more cell cycle without EdU. Metaphase spreads from labelled cells were prepared and EdU was visualised by Click-It reaction. Cells were visualised under 1000 x magnification and SCEs in each cell line were scored (Figure 5.8 D). Since the T-REx Flp-In 293 cell line does not have a stable diploid karyotype, the number of SCEs was expressed as an average number of SCE per chromosome for each cell line. The preliminary data pinpointed an apparent increase in SCE per chromosome in the NSMCE4a shut off cell line, in comparison to the WT control (Figure 5.8 E). The NSMCE4a shut off cell line had an average number of 4.55 SCE/chromosome, whereas the WT control had 2.61 SCE/chromosome. Interestingly, the NSMCE4a ON control cells also displayed an increase in SCE formation (3.73 SCE/chromosome). Our preliminary results indicate that a destabilisation of the SMC5/6 complex increases the number of SCEs. However, our experiment is missing biological replicates, therefore, in order to confidently interpret the results, additional replicates will have to be performed.

5.3.4.3 Depletion of NSMCE4a leads to aneuploidy

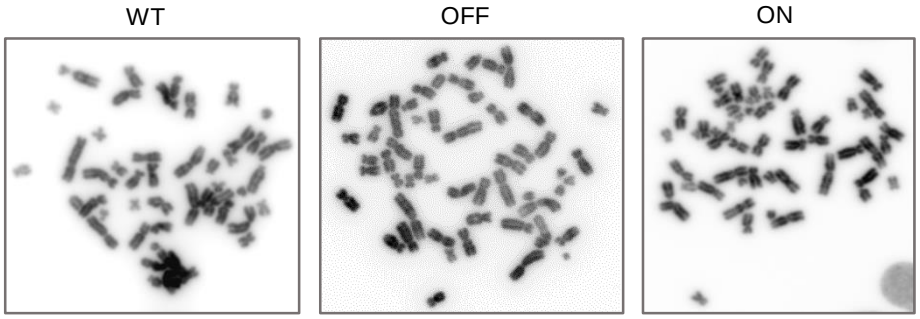
Based on the observed increase in micronuclei upon NSMCE4a shut off, the next aim was to explore the effects of long term NSMCE4a depletion on the karyotype of T-REx Flp-In 293 cells. The karyotype of the original HEK293 cell line created by adenovirus transformation likely evolved through tetraploidy and it is known to be unstable (Bylund et al., 2004; Russell et al., 1977). According to American Type Culture Collection (ATCC), the karyotype of the HEK293 cell line (CRL-1573) is hypotriploid, the modal chromosome number is 64 and is present in approximately 30% of cells. However, different studies report different karyotypes, which points towards a large variability of the HEK293 karyotype (reviewed in: Stepanenko and Dmitrenko, 2015). Therefore, we wanted to map the karyotype of the T-REx Flp-In 293 cell lines with and without long term NSMCE4a shut off. The three cell lines (NSMCE4a ON, OFF and WT) were grown in the presence (WT and OFF) or absence (ON) of 10 µg/ml Blasticidin for 17-23 days, before metaphase spreads were prepared. Metaphase spreads from each cell line were imaged under 1000x magnification and the number of chromosomes in a minimum of 58

spreads per repeat was counted by blind scoring (Figure 5.9 A). Modal and median number of chromosomes in each cell line was calculated and averaged. The cell line with long term NSMCE4a shut off (NSMCE4a OFF) had a modal number of 51.3 chromosomes per spread and a median number of 50 chromosome per spread. This was lower in comparison to WT control (53 mode, 52.7 median) and NSMCE4a ON control (54.5 mode, 55 median) (Figure 5.9 B). Cumulative distributions of chromosome number showed a difference in distribution of chromosome number in the cell line that had undergone long term NSMCE4a shut off (NSMCE4a OFF). This cell line displayed a significant increase in the number of spreads with low numbers of chromosomes, in comparison to both controls (NSMCE4a ON and WT) (Figure 5.9 C). These results indicate that long term shut off of the NSMCE4a influences the karyotype of transformed immortalised T-REx Flp-In 293 cells. This points towards a more frequent chromosome loss, when the stability of the SMC5/6 complex is compromised. Our observations are in accordance with previously reported increase in chromosome instability and micronuclei formation. The explanation for the loss of genetic material upon NSMCE4a shut off corresponds to the increased micronuclei formation, likely caused by abnormal chromosome segregation (reviewed in: Fenech et al., 2011).

5.3.4.4 NSMCE4a shut off leads to an increased level of γ-H2AX foci formation

Increased replication stress and genome instability can result in higher levels of DNA damage markers and checkpoint signalling. Phosphorylation of histone variant H2AX at Serine 139 (γ-H2AX) is one of the first steps in response to DNA damage. γ-H2AX is mediated by the members of PI3 kinase family, DNA-PKcs, ATM and ATR in response to DNA double strand breaks, as well as replication stress (Burma et al., 2001; Rogakou et al., 1998; Ward and Chen, 2001). Phosphorylation of histone H2AX is a sensitive biomarker of DNA damage, or increased replication stress (reviewed in: Kuo and Yang). Since the long term shut off of NSMCE4a confers increased genomic instability and changes in karyotype, it is likely that an accumulation of DNA damage would also be present. Phosphorylated H2AX forms distinct foci in the vicinity of the DNA lesions, which can be visualised and quantified using immunostaining with γ-H2AX specific antibodies (Kinner et al., 2008). Therefore, cells containing endogenous NSMCE4a (WT), or ectopic NSMCE4a with (OFF), or without (ON) long term shut off, were subjected to an immunofluorescence assay with an antibody recognizing phosphorylated Serine 139

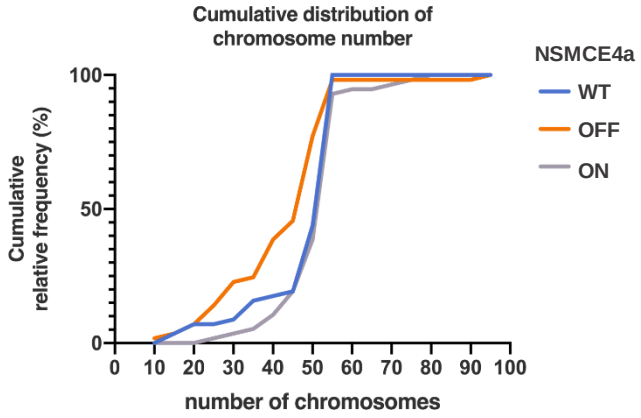
A



B

Number of chromosomes/spread	WT	OFF	ON
median	52.7	50.0	54.5
mode	53.0	51.3	55.0

C



Kolmogorov-Smirnov test	p - value	significance
WT vs OFF	0.0009	***
OFF vs ON	<0.0001	****
WT vs ON	0.7833	ns

Figure 5.9: Long term NSMCE4a shut off leads to chromosome loss
A. Example of metaphase spreads in three cell lines. **B.** Mode and median chromosome number, table shows average of three independent experiments. **C.** Representative example of cumulative distribution of chromosome number in cell lines with or with NSMCE4a shut off, in each experiment a minimum of 58 spreads was scored, WT: T-REx Flp-In 293 cell line, OFF: -/-;NSMCE4a cell line after 15 -20 days of BSR selection, ON: -/-;NSMCE4a cell line without Blasticidin selection, Kolmogorov-Smirnov test was used to calculate statistical significance.

residue of H2AX (γ-H2AX). The NSMCE3 patient cells showed a defect in S-G2 phase of the cell cycle, which might correspond to a problem with homologous recombination or problems during DNA replication. Therefore, scored cells were divided into populations of G1 and S-G2 by gating based on DAPI intensity. The imaging of cells and quantification of γ-H2AX foci was performed using the Olympus ScanR platform with an incorporated software for automated foci scoring (Figure 5.10 A). The number of γ-H2AX foci in each cell line (NSMCE4a WT, OFF and ON) in G1 and S-G2 was scored. The overall number of γ-H2AX foci in G1 phase was lower than in S-G2 (Figure 5.8 B, C). This is expected, as the majority of endogenous γ-H2AX foci are formed during DNA replication, when endogenous replication stress is increased. The increase in endogenous replication stress typically occurs during rDNA replication, or collision between replication and transcription machinery (reviewed in: Zeman and Cimprich, 2014). The number of foci in G1 was slightly increased in the NSMCE4a shut off cell line (OFF), in comparison to the cell line with endogenous NSMCE4a (WT). However, the observed increase was not significant in comparison to the isogenic control without NSMCE4a shut off (ON) (Figure 5.8 B). During the S-G2 phase, the cell line depleted of NSMCE4a displayed elevated levels of endogenous γ-H2AX foci, with an average of 1.6 foci/nucleus, in comparison to control cells containing endogenous levels of NSMCE4a (average of 0.5 foci/nucleus). This increase was moderate but not significant, when compared to the control without shut off of the ectopic NSMCE4a (ON), with an average number of foci being 1.0 foci/nucleus (Figure 5.10 C). The intermediate phenotype of the NSMCE4a ON cell line may be explained by the aforementioned heterogeneity in the population of cells (Figure 5.6). To further validate the immunofluorescence results, western blot with anti-γ-H2AX was performed on the whole cell extract to monitor the overall levels of H2AX phosphorylation (Figure 5.11 A). The western blot results confirmed a slight increase in the endogenous levels of γ-H2AX upon long term NSMCE4a shut off, in comparison to both control cell lines (NSMCE4a ON and WT). These data imply that long term shut off of NSMCE4a results in increased DNA damage signalling. This could be due to higher levels of DNA damage or impaired kinetics of DNA damage repair, as well as increased replication stress or inability to protect replication forks.

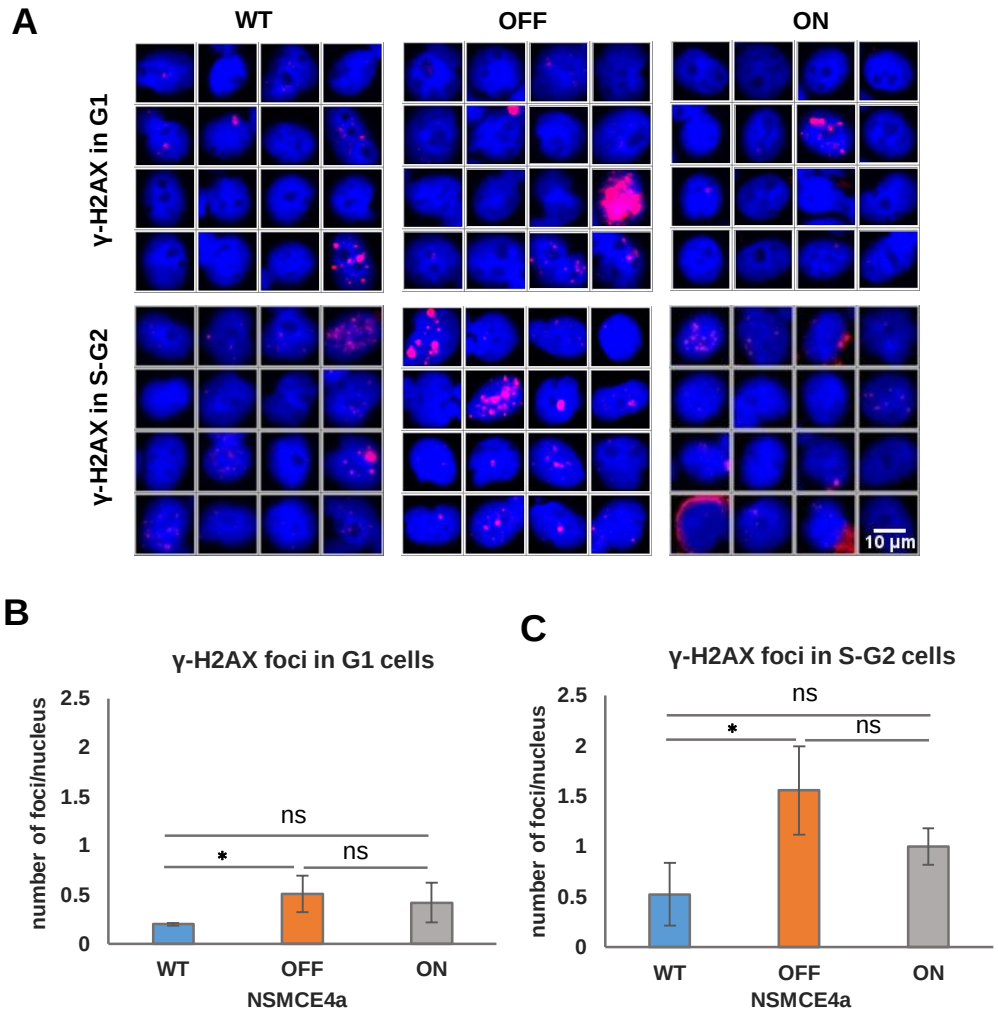


Figure 5.10: Long term NSMCE4a shut off leads to an increase in endogenous γ-H2AX foci

A. Panel of γ-H2AX foci in G1 phase cells and S-G2 phase cells, cell lines with different levels of NSMCE4a were imaged using 40 x dry objective on Olympus ScanR microscope, number of foci in cells were scored using the ScanR incorporated software, panel shows examples of cells from gated population randomly chosen by the ScanR analysis program, scale bar represents 10 µm. **B - C.** Quantification of endogenous level of γ-H2AX foci in G1 (**B**) and S-G2 (**C**) in cell lines with different NSMCE4a levels, number of foci per nucleus was scored using Olympus ScanR microscope coupled with ScnaR analysis software, error bars show +/- standard deviation of 3 independent biological repeats, two-tailed Student t-test was used to calculate statistical significance * $p \leq 0.05$. **A – C.** WT: T-REx Flp-In 293 parental cell line, OFF: -/-;NSMCE4a cell line after 15 -20 days of BSR selection, ON: -/-;NSMCE4a cell line without Blasticidin selection.

5.3.4.5 Depletion of NSMCE4a increases replication stress

Since γ-H2AX becomes phosphorylated in response to a variety of DNA lesions (reviewed in: Turinetto and Giachino, 2015), it does not allow to determine the exact origin or character of the DNA damage. To narrow down the DNA damage response pathways activated during long term NSMCE4a shut off, we decided to assess the phosphorylation levels of RPA. RPA is a heterotrimeric single stranded DNA binding protein, which plays a key role in DNA metabolism (reviewed in: Chen and Wold, 2014). During replication stress, the 32 kDa subunit of RPA, RPA2, becomes phosphorylated specifically by ATR kinase on Serine33 (RPA2 [pSer33]) (Olson et al., 2006). Phosphorylation of RPA2 on Serine33 therefore is implicated in the replication stress response. The RPA2 [pSer33] levels were assessed by western blot in the NSMCE4a shut off cell line (OFF), as well as both control cell lines (WT and ON). The results revealed an increase in endogenous RPA2 [pSer33], specifically in the NSMCE4 shut off cell line (OFF) (Figure 5.11 B). RPA2 [pSer33] was not detected in either of the control cell lines. Importantly, this increase in RPA2 [pSer33] was not due to increased levels of total RPA in the NSMCE4a shut off cell line, which was demonstrated by probing for total RPA (RPA70 subunit) (Figure 5.11 B, middle panel). Together, our data implies that the SMC5/6 destabilisation leads to an increase in endogenous replication stress. These observations are in line with previous studies implicating SMC5/6 in DNA replication during an unperturbed cell cycle (Ampatzidou et al., 2006; Gallego-Paez et al., 2014; Menolfi et al., 2015; Torres-Rosell et al., 2005b, 2005a).

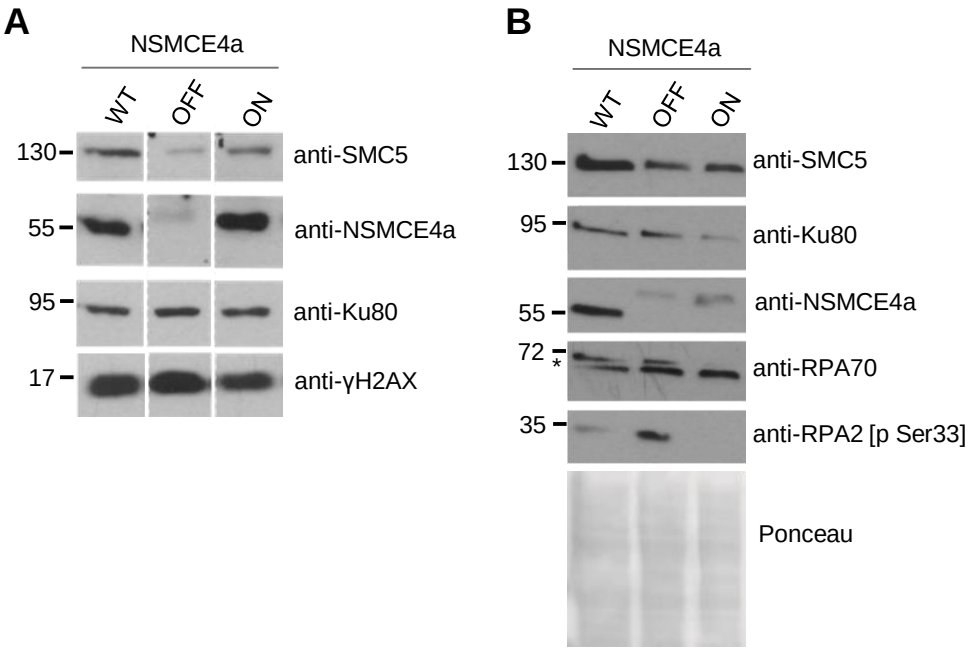


Figure 5.11: Long term NSMCE4a shut off leads to increase in endogenous γ-H2AX signalling and phosphorylation RPA2 on Serine 33
A. Western blot demonstrating increase in total γ-H2AX after long term NSMCE4a shut off (OFF) in comparison to control cell lines (ON and WT), Ku80 is a loading control. **B.** Western blot showing increase in phosphorylation of RPA2 on Serine 33 (ATR substrate) in NSMCE4a shut off cell line, Ku80 is a loading control, anti-RPA70 is a control for total RPA levels, asterisk (*) marks a membrane cut. **A - B.** WT: T-REx Flp-In 293 cell line, OFF: -/-;NSMCE4a cell line after 15 -20 days of BSR selection, ON: -/-;NSMCE4a cell line without Blasticidin selection.

5.4 Discussion

This chapter describes a detailed characterisation of the NSMCE4a shut off cell line using the inducible Flp-In T-REx system. First, the conditions of the NSMCE4a shut off were established. In order to decrease the protein levels of NSMCE4a the -/-;NSMCE4a cells have to be maintained under Blasticidin selection, to ensure stable expression of the TetR protein. Since the TetR protein is expressed together with the Blasticidin resistance gene, it can be speculated that the promoter driving expression of the TetR/Blasticidin becomes silenced, likely by DNA methylation. The silencing of the TetR/Blasticidin resistance genes might have occurred during insertion of the ectopic NSMCE4a into the Flp-In T-REx 293 cell line. Single clones that displayed close-to-endogenous levels of the ectopic NSMCE4a were purposely selected in order to ensure viability during CRSPR/Cas9 knock out of endogenous NSMCE4a.

Secondly, we showed that NSMCE4a shut off gradually leads to the destabilisation of other SMC5/6 components. While NSMCE4a is rapidly degraded 24 hours after shut off, the levels of SMC5 continue to decrease to a minimal level only after 12 days. This could be due to the fact that the expression of the SMC5 subunit is not directly regulated by the Tet-ON system. Therefore, the depletion of other components most likely relies on degradation by the ubiquitin-proteasome pathway (reviewed in: Rothman, 2010), due to the inability to form a stable SMC5/6 complex in the absence of NSMCE4a. Further, we showed that shut off of the ectopic NSMCE4a results in decreased viability in -/-;NSMCE4a cells, which emphasises the essential function of the SMC5/6 complex in human cells.

Growth of the -/-;NSMCE4a cells in non-permissive conditions for more than 14 days (long term shut off) results in an decrease of NSMCE4a protein levels to 11%, whereas the level of SMC5 is down to 18% of the endogenous protein levels. This data suggests that even though the SMC5 subunit of the SMC5/6 complex is more stable, it eventually becomes destabilised, if cells are grown under continuous Blasticidin selection. Long term NSMCE4a shut off results in a modest slow growth phenotype in the -/-;NSMCE4a cell line, which is in accordance with the loss of viability after the shut off of NSMCE4a by media change.

NSMCE4a is required to maintain chromosome stability, which is reflected by the fact that low levels of NSMCE4a leads to an increased number of micronuclei and

chromosome loss. Overall, these results support previous studies in human cells using siRNA for SMC5/6. However, we failed to observe any significant difference in chromosome morphology, or significantly, a different number of 'curly' chromosomes (Gallego-Paez et al., 2014). The increase in chromosome loss in the -/-;NSMCE4a cell line was significant in comparison to both control cell lines (WT and the isogenic NSMCE4a ON control). This implies that the chromosome loss is specifically connected with the destabilisation of the SMC5/6 complex.

Initial scoring of SCEs indicates that a destabilisation of the SMC5/6 complex, by NSMCE4a shut off, results in increased SCEs. Our preliminary data is in line with previous studies that used chicken DT40 cells, where Smc5 knock out has been shown to increase the frequency of SCEs during a normal cell cycle. On the other hand, our observations differ from previously published studies on human SMC5/6, which showed that knock out of NSMCE2, as well as deficiency in its SUMO-ligase activity, does not significantly change the frequency of SCEs during an unperturbed cell cycle (Payne et al., 2014; Pond et al., 2019). However, in contrast to NSMCE4a, depletion of NSMCE2 does not cause a destabilisation of the SMC5/6 complex (Payne et al., 2014; Taylor et al., 2008). Therefore, these results can also pinpoint the pleiotropic phenotype of SMC5/6 deficiency, which has been shown to vary, depending on what function of the complex is compromised.

Lastly, we monitored the levels of DNA damage markers γ-H2AX and phosphorylation of RPA. Cells with long term NSMCE4a shut off had significantly increased levels of γ-H2AX in both G1 and G2 phases. The increased γ-H2AX was more prominent in G2 phase, which supports the observations in NSMCE3 patient cells (van der Crabben et al., 2016). Importantly, cells with destabilised SMC5/6 (long term NSMCE4a shut off) display increased phosphorylation of Ser33 of the 32 kDa subunit of RPA, which is a specific ATR substrate. This implies that normal levels of SMC5/6 are important to prevent chronic replication stress. Together, this chapter provides a characterisation of the isogenic T-REx Flp-In 293 cell lines upon induced depletion of an essential SMC5/6 subunit, without using RNA interference.

6 Chapter 6

Results IV

Investigation of the response of NSMCE4a shut off cells to DNA damage

6.1 Introduction

Mutation of any components of the yeast Smc5/6 complex renders cells sensitive to DNA damaging agents, such as hydroxyurea, methyl methanesulfonate, ionizing radiation and UV (Verkade et al., 1999; Ampatzidou et al., 2006; Cost and Cozzarelli, 2006; Morikawa et al., 2004; Zhao and Blobel, 2005, reviewed in: Kegel and Sjorgen, 2010). Experiments in yeast showed that DNA double strand breaks induced during G2 remain unrepaired in *smc5/6* hypomorphic mutants (Lindroos et al., 2006). Furthermore, the *smc5/6* mutants fail to properly segregate their DNA in mitosis after perturbation of DNA replication by hydroxyurea. The resulting catastrophic mitosis can be alleviated by loss of homologous recombination (Ampatzidou et al., 2006; Lindroos et al., 2006; Miyabe et al., 2006; reviewed in: Murray and Carr, 2008). The genetic interactions studies of Smc5/6 in yeasts established its role in homologous recombination and DNA replication. Similarly, work in chicken DT40 cells confirmed the Smc5/6 role in regulation of homologous recombination (Stephan et al., 2011). Therefore, the role of the Smc5/6 in HR is likely to be conserved in mammalian systems. Treatment of the NSMCE2 patient cells (SUMO-ligase dead) with hydroxyurea results in defect in replication recovery after induced stalling and induction of nuclear abnormalities (Payne et al., 2014). The NSMCE3 patient fibroblasts displayed DNA repair defect in S/G2 after treatment with ionizing radiation and similarly to NSMCE2 patient cells, impaired recovery of replication after prolonged hydroxyurea treatment. Similarly, a recent study proposed that NSMCE2 is important for effective rescue of collapsed replication forks after prolonged HU treatment (Pond et al., 2019). In contrast to hypomorphic Smc5/6 mutants in yeasts, the NSMCE3 patient cells showed only mild sensitivity to UV, ionizing radiation and hydroxyurea (van der Crabben et al., 2016). This suggests that the low levels of NSMCE3 are sufficient to cope with certain DNA damage. While the SMC5/6 complex has been implicated in regulating HR,

there is no evidence suggesting that SMC5/6 plays roles in non-homologous end joining (NHEJ). While NSMCE3 patients died during infancy due to immunodeficiency, they had normal levels of B-lymphocytes and no signs of defective variable diversity joining (V(D)J) recombination (van der Crabben et al., 2016). Likewise, work in chicken DT40 cells also implies that Smc5/6 does not play a direct role in NHEJ pathway since knock out of an essential NHEJ factor, Ku70, exacerbates Smc5-/- cells sensitivity to ionising radiation (Stephan et al., 2011).

To validate and expand the knowledge of the role of human SMC5/6 in DNA damage repair, we used the constructed NSMCE4a shut off cell line. Studying nuclear processes *in vivo* in mammalian systems have advantages over yeast models; the nucleus is bigger, therefore, allows direct visualisation of DNA repair processes by molecular markers, such as DNA repair foci. This chapter characterises the cell phenotype after the SMC5/6 complex destabilisation upon exposure to a range of DNA damaging agents. The kinetics of DNA double strand break repair after NSMCE4a shut off, as well as the ability to repair induced DNA double strand breaks was assessed.

6.2 Aims

i) To investigate cellular responses in NSMCE4a shut off cell line after exposure to different types of DNA damage

ii) To monitor HR repair and its kinetics in the NSMCE4a shut off cell line

6.3 Results

6.3.1 NSMCE4a shut off and replication stress

Number of studies implicate the role of Smc5/6 in programmed replication fork pausing, such as in replication of rDNA and in repair of collapsed replication forks (Ampatzidou et al., 2006; Peng et al., 2018). Hypomorphic *smc5/6* mutants in yeast show sensitivity on spot-test assay to replication inhibitor, hydroxyurea (Ampatzidou et al., 2006; Cost and Cozzarelli, 2006; Morikawa et al., 2004; Pebernard et al., 2004; Zhao and Blobel, 2005). Hydroxyurea is commonly used as a replication inhibitor; it selectively inhibits ribonucleotide reductase enzyme, which leads to decrease of dNTP pool and results in replication fork stalling (Bianchi et al., 1986; reviewed in: Vesela et al., 2017). Treatment with hydroxyurea can result in different outcomes, depending on the time of exposure and its dose. During short term exposure to hydroxyurea (up to 2 hours), the depletion of dNTP pool will lead to uncoupling of the replicative polymerase and helicase. This will generate stretches of DNA bound by RPA, this will signal the checkpoint activation (Zou, 2003). The S-phase checkpoint stabilised replication forks can in most cases resume replication after the removal of hydroxyurea (Petermann et al., 2010, reviewed in: Friedel et al., 2009). Whereas long term exposure to hydroxyurea (more than 18 hours in mammalian cells) results in replication fork collapse and generation of Mus81 dependent DNA double-strand breaks (Hanada et al., 2007). During the spot-test assay, yeast cells are usually grown for many cell cycles in the presence of hydroxyurea, which inevitably leads to replication fork collapse. Therefore, the sensitivity of yeast *smc5/6* hypomorphs to hydroxyurea can reflect a defect in collapsed fork processing, as well as maintenance of stalled replication forks.

6.3.1.1 Cell viability after short time and prolonged hydroxyurea treatment

To explore the requirements for SMC5/6 for the maintenance of stalled forks and for collapsed fork processing we therefore examined the effects of depletion of the SMC5/6 complex during

i) replication fork stalling (2 hours exposure to 2mM hydroxyurea)
ii) replication fork collapse (24 hours exposure to 2mM hydroxyurea

Initially, cell viability after short and prolonged replication fork stalling was assessed using clonogenics viability assay. FRT-NSCE4a-/- cells were grown in Blasticidin

containing media for 7 – 10 days to render NSMCE4a shut off. To confirm the NSMCE4a shut off, protein levels of NSMCE4a were monitored by Western blot at the day of hydroxyurea treatment (Figure 6.1 D). Cells were exposed 2mM hydroxyurea for 2 or 24 hours, after which they were plated into 10 cm plates containing Tetracycline free media with 10 µg/ml Blasticidin. The T-REx Flp-In cell line, which has endogenous protein levels of NSMCE4a, was used as a control. To validate the hydroxyurea efficiency, cell cycle profiles of treated and non-treated cells were analysed by flow cytometry in parallel. Cell cycle profiles of the hydroxyurea treated cells show disappearance of the G2/M peak indicating the gradual accumulation of cells in G1/S, confirming the drug efficiency (Figure 6.1 E). Cells were allowed to form macroscopic colonies for 12 – 14 days and number of colonies in each plate was scored. The ability of NSMCE4a shut off cell line to form colonies after exposure to 2mM hydroxyurea was decreased in case of both replication fork stalling (2h) and collapse (24h) in comparison to the control cell line (Figure 6.1 A). To assess whether the observed phenotype was specific for NSMCE4a shut off, similar experiment was performed with cells grown for 7-10 days in the presence of 10 ng/ml Doxycycline and 10 µg/ml Blasticidin. In this set up, the ectopic NSMCE4a is overexpressed. No difference in the ability to form colonies after fork stalling or fork collapse was observed (Figure 6.1 B). This experiment confirmed, that the observed colony formation defect is indeed due to destabilisation of the SMC5/6 complex in the NSMCE4a shut off cell line. Interestingly, hydroxyurea treated NSMCE4a shut off cells displayed higher number of small colonies than the control cell line (Figure 6.1 C). This small colony phenotype can be explained by chromosome missegregation resulting in cell death over multiple generations indicative of unstable karyotype.

6.3.1.2 Replication fork recovery after replication fork stalling

Since the NSMCE4a shut off cell line showed sensitivity to both short and long time exposure to hydroxyurea, the next goal was to investigate what is the cause of cell death/defect in colony formation in NSMCE4a shut off cell line. It has been established that upon 2 hours treatment with 2mM hydroxyurea, most replication forks can resume replication (Petermann et al., 2010). Therefore, we wanted to validate, whether this is the case for cells with NSMCE4a shut off cells. FRT-NSMCE4a and the control T-REx Flp-In cell lines were grown in media with 10 µg/ml Blasticidin before being experiment. Cells were treated with 2mM hydroxyurea for 2 hours after which the cells were washed

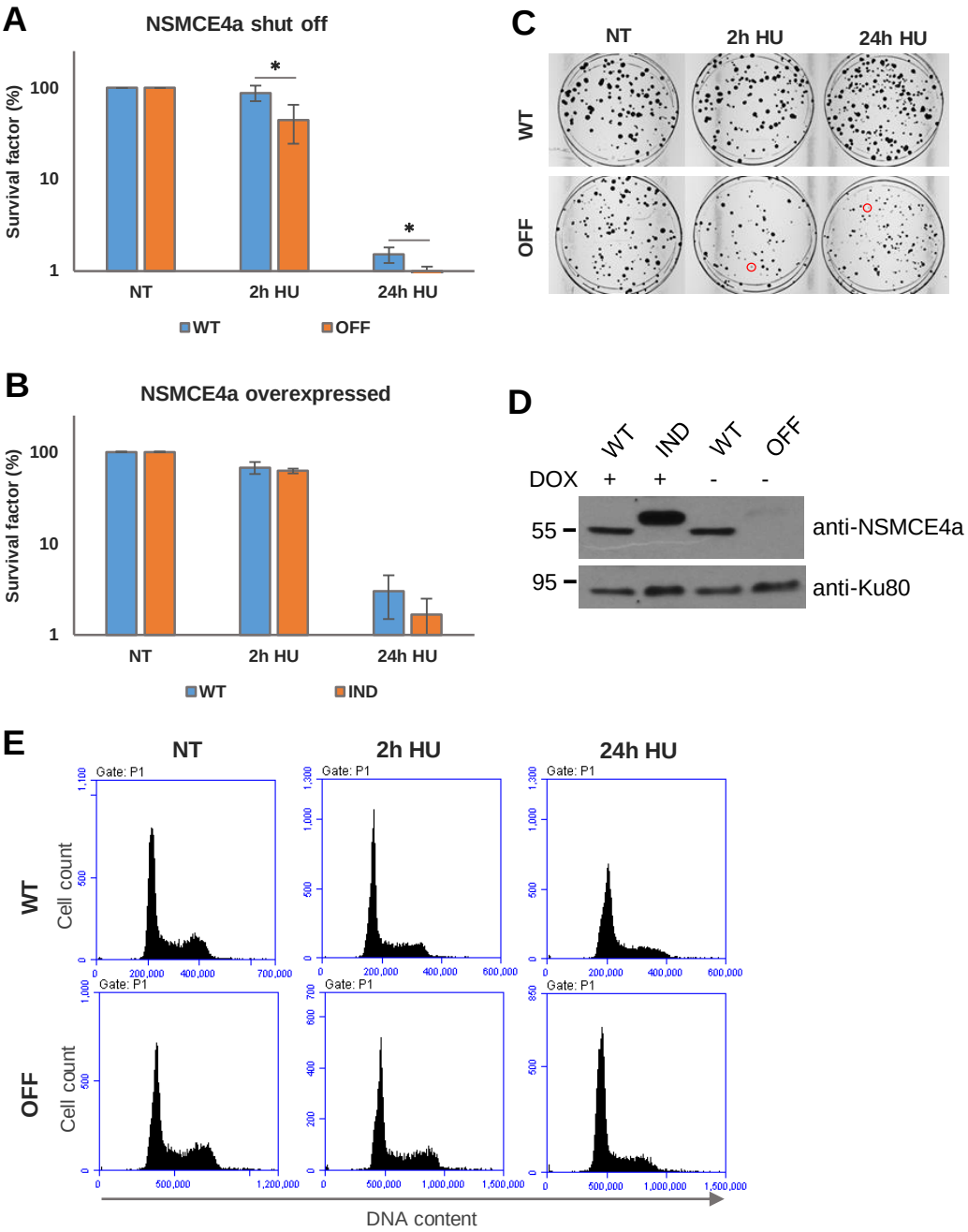


Figure 6.1: **NSMCE4a shut off confers sensitivity to replication fork stalling and collapse**

A – B. Clonogenics viability assay of cell line with endogenous NSMCE4a (WT), overexpressed NSMCE4a (IND) and NSMCE4a shut off (OFF) protein levels, cells were treated for 2 and 24 hours with 2mM Hydroxyurea before being plated out into 10 cm dishes, survival factor was counted as a plating efficiency of treated cells divided by plating efficiency of non-treated cells (NT), error bars represent +/- standard deviation of three independent experiments, two-tailed Student t-test was used to calculate statistical significance * $p \leq 0.05$. **C.** Colony phenotype of NSMCE4a shut off (OFF) and T-Rex Flp-In cell line (WT), rec circles indicate small colonies. **D.** Western blot showing NSMCE4a levels in different cell lines on the day of experiment A and B. **E.** Flow cytometry profiles of NSMCE4a shut off (OFF) and T-REx Flp-In cell line after treatment with 2mM Hydroxyurea for 2 and 24 hours.

and released into a fresh media and chased for 40 minutes with 10 μM EdU. The percentage of EdU positive cells in non-treated and hydroxyurea treated cells was scored (Figure 6.2 A). Cells with NSMCE4a shut off did not show any significant difference in EdU incorporation after hydroxyurea block. This indicates that the viability loss after replication fork stalling is not due to the inability of NSMCE4a shut off cells to resume replication after stalling. Therefore, the SMC5/6 absence does not seem to affect replication kinetics after short-time exposure to replication stress.

6.3.2 DNA double strand breaks repair kinetics in SMC5/6 deficient cell line

Ionizing radiation has a character of high energy electromagnetic waves (γ-rays, X-rays) or particles (α-particles, β-particles or neutrons). Exposure to ionizing radiation has different effects on DNA; it directly affects the DNA structure by introducing double strand and single strand breaks. Secondly, it ionises water molecules creating hydroxyl radicals, highly reactive species that react with DNA and create lesions, such as abasic sites or nucleotid base deamination. It has been found that the majority (around 70%) of DNA lesions caused by ionizing radiation is caused by the indirect effects, by hydroxyl radicals (reviewed in: Desouky et al., 2015). Importantly, majority of DNA double strand breaks formed after IR exposure occur during the next S-phase, as a result of replication fork collision with IR-dependent DNA lesions (Groth et al., 2012).

Multiple studies implicate the Smc5/6 in repair of DNA double strand break by homologous recombination (Betts Lindroos et al., 2006; van der Crabben et al., 2016; De Piccoli et al., 2006; Stephan et al., 2011; Torres-Rosell et al., 2007). Moreover, the *smc6-X* and *smc6-74* hypomorphic mutants in *S. pombe* are both defective in resolution of HR-dependent structures (Ampatzidou et al., 2006; Irmisch et al., 2009). To understand the exact role of SMC5/6 complex in double-strand break repair, we decided to map the kinetics of DSB and HR markers in the NSMCE4a shut off cell line.

6.3.2.1 NSMCE4a shut off alters DNA repair kinetics in S-G2

Ionizing radiation triggers cellular DNA damage response, which is characterised by activation of the ATR and ATM checkpoint kinases. A sensitive marker or DNA damage response and checkpoint activation is phosphorylation of histone H2AX (γ-H2AX). H2AX becomes rapidly phosphorylated by the ATM/DNA-PKcs kinase and forms distinct nuclear foci following exposure to ionizing radiation (Stiff et al., 2004). The

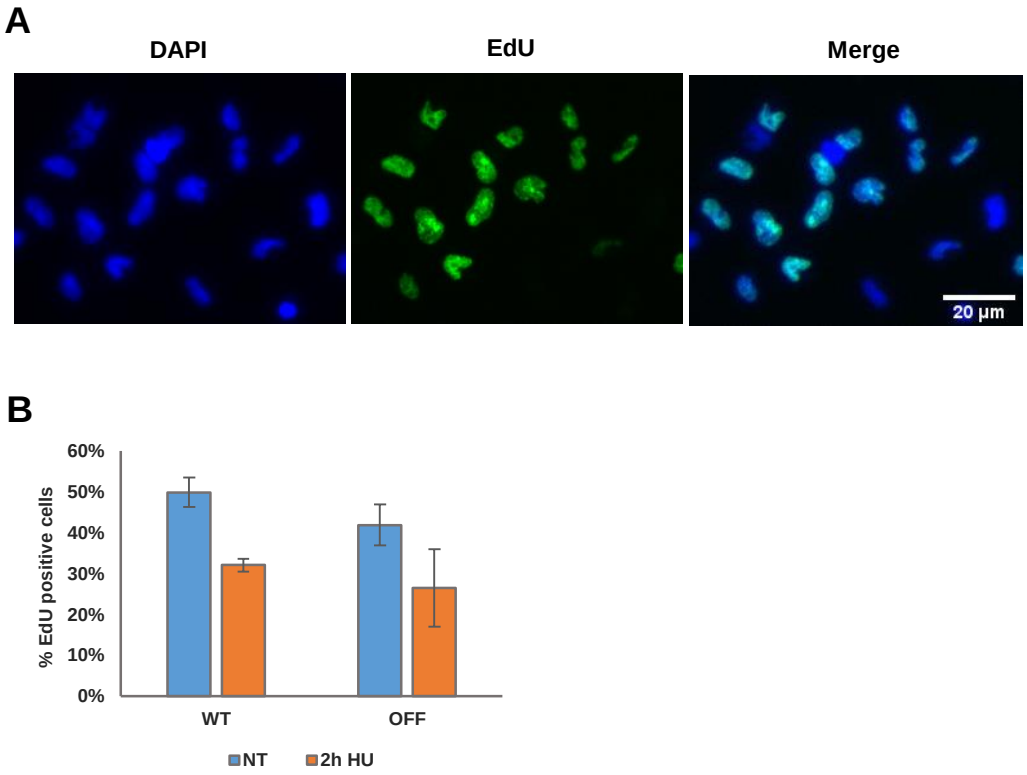


Figure 6.2: NSMCE4a shut off does not result in replication defects after short-time exposure to replication stress

A. Representative example of EdU positive cells scored in (B), cells were imaged using 100 x magnification, scale bar represents 20 µm. **B.** Analysis of replication fork recovery after 2 hours treatment with Hydroxyurea in asynchronous NSMCE4a shut off (OFF) and control T-REx Flp-In cell lines (WT), cells were treated with 2mM hydroxyurea after which cells were washed and released for 40 minutes into fresh media containing 10 µM EdU, percentage of EdU positive cells for each condition was determined as a number of EdU positive cells normalised on number of cells scored, in each experiment a minimum of 250 cells were scored, error bars represent +/- standard deviation of three independent experiments.

levels of γ-H2AX after IR exposure are dose dependent and typically peak around 30 minutes after exposure to IR and in normal cells gradually decrease to basal levels within 24 hours. Therefore, γ-H2AX can be used as a readout of DNA repair kinetics (Mariotti et al., 2013; reviewed in: Kinner et al., 2008). The level of γ-H2AX can be quantified in whole cell extract by immunoblotting, or by immunofluorescence in fixed cells, as a number of γ-H2AX foci per nucleus. After exposure to ionizing radiation, the NSMCE3 patient fibroblasts showed a mild increased number of γ-H2AX foci in G2 phase consistent with a defect in DNA repair by homologous recombination (van der Crabben et al., 2016). To assess whether the DNA repair kinetics in the NSMCE4a shut off cell line is also affected, we exposed the cells to ionizing radiation and monitored the level of γ-H2AX at different time points after exposure. Cells were exposed to 3 Gy ionizing radiation and fixed for immunofluorescence analysis at indicated time points (Figure 6.3 A). Cells were subjected to immunofluorescence with anti-γ-H2AX antibody, imaging and foci scoring was performed using the Olympus ScanR wide-field microscope with an integrated automated ScanR software. In human cells DSB repair by NHEJ occurs throughout the whole cell cycle and is faster and more efficient that HR. In contrast, HR is slower than NHEJ and occurs only during the S-G2 phase, when the sister chromatid template is present (Mao et al., 2008; Rothkamm et al., 2003). To determine, whether the NSMCE4a shut off cells have altered homologous recombination kinetics, the cell fraction in S-G2 phase was analysed. As a readout of DNA repair kinetics, the average number of γ-H2AX foci per nucleus at different time points were scored. Both the NSMCE4a shut off (OFF), and an isogenic cell line without NSMCE4a shut off (ON), cell lines displayed increase in γ-H2AX foci number at time point 8 and 12 hours in comparison to the parental cell line (WT) (Figure 6.3 B, C). This indicates that the -/-;NSMCE4a knock out cell line has an intermediate phenotype even without NSMCE4a shut off and displays altered kinetics of DNA repair in S-G2 phase. Importantly, 24 hours after exposure to IR, there was a moderate increase in the number of γ-H2AX foci in NSMCE4a shut off cells. This indicates, unrepaired or unresolved DNA lesions marked by persisting γ-H2AX signalling. These data are consistent with the G2 repair defect in NSMCE3 patient cells (van der Crabben et al., 2016) and supports the model based on yeast work, where Smc5/6 is required for correct resolution of DNA intermediates originating from homologous recombination (Copsey et al., 2013; Irmisch et al., 2009; Xaver et al., 2013).

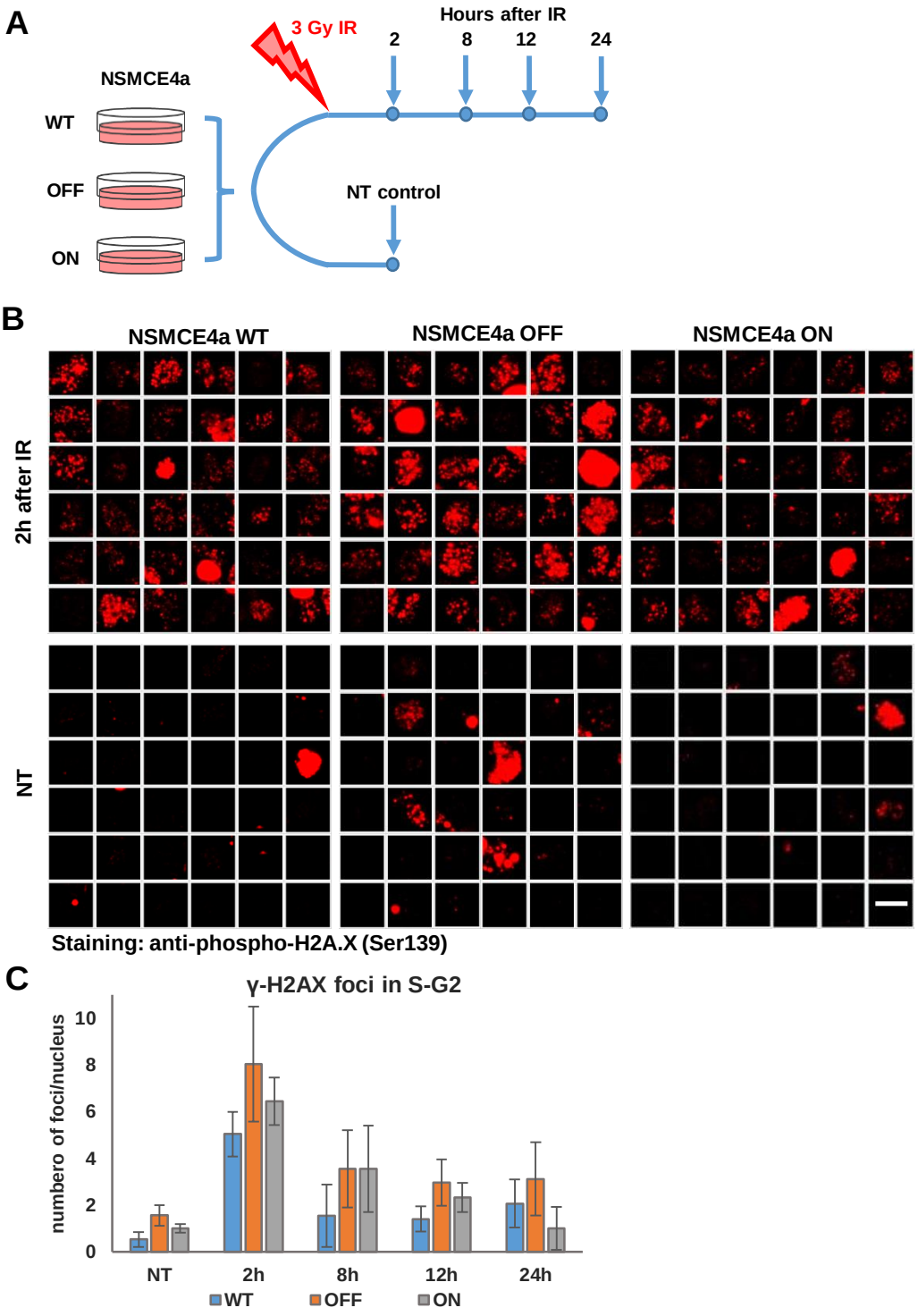


Figure 6.3: **Dynamics of γ-H2AX foci after ionizing radiation treatment**
A. Experimental outline, cell lines were treated with 3 Gy ionizing radiation using γ-rays, cells were fixed at different time points after exposure and subjected to immunofluorescence staining for γ-H2AX, NT – non-treated control. **B.** Example of immunofluorencence staining in different cell lines, images were taken using Olympus ScanR microscope, scale bar represents 10 µm. **C.** Quantification of γ-H2AX using automated ScanR software, cells in S-G2 were gated and the number of foci was plotted, error bars represent +/- standard deviation of three independent experiments; WT: parental Flp-In T-REx 293 cell line, ON: isogenic control, -/-;NSMCE4a without NSMCE4a shut off, OFF: -/-;NSMCE4a cell line with NSMCE4a shut off.

6.3.2.2 Rad51 foci formation in NSMCE4a shut off cell line

Smc5/6 hypomorphic mutants in yeast have been associated with defects in homologous recombination (HR) (Ampatzidou et al., 2006; Onoda et al., 2004; Verkade et al., 1999; Zhao and Blobel, 2005; reviewed in: Kegel and Sjögren, 2010). During double strand break repair by HR, DNA around the DSB is detected and initially resected by the MRN complex, RPA coated ssDNA ends are than displaced by the Rad51 recombinase (reviewed in: San Filippo et al., 2008). Therefore, the sites of homologous recombination repair (HRR) can be monitored by the presence of Rad51 foci (Badie et al., 2009; Cruz et al., 2018).

To check whether human SMC5/6 is important for recruitment and loading of Rad51, we assessed the ability of the NSMCE4a shut off cell line to form Rad51 foci after IR treatment. Cells were irradiated with 3 Gy IR and stained with Rad51 antibody, the presence of Rad51 foci was visualised 4 hours post exposure. Since Rad51 forms foci during S and G2 phase, cell population in S-G2 was gated (Figure 6.4). The results argue that the NSMCE4a shut off cell line is well capable of forming Rad51 foci as a consequence of DSB induction. These results are in accordance with previously published results in yeast and human cells, which showed that Smc5/6 deficient cells are capable of recruitment of HR machinery to DNA lesions (Ampatzidou et al., 2006; Potts et al., 2006).

The next aim was to map the kinetics of Rad51 foci formation, as well as the number of Rad51 foci in NSMCE4a shut off cell line. Cells were exposed to 3 Gy ionizing radiation and collected at different time points after exposure for immunofluorescence staining (Figure 6.5 A). The number of foci per nucleus was scored manually using 1000 x magnification on Nikon E400 wide-field microscope. Quantification of Rad51 foci was performed by calculating the percentage of cells with different number of Rad51 foci per nucleus in categories: 0, 1-5, 6 – 15, more than 15 foci per nucleus (Figure 6.5 B). Based on the data, the NSMCE4a shut off cell line displayed slight decrease in Rad51 foci, which was however, not significant. For more obvious visualisation, the same data set was plotted in two groups, as cells containing more than 5 foci per nucleus and cells not containing Rad51 foci. The average moderate decrease in Rad51 foci in the NSMCE4a shut off cell line, in comparison to both control cell lines, was observed (Figure 6.5 C).

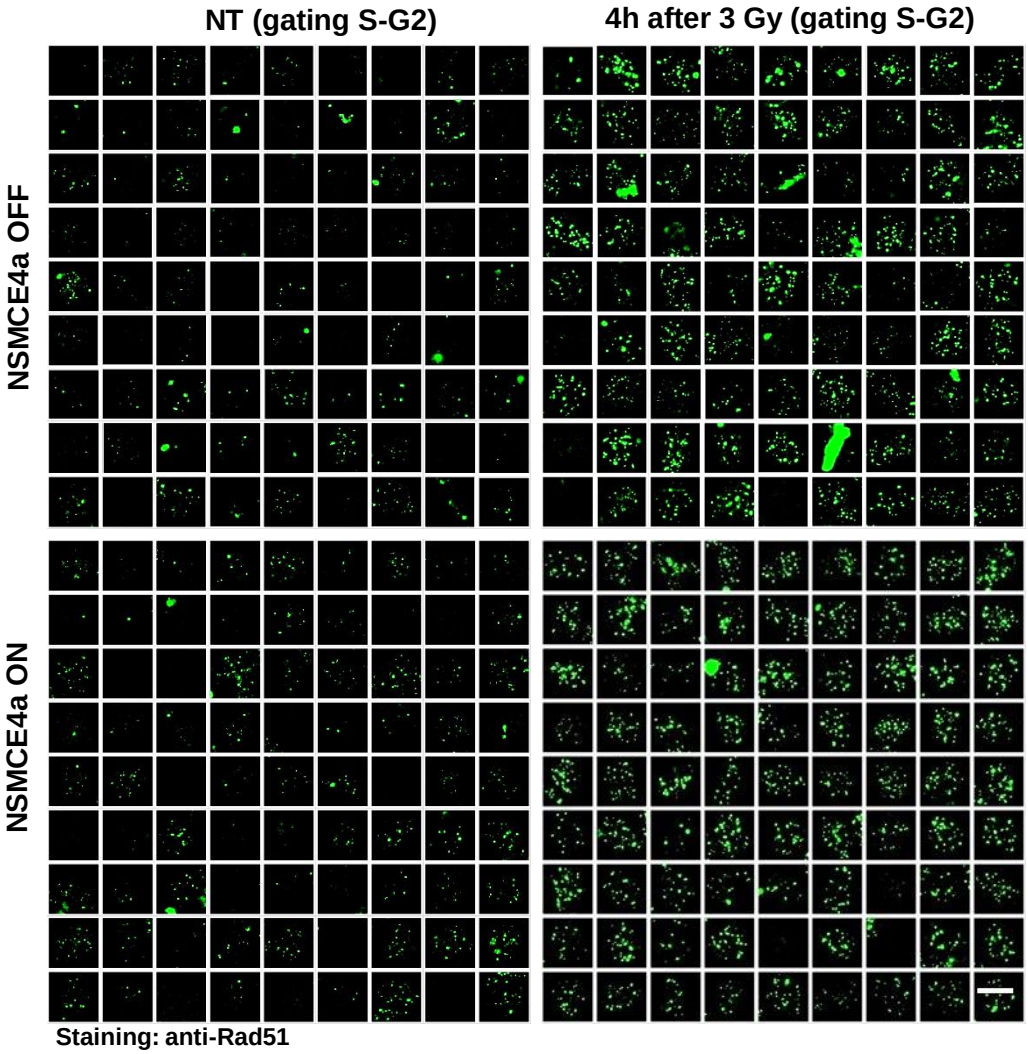


Figure 6.4: NSMCE4a shut off cell line is proficient in Rad51 foci formation
Example of Rad51 foci, cells were exposed to 3 Gy of ionizing radiation and pre-extracted for 1 minute with 0.1% Tritone X before being fixed; images were taken using Olympus ScanR wide-field microscope with 40 x objective (400 x magnification), galleries of typical cells in S-G2 phase were generated using ScanR software; NSMCE4a ON: isogenic control, -/-;NSMCE4a without NSMCE4a shut off, NSMCE4a OFF: -/-;NSMCE4a cell line with NSMCE4a shut off, scale bar represents 10 µm.

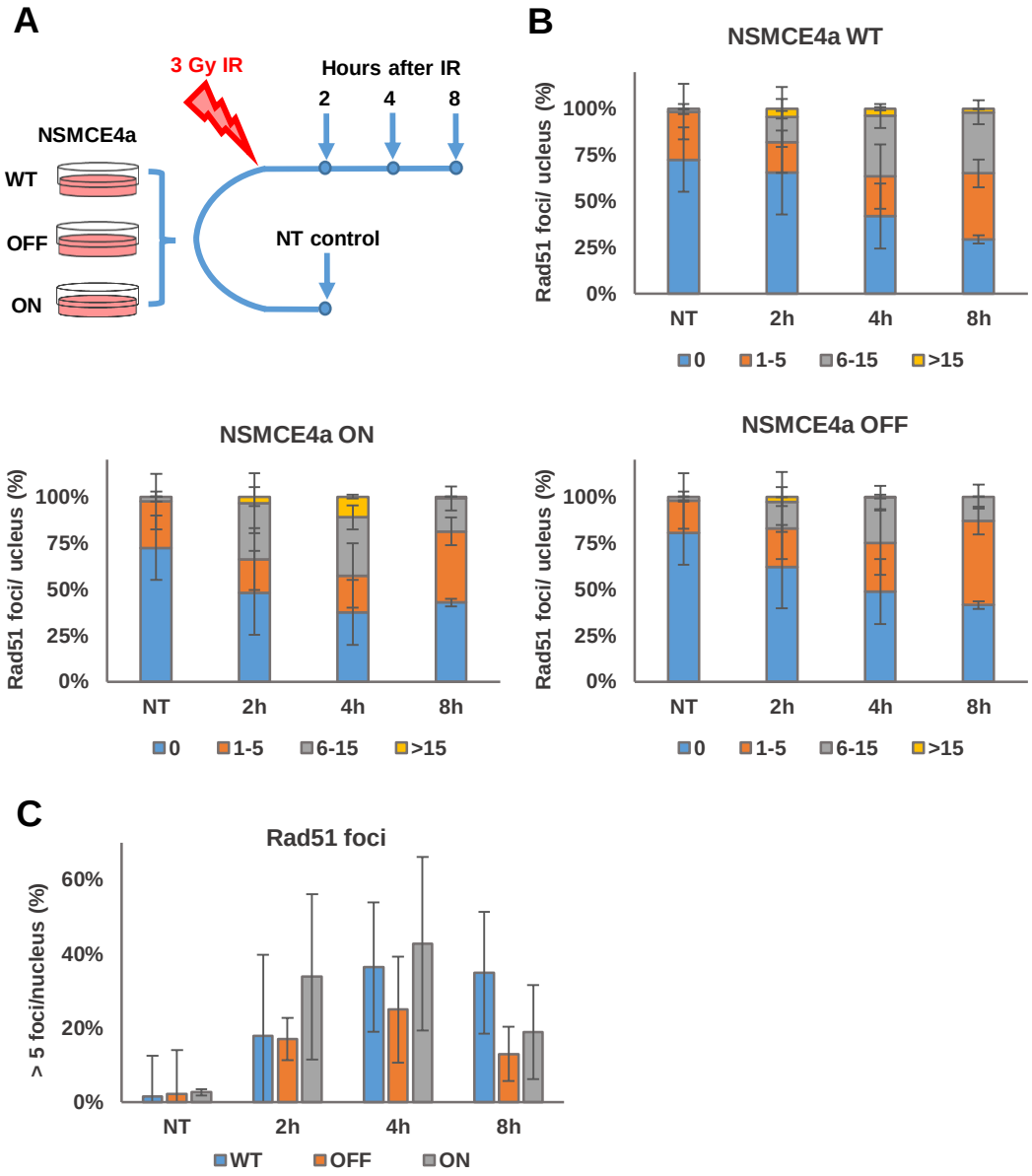


Figure 6.5: Moderate decrease in Rad51 foci formation in NSMCE4a shut off cell line

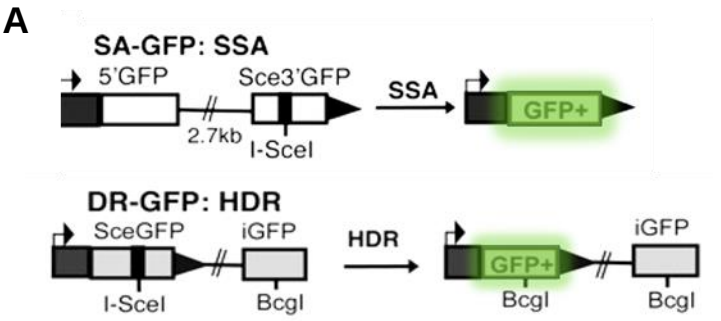
A. Experimental outline, cells were fixed at different time points after exposure to 3 Gy ionizing radiation using γ-rays and subjected to immunofluorescence staining for Rad51 antibody, NT: non-treated control. **B.** Quantification of Rad51 foci, graph shows percentage of cells containing 0 foci (blue), 1-5 foci (orange), 6-15 foci (grey) and more than 15 foci (yellow), minimum of 50 cells for each condition was scored, error bars represent +/- standard deviation of three independent experiments. **C.** Quantification of cells containing more than five Rad51 foci per nucleus, minimum of 50 cells for each condition was scored, error bars represent +/- standard deviation of three independent experiments; WT: parental Flp-In T-REx 293 cell line, ON: isogenic control, -/-;NSMCE4a without NSMCE4a shut off, OFF: -/-;NSMCE4a cell line with NSMCE4a shut off.

Together, our data indicate, that destabilisation of the SMC5/6 complex does not compromise the ability to perform HR up to the formation of pre-synaptic filament. The mild decrease in Rad51 foci formation might point towards a certain HR defect.

6.3.3 The role of SMC5/6 in DNA double strand break repair of ectopic template

To further investigate the role of SMC5/6 in HR, the approach was to transfect the NSMCE4a shut off cell line with DNA damage repair reporters (Pierce et al., 1999; Stark et al., 2004). These are GFP based reporters, which allow quantitative measurement of DNA repair pathway directly by flow cytometry. The principal of the repair reporters is a plasmid containing two non-functional GFP truncations, one of them contains an I-SceI-recognition target site (Figure 6.6 A). I-SceI is a site-specific endonuclease, which will cleave within the I-SceI site, generating a DNA double-strand break, the fate of which is determined by the DNA repair pathway choice. If the I-SceI generated DSB utilises the repair pathway measured by the reporter, it will result in generation of functional GFP protein, which can be quantified.

The SA-GFP reporter measures single-strand annealing pathway; it consists of a 5' and a 3' fragment of a functional GFP gene separated by 2.7 kb and share 266 bp homology. The I-SceI site is localised within the 3' GFP fragment, which, when cleaved, can get resected exposing the 266 bp homologous sequence of both GFP fragments. If the I-SceI generated DSB utilises SSA as a repair pathway, it will lead to restoration of a functional GFP gene (Figure 6.6 A) (Gunn and Stark, 2012; Stark et al., 2004). However, the SA-GFP reporter can also be repaired using non-allelic homologous recombination (NAHR); if the I-SceI cut sites of 3' GFP gets partially resected, it can invade the 5' fragment and use it as a homologous template. Therefore, it has to be kept in mind that NAHR repair pathway can also give a positive GFP readout in SA-GFP assay. The DR-GFP reporter, on the other hand, contains a GFP gene which functionality is compromised by insertion of the 18-bp I-SceI site, generating two in-frame stop codons. The second GFP copy is a 5' and 3' truncated non-functional GFP gene (iGFP), the homologous sequences between both GFP fragments are separated by 3.7 kb. The I-SceI containing GFP is cut and the generates DSB. If the break is repaired by homology directed repair (HDR) using part of the iGFP as a template, it will lead to restoration of a functional GFP gene (Figure 6.6 A) (Gunn and Stark, 2012; Pierce et al., 1999).



Adapted from: Gunn and Stark, 2012

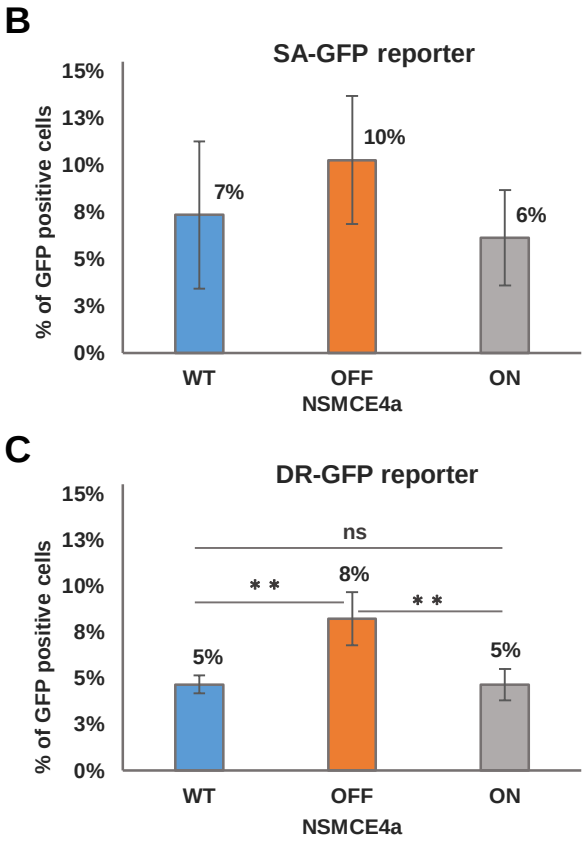


Figure 6.6: **NSMCE4a shut off leads to increase in ectopic homologous recombination**

A. Scheme of a single-strand annealing GFP reporter (SA-GFP) (Stark et al., 2004) and homologous directed repair reporter (DR-GFP) (Pierce et al., 1999), I-Sce expression plasmid is co-transfected with the GFP reporter plasmid, GFP reporter contains non-functional GFP protein, which function is restored if an examined repair pathway is used; SA-GFP: the I-Sce cut site can be resected to expose the sequence homology of the functional 5' GFP truncation, if SSA is used for repair of the induced DSB, a functional GFP gene is expressed; DR-GFP: if the I-Sce cut is repaired by non-allelic homologous recombination between/within DR-GFP plasmid, it gives rise to a functional GFP gene. **B.** NSMCE4a shut off leads to moderate but not significant increase in single strand annealing. **C.** NSMCE4a shut off leads to increase in homologous recombination within/between DR-GFP plasmids. **B – C.** Error bars +/- SD of three independent experiments, two-tailed Student t-test was used to calculate statistical significance * $p \leq 0.05$, ** $p \leq 0.01$; WT: parental Flp-In T-REx 293 cell line, ON: isogenic control, -/-;NSMCE4a without NSMCE4a shut off, OFF: -/-;NSMCE4a cell line with NSMCE4a shut off.

Both reporters can be stably inserted into the genome to map DNA repair on chromatinised DNA or transiently transfected into cells to track DNA repair pathways on ectopic DNA templates.

In order to assess whether NSMCE4a shut off alters the repair pathway of the I-SceI generated DSB, the cells were co-transfected with the GFP reporter plasmid together with I-SceI expression plasmid. Cells were incubated for 48 after transfection to allow the I-SceI induction and DNA repair. Cells were harvested and the percentage of GFP positive cells was quantified using flow cytometry. The percentage of GFP positive cells originated from GFP reporter was normalised on transfection efficiency (Figure 6.6 B, C). In case of the SSA reporter (SA-GFP), we observed moderate yet not significant increase in SSA in the NSMCE4a shut off cell line (Figure 6.6 B). The increase of SSA annealing might indicate misregulation of DNA end resection. However, it can also mean that the SA-GFP reporter was repaired by NAHR. In case of DR-GFP reporter, a significant increase in HDR in the NSMCE4a shut off in comparison to both control cell lines was observed (Figure 6.6 C). Since in each cell there might be one or more copies of the reporter plasmid, it cannot be distinguished whether the HDR happen within one or between more plasmids. Based on these results, we conclude that destabilisation of the SMC5/6 complex by NSMCE4a shut off leads to increase of HDR between or within ectopic template. If this is true, than the moderate increase in SSA in the NSMCE4a shut off cell line could be also explained by increased NAHR.

6.3.4 Viability of NSMCE4a shut off cells upon different DNA damaging agents

DNA damaging agents cause specific DNA lesions, each of them affects the DNA structure in different way and in specific cell cycle phase. Human NSMCE2 knock out U2OS cells showed only mild sensitivity to IR in comparison to wild type cells (Verver et al., 2016a). Further, NSMCE2 mutant (SUMO-ligase dead) patient lymphoblastoid cells do not display hypersensitivity to Camptothecin, or alkylating agent Mechlorethamine, in comparison to BLM-deficient lymphoblastoid cells (Payne et al., 2014). Similarly, destabilisation of the SMC5/6 complex in the NSMCE3 patient fibroblasts results only in moderate sensitivity to IR, UV and Camptothecin (van der Crabben et al., 2016). Hence, the phenotype of SMC5/6 deficiency is hugely variable and depends on the character of mutation, as well as the SMC5/6 subunit mutated. To understand which DNA repair pathway is affected in the presence of low levels of the

human SMC5/6 complex caused by its destabilisation, we subjected the NSMCE4a shut off cells to viability assay after exposure to a range of DNA damaging agents.

6.3.4.1 NSMCE4a shut off cell line does not display increased sensitivity to IR

To assess whether NSMCE4a shut off alters the viability of cells after exposure to IR, cells were treated with 2, 4 and 6 Gy of IR. To validate the SMC5/6 complex destabilisation, protein levels of NSMCE4a and SMC5 were determined by western blot on the day of the experiment (Figure 6.7 B). After the exposure to IR, cells were plated and allowed to form macroscopic colonies. The colony phenotype after fixing and staining with crystal violet is displayed in Figure 6.7 C. Clonogenics viability assay revealed that NSMCE4a shut off results only in mild, yet not significant sensitivity to IR (Figure 6.7 A). The viability assays validate the phenotype of NSMCE3 patient cells (van der Crabben et al., 2016) and are in line with our previous data showing that NSMCE4a shut off cells are capable of DNA damage signalling and repair by HR (Figure 6.3 and 6.4). These results indicate that low levels of functional SMC5/6 complex do not fully compromise repair of DSBs and other DNA lesions created by IR.

6.3.4.2 NSMCE4a shut off cell line is sensitive to Camptothecin

Topoisomerase 1 (Top1) is an essential enzyme in vertebrates and flies, but not in yeast. Top1 regulates DNA topology and manages torsional stress, it can transiently bind and relax DNA supercoils created by transcription or replication. It does so, by generating single-strand DNA break by transient attachment of the Top1 catalytic tyrosine residue to the phosphate of the sugar-phosphate backbone. Camptothecin is a Topoisomerase I inhibitor, which reversibly traps the Top1enzyme on DNA creating a stable covalently attached Top1 cleavage complex (Top1-cc). Upon collision with replication or transcription machinery, the Top1-cc complex is converted into a single ended DSB. The repair of the Top1-cc mediated DNA damage requires (i) excision of the Top1-cc and (ii) repair of the one-ended DSB (reviewed in: Pommier, 2006). It is generally accepted that the most cytotoxic effect of Camptothecin in proliferating cells is generation of replication dependent DSBs (Hsiang et al., 1989). However, inhibition of Top1 by Camptothecin also leads to accumulation of positive supercoils ahead of the replication fork (Koster et al., 2007). Low dose of Camptothecin (up to 25 nm in human cells) have been shown to cause DSB independent replication fork stalling, resulting in replication

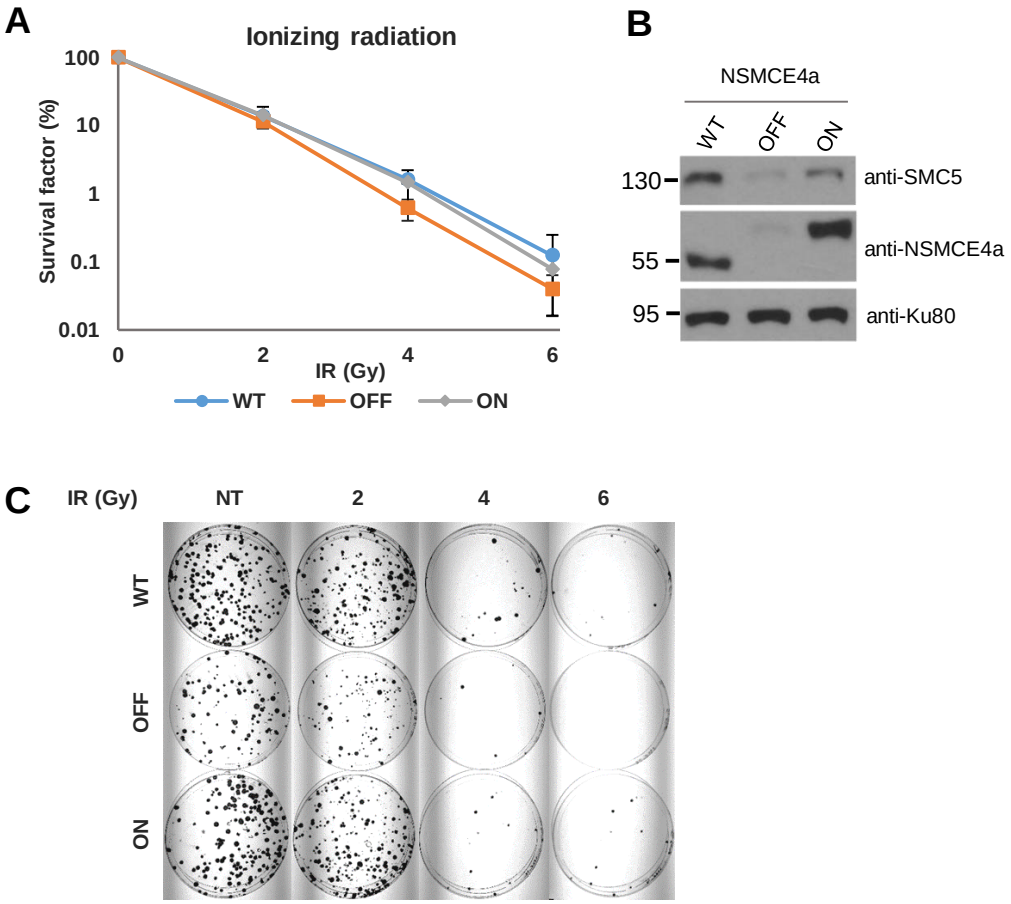


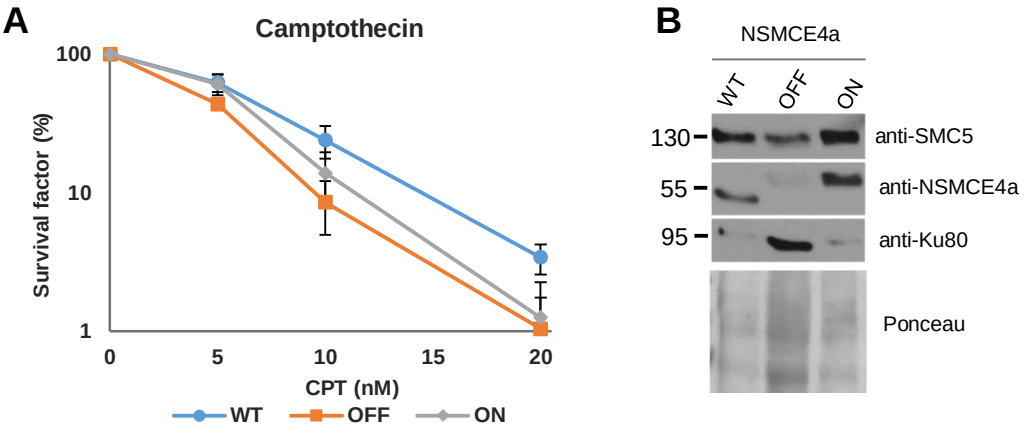
Figure 6.7: **NSMCE4a shut off does not sensitise cells to ionizing radiation**
A. Clonogenics viability assay, cells were plated out in 10 cm dishes, exposed to indicated dose of IR (X-ray) and grown until macroscopic colonies were formed, error bars represent +/- standard deviation of three independent experiments. **B.** Example of western blot showing protein levels of NSMCE4a and SMC5 on the day of exposure to IR, Ku80 is a loading control. **C.** Colony phenotype of cells after exposure to IR; . WT: parental Flp-In T-REx 293 cell line, ON: isogenic control, -/-;NSMCE4a without NSMCE4a shut off, OFF: -/-;NSMCE4a cell line with NSMCE4a shut off**.**

fork reversal to sustain fork stability (Ray Chaudhuri et al., 2012). Therefore, the cytotoxicity of Camptothecin might not only be caused by replication-dependent DSBs, but also by the inability to relax positive supercoiling leading to replication fork stalling.

Both the NSMCE3 patient fibroblasts and NSMCE2 patient lymphoblastoid cells showed only very modest sensitivity to Camptothecin (van der Crabben et al., 2016; Payne et al., 2014). To assay the viability of the NSMCE4a shut off cell line after transient exposure Top1-cc, the cells were exposed to 5, 10 and 20nM Camptothecin and allowed to form macroscopic colonies (Figure 6.8 B). Our results revealed that both -/-;NSMCE4a cell lines (NSMCE4a ON and NSMCE4a OFF) had a reproducible sensitivity to Camptothecin in comparison with the parental T-REx Flp-In 293 cell line (NSMCE4a WT) (Figure 6.8 A). The NSMCE4a shut off cell line (OFF) displayed more severe viability loss than the isogenic NSMCE4a cell line without shut off (ON). The viability loss observed in the NSMCE4a ON control cell line could be explained by the variability in protein levels of ectopic NSMCE4a that is some cells could lead to destabilisation of the SMC5/6 complex (Figure 5.4 C). Since the Flp-In T-REx 293 cell lines are highly proliferative, the observed sensitivity of cells with low levels of the SMC5/6 complex is likely linked to S-phase. The viability loss might originate from dysfunctional repair of replication-coupled DSBs, as well as from the lack of ability to stabilise replication forks during stalling.

6.3.4.3 NSMCE4a shut off cell line is synthetic lethal with PARP inhibition

The poly (ADP-ribose) polymerase (PARP) is an abundant nuclear protein that plays an essential role in DNA single strand break (SSB) repair. It readily binds broken DNA and hydrolyzes the NAD^+ to produce Poly (ADP-ribose) chains, which serves to recruit DNA repair proteins to the site of break (reviewed in: Shen et al., 2015). The clinical potential of inhibition of PARP enzymes has been exploited in cancer treatment. PARP inhibition results in inability to repair SSBs. This will lead to formation of DSBs during S-phase, when the replication fork encounters the single strand break bound by blocked PARP enzyme. PARP1 is the most abundant of PARP enzymes, its inhibition is known to produce synthetically lethal with deficiency in homologous recombination. This has been used in clinical research and treatment of BRCA1/BRCA2 deficient cancers (Bryant et al., 2009). Originally, the toxicity of PARP inhibitors (PARPi) was believed to be caused by the inability of PARP1 to repair DNA SSBs, which would be converted to DSBs upon



Student t-test		5nM		10nM		20nM	
WT vs OFF	P(T<=t) two-tail	0.004	**	0.022	*	0.014	*
WT vs ON	P(T<=t) two-tail	0.874	ns	0.112	ns	0.047	*
OFF vs ON	P(T<=t) two-tail	0.007	**	0.254	ns	0.922	ns

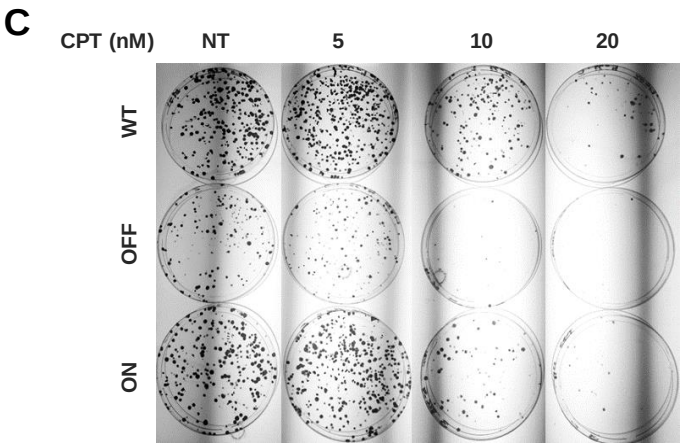


Figure 6.8: **NSMCE4a shut off sensitises cells to Camptothecin**
A. Clonogenics viability assay, cells were plated out in 10 cm dishes, exposed to indicated dose of Camptothecin for 24 hours, after which a fresh media was added and cells were grown until macroscopic colonies were formed, error bars represent +/- standard deviation of three independent experiments two-tailed Student t-test was used to calculate statistical significance * $p \leq 0.05$, ** $p \leq 0.01$. **B.** Example of western blot showing protein levels of NSMCE4a and SMC5 on the day of exposure to Camptothecin, Ku80 and Ponceau are loading controls. **C.** Colony phenotype of cells after exposure to Camptothecin; WT: parental Flp-In T-REx 293 cell line, ON: isogenic control, -/-;NSMCE4a without NSMCE4a shut off, OFF: -/-;NSMCE4a cell line with NSMCE4a shut off.

collision with replication machinery. Newer model of PARPi explain the cytotoxicity of PARPi by physical trapping of the PARP1 enzyme on DNA, creating lesions after replication fork collision with PARP1 enzyme (Ström et al., 2011). This model has been supported by multiple studies (Murai et al., 2012, 2014; reviewed in: Shen et al., 2015). The latest model of PARPi cytotoxicity is based on the observations that PARP1 plays a role in replication fork stabilisation during stalling (reviewed in: Helleday, 2011). It is known that both PARP1 and BRCA1/BRCA2 play an important role in replication fork stabilisation by protecting it from MRN nucleolytic degradation (Schlacher et al., 2011; Ying et al., 2012). Hence, it has been recently proposed that the synthetic lethality of BRCA2 deficient cells with PARP inhibition can also be caused by the inability to protect replication fork (reviewed in: Schlacher, 2017). The role of PARP in replication fork stabilisation by facilitation of replication fork reversal has been established by multiple studies (Berti et al., 2013; Ray Chaudhuri et al., 2012b; Ronson et al., 2018; reviewed in: Ray Chaudhuri and Nussenzweig, 2017).

Based on studies that reported the role of PARP in replication fork protection and the SMC5/6 in recombination-mediated restart of replication forks, we decided to assay the viability after NSMCE4a shut off cells after exposure to PARP inhibitors (PARPi). Cells were exposed to 0.5, 1 and 2 μM PARPi (KU0058948) for 24 hours before plating out for clonogenics viability assay. After forming macroscopic colonies, the number of cells was scored. From the colony phenotype it was apparent that the NSMCE4a shut off cell line (OFF) was hypersensitive to PARPi (Figure 6.9 B). Quantification and statistical evaluation of clonogenics survival assays confirmed strong synthetic sick phenotype of NSMCE4a shut off cell line with PARP inhibition (Figure 6.9 A). Importantly, the phenotype was specific for NSMCE4a shut off cell line (OFF). The viability of the isogenic NSMCE4a (ON) control cell line was similar to the T-REx Flp-In 293 cell line (WT). This indicates that the severe viability defect after PARPi is specifically connected with the low levels of the SMC5/6 complex in the NSMCE4a shut off cell line. Given the role of PARP1 in replication fork stabilisation during stalling, it can be speculated that the human SMC5/6 complex plays a role in the same pathway.

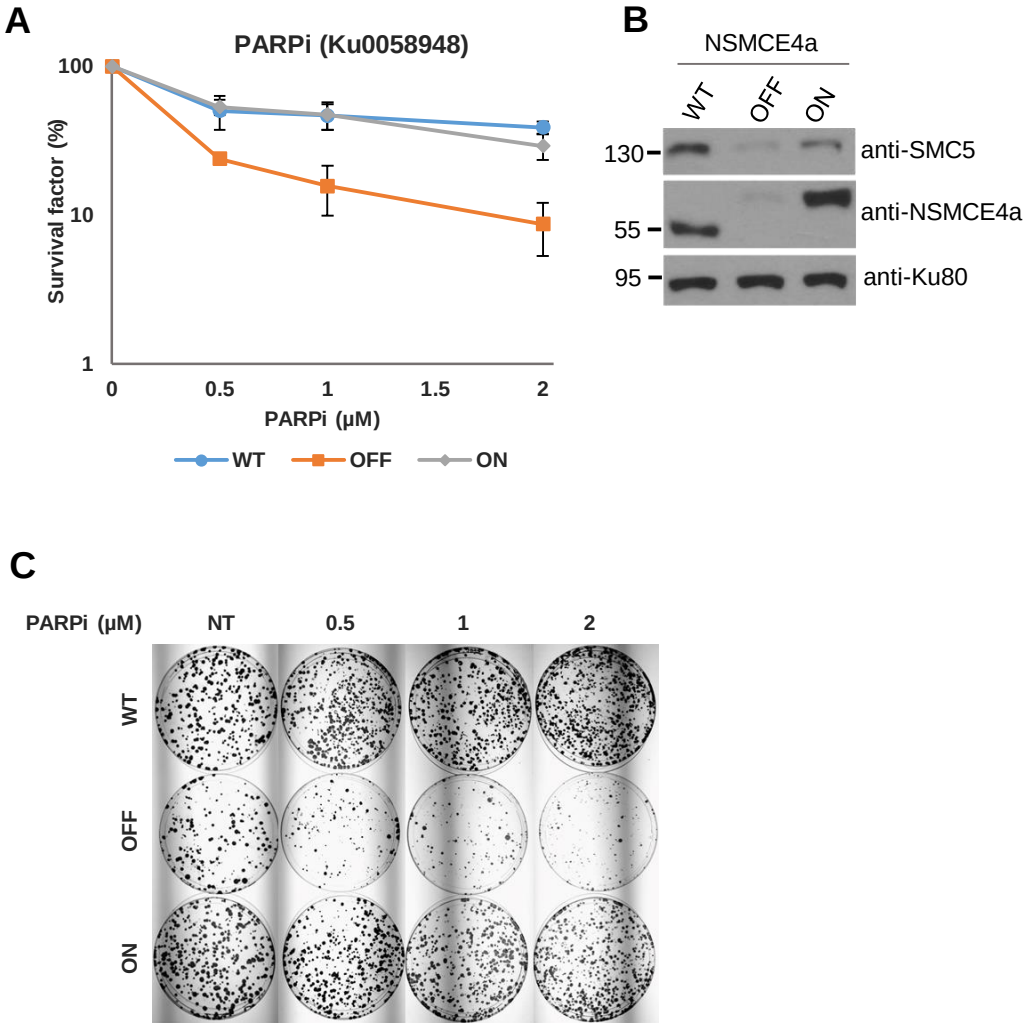


Figure 6.9: **NSMCE4a shut off confers hypersensitivity to PARP inhibitor**
A. Clonogenics viability assay, cells were plated out in 10 cm dishes, exposed to indicated dose of PARPi (KU0058948) for 24 hours, after which a fresh media was added and cells were grown until macroscopic colonies were formed, error bars represent +/- standard deviation of three independent experiments two-tailed Student t-test was used to calculate statistical significance * $p \leq 0.05$, ** $p \leq 0.01$. **B.** Example of western blot showing protein levels of NSMCE4a and SMC5 on the day of exposure to PARPi, Ku80 is a loading control. **C.** Colony phenotype of cells after exposure to PARPi; WT: parental Flp-In T-REx 293 cell line, ON: isogenic control, -/-;NSMCE4a without NSMCE4a shut off, OFF: -/-;NSMCE4a cell line with NSMCE4a shut off.

6.3.5 PARP inhibition in NSMCE4a shut off cell line decreases the number of replicating cells and leads to increase in G2/M population

Based on the observed hypersensitivity of NSMCE4a shut off cell line to PARP inhibition, the next aim was to explore in more detail the cellular processes that precede the cell death. At first, it had to be determined whether PARP inhibition affects the cell ability to progress through the cell cycle. Therefore, the ability of cells to replicate DNA after PARP inhibition treatment was measured using EdU incorporation assay. Exponentially growing cells were treated with 1μM PARPi for 24 hours, washed and released into fresh media containing 10μM EdU for 60 minutes. EdU signal was visualised by conjugation with fluorescence azide in Click-IT reaction and the number of EdU positive cells were scored (Figure 6.10 A). Number of replicating cells after 24 hours of PARPi treatment was normalised to number of replicating cells in non-treated population. The number of S-phase cells in NSMCE4a shut off cell line after PARPi treatment was decreased in comparison to both control cell lines (Figure 6.10 B). In order to assess whether PARP inhibition leads to formation of more DSB or other DNA structures recognised by DNA damage checkpoint, western blot analysis to determine γ-H2AX levels was performed (Figure 6.10 C). The γ-H2AX levels in NSMCE4a shut off cell line were slightly increased in comparison to NSMCE4a ON (non-shut off NSMCE4a control) even during the unperturbed cell cycle. This was consistent with the results in Chapter 5, however, the T-REx Flp-In 293 control also showed increase in γ-H2AX. This might be caused by difference in loading. On the other hand, all cell lines showed increase in γ-H2AX after 24 hours of PARPi treatment. However, in comparison to both controls, the NSMCE4a shut off cell line (OFF) showed an increase in γ-H2AX levels 24 hours after PARPi treatment, indicating presence of elevated levels of DSBs or other DNA structures recognised by the DNA damage checkpoint. All experiments in Figure 6.10 are only preliminary and need to be validated in multiple repeats before any conclusion can be drawn.

The initial EdU incorporation assay results indicated that the NSMCE4a shut off cell line has a decrease in S-phase cells after PARPi treatment (Figure 6.10 B). To get more quantitative and robust readout, we decided to quantify the percentage of cells in each cell cycle phase by flow cytometry. The experimental set up was similar as described for Figure 6.10 B, exponentially growing cells were treated with 1μM PARPi for 24 hours before being washed and chased for 60 minutes by 10μM EdU. Click-iT chemistry was

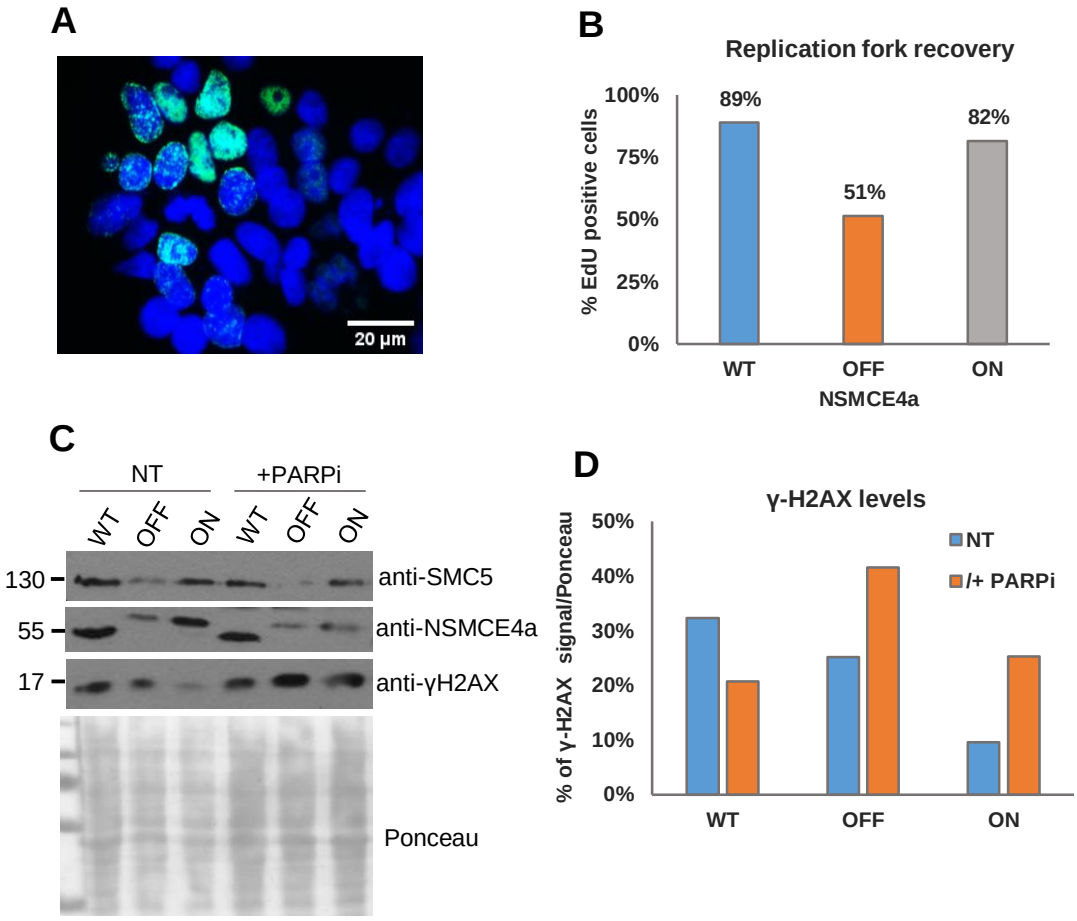


Figure 6.10: **Replication recovery defect in NSMCE4a shut off cell line upon PARPi treatment**

A. Example of EdU incorporation assay, green signal (EdU) marks replicating cells, scale bar represents 20 µm. **B.** Quantification of EdU incorporation assay (showed in A), exponentially growing cells were treated for 24 hours with 1µM PARPi, washed and released into fresh media containing 10µM EdU for 60 minutes, Click-iT chemistry was performed to conjugate Alexa Fluor 488 reporter dye to EdU, the percentage of EdU positive cells after PARPi treatment was normalised to non-treated control. **C.** Example of western blot showing increase in γ-H2AX signalling after 24 hours of PARPi treatment, 30 µg of whole cell extract was loaded per lane, treated and non-treated cells were harvested 24 hours after PARPi treatment. **D.** Quantification of (C); WT: parental Flp-In T-REx 293 cell line, ON: isogenic control, -/-;NSMCE4a without NSMCE4a shut off, OFF: -/-;NSMCE4a cell line with NSMCE4a shut off.

performed to visualise the EdU and cells were stained by propidium iodide to quantify the DNA content. The EdU positive cells were either entering or actively replicating during the 60 minutes EdU chase window (Figure 6.11 A). Quantification of cell cycle profiles revealed that the NSMCE4a shut off cell line has a reproducible decrease in percentage of S-phase population in comparison to both controls (Figure 6.11 B). Simultaneously, an increase in G2/M population has been observed in case of the NSMCE4a shut off cell line. These results indicate that SMC5/6 destabilisation in the NSMCE4a shut off cell line prevents normal recovery after PARP inhibition. In other words, PARP inhibition in the NSMCE4a shut off cell line is likely to result in cell cycle arrest.

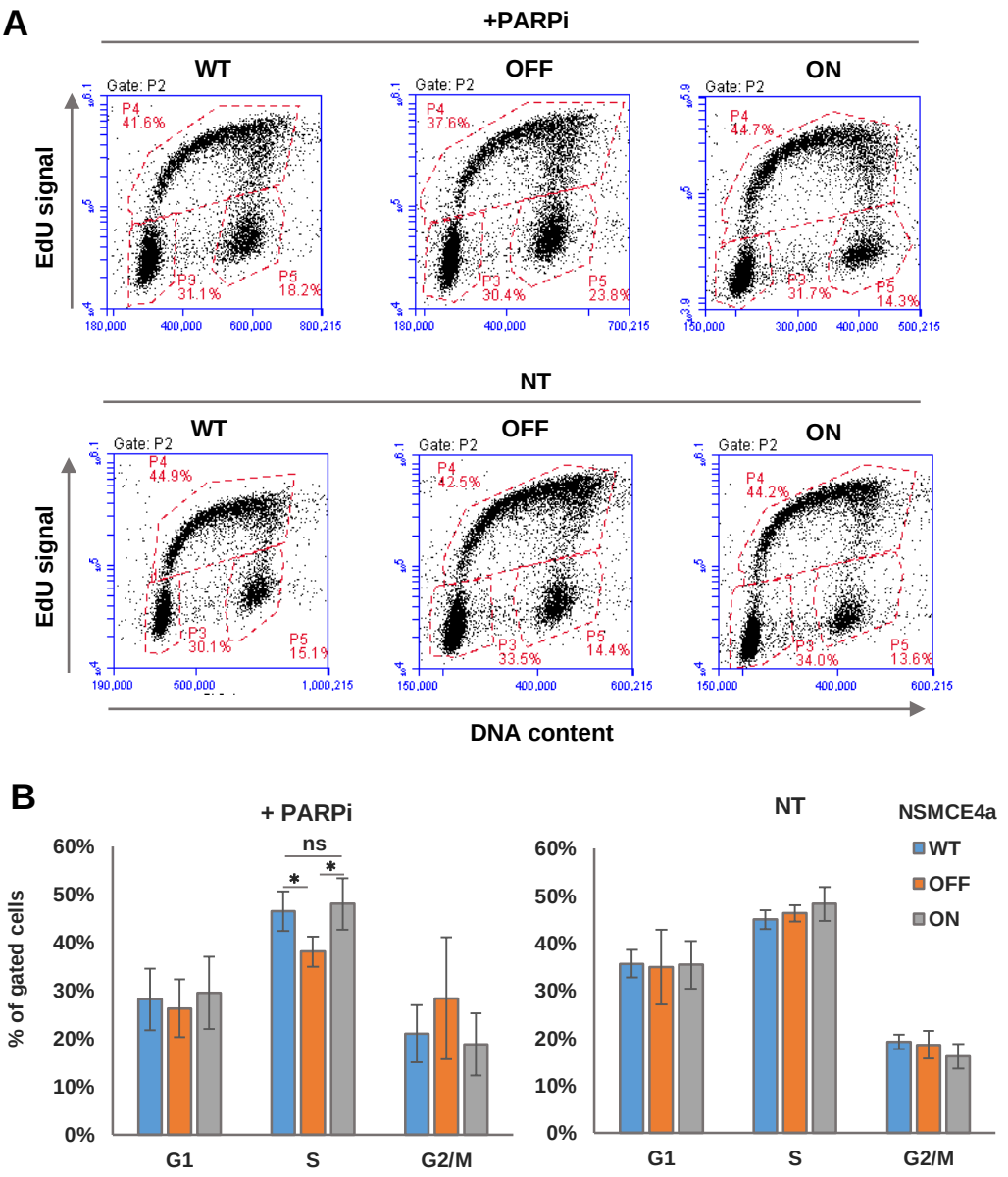


Figure 6.11: **PARP inhibition leads to decrease in S-phase population and increase of in G2/M population in NSMCE4a shut off cells**

A. Example of flow cytometry analysis to quantify percentage of cells in different cell cycle phases; exponentially growing cells were treated with PARPi for 24 hours, washed and released into fresh media with 10μM EdU for 60 minutes, Click-iT chemistry was performed to conjugate Alexa Fluor 488 reporter dye to EdU, cells were analysed by flow cytometry, cell populations in G1, S and G2/M were gated. **B.** Quantification of (A), gating was performed to quantify the percentage of cells in different cell cycle phases, error bars show +/- standard deviation of three independent repeats; two-tailed Student t-test was used to calculate statistical significance * $p \leq 0.05$; WT: parental Flp-In T-REx 293 cell line, ON: isogenic control, -/-;NSMCE4a without NSMCE4a shut off, OFF: -/-;NSMCE4a cell line with NSMCE4a shut off.

6.4 Discussion

This chapter aimed to elucidate the cellular responses in cell line with SMC5/6 complex destabilisation upon exposure to a range of DNA damaging agents. We utilised the NSMCE4a shut off cell line to validate and expand the knowledge about human SMC5/6 in DNA repair. Clonogenics viability assay after hydroxyurea treatment revealed that both short-time (RF stalling) and prolonged (RF collapse) exposure of NSMCE4a shut off cell line to hydroxyurea decreases cell survival. Our results, however, argue that destabilisation of SMC5/6 in T-REx Flp-In 293 cell line does not compromise the ability of replication forks to resume replication after short term stalling (2h 2mM hydroxyurea). This is seemingly in contrast with the results performed on NSMCE2 and NSMCE3 patient cells. However, the NSMCE3 patient cells were treated with low dose of hydroxyurea (250 μM) for 6 hours and the NSMCE3 patient cells were treated with hydroxyurea for prolonged period (18 hours). This could have led to replication fork collapse, which is a very different situation in comparison to replication fork stalling. On the other hand, our results were in line with the recent observations made by Pond and colleagues, who showed NSMCE2 knock down cell line treated with 2mM hydroxyurea for 5 hours, does not show any difference in replication fork restart and collapse in comparison to control (Pond et al., 2019).

Dynamics of γ-H2AX signalling after exposure to IR showed a moderate increase of γ-H2AX foci in S/G2 in later time points after exposure, consistent with an HRR defect. The formation of Rad51 foci after IR exposure was not impaired in NSMCE4a shut off cell line. However, the number of Rad51 foci seemed slightly decreased. These results

indicate that low levels of the SMC5/6 complex are sufficient to perform most steps of homologous recombination. Nevertheless, when homologous recombination was measured using ectopic templates reporters (DR-GFP and SA-GFP), the percentage of gene conversions between between/within DR-GFP reporters was increased in NSMCE4a shut off cell line. In line with that, an increase in gene targeting upon SMC5/6 knock down by siRNA has been previously reported (Potts et al., 2006) (although the siRNAs used in this paper were subsequently reported to have off target effects (Wu et al, 2012)). Moreover, the NSMCE2 patient cells showed increase in sister chromatid exchanges after UV treatment (Payne et al., 2014). Together with increase in sister-chromatic exchanges and chromosome instability (Chapter 5), our data confirm the role of SMC5/6 in regulation the correct template choice and the outcomes of HR. To gain a deeper understanding in SMC5/6 and regulation of HR, the same assay should be performed with stably inserted GFP reporters on chromatinised DNA.

Viability assays after exposure of NSMCE4a shut off cell line revealed only mild sensitivity to IR. These observations are in agreement with the previous experiments showing that NSMCE4a shut off cells are proficient of Rad51 foci formation and HR within HDR reporters. However, NSMCE4a showed sensitivity to the Top1 poison, Camptothecin and synthetic lethality to PARP inhibitor (KU0058948). Our observations further indicate that NSMCE4a shut off cells cannot correctly progress through the cell cycle and become arrested in G2 following PARPi treatment. Based on our results, the lesions created by PARP inhibition in human cells with destabilised SMC5/6 complex become lethal. Therefore, PARP might play an essential role in replication fork protection and stability, which, in the absence of functional SMC5/6, becomes synthetically lethal. Importantly, this emphasises the potential of SMC5/6 complex in cancer treatment.

Despite many studies focusing on the SMC5/6 role in recombination, similar defects can be ascribed to cohesin and condensin mutants (reviewed in: Tapia-Alveal et al., 2014). Remarkably, it has been shown that mutation in cohesin subunit STAG2 also confers sensitivity to PARPi (Bailey et al., 2014; Mondal et al., 2019). There is a tight functional overlap between cohesin and the SMC5/6 complex. It is therefore crucial to establish, whether the observed synthetic sensitivity of SMC5/6 destabilisation with PARPi is due to a separate or epistatic function of the SMC5/6 and cohesin.

7 Chapter 7

Discussion

7.1 Usage of the Flp-In T-REx 293 system to generate regulatable SMC5/6 cell lines

The thesis describes the usage of a commercially available T-REx Flp-In 293 cell line to engineer a system that allows characterisation of the human SMC5/6 complex. The principal of our approach is to complement a gene of interest with a regulatable cDNA, prior to its knock out. This is a more controlled way to create human cell lines, especially while working with genes that are suspected to be/ are essential. In these cases a direct CRISPR/Cas9 gene knock out is either not viable, or may lead to the generation of truncations or heterozygous mutations, rather than full knockouts. Recent studies in human cells indicate that CRISPR/Cas9 knock out of the NSMCE2 is viable (Pond et al., 2019; Verver et al., 2016b). However, it is possible that, despite the absence of protein product showed by western blotting, a residual truncation of the NSMCE2 protein, sufficient to stabilise the SMC5 arm might be present in these cell lines. Using the Flp-In T-REx system, we were able to show that full deletion of NSMCE4a in human cells is not viable. This is likely to be due to the destabilisation of the whole SMC5/6 complex. Equally, downregulation of the NSMCE4a using the Tetracycline regulatable promoter leads to destabilisation of the SMC5/6 complex demonstrated by low levels of the other components (Chapter 5 and 6). We further demonstrated that the Strep-6xHis tag on the C-terminus of human NSMCE4a does not interfere with functionality of the protein.

The drawback of the Flp-In T-REx system is that the depletion of the whole SMC5/6 complex takes relatively long time (over ten days). The T-REx Flp-In 293 cell line was used since it was the available system at the start of the project. Since then, human degron systems enabling much faster depletion of a protein of interest, such as the auxin-inducible degradation (AID), or Small Molecule-Assisted Shutoff (SMASh) tag, have become available (Chung et al., 2015; Natsume et al., 2016).

Rapid condensin depletion using the auxin inducible degron (AID) has been shown to have much more dramatic chromosome morphological defects (Samejima et al., 2018) than a gradual condensin depletion induced by conditional knock out, or RNAi (Hudson et al., 2003; Ono et al., 2003). Cells might be adapting to a gradual lower levels of condensin, thus the phenotype of a gradual condensin loss might be largely different from an acute condensin depletion. Another advantage of the AID system used to deplete condensin, is that it allows differential protein levels of the complex by auxin titration (Samejima et al., 2018).

Similarly, depletion of cohesin on protein level by AID also uncovered that acute depletion results in loss of topological domains (Rao et al., 2017). Whereas previous studies using conditional knock outs of Rad21 by the Cre/Lox system, showed that topological domains are resilient to cohesin depletion (Seitan et al., 2013). Therefore, it is crucial to establish an AID-system for SMC5/6 and compare the phenotypes of acute depletion with RNAi methods, or the presented Tet-ON system.

An advantage of the -/-;NSMCE4a[7] cell line is that the FRT-inserted cDNA can be exchanged using the FRT-expression vector with a different selection marker. This allows fast and straightforward creation of new cell lines bearing differentially tagged NSMCE4a, which can be tested for viability before tagging the endogenous locus. A SMASh-tagged NSMCE4a has been integrated in the -/-;NSMCE4a cell line in the lab. The tag does not affect growth rates and enables d NSMCE4a within 48 hours (Owen Wells, personal communication). Another use for the Flp-In T-REx system is to generate cell lines carrying mutated version of the SMC5/6 subunits. Structure informed mutations in NSMCE4a, which, similarly to the patient mutation in NSMCE3, are predicted to disrupt the interaction between NSMCE4a and NSMCE3, are currently being characterised (Desiree Villahermosa-Caballero, personal communication). Thus, the current Flp-In T-REx 293 cell line can be used to complement the structural analysis of the SMC5/6 complex.

7.1.1 Regulation of the NSMCE4a levels using the Flp-In T-Rex system

During the first attempts to downregulate the NSMCE4a, we found out that the -/-;NSMCE4a cell line had to be continuously grown in the presence of Blasticidin. The

[7] Endogenous NSMCE4a knock out cell line with ectopic FRT-inserted NSMCE4a-Strep-6xHis

need for continuous selection might either be caused by heterogeneity in the cell population (cells differentially expressing the regulatable NSMCE4a gene), or by active silencing of the genome inserted pcDNA6/TR containing both the Blasticidin resistance gene and the Tet repressor cDNA. Since the NSMCE4a is an essential gene, it is likely that there is a high selection pressure on the cells to express the NSMCE4a gene. Further, we demonstrated that low levels of the SMC5/6 complex led to slow growth and resulted in genome instability; even with no treatment, the NSMCE4a shut off cell line displays increased number of micronuclei and aneuploidy. The NSMCE4a shut off cells also display elevated markers of DNA damage and replication stress (Chapter 5).

7.2 Search for interactors of the SMC5/6 complex using AP-MS

Another project aim was to use the constructed -/-;NSMCE4a cell line to affinity purify the SMC5/6 complex. Using the 6xHis tag of the NSMCE4a-Strep-6xHis we were able to recover the SMC5/6 complex, as confirmed by the mass spectrometry analysis (Chapter 4). We aimed to identify protein interactors of the SMC5/6 complex under unperturbed condition and after replication stress. In order to do so, the native elution fractions from the IMAC affinity purification were subjected to mass spectrometry analysis. To quantify the identified proteins, label-free approach coupled with MaxQuant search was applied. Based on statistical analysis using the Perseus platform, the only significant hits after FDR corrections were the components of the SMC5/6 complex. The fact that there were no more statistically significant interactors of the SMC5/6 complex is likely to be caused by: (i) relatively low yield of the SMC5/6 in the examined elution fractions and (ii) only a small number of highly reproducible replicates analysed by mass spectrometry. The solution to this problem would be to increase the number of replicates from each mass spectrometry sample. The MaxQuant software used to perform the database search, has improved significantly and offers many features that allow accurate quantification of proteins in the sample even using label-free approaches. Another option to search for interactors of the SMC5/6 complex would be usage of labelling methods, such as metabolic or chemical labelling, which provide higher quantitative accuracy (reviewed in: Bantscheff et al., 2007).

Since SMC5/6 is a DNA binding complex, its function is likely to be executed mainly when it becomes bound to chromatin. Therefore, most of the interacting partners are predicted to interact with the SMC5/6 complex in its chromatin-bound state. We repeatedly attempted to purify chromatin-bound SMC5/6, however, no protocol which would allow the downstream mass spectrometry analysis was successfully optimised. An alternative solution would be re-tagging the NSMCE4a-Strep-6xHis with a BioID tag, which allows proximity ligation of biotin to all proteins in the vicinity of the bait protein (Roux et al., 2013). This approach could bring novel information about cellular processes involving SMC5/6. However, it has to be noted that the BioID approach does not distinguish covalent interactors from transient interactors, or proteins in the vicinity of the bait protein.

7.3 SMC5/6 and regulation of homologous recombination

The role of SMC5/6 in regulation of DNA DSB repair by homologous recombination during meiosis and mitosis has been implicated by many studies in yeasts (Ampatzidou et al., 2006; Copsey et al., 2013; Cost and Cozzarelli, 2006; Farmer et al., 2011; Lehmann et al., 1995; Lilienthal et al., 2013; Onoda et al., 2004; Torres-Rosell et al., 2005a). The project investigated the role of SMC5/6 in HRR repair by looking at the kinetics of DNA damage and HR markers, such as γ-H2AX and Rad51 foci upon depletion of the SMC5/6 complex. The NSMCE4a shut off cells displayed elevated endogenous levels of γ-H2AX; after IR treatment, the kinetics of γ-H2AX foci in the SMC5/6 depleted cell line was only mildly altered, which was the most apparent during later timepoints in S/G2 and the cell viability after IR treatment was only mildly decreased. Equally, Rad51 foci formation in S/G2 after IR treatment was only slightly decreased upon NSMCE4a shut off. However, after IR treatment, NHEJ is the most prevalent DNA double strand break repair pathway throughout the whole cell cycle (reviewed in: Löbrich and Jeggo, 2017). Since SMC5/6 deficiency has been shown to specifically affect the HRR pathway of DNA double strand break repair (Stephan et al., 2011b), IR induced damage might not provide the most sensitive readout of HR deficiency in our system.

The results in Chapter 6 showed an increase in non-allelic homologous recombination in the NSMCE4a shut off cell line using the HR GFP-reporter assay (Gunn and Stark, 2012; Pierce et al., 1999). The fact that the NSMCE4a shut off cells are capable of completing the HR repair, to gives rise to a functional GFP gene, further confirms that the SMC5/6 deficiency does not result in HR-deficiency but rather misregulation of the HRR pathway (Figure 6.6). It should be noted that the GFP-reporters were located on the transfected plasmids; the homology-directed repair might differ depending on whether the HR-reporters are stably inserted in the genome or transiently transfected.

We observed increased sensitivity of the SMC5/6 depleted cells to higher doses of damaging agents producing replication dependent lesions, such as the Top1 poison, Camptothecin (Chapter 6). This could indicate a specific defect in processing of one-ended DSB created when the replication fork collides with the DNA bound Top1-cc. Alternatively, the Camptothecin sensitivity of the NSMCE4a shut off cell line may reflect a defect in stabilizing the replication fork at the site of the lesion. In line with this

hypothesis are the observations that low doses of Camptothecin treatment leads to replication fork slowing and reversal (Ray Chaudhuri et al., 2012). Therefore, the sensitivity of the NSMCE4a shut off cell line to replication dependent lesions may reflect the role of the complex in maintenance of replication fork stability.

7.3.1 Interplay between the SMC5/6 complex and PARP

The role in stabilising stalled replication forks was investigated using PARP[8] inhibitors. PARP1 and PARP2 have been implicated in stabilisation of replication forks, by maintaining them stalled at DNA lesions (Ronson et al., 2018). Equally, it has been shown that PARP inhibition abolishes the replication fork slowing observed upon Top1 poisoning by Camptothecin (Ray Chaudhuri et al., 2012). Therefore, it can be speculated that upon Top1 inhibition by Camptothecin treatment, replication forks require PARP for stabilisation by RF reversal. The sensitivity of NSMCE4a shut off cell line to Camptothecin could be explained by the role of SMC5/6 in replication fork stabilisation by reversal, similarly to PARP1/2. PARP enzymes have recently been proposed to play a role during replication fork stalling by stabilisation of Rad51 nucleofilament at reversed forks (reviewed in: Haynes et al., 2018 and Liao et al., 2018). Human cells with knock out of both PARP1 and PARP2 display less Rad51 and more RPA foci after MMS treatment. PARP inhibition in these knock out cell lines also inhibits Rad51 foci formation (Ronson et al., 2018). The Rad51 foci formation defect can be rescued by deletion of Fbh1 helicase, a homologous recombination regulator, which can displace Rad51 from nucleofilament (Fugger et al., 2009). Therefore, the role of PARP at stalled replication forks stabilised by fork reversal, is likely to be protection of the Rad51 nucleofilament from nucleolytic degradation or helicase-mediated displacement (Ronson et al., 2018) (Figure 7.1 A). Upon PARP inhibition, (i) cells are exposed to replication roadblocks created by PARP trapping on DNA (Murai et al., 2012) and (ii) PARP function in replication fork stabilisation by Rad51-dependent mechanism is compromised (Figure 7.1 B). Therefore, cells treated with PARPi will have to rely on homologous recombination to rescue the unprotected and damaged replication forks.

[8] PARP1 and PARP2

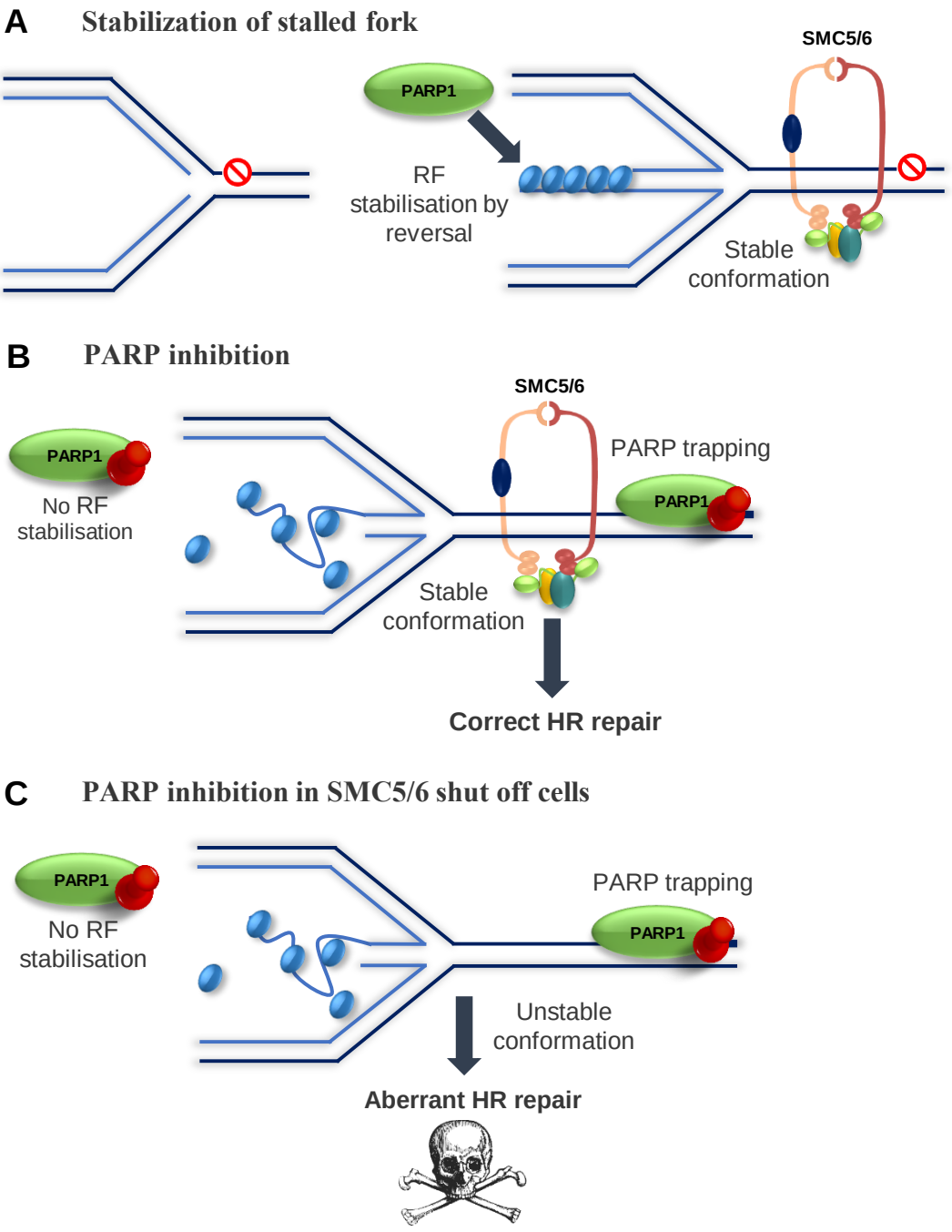


Figure 7.1: **Model of SMC5/6 function during replication fork stabilisation and repair**

A. Following perturbation, the replication fork can be remodelled into a four way junction (replication fork reversal), PARP1 is responsible for stabilisation of Rad51 (blue ovals) at reversed replication fork; Rad51 protects DNA at the stalled replication fork from nucleolytic degradation; SMC5/6 maintains the stalled fork in a stable conformation. **B.** PARP inhibition (red pin) leads to: (i) DNA lesions by PARP1 trapping at the site if ssDNA breaks, trapped PARP1-DNA create a roadblock for replication fork progression; when replication fork cannot be properly stabilised by fork reversal, homologous recombination (HR) will become crucial for the replication fork rescue, SMC5/6 enables correct HR repair, either by regulating appropriate template choice and/or by facilitating resolution of HR-dependent intermediates prior to mitosis; in the absence of SMC5/6 (shut off), the non-stabilised replication fork undergoes aberrant HR leading to cell death.

The role of SMC5/6 at stably stalled replication forks is much less clear. Studies in yeast showed that Smc5/6 hypomorphs carrying mutation in the ATPase domain (*smc6-74*) fail to recruit Rad52 to replication forks and display decrease in Rad51 and RPA chromatin association after hydroxyurea treatment (Irmisch et al., 2009). This led to a proposal of two independent functions of Smc5/6 during replication fork stalling and collapse: (i) the early function, which acts to stabilise stalled replication forks and maintain them in a conformation, which allows correct repair by homologous recombination (ii) the late function of the Smc5/6 complex is attributed to resolution of HR-dependent intermediates (Ampatzidou et al., 2006; Irmisch et al., 2009). The role of Smc5/6 at replication forks, or during resolution of HR-dependent intermediates is further supported by *in vitro* observations; the Smc5 and Smc6 heterodimer binds DNA structures arising during HR repair, such as Holliday junctions and replication forks (Roy et al., 2015) and to DNA intermediates arising during replication, such as ssDNA tracts (Alt et al., 2017; Roy et al., 2011). While our data do not provide a mechanistic detail of the Smc5/6 function at the sites of DNA-protein barriers (PARP enzyme trapped on DNA), it does enable us to propose the following model, based on our data and previous studies: (i) upon PARP inhibition, the complex acts to stabilise the blocked replication fork, (ii) and/or the SMC5/6 ensures appropriate DNA intermediates resolution after HR-mediated repair of replication fork damaged by PARPi treatment (Figure 7.1 C). Inappropriate stabilisation of the blocked replication fork together with a deficiency to perform correct HRR ultimately leads to cell death.

The model raises many questions, which could be answered by future experiments; at first it would be interesting to map the replication fork progression after PARP inhibition in the NSMCE4a shut off cell line. For this reason, it would be necessary to use techniques, which can distinguish a single fork, such as DNA combing or electron microscopy. To determine, which repair step at the stalled fork is affected, it is crucial to track the kinetics of formation and the phenotype of Rad51 and RPA foci after PARP inhibition in the NSMCE4a shut off cells. Equally, it would be interesting to deplete the SMC5/6 complex in a cell line with PARP1 deficiency, to validate, whether the observed phenotype is specific for PARP trapping or PARP depletion. Lastly, it would be interesting to perform the above mentioned experiments in a cell line that can be synchronised in a specific cell

cycle phase. This would determine, when the effects of SMC5/6 deficiency upon PARP inhibition become lethal.

7.4 Conclusion

In conclusion, this work describes the construction of a human system allowing regulatable expression of the NSMCE4a subunit of the SMC5/6 complex. First, we showed a successful insertion of C-terminally tagged NSMCE4a-Strep-6xHis into the genome using Flp-FRT mediated recombination. Secondly, knock out of the endogenous NSMCE4a gene using CRISPR/Cas9 approach was described. We demonstrated that the only functional copy of NSMCE4a in the knock out cell line is the ectopic NSMCE4a-Strep-6xHis. Importantly, we have demonstrated that the full deletion of NSMCE4a, by Flp-out of the ectopic NSMCE4a, is not viable, hence the NSMCE4a is an essential gene in human cells. The NSMCE4a-Strep-6xHis subunit in the created knock-out cell line, was shown to stably integrate into and create a functional SMC5/6 complex. The project further provided a detailed characterisation of NSMCE4a shut off cell line, including the shut off conditions, kinetics and protein levels of NSMCE4a and SMC5. Our results establish that depletion of the SMC5/6 induced by the NSMCE4a shut off, results in increased genome instability, manifesting in aneuploidy, high number or micronuclei and elevated levels of DNA damage and replication stress. NSMCE4a shut off leads to an increase in non-allelic homologous recombination within/between the HR-reporter plasmids. Further, the NSMCE4a shut off cell line displayed increased sensitivity to both short and prolonged exposure to replication fork stalling, and strong sensitivity to PARP inhibition. The strong sensitivity of SMC5/6 depleted cells to PARP inhibition was coupled to replication recovery.

Bibliography

Abdul, F., Filleton, F., Gerossier, L., Paturel, A., Hall, J., Strubin, M., and Etienne, L. (2018). Smc5/6 Antagonism by HBx Is an Evolutionarily Conserved Function of Hepatitis B Virus Infection in Mammals. J. Virol. *92*.

Ahnesorg, P., Smith, P., and Jackson, S.P. (2006). XLF interacts with the XRCC4-DNA Ligase IV complex to promote DNA nonhomologous end-joining. Cell *124*, 301–313.

al-Khodairy, F., and Carr, A.M. (1992). DNA repair mutants defining G2 checkpoint pathways in Schizosaccharomyces pombe. EMBO J. *11*, 1343–1350.

Allison, D.F., and Wang, G.G. (2019). R-loops: formation, function, and relevance to cell stress. Cell Stress *3*, 38–46.

Alt, Aaron, Dang, H.Q., Wells, O.S., Smith, L.M., Mcgregor, M.A., Welte, G.A., Thomas, Lehmann, A.R., Pearl, L.H., et al. (2017). Specialized interfaces of Smc5/6 control hinge stability and DNA association) Specialized interfaces of Smc5/6 control hinge stability and DNA association. Nat. Commun. *8*, 14011.

Ampatzidou, E., Irmisch, A., O'Connell, M.J., and Murray, J.M. (2006). Smc5/6 is required for repair at collapsed replication forks. Mol. Cell. Biol. *26*, 9387–9401.

Amunugama, R., Willcox, S., Wu, R.A., Abdullah, U.B., El-Sagheer, A.H., Brown, T., McHugh, P.J., Griffith, J.D., and Walter, J.C. (2018). Replication Fork Reversal during DNA Interstrand Crosslink Repair Requires CMG Unloading. Cell Rep. *23*, 3419–3428.

Andrews, E.A., Palecek, J., Sergeant, J., Taylor, E., Lehmann, A.R., and Watts, F.Z. (2005). Nse2, a Component of the Smc5-6 Complex, Is a SUMO Ligase Required for the Response to DNA Damage. Mol. Cell. Biol. *25*, 185–196.

Badie, S., Liao, C., Thanasoula, M., Barber, P., Hill, M.A., and Tarsounas, M. (2009). RAD51C facilitates checkpoint signaling by promoting CHK2 phosphorylation. J. Cell Biol. *185*, 587–600.

Bailey, M.L., O'neil, N.J., Van Pel, D.M., Solomon, D.A., Waldman, T., and Hieter, P. (2014). Cancer Biology and Signal Transduction Glioblastoma Cells Containing Mutations in the Cohesin Component STAG2 Are Sensitive to PARP Inhibition.

Bantscheff, M., Schirle, M., Sweetman, G., Rick, J., and Kuster, B. (2007). Quantitative mass spectrometry in proteomics: A critical review. Anal. Bioanal. Chem. *389*, 1017–1031.

Baxter, J., Sen, N., López Martínez, V., Monturus De Carandini, M.E., Schvartzman, J.B., Diffley, J.F.X., and Aragón, L. (2011). Positive supercoiling of mitotic DNA drives decatenation by topoisomerase II in eukaryotes. Science (80-.). *331*, 1328–1332.

Ben-Shahar, T.R., Heeger, S., Lehane, C., East, P., Flynn, H., Skehel, M., and Uhlmann, F. (2008). Eco1-dependent cohesin acetylation during establishment of sister chromatid cohesion. Science (80-.). *321*, 563–566.

Benjamini, Yoav ; Hochberg, Y. (1995). Controlling the False Discovery Rate - a Practical and Powerful Approach to Multiple Testing. Journal of the Royal Statistical Society Series B-Methodological 1995.pdf. J. R. Stat. Soc. Ser. B *57*, 289–300.

Bentley, N.J., Holtzman, D.A., Flaggs, G., Keegan, K.S., DeMaggio, A., Ford, J.C., Hoekstra, M., and Carr, A.M. (1996). The Schizosaccharomyces pombe rad3 checkpoint gene. EMBO J. *15*, 6641–6651.

Bentley, P., Tan, M.J.A., McBride, A.A., White, E.A., and Howley, P.M. (2018). The SMC5/6 Complex Interacts with the Papillomavirus E2 Protein and Influences Maintenance of Viral Episomal DNA. J. Virol. *92*.

Bermejo, R., Doksani, Y., Capra, T., Katou, Y.M., Tanaka, H., Shirahige, K., and Foiani, M. (2007). Top1- and Top2-mediated topological transitions at replication forks ensure fork progression and stability and prevent DNA damage checkpoint activation. Genes Dev *21*, 1921–1936.

Bermúdez-López, M., Ceschia, A., de Piccoli, G., Colomina, N., Pasero, P., Aragón, L., and Torres-Rosell, J. (2010). The Smc5/6 complex is required for dissolution of DNA-mediated sister chromatid linkages. Nucleic Acids Res. *38*, 6502–6512.

Berti, M., Ray Chaudhuri, A., Thangavel, S., Gomathinayagam, S., Kenig, S., Vujanovic, M., Odreman, F., Glatter, T., Graziano, S., Mendoza-Maldonado, R., et al. (2013). Human RECQ1 promotes restart of replication forks reversed by DNA topoisomerase I inhibition. Nat. Struct. Mol. Biol. *20*, 347–354.

Bianchi, V., Pontis, E., and Reichard, P. (1986). Changes of deoxyribonucleoside triphosphate pools induced by hydroxyurea and their relation to DNA synthesis. J. Biol. Chem. *261*, 16037–16042.

Bickel, J.S., Chen, L., Hayward, J., Yeap, S.L., Alkers, A.E., and Chan, R.C. (2010). Structural Maintenance of Chromosomes (SMC) Proteins Promote Homolog-Independent Recombination Repair in Meiosis Crucial for Germ Cell Genomic Stability. PLoS Genet *6*, e1001028.

Blackford, A.N., and Jackson, S.P. (2017). ATM, ATR, and DNA-PK: The Trinity at the Heart of the DNA Damage Response. Mol. Cell *66*, 801–817.

Boddy, M.N., Shanahan, P., Hayes McDonald, W., Lopez-Girona, A., Noguchi, E., Yates Iii, J.R., and Russell, P. (2003). Replication Checkpoint Kinase Cds1 Regulates Recombinational Repair Protein Rad60. Mol. Cell. Biol. *23*, 5939–5946.

Bornhorst, J.A., and Falke, J.J. (2000). Purification of proteins using polyhistidine affinity tags. Methods Enzymol. *326*, 245–254.

Branzei, D., Sollier, J., Liberi, G., Zhao, X., Maeda, D., Seki, M., Enomoto, T., Ohta, K., and Foiani, M. (2006). Ubc9- and Mms21-Mediated Sumoylation Counteracts Recombinogenic Events at Damaged Replication Forks. Cell *127*, 509–522.

Bryant, H.E., Petermann, E., Schultz, N., Jemth, A.-S., Loseva, O., Issaeva, N., Johansson, F., Fernandez, S., McGlynn, P., and Helleday, T. (2009). PARP is activated at stalled forks to mediate Mre11-dependent replication restart and recombination. EMBO J. *28*, 2601–2615.

Buisson, R., Boisvert, J.L., Benes, C.H., and Zou, L. (2015). Distinct but Concerted Roles of ATR, DNA-PK, and Chk1 in Countering Replication Stress during S Phase. Mol. Cell *59*, 1011–1024.

Burma, S., Chen, B.P., Murphy, M., Kurimasa, A., and Chen, D.J. (2001). ATM Phosphorylates Histone H2AX in Response to DNA Double-strand Breaks. J. Biol. Chem.

276, 42462–42467.

Bustard, D.E., Menolfi, D., Jeppsson, K., Ball, L.G., Dewey, S.C., Shirahige, K., Sjögren, C., Branzei, D., and Cobb, J.A. (2012). During replication stress Non-Smc-Element 5 is required for Smc5/6 complex functionality at stalled forks.

Bylund, L., Kytölä, S., Lui, W.-O., Larsson, C., and Weber, G. (2004). Analysis of the cytogenetic stability of the human embryonal kidney cell line 293 by cytogenetic and STR profiling approaches. Cytogenet. Genome Res. *106*, 28–32.

Byun, T.S., Pacek, M., Yee, M.C., Walter, J.C., and Cimprich, K.A. (2005). Functional uncoupling of MCM helicase and DNA polymerase activities activates the ATR-dependent checkpoint. Genes Dev. *19*, 1040–1052.

Celeste, A., Petersen, S., Romanienko, P.J., Fernandez-Capetillo, O., Chen, H.T., Sedelnikova, O.A., Reina-San-Martin, B., Coppola, V., Meffre, E., Difilippantonio, M.J., et al. (2002). Genomic instability in mice lacking histone H2AX. Science *296*, 922–927.

Chapman, J.R., and Jackson, S.P. (2008). Phospho-dependent interactions between NBS1 and MDC1 mediate chromatin retention of the MRN complex at sites of DNA damage. EMBO Rep. *9*, 795–801.

Chavez, A., Agrawal, V., and Johnson, F.B. (2011). Homologous recombination-dependent rescue of deficiency in the structural maintenance of chromosomes (Smc) 5/6 complex. J. Biol. Chem. *286*, 5119–5125.

Chen, R., and Wold, M.S. (2014). Replication protein A: Single-stranded DNA's first responder: Dynamic DNA-interactions allow replication protein A to direct single-strand DNA intermediates into different pathways for synthesis or repair Prospects & Overviews R. Chen and M. S. Wold. BioEssays *36*, 1156–1161.

Chen, Y.-H., Choi, K., Szakal, B., Arenz, J., Duan, X., Ye, H., Branzei, D., and Zhao, X. (2009). Interplay between the Smc5/6 Complex and the Mph1 Helicase in Recombinational Repair. Proc. Natl. Acad. Sci. U. S. A. *106*, 21252–21257.

Chomez, P., De Backer, O., Bertrand, M., De Plaen, E., Boon, T., and Lucas, S. (2001). An overview of the MAGE gene family with the identification of all human members of the family. Cancer Res. *61*, 5544–5551.

Chowdhury, D., Keogh, M.C., Ishii, H., Peterson, C.L., Buratowski, S., and Lieberman, J. (2005). γ-H2AX dephosphorylation by protein phosphatase 2A facilitates DNA double-strand break repair. Mol. Cell *20*, 801–809.

Chuang, P.T., Albertson, D.G., and Meyer, B.J. (1994). DPY-27: A chromosome condensation protein homolog that regulates C. elegans dosage compensation through association with the X chromosome. Cell *79*, 459–474.

Chung, H.K., Jacobs, C.L., Huo, Y., Yang, J., Krumm, S.A., Plemper, R.K., Tsien, R.Y., and Lin, M.Z. (2015). Tunable and reversible drug control of protein production via a self-excising degron. Nat. Chem. Biol. *11*, 713–720.

Ciosk, R., Shirayama, M., Shevchenko, A., Tanaka, T., Toth, A., Shevchenko, A., and Nasmyth, K. (2000). Cohesin's binding to chromosomes depends on a separate complex consisting of Scc2 and Scc4 proteins. Mol. Cell *5*, 243–254.

Cobb, J.A., Bjergbaek, L., Shimada, K., Frei, C., and Gasser, S.M. (2003). DNA polymerase stabilization at stalled replication forks requires Mec1 and the RecQ helicase Sgs1. Embo J *22*, 4325–4336.

Copsey, A., Tang, S., Jordan, P.W., Blitzblau, H.G., Newcombe, S., Chan, A.C. ho, Newnham, L., Li, Z., Gray, S., Herbert, A.D., et al. (2013). Smc5/6 Coordinates Formation and Resolution of Joint Molecules with Chromosome Morphology to Ensure Meiotic Divisions. PLoS Genet. *9*.

Cortez, D. (2015). Preventing replication fork collapse to maintain genome integrity. DNA Repair (Amst). *32*, 149–157.

Cost, G.J., and Cozzarelli, N.R. (2006). Smc5p Promotes Faithful Chromosome Transmission and DNA Repair in Saccharomyces cerevisiae. Genetics *172*, 2185–2200.

Costanzo, V., Shechter, D., Lupardus, P.J., Cimprich, K.A., Gottesman, M., and Gautier, J. (2003). An ATR- and Cdc7-dependent DNA damage checkpoint that inhibits initiation of DNA replication. Mol. Cell *11*, 203–213.

Cox, J., and Mann, M. (2008). MaxQuant enables high peptide identification rates, individualized p.p.b.-range mass accuracies and proteome-wide protein quantification. Nat. Biotechnol. *26*, 1367–1372.

Cox, J., Hein, M.Y., Luber, C.A., Paron, I., Nagaraj, N., and Mann, M. (2014). Accurate Proteome-wide Label-free Quantification by Delayed Normalization and Maximal Peptide Ratio Extraction, Termed MaxLFQ* □ S Technological Innovation and Resources. Mol. Cell. Proteomics *13*, 2513–2526.

van der Crabben, S.N., Hennus, M.P., McGregor, G.A., Ritter, D.I., Nagamani, S.C.S., Wells, O.S., Harakalova, M., Chinn, I.K., Alt, A., Vondrova, L., et al. (2016). Destabilized SMC5/6 complex leads to chromosome breakage syndrome with severe lung disease. J. Clin. Invest. *126*, 2881–2892.

Cruz, C., Castroviejo-Bermejo, M., Gutiérrez-Enríquez, S., Llop-Guevara, A., Ibrahim, Y.H., Gris-Oliver, A., Bonache, S., Morancho, B., Bruna, A., Rueda, O.M., et al. (2018). RAD51 foci as a functional biomarker of homologous recombination repair and PARP inhibitor resistance in germline BRCA-mutated breast cancer. Ann. Oncol. Off. J. Eur. Soc. Med. Oncol. *29*, 1203–1210.

Csankovszki, G., Petty, E.L., and Collette, K.S. (2009). The worm solution: A chromosome-full of condensin helps gene expression go down. Chromosom. Res. *17*, 621–635.

Decorsière, A., Mueller, H., Van Breugel, P.C., Abdul, F., Gerossier, L., Beran, R.K., Livingston, C.M., Niu, C., Fletcher, S.P., Hantz, O., et al. (2016). Hepatitis B virus X protein identifies the Smc5/6 complex as a host restriction factor. Nature *531*, 386–389.

Desouky, O., Ding, N., and Zhou, G. (2015). Targeted and non-targeted effects of ionizing radiation. J. Radiat. Res. Appl. Sci. *8*, 247–254.

Díaz, M., Pečinková, P., Nowicka, A., Baroux, C., Sakamoto, T., Gandha, P.Y., Jeřábková, H., Matsunaga, S., Grossniklaus, U., and Pecinka, A. (2019). The SMC5/6 complex subunit NSE4A is involved in DNA damage repair and seed development. Plant Cell *31*, 1579–1597.

Dixon, J.R., Selvaraj, S., Yue, F., Kim, A., Li, Y., Shen, Y., Hu, M., Liu, J.S., and Ren,

B. (2012). Topological domains in mammalian genomes identified by analysis of chromatin interactions. Nature *485*, 376–380.

Doyle, J.M., Gao, J., Wang, J., Yang, M., and Potts, P.R. (2010). MAGE-RING protein complexes comprise a family of E3 ubiquitin ligases. Mol. Cell *39*, 963–974.

Duan, X., Sarangi, P., Liu, X., Rangi, G.K., Zhao, X., and Ye, H. (2009a). Structural and functional insights into the roles of the Mms21 subunit of the Smc5/6 complex. Mol. Cell *35*, 657–668.

Duan, X., Yang, Y., Chen, Y.-H., Arenz, J., Rangi, G.K., Zhao, X., and Ye, H. (2009b). Architecture of the Smc5/6 Complex of *Saccharomyces cerevisiae* Reveals a Unique Interaction between the Nse5-6 Subcomplex and the Hinge Regions of Smc5 and Smc6. J. Biol. Chem. *284*, 8507–8515.

Enomoto, M., Sawano, Y., Kosuge, S., Yamano, Y., Kuroki, K., and Ohtsuki, K. (2006). High phosphorylation of HBV core protein by two α-type CK2-activated cAMP-dependent protein kinases in vitro. FEBS Lett. *580*, 894–899.

Falck, J., Coates, J., and Jackson, S.P. (2005). Conserved modes of recruitment of ATM, ATR and DNA-PKcs to sites of DNA damage. Nature *434*, 605–611.

Farmer, S., San-Segundo, P.A., and Aragón, L. (2011). The Smc5–Smc6 Complex Is Required to Remove Chromosome Junctions in Meiosis. PLoS One *6*, e20948.

Fenech, M., and Morley, A.A. (1989). Kinetochore detection in micronuclei: an alternative method for measuring chromosome loss. Mutagenesis *4*, 98–104.

Fenech, M., Kirsch-Volders, M., Natarajan, A.T., Surralles, J., Crott, J.W., Parry, J., Norppa, H., Eastmond, D.A., Tucker, J.D., and Thomas, P. (2011). Molecular mechanisms of micronucleus, nucleoplasmic bridge and nuclear bud formation in mammalian and human cells. Mutagenesis *26*, 125–132.

Ford, J.H., Schultz, C.J., and Correll, A.T. (1988). Chromosome elimination in micronuclei: a common cause of hypoploidy. Am. J. Hum. Genet. *43*, 733–740.

Forment, J. V., Blasius, M., Guerini, I., and Jackson, S.P. (2011). Structure-Specific DNA Endonuclease Mus81/Eme1 Generates DNA Damage Caused by Chk1 Inactivation. PLoS One *6*, e23517.

Fousteri, M.I., and Lehmann, A.R. (2000). A novel SMC protein complex in Schizosaccharomyces pombe contains the Rad18 DNA repair protein. EMBO J. *19*, 1691–1702.

Friedel, A.M., Pike, B.L., and Gasser, S.M. (2009). ATR/Mec1: coordinating fork stability and repair. Curr. Opin. Cell Biol. *21*, 237–244.

Fudenberg, G., Imakaev, M., Lu, C., Goloborodko, A., Abdennur, N., and Mirny, L.A. (2016). Formation of Chromosomal Domains by Loop Extrusion. Cell Rep. *15*, 2038–2049.

Fugger, K., Mistrik, M., Danielsen, J.R., Dinant, C., Falck, J., Bartek, J., Lukas, J., and Mailand, N. (2009). Human Fbh1 helicase contributes to genome maintenance via pro- and anti-recombinase activities. J. Cell Biol. *186*, 655–663.

Gallego-Paez, L.M., Tanaka, H., Bando, M., Takahashi, M., Nozaki, N., Nakato, R., Shirahige, K., and Hirota, T. (2014). Smc5/6-mediated regulation of replication

progression contributes to chromosome assembly during mitosis in human cells. Mol. Biol. Cell *25*, 302–317.

Ganji, M., Shaltiel, I.A., Bisht, S., Kim, E., Kalichava, A., Haering, C.H., and Dekker, C. (2018). Real-time imaging of DNA loop extrusion by condensin. Science (80-.). *360*, 102–105.

Gerlich, D., Koch, B., Dupeux, F., Peters, J.M., and Ellenberg, J. (2006). Live-Cell Imaging Reveals a Stable Cohesin-Chromatin Interaction after but Not before DNA Replication. Curr. Biol. *16*, 1571–1578.

Goloborodko, A., Imakaev, M. V., Marko, J.F., and Mirny, L. (2016). Compaction and segregation of sister chromatids via active loop extrusion. Elife *5*.

Gómez, R., Jordan, P.W., Viera, A., Alsheimer, M., Fukuda, T., Jessberger, R., Llano, E., Pendás, A.M., Handel, M.A., and Suja, J.A. (2013). Dynamic localization of SMC5/6 complex proteins during mammalian meiosis and mitosis suggests functions in distinct chromosome processes. J. Cell Sci. *126*, 4239–4252.

Gosling, K.M., Goodnow, C.C., Verma, N.K., and Fahrer, A.M. (2008). Defective T-cell function leading to reduced antibody production in a *kleisin-β* mutant mouse. Immunology *125*, 208–217.

Gottlieb, T.M., and Jackson, S.P. (1993). The DNA-dependent protein kinase: requirement for DNA ends and association with Ku antigen. Cell *72*, 131–142.

Greene, E.C. (2016). DNA sequence alignment during homologous recombination. J. Biol. Chem. *291*, 11572–11580.

Griese, J.J., Witte, G., and Hopfner, K.P. (2010). Structure and DNA binding activity of the mouse condensin hinge domain highlight common and diverse features of SMC proteins. Nucleic Acids Res. *38*, 3454–3465.

Gronostajski, R.M., and Sadowski, P.D. (1985). Determination of DNA sequences essential for FLP-mediated recombination by a novel method. J. Biol. Chem. *260*, 12320–12327.

Groth, P., Orta, M.L., Elvers, I., Majumder, M.M., Lagerqvist, A., and Helleday, T. (2012). Homologous recombination repairs secondary replication induced DNA double-strand breaks after ionizing radiation. Nucleic Acids Res. *40*, 6585–6594.

Guerineau, M., Kriz, Z., Kozakova, L., Bednarova, K., Janos, P., and Palecek, J. (2012). Analysis of the Nse3/MAGE-binding domain of the Nse4/EID family proteins. PLoS One *7*.

Gunn, A., and Stark, J.M. (2012). I-SceI-Based Assays to Examine Distinct Repair Outcomes of Mammalian Chromosomal Double Strand Breaks. In Methods in Molecular Biology (Clifton, N.J.), pp. 379–391.

Haering, C.H., Löwe, J., Hochwagen, A., and Nasmyth, K. (2002). Molecular Architecture of SMC Proteins and the Yeast Cohesin Complex. Mol. Cell *9*, 773–788.

Haering, C.H., Farcas, A.-M., Arumugam, P., Metson, J., and Nasmyth, K. (2008). The cohesin ring concatenates sister DNA molecules. Nature *454*, 297–301.

Hamperl, S., Bocek, M.J., Saldivar, J.C., Swigut, T., and Cimprich, K.A. (2017). Transcription-Replication Conflict Orientation Modulates R-Loop Levels and Activates

Distinct DNA Damage Responses. Cell *170*, 774-786.e19.

Hanada, K., Budzowska, M., Davies, S.L., van Drunen, E., Onizawa, H., Beverloo, H.B., Maas, A., Essers, J., Hickson, I.D., and Kanaar, R. (2007). The structure-specific endonuclease Mus81 contributes to replication restart by generating double-strand DNA breaks. Nat. Struct. Mol. Biol. *14*, 1096–1104.

Hargreaves, D.C., and Crabtree, G.R. (2011). ATP-dependent chromatin remodeling: Genetics, genomics and mechanisms. Cell Res. *21*, 396–420.

Harvey, S.H., Sheedy, D.M., Cuddihy, A.R., and O'Connell, M.J. (2004). Coordination of DNA Damage Responses via the Smc5/Smc6 Complex. Mol. Cell. Biol. *24*, 662–674.

Hauf, S., Roitinger, E., Koch, B., Dittrich, C.M., Mechtler, K., and Peters, J.-M. (2005). Dissociation of cohesin from chromosome arms and loss of arm cohesion during early mitosis depends on phosphorylation of SA2. PLoS Biol. *3*, e69.

Hayashi, M.T., Takahashi, T.S., Nakagawa, T., Nakayama, J.I., and Masukata, H. (2009). The heterochromatin protein Swi6/HP1 activates replication origins at the pericentromeric region and silent mating-type locus. Nat. Cell Biol. *11*, 357–362.

Haynes, B., Murai, J., and Lee, J.-M. (2018). Restored replication fork stabilization, a mechanism of PARP inhibitor resistance, can be overcome by cell cycle checkpoint inhibition. Cancer Treat. Rev. *71*, 1–7.

Hegemann, B., Hutchins, J.R.A., Hudecz, O., Novatchkova, M., Rameseder, J., Sykora, M.M., Liu, S., Mazanek, M., Lénárt, P., Hériché, J.K., et al. (2011). Systematic phosphorylation analysis of human mitotic protein complexes. Sci. Signal. *4*.

Helleday, T. (2011). The underlying mechanism for the PARP and BRCA synthetic lethality: Clearing up the misunderstandings. Mol. Oncol. *5*, 387–393.

Helmrich, A., Ballarino, M., and Tora, L. (2011). Collisions between Replication and Transcription Complexes Cause Common Fragile Site Instability at the Longest Human Genes. Mol. Cell *44*, 966–977.

Heyer, W.D. (2015). Regulation of recombination and genomic maintenance. Cold Spring Harb Perspect Biol *7*, a016501.

Hirano, T. (2002). The ABCs of SMC proteins: two-armed ATPases for chromosome condensation, cohesion, and repair. Genes Dev. *16*, 399–414.

Hirano, T. (2012). Condensins: Universal organizers of chromosomes with diverse functions. Genes Dev. *26*, 1659–1678.

Hirano, T., and Mitchison, T.J. (1994). A heterodimeric coiled-coil protein required for mitotic chromosome condensation in vitro. Cell *79*, 449–458.

Hochstrasser, M. (2001). SP-RING for SUMO: new functions bloom for a ubiquitin-like protein. Cell *107*, 5–8.

Hsiang, Y.H., Lihou, M.G., and Liu, L.F. (1989). Arrest of Replication Forks by Drug-stabilized Topoisomerase I-DNA Cleavable Complexes as a Mechanism of Cell Killing by Camptothecin. Cancer Res. *49*, 5077–5082.

Hudson, D.F., Vagnarelli, P., Gassmann, R., and Earnshaw, W.C. (2003). Condensin is required for nonhistone protein assembly and structural integrity of vertebrate mitotic

chromosomes. Dev. Cell *5*, 323–336.

Hudson, J.J.R., Bednarova, K., Kozakova, L., Liao, C., Guerineau, M., Colnaghi, R., Vidot, S., Marek, J., Bathula, S.R., Lehmann, A.R., et al. (2011). Interactions between the Nse3 and Nse4 components of the SMC5-6 complex identify evolutionarily conserved interactions between MAGE and EID families. PLoS One *6*.

Irmisch, A., Ampatzidou, E., Mizuno, K., O'Connell, M.J., and Murray, J.M. (2009). Smc5/6 maintains stalled replication forks in a recombination-competent conformation. EMBO J. *28*, 144–155.

Ivessa, A.S., Lenzmeier, B.A., Bessler, J.B., Goudsouzian, L.K., Schnakenberg, S.L., and Zakian, V.A. (2003). The Saccharomyces cerevisiae helicase Rrm3p facilitates replication past nonhistone protein-DNA complexes. Mol Cell *12*, 1525–1536.

Jackson, S.P., and Bartek, J. (2009). The DNA-damage response in human biology and disease. Nature *461*, 1071.

Jacome, A., Gutierrez-Martinez, P., Schiavoni, F., Tenaglia, E., Martinez, P., Rodríguez-Acebes, S., Lecona, E., Murga, M., Méndez, J., Blasco, M.A., et al. (2015). NSMCE2 suppresses cancer and aging in mice independently of its SUMO ligase activity. EMBO J. *34*, 2604–2619.

Jang, M.K., Anderson, D.E., van Doorslaer, K., and Mcbride, A.A. (2015). A proteomic approach to discover and compare interacting partners of papillomavirus E2 proteins from diverse phylogenetic groups. Proteomics *15*, 2038–2050.

Jensen, R.B., Carreira, A., and Kowalczykowski, S.C. (2010). Purified human BRCA2 stimulates RAD51-mediated recombination. Nature *467*, 678–683.

Jeppsson, K., Carlborg, K.K., Nakato, R., Berta, D.G., Lilienthal, I., Kanno, T., Lindqvist, A., Brink, M.C., Dantuma, N.P., Katou, Y., et al. (2014). The Chromosomal Association of the Smc5/6 Complex Depends on Cohesion and Predicts the Level of Sister Chromatid Entanglement. PLoS Genet. *10*.

Jimenez, G., Yucel, J., Rowley, R., and Subramani, S. (1992). The rad3+ gene of Schizosaccharomyces pombe is involved in multiple checkpoint functions and in DNA repair. Proc. Natl. Acad. Sci. U. S. A. *89*, 4952–4956.

Johnson, R.D., and Jasin, M. (2000). Sister chromatid gene conversion is a prominent double-strand break repair pathway in mammalian cells. Embo J *19*, 3398–3407.

Johzuka, K., and Horiuchi, T. (2009). The cis Element and Factors Required for Condensin Recruitment to Chromosomes. Mol. Cell *34*, 26–35.

Johzuka, K., Terasawa, M., Ogawa, H., Ogawa, T., and Horiuchi, T. (2006). Condensin Loaded onto the Replication Fork Barrier Site in the rRNA Gene Repeats during S Phase in a FOB1-Dependent Fashion To Prevent Contraction of a Long Repetitive Array in Saccharomyces cerevisiae. Mol. Cell. Biol. *26*, 2226–2236.

Ju, L., Wing, J., Taylor, E., Brandt, R., Slijepcevic, P., Horsch, M., Rathkolb, B., Racz, I., Becker, L., Hans, W., et al. (2013). SMC6 is an essential gene in mice, but a hypomorphic mutant in the ATPase domain has a mild phenotype with a range of subtle abnormalities. DNA Repair *12*, 356–366.

Kanno, T., Berta, D.G., and Sjogren, C. (2015). The Smc5/6 Complex Is an ATP-Dependent Intermolecular DNA Linker. Cell Rep *12*, 1471–1482.

Kaseb, H., and Hozayen, S. (2019). Chromosome Instability Syndromes.

Kato, H. (1974). Spontaneous sister chromatid exchanges detected by a BUdR-labelling method. Nature *251*, 70–72.

Kegel, A., and Sjögren, C. (2010). The Smc5/6 complex: more than repair? Cold Spring Harb. Symp. Quant. Biol. *75*, 179–187.

Kegel, A., Betts-Lindroos, H., Kanno, T., Jeppsson, K., Strom, L., Katou, Y., Itoh, T., Shirahige, K., and Sjogren, C. (2011). Chromosome length influences replication-induced topological stress. Nature *471*, 392–396.

Kinner, A., Wu, W., Staudt, C., and Iliakis, G. (2008). -H2AX in recognition and signaling of DNA double-strand breaks in the context of chromatin. Nucleic Acids Res. *36*, 5678–5694.

Koffa, M.D., Kean, J., Zachos, G., Rice, S.A., and Clements, J.B. (2003). CK2 Protein Kinase Is Stimulated and Redistributed by Functional Herpes Simplex Virus ICP27 Protein. J. Virol. *77*, 4315–4325.

Kolinjivadi, A.M., Sannino, V., De Antoni, A., Zadorozhny, K., Kilkenny, M., Técher, H., Baldi, G., Shen, R., Ciccia, A., Pellegrini, L., et al. (2017). Smarcal1-Mediated Fork Reversal Triggers Mre11-Dependent Degradation of Nascent DNA in the Absence of Brca2 and Stable Rad51 Nucleofilaments. Mol. Cell *67*, 867-881.e7.

Koster, D.A., Palle, K., Bot, E.S.M., Bjornsti, M.A., and Dekker, N.H. (2007). Antitumour drugs impede DNA uncoiling by topoisomerase I. Nature *448*, 213–217.

Kozakova, L., Vondrova, L., Stejskal, K., Charalabous, P., Kolesar, P., Lehmann, A.R., Uldrijan, S., Sanderson, C.M., Zdrahal, Z., and Palecek, J.J. (2015). The melanoma-associated antigen 1 (MAGEA1) protein stimulates the E3 ubiquitin-ligase activity of trim31 within a TRIM31-MAGEA1-NSE4 complex. Cell Cycle *14*, 920–930.

Krejci, L., Altmannova, V., Spirek, M., and Zhao, X. (2012). Homologous recombination and its regulation. Nucleic Acids Res. *40*, 5795–5818.

Kueng, S., Hegemann, B., Peters, B.H., Lipp, J.J., Schleiffer, A., Mechtler, K., and Peters, J.-M. (2006). Wapl controls the dynamic association of cohesin with chromatin. Cell *127*, 955–967.

Kumagai, A., Lee, J., Yoo, H.Y., and Dunphy, W.G. (2006). TopBP1 activates the ATR-ATRIP complex. Cell *124*, 943–955.

Kuo, L.J., and Yang, L.-X. Gamma-H2AX - a novel biomarker for DNA double-strand breaks. In Vivo *22*, 305–309.

Kurze, A., Michie, K.A., Dixon, S.E., Mishra, A., Itoh, T., Khalid, S., Strmecki, L., Shirahige, K., Haering, C.H., Löwe, J., et al. (2011). A positively charged channel within the Smc1/Smc3 hinge required for sister chromatid cohesion. EMBO J. *30*, 374–378.

Kustatscher, G., Wills, K.L.H., Furlan, C., and Rappsilber, J. (2014). Chromatin enrichment for proteomics. Nat. Protoc. *9*, 2090–2099.

Laursen, L. V, Ampatzidou, E., Andersen, A.H., and Murray, J.M. (2003). Role for the fission yeast RecQ helicase in DNA repair in G2. Mol Cell Biol *23*, 3692–3705.

Lee, J., Kumagai, A., and Dunphy, W.G. (2007a). The Rad9-Hus1-Rad1 checkpoint clamp regulates interaction of TopBP1 with ATR. J. Biol. Chem. *282*, 28036–28044.

Lee, K.M., Nizza, S., Hayes, T., Bass, K.L., Irmisch, A., Murray, J.M., and O'Connell, M.J. (2007b). Brc1-mediated rescue of Smc5/6 deficiency: requirement for multiple nucleases and a novel Rad18 function. Genetics *175*, 1585–1595.

Lee, S.Y., Rozenzhak, S., and Russell, P. (2013). gammaH2A-binding protein Brc1 affects centromere function in fission yeast. Mol Cell Biol *33*, 1410–1416.

Lehmann, A.R., Walicka, M., Griffiths, D.J., Murray, J.M., Watts, F.Z., McCready, S., and Carr, A.M. (1995). The rad18 gene of Schizosaccharomyces pombe defines a new subgroup of the SMC superfamily involved in DNA repair. Mol. Cell. Biol. *15*, 7067–7080.

Lengronne, A., Katou, Y., Mori, S., Yokobayashi, S., Kelly, G.P., Itoh, T., Watanabe, Y., Shirahige, K., and Uhlmann, F. (2004). Cohesin relocation from sites of chromosomal loading to places of convergent transcription. Nature *430*, 573–578.

Leupin, O., Bontron, S., and Strubin, M. (2003). Hepatitis B virus X protein and simian virus 5 V protein exhibit similar UV-DDB1 binding properties to mediate distinct activities. J Virol *77*, 6274–6283.

Liao, H., Ji, F., Helleday, T., and Ying, S. (2018). Mechanisms for stalled replication fork stabilization: new targets for synthetic lethality strategies in cancer treatments. EMBO Rep. *19*.

Lilienthal, I., Kanno, T., and Sjogren, C. (2013). Inhibition of the Smc5/6 complex during meiosis perturbs joint molecule formation and resolution without significantly changing crossover or non-crossover levels. PLoS Genet *9*, e1003898.

Limbo, O., Chahwan, C., Yamada, Y., de Bruin, R.A.M., Wittenberg, C., and Russell, P. (2007). Ctp1 Is a Cell-Cycle-Regulated Protein that Functions with Mre11 Complex to Control Double-Strand Break Repair by Homologous Recombination. Mol. Cell *28*, 134–146.

Lin, Y.-C., Boone, M., Meuris, L., Lemmens, I., Van Roy, N., Soete, A., Reumers, J., Moisse, M., Plaisance, S., Drmanac, R., et al. (2014). Genome dynamics of the human embryonic kidney 293 lineage in response to cell biology manipulations. Nat. Commun. *5*, 4767.

Lindroos, H.B., Strom, L., Itoh, T., Katou, Y., Shirahige, K., and Sjogren, C. (2006). Chromosomal association of the Smc5/6 complex reveals that it functions in differently regulated pathways. Mol Cell *22*, 755–767.

Lisby, M., Barlow, J.H., Burgess, R.C., and Rothstein, R. (2004). Choreography of the DNA damage response: spatiotemporal relationships among checkpoint and repair proteins. Cell *118*, 699–713.

Litchfield, D.W. (2003). Protein kinase CK2: Structure, regulation and role in cellular decisions of life and death. Biochem. J. *369*, 1–15.

Löbrich, M., and Jeggo, P. (2017). A Process of Resection-Dependent Nonhomologous End Joining Involving the Goddess Artemis. Trends Biochem. Sci. *42*, 690–701.

Lopes, M., Cotta-Ramusino, C., Pellicioli, A., Liberi, G., Plevani, P., Muzi-Falconi, M., Newlon, C.S., and Foiani, M. (2001). The DNA replication checkpoint response stabilizes stalled replication forks. Nature *412*, 557–561.

Losada, A., and Hirano, T. (2005). Dynamic molecular linkers of the genome: the first decade of SMC proteins. Genes Dev *19*, 1269–1287.

Losada, A., Hirano, M., and Hirano, T. (2002). Cohesin release is required for sister chromatid resolution, but not for condensin-mediated compaction, at the onset of mitosis. Genes Dev. *16*, 3004–3016.

Ma, Y., Pannicke, U., Schwarz, K., and Lieber, M.R. (2002). Hairpin opening and overhang processing by an Artemis/DNA-dependent protein kinase complex in nonhomologous end joining and V(D)J recombination. Cell *108*, 781–794.

Makrantoni, V., and Marston, A.L. (2018). Cohesin and chromosome segregation. Curr. Biol. *28*, R688–R693.

Maloisel, L., Fabre, F., and Gangloff, S. (2008). DNA Polymerase Is Preferentially Recruited during Homologous Recombination To Promote Heteroduplex DNA Extension. Mol. Cell. Biol. *28*, 1373–1382.

Malu, S., Malshetty, V., Francis, D., and Cortes, P. (2012). Role of non-homologous end joining in V(D)J recombination. Immunol. Res. *54*, 233–246.

Mao, Z., Bozzella, M., Seluanov, A., and Gorbunova, V. (2008). Comparison of nonhomologous end joining and homologous recombination in human cells. DNA Repair (Amst). *7*, 1765–1771.

Mariotti, L.G., Pirovano, G., Savage, K.I., Ghita, M., Ottolenghi, A., Prise, K.M., and Schettino, G. (2013). Use of the γ-H2AX Assay to Investigate DNA Repair Dynamics Following Multiple Radiation Exposures. PLoS One *8*, e79541.

Martinez-Perez, E., and Colaiacovo, M.P. (2009). Distribution of meiotic recombination events: talking to your neighbors. Curr Opin Genet Dev *19*, 105–112.

Mayle, R., Campbell, I.M., Beck, C.R., Yu, Y., Wilson, M., Shaw, C.A., Bjergbaek, L., Lupski, J.R., and Ira, G. (2015). Mus81 and converging forks limit the mutagenicity of replication fork breakage. Science (80-.). *349*, 742–747.

Maynard, S., Schurman, S.H., Harboe, C., de Souza-Pinto, N.C., and Bohr, V.A. (2009). Base excision repair of oxidative DNA damage and association with cancer and aging. Carcinogenesis *30*, 2–10.

McDonald, W.H., Pavlova, Y., Yates 3rd, J.R., and Boddy, M.N. (2003). Novel essential DNA repair proteins Nse1 and Nse2 are subunits of the fission yeast Smc5-Smc6 complex. J Biol Chem *278*, 45460–45467.

McVey, M., Khodaverdian, V.Y., Meyer, D., Cerqueira, P.G., and Heyer, W.-D. (2016). Eukaryotic DNA Polymerases in Homologous Recombination. Annu. Rev. Genet. *50*, 393–421.

Meng, X., Wei, L., Peng, X.P., and Zhao, X. (2019). Sumoylation of the DNA polymerase ε by the Smc5/6 complex contributes to DNA replication. PLOS Genet. *15*, e1008426.

Menolfi, D., Delamarre, A., Lengronne, A., Pasero, P., and Branzei, D. (2015). Essential Roles of the Smc5/6 Complex in Replication through Natural Pausing Sites and Endogenous DNA Damage Tolerance. Mol. Cell *60*, 835–846.

Mimitou, E.P., and Symington, L.S. (2008). Sae2, Exo1 and Sgs1 collaborate in DNA double-strand break processing. Nature *455*, 770–774.

Miyabe, I., Morishita, T., Hishida, T., Yonei, S., and Shinagawa, H. (2006). Rhp51-dependent recombination intermediates that do not generate checkpoint signal are accumulated in Schizosaccharomyces pombe rad60 and smc5/6 mutants after release from replication arrest. Mol. Cell. Biol. *26*, 343–353.

Mondal, G., Stevers, M., Goode, B., Ashworth, A., and Solomon, D.A. (2019). A requirement for STAG2 in replication fork progression creates a targetable synthetic lethality in cohesin-mutant cancers. Nat. Commun. *10*.

Moradi-Fard, S., Sarthi, J., Tittel-Elmer, M., Lalonde, M., Cusanelli, E., Chartrand, P., and Cobb, J.A. (2016). Smc5/6 Is a Telomere-Associated Complex that Regulates Sir4 Binding and TPE. PLOS Genet. *12*, e1006268.

Morikawa, H., Morishita, T., Kawane, S., Iwasaki, H., Carr, A.M., and Shinagawa, H. (2004). Rad62 Protein Functionally and Physically Associates with the Smc5/Smc6 Protein Complex and Is Required for Chromosome Integrity and Recombination Repair in Fission Yeast. Mol. Cell. Biol. *24*, 9401–9413.

Murai, J., Huang, S.N., Das, B.B., Renaud, A., Zhang, Y., Doroshow, J.H., Ji, J., Takeda, S., and Pommier, Y. (2012). Trapping of PARP1 and PARP2 by Clinical PARP Inhibitors. Cancer Res. *72*, 5588–5599.

Murai, J., Zhang, Y., Morris, J., Ji, J., Takeda, S., Doroshow, J.H., and Pommier, Y. (2014). Rationale for Poly(ADP-ribose) Polymerase (PARP) Inhibitors in Combination Therapy with Camptothecins or Temozolomide Based on PARP Trapping versus Catalytic Inhibition. J. Pharmacol. Exp. Ther. *349*, 408–416.

Murphy, C.M., Xu, Y., Li, F., Nio, K., Reszka-Blanco, N., Li, X., Wu, Y., Yu, Y., Xiong, Y., and Su, L. (2016). Hepatitis B Virus X Protein Promotes Degradation of SMC5/6 to Enhance HBV Replication. Cell Rep. *16*, 2846–2854.

Murray, J.M., and Carr, A.M. (2008). Smc5/6: a link between DNA repair and unidirectional replication? Nat. Rev. Mol. Cell Biol. *9*, 177–182.

Nakajima, M., Kumada, K., Hatakeyama, K., Noda, T., Peters, J.M., and Hirota, T. (2007). The complete removal of cohesin from chromosome arms depends on separase. J. Cell Sci. *120*, 4188–4196.

Nasim, A., and Smith, B.P. (1975). Genetic control of radiation sensitivity in Schizosaccharomyces pombe. Genetics *79*, 573–582.

Natsume, T., Kiyomitsu, T., Saga, Y., and Kanemaki, M.T. (2016). Rapid Protein Depletion in Human Cells by Auxin-Inducible Degron Tagging with Short Homology Donors. Cell Rep. *15*, 210–218.

Neelsen, K.J., and Lopes, M. (2015). Replication fork reversal in eukaryotes: from dead end to dynamic response. Nat. Rev. Mol. Cell Biol. *16*, 207–220.

Nora, E.P., Goloborodko, A., Valton, A.L., Gibcus, J.H., Uebersohn, A., Abdennur, N.,

Dekker, J., Mirny, L.A., and Bruneau, B.G. (2017). Targeted Degradation of CTCF Decouples Local Insulation of Chromosome Domains from Genomic Compartmentalization. Cell *169*, 930-944.e22.

Nordlund, P., and Reichard, P. (2006). Ribonucleotide Reductases. Annu. Rev. Biochem. *75*, 681–706.

Nuebler, J., Fudenberg, G., Imakaev, M., Abdennur, N., and Mirny, L.A. (2018). Chromatin organization by an interplay of loop extrusion and compartmental segregation. Proc. Natl. Acad. Sci. U. S. A. *115*, E6697–E6706.

O'Gorman, S., Fox, D., and Wahl, G. (1991). Recombinase-mediated gene activation and site-specific integration in mammalian cells. Science (80-.). *251*, 1351–1355.

Ocampo-Hafalla, M., Muñoz, S., Samora, C.P., and Uhlmann, F. (2016). Evidence for cohesin sliding along budding yeast chromosomes. Open Biol. *6*.

Ochi, T., Blackford, A.N., Coates, J., Jhujh, S., Mehmood, S., Tamura, N., Travers, J., Wu, Q., Draviam, V.M., Robinson, C. V., et al. (2015). PAXX, a paralog of XRCC4 and XLF, interacts with Ku to promote DNA double-strand break repair. Science (80-.). *347*, 185–188.

Olson, E., Nievera, C.J., Klimovich, V., Fanning, E., and Wu, X. (2006). RPA2 Is a Direct Downstream Target for ATR to Regulate the S-phase Checkpoint * □ S.

Ono, T., Losada, A., Hirano, M., Myers, M.P., Neuwald, A.F., and Hirano, T. (2003). Differential contributions of condensin I and condensin II to mitotic chromosome architecture in vertebrate cells. Cell *115*, 109–121.

Ono, T., Fang, Y., Spector, D.L., and Hirano, T. (2004). Spatial and temporal regulation of condensins I and II in mitotic chromosome assembly in human cells. Mol. Biol. Cell *15*, 3296–3308.

Onoda, F., Takeda, M., Seki, M., Maeda, D., Tajima, J., Ui, A., Yagi, H., and Enomoto, T. (2004). SMC6 is required for MMS-induced interchromosomal and sister chromatid recombinations in Saccharomyces cerevisiae. DNA Repair (Amst). *3*, 429–439.

Oravcová, M., Gadaleta, M.C., Nie, M., Reubens, M.C., Limbo, O., Russell, P., and Boddy, M.N. (2019). Brc1 Promotes the Focal Accumulation and SUMO Ligase Activity of Smc5-Smc6 during Replication Stress.

Osman, F., Ahn, J.S., Lorenz, A., and Whitby, M.C. (2016). The RecQ DNA helicase Rqh1 constrains Exonuclease 1-dependent recombination at stalled replication forks. Sci Rep *6*, 22837.

Outwin, E.A., Irmisch, A., Murray, J.M., and O'Connell, M.J. (2009). Smc5-Smc6-dependent removal of cohesin from mitotic chromosomes. Mol. Cell. Biol. *29*, 4363–4375.

Palecek, J.J., and Gruber, S. (2015). Kite Proteins: A Superfamily of SMC/Kleisin Partners Conserved Across Bacteria, Archaea, and Eukaryotes. Structure *23*, 2183–2190.

Palecek, J., Vidot, S., Feng, M., Doherty, A.J., and Lehmann, A.R. (2006). The Smc5-Smc6 DNA repair complex. bridging of the Smc5-Smc6 heads by the KLEISIN, Nse4, and non-Kleisin subunits. J Biol Chem *281*, 36952–36959.

Parelho, V., Hadjur, S., Spivakov, M., Leleu, M., Sauer, S., Gregson, H.C., Jarmuz, A., Canzonetta, C., Webster, Z., Nesterova, T., et al. (2008). Cohesins Functionally Associate with CTCF on Mammalian Chromosome Arms. Cell *132*, 422–433.

Parrilla-Castellar, E.R., Arlander, S.J.H., and Karnitz, L. (2004). Dial 9-1-1 for DNA damage: The Rad9-Hus1-Rad1 (9-1-1) clamp complex. DNA Repair (Amst). *3*, 1009–1014.

Paull, T.T., Rogakou, E.P., Yamazaki, V., Kirchgessner, C.U., Gellert, M., and Bonner, W.M. (2000). A critical role for histone H2AX in recruitment of repair factors to nuclear foci after DNA damage. Curr. Biol. *10*, 886–895.

Payne, F., Colnaghi, R., Rocha, N., Seth, A., Harris, J., Carpenter, G., Bottomley, W.E., Wheeler, E., Wong, S., Saudek, V., et al. (2014). Hypomorphism in human NSMCE2 linked to primordial dwarfism and insulin resistance. J. Clin. Invest. *124*, 4028–4038.

Pebernard, S., McDonald, W.H., Pavlova, Y., Yates, J.R., Boddy, M.N., and Boddy, M.N. (2004). Nse1, Nse2, and a novel subunit of the Smc5-Smc6 complex, Nse3, play a crucial role in meiosis. Mol. Biol. Cell *15*, 4866–4876.

Pebernard, S., Wohlschlegel, J., McDonald, W.H., Yates, J.R., and Boddy, M.N. (2006). The Nse5-Nse6 Dimer Mediates DNA Repair Roles of the Smc5-Smc6 Complex. Mol. Cell. Biol. *26*, 3336–3336.

Pebernard, S., Schaffer, L., Campbell, D., Head, S.R., and Boddy, M.N. (2008a). Localization of Smc5/6 to centromeres and telomeres requires heterochromatin and SUMO, respectively. Embo J *27*, 3011–3023.

Pebernard, S., Perry, J.J.P., Tainer, J.A., and Boddy, M.N. (2008b). Nse1 RING-like Domain Supports Functions of the Smc5-Smc6 Holocomplex in Genome Stability. Mol. Biol. Cell *19*, 4099–4109.

Peng, X.P., Lim, S., Li, S., Marjavaara, L., Chabes, A., and Zhao, X. (2018). Acute Smc5/6 depletion reveals its primary role in rDNA replication by restraining recombination at fork pausing sites. PLOS Genet. *14*, e1007129.

Petermann, E., Orta, M.L., Issaeva, N., Schultz, N., and Helleday, T. (2010). Hydroxyurea-Stalled Replication Forks Become Progressively Inactivated and Require Two Different RAD51-Mediated Pathways for Restart and Repair. Mol. Cell *37*, 492–502.

De Piccoli, G., Cortes-Ledesma, F., Ira, G., Torres-Rosell, J., Uhle, S., Farmer, S., Hwang, J.-Y., Machin, F., Ceschia, A., McAleenan, A., et al. (2006). Smc5–Smc6 mediate DNA double-strand-break repair by promoting sister-chromatid recombination. Nat. Cell Biol. *8*, 1032–1034.

De Piccoli, G., Torres-Rosell, J., and Aragón, L. (2009). The unnamed complex: What do we know about Smc5-Smc6? Chromosom. Res.

Pierce, A.J., Johnson, R.D., Thompson, L.H., and Jasin, M. (1999). XRCC3 promotes homology-directed repair of DNA damage in mammalian cells. Genes Dev. *13*, 2633–2638.

Pommier, Y. (2006). Topoisomerase I inhibitors: Camptothecins and beyond. In Nature Reviews Cancer, pp. 789–802.

Pond, K.W., de Renty, C., Yagle, M.K., and Ellis, N.A. (2019). Rescue of collapsed replication forks is dependent on NSMCE2 to prevent mitotic DNA damage. PLOS Genet. *15*, e1007942.

Potapova, T., and Gorbsky, G.J. (2017). biology The Consequences of Chromosome Segregation Errors in Mitosis and Meiosis.

Potts, P.R., and Yu, H. (2005). Human MMS21/NSE2 is a SUMO ligase required for DNA repair. Mol Cell Biol *25*, 7021–7032.

Potts, P.R., and Yu, H. (2007). The SMC5/6 complex maintains telomere length in ALT cancer cells through SUMOylation of telomere-binding proteins. Nat. Struct. Mol. Biol. *14*, 581–590.

Potts, P.R., Porteus, M.H., and Yu, H. (2006). Human SMC5/6 complex promotes sister chromatid homologous recombination by recruiting the SMC1/3 cohesin complex to double-strand breaks. EMBO J. *25*, 3377–3388.

Prakash, R., Krejci, L., Van Komen, S., Anke Schurer, K., Kramer, W., and Sung, P. (2005). Saccharomyces cerevisiae MPH1 gene, required for homologous recombination-mediated mutation avoidance, encodes a 3' to 5' DNA helicase. J Biol Chem *280*, 7854–7860.

Pryzhkova, M. V., and Jordan, P.W. (2016). Conditional mutation of *Smc5* in mouse embryonic stem cells perturbs condensin localization and mitotic progression. J. Cell Sci. *129*, 1619–1634.

Puget, N., Knowlton, M., and Scully, R. (2005). Molecular analysis of sister chromatid recombination in mammalian cells. DNA Repair *4*, 149–161.

Rao, S.S.P., Huang, S.C., Glenn St Hilaire, B., Engreitz, J.M., Perez, E.M., Kieffer-Kwon, K.R., Sanborn, A.L., Johnstone, S.E., Bascom, G.D., Bochkov, I.D., et al. (2017). Cohesin Loss Eliminates All Loop Domains. Cell *171*, 305-320.e24.

Räschle, M., Smeenk, G., Hansen, R.K., Temu, T., Oka, Y., Hein, M.Y., Nagaraj, N., Long, D.T., Walter, J.C., Hofmann, K., et al. (2015). Proteomics reveals dynamic assembly of repair complexes during bypass of DNA cross-links. Science (80-.). *348*.

Ray Chaudhuri, A., and Nussenzweig, A. (2017). The multifaceted roles of PARP1 in DNA repair and chromatin remodelling. Nat. Rev. Mol. Cell Biol. *18*, 610–621.

Ray Chaudhuri, A., Hashimoto, Y., Herrador, R., Neelsen, K.J., Fachinetti, D., Bermejo, R., Cocito, A., Costanzo, V., and Lopes, M. (2012). Topoisomerase I poisoning results in PARP-mediated replication fork reversal. Nat. Struct. Mol. Biol. *19*, 417–423.

Remeseiro, S., Cuadrado, A., Gómez-López, G., Pisano, D.G., and Losada, A. (2012). A unique role of cohesin-SA1 in gene regulation and development. EMBO J. *31*, 2090–2102.

Revenkova, E., and Jessberger, R. (2005). Keeping sister chromatids together: cohesins in meiosis. Reproduction *130*, 783–790.

Rogakou, E.P., Pilch, D.R., Orr, A.H., Ivanova, V.S., and Bonner, W.M. (1998). DNA Double-stranded Breaks Induce Histone H2AX Phosphorylation on Serine 139. J. Biol. Chem. *273*, 5858–5868.

Ronson, G.E., Piberger, A.L., Higgs, M.R., Olsen, A.L., Stewart, G.S., McHugh, P.J., Petermann, E., and Lakin, N.D. (2018). PARP1 and PARP2 stabilise replication forks at base excision repair intermediates through Fbh1-dependent Rad51 regulation. Nat. Commun. *9*.

Rothkamm, K., Krüger, I., Thompson, L.H., and Löbrich, M. (2003). Pathways of DNA double-strand break repair during the mammalian cell cycle. Mol. Cell. Biol. *23*, 5706–5715.

Rothman, S. (2010). How is the balance between protein synthesis and degradation achieved? Theor. Biol. Med. Model. *7*.

Rothstein, R., Michel, B., and Gangloff, S. (2000). Replication fork pausing and recombination or "gimme a break." Genes Dev. *14*, 1–10.

Roumeliotis, T.I., Williams, S.P., Gonçalves, E., Alsinet, C., Del Castillo Velasco-Herrera, M., Aben, N., Ghavidel, F.Z., Michaut, M., Schubert, M., Price, S., et al. (2017). Genomic Determinants of Protein Abundance Variation in Colorectal Cancer Cells. Cell Rep. *20*, 2201–2214.

Roux, K.J., Kim, D.I., and Burke, B. (2013). BioID: A screen for protein-protein interactions. Curr. Protoc. Protein Sci. *2013*, 19.23.1-19.23.14.

Roy, M.-A., Siddiqui, N., and Amours, D.D.' (2011). Cell Cycle Dynamic and selective DNA-binding activity of Smc5, a core component of the Smc5-Smc6 complex.

Roy, M.A., Dhanaraman, T., and D'Amours, D. (2015). The Smc5-Smc6 heterodimer associates with DNA through several independent binding domains. Sci. Rep. *5*.

Russell, W.C., Graham, F.L., Smiley, J., and Nairn, R. (1977). Characteristics of a Human Cell Line Transformed by DNA from Human Adenovirus Type 5. J. Gen. Virol. *36*, 59–72.

Saini, N., Ramakrishnan, S., Elango, R., Ayyar, S., Zhang, Y., Deem, A., Ira, G., Haber, J.E., Lobachev, K.S., and Malkova, A. (2013). Migrating bubble during break-induced replication drives conservative DNA synthesis. Nature *502*, 389–392.

Samejima, K., Booth, D.G., Ogawa, H., Paulson, J.R., Xie, L., Watson, C.A., Platani, M., Kanemaki, M.T., and Earnshaw, W.C. (2018). Functional analysis after rapid degradation of condensins and 3D-EM reveals chromatin volume is uncoupled from chromosome architecture in mitosis. J. Cell Sci. *131*.

San Filippo, J., Sung, P., and Klein, H. (2008). Mechanism of Eukaryotic Homologous Recombination. Annu. Rev. Biochem. *77*, 229–257.

Satoh, M.S., and Lindahl, T. (1992). Role of poly(ADP-ribose) formation in DNA repair. Nature *356*, 356–358.

Sauer, B. (1994). Site-specific recombination: developments and applications. Curr. Opin. Biotechnol. *5*, 521–527.

Schalbetter, S.A., Mansoubi, S., Chambers, A.L., Downs, J.A., and Baxter, J. (2015). Fork rotation and DNA precatenation are restricted during DNA replication to prevent chromosomal instability. Proc Natl Acad Sci U S A *112*, E4565-70.

Schlacher, K. (2017). PARPi focus the spotlight on replication fork protection in cancer. Nat. Cell Biol. *19*, 1309–1310.

Schlacher, K., Christ, N., Siaud, N., Egashira, A., Wu, H., and Jasin, M. (2011). Double-strand break repair-independent role for BRCA2 in blocking stalled replication fork degradation by MRE11. Cell *145*, 529–542.

Schmidt, T.G.M., and Skerra, A. (2007). The Strep-tag system for one-step purification and high-affinity detection or capturing of proteins. Nat. Protoc. *2*, 1528–1535.

Schmitt, J., Hess, H., and Stunnenberg, H.G. (1993). Affinity purification of histidine-tagged proteins.

Schurer, K.A., Rudolph, C., Ulrich, H.D., and Kramer, W. (2004). Yeast MPH1 gene functions in an error-free DNA damage bypass pathway that requires genes from Homologous recombination, but not from postreplicative repair. Genetics *166*, 1673–1686.

Scully, R., Panday, A., Elango, R., and Willis, N.A. (2019). DNA double-strand break repair-pathway choice in somatic mammalian cells. Nat. Rev. Mol. Cell Biol. *20*, 698–714.

Seitan, V.C., Faure, A.J., Zhan, Y., McCord, R.P., Lajoie, B.R., Ing-Simmons, E., Lenhard, B., Giorgetti, L., Heard, E., Fisher, A.G., et al. (2013). Cohesin-Based chromatin interactions enable regulated gene expression within preexisting architectural compartments. Genome Res. *23*, 2066–2077.

Sergeant, J., Taylor, E., Palecek, J., Fousteri, M., Andrews, E.A., Sweeney, S., Shinagawa, H., Watts, F.Z., and Lehmann, A.R. (2005). Composition and architecture of the Schizosaccharomyces pombe Rad18 (Smc5-6) complex. Mol Cell Biol *25*, 172–184.

Sharma, A., Singh, K., and Almasan, A. (2012). Histone H2AX Phosphorylation: A Marker for DNA Damage. pp. 613–626.

Sharma, P.M., Ponnaiya, B., Taveras, M., Shuryak, I., Turner, H., and Brenner, D.J. (2015). High throughput measurement of γH2AX DSB repair kinetics in a healthy human population. PLoS One *10*.

Sheedy, D.M., Dimitrova, D., Rankin, J.K., Bass, K.L., Lee, K.M., Tapia-Alveal, C., Harvey, S.H., Murray, J.M., and O'Connell, M.J. (2005). Brc1-mediated DNA repair and damage tolerance. Genetics *171*, 457–468.

Shen, T., and Huang, S. (2012). The role of Cdc25A in the regulation of cell proliferation and apoptosis. Anticancer. Agents Med. Chem. *12*, 631–639.

Shen, Y., Aoyagi-Scharber, M., and Wang, B. (2015). Trapping Poly(ADP-Ribose) Polymerase. J. Pharmacol. Exp. Ther. *353*, 446–457.

Shintomi, K., and Hirano, T. (2011). The relative ratio of condensing I to II determines chromosome shapes. Genes Dev. *25*, 1464–1469.

Simbulan-Rosenthal, C.M., Rosenthal, D.S., Hilz, H., Hickey, R., Malkas, L., Applegren, N., Wu, Y., Bers, G., and Smulson, M.E. (1996). The expression of poly(ADP-ribose) polymerase during differentiation- linked dna replication reveals that it is a component of the multiprotein dna replication complex. Biochemistry *35*, 11622–11633.

Skerra, A., and Schmidt, T.G.M. (2000). Use of the Strep-tag and streptavidin for detection and purification of recombinant proteins. Methods Enzymol. *326*, 271–304.

Smith, C.E., Llorente, B., and Symington, L.S. (2007). Template switching during break-induced replication. Nature *447*, 102–105.

Sollier, J., Driscoll, R., Castellucci, F., Foiani, M., Jackson, S.P., and Branzei, D. (2009). The Saccharomyces cerevisiae Esc2 and Smc5-6 Proteins Promote Sister Chromatid Junction-mediated Intra-S Repair. Mol. Biol. Cell *20*, 1671–1682.

Song, J., Lafont, A., Chen, J., Wu, F.M., Shirahige, K., and Rankin, S. (2012). Cohesin acetylation promotes sister chromatid cohesion only in association with the replication machinery. J. Biol. Chem. *287*, 34325–34336.

Sonoda, E., Sasaki, M.S., Morrison, C., Yamaguchi-Iwai, Y., Takata, M., and Takeda, S. (1999). Sister Chromatid Exchanges Are Mediated by Homologous Recombination in Vertebrate Cells. Mol. Cell. Biol. *19*, 5166–5169.

Soppa, J. (2001). Prokaryotic structural maintenance of chromosomes (SMC) proteins: distribution, phylogeny, and comparison with MukBs and additional prokaryotic and eukaryotic coiled-coil proteins. Gene *278*, 253–264.

Sparks, J.L., Chon, H., Cerritelli, S.M., Kunkel, T.A., Johansson, E., Crouch, R.J., and Burgers, P.M. (2012). RNase H2-Initiated Ribonucleotide Excision Repair. Mol. Cell *47*, 980–986.

Stark, J.M., Pierce, A.J., Oh, J., Pastink, A., and Jasin, M. (2004). Genetic Steps of Mammalian Homologous Repair with Distinct Mutagenic Consequences. Mol. Cell. Biol. *24*, 9305–9316.

Stepanenko, A.A., and Dmitrenko, V.V. (2015). HEK293 in cell biology and cancer research: phenotype, karyotype, tumorigenicity, and stress-induced genome-phenotype evolution. Gene *569*, 182–190.

Stephan, A.K., Kliszczak, M., Dodson, H., Cooley, C., and Morrison, C.G. (2011a). Roles of Vertebrate Smc5 in Sister Chromatid Cohesion and Homologous Recombinational Repair. Mol. Cell. Biol. *31*, 1369–1381.

Stephan, A.K., Kliszczak, M., Dodson, H., Cooley, C., and Morrison, C.G. (2011b). Roles of Vertebrate Smc5 in Sister Chromatid Cohesion and Homologous Recombinational Repair. Mol. Cell. Biol. *31*, 1369–1381.

Stiff, T., O'Driscoll, M., Rief, N., Iwabuchi, K., Löbrich, M., and Jeggo, P.A. (2004). ATM and DNA-PK function redundantly to phosphorylate H2AX after exposure to ionizing radiation. Cancer Res. *64*, 2390–2396.

Stoop-Myer, C., and Amon, A. (1999). Meiosis: Rec8 is the reason for cohesion. Nat. Cell Biol. *1*, E125–E127.

Strom, L., Karlsson, C., Lindroos, H.B., Wedahl, S., Katou, Y., Shirahige, K., and Sjogren, C. (2007). Postreplicative formation of cohesion is required for repair and induced by a single DNA break. Science (80-.). *317*, 242–245.

Ström, C.E., Johansson, F., Uhlén, M., Szigyarto, C.A.-K., Erixon, K., and Helleday, T. (2011). Poly (ADP-ribose) polymerase (PARP) is not involved in base excision repair but PARP inhibition traps a single-strand intermediate. Nucleic Acids Res. *39*, 3166–3175.

Ström, L., Lindroos, H.B., Shirahige, K., and Sjögren, C. (2004). Postreplicative recruitment of cohesin to double-strand breaks is required for DNA repair. Mol. Cell *16*,

1003–1015.

Stucki, M., and Jackson, S.P. (2006). γH2AX and MDC1: Anchoring the DNA-damage-response machinery to broken chromosomes. DNA Repair (Amst). *5*, 534–543.

Szczesny, R.J., Kowalska, K., Klosowska-Kosicka, K., Chlebowski, A., Owczarek, E.P., Warkocki, Z., Kulinski, T.M., Adamska, D., Affek, K., Jedroszkowiak, A., et al. (2018). Versatile approach for functional analysis of human proteins and efficient stable cell line generation using FLP-mediated recombination system. PLoS One *13*, e0194887.

Tapia-Alveal, C., Lin, S.-J., and O'Connell, M.J. (2014). Functional interplay between cohesin and Smc5/6 complexes. Chromosoma *123*, 437–445.

Tashiro, S., Kotomura, N., Shinohara, A., Tanaka, K., Ueda, K., and Kamada, N. (1996). S phase specific formation of the human Rad51 protein nuclear foci in lymphocytes. Oncogene *12*, 2165–2170.

Tashiro, S., Walter, J., Shinohara, A., Kamada, N., and Cremer, T. (2000). Rad51 accumulation at sites of DNA damage and in postreplicative chromatin. J. Cell Biol. *150*, 283–291.

Tavares, E.M., Wright, W.D., Heyer, W.D., Le Cam, E., and Dupaigne, P. (2019). In vitro role of Rad54 in Rad51-ssDNA filament-dependent homology search and synaptic complexes formation. Nat. Commun. *10*.

Taylor, E.M., Moghraby, J.S., Lees, J.H., Smit, B., Moens, P.B., and Lehmann, A.R. (2001). Characterization of a Novel Human SMC Heterodimer Homologous to the Schizosaccharomyces pombe Rad18/Spr18 Complex. Mol. Biol. Cell *12*, 1583–1594.

Taylor, E.M., Copsey, A.C., Hudson, J.J.R., Vidot, S., and Lehmann, A.R. (2008). Identification of the Proteins, Including MAGEG1, That Make Up the Human SMC5-6 Protein Complex. Mol. Cell. Biol. *28*, 1197–1206.

Terakawa, T., Bisht, S., Eeftens, J.M., Dekker, C., Haering, C.H., and Greene, E.C. (2017). The condensin complex is a mechanochemical motor that translocates along DNA. Science (80-.). *358*, 672–676.

Tercero, J.A., and Diffley, J.F.X. (2001). Regulation of DNA replication fork progression through damaged DNA by the Mec1/Rad53 checkpoint. Nature *412*, 553–557.

Terradas, M., Martín, M., Tusell, L., and Genescà, A. (2010). Genetic activities in micronuclei: Is the DNA entrapped in micronuclei lost for the cell? Mutat. Res. Mutat. Res. *705*, 60–67.

Toledo, L.I., Altmeyer, M., Rask, M.B., Lukas, C., Larsen, D.H., Povlsen, L.K., Bekker-Jensen, S., Mailand, N., Bartek, J., and Lukas, J. (2013). XATR prohibits replication catastrophe by preventing global exhaustion of RPA. Cell *155*, 1088.

Torres-Rosell, J., Mahín, F., Farmer, S., Jarmuz, A., Eydmann, T., Dalgaard, J.Z., and Aragón, L. (2005a). SMC5 and SMC6 genes are required for the segregation of repetitive chromosome regions. Nat. Cell Biol.

Torres-Rosell, J., Machín, F., and Aragón, L. (2005b). Smc5-Smc6 Complex Preserves Nucleolar Integrity in *S. cerevisiae*. Cell Cycle *4*, 868–872.

Torres-Rosell, J., Sunjevaric, I., De Piccoli, G., Sacher, M., Eckert-Boulet, N., Reid, R., Jentsch, S., Rothstein, R., Aragón, L., and Lisby, M. (2007). The Smc5-Smc6 complex

and SUMO modification of Rad52 regulates recombinational repair at the ribosomal gene locus. Nat. Cell Biol. *9*, 923–931.

Trenz, K., Errico, A., and Costanzo, V. (2008). Plx1 is required for chromosomal DNA replication under stressful conditions. EMBO J. *27*, 876–885.

Tsuyama, T., Inou, K., Seki, M., Seki, T., Kumata, Y., Kobayashi, T., Kimura, K., Hanaoka, F., Enomoto, T., and Tada, S. (2006). Chromatin loading of Smc5/6 is induced by DNA replication but not by DNA double-strand breaks. Biochem Biophys Res Commun *351*, 935–939.

Tubbs, A., and Nussenzweig, A. (2017). Endogenous DNA Damage as a Source of Genomic Instability in Cancer. Cell *168*, 644–656.

Turinetto, V., and Giachino, C. (2015). Multiple facets of histone variant H2AX: a DNA double-strand-break marker with several biological functions. Nucleic Acids Res. *43*, 2489–2498.

Tyanova, S., Temu, T., Sinitcyn, P., Carlson, A., Hein, M.Y., Geiger, T., Mann, M., and Cox, J. (2016). The Perseus computational platform for comprehensive analysis of (prote)omics data. Nat. Methods *13*, 731–740.

Ünal, E., Arbel-Eden, A., Sattler, U., Shroff, R., Lichten, M., Haber, J.E., and Koshland, D. (2004). DNA damage response pathway uses histone modification to assemble a double-strand break-specific cohesin domain. Mol. Cell *16*, 991–1002.

Ünal, E., Heidinger-Pauli, J.M., and Koshland, D. (2007). DNA double-strand breaks trigger genome-wide sister-chromatid cohesion through Eco1 (Ctf7). Science (80-.). *317*, 245–248.

Vassin, V.M., Anantha, R.W., Sokolova, E., Kanner, S., and Borowiec, J.A. (2009). Human RPA phosphorylation by ATR stimulates DNA synthesis and prevents ssDNA accumulation during DNA-replication stress. J. Cell Sci. *122*, 4070–4080.

Verkade, H.M., Bugg, S.J., Lindsay, H.D., Carr, A.M., and O'Connell, M.J. (1999). Rad18 is required for DNA repair and checkpoint responses in fission yeast. Mol. Biol. Cell *10*, 2905–2918.

Verver, D.E., Hwang, G.H., Jordan, P.W., and Hamer, G. (2016a). Resolving complex chromosome structures during meiosis: versatile deployment of Smc5/6. Chromosoma *125*, 15–27.

Verver, D.E., Zheng, Y., Speijer, D., Hoebe, R., Dekker, H.L., Repping, S., Stap, J., and Hamer, G. (2016b). Non-SMC element 2 (NSMCE2) of the SMC5/6 complex helps to resolve topological stress. Int. J. Mol. Sci. *17*.

Vesela, E., Chroma, K., Turi, Z., and Mistrik, M. (2017). Common Chemical Inductors of Replication Stress: Focus on Cell-Based Studies. Biomolecules *7*.

Vian, L., Pękowska, A., Rao, S.S.P., Kieffer-Kwon, K.R., Jung, S., Baranello, L., Huang, S.C., El Khattabi, L., Dose, M., Pruett, N., et al. (2018). The Energetics and Physiological Impact of Cohesin Extrusion. Cell *173*, 1165-1178.e20.

Vos, S.M., Tretter, E.M., Schmidt, B.H., and Berger, J.M. (2011). All tangled up: how cells direct, manage and exploit topoisomerase function. Nat Rev Mol Cell Biol *12*, 827–841.

Waizenegger, I.C., Hauf, S., Meinke, A., and Peters, J.M. (2000). Two distinct pathways remove mammalian cohesin from chromosome arms in prophase and from centromeres in anaphase. Cell *103*, 399–410.

Walker, J.R., Corpina, R.A., and Goldberg, J. (2001). Structure of the Ku heterodimer bound to dna and its implications for double-strand break repair. Nature *412*, 607–614.

Ward, I.M., and Chen, J. (2001). Histone H2AX is phosphorylated in an ATR-dependent manner in response to replicational stress. J. Biol. Chem. *276*, 47759–47762.

Watanabe, K., Pacher, M., Dukowic, S., Schubert, V., Puchta, H., and Schubert, I. (2009). The STRUCTURAL MAINTENANCE OF CHROMOSOMES 5/6 complex promotes sister chromatid alignment and homologous recombination after DNA damage in Arabidopsis thaliana. Plant Cell *21*, 2688–2699.

Watrin, E., Schleiffer, A., Tanaka, K., Eisenhaber, F., Nasmyth, K., and Peters, J.-M. (2006). Human Scc4 is required for cohesin binding to chromatin, sister-chromatid cohesion, and mitotic progression. Curr. Biol. *16*, 863–874.

Wehrkamp-Richter, S., Hyppa, R.W., Prudden, J., Smith, G.R., and Boddy, M.N. (2012). Meiotic DNA joint molecule resolution depends on Nse5–Nse6 of the Smc5–Smc6 holocomplex. Nucleic Acids Res. *40*, 9633–9646.

Weinert, T.A., Kiser, G.L., and Hartwell, L.H. (1994). Mitotic checkpoint genes in budding yeast and the dependence of mitosis on DNA replication and repair. Genes Dev. *8*, 652–665.

Wells, J.N., Gligoris, T.G., Nasmyth, K.A., and Marsh, J.A. (2017). Evolution of condensin and cohesin complexes driven by replacement of Kite by Hawk proteins. Curr. Biol. *27*, R17–R18.

Wilson, D.M., and Thompson, L.H. (2007). Molecular mechanisms of sister-chromatid exchange. Mutat. Res. - Fundam. Mol. Mech. Mutagen. *616*, 11–23.

Winczura, A., Appanah, R., Tatham, M.H., Hay, R.T., and De Piccoli, G. (2019). The S phase checkpoint promotes the Smc5/6 complex dependent SUMOylation of Pol2, the catalytic subunit of DNA polymerase ε. PLOS Genet. *15*, e1008427.

de Wit, E., Vos, E.S.M., Holwerda, S.J.B., Valdes-Quezada, C., Verstegen, M.J.A.M., Teunissen, H., Splinter, E., Wijchers, P.J., Krijger, P.H.L., and de Laat, W. (2015). CTCF Binding Polarity Determines Chromatin Looping. Mol. Cell *60*, 676–684.

Wong, A.K.C., Shanahan, F., Chen, Y., Lian, L., Ha, P., Hendricks, K., Ghaffari, S., Iliev, D., Penn, B., Woodland, A.M., et al. (2000). BRG1, a component of the SWI-SNF complex, is mutated in multiple human tumor cell lines. Cancer Res. *60*, 6171–6177.

Wu, L. (2008). Wrestling off RAD51: a novel role for RecQ helicases. BioEssays *30*, 291–295.

Wu, N., Kong, X., Ji, Z., Zeng, W., Potts, P.R., Yokomori, K., and Yu, H. (2012). Scc1 sumoylation by Mms21 promotes sister chromatid recombination through counteracting Wapl. Genes Dev. *26*, 1473–1485.

Wu, S.Y., Lee, A.Y., Hou, S.Y., Kemper, J.K., Erdjument-Bromage, H., Tempst, P., and Chiang, C.M. (2006). Brd4 links chromatin targeting to HPV transcriptional silencing. Genes Dev. *20*, 2383–2396.

Xaver, M., Huang, L., Chen, D., and Klein, F. (2013). Smc5/6-Mms21 prevents and eliminates inappropriate recombination intermediates in meiosis. PLoS Genet *9*, e1004067.

Xu, Y., Leung, C.G., Lee, D.C., Kennedy, B.K., and Crispino, J.D. (2006). MTB, the murine homolog of condensin II subunit CAP-G2, represses transcription and promotes erythroid cell differentiation. Leukemia *20*, 1261–1269.

Xue, X., Choi, K., Bonner, J., Chiba, T., Kwon, Y., Xu, Y., Sanchez, H., Wyman, C., Niu, H., Zhao, X., et al. (2014). Restriction of replication fork regression activities by a conserved SMC complex. Mol. Cell.

Yang, H., Li, Q., Fan, J., Holloman, W.K., and Pavletich, N.P. (2005). The BRCA2 homologue Brh2 nucleates RAD51 filament formation at a dsDNA-ssDNA junction. Nature *433*, 653–657.

Yano, K.I., Morotomi-Yano, K., Wang, S.Y., Uematsu, N., Lee, K.J., Asaithamby, A., Weterings, E., and Chen, D.J. (2008). Ku recruits XLF to DNA double-strand breaks. EMBO Rep. *9*, 91–96.

Yatskevich, S., Rhodes, J., and Nasmyth, K. (2019). Organization of Chromosomal DNA by SMC Complexes.

Ying, S., Hamdy, F.C., and Helleday, T. (2012). Mre11-dependent degradation of stalled DNA replication forks is prevented by BRCA2 and PARP1. Cancer Res. *72*, 2814–2821.

Yu, H.G., and Koshland, D.E. (2003). Meiotic condensin is required for proper chromosome compaction, SC assembly, and resolution of recombination-dependent chromosome linkages. J Cell Biol *163*, 937–947.

Zabrady, K., Adamus, M., Vondrova, L., Liao, C., Skoupilova, H., Novakova, M., Jurcisinova, L., Alt, A., Oliver, A.W., Lehmann, A.R., et al. (2016). Chromatin association of the SMC5/6 complex is dependent on binding of its NSE3 subunit to DNA. Nucleic Acids Res. *44*, 1064–1079.

Zapatka, M., Pociño-Merino, I., Heluani-Gahete, H., Bermúdez-López, M., Tarrés, M., Ibars, E., Solé-Soler, R., Gutiérrez-Escribano, P., Apostolova, S., Casas, C., et al. (2019). Sumoylation of Smc5 Promotes Error-free Bypass at Damaged Replication Forks. Cell Rep.

Zellweger, R., Dalcher, D., Mutreja, K., Berti, M., Schmid, J.A., Herrador, R., Vindigni, A., and Lopes, M. (2015). Rad51-mediated replication fork reversal is a global response to genotoxic treatments in human cells. J. Cell Biol. *208*, 563–579.

Zeman, M.K., and Cimprich, K.A. (2014). Causes and consequences of replication stress. Nat. Cell Biol. *16*, 2–9.

Zhang, Y., Fonslow, B.R., Shan, B., Baek, M.-C., Yates, J.R., and III (2013). Protein analysis by shotgun/bottom-up proteomics. Chem. Rev. *113*, 2343–2394.

Zhang, Z., Schwartz, S., Wagner, L., and Miller, W. (2000). A Greedy Algorithm for Aligning DNA Sequences. J. Comput. Biol. *7*, 203–214.

Zhao, X., and Blobel, G. (2005). A SUMO ligase is part of a nuclear multiprotein complex that affects DNA repair and chromosomal organization. Proc. Natl. Acad. Sci. U. S. A. *102*, 4777–4782.

Zhao, W., Steinfeld, J.B., Liang, F., Chen, X., Maranon, D.G., Jian Ma, C., Kwon, Y., Rao, T., Wang, W., Sheng, C., et al. (2017). BRCA1-BARD1 promotes RAD51-mediated homologous DNA pairing. Nature *550*.

Zou, L. (2003). Sensing DNA Damage Through ATRIP Recognition of RPA-ssDNA Complexes. Science (80-.). *300*, 1542–1548.

Zou, Y., Liu, Y., Wu, X., and Shell, S.M. (2006). Functions of human replication protein A (RPA): From DNA replication to DNA damage and stress responses. J. Cell. Physiol. *208*, 267–273.

Appendix

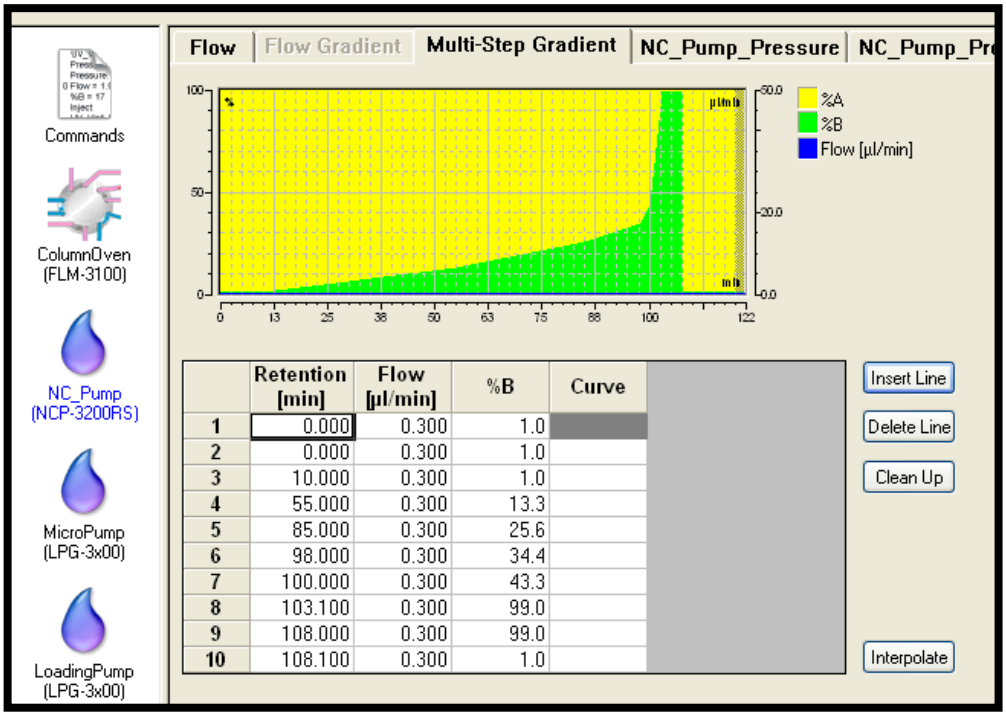
The appendix contains description of the used HPLC method and the number of scan events during the mass spectrometry analysis. Further, the appendix contains a list of identified peptides in each/subset of samples described in Chapter 4, as well as the search parameters and the used version of the search engine. The list of identified peptides is used, as an approximate measure to estimate purity and yield of the SMC5/6 complex in the elution fractions of a pull down experiment. Subunits of the SMC5/6 complex in the search results are marked in yellow.

In the MASCOT search results (Table A.3), the number of identified peptides was used to estimate the efficiency of the SMC5/6 recovery and the purity of the analysed sample. In the MaxQuant search results (Table A.2, A.4, A.6), the LFQ intensities[9] are used as a quantitative measure of the identified proteins in the sample.

To look for identified SMC5/6 interactors, the reader should focus on the lists Perseus processed samples (Table A.5, A.7 and A.8), these show statistically significant interactors (-Log Student's T-test p-value) of identified proteins in replicate samples. Due to the lack of biological and technical replicates, in the SILAC MaxQuant search results, only light (L) and heavy (H) intensity values are used as an approximate quantitative measure of identified proteins in each sample (Table A.9).

[9] MaxLFQ is a set of algorithms, which are part of the MaxQuant suite and apply delayed normalisation to make the label-free quantification more quantitative

A



B

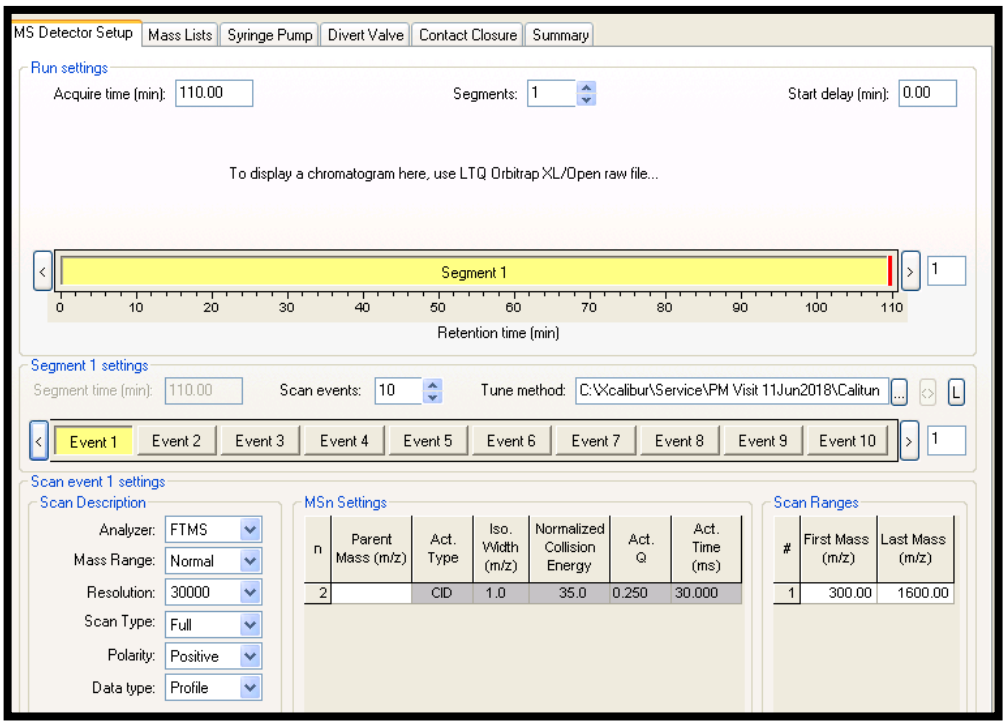


Figure A.1: Illustration of multi-step gradient method for peptide elution
A. Peptides were eluted in 90% acetonitrile gradient (%B) depicted in green, solution A: 0.1% formic acid, Retention [min]: the time between sample injection and its elution from the analytical column. Flow: flow rate by which the peptides are separated on the analytical column. **B.** Description of the mass spectra detector parameters; for sample identification, ten scan events ranging from 300 (m/z) to 1600 (m/z) were performed.

Table A.2: MaxQuant search parameters and identified proteins for initial NSMCE4a affinity purification using IMAC (Figure 4.1 C)
A. MaxQuant search parameters used to identify peptides in the sample, LFQ intensities were used for quantitative measurements. **B.** Proteins identified by MaxQuant search on control and bait cell lines, search results were filtered and proteins with peptides only identified by site, reverse and potential contaminants were excluded from the list.

A

MaxQuant search parameters LFQ (1)

Parameter	Value
Version	1.6.3.3
User name	ab797
Machine name	GC04007378
Date of writing	08/27/2019 13:23:53
Include contaminants	TRUE
PSM FDR	0.01
PSM FDR Crosslink	0.01
Protein FDR	0.01
Site FDR	0.01
Use Normalized Ratios For Occupancy	TRUE
Min. peptide Length	7
Min. score for unmodified peptides	0
Min. score for modified peptides	40
Min. delta score for unmodified peptides	0
Min. delta score for modified peptides	6
Min. unique peptides	0
Min. razor peptides	1
Min. peptides	1
Use only unmodified peptides and	TRUE
Modifications included in protein quantification	Oxidation (M);Acetyl (Protein N-term)
Peptides used for protein quantification	Razor
Discard unmodified counterpart peptides	TRUE
Label min. ratio count	2
Use delta score	FALSE
iBAQ	FALSE
iBAQ log fit	FALSE
Match between runs	FALSE
Find dependent peptides	FALSE
Fasta file	N:\Documents\Programmes\MaxQuantHuman_Swiss_Uniprot_20200_June2017.fasta
Decoy mode	revert
Include contaminants	TRUE
Advanced ratios	TRUE
Fixed andromeda index folder	
Temporary folder	
Combined folder location	
Second peptides	TRUE
Stabilize large LFQ ratios	TRUE
Separate LFQ in parameter groups	FALSE
Require MS/MS for LFQ comparisons	TRUE
Calculate peak properties	FALSE
Main search max. combinations	200
Advanced site intensities	TRUE
Write msScans table	FALSE
Write msmsScans table	TRUE
Write ms3Scans tableA	TRUE
Write allPeptides table	TRUE
Write mzRange table	TRUE
Write pasefMsmsScans table	TRUE
Write accumulatedPasefMsmsScans table	TRUE
Max. peptide mass [Da]	4600
Min. peptide length for unspecific search	8
Max. peptide length for unspecific search	25
Razor protein FDR	TRUE
Disable MD5	FALSE
Max mods in site table	3
Match unidentified features	FALSE
Epsilon score for mutations	
Evaluate variant peptides separately	TRUE
Variation mode	None
MS/MS tol. (FTMS)	20 ppm
Top MS/MS peaks per Da interval. (FTMS)	12
Da interval. (FTMS)	100
MS/MS deisotoping (FTMS)	TRUE
MS/MS deisotoping tolerance (FTMS)	7
MS/MS deisotoping tolerance unit (FTMS)	ppm

MaxQuant search parameters LFQ (1)

Parameter	Value
MS/MS higher charges (FTMS)	TRUE
MS/MS water loss (FTMS)	TRUE
MS/MS ammonia loss (FTMS)	TRUE
MS/MS dependent losses (FTMS)	TRUE
MS/MS recalibration (FTMS)	FALSE
MS/MS tol. (ITMS)	0.5 Da
Top MS/MS peaks per Da interval. (ITMS)	8
Da interval. (ITMS)	100
MS/MS deisotoping (ITMS)	FALSE
MS/MS deisotoping tolerance (ITMS)	0.15
MS/MS deisotoping tolerance unit (ITMS)	Da
MS/MS higher charges (ITMS)	TRUE
MS/MS water loss (ITMS)	TRUE
MS/MS ammonia loss (ITMS)	TRUE
MS/MS dependent losses (ITMS)	TRUE
MS/MS recalibration (ITMS)	FALSE
MS/MS tol. (TOF)	40 ppm
Top MS/MS peaks per Da interval. (TOF)	10
Da interval. (TOF)	100
MS/MS deisotoping (TOF)	TRUE
MS/MS deisotoping tolerance (TOF)	0.01
MS/MS deisotoping tolerance unit (TOF)	Da
MS/MS higher charges (TOF)	TRUE
MS/MS water loss (TOF)	TRUE
MS/MS ammonia loss (TOF)	TRUE
MS/MS dependent losses (TOF)	TRUE
MS/MS recalibration (TOF)	FALSE
MS/MS tol. (Unknown)	0.5 Da
Top MS/MS peaks per Da interval. (Unknown)	8
Da interval. (Unknown)	100
MS/MS deisotoping (Unknown)	FALSE
MS/MS deisotoping tolerance (Unknown)	0.15
MS/MS deisotoping tolerance unit (Unknown)	Da
MS/MS higher charges (Unknown)	TRUE
MS/MS water loss (Unknown)	TRUE
MS/MS ammonia loss (Unknown)	TRUE
MS/MS dependent losses (Unknown)	TRUE
MS/MS recalibration (Unknown)	FALSE
Site tables	Oxidation (M)Sites.txt

B

MaxQuant search results 1 (LFQ)

id	Protein names	Unique peptides Bait	Unique peptides Control	Sequence coverage Bait [%]	Sequence coverage Control [%]	LFQ intensity Bait	LFQ intensity Control
1	BTBDB_HUMAN	4	2	6.1	1.8	1.47E+07	0.00E+00
2	NUD19_HUMAN	5	4	17.9	12.8	5.23E+07	6.37E+07
3	MCRI1_HUMAN	3	4	32	50.5	2.09E+07	3.23E+07
4	IMA4_HUMAN;sp|O00	4	1	13.4	6.3	1.40E+07	0.00E+00
5	DDX3Y_HUMAN;sp|O0	1	0	1.5	0	2.00E+06	0.00E+00
6	MEIS2_HUMAN;sp|O0(	2	0	6.5	0	5.02E+06	0.00E+00
7	BCKD_HUMAN	6	4	25.7	17.5	8.16E+07	6.98E+07
8	SR140_HUMAN	14	11	17.1	16	1.28E+08	1.39E+08
9	NKRF_HUMAN	4	0	7.4	0	1.02E+07	0.00E+00
10	TYY2_HUMAN	1	1	14.8	11.8	0.00E+00	1.61E+07
11	DHX15_HUMAN	29	29	44.9	46.5	1.04E+09	1.09E+09
12	ARK72_HUMAN;sp|Q8	9	8	44.8	41.5	3.60E+08	3.44E+08
13	CPSF5_HUMAN	12	9	55.9	48.5	7.42E+08	5.04E+08
14	CCNT1_HUMAN	6	3	14.3	8.8	5.80E+07	3.76E+07
15	CCNT2_HUMAN	1	0	1.8	0	1.07E+06	0.00E+00
16	H2B1L_HUMAN;sp|Q9	1	0	15.1	7.1	1.15E+08	0.00E+00
17	BRD4_HUMAN;sp|Q15	10	7	10.8	7.5	1.25E+08	1.21E+08
18	BRE1B_HUMAN	1	1	5.7	3.8	0.00E+00	9.23E+06
19	H2AY_HUMAN	2	0	8.1	0	6.86E+06	0.00E+00
20	SRS10_HUMAN	0	1	0	6.1	0.00E+00	5.73E+06
21	BAF_HUMAN	1	0	13.5	0	4.13E+06	0.00E+00
22	SF3B1_HUMAN	33	27	37.9	31.7	5.52E+08	4.63E+08
23	U520_HUMAN	1	1	0.7	0.7	0.00E+00	1.73E+06
24	CCNK_HUMAN	3	2	9.5	6.6	1.69E+07	2.20E+07
25	DNJC8_HUMAN	3	5	20.9	27.7	3.53E+07	5.66E+07
26	SPF30_HUMAN	1	1	4.2	4.2	0.00E+00	4.05E+06
27	TOX4_HUMAN;sp|O94	6	5	14.8	11.6	4.54E+07	3.51E+07
28	FBX21_HUMAN	4	1	11.9	3.7	2.54E+07	0.00E+00
29	LDHA_HUMAN	10	10	27.4	31	9.34E+07	1.28E+08
30	DHE3_HUMAN;sp|P49	7	12	17.7	28.7	9.61E+07	2.47E+08
31	LMNA_HUMAN	1	1	1.4	1.4	2.20E+06	0.00E+00
32	H2A1J_HUMAN;sp|Q9	1	1	27.3	20.3	2.69E+08	1.11E+08
33	ADT2_HUMAN;sp|P12	4	0	14.4	0	2.15E+07	0.00E+00
34	RLA1_HUMAN	1	0	14	0	6.64E+06	0.00E+00
35	JUN_HUMAN	1	0	4.5	0	0.00E+00	0.00E+00
36	AP2A_HUMAN;sp|Q6V	5	1	17.8	4.6	2.59E+07	0.00E+00
37	NPM_HUMAN	1	0	12.6	0	4.90E+06	0.00E+00
38	LDHB_HUMAN;sp|Q6Z	11	10	40.7	43.7	1.35E+08	2.31E+08
39	TBB5_HUMAN;sp|Q13	2	2	30.2	25.9	7.48E+07	6.05E+07
40	HNRPC_HUMAN;sp|P0	2	0	7.5	0	4.74E+06	0.00E+00
41	RSSA_HUMAN	2	0	14.2	0	7.47E+06	0.00E+00
42	PARP1_HUMAN	2	0	2.8	0	6.60E+06	0.00E+00
43	H2AV_HUMAN;sp|P0C(	1	0	23.4	5.5	5.39E+06	0.00E+00
44	HS71B_HUMAN;sp|P0I	9	9	43.2	36.8	5.47E+08	5.87E+08
45	CH60_HUMAN	5	2	14.7	6.8	1.74E+07	1.54E+07
46	GRP78_HUMAN	8	4	21.9	11.3	2.18E+07	3.12E+07
47	HSP7C_HUMAN;sp|P54	13	12	34.5	31.4	1.76E+08	2.26E+08
48	TOP1_HUMAN;sp|Q96	26	21	37.1	32.9	9.12E+08	7.97E+08
49	PABP1_HUMAN;sp|Q9	2	1	3.9	1.3	8.71E+06	0.00E+00
50	TPR_HUMAN	7	7	4.1	4.1	2.32E+07	3.92E+07
51	KCRU_HUMAN;sp|P17	3	4	12.9	15.6	2.31E+07	4.38E+07
52	HNRPL_HUMAN;sp|Q8	30	26	80.3	65.4	3.72E+09	2.86E+09
53	H2A1A_HUMAN;sp|P1(	1	0	29.8	5.3	1.39E+07	0.00E+00
54	HSP76_HUMAN;sp|P48	1	1	12	12	0.00E+00	1.96E+07
55	DDX5_HUMAN;sp|Q92	2	0	4.1	0	4.83E+06	0.00E+00
56	NUCL_HUMAN	9	4	15.4	6.3	9.07E+07	2.91E+07
57	TBP_HUMAN;sp|Q6SJ9	2	0	11.8	0	1.08E+07	0.00E+00

id	Protein names	Unique peptides Bait	Unique peptides Control	Sequence coverage Bait [%]	Sequence coverage Control [%]	LFQ intensity Bait	LFQ intensity Control
58	PO3F2_HUMAN;sp|Q0	2	1	4.1	4.5	1.57E+07	0.00E+00
59	CBL_HUMAN	5	1	8.2	2.1	2.89E+07	0.00E+00
60	SFPQ_HUMAN	23	14	41.6	31.3	5.23E+09	3.21E+09
61	RS12_HUMAN	2	0	18.9	0	7.70E+06	0.00E+00
62	TYY1_HUMAN;sp|Q96M	6	5	29.5	19.6	2.02E+08	1.61E+08
63	ATPA_HUMAN	0	1	0	2.9	0.00E+00	2.57E+06
64	DDX6_HUMAN	17	13	46	38.7	2.89E+08	2.44E+08
65	1433T_HUMAN	1	0	4.9	0	5.50E+06	0.00E+00
66	2AAA_HUMAN	1	0	3.4	0	5.21E+06	0.00E+00
67	AMRP_HUMAN	5	3	13.2	10.6	2.10E+07	2.14E+07
68	HNRH1_HUMAN;sp|P5	2	1	11.1	7.3	2.24E+07	8.33E+06
69	FUS_HUMAN;sp|Q9280	1	0	2.7	0	1.69E+06	0.00E+00
70	PP1G_HUMAN	2	2	46.4	42.4	1.98E+08	2.47E+08
71	RBMX_HUMAN;sp|Q96	1	3	3.3	10.2	0.00E+00	2.51E+07
72	GRP75_HUMAN	7	5	15.8	9.9	3.80E+07	3.11E+07
73	AN32A_HUMAN;sp|Q9	1	0	6.4	0	4.90E+06	0.00E+00
74	HELZ_HUMAN	3	1	3.3	0.8	1.10E+07	0.00E+00
75	MATR3_HUMAN	2	3	3.8	6.3	1.00E+07	1.38E+07
76	RS5_HUMAN	1	0	7.4	0	7.80E+06	0.00E+00
77	TCPE_HUMAN	3	1	8.7	3	6.92E+06	0.00E+00
78	LMAN1_HUMAN	13	11	28.6	28.2	3.17E+08	3.05E+08
79	TCPG_HUMAN	1	1	2	2.4	1.67E+06	0.00E+00
80	EFTU_HUMAN	3	1	10	4.2	1.32E+07	0.00E+00
81	YLPM1_HUMAN	6	6	5.3	5.4	3.08E+07	3.15E+07
82	CLK3_HUMAN	1	0	3.1	0	4.37E+06	0.00E+00
83	CDK9_HUMAN	6	3	20.4	11.6	5.16E+07	4.69E+07
84	TCPQ_HUMAN	1	2	2.2	4.9	0.00E+00	6.79E+06
85	MECP2_HUMAN	10	7	26.5	21.6	6.57E+07	5.97E+07
86	HNRPF_HUMAN	1	0	8.2	4.1	6.23E+06	0.00E+00
87	TF2AA_HUMAN	2	2	7.4	7.4	2.82E+07	3.88E+07
88	T2AG_HUMAN	1	2	14.7	22.9	0.00E+00	1.19E+07
89	TCP4_HUMAN	2	2	18.9	18.9	3.10E+07	2.10E+07
90	ATN1_HUMAN	4	2	8.2	3.6	1.65E+07	1.52E+07
91	MAZ_HUMAN	5	2	13.4	6.7	5.93E+07	3.97E+07
92	ACTG_HUMAN;sp|P607	2	1	7.5	4.8	1.42E+07	0.00E+00
93	DCAF7_HUMAN	7	8	29.2	30.1	9.05E+07	1.01E+08
94	WDR5_HUMAN	6	4	25.1	13.5	2.94E+07	3.02E+07
95	HNRPK_HUMAN	3	0	11	0	1.13E+07	0.00E+00
96	PP1A_HUMAN	1	2	40.9	42.4	5.85E+06	0.00E+00
97	PP1B_HUMAN	3	2	43.4	32.7	1.21E+07	1.35E+07
98	1433E_HUMAN	1	2	4.7	9	0.00E+00	7.55E+06
99	SMD1_HUMAN	1	1	16.8	16.8	0.00E+00	2.84E+07
100	TBPL1_HUMAN	3	3	25.3	25.3	4.04E+07	4.22E+07
101	PP2AA_HUMAN;sp|P62	1	0	3.6	0	2.15E+06	0.00E+00
102	H4_HUMAN	4	4	38.8	38.8	3.21E+08	1.51E+08
103	RS28_HUMAN	1	0	17.4	0	7.22E+06	0.00E+00
104	TRA2B_HUMAN	2	2	10.4	10.4	9.91E+06	1.04E+07
105	GAK24_HUMAN	0	1	0	2.3	0.00E+00	4.86E+06
106	DYL2_HUMAN;sp|P631	1	1	12.4	12.4	0.00E+00	1.66E+06
107	SKP1_HUMAN	3	1	26.4	7.4	1.50E+07	0.00E+00
108	CSK2B_HUMAN	3	1	19.1	5.1	1.86E+07	0.00E+00
109	EF1A3_HUMAN;sp|P68	1	0	2.4	0	3.68E+06	0.00E+00
110	TBA1C_HUMAN;sp|P68	8	8	28.3	27.8	1.26E+08	1.42E+08
111	TBB4B_HUMAN;sp|P04	1	1	23.4	19.1	1.35E+07	0.00E+00
112	CSK21_HUMAN;sp|Q8N	2	0	10.2	0	1.28E+07	0.00E+00
113	H31_HUMAN;sp|Q6NX	1	0	35.3	11.8	1.11E+07	0.00E+00
114	ERH_HUMAN	1	1	10.6	10.6	0.00E+00	8.06E+06
115	SRSF3_HUMAN	1	0	5.5	0	2.53E+06	0.00E+00

id	Protein names	Unique peptides Bait	Unique peptides Control	Sequence coverage Bait [%]	Sequence coverage Control [%]	LFQ intensity Bait	LFQ intensity Control
116	H33_HUMAN	1	1	35.3	35.3	7.45E+07	5.05E+07
117	SATB1_HUMAN	1	0	6.7	2.8	5.56E+06	0.00E+00
118	CREB5_HUMAN	2	0	4.9	0	3.57E+06	0.00E+00
119	TLE1_HUMAN;sp|Q047	7	3	24	13.6	8.75E+07	3.24E+07
120	TLE3_HUMAN	11	10	31.3	31	2.41E+08	2.02E+08
121	RING1_HUMAN;sp|Q9	2	1	6.2	3.4	9.27E+06	0.00E+00
122	PRDX1_HUMAN	1	1	11.1	11.1	0.00E+00	2.69E+06
123	C1QBP_HUMAN	2	1	16.7	9.6	1.15E+07	0.00E+00
124	CKAP4_HUMAN	20	19	48.5	39.5	2.17E+08	2.66E+08
125	KHDR1_HUMAN	1	0	3.2	0	5.22E+06	0.00E+00
126	DLX2_HUMAN	1	0	11.6	0	6.38E+06	0.00E+00
127	SRSF1_HUMAN	0	1	0	4	0.00E+00	4.37E+06
128	AES_HUMAN	3	1	27.4	6.1	3.09E+07	0.00E+00
129	CPSF1_HUMAN	17	12	15.7	10.2	7.30E+07	9.96E+07
130	SF3A3_HUMAN	10	10	23	22.8	9.25E+07	1.18E+08
131	ILF2_HUMAN	4	5	18.7	19	2.37E+07	2.33E+07
132	ILF3_HUMAN;sp|Q96SI	2	2	3.6	3.5	0.00E+00	1.29E+07
133	TIF1B_HUMAN	3	3	7.5	7.5	1.38E+07	1.54E+07
134	SF3B2_HUMAN	21	20	27.8	29.1	3.85E+08	3.32E+08
135	SMAD4_HUMAN	10	5	24.3	16.7	1.21E+08	6.72E+07
136	PRP4B_HUMAN	7	6	6.9	5.9	4.51E+07	4.80E+07
137	HDAC1_HUMAN;sp|Q9	0	1	0	2.5	0.00E+00	7.62E+06
138	STIM1_HUMAN	1	2	2	4.8	0.00E+00	5.70E+06
139	DYR1A_HUMAN	4	3	7.9	5.5	1.93E+07	1.94E+07
140	SAFB2_HUMAN	2	3	13.7	15.3	1.11E+07	1.04E+07
141	ARHG7_HUMAN	3	1	6.4	1.5	1.07E+07	0.00E+00
142	IMB1_HUMAN	1	0	1.7	0	2.20E+06	0.00E+00
143	FL2D_HUMAN	3	1	9.1	3	1.22E+07	0.00E+00
144	HERC3_HUMAN	1	0	1.2	0	2.90E+06	0.00E+00
145	PLCB4_HUMAN	1	0	1.3	0	2.24E+06	0.00E+00
146	NONO_HUMAN	22	21	51	48.6	4.22E+09	3.25E+09
147	ELOB_HUMAN	1	1	21.2	21.2	0.00E+00	9.49E+06
148	SF3B3_HUMAN	30	33	35.2	37.1	6.59E+08	7.98E+08
149	SAFB1_HUMAN	5	4	19.6	16.3	3.55E+08	4.03E+08
150	SF3B4_HUMAN	4	4	19.1	19.1	1.22E+08	1.27E+08
151	SF3A2_HUMAN	2	2	8	5.8	2.59E+07	0.00E+00
152	SF3A1_HUMAN	14	13	23.3	20.9	1.20E+08	2.16E+08
153	SF01_HUMAN	7	7	17.5	16.3	5.56E+07	6.28E+07
154	ITSN1_HUMAN	1	0	0.8	0	1.79E+06	0.00E+00
155	RBBP7_HUMAN;sp|Q0	3	2	12.2	8.2	1.19E+07	0.00E+00
156	SRSF7_HUMAN	1	0	8.8	0	7.58E+06	0.00E+00
157	CPSF6_HUMAN	7	5	18	15.1	1.85E+08	1.75E+08
158	SMU1_HUMAN	0	2	0	6.4	0.00E+00	1.89E+06
159	LSM12_HUMAN	3	4	28.2	34.9	8.19E+07	6.96E+07
160	LARP7_HUMAN	8	10	19.2	25.9	5.87E+07	8.17E+07
161	AMOT_HUMAN	0	5	0	7.2	0.00E+00	2.09E+07
162	P5CR3_HUMAN	3	1	17.5	4	2.55E+07	0.00E+00
163	ACTBL_HUMAN	1	1	4.8	4.8	0.00E+00	1.06E+07
164	FA76B_HUMAN	1	0	3.2	0	2.87E+06	0.00E+00
165	LRRK2_HUMAN	1	1	0.4	0.4	0.00E+00	1.57E+07
166	CE170_HUMAN	2	0	2	0	5.08E+06	0.00E+00
167	BRE1A_HUMAN	1	1	2.6	2.6	0.00E+00	3.69E+06
168	VIR_HUMAN	5	1	4.2	0.7	9.53E+06	0.00E+00
169	TAF2_HUMAN	1	0	0.9	0	4.44E+06	0.00E+00
170	FIP1_HUMAN	6	5	21.2	14.8	5.75E+07	6.07E+07
171	WDR82_HUMAN	10	10	42.8	42.8	9.49E+07	1.12E+08
172	DPP8_HUMAN	1	1	1.7	1.7	0.00E+00	2.36E+07
173	H32_HUMAN	1	0	35.3	11.8	2.26E+07	0.00E+00

id	Protein names	Unique peptides Bait	Unique peptides Control	Sequence coverage Bait [%]	Sequence coverage Control [%]	LFQ intensity Bait	LFQ intensity Control
174	HAKAI_HUMAN	1	1	4.1	4.1	0.00E+00	7.07E+06
175	DHX30_HUMAN	1	2	1	3	0.00E+00	8.63E+06
176	MEPCE_HUMAN	10	6	25.1	12	4.16E+07	3.28E+07
177	PHF5A_HUMAN	3	4	36.4	48.2	5.97E+07	7.48E+07
178	NUFP2_HUMAN	9	8	20.4	18.8	8.30E+07	6.33E+07
179	PEG10_HUMAN	7	4	12.4	7.5	6.22E+07	5.55E+07
180	DPP9_HUMAN	22	16	35.7	27.8	2.87E+08	3.27E+08
181	DDX42_HUMAN	35	25	51.3	42	9.04E+08	5.42E+08
182	CHERP_HUMAN	7	5	10.8	7.5	5.53E+07	5.50E+07
183	DJC10_HUMAN	3	1	4.9	2.1	1.13E+07	0.00E+00
184	SMC5_HUMAN	2	0	2.5	0	5.12E+06	0.00E+00
185	SUV3_HUMAN	1	0	1.7	0	8.41E+07	0.00E+00
186	P20D2_HUMAN	15	13	45.6	42.9	4.58E+08	2.81E+08
187	CMTR1_HUMAN	6	1	13.2	1.9	3.49E+07	0.00E+00
188	CMYA5_HUMAN	1	0	0.3	0	2.49E+07	0.00E+00
189	RIBC1_HUMAN	1	0	4.7	0	8.11E+07	0.00E+00
190	CPSF7_HUMAN	11	10	29.5	25.5	3.64E+08	2.79E+08
191	FA98A_HUMAN;sp|Q5	5	0	15.4	0	2.39E+07	0.00E+00
192	ZNT7_HUMAN	2	2	8.2	6.6	1.90E+07	0.00E+00
193	ARI1B_HUMAN	0	1	0	1.3	0.00E+00	5.70E+06
194	PPIL4_HUMAN	14	11	38	32.3	2.17E+08	1.88E+08
195	ATX2L_HUMAN	12	11	17.4	17	1.15E+08	1.31E+08
196	PSPC1_HUMAN	15	10	33.7	21.6	1.20E+09	7.05E+08
197	DDX1_HUMAN	13	9	26.4	18.4	1.02E+08	7.60E+07
198	S39A7_HUMAN	1	1	3	3	0.00E+00	6.16E+06
199	HS105_HUMAN	1	0	1.7	0	2.46E+06	0.00E+00
200	GATA6_HUMAN	1	1	2.4	2.4	0.00E+00	8.81E+06
201	DVL3_HUMAN	1	0	2.1	0	2.89E+06	0.00E+00
202	USP9X_HUMAN;sp|O0	2	9	1.2	5.1	0.00E+00	4.74E+07
203	UBP7_HUMAN	1	0	2	0	4.55E+06	0.00E+00
204	PBIP1_HUMAN	2	1	3.7	1.5	3.86E+06	0.00E+00
205	SEH1_HUMAN	1	0	5.3	0	2.59E+06	0.00E+00
206	F120B_HUMAN	3	0	4.1	0	9.55E+06	0.00E+00
207	RBM33_HUMAN	12	8	16.8	11.5	1.17E+08	9.05E+07
208	SPF45_HUMAN	6	5	16	15.7	3.79E+07	4.33E+07
209	NSE2_HUMAN	2	0	10.9	0	5.12E+06	0.00E+00
210	NSE3_HUMAN	1	0	5.3	0	2.42E+06	0.00E+00
211	JKIP1_HUMAN	1	0	1.4	0	1.86E+06	0.00E+00
212	DOCK7_HUMAN;sp|Q8	8	1	5.7	0.5	3.81E+07	0.00E+00
213	ADCYA_HUMAN	1	0	0.8	0	4.31E+06	0.00E+00
214	PP1RA_HUMAN	15	8	20.6	11.7	1.38E+08	1.07E+08
215	NUDC1_HUMAN	2	2	5.5	5.5	7.47E+06	1.03E+07
216	SMC6_HUMAN	4	0	6.5	0	1.21E+07	0.00E+00
217	SIN3A_HUMAN	2	1	3.2	1	5.58E+06	0.00E+00
218	ZIC5_HUMAN	1	0	5.1	0	8.24E+06	0.00E+00
219	LGMN_HUMAN	2	1	10.9	3.9	9.58E+06	0.00E+00
220	ATX2_HUMAN	9	8	11.7	10.5	6.78E+07	5.52E+07
221	ERP44_HUMAN	7	6	31.8	20.4	6.97E+07	8.12E+07
222	MMTA2_HUMAN	2	1	8.7	4.9	7.08E+06	0.00E+00
223	MCRI2_HUMAN	1	0	19.4	0	3.87E+06	0.00E+00
224	SF3B5_HUMAN	2	2	32.6	32.6	4.18E+07	5.02E+07
225	DPY30_HUMAN	1	0	16.2	0	1.50E+06	0.00E+00
226	WDR33_HUMAN	3	1	3.1	0.9	1.03E+07	0.00E+00
227	CT027_HUMAN	9	8	72.4	65.5	4.51E+08	3.72E+08
228	PITH1_HUMAN	2	1	14.2	8.5	1.43E+07	0.00E+00
229	XRN2_HUMAN	3	0	4.5	0	1.21E+07	0.00E+00
230	NSRP1_HUMAN	5	4	8.2	7.9	3.74E+07	3.22E+07
231	NT5D2_HUMAN	8	9	21.7	26	5.76E+07	8.72E+07

id	Protein names	Unique peptides Bait	Unique peptides Control	Sequence coverage Bait [%]	Sequence coverage Control [%]	LFQ intensity Bait	LFQ intensity Control
232	CHD8_HUMAN;sp|Q8T	5	2	3.4	1.3	1.40E+07	1.54E+07
233	MIO_HUMAN	4	0	6.3	0	1.07E+07	0.00E+00
234	NSE4A_HUMAN	2	0	11.2	0	1.38E+07	0.00E+00
235	CDK12_HUMAN;sp|Q0	5	2	6.6	2.6	1.79E+07	0.00E+00
236	CPSF2_HUMAN	5	2	9.1	3.3	1.71E+07	1.63E+07
237	RERE_HUMAN	1	0	1.8	0	3.41E+06	0.00E+00
238	AASS_HUMAN	18	17	29.9	27.6	2.23E+08	2.56E+08
239	BI2L1_HUMAN	6	5	19.6	16.4	4.90E+07	4.31E+07
240	NRBP_HUMAN	1	0	3	0	5.78E+06	0.00E+00
241	CPSF3_HUMAN	3	4	8.3	7.5	0.00E+00	2.43E+07
242	ZN214_HUMAN	1	0	1.5	0	1.90E+06	0.00E+00
243	S39AA_HUMAN	1	2	1.2	2.9	0.00E+00	1.27E+07
244	CHIP_HUMAN	3	2	10.9	8.3	1.59E+07	1.76E+07
245	FOXJ3_HUMAN	2	0	6.4	0	9.39E+06	0.00E+00
246	SATB2_HUMAN	1	1	7.2	5.9	1.79E+07	2.05E+07
247	CN166_HUMAN	7	4	39.3	25.4	5.18E+07	4.06E+07
248	RUVB2_HUMAN	1	1	1.9	2.4	0.00E+00	2.88E+06
249	RUVB1_HUMAN	2	3	7	9.6	1.09E+07	1.48E+07
250	GIT1_HUMAN	2	1	3.3	1.4	6.77E+06	0.00E+00
251	LC7L2_HUMAN;sp|Q9N	3	4	9.9	12.5	7.53E+06	1.15E+07
252	SF3B6_HUMAN	4	4	40.8	39.2	5.03E+07	5.38E+07
253	RTCB_HUMAN	7	3	24	9.5	4.66E+07	3.80E+07
254	CCDC9_HUMAN	1	1	1.3	1.3	0.00E+00	8.21E+07

Table A.3: Proteins identified in MASCOT search using one-step TALON or two-step TALON/StrepTactin NSMCE4a affinity purification (Figure 4.5)

A. MASCOT search parameters used to identified peptides in the both Control and Bait samples using one-step TALON column. **B.** MASCOT search results using parameters described in A, table shows search results for both Bait and Control cell lines and number of all peptides identified for each protein hit for affinity purification using one-step TALON column; BAIT (NSMCE4a-Strep-6xHis), CONTROL (Flp-In T-REx 293 cell line with no tag). **C.** MASCOT search parameters used to identified peptides in the both Control and Bait samples using two-step TALON and StrepTactin columns. **D.** MASCOT search results using parameters described in C, table shows search results for both Bait and Control cell lines and number of all peptides identified for each protein hit for affinity purification using two-step TALON and StrepTactin columns.

A

2017_11_16 MASCOT search parameters; experiment: TALON

Search title	
Timestamp	2017-11-16T12:57:02Z
User	Zuzanna Kozik
Email	zkk21@sussex.ac.uk
Report URI	http://139.184.166.59/mascot/cgi/master_results.pl?file=../data/20171116/F0
Peak list data path	C:\MGF files\Zuza Kozik\Anita_MS data\TEMP Anita\Anita_clone2_TALON_171
Peak list format	Mascot generic
Search type	MIS
Mascot version	2.3.02
Database	SwissProt
Fasta file	SwissProt_Jan2017_custom_v3.FASTA
Total sequences	553657
Total residues	198178534
Sequences after taxonomy filter	20169
Number of queries	14506

Fixed modifications ----------

Identifier	Name	Delta	Neutral loss
1	Carbamidomethyl (C)	57.02146	

Variable modifications ----------

Identifier	Name	Delta	Neutral loss(es)	
1	Acetyl (Protein N-term)	42.01057		
2	Oxidation (M)	15.99492	0	63.99829

Search Parameters ----------

Taxonomy filter	. . . . . Homo sapiens (human)
Enzyme	Trypsin
Maximum Missed Cleavages	2
Fixed modifications	Carbamidomethyl (C)
Variable modifications	Acetyl (Protein N-term),Oxidation (M)
Peptide Mass Tolerance	6
Peptide Mass Tolerance Units	ppm
Fragment Mass Tolerance	0.7
Fragment Mass Tolerance Units	Da
Mass values	Monoisotopic
Instrument type	Default

Format parameters ----------

Significance threshold	0.05
Max. number of hits	0
Use MudPIT protein scoring	1
Ions score cut-off	0
Include same-set proteins	
Include sub-set proteins	0
Include unassigned	0
Require bold red	0

2017_11_16 MASCOT search parameters; experiment: TALON	
Use homology threshold	0
Group protein families	0

B

2017_11_16 MASCOT search; experiment: TALON

BAIT			CONTROL		
prot_hit_num	prot_acc	# peptides_all	prot_hit_num	prot_acc	# peptides_all
1	Q15233|NONO_HUMAN	308	1	Q15233|NONO_HUMAN	366
2	P23246|SFPQ_HUMAN	235	2	P23246|SFPQ_HUMAN	370
3	P14866|HNRPL_HUMAN	146	3	P14866|HNRPL_HUMAN	130
4	O43143|DHX15_HUMAN	117	4	P11387|TOP1_HUMAN	159
5	P11387|TOP1_HUMAN	154	5	O43143|DHX15_HUMAN	95
6	P0DMV8|HS71A_HUMAN	87	6	Q13435|SF3B2_HUMAN	129
7	Q8WXF1|PSPC1_HUMAN	164	7	P0DMV8|HS71A_HUMAN	81
8	Q13435|SF3B2_HUMAN	96	8	Q86XP3|DDX42_HUMAN	97
9	Q86XP3|DDX42_HUMAN	89	9	Q8WXF1|PSPC1_HUMAN	161
10	Q15393|SF3B3_HUMAN	62	10	Q15459|SF3A1_HUMAN	84
11	P11142|HSP7C_HUMAN	73	11	P11142|HSP7C_HUMAN	74
12	Q15459|SF3A1_HUMAN	75	12	Q12874|SF3A3_HUMAN	67
13	O75533|SF3B1_HUMAN	96	13	Q15393|SF3B3_HUMAN	55
14	P51608|MECP2_HUMAN	54	14	O60885|BRD4_HUMAN	95
15	O60885|BRD4_HUMAN	91	15	Q8WWM7|ATX2L_HUMAN	90
16	Q12874|SF3A3_HUMAN	63	16	O75533|SF3B1_HUMAN	83
17	Q93008|USP9X_HUMAN	72	17	P51608|MECP2_HUMAN	55
18	Q8WWM7|ATX2L_HUMAN	83	18	Q99700|ATX2_HUMAN	52
19	P34931|HS71L_HUMAN	39	19	P34931|HS71L_HUMAN	38
20	Q99700|ATX2_HUMAN	44	20	Q15424|SAFB1_HUMAN	103
21	P07437|TBB5_HUMAN	32	21	P17066|HSP76_HUMAN	31
22	Q15637|SF01_HUMAN	54	22	P11940|PABP1_HUMAN	40
23	P17066|HSP76_HUMAN	34	23	P04406|G3P_HUMAN	41
24	P11940|PABP1_HUMAN	41	24	Q9Y3I0|RTCB_HUMAN	51
25	P04406|G3P_HUMAN	37	25	Q15007|FL2D_HUMAN	38
26	Q8N684|CPSF7_HUMAN	38	26	Q9H0G5|NSRP1_HUMAN	65
27	Q8IYS1|P20D2_HUMAN	54	27	Q8N684|CPSF7_HUMAN	43
28	Q15424|SAFB1_HUMAN	86	28	P25490|TYY1_HUMAN	52
29	P25490|TYY1_HUMAN	52	29	Q16630|CPSF6_HUMAN	39
30	Q9Y3I0|RTCB_HUMAN	45	30	Q15637|SF01_HUMAN	53
31	Q15007|FL2D_HUMAN	35	31	Q8IYS1|P20D2_HUMAN	59
32	Q8N163|CCAR2_HUMAN	50	32	Q9Y224|CN166_HUMAN	32
33	P68371|TBB4B_HUMAN	29	33	Q9BS26|ERP44_HUMAN	24
34	O15042|SR140_HUMAN	80	34	Q04726|TLE3_HUMAN	35
35	Q13509|TBB3_HUMAN	21	35	Q92499|DDX1_HUMAN	48
36	Q9BS26|ERP44_HUMAN	31	36	P38646|GRP75_HUMAN	34
37	Q04726|TLE3_HUMAN	41	37	Q8WUA2|PPIL4_HUMAN	30
38	P04264|K2C1_HUMAN	18	38	O15042|SR140_HUMAN	60
39	Q86TG7|PEG10_HUMAN	29	39	Q14151|SAFB2_HUMAN	68
40	P11021|GRP78_HUMAN	37	40	Q93008|USP9X_HUMAN	49
41	P38646|GRP75_HUMAN	41	41	Q4VCS5|AMOT_HUMAN	48
42	Q16630|CPSF6_HUMAN	33	42	Q86TG7|PEG10_HUMAN	23
43	P49750|YLPM1_HUMAN	46	43	Q96EV2|RBM33_HUMAN	37
44	Q9H361|PABP3_HUMAN	30	44	P26196|DDX6_HUMAN	29
45	Q96EV2|RBM33_HUMAN	50	45	P11021|GRP78_HUMAN	27
46	Q9Y224|CN166_HUMAN	27	46	Q13310|PABP4_HUMAN	29
47	O95817|BAG3_HUMAN	32	47	P07437|TBB5_HUMAN	17

BAIT			CONTROL		
prot_hit_num	prot_acc	# peptides_all	prot_hit_num	prot_acc	# peptides_all
48	Q5SW79|CE170_HUMAN	50	48	O43809|CPSF5_HUMAN	33
49	Q53H96|P5CR3_HUMAN	23	49	Q9H361|PABP3_HUMAN	29
50	Q8IWX8|CHERP_HUMAN	45	50	Q9Y3B4|SF3B6_HUMAN	19
51	P68363|TBA1B_HUMAN	21	51	Q15427|SF3B4_HUMAN	16
52	P50750|CDK9_HUMAN	18	52	Q96QC0|PP1RA_HUMAN	50
53	Q13310|PABP4_HUMAN	28	53	Q15428|SF3A2_HUMAN	39
54	Q15427|SF3B4_HUMAN	11	54	Q8IVS2|FABD_HUMAN	15
55	Q4G0J3|LARP7_HUMAN	30	55	P50750|CDK9_HUMAN	19
56	Q96QC0|PP1RA_HUMAN	49	56	Q9C0J8|WDR33_HUMAN	39
57	Q9H0G5|NSRP1_HUMAN	54	57	P32929|CGL_HUMAN	19
58	Q9GZN8|CT027_HUMAN	23	58	P68363|TBA1B_HUMAN	12
59	Q7RTV0|PHF5A_HUMAN	15	59	Q8IXB1|DJC10_HUMAN	27
60	Q9Y3B4|SF3B6_HUMAN	20	60	Q86X55|CARM1_HUMAN	19
61	O00507|USP9Y_HUMAN	34	61	P49750|YLPM1_HUMAN	40
62	Q14151|SAFB2_HUMAN	62	62	Q9NTM9|CUTC_HUMAN	13
63	P22681|CBL_HUMAN	34	63	Q53H96|P5CR3_HUMAN	15
64	Q8IXB1|DJC10_HUMAN	26	64	Q5SW79|CE170_HUMAN	45
65	Q86X55|CARM1_HUMAN	22	65	Q7RTV0|PHF5A_HUMAN	17
66	Q8N1G2|CMTR1_HUMAN	34	66	P30048|PRDX3_HUMAN	11
67	Q9P2N5|RBM27_HUMAN	25	67	Q8IVM0|CCD50_HUMAN	22
68	Q15428|SF3A2_HUMAN	37	68	P68371|TBB4B_HUMAN	16
69	O43809|CPSF5_HUMAN	28	69	Q8N1G2|CMTR1_HUMAN	23
70	Q8IVS2|FABD_HUMAN	19	70	P22681|CBL_HUMAN	28
71	Q92499|DDX1_HUMAN	42	71	O95817|BAG3_HUMAN	19
72	O60563|CCNT1_HUMAN	33	72	Q9P2N5|RBM27_HUMAN	21
73	O15226|NKRF_HUMAN	49	73	O15226|NKRF_HUMAN	44
74	Q8WUA2|PPIL4_HUMAN	16	74	Q969P6|TOP1M_HUMAN	23
75	Q9H0D6|XRN2_HUMAN	39	75	P61964|WDR5_HUMAN	17
76	Q9UPW6|SATB2_HUMAN	11	76	Q86TI2|DPP9_HUMAN	41
77	Q9BQE3|TBA1C_HUMAN	18	77	Q8NCA5|FA98A_HUMAN	14
78	Q969P6|TOP1M_HUMAN	29	78	Q9GZN8|CT027_HUMAN	25
79	Q9UNE7|CHIP_HUMAN	19	79	Q4G0J3|LARP7_HUMAN	28
80	Q8NCA5|FA98A_HUMAN	13	80	O15391|TYY2_HUMAN	20
81	O15391|TYY2_HUMAN	21	81	Q96I25|SPF45_HUMAN	31
82	Q7Z417|NUFP2_HUMAN	18	82	Q8N163|CCAR2_HUMAN	31
83	Q9NTM9|CUTC_HUMAN	10	83	Q10570|CPSF1_HUMAN	19
84	Q86TI2|DPP9_HUMAN	35	84	Q13509|TBB3_HUMAN	11
85	O94842|TOX4_HUMAN	17	85	Q4VXU2|PAP1L_HUMAN	12
86	O00193|SMAP_HUMAN	11	86	O60563|CCNT1_HUMAN	22
87	Q96I25|SPF45_HUMAN	34	87	P52655|TF2AA_HUMAN	12
88	P30048|PRDX3_HUMAN	8	88	C9JLW8|MCRI1_HUMAN	11
89	Q9BUF5|TBB6_HUMAN	7	89	O00507|USP9Y_HUMAN	20
90	Q92908|GATA6_HUMAN	7	90	Q96ST3|SIN3A_HUMAN	18
91	Q9BTA9|WAC_HUMAN	16	91	Q14247|SRC8_HUMAN	23
92	Q9BU76|MMTA2_HUMAN	6	92	P36873|PP1G_HUMAN	9
93	P42694|HELZ_HUMAN	6	93	Q8IWX8|CHERP_HUMAN	32
94	Q3ZCM7|TBB8_HUMAN	9	94	Q9H0D6|XRN2_HUMAN	34
95	P52655|TF2AA_HUMAN	11	95	Q7Z417|NUFP2_HUMAN	21

BAIT			CONTROL		
prot_hit_num	prot_acc	# peptides_all	prot_hit_num	prot_acc	# peptides_all
96	P35908|K22E_HUMAN	6	96	Q96N67|DOCK7_HUMAN	23
97	P26196|DDX6_HUMAN	20	97	P63261|ACTG_HUMAN	10
98	Q96ST3|SIN3A_HUMAN	22	98	P02545|LMNA_HUMAN	19
99	P12532|KCRU_HUMAN	23	99	P61962|DCAF7_HUMAN	11
100	Q4VXU2|PAP1L_HUMAN	14	100	P68871|HBB_HUMAN	5
101	P62805|H4_HUMAN	10	101	O94842|TOX4_HUMAN	12
102	P61962|DCAF7_HUMAN	12	102	Q9UNE7|CHIP_HUMAN	15
103	Q96N67|DOCK7_HUMAN	27	103	P31943|HNRH1_HUMAN	14
104	Q8IY18|SMC5_HUMAN	18	104	Q7L2J0|MEPCE_HUMAN	19
105	Q01826|SATB1_HUMAN	10	105	Q9HCK8|CHD8_HUMAN	17
106	Q69YN4|VIR_HUMAN	16	106	Q13485|SMAD4_HUMAN	24
107	P20265|PO3F2_HUMAN	11	107	P62380|TBPL1_HUMAN	10
108	P61964|WDR5_HUMAN	14	108	Q07955|SRSF1_HUMAN	13
109	Q96MG7|NSE3_HUMAN	10	109	Q15059|BRD3_HUMAN	17
110	P49411|EFTU_HUMAN	15	110	P52657|T2AG_HUMAN	10
111	Q07021|C1QBP_HUMAN	5	111	Q04724|TLE1_HUMAN	16
112	P13645|K1C10_HUMAN	12	112	Q9UHB7|AFF4_HUMAN	16
113	Q5JTD0|TJAP1_HUMAN	16	113	Q9BTA9|WAC_HUMAN	9
114	Q9UHB7|AFF4_HUMAN	15	114	Q6UN15|FIP1_HUMAN	14
115	Q5T200|ZC3HD_HUMAN	26	115	Q9NQX3|GEPH_HUMAN	9
116	Q7L2J0|MEPCE_HUMAN	28	116	O00193|SMAP_HUMAN	10
117	Q9BWJ5|SF3B5_HUMAN	15	117	P60709|ACTB_HUMAN	10
118	P04259|K2C6B_HUMAN	4	118	P20265|PO3F2_HUMAN	9
119	Q9C0J8|WDR33_HUMAN	31	119	P62140|PP1B_HUMAN	11
120	Q6UN15|FIP1_HUMAN	14	120	Q3MHD2|LSM12_HUMAN	11
121	P32929|CGL_HUMAN	15	121	Q9BWJ5|SF3B5_HUMAN	12
122	Q5VTE0|EF1A3_HUMAN	12	122	O95479|G6PE_HUMAN	6
123	Q9HCK8|CHD8_HUMAN	11	123	Q9UPW6|SATB2_HUMAN	6
124	P98175|RBM10_HUMAN	12	124	P33240|CSTF2_HUMAN	15
125	Q14247|SRC8_HUMAN	17	125	P12270|TPR_HUMAN	13
126	O95409|ZIC2_HUMAN	7	126	Q15717|ELAV1_HUMAN	6
127	Q15717|ELAV1_HUMAN	11	127	Q04727|TLE4_HUMAN	14
128	Q13523|PRP4B_HUMAN	10	128	Q6S8J3|POTEE_HUMAN	10
129	P84090|ERH_HUMAN	5	129	Q6NT76|HMBX1_HUMAN	4
130	Q8IVM0|CCD50_HUMAN	9	130	P98175|RBM10_HUMAN	12
131	Q9H4B7|TBB1_HUMAN	7	131	Q9Y2L9|LRCH1_HUMAN	4
132	O95487|SC24B_HUMAN	4	132	Q01826|SATB1_HUMAN	6
133	P52657|T2AG_HUMAN	9	133	P04075|ALDOA_HUMAN	8
134	Q9P2R6|RERE_HUMAN	8	134	A6NKD9|CC85C_HUMAN	6
135	Q15059|BRD3_HUMAN	14	135	Q96DU9|PABP5_HUMAN	4
136	A6NKD9|CC85C_HUMAN	7	136	Q5T200|ZC3HD_HUMAN	16
137	P50990|TCPQ_HUMAN	11	137	B1AK53|ESPN_HUMAN	8
138	P04075|ALDOA_HUMAN	8	138	P63208|SKP1_HUMAN	12
139	Q9BRR6|ADPGK_HUMAN	5	139	P12532|KCRU_HUMAN	20
140	Q05639|EF1A2_HUMAN	6	140	Q5JQF8|PAP1M_HUMAN	6
141	Q8WVV9|HNRLL_HUMAN	9	141	P54259|ATN1_HUMAN	7
142	P60891|PRPS1_HUMAN	9	142	Q5T6F2|UBAP2_HUMAN	7
143	P11908|PRPS2_HUMAN	9	143	Q9P2R6|RERE_HUMAN	5

BAIT			CONTROL		
prot_hit_num	prot_acc	# peptides_all	prot_hit_num	prot_acc	# peptides_all
144	Q92841|DDX17_HUMAN	5	144	Q8WVV9|HNRLL_HUMAN	8
145	Q04724|TLE1_HUMAN	18	145	Q9UII2|ATIF1_HUMAN	13
146	P02538|K2C6A_HUMAN	6	146	Q6UXN9|WDR82_HUMAN	18
147	Q7Z794|K2C1B_HUMAN	3	147	P62136|PP1A_HUMAN	7
148	P54259|ATN1_HUMAN	9	148	P62805|H4_HUMAN	7
149	Q75N03|HAKAI_HUMAN	12	149	O95487|SC24B_HUMAN	3
150	Q10570|CPSF1_HUMAN	9	150	Q5VTE0|EF1A3_HUMAN	4
151	Q9HAH7|FBRS_HUMAN	14	151	Q9GZP4|PITH1_HUMAN	14
152	P05549|AP2A_HUMAN	6	152	Q9H4B7|TBB1_HUMAN	6
153	Q13485|SMAD4_HUMAN	17	153	Q3ZCM7|TBB8_HUMAN	5
154	C9JLW8|MCRI1_HUMAN	5	154	P30533|AMRP_HUMAN	17
155	Q96SB8|SMC6_HUMAN	19	155	Q5QNW6|H2B2F_HUMAN	4
156	Q9UII2|ATIF1_HUMAN	10	156	Q05682|CALD1_HUMAN	7
157	Q9Y6M1|IF2B2_HUMAN	20	157	Q92997|DVL3_HUMAN	4
158	O00470|MEIS1_HUMAN	7	158	P84090|ERH_HUMAN	3
159	P33240|CSTF2_HUMAN	15	159	Q5ST30|SYVM_HUMAN	10
160	Q7Z4S6|KI21A_HUMAN	17	160	Q15599|NHRF2_HUMAN	4
161	Q9NXX6|NSE4A_HUMAN	6	161	P63167|DYL1_HUMAN	5
162	P31943|HNRH1_HUMAN	7	162	Q01105|SET_HUMAN	6
163	O14770|MEIS2_HUMAN	6	163	Q5VTR2|BRE1A_HUMAN	10
164	Q5JQF8|PAP1M_HUMAN	6	164	Q8WW12|PCNP_HUMAN	9
165	Q07955|SRSF1_HUMAN	6	165	Q69YN4|VIR_HUMAN	11
166	P13647|K2C5_HUMAN	3	166	Q5JTD0|TJAP1_HUMAN	16
167	Q9UPW0|FOXJ3_HUMAN	4	167	P62158|CALM_HUMAN	9
168	Q5T6F2|UBAP2_HUMAN	6	168	O15027|SC16A_HUMAN	12
169	Q5ST30|SYVM_HUMAN	11	169	Q99583|MNT_HUMAN	5
170	P48643|TCPE_HUMAN	8	170	O75937|DNJC8_HUMAN	9
171	O94992|HEXI1_HUMAN	2	171	O96019|ACL6A_HUMAN	5
172	O75937|DNJC8_HUMAN	18	172	P67870|CSK2B_HUMAN	9
173	Q8WW12|PCNP_HUMAN	9	173	Q14244|MAP7_HUMAN	10
174	Q5QNW6|H2B2F_HUMAN	4	174	O00294|TULP1_HUMAN	13
175	Q96F86|EDC3_HUMAN	10	175	P69905|HBA_HUMAN	9
176	P05412|JUN_HUMAN	2	176	O14770|MEIS2_HUMAN	4
177	P08651|NFIC_HUMAN	9	177	O00712|NFIB_HUMAN	4
178	Q14157|UBP2L_HUMAN	7	178	Q9P2I0|CPSF2_HUMAN	6
179	Q04727|TLE4_HUMAN	14	179	Q9P2D1|CHD7_HUMAN	11
180	P63208|SKP1_HUMAN	10	180	P84103|SRSF3_HUMAN	3
181	P19784|CSK22_HUMAN	4	181	Q8TAQ2|SMRC2_HUMAN	16
182	O95479|G6PE_HUMAN	5	182	Q13642|FHL1_HUMAN	5
183	Q9Y2L9|LRCH1_HUMAN	8	183	Q8NEV1|CSK23_HUMAN	8
184	Q6VUC0|AP2E_HUMAN	5	184	P07910|HNRPC_HUMAN	4
185	P15104|GLNA_HUMAN	6	185	P61978|HNRPK_HUMAN	11
186	P68400|CSK21_HUMAN	5	186	O75150|BRE1B_HUMAN	17
187	Q99832|TCPH_HUMAN	11	187	Q8IY63|AMOL1_HUMAN	7
188	Q15102|PA1B3_HUMAN	3	188	O60231|DHX16_HUMAN	3
189	O15405|TOX3_HUMAN	3	189	O95409|ZIC2_HUMAN	4
190	P49368|TCPG_HUMAN	5	190	Q9HAH7|FBRS_HUMAN	9
191	O14874|BCKD_HUMAN	3	191	O15405|TOX3_HUMAN	3

BAIT			CONTROL		
prot_hit_num	prot_acc	# peptides_all	prot_hit_num	prot_acc	# peptides_all
192	A6QL63|BTBDB_HUMAN	7	192	Q13972|RGRF1_HUMAN	7
193	Q9Y2X7|GIT1_HUMAN	6	193	O14827|RGRF2_HUMAN	5
194	Q6V1X1|DPP8_HUMAN	2	194	B3EWG3|FM25A_HUMAN	2
195	B1AK53|ESPN_HUMAN	9	195	Q7RTR2|NLRC3_HUMAN	2
196	Q6NT76|HMBX1_HUMAN	2	196	Q8NF91|SYNE1_HUMAN	23
197	Q9NQX3|GEPH_HUMAN	4	197	Q15149|PLEC_HUMAN	31
198	Q6P6B7|ANR16_HUMAN	2	198	Q8NDA2|HMCN2_HUMAN	12
199	P62136|PP1A_HUMAN	12	199	Q9NR48|ASH1L_HUMAN	9
200	Q9NRL2|BAZ1A_HUMAN	10	200	Q5JRA6|MIA3_HUMAN	12
201	Q66GS9|CP135_HUMAN	10	201	Q9BXT5|TEX15_HUMAN	12
202	Q4G0X9|CCD40_HUMAN	9	202	Q9H2F9|CCD68_HUMAN	7
203	Q8IYB8|SUV3_HUMAN	5	203	Q14CN2|CLCA4_HUMAN	4
204	Q96NL6|SCLT1_HUMAN	6	204	P43034|LIS1_HUMAN	3
205	P36873|PP1G_HUMAN	14	205	Q9Y2X7|GIT1_HUMAN	7
206	P67870|CSK2B_HUMAN	11	206	P55011|S12A2_HUMAN	6
207	P43034|LIS1_HUMAN	3	207	P49257|LMAN1_HUMAN	6
208	Q13642|FHL1_HUMAN	3	208	Q08117|AES_HUMAN	6
209	O60583|CCNT2_HUMAN	6	209	O14874|BCKD_HUMAN	3
210	B3EWG3|FM25A_HUMAN	2	210	Q13523|PRP4B_HUMAN	4
211	Q7RTR2|NLRC3_HUMAN	2	211	P53999|TCP4_HUMAN	7
212	Q99626|CDX2_HUMAN	8	212	Q99626|CDX2_HUMAN	6
213	P78371|TCPB_HUMAN	3	213	P47928|ID4_HUMAN	2
214	P20226|TBP_HUMAN	6	214	Q13586|STIM1_HUMAN	3
215	O00712|NFIB_HUMAN	8	215	Q9Y230|RUVB2_HUMAN	6
216	Q7Z6R9|AP2D_HUMAN	3	216	O95639|CPSF4_HUMAN	4
217	Q14155|ARHG7_HUMAN	7	217	P20226|TBP_HUMAN	6
218	Q15052|ARHG6_HUMAN	5	218	Q6SJ96|TBPL2_HUMAN	4
219	Q99583|MNT_HUMAN	7	219	Q66GS9|CP135_HUMAN	10
220	Q14938|NFIX_HUMAN	10	220	Q8IYB8|SUV3_HUMAN	5
221	Q05682|CALD1_HUMAN	5	221	Q4G0X9|CCD40_HUMAN	5
222	Q96DU9|PABP5_HUMAN	3	222	Q9NRL2|BAZ1A_HUMAN	9
223	Q14241|ELOA1_HUMAN	13	223	Q96NL6|SCLT1_HUMAN	5
224	Q6Y7W6|PERQ2_HUMAN	15	224	P40227|TCPZ_HUMAN	5
225	Q9NYV4|CDK12_HUMAN	6	225	P55735|SEC13_HUMAN	2
226	P11362|FGFR1_HUMAN	5	226	P52597|HNRPF_HUMAN	9
227	P20794|MAK_HUMAN	6	227	P0CB38|PAB4L_HUMAN	6
228	Q14004|CDK13_HUMAN	4	228	Q6V1X1|DPP8_HUMAN	1
229	Q00534|CDK6_HUMAN	3	229	Q9BUT9|MCRI2_HUMAN	5
230	P06241|FYN_HUMAN	3	230	Q14155|ARHG7_HUMAN	6
231	P06493|CDK1_HUMAN	4	231	Q7Z4S6|KI21A_HUMAN	13
232	P11802|CDK4_HUMAN	4	232	Q9UPW0|FOXJ3_HUMAN	1
233	Q07002|CDK18_HUMAN	3	233	Q92908|GATA6_HUMAN	6
234	Q15714|T22D1_HUMAN	6	234	P34897|GLYM_HUMAN	5
235	A6NDR6|ME3L1_HUMAN	5	235	Q14938|NFIX_HUMAN	9
236	P40227|TCPZ_HUMAN	2	236	Q5UIP0|RIF1_HUMAN	7
237	Q6UXN9|WDR82_HUMAN	13	237	Q6PI26|SHQ1_HUMAN	2
238	Q6PI26|SHQ1_HUMAN	2	238	Q6Y7W6|PERQ2_HUMAN	17
239	Q92997|DVL3_HUMAN	4	239	Q96HP0|DOCK6_HUMAN	4

BAIT			CONTROL		
prot_hit_num	prot_acc	# peptides_all	prot_hit_num	prot_acc	# peptides_all
240	P42858|HD_HUMAN	6	240	Q9NZ56|FMN2_HUMAN	4
241	O15027|SC16A_HUMAN	9	241	P39687|AN32A_HUMAN	2
242	Q9NZ56|FMN2_HUMAN	6	242	Q14157|UBP2L_HUMAN	10
243	Q9UJU2|LEF1_HUMAN	4	243	Q9HCM7|FBSL_HUMAN	3
244	Q5T9S5|CCD18_HUMAN	7	244	P48200|IREB2_HUMAN	4
245	O95447|LCA5L_HUMAN	5	245	Q14241|ELOA1_HUMAN	11
246	Q9NYU2|UGGG1_HUMAN	7	246	P51532|SMCA4_HUMAN	9
247	Q5EBN2|TRI61_HUMAN	3	247	P78386|KRT85_HUMAN	3
248	Q13586|STIM1_HUMAN	9	248	A6NDR6|ME3L1_HUMAN	4
249	Q12857|NFIA_HUMAN	8	249	Q07021|C1QBP_HUMAN	3
250	Q9UQ35|SRRM2_HUMAN	15	250	P17987|TCPA_HUMAN	4
251	Q06830|PRDX1_HUMAN	2	251	O60583|CCNT2_HUMAN	4
252	P49257|LMAN1_HUMAN	8	252	Q9Y512|SAM50_HUMAN	4
253	Q6SJ96|TBPL2_HUMAN	4	253	P08651|NFIC_HUMAN	5
254	P30533|AMRP_HUMAN	12	254	P50991|TCPD_HUMAN	6
255	P0C0S8|H2A1_HUMAN	5	255	P56178|DLX5_HUMAN	3
256	Q9BUT9|MCRI2_HUMAN	5	256	Q07687|DLX2_HUMAN	3
257	Q9NQB0|TF7L2_HUMAN	4	257	P42858|HD_HUMAN	7
258	Q9H9Y6|RPA2_HUMAN	6	258	A6NM62|LRC53_HUMAN	4
259	Q9Y2R4|DDX52_HUMAN	4	259	Q13191|CBLB_HUMAN	5
260	Q15599|NHRF2_HUMAN	2	260	Q92922|SMRC1_HUMAN	7
261	P62140|PP1B_HUMAN	11	261	Q75N03|HAKAI_HUMAN	8
262	Q8NF91|SYNE1_HUMAN	24	262	Q6KC79|NIPBL_HUMAN	4
263	P12270|TPR_HUMAN	8	263	P24534|EF1B_HUMAN	2
264	Q9NX05|F120C_HUMAN	4	264	Q15052|ARHG6_HUMAN	5
265	P40424|PBX1_HUMAN	3	265	P0DMR1|HNRC4_HUMAN	2
266	Q9UPT8|ZC3H4_HUMAN	9	266	Q9UGU0|TCF20_HUMAN	5
267	A6NM62|LRC53_HUMAN	5	267	Q8N954|GPT11_HUMAN	3
268	P52597|HNRPF_HUMAN	5	268	P78371|TCPB_HUMAN	2
269	Q96MF7|NSE2_HUMAN	5	269	Q15369|ELOC_HUMAN	3
270	Q92769|HDAC2_HUMAN	5	270	Q05048|CSTF1_HUMAN	1
271	Q13547|HDAC1_HUMAN	5	271	P49368|TCPG_HUMAN	5
272	Q5TCS8|KAD9_HUMAN	7	272	Q01082|SPTB2_HUMAN	5
273	Q9BUQ8|DDX23_HUMAN	6	273	O60683|PEX10_HUMAN	3
274	P0DN76|U2AF5_HUMAN	2	274	Q8NCG7|DGLB_HUMAN	2
275	Q8N954|GPT11_HUMAN	3	275	P11532|DMD_HUMAN	16
276	P84103|SRSF3_HUMAN	3	276	Q6BDS2|URFB1_HUMAN	6
277	Q9HCM7|FBSL_HUMAN	3	277	Q96Q15|SMG1_HUMAN	6
278	Q8NDA2|HMCN2_HUMAN	10	278	O14556|G3PT_HUMAN	3
279	Q15149|PLEC_HUMAN	13	279	P49756|RBM25_HUMAN	11
280	Q5JRA6|MIA3_HUMAN	9	280	P50990|TCPQ_HUMAN	4
281	Q9BXT5|TEX15_HUMAN	6	281	Q9NRC6|SPTN5_HUMAN	13
282	Q9H9F9|ARP5_HUMAN	3	282	Q03001|DYST_HUMAN	15
283	Q9NR48|ASH1L_HUMAN	5	283	Q5TZA2|CROCC_HUMAN	11
284	Q8IV61|GRP3_HUMAN	3	284	O15078|CE290_HUMAN	11
285	Q9H2F9|CCD68_HUMAN	5	285	Q96JP2|MY15B_HUMAN	5
286	Q9H0P0|5NT3A_HUMAN	4	286	Q76LX8|ATS13_HUMAN	3
287	Q14CN2|CLCA4_HUMAN	3	287	Q8N9V3|WSDU1_HUMAN	3

BAIT			CONTROL		
prot_hit_num	prot_acc	# peptides_all	prot_hit_num	prot_acc	# peptides_all
288	Q5UIP0|RIF1_HUMAN	7	288	Q3SY00|T10IP_HUMAN	3
289	Q9BXF6|RFIP5_HUMAN	5	289	P42892|ECE1_HUMAN	3
290	P63261|ACTG_HUMAN	7	290	Q2VIQ3|KIF4B_HUMAN	3
291	Q7Z3Z0|K1C25_HUMAN	4	291	O95239|KIF4A_HUMAN	4
292	Q8WV22|NSE1_HUMAN	4	292	P20774|MIME_HUMAN	2
293	O60683|PEX10_HUMAN	3	293	Q8TAV0|FA76A_HUMAN	1
294	Q8NCG7|DGLB_HUMAN	3	294	O43663|PRC1_HUMAN	2
295	Q01082|SPTB2_HUMAN	4	295	Q86SE9|PCGF5_HUMAN	2
296	Q8IY37|DHX37_HUMAN	8	296	Q9NXC2|GFOD1_HUMAN	3
297	Q96F63|CCD97_HUMAN	3	297	Q8IY37|DHX37_HUMAN	9
298	P34897|GLYM_HUMAN	5	298	Q05519|SRS11_HUMAN	4
299	Q6KC79|NIPBL_HUMAN	11	299	O94979|SC31A_HUMAN	8
300	Q9UHR4|BI2L1_HUMAN	2	300	P10074|ZBT48_HUMAN	3
301	P48200|IREB2_HUMAN	9	301	Q8IVF7|FMNL3_HUMAN	4
302	O14556|G3PT_HUMAN	3	302	Q06830|PRDX1_HUMAN	4
303	Q86W92|LIPB1_HUMAN	4	303	Q5T9S5|CCD18_HUMAN	10
304	P17987|TCPA_HUMAN	7	304	O94804|STK10_HUMAN	9
305	Q8NE31|FA13C_HUMAN	2	305	Q96NM4|TOX2_HUMAN	3
306	P0CB38|PAB4L_HUMAN	5	306	Q14204|DYHC1_HUMAN	17
307	A6NFZ4|FA24A_HUMAN	3	307	Q9UJV8|PURG_HUMAN	2
308	P11532|DMD_HUMAN	13	308	P15104|GLNA_HUMAN	4
309	Q6BDS2|URFB1_HUMAN	9	309	Q4ADV7|RIC1_HUMAN	6
310	Q96Q15|SMG1_HUMAN	6	310	Q8IYX3|CC116_HUMAN	4
311	Q9ULT8|HECD1_HUMAN	7	311	Q5VU43|MYOME_HUMAN	10
312	Q9HCE3|ZN532_HUMAN	5	312	Q86UU0|BCL9L_HUMAN	6
313	Q14533|KRT81_HUMAN	3	313	Q9BUQ8|DDX23_HUMAN	7
314	P10074|ZBT48_HUMAN	6	314	Q5TCS8|KAD9_HUMAN	5
315	Q6ZTR5|CFA47_HUMAN	8	315	O15455|TLR3_HUMAN	3
316	P12111|CO6A3_HUMAN	5	316	Q9BQ52|RNZ2_HUMAN	10
317	Q4ADV7|RIC1_HUMAN	6	317	Q8IZT6|ASPM_HUMAN	23
318	P62258|1433E_HUMAN	4	318	P51665|PSMD7_HUMAN	4
319	Q8IZP0|ABI1_HUMAN	1	319	Q6NSJ2|PHLB3_HUMAN	4
320	Q9NU02|ANKE1_HUMAN	3	320	Q8N531|FBXL6_HUMAN	2
321	Q13191|CBLB_HUMAN	9	321	Q9H3R5|CENPH_HUMAN	4
322	Q9UJV8|PURG_HUMAN	3	322	P52630|STAT2_HUMAN	3
323	Q9NRC6|SPTN5_HUMAN	16	323	Q6PCT2|FXL19_HUMAN	2
324	Q14244|MAP7_HUMAN	15	324	Q6P3X3|TTC27_HUMAN	2
325	Q6IS14|IF5AL_HUMAN	1	325	Q9HCS7|SYF1_HUMAN	3
326	Q96Q89|KI20B_HUMAN	12	326	P38405|GNAL_HUMAN	3
327	Q05519|SRS11_HUMAN	6	327	O14948|TFEC_HUMAN	4
328	Q8WXA9|SREK1_HUMAN	7	328	P61244|MAX_HUMAN	3
329	P02768|ALBU_HUMAN	3	329	Q96N23|CFA54_HUMAN	6
330	Q8WY91|THAP4_HUMAN	3	330	Q96Q89|KI20B_HUMAN	6
331	O75683|SURF6_HUMAN	4	331	O75683|SURF6_HUMAN	5
332	Q96JG6|VPS50_HUMAN	3	332	P02768|ALBU_HUMAN	4
333	Q86Z14|KLOTB_HUMAN	2	333	Q8WY91|THAP4_HUMAN	5
334	Q6PKG0|LARP1_HUMAN	5	334	Q8WXA9|SREK1_HUMAN	3
335	Q8TAV0|FA76A_HUMAN	2	335	Q96JG6|VPS50_HUMAN	3

BAIT			CONTROL		
prot_hit_num	prot_acc	# peptides_all	prot_hit_num	prot_acc	# peptides_all
336	Q9NSY1|BMP2K_HUMAN	1	336	Q86Z14|KLOTB_HUMAN	2
337	A6NJL1|ZSA5B_HUMAN	4	337	Q13547|HDAC1_HUMAN	3
338	Q5TZA2|CROCC_HUMAN	18	338	Q8NE31|FA13C_HUMAN	2
339	Q03001|DYST_HUMAN	16	339	P19429|TNNI3_HUMAN	10
340	O15078|CE290_HUMAN	11	340	Q969V6|MKL1_HUMAN	12
341	Q16512|PKN1_HUMAN	4	341	Q15910|EZH2_HUMAN	7
342	Q9UL16|CFA45_HUMAN	5	342	O00338|ST1C2_HUMAN	8
343	Q8N9V3|WSDU1_HUMAN	5	343	Q9BXU7|UBP26_HUMAN	6
344	Q5VTR2|BRE1A_HUMAN	3	344	Q99741|CDC6_HUMAN	6
345	O95239|KIF4A_HUMAN	7	345	Q92800|EZH1_HUMAN	5
346	Q96JP2|MY15B_HUMAN	4	346	Q9BY12|SCAPE_HUMAN	6
347	Q76LX8|ATS13_HUMAN	4	347	O75347|TBCA_HUMAN	4
348	P42892|ECE1_HUMAN	3	348	Q5VT52|RPRD2_HUMAN	3
349	P20774|MIME_HUMAN	2	349	Q86UP2|KTN1_HUMAN	12
350	Q96J88|ESIP1_HUMAN	5	350	Q8N8D1|PDCD7_HUMAN	7
351	O95801|TTC4_HUMAN	5	351	P12821|ACE_HUMAN	6
352	Q05048|CSTF1_HUMAN	2	352	O60749|SNX2_HUMAN	5
353	Q9H720|PG2IP_HUMAN	4	353	Q9NQ66|PLCB1_HUMAN	7
354	P08048|ZFY_HUMAN	4	354	O75762|TRPA1_HUMAN	5
355	Q5VWQ0|RSBN1_HUMAN	2	355	Q0ZGT2|NEXN_HUMAN	6
356	Q9NRH3|TBG2_HUMAN	1	356	Q92835|SHIP1_HUMAN	5
357	Q2T9J0|TYSD1_HUMAN	3	357	P28288|ABCD3_HUMAN	4
358	Q58F21|BRDT_HUMAN	6	358	Q17RS7|GEN_HUMAN	3
359	Q8WZ74|CTTB2_HUMAN	5	359	Q99959|PKP2_HUMAN	3
360	P20908|CO5A1_HUMAN	11	360	Q96QV1|HHIP_HUMAN	2
361	Q5HYJ3|FA76B_HUMAN	1	361	Q86W92|LIPB1_HUMAN	5
362	Q9UKJ3|GPTC8_HUMAN	9	362	Q76M96|CCD80_HUMAN	5
363	Q14166|TTL12_HUMAN	2	363	Q7Z7G8|VP13B_HUMAN	2
364	O00294|TULP1_HUMAN	6	364	Q6P6B7|ANR16_HUMAN	7
365	Q8IYX3|CC116_HUMAN	4	365	A6NMK7|CPS4L_HUMAN	3
366	Q96N23|CFA54_HUMAN	10	366	Q6PKG0|LARP1_HUMAN	4
367	Q15067|ACOX1_HUMAN	4	367	P50219|MNX1_HUMAN	4
368	O14948|TFEC_HUMAN	2	368	Q92526|TCPW_HUMAN	6
369	Q8NEW0|ZNT7_HUMAN	4	369	Q53GS7|GLE1_HUMAN	3
370	Q8N7J2|AMER2_HUMAN	3	370	Q9NU02|ANKE1_HUMAN	6
371	Q8IVL6|P3H3_HUMAN	3	371	O95801|TTC4_HUMAN	6
372	Q06587|RING1_HUMAN	4	372	Q8IVE3|PKHH2_HUMAN	2
373	Q99496|RING2_HUMAN	2	373	Q96QP1|ALPK1_HUMAN	5
374	O94804|STK10_HUMAN	9	374	Q8N393|ZN786_HUMAN	3
375	Q9NWH9|SLTM_HUMAN	13	375	P0C0S8|H2A1_HUMAN	4
376	Q15327|ANKR1_HUMAN	3	376	Q86XP0|PA24D_HUMAN	4
377	Q9Y2D9|ZN652_HUMAN	4	377	Q9UPR6|ZFR2_HUMAN	6
378	P27824|CALX_HUMAN	3	378	Q676U5|A16L1_HUMAN	6
379	Q5CZC0|FSIP2_HUMAN	26	379	Q709C8|VP13C_HUMAN	9
380	Q99435|NELL2_HUMAN	1	380	P14868|SYDC_HUMAN	9
381	P62380|TBPL1_HUMAN	9	381	Q8NAA4|A16L2_HUMAN	7
382	P25391|LAMA1_HUMAN	6	382	Q86UB2|BIVM_HUMAN	4
383	P04839|CY24B_HUMAN	5	383	Q9H8V3|ECT2_HUMAN	6

BAIT			CONTROL		
prot_hit_num	prot_acc	# peptides_all	prot_hit_num	prot_acc	# peptides_all
384	Q07954|LRP1_HUMAN	5	384	O60281|ZN292_HUMAN	4
385	Q9Y276|BCS1_HUMAN	2	385	Q659C4|LAR1B_HUMAN	5
386	Q8IVE3|PKHH2_HUMAN	3	386	Q99569|PKP4_HUMAN	6
387	Q9P281|BAHC1_HUMAN	7	387	P32455|GBP1_HUMAN	2
388	O43272|PROD_HUMAN	7	388	Q9C0D2|CE295_HUMAN	9
389	Q9BWS9|CHID1_HUMAN	2	389	Q8WXH0|SYNE2_HUMAN	20
390	Q9UPW5|CBPC1_HUMAN	6	390	Q5VTM2|AGAP9_HUMAN	4
391	P63167|DYL1_HUMAN	4	391	P25440|BRD2_HUMAN	12
392	Q5JU85|IQEC2_HUMAN	3	392	P08048|ZFY_HUMAN	5
393	Q9Y6N8|CAD10_HUMAN	2	393	P61160|ARP2_HUMAN	4
394	Q99569|PKP4_HUMAN	6	394	Q9Y6N8|CAD10_HUMAN	2
395	P32455|GBP1_HUMAN	2	395	P07919|QCR6_HUMAN	1
396	P14416|DRD2_HUMAN	2	396	O95670|VATG2_HUMAN	4
397	P61160|ARP2_HUMAN	6	397	P19338|NUCL_HUMAN	2
398	Q8N443|RIBC1_HUMAN	5	398	Q8NI35|INADL_HUMAN	3
399	Q6ZU35|K1211_HUMAN	11	399	P49585|PCY1A_HUMAN	3
400	Q86WI3|NLRC5_HUMAN	7	400	Q8TDI7|TMC2_HUMAN	8
401	P39880|CUX1_HUMAN	4	401	O94886|CSCL1_HUMAN	4
402	P55735|SEC13_HUMAN	4	402	Q6ZTR5|CFA47_HUMAN	8
403	O75150|BRE1B_HUMAN	12	403	Q9UPW5|CBPC1_HUMAN	5
404	Q9GZP4|PITH1_HUMAN	12	404	Q96JG9|ZN469_HUMAN	4
405	Q8TB68|PRR7_HUMAN	9	405	P62258|1433E_HUMAN	2
406	Q86SE9|PCGF5_HUMAN	3	406	A6NCC3|GOG8O_HUMAN	15
407	P54845|NRL_HUMAN	3	407	A6NEM1|GG6L9_HUMAN	12
408	A6NCC3|GOG8O_HUMAN	12	408	A6NEF3|GG6L4_HUMAN	13
409	A6NEY3|GG6L3_HUMAN	13	409	A6NEY3|GG6L3_HUMAN	13
410	A6NEM1|GG6L9_HUMAN	12	410	Q15370|ELOB_HUMAN	4
411	Q8TCU4|ALMS1_HUMAN	13	411	Q9BQG2|NUD12_HUMAN	6
412	P82279|CRUM1_HUMAN	1	412	Q8WZ74|CTTB2_HUMAN	3
413	P25440|BRD2_HUMAN	11	413	Q9H2S9|IKZF4_HUMAN	2
414	P22003|BMP5_HUMAN	8	414	Q5T4S7|UBR4_HUMAN	9
415	Q7Z7G8|VP13B_HUMAN	4	415	Q9Y5A7|NUB1_HUMAN	6
416	Q96A00|PP14A_HUMAN	4	416	Q9UNY4|TTF2_HUMAN	4
417	Q494V2|CP100_HUMAN	4	417	Q8NEE8|TTC16_HUMAN	5
418	Q9Y2A7|NCKP1_HUMAN	4	418	Q58FF7|H90B3_HUMAN	6
419	Q6NT04|TIGD7_HUMAN	2	419	P22003|BMP5_HUMAN	6
420	Q8TDW5|SYTL5_HUMAN	5	420	Q96A00|PP14A_HUMAN	5
421	Q96LM6|TEX37_HUMAN	2	421	Q494V2|CP100_HUMAN	7
422	P51825|AFF1_HUMAN	4	422	Q14511|CASL_HUMAN	3
423	Q8TF46|DI3L1_HUMAN	3	423	Q92576|PHF3_HUMAN	6
424	Q96M83|CCDC7_HUMAN	5	424	Q9ULT8|HECD1_HUMAN	9
425	Q9C0B0|UNK_HUMAN	4	425	Q14997|PSME4_HUMAN	4
426	O00429|DNM1L_HUMAN	2	426	Q9Y566|SHAN1_HUMAN	3
427	Q9Y3S2|ZN330_HUMAN	3	427	Q9HCE0|EPG5_HUMAN	2
428	Q5T4T6|SYC2L_HUMAN	3	428	Q9NTG1|PKDRE_HUMAN	5
429	Q14997|PSME4_HUMAN	3	429	Q5C9Z4|NOM1_HUMAN	7
430	Q9Y566|SHAN1_HUMAN	3	430	Q15154|PCM1_HUMAN	4
431	Q9HCE0|EPG5_HUMAN	4	431	Q6NXR0|IIGP5_HUMAN	8

BAIT			CONTROL		
prot_hit_num	prot_acc	# peptides_all	prot_hit_num	prot_acc	# peptides_all
432	Q86UP2|KTN1_HUMAN	9	432	P26368|U2AF2_HUMAN	4
433	P12821|ACE_HUMAN	5	433	Q8TB68|PRR7_HUMAN	9
434	Q8N8D1|PDCD7_HUMAN	4	434	O95447|LCA5L_HUMAN	4
435	Q9NQ66|PLCB1_HUMAN	8	435	Q495X7|TRI60_HUMAN	3
436	O75762|TRPA1_HUMAN	3	436	Q68DK2|ZFY26_HUMAN	6
437	O60749|SNX2_HUMAN	2	437	O75940|SPF30_HUMAN	3
438	Q6UB99|ANR11_HUMAN	18	438	Q86VF7|NRAP_HUMAN	6
439	Q96T25|ZIC5_HUMAN	7	439	Q5THR3|EFCB6_HUMAN	5
440	Q86XP0|PA24D_HUMAN	2	440	Q86YR7|MF2L2_HUMAN	5
441	Q5C9Z4|NOM1_HUMAN	6	441	Q8NDM7|CFA43_HUMAN	4
442	Q31610|1B81_HUMAN	6	442	Q8NB25|F184A_HUMAN	9
443	P26440|IVD_HUMAN	1	443	Q96EK4|THA11_HUMAN	6
444	Q96QP1|ALPK1_HUMAN	6	444	Q8IYN2|TCAL8_HUMAN	4
445	Q8N393|ZN786_HUMAN	3	445	P33908|MA1A1_HUMAN	4
446	Q8TAT5|NEIL3_HUMAN	3	446	Q9UBB5|MBD2_HUMAN	3
447	Q96CT7|CC124_HUMAN	3	447	Q2M243|CCD27_HUMAN	8
448	Q5T4S7|UBR4_HUMAN	13	448	Q9UHV7|MED13_HUMAN	6
449	Q9UNY4|TTF2_HUMAN	4	449	Q9NRH3|TBG2_HUMAN	1
450	Q9Y5A7|NUB1_HUMAN	4	450	Q96A08|H2B1A_HUMAN	5
451	O60281|ZN292_HUMAN	7	451	Q96T25|ZIC5_HUMAN	7
452	Q659C4|LAR1B_HUMAN	3	452	O14492|SH2B2_HUMAN	4
453	O14827|RGRF2_HUMAN	2	453	P54845|NRL_HUMAN	3
454	Q9UGU0|TCF20_HUMAN	6	454	O43303|CP110_HUMAN	2
455	Q96EK7|F120B_HUMAN	4	455	Q8IWZ6|BBS7_HUMAN	2
456	Q3B7J2|GFOD2_HUMAN	2	456	P26440|IVD_HUMAN	2
457	Q9BSF8|BTBDA_HUMAN	2	457	Q8N5D0|WDTC1_HUMAN	5
458	Q7Z5Y7|KCD20_HUMAN	2	458	Q5JSH3|WDR44_HUMAN	3
459	Q68DK2|ZFY26_HUMAN	4	459	Q6Q759|SPG17_HUMAN	6
460	Q7Z5L9|I2BP2_HUMAN	6	460	Q7Z6E9|RBBP6_HUMAN	5
461	Q7Z4Q2|HEAT3_HUMAN	5	461	Q96HJ3|CCD34_HUMAN	4
462	Q53T94|TAF1B_HUMAN	5	462	Q8IYB3|SRRM1_HUMAN	4
463	Q96JG9|ZN469_HUMAN	7	463	Q5VWG9|TAF3_HUMAN	5
464	P04424|ARLY_HUMAN	5	464	Q12802|AKP13_HUMAN	4
465	Q8NHY3|GA2L2_HUMAN	5	465	Q9BWT7|CAR10_HUMAN	7
466	Q08AM6|VAC14_HUMAN	4	466	O60216|RAD21_HUMAN	3
467	P82675|RT05_HUMAN	2	467	O43310|CTIF_HUMAN	2
468	O14646|CHD1_HUMAN	2	468	Q8N5P1|ZC3H8_HUMAN	3
469	Q8NGX5|O10K1_HUMAN	2	469	Q99832|TCPH_HUMAN	10
470	Q5VTM2|AGAP9_HUMAN	2	470	Q96F63|CCD97_HUMAN	2
471	O15015|ZN646_HUMAN	3	471	Q8NCM8|DYHC2_HUMAN	8
472	Q9P1Y6|PHRF1_HUMAN	2	472	Q9HBX8|LGR6_HUMAN	2
473	Q8IZT6|ASPM_HUMAN	26	473	P46977|STT3A_HUMAN	1
474	Q6PCT2|FXL19_HUMAN	6	474	Q9ULL5|PRR12_HUMAN	4
475	P51665|PSMD7_HUMAN	4	475	Q9P1Y6|PHRF1_HUMAN	2
476	Q6P3X3|TTC27_HUMAN	5	476	Q58F21|BRDT_HUMAN	9
477	P52630|STAT2_HUMAN	3	477	Q0VF49|K2012_HUMAN	4
478	Q6NSJ2|PHLB3_HUMAN	3	478	O43166|SI1L1_HUMAN	8
479	P38405|GNAL_HUMAN	2	479	O60292|SI1L3_HUMAN	4

BAIT			CONTROL		
prot_hit_num	prot_acc	# peptides_all	prot_hit_num	prot_acc	# peptides_all
480	Q96HP0|DOCK6_HUMAN	7	480	Q9P2F8|SI1L2_HUMAN	5
481	Q8WXH0|SYNE2_HUMAN	19	481	Q8IYT1|FA71A_HUMAN	5
482	Q7Z5J8|ANKAR_HUMAN	7	482	O14732|IMPA2_HUMAN	2
483	P14678|RSMB_HUMAN	4	483	Q09028|RBBP4_HUMAN	1
484	Q7Z6G8|ANS1B_HUMAN	3	484	Q7Z6Z7|HUWE1_HUMAN	9
485	P50748|KNTC1_HUMAN	3	485	H3BSY2|GOG8M_HUMAN	12
486	P29728|OAS2_HUMAN	2	486	A6NC78|GOG8I_HUMAN	9
487	Q6UX04|CWC27_HUMAN	2	487	Q06609|RAD51_HUMAN	3
488	Q9UQ49|NEUR3_HUMAN	2	488	Q9Y276|BCS1_HUMAN	2
489	Q86XX4|FRAS1_HUMAN	7	489	P51648|AL3A2_HUMAN	5
490	Q9Y483|MTF2_HUMAN	5	490	E7EW31|PROB1_HUMAN	5
491	Q70E73|RAPH1_HUMAN	3	491	Q6ZUA9|MROH5_HUMAN	2
492	P59051|BRAS2_HUMAN	4	492	A8TX70|CO6A5_HUMAN	11
493	P02686|MBP_HUMAN	6	493	Q6NT04|TIGD7_HUMAN	2
494	Q8NI35|INADL_HUMAN	4	494	Q9Y2A7|NCKP1_HUMAN	2
495	Q86Z20|CC125_HUMAN	3	495	P08240|SRPRA_HUMAN	3
496	P56270|MAZ_HUMAN	6	496	Q8NC51|PAIRB_HUMAN	4
497	P50991|TCPD_HUMAN	9	497	P42694|HELZ_HUMAN	4
498	Q3MHD2|LSM12_HUMAN	4	498	Q9BWL3|CA043_HUMAN	2
499	A8MYJ7|TTC34_HUMAN	2	499	P20929|NEBU_HUMAN	19
500	Q96A08|H2B1A_HUMAN	6	500	Q14123|PDE1C_HUMAN	9
501	Q96N76|HUTU_HUMAN	4	501	P31641|SC6A6_HUMAN	2
502	P26368|U2AF2_HUMAN	3	502	Q5VWQ0|RSBN1_HUMAN	4
503	P61586|RHOA_HUMAN	2	503	P09525|ANXA4_HUMAN	5
504	Q5VUJ6|LRCH2_HUMAN	3	504	Q8N239|KLH34_HUMAN	2
505	O14492|SH2B2_HUMAN	4	505	P48764|SL9A3_HUMAN	5
506	Q86UU1|PHLB1_HUMAN	11	506	P05976|MYL1_HUMAN	2
507	O00555|CAC1A_HUMAN	6	507	P26010|ITB7_HUMAN	2
508	Q9NXE8|CWC25_HUMAN	2	508	Q9Y3X0|CCDC9_HUMAN	8
509	P29973|CNGA1_HUMAN	6	509	P11908|PRPS2_HUMAN	5
510	O75376|NCOR1_HUMAN	9	510	P22102|PUR2_HUMAN	3
511	Q8IUZ0|LRC49_HUMAN	3	511	Q9Y2J4|AMOL2_HUMAN	5
512	Q9P2I0|CPSF2_HUMAN	7	512	Q9BQ04|RBM4B_HUMAN	2
513	Q9UN71|PCDGG_HUMAN	3	513	P19224|UD16_HUMAN	10
514	Q9Y5G1|PCDGF_HUMAN	3	514	Q14166|TTL12_HUMAN	2
515	P12259|FA5_HUMAN	5	515	Q8IWV7|UBR1_HUMAN	3
516	Q96I34|PP16A_HUMAN	6	516	Q6NUN7|CK063_HUMAN	3
517	O43166|SI1L1_HUMAN	13	517	P22626|ROA2_HUMAN	3
518	Q0VF49|K2012_HUMAN	6	518	P14416|DRD2_HUMAN	3
519	Q8IYT1|FA71A_HUMAN	4	519	Q6ZTQ3|RASF6_HUMAN	4
520	Q9P2F8|SI1L2_HUMAN	7	520	Q16206|ENOX2_HUMAN	16
521	O60292|SI1L3_HUMAN	3	521	Q5TB30|DEP1A_HUMAN	3
522	O14732|IMPA2_HUMAN	2	522	Q9Y483|MTF2_HUMAN	5
523	Q05C16|LRC63_HUMAN	2	523	P59051|BRAS2_HUMAN	3
524	P61968|LMO4_HUMAN	2	524	P06748|NPM_HUMAN	3
525	Q7Z4V0|ZN438_HUMAN	4	525	Q86W26|NAL10_HUMAN	4
526	Q8NGS6|O13C3_HUMAN	2	526	Q9H0C8|ILKAP_HUMAN	4
527	Q9Y6G9|DC1L1_HUMAN	2	527	Q9NVN8|GNL3L_HUMAN	2

BAIT			CONTROL		
prot_hit_num	prot_acc	# peptides_all	prot_hit_num	prot_acc	# peptides_all
528	P46020|KPB1_HUMAN	3	528	Q13362|2A5G_HUMAN	2
529	Q8N5D0|WDTC1_HUMAN	3	529	P12259|FA5_HUMAN	2
530	Q15154|PCM1_HUMAN	3	530	P78559|MAP1A_HUMAN	10
531	Q4VCS5|AMOT_HUMAN	18	531	Q9BXF6|RFIP5_HUMAN	3
532	Q8IY63|AMOL1_HUMAN	4	532	O14529|CUX2_HUMAN	2
533	Q9BWL3|CA043_HUMAN	2	533	A6NC57|ANR62_HUMAN	6
534	Q8NB25|F184A_HUMAN	8	534	O14776|TCRG1_HUMAN	5
535	Q9Y247|FA50B_HUMAN	4	535	Q96NW7|LRRC7_HUMAN	7
536	Q14320|FA50A_HUMAN	3	536	Q9BZA7|PC11X_HUMAN	3
537	Q96EK4|THA11_HUMAN	3	537	Q13009|TIAM1_HUMAN	4
538	Q8IYN2|TCAL8_HUMAN	2	538	O43781|DYRK3_HUMAN	3
539	Q13200|PSMD2_HUMAN	4	539	Q96I15|SCLY_HUMAN	7
540	Q9HBX8|LGR6_HUMAN	3	540	Q9BXT6|M10L1_HUMAN	2
541	P15538|C11B1_HUMAN	2	541	Q9Y2G8|DJC16_HUMAN	2
542	Q96T37|RBM15_HUMAN	4	542	Q99527|GPER1_HUMAN	2
543	Q5VT52|RPRD2_HUMAN	2	543	P0C7V9|ME15P_HUMAN	2
544	Q8TAQ2|SMRC2_HUMAN	6	544	Q9NWH9|SLTM_HUMAN	10
545	P35527|K1C9_HUMAN	6	545	Q09666|AHNK_HUMAN	17
546	Q71DI3|H32_HUMAN	7	546	Q92785|REQU_HUMAN	2
547	Q9C0D2|CE295_HUMAN	10	547	P08183|MDR1_HUMAN	4
548	Q9Y512|SAM50_HUMAN	6	548	O15014|ZN609_HUMAN	3
549	Q92526|TCPW_HUMAN	3	549	Q9Y580|RBM7_HUMAN	3
550	O95670|VATG2_HUMAN	4	550	P25189|MYP0_HUMAN	2
551	P05305|EDN1_HUMAN	3	551	Q6TFL3|CC171_HUMAN	5
552	Q92536|YLAT2_HUMAN	2	552	O00555|CAC1A_HUMAN	7
553	Q5JWR5|DOP1_HUMAN	5	553	Q00975|CAC1B_HUMAN	10
554	Q15043|S39AE_HUMAN	1	554	O75381|PEX14_HUMAN	3
555	Q16629|SRSF7_HUMAN	9	555	P11226|MBL2_HUMAN	5
556	Q008S8|ECT2L_HUMAN	8	556	Q8WZ42|TITIN_HUMAN	57
557	P30519|HMOX2_HUMAN	5	557	Q8IYD2|KLD8A_HUMAN	1
558	P56182|RRP1_HUMAN	3	558	P18859|ATP5J_HUMAN	2
559	H3BSY2|GOG8M_HUMAN	12	559	Q15067|ACOX1_HUMAN	2
560	A6NMD2|GOG8J_HUMAN	10	560	Q8NEW0|ZNT7_HUMAN	4
561	A6NC78|GOG8I_HUMAN	10	561	Q8N7J2|AMER2_HUMAN	2
562	Q9NZN9|AIPL1_HUMAN	5	562	Q8N2G8|GHDC_HUMAN	2
563	Q9UKF6|CPSF3_HUMAN	2	563	Q9NYV4|CDK12_HUMAN	5
564	P50219|MNX1_HUMAN	4	564	P11362|FGFR1_HUMAN	7
565	Q9BQG2|NUD12_HUMAN	7	565	P20794|MAK_HUMAN	5
566	Q9Y2J4|AMOL2_HUMAN	2	566	O94921|CDK14_HUMAN	3
567	P53999|TCP4_HUMAN	2	567	Q14004|CDK13_HUMAN	4
568	Q9Y6V0|PCLO_HUMAN	9	568	P07948|LYN_HUMAN	4
569	Q9H3E2|SNX25_HUMAN	2	569	Q00534|CDK6_HUMAN	4
570	P09525|ANXA4_HUMAN	5	570	P06239|LCK_HUMAN	3
571	P19429|TNNI3_HUMAN	9	571	P24941|CDK2_HUMAN	3
572	Q969V6|MKL1_HUMAN	10	572	P06493|CDK1_HUMAN	3
573	Q15910|EZH2_HUMAN	6	573	Q00536|CDK16_HUMAN	3
574	Q9BXU7|UBP26_HUMAN	7	574	Q9H720|PG2IP_HUMAN	5
575	O00338|ST1C2_HUMAN	9	575	Q15915|ZIC1_HUMAN	4

BAIT			CONTROL		
prot_hit_num	prot_acc	# peptides_all	prot_hit_num	prot_acc	# peptides_all
576	Q9BY12|SCAPE_HUMAN	5	576	Q9Y2Z9|COQ6_HUMAN	5
577	Q92800|EZH1_HUMAN	5	577	P55060|XPO2_HUMAN	2
578	O75347|TBCA_HUMAN	3	578	Q96M42|CU129_HUMAN	1
579	Q99741|CDC6_HUMAN	3	579	P05305|EDN1_HUMAN	5
580	P20719|HXA5_HUMAN	3	580	Q04721|NOTC2_HUMAN	7
581	Q96BK5|PINX1_HUMAN	1	581	P49411|EFTU_HUMAN	1
582	P22102|PUR2_HUMAN	1	582	Q86Z20|CC125_HUMAN	8
583	Q86Y38|XYLT1_HUMAN	5	583	Q14839|CHD4_HUMAN	3
584	Q96DT7|ZBT10_HUMAN	3	584	O75052|CAPON_HUMAN	3
585	O75446|SAP30_HUMAN	2	585	A8MYJ7|TTC34_HUMAN	4
586	O95672|ECEL1_HUMAN	2	586	Q9HAY2|MAGF1_HUMAN	2
587	Q9UBF2|COPG2_HUMAN	2	587	O00629|IMA3_HUMAN	2
588	Q9Y678|COPG1_HUMAN	2	588	Q9BR77|CCD77_HUMAN	3
589	P18859|ATP5J_HUMAN	2	589	Q86X67|NUD13_HUMAN	1
590	Q76M96|CCD80_HUMAN	4	590	Q15714|T22D1_HUMAN	6
591	Q6P3S1|DEN1B_HUMAN	3	591	Q8NHP7|EXD1_HUMAN	2
592	Q96JB1|DYH8_HUMAN	9	592	Q12996|CSTF3_HUMAN	2
593	Q6ZQQ6|WDR87_HUMAN	10	593	Q6P3S1|DEN1B_HUMAN	3
594	Q96IX9|A26L1_HUMAN	3	594	Q9BWU0|NADAP_HUMAN	1
595	O43314|VIP2_HUMAN	6	595	Q9Y6Y8|S23IP_HUMAN	2
596	Q8TE73|DYH5_HUMAN	9	596	O00425|IF2B3_HUMAN	5
597	Q8N568|DCLK2_HUMAN	4	597	Q9Y6M1|IF2B2_HUMAN	2
598	Q96D46|NMD3_HUMAN	4	598	O15195|VILL_HUMAN	4
599	Q9Y2Z9|COQ6_HUMAN	4			0
600	Q86VF7|NRAP_HUMAN	7			
601	P55060|XPO2_HUMAN	5			
602	Q8N239|KLH34_HUMAN	3			
603	Q8TDI7|TMC2_HUMAN	1			
604	Q09028|RBBP4_HUMAN	1			
605	Q92922|SMRC1_HUMAN	2			
606	Q14168|MPP2_HUMAN	5			
607	P56179|DLX6_HUMAN	2			
608	Q9BQ52|RNZ2_HUMAN	3			
609	Q9NVN8|GNL3L_HUMAN	3			
610	Q15369|ELOC_HUMAN	3			
611	Q9H2S9|IKZF4_HUMAN	2			
612	P22626|ROA2_HUMAN	3			
613	P30622|CLIP1_HUMAN	8			
614	Q7Z5J4|RAI1_HUMAN	4			
615	P04085|PDGFA_HUMAN	2			
616	O76021|RL1D1_HUMAN	2			
617	Q96M42|CU129_HUMAN	2			
618	P02786|TFR1_HUMAN	4			
619	Q9NRY2|SOSSC_HUMAN	1			
620	Q13243|SRSF5_HUMAN	5			
621	Q13247|SRSF6_HUMAN	2			
622	O95402|MED26_HUMAN	5			
623	P08183|MDR1_HUMAN	4			

BAIT			CONTROL		
prot_hit_num	prot_acc	# peptides_all	prot_hit_num	prot_acc	# peptides_all
624	Q15436|SC23A_HUMAN	2			
625	Q6SZW1|SARM1_HUMAN	3			
626	O00425|IF2B3_HUMAN	5			
627	Q9NPC6|MYOZ2_HUMAN	3			
628	P07910|HNRPC_HUMAN	3			
629	Q07912|ACK1_HUMAN	2			
630	Q9C0H6|KLHL4_HUMAN	2			
631	Q7Z570|Z804A_HUMAN	3			
632	A4D1E1|Z804B_HUMAN	3			
633	O75400|PR40A_HUMAN	6			
634	Q8TB05|UBAD1_HUMAN	2			
635	Q6XYB7|LBX2_HUMAN	1			
636	O60353|FZD6_HUMAN	5			
637	Q9Y426|CU025_HUMAN	2			
638	Q75VX8|GARE2_HUMAN	5			
639	Q96NB3|ZN830_HUMAN	2			
640	P0CG23|ZN853_HUMAN	4			
641	Q9UN42|AT1B4_HUMAN	2			
642	Q9NYF8|BCLF1_HUMAN	6			
643	Q9H6P5|TASP1_HUMAN	3			
644	Q9H583|HEAT1_HUMAN	2			

C

2017_11_21 MASCOT search parameters; experiment: TALON-StrepTactin

Search title	
Timestamp	2017-11-21T12:12:23Z
User	Zuzanna Kozik
Email	zkk21@sussex.ac.uk
Report URI	http://139.184.166.59/mascot/cgi/master_results.pl?file=../d
Peak list data path	E:\Anita lab work\Anita_MS data\19_11_2017\AB_2017-11-1
Peak list format	Mascot generic
Search type	MIS
Mascot version	2.3.02
Database	SwissProt
Fasta file	SwissProt_Jan2017_custom_v3.FASTA
Total sequences	553657
Total residues	198178534
Sequences after taxonomy filter	20169
Number of queries	14914

Fixed modifications ----------

Identifier	Name	Delta	Neutral loss
1	Carbamidomethyl (C)	57.02146	

Variable modifications ----------

Identifier	Name	Delta	Neutral loss(es)
1	Acetyl (Protein N-term)	42.01057	
2	Oxidation (M)	15.99492	0 63.99829

Search Parameters ----------

Taxonomy filter	. . . . . Homo sapiens (human)
Enzyme	Trypsin
Maximum Missed Cleavages	2
Fixed modifications	Carbamidomethyl (C)
Variable modifications	Acetyl (Protein N-term),Oxidation (M)
Peptide Mass Tolerance	6
Peptide Mass Tolerance Units	ppm
Fragment Mass Tolerance	0.7
Fragment Mass Tolerance Units	Da
Mass values	Monoisotopic
Instrument type	Default

Format parameters ----------

Significance threshold	0.05
Max. number of hits	0

2017_11_21 MASCOT search parameters; experiment: TALON-StrepTactin	
Use MudPIT protein scoring	1
Ions score cut-off	0
Include same-set proteins	
Include sub-set proteins	0
Include unassigned	0
Require bold red	0
Use homology threshold	0
Group protein families	0

D

2017_11_21 MASCOT search; experiment: TALON-StrepTactin

BAIT			CONTROL		
prot_hit_num	prot_acc	# peptides_all	prot_hit_num	prot_acc	# peptides_all
1	Q15233|NONO_HUMAN	236	1	Q15233|NONO_HUMAN	250
2	P23246|SFPQ_HUMAN	230	2	P23246|SFPQ_HUMAN	282
3	P14866|HNRPL_HUMAN	161	3	P14866|HNRPL_HUMAN	98
4	O43143|DHX15_HUMAN	76	4	O43143|DHX15_HUMAN	76
5	P11142|HSP7C_HUMAN	52	5	P11387|TOP1_HUMAN	106
6	P0DMV8|HS71A_HUMAN	55	6	Q13435|SF3B2_HUMAN	121
7	Q13435|SF3B2_HUMAN	80	7	P0DMV8|HS71A_HUMAN	55
8	Q15459|SF3A1_HUMAN	50	8	Q8WXF1|PSPC1_HUMAN	121
9	P11387|TOP1_HUMAN	82	9	Q86XP3|DDX42_HUMAN	55
10	P34931|HS71L_HUMAN	30	10	P11142|HSP7C_HUMAN	45
11	Q86XP3|DDX42_HUMAN	52	11	Q15459|SF3A1_HUMAN	61
12	Q8WXF1|PSPC1_HUMAN	96	12	Q8WWM7|ATX2L_HUMAN	60
13	Q99700|ATX2_HUMAN	37	13	O60885|BRD4_HUMAN	62
14	O75533|SF3B1_HUMAN	64	14	P34931|HS71L_HUMAN	31
15	P51608|MECP2_HUMAN	45	15	Q15393|SF3B3_HUMAN	40
16	Q8WWM7|ATX2L_HUMAN	49	16	Q99700|ATX2_HUMAN	35
17	O60885|BRD4_HUMAN	56	17	P51608|MECP2_HUMAN	49
18	Q15393|SF3B3_HUMAN	47	18	O75533|SF3B1_HUMAN	59
19	P11021|GRP78_HUMAN	25	19	Q15637|SF01_HUMAN	44
20	Q04726|TLE3_HUMAN	27	20	Q9H0G5|NSRP1_HUMAN	67
21	P04264|K2C1_HUMAN	26	21	Q12874|SF3A3_HUMAN	44
22	P11940|PABP1_HUMAN	29	22	P17066|HSP76_HUMAN	26
23	Q12874|SF3A3_HUMAN	36	23	Q15007|FL2D_HUMAN	26
24	P04406|G3P_HUMAN	23	24	Q9Y3I0|RTCB_HUMAN	33
25	P49750|YLPM1_HUMAN	34	25	P54652|HSP72_HUMAN	26
26	Q8N684|CPSF7_HUMAN	33	26	P25490|TYY1_HUMAN	45
27	P25490|TYY1_HUMAN	46	27	Q15424|SAFB1_HUMAN	90
28	P17066|HSP76_HUMAN	19	28	P04264|K2C1_HUMAN	26
29	Q8N163|CCAR2_HUMAN	25	29	Q8N684|CPSF7_HUMAN	39
30	Q53H96|P5CR3_HUMAN	14	30	Q8IYS1|P20D2_HUMAN	35
31	Q15637|SF01_HUMAN	28	31	P04406|G3P_HUMAN	23
32	Q15007|FL2D_HUMAN	20	32	P11021|GRP78_HUMAN	19
33	Q86TG7|PEG10_HUMAN	16	33	Q04726|TLE3_HUMAN	22
34	P35527|K1C9_HUMAN	12	34	Q86TG7|PEG10_HUMAN	23
35	Q92499|DDX1_HUMAN	26	35	Q4VCS5|AMOT_HUMAN	35
36	Q9Y3I0|RTCB_HUMAN	29	36	P11940|PABP1_HUMAN	22
37	Q9H361|PABP3_HUMAN	17	37	P35527|K1C9_HUMAN	15
38	O15042|SR140_HUMAN	27	38	P26196|DDX6_HUMAN	20
39	Q8IYS1|P20D2_HUMAN	30	39	P13645|K1C10_HUMAN	25
40	Q5SW79|CE170_HUMAN	28	40	Q96QC0|PP1RA_HUMAN	39
41	Q04724|TLE1_HUMAN	15	41	Q8WUA2|PPIL4_HUMAN	16
42	Q96QC0|PP1RA_HUMAN	30	42	Q86X55|CARM1_HUMAN	22
43	P07437|TBB5_HUMAN	16	43	Q14151|SAFB2_HUMAN	46
44	Q13310|PABP4_HUMAN	21	44	Q53H96|P5CR3_HUMAN	12
45	P50750|CDK9_HUMAN	11	45	Q96EV2|RBM33_HUMAN	24
46	Q86X55|CARM1_HUMAN	21	46	Q9Y224|CN166_HUMAN	18
47	P38646|GRP75_HUMAN	23	47	Q5SW79|CE170_HUMAN	31
48	Q96EV2|RBM33_HUMAN	21	48	Q93008|USP9X_HUMAN	21
49	P04350|TBB4A_HUMAN	12	49	Q7RTV0|PHF5A_HUMAN	14
50	P26196|DDX6_HUMAN	13	50	O43809|CPSF5_HUMAN	16

BAIT			CONTROL		
prot_hit_num	prot_acc	# peptides_all	prot_hit_num	prot_acc	# peptides_all
51	Q86TI2|DPP9_HUMAN	19	51	O15042|SR140_HUMAN	35
52	Q15424|SAFB1_HUMAN	42	52	P38646|GRP75_HUMAN	29
53	O60583|CCNT2_HUMAN	13	53	Q16630|CPSF6_HUMAN	21
54	O43809|CPSF5_HUMAN	13	54	P52655|TF2AA_HUMAN	12
55	Q969P6|TOP1M_HUMAN	22	55	Q8IWX8|CHERP_HUMAN	16
56	O94842|TOX4_HUMAN	7	56	Q13310|PABP4_HUMAN	13
57	Q8IWX8|CHERP_HUMAN	21	57	Q15427|SF3B4_HUMAN	6
58	Q16630|CPSF6_HUMAN	19	58	Q969P6|TOP1M_HUMAN	21
59	O95817|BAG3_HUMAN	19	59	P50750|CDK9_HUMAN	11
60	P04259|K2C6B_HUMAN	8	60	O94842|TOX4_HUMAN	12
61	Q7L2J0|MEPCE_HUMAN	14	61	Q92499|DDX1_HUMAN	20
62	P35908|K22E_HUMAN	9	62	Q9BS26|ERP44_HUMAN	18
63	P22681|CBL_HUMAN	15	63	O60563|CCNT1_HUMAN	19
64	Q7RTV0|PHF5A_HUMAN	10	64	P32929|CGL_HUMAN	13
65	Q15427|SF3B4_HUMAN	8	65	Q7L2J0|MEPCE_HUMAN	24
66	O15391|TYY2_HUMAN	18	66	Q96I25|SPF45_HUMAN	21
67	Q9H0G5|NSRP1_HUMAN	28	67	Q6UN15|FIP1_HUMAN	12
68	Q8IVS2|FABD_HUMAN	11	68	Q4G0J3|LARP7_HUMAN	14
69	Q9BU76|MMTA2_HUMAN	8	69	Q8IVS2|FABD_HUMAN	8
70	P32929|CGL_HUMAN	12	70	Q9P2N5|RBM27_HUMAN	19
71	Q6UN15|FIP1_HUMAN	10	71	Q9H361|PABP3_HUMAN	16
72	Q96I25|SPF45_HUMAN	17	72	Q15428|SF3A2_HUMAN	22
73	Q15059|BRD3_HUMAN	14	73	Q15059|BRD3_HUMAN	12
74	Q15428|SF3A2_HUMAN	16	74	A6NKD9|CC85C_HUMAN	12
75	Q93008|USP9X_HUMAN	32	75	Q3MHD2|LSM12_HUMAN	6
76	Q75N03|HAKAI_HUMAN	11	76	O15391|TYY2_HUMAN	14
77	P13645|K1C10_HUMAN	12	77	C9JLW8|MCRI1_HUMAN	8
78	O60563|CCNT1_HUMAN	23	78	P02545|LMNA_HUMAN	5
79	Q9P2N5|RBM27_HUMAN	19	79	Q7Z417|NUFP2_HUMAN	21
80	Q9GZN8|CT027_HUMAN	15	80	Q86TI2|DPP9_HUMAN	24
81	Q9UNE7|CHIP_HUMAN	10	81	Q9BQE3|TBA1C_HUMAN	5
82	O15226|NKRF_HUMAN	31	82	P35908|K22E_HUMAN	6
83	A6NKD9|CC85C_HUMAN	5	83	P53999|TCP4_HUMAN	10
84	Q9P2R6|RERE_HUMAN	4	84	P07437|TBB5_HUMAN	8
85	Q9Y224|CN166_HUMAN	6	85	Q13485|SMAD4_HUMAN	14
86	Q8WVV9|HNRLL_HUMAN	6	86	P98175|RBM10_HUMAN	10
87	Q9Y2L9|LRCH1_HUMAN	6	87	P04259|K2C6B_HUMAN	6
88	Q4G0J3|LARP7_HUMAN	14	88	Q04724|TLE1_HUMAN	15
89	Q96N67|DOCK7_HUMAN	12	89	Q9H0D6|XRN2_HUMAN	16
90	Q9NXX6|NSE4A_HUMAN	4	90	Q8IVM0|CCD50_HUMAN	10
91	Q5VTE0|EF1A3_HUMAN	6	91	Q9UPW6|SATB2_HUMAN	7
92	Q3ZCM7|TBB8_HUMAN	6	92	P22681|CBL_HUMAN	12
93	Q9NQX3|GEPH_HUMAN	4	93	O15226|NKRF_HUMAN	14
94	Q9HCK8|CHD8_HUMAN	7	94	O95817|BAG3_HUMAN	10
95	Q04727|TLE4_HUMAN	9	95	Q8NCA5|FA98A_HUMAN	9
96	Q04725|TLE2_HUMAN	9	96	Q04727|TLE4_HUMAN	9
97	Q15717|ELAV1_HUMAN	7	97	Q9BTA9|WAC_HUMAN	10
98	P20265|PO3F2_HUMAN	7	98	Q13523|PRP4B_HUMAN	8
99	Q9BS26|ERP44_HUMAN	14	99	P42694|HELZ_HUMAN	3
100	P67870|CSK2B_HUMAN	8	100	Q9GZN8|CT027_HUMAN	12
101	Q5JQF8|PAP1M_HUMAN	6	101	Q8N163|CCAR2_HUMAN	12

BAIT			CONTROL		
prot_hit_num	prot_acc	# peptides_all	prot_hit_num	prot_acc	# peptides_all
102	Q7Z417|NUFP2_HUMAN	7	102	Q9Y3B4|SF3B6_HUMAN	10
103	P52657|T2AG_HUMAN	5	103	Q9BWJ5|SF3B5_HUMAN	5
104	Q96MG7|NSE3_HUMAN	4	104	P61964|WDR5_HUMAN	7
105	Q9UJU2|LEF1_HUMAN	8	105	P52657|T2AG_HUMAN	10
106	P02538|K2C6A_HUMAN	7	106	P49750|YLPM1_HUMAN	18
107	P48668|K2C6C_HUMAN	6	107	P62805|H4_HUMAN	3
108	P53999|TCP4_HUMAN	3	108	Q8WVV9|HNRLL_HUMAN	6
109	Q92841|DDX17_HUMAN	4	109	Q9UNE7|CHIP_HUMAN	9
110	O95409|ZIC2_HUMAN	5	110	Q96N67|DOCK7_HUMAN	8
111	Q13485|SMAD4_HUMAN	11	111	P20265|PO3F2_HUMAN	7
112	Q5T6F2|UBAP2_HUMAN	9	112	P54259|ATN1_HUMAN	8
113	Q9C0J8|WDR33_HUMAN	13	113	P30048|PRDX3_HUMAN	6
114	O95487|SC24B_HUMAN	2	114	P50219|MNX1_HUMAN	7
115	P0C0S8|H2A1_HUMAN	3	115	Q9UHB7|AFF4_HUMAN	9
116	P54259|ATN1_HUMAN	6	116	O95409|ZIC2_HUMAN	3
117	Q14151|SAFB2_HUMAN	25	117	P31943|HNRH1_HUMAN	4
118	Q5VT52|RPRD2_HUMAN	3	118	Q14157|UBP2L_HUMAN	8
119	P62805|H4_HUMAN	5	119	Q01826|SATB1_HUMAN	5
120	O15027|SC16A_HUMAN	8	120	P07910|HNRPC_HUMAN	4
121	P47928|ID4_HUMAN	2	121	Q9NQX3|GEPH_HUMAN	4
122	P52655|TF2AA_HUMAN	7	122	Q5VTE0|EF1A3_HUMAN	7
123	P61964|WDR5_HUMAN	8	123	Q9HCK8|CHD8_HUMAN	13
124	Q96QV6|H2A1A_HUMAN	4	124	Q75N03|HAKAI_HUMAN	7
125	P0C0S5|H2AZ_HUMAN	4	125	P02533|K1C14_HUMAN	7
126	P02533|K1C14_HUMAN	5	126	P08779|K1C16_HUMAN	7
127	Q92908|GATA6_HUMAN	6	127	Q9P2R6|RERE_HUMAN	6
128	Q08117|AES_HUMAN	6	128	P09234|RU1C_HUMAN	2
129	Q9UPW6|SATB2_HUMAN	5	129	Q14241|ELOA1_HUMAN	16
130	P84090|ERH_HUMAN	2	130	P62380|TBPL1_HUMAN	5
131	Q9BTA9|WAC_HUMAN	10	131	P04350|TBB4A_HUMAN	4
132	P12532|KCRU_HUMAN	8	132	O95487|SC24B_HUMAN	2
133	P98175|RBM10_HUMAN	5	133	O43290|SNUT1_HUMAN	7
134	Q9UHB7|AFF4_HUMAN	12	134	P61962|DCAF7_HUMAN	3
135	P19013|K2C4_HUMAN	3	135	Q4VXU2|PAP1L_HUMAN	7
136	Q9BQE3|TBA1C_HUMAN	9	136	P36873|PP1G_HUMAN	7
137	Q7Z5L9|I2BP2_HUMAN	6	137	Q15714|T22D1_HUMAN	5
138	P49368|TCPG_HUMAN	6	138	Q7Z5L9|I2BP2_HUMAN	5
139	Q8N1G2|CMTR1_HUMAN	17	139	Q9C0J8|WDR33_HUMAN	12
140	Q8IY37|DHX37_HUMAN	15	140	Q8N954|GPT11_HUMAN	3
141	Q9UPW0|FOXJ3_HUMAN	3	141	Q5T6F2|UBAP2_HUMAN	5
142	Q01826|SATB1_HUMAN	5	142	O00470|MEIS1_HUMAN	3
143	Q14157|UBP2L_HUMAN	3	143	Q10570|CPSF1_HUMAN	5
144	Q6VUC0|AP2E_HUMAN	3	144	Q2M2I5|K1C24_HUMAN	5
145	Q7Z6R9|AP2D_HUMAN	3	145	P13646|K1C13_HUMAN	5
146	Q92754|AP2C_HUMAN	3	146	Q8IUE6|H2A2B_HUMAN	4
147	P43034|LIS1_HUMAN	2	147	B1AK53|ESPN_HUMAN	7
148	Q9H0D6|XRN2_HUMAN	21	148	Q16777|H2A2C_HUMAN	8
149	Q7Z3Z0|K1C25_HUMAN	4	149	O60231|DHX16_HUMAN	6
150	P84103|SRSF3_HUMAN	2	150	Q92908|GATA6_HUMAN	3
151	Q96ST3|SIN3A_HUMAN	6	151	Q05682|CALD1_HUMAN	6
152	P50219|MNX1_HUMAN	5	152	Q5JTD0|TJAP1_HUMAN	6

BAIT			CONTROL		
prot_hit_num	prot_acc	# peptides_all	prot_hit_num	prot_acc	# peptides_all
153	Q8IXB1|DJC10_HUMAN	7	153	Q6V1X1|DPP8_HUMAN	1
154	O60231|DHX16_HUMAN	6	154	Q9BUT9|MCRI2_HUMAN	3
155	Q14562|DHX8_HUMAN	3	155	P81605|DCD_HUMAN	2
156	Q58F21|BRDT_HUMAN	6	156	Q5VT52|RPRD2_HUMAN	6
157	Q10570|CPSF1_HUMAN	6	157	P62136|PP1A_HUMAN	7
158	O75940|SPF30_HUMAN	2	158	P62140|PP1B_HUMAN	7
159	Q4VCS5|AMOT_HUMAN	13	159	O15027|SC16A_HUMAN	10
160	Q05682|CALD1_HUMAN	7	160	Q96NM4|TOX2_HUMAN	2
161	Q9Y6M1|IF2B2_HUMAN	9	161	P67870|CSK2B_HUMAN	2
162	Q9NZI8|IF2B1_HUMAN	3	162	Q7Z3Y9|K1C26_HUMAN	3
163	Q8N0Y2|ZN444_HUMAN	2	163	P50990|TCPQ_HUMAN	3
164	P20226|TBP_HUMAN	6	164	Q7RTR2|NLRC3_HUMAN	5
165	Q9BRR6|ADPGK_HUMAN	1	165	B3EWG3|FM25A_HUMAN	4
166	Q7Z4S6|KI21A_HUMAN	8	166	Q99626|CDX2_HUMAN	8
167	Q9BWJ5|SF3B5_HUMAN	8	167	Q7Z4S6|KI21A_HUMAN	11
168	Q08AD1|CAMP2_HUMAN	7	168	O95447|LCA5L_HUMAN	3
169	O75843|AP1G2_HUMAN	3	169	Q9NYU2|UGGG1_HUMAN	3
170	Q05D60|DEUP1_HUMAN	3	170	Q9Y2J4|AMOL2_HUMAN	5
171	Q5ST30|SYVM_HUMAN	4	171	Q9UPT8|ZC3H4_HUMAN	11
172	Q6UXN9|WDR82_HUMAN	14	172	P33240|CSTF2_HUMAN	5
173	Q9P2D1|CHD7_HUMAN	7	173	Q08AD1|CAMP2_HUMAN	7
174	Q53ET0|CRTC2_HUMAN	1	174	Q05D60|DEUP1_HUMAN	6
175	Q3MHD2|LSM12_HUMAN	5	175	O75843|AP1G2_HUMAN	2
176	Q8IY18|SMC5_HUMAN	7	176	Q66GS9|CP135_HUMAN	10
177	Q66GS9|CP135_HUMAN	9	177	Q8IYB8|SUV3_HUMAN	5
178	Q9NRL2|BAZ1A_HUMAN	5	178	Q9NRL2|BAZ1A_HUMAN	5
179	Q8IYB8|SUV3_HUMAN	3	179	Q4G0X9|CCD40_HUMAN	5
180	Q4G0X9|CCD40_HUMAN	5	180	Q96NL6|SCLT1_HUMAN	4
181	Q96NL6|SCLT1_HUMAN	2	181	O00507|USP9Y_HUMAN	10
182	Q6PI26|SHQ1_HUMAN	4	182	Q8IY63|AMOL1_HUMAN	9
183	Q9UPT8|ZC3H4_HUMAN	8	183	Q5T9S5|CCD18_HUMAN	7
184	Q6SJ96|TBPL2_HUMAN	4	184	Q6PI26|SHQ1_HUMAN	5
185	O75150|BRE1B_HUMAN	9	185	P34897|GLYM_HUMAN	1
186	B3EWG3|FM25A_HUMAN	4	186	P84103|SRSF3_HUMAN	3
187	Q7RTR2|NLRC3_HUMAN	4	187	P08727|K1C19_HUMAN	8
188	Q9Y3B4|SF3B6_HUMAN	7	188	Q04695|K1C17_HUMAN	6
189	Q14241|ELOA1_HUMAN	11	189	P19012|K1C15_HUMAN	5
190	Q5T200|ZC3HD_HUMAN	13	190	O00193|SMAP_HUMAN	3
191	Q69YN4|VIR_HUMAN	6	191	P47928|ID4_HUMAN	1
192	Q9BUT9|MCRI2_HUMAN	1	192	Q8IUD2|RB6I2_HUMAN	4
193	Q9NZ56|FMN2_HUMAN	4	193	O75940|SPF30_HUMAN	5
194	Q96SB8|SMC6_HUMAN	7	194	P42858|HD_HUMAN	4
195	Q9H9Y6|RPA2_HUMAN	8	195	Q3ZCM7|TBB8_HUMAN	3
196	Q9Y2R4|DDX52_HUMAN	2	196	Q9Y2L9|LRCH1_HUMAN	2
197	P04075|ALDOA_HUMAN	4	197	Q99583|MNT_HUMAN	5
198	P42858|HD_HUMAN	7	198	P78386|KRT85_HUMAN	4
199	Q15714|T22D1_HUMAN	2	199	Q14533|KRT81_HUMAN	3
200	P56270|MAZ_HUMAN	9	200	O75400|PR40A_HUMAN	6
201	Q6KC79|NIPBL_HUMAN	7	201	Q07021|C1QBP_HUMAN	3
202	A6NM62|LRC53_HUMAN	6	202	Q13547|HDAC1_HUMAN	3
203	P51991|ROA3_HUMAN	3	203	A6NM62|LRC53_HUMAN	7

BAIT			CONTROL		
prot_hit_num	prot_acc	# peptides_all	prot_hit_num	prot_acc	# peptides_all
204	Q86W92|LIPB1_HUMAN	5	204	Q06587|RING1_HUMAN	4
205	O75400|PR40A_HUMAN	4	205	Q6P1X5|TAF2_HUMAN	6
206	Q07687|DLX2_HUMAN	5	206	Q15149|PLEC_HUMAN	24
207	P08651|NFIC_HUMAN	5	207	P46977|STT3A_HUMAN	2
208	P13647|K2C5_HUMAN	3	208	Q14247|SRC8_HUMAN	5
209	P48200|IREB2_HUMAN	5	209	Q96ST3|SIN3A_HUMAN	3
210	P33240|CSTF2_HUMAN	6	210	Q5UIP0|RIF1_HUMAN	12
211	Q8NFD5|ARI1B_HUMAN	9	211	Q9BXT6|M10L1_HUMAN	6
212	P30533|AMRP_HUMAN	4	212	Q53ET0|CRTC2_HUMAN	1
213	Q76M96|CCD80_HUMAN	8	213	Q9NYV4|CDK12_HUMAN	3
214	P46977|STT3A_HUMAN	2	214	Q14525|KT33B_HUMAN	5
215	P10074|ZBT48_HUMAN	4	215	O76013|KRT36_HUMAN	4
216	P55011|S12A2_HUMAN	3	216	P05783|K1C18_HUMAN	3
217	Q13107|UBP4_HUMAN	5	217	Q5JQF8|PAP1M_HUMAN	4
218	P78386|KRT85_HUMAN	6	218	Q0ZGT2|NEXN_HUMAN	3
219	O95639|CPSF4_HUMAN	2	219	Q96J88|ESIP1_HUMAN	5
220	Q00536|CDK16_HUMAN	7	220	Q9UBB9|TFP11_HUMAN	2
221	P20794|MAK_HUMAN	6	221	Q8NF91|SYNE1_HUMAN	38
222	P21802|FGFR2_HUMAN	3	222	Q5JRA6|MIA3_HUMAN	11
223	Q14004|CDK13_HUMAN	4	223	Q8NDA2|HMCN2_HUMAN	8
224	Q9NYV4|CDK12_HUMAN	3	224	Q9NR48|ASH1L_HUMAN	9
225	P22607|FGFR3_HUMAN	3	225	Q9BXT5|TEX15_HUMAN	9
226	P07948|LYN_HUMAN	3	226	Q9H2F9|CCD68_HUMAN	5
227	Q9UPZ9|ICK_HUMAN	3	227	Q9H0P0|5NT3A_HUMAN	5
228	Q8NF91|SYNE1_HUMAN	25	228	Q9H9F9|ARP5_HUMAN	4
229	Q15149|PLEC_HUMAN	17	229	Q14CN2|CLCA4_HUMAN	4
230	Q8NDA2|HMCN2_HUMAN	5	230	P01011|AACT_HUMAN	2
231	Q5JRA6|MIA3_HUMAN	7	231	Q7Z408|CSMD2_HUMAN	7
232	Q9NR48|ASH1L_HUMAN	8	232	Q5T4S7|UBR4_HUMAN	16
233	Q9BXT5|TEX15_HUMAN	10	233	Q96Q15|SMG1_HUMAN	5
234	Q9H2F9|CCD68_HUMAN	4	234	O75970|MPDZ_HUMAN	5
235	Q9H0P0|5NT3A_HUMAN	4	235	Q9BZ23|PANK2_HUMAN	3
236	Q14CN2|CLCA4_HUMAN	3	236	A2RRP1|NBAS_HUMAN	4
237	P31946|1433B_HUMAN	5	237	Q9UPS6|SET1B_HUMAN	3
238	P50990|TCPQ_HUMAN	3	238	O43903|GAS2_HUMAN	4
239	P08727|K1C19_HUMAN	3	239	Q9UN71|PCDGG_HUMAN	2
240	Q04695|K1C17_HUMAN	5	240	Q7Z6E9|RBBP6_HUMAN	5
241	P19012|K1C15_HUMAN	3	241	Q8IXB1|DJC10_HUMAN	6
242	Q9HD26|GOPC_HUMAN	1	242	O14827|RGRF2_HUMAN	4
243	O14827|RGRF2_HUMAN	4	243	Q13972|RGRF1_HUMAN	3
244	Q13972|RGRF1_HUMAN	3	244	Q15884|F1892_HUMAN	4
245	P30048|PRDX3_HUMAN	2	245	Q8NDM7|CFA43_HUMAN	4
246	Q9UJV8|PURG_HUMAN	3	246	Q9NTJ4|MA2C1_HUMAN	6
247	Q5UIP0|RIF1_HUMAN	6	247	Q15526|SURF1_HUMAN	2
248	Q9Y512|SAM50_HUMAN	4	248	Q07687|DLX2_HUMAN	3
249	P55735|SEC13_HUMAN	3	249	O43150|ASAP2_HUMAN	5
250	P36873|PP1G_HUMAN	6	250	Q9NRC6|SPTN5_HUMAN	16
251	Q8TCU6|PREX1_HUMAN	4	251	Q5TZA2|CROCC_HUMAN	14
252	O00470|MEIS1_HUMAN	1	252	Q03001|DYST_HUMAN	20
253	Q14204|DYHC1_HUMAN	12	253	O15078|CE290_HUMAN	13
254	O95479|G6PE_HUMAN	5	254	Q96JP2|MY15B_HUMAN	7

BAIT			CONTROL		
prot_hit_num	prot_acc	# peptides_all	prot_hit_num	prot_acc	# peptides_all
255	Q9HAH7|FBRS_HUMAN	6	255	Q92609|TBCD5_HUMAN	5
256	Q8NCA5|FA98A_HUMAN	9	256	Q3SY00|T10IP_HUMAN	3
257	Q14687|GSE1_HUMAN	1	257	Q8N9V3|WSDU1_HUMAN	3
258	Q7Z3Z3|PIWL3_HUMAN	4	258	Q76LX8|ATS13_HUMAN	4
259	O15078|CE290_HUMAN	15	259	O95239|KIF4A_HUMAN	7
260	Q03001|DYST_HUMAN	20	260	P20774|MIME_HUMAN	3
261	Q5TZA2|CROCC_HUMAN	9	261	Q16512|PKN1_HUMAN	3
262	Q9Y315|DEOC_HUMAN	3	262	Q9UL16|CFA45_HUMAN	3
263	Q96JP2|MY15B_HUMAN	6	263	Q9NWM3|CUED1_HUMAN	2
264	O95239|KIF4A_HUMAN	4	264	Q9ULD9|ZN608_HUMAN	11
265	Q92609|TBCD5_HUMAN	3	265	Q13107|UBP4_HUMAN	5
266	Q8N9V3|WSDU1_HUMAN	4	266	P43034|LIS1_HUMAN	2
267	Q2VIQ3|KIF4B_HUMAN	3	267	Q9UJV8|PURG_HUMAN	4
268	P20774|MIME_HUMAN	2	268	Q9Y512|SAM50_HUMAN	5
269	Q01082|SPTB2_HUMAN	6	269	Q14204|DYHC1_HUMAN	15
270	Q8NCG7|DGLB_HUMAN	2	270	Q96RS6|NUDC1_HUMAN	2
271	O60683|PEX10_HUMAN	2	271	Q15067|ACOX1_HUMAN	3
272	O15169|AXIN1_HUMAN	1	272	Q13642|FHL1_HUMAN	2
273	Q9ULT8|HECD1_HUMAN	5	273	O14556|G3PT_HUMAN	3
274	Q99626|CDX2_HUMAN	9	274	O60765|Z354A_HUMAN	3
275	P09848|LPH_HUMAN	5	275	Q01082|SPTB2_HUMAN	4
276	P28062|PSB8_HUMAN	2	276	O60683|PEX10_HUMAN	3
277	Q9NRC6|SPTN5_HUMAN	15	277	Q8NCG7|DGLB_HUMAN	2
278	Q96HP0|DOCK6_HUMAN	4	278	Q86W92|LIPB1_HUMAN	6
279	Q15327|ANKR1_HUMAN	5	279	Q8N1F8|S11IP_HUMAN	7
280	P30954|O10J1_HUMAN	2	280	P31153|METK2_HUMAN	1
281	O94804|STK10_HUMAN	8	281	Q9ULT8|HECD1_HUMAN	7
282	P23588|IF4B_HUMAN	5	282	Q9UII2|ATIF1_HUMAN	4
283	Q7Z3E5|ARMC9_HUMAN	3	283	Q6Y7W6|PERQ2_HUMAN	9
284	Q7Z5J4|RAI1_HUMAN	4	284	Q6PKG0|LARP1_HUMAN	7
285	P55081|MFAP1_HUMAN	2	285	Q8WW12|PCNP_HUMAN	2
286	Q5THK1|PR14L_HUMAN	8	286	Q9NWH9|SLTM_HUMAN	10
287	Q8NBT2|SPC24_HUMAN	3	287	Q8NFD5|ARI1B_HUMAN	2
288	Q9NRM1|ENAM_HUMAN	6	288	Q5C9Z4|NOM1_HUMAN	8
289	P16189|1A31_HUMAN	5	289	O94804|STK10_HUMAN	11
290	Q31610|1B81_HUMAN	4	290	Q9BR77|CCD77_HUMAN	3
291	P49585|PCY1A_HUMAN	4	291	Q9Y6M1|IF2B2_HUMAN	3
292	P17987|TCPA_HUMAN	4	292	O00425|IF2B3_HUMAN	3
293	P09086|PO2F2_HUMAN	2	293	Q9BUQ8|DDX23_HUMAN	6
294	C9JLW8|MCRI1_HUMAN	5	294	O15455|TLR3_HUMAN	4
295	P62136|PP1A_HUMAN	5	295	Q5TCS8|KAD9_HUMAN	3
296	Q9H853|TBA4B_HUMAN	2	296	P25705|ATPA_HUMAN	3
297	Q14643|ITPR1_HUMAN	6	297	Q9GZP4|PITH1_HUMAN	2
298	Q96M42|CU129_HUMAN	2	298	Q15139|KPCD1_HUMAN	2
299	O60765|Z354A_HUMAN	2	299	P57081|WDR4_HUMAN	2
300	Q8IXK0|PHC2_HUMAN	2	300	Q8IY37|DHX37_HUMAN	5
301	A6NJL1|ZSA5B_HUMAN	2	301	Q9BWS9|CHID1_HUMAN	2
302	Q8N5C6|SRBD1_HUMAN	4	302	Q76M96|CCD80_HUMAN	9
303	P26368|U2AF2_HUMAN	3	303	Q96A08|H2B1A_HUMAN	6
304	Q8N693|ESX1_HUMAN	2	304	Q8N257|H2B3B_HUMAN	3
305	Q9GZP4|PITH1_HUMAN	5	305	P57053|H2BFS_HUMAN	3

BAIT			CONTROL		
prot_hit_num	prot_acc	# peptides_all	prot_hit_num	prot_acc	# peptides_all
306	Q9BXF6|RFIP5_HUMAN	3	306	Q13586|STIM1_HUMAN	6
307	A8MT82|AG14P_HUMAN	3	307	P09848|LPH_HUMAN	2
308	Q96F63|CCD97_HUMAN	1	308	P28062|PSB8_HUMAN	2
309	Q15067|ACOX1_HUMAN	1	309	Q08117|AES_HUMAN	2
310	O43272|PROD_HUMAN	4	310	Q99456|K1C12_HUMAN	3
311	Q9P281|BAHC1_HUMAN	3	311	Q8NE31|FA13C_HUMAN	2
312	A6NMZ7|CO6A6_HUMAN	14	312	Q5H9U9|DDX6L_HUMAN	4
313	Q9BWT7|CAR10_HUMAN	6	313	Q86XP0|PA24D_HUMAN	3
314	Q5BLP8|CD048_HUMAN	1	314	P08651|NFIC_HUMAN	3
315	Q15262|PTPRK_HUMAN	5	315	Q5CZC0|FSIP2_HUMAN	21
316	Q14152|EIF3A_HUMAN	5	316	Q17RN3|FA98C_HUMAN	6
317	Q8NHY3|GA2L2_HUMAN	4	317	P56270|MAZ_HUMAN	4
318	P04424|ARLY_HUMAN	3	318	O75473|LGR5_HUMAN	3
319	P40938|RFC3_HUMAN	4	319	P08048|ZFY_HUMAN	3
320	P82675|RT05_HUMAN	2	320	P0C263|SBK2_HUMAN	2
321	Q9NXV6|CARF_HUMAN	2	321	Q92997|DVL3_HUMAN	2
322	Q9UQ35|SRRM2_HUMAN	11	322	Q6ZTR5|CFA47_HUMAN	6
323	Q99583|MNT_HUMAN	4	323	O60293|ZC3H1_HUMAN	3
324	O14654|IRS4_HUMAN	4	324	Q14244|MAP7_HUMAN	2
325	Q9Y3X0|CCDC9_HUMAN	2	325	Q9UKU0|ACSL6_HUMAN	5
326	Q9BZW7|TSG10_HUMAN	5	326	Q5ST30|SYVM_HUMAN	5
327	Q7Z408|CSMD2_HUMAN	4	327	Q9Y2Z9|COQ6_HUMAN	3
328	Q9UGU0|TCF20_HUMAN	4	328	P55060|XPO2_HUMAN	4
329	Q9HBE1|PATZ1_HUMAN	7	329	Q96M42|CU129_HUMAN	2
330	Q96JB1|DYH8_HUMAN	8	330	A6QL63|BTBDB_HUMAN	8
331	Q6ZQQ6|WDR87_HUMAN	5	331	Q86UP2|KTN1_HUMAN	9
332	Q5TIA1|MEI1_HUMAN	2	332	P12821|ACE_HUMAN	3
333	A0MZ66|SHOT1_HUMAN	3	333	Q9NQ66|PLCB1_HUMAN	3
334	O14874|BCKD_HUMAN	2	334	O75762|TRPA1_HUMAN	3
335	P54845|NRL_HUMAN	3	335	O14948|TFEC_HUMAN	2
336	Q9H871|RMD5A_HUMAN	4	336	O60749|SNX2_HUMAN	3
337	Q9NWH9|SLTM_HUMAN	9	337	Q15517|CDSN_HUMAN	2
338	Q14247|SRC8_HUMAN	4	338	Q9Y625|GPC6_HUMAN	3
339	P08048|ZFY_HUMAN	2	339	Q5FWF5|ESCO1_HUMAN	17
340	Q5SQS7|SH24B_HUMAN	2	340	Q99832|TCPH_HUMAN	3
341	O43150|ASAP2_HUMAN	4	341	Q8NI35|INADL_HUMAN	3
342	O60524|NEMF_HUMAN	4	342	Q8NEY8|PPHLN_HUMAN	3
343	Q9NZV7|ZIM2_HUMAN	4	343	Q8N693|ESX1_HUMAN	2
344	Q86XP0|PA24D_HUMAN	3	344	Q92794|KAT6A_HUMAN	4
345	Q8NB25|F184A_HUMAN	7	345	P22102|PUR2_HUMAN	3
346	Q96EK4|THA11_HUMAN	3	346	P51825|AFF1_HUMAN	6
347	Q14320|FA50A_HUMAN	3	347	Q8IZT6|ASPM_HUMAN	14
348	Q9Y247|FA50B_HUMAN	3	348	P51884|LUM_HUMAN	3
349	Q8IYN2|TCAL8_HUMAN	2	349	P17987|TCPA_HUMAN	5
350	P62380|TBPL1_HUMAN	2	350	P19367|HXK1_HUMAN	4
351	P48643|TCPE_HUMAN	2	351	Q96CN9|GCC1_HUMAN	8
352	Q9NPC6|MYOZ2_HUMAN	7	352	Q9Y490|TLN1_HUMAN	7
353	O95447|LCA5L_HUMAN	4	353	Q86YF9|DZIP1_HUMAN	4
354	Q5EBN2|TRI61_HUMAN	2	354	P10070|GLI2_HUMAN	4
355	Q6P5Q4|LMOD2_HUMAN	2	355	Q9Y4G6|TLN2_HUMAN	6
356	Q14119|VEZF1_HUMAN	5	356	Q68BL7|OLM2A_HUMAN	6

BAIT			CONTROL		
prot_hit_num	prot_acc	# peptides_all	prot_hit_num	prot_acc	# peptides_all
357	Q02388|CO7A1_HUMAN	4	357	Q08881|ITK_HUMAN	4
358	Q96T25|ZIC5_HUMAN	5	358	Q13200|PSMD2_HUMAN	4
359	O43776|SYNC_HUMAN	3	359	A2RUS2|DEND3_HUMAN	7
360	Q5CZC0|FSIP2_HUMAN	19	360	Q5THK1|PR14L_HUMAN	9
361	Q17RN3|FA98C_HUMAN	4	361	Q8NBT2|SPC24_HUMAN	3
362	Q9Y2X7|GIT1_HUMAN	4	362	Q9UBX7|KLK11_HUMAN	1
363	Q6ZRR7|LRRC9_HUMAN	4	363	Q9BWL3|CA043_HUMAN	2
364	Q9H334|FOXP1_HUMAN	2	364	Q9NXV6|CARF_HUMAN	3
365	Q9BYG4|PAR6G_HUMAN	2	365	Q8N0X7|SPG20_HUMAN	1
366	Q3B7J2|GFOD2_HUMAN	1	366	Q9BU76|MMTA2_HUMAN	2
367	Q9Y5P8|P2R3B_HUMAN	5	367	Q07912|ACK1_HUMAN	6
368	Q9Y5A7|NUB1_HUMAN	4	368	C9JTQ0|ANR63_HUMAN	6
369	Q96MF7|NSE2_HUMAN	5	369	Q8TF76|HASP_HUMAN	9
370	E7ETH6|Z587B_HUMAN	2	370	Q9UBW7|ZMYM2_HUMAN	6
371	Q8N7H5|PAF1_HUMAN	1	371	P62258|1433E_HUMAN	2
372	Q9Y625|GPC6_HUMAN	5	372	A6NM43|TCPQL_HUMAN	2
373	Q96ND8|ZN583_HUMAN	2	373	P49585|PCY1A_HUMAN	3
374	Q9BUQ8|DDX23_HUMAN	4	374	Q674X7|KAZRN_HUMAN	2
375	Q5TCS8|KAD9_HUMAN	2	375	A6NC57|ANR62_HUMAN	4
376	Q9Y6N8|CAD10_HUMAN	2	376	Q68CZ2|TENS3_HUMAN	4
377	P82930|RT34_HUMAN	4	377	P19338|NUCL_HUMAN	6
378	O00193|SMAP_HUMAN	6	378	Q9HCQ5|GALT9_HUMAN	3
379	Q68DK2|ZFY26_HUMAN	5	379	Q8NB25|F184A_HUMAN	6
380	P15169|CBPN_HUMAN	2	380	Q9Y247|FA50B_HUMAN	5
381	O60293|ZC3H1_HUMAN	7	381	Q14320|FA50A_HUMAN	3
382	Q96A08|H2B1A_HUMAN	6	382	Q8IYN2|TCAL8_HUMAN	2
383	Q8N257|H2B3B_HUMAN	4	383	Q14692|BMS1_HUMAN	6
384	Q9Y2Z9|COQ6_HUMAN	2	384	P51649|SSDH_HUMAN	2
385	P55060|XPO2_HUMAN	2	385	Q9NU02|ANKE1_HUMAN	7
386	P78536|ADA17_HUMAN	5	386	Q8N239|KLH34_HUMAN	3
387	P0CB38|PAB4L_HUMAN	8	387	Q8NCU7|C2C4A_HUMAN	4
388	P51825|AFF1_HUMAN	6	388	A6NLJ0|C2C4B_HUMAN	5
389	O43365|HXA3_HUMAN	4	389	P15169|CBPN_HUMAN	2
390	P20700|LMNB1_HUMAN	3	390	O75446|SAP30_HUMAN	1
391	P11717|MPRI_HUMAN	10	391	Q9BXM0|PRAX_HUMAN	3
392	O75446|SAP30_HUMAN	2	392	Q5T200|ZC3HD_HUMAN	11
393	Q2NL98|VMAC_HUMAN	3	393	Q53T94|TAF1B_HUMAN	4
394	Q6SZW1|SARM1_HUMAN	3	394	Q7Z4Q2|HEAT3_HUMAN	2
395	Q6P2S7|TTC41_HUMAN	2	395	O60673|REV3L_HUMAN	11
396	Q8NFH3|NUP43_HUMAN	2	396	Q6I9Y2|THOC7_HUMAN	2
397	Q9BX10|GTPB2_HUMAN	2	397	Q9H2S9|IKZF4_HUMAN	1
398	Q9NWM3|CUED1_HUMAN	2	398	P09525|ANXA4_HUMAN	6
399	Q8IZT6|ASPM_HUMAN	24	399	A4GXA9|EME2_HUMAN	2
400	Q9Y2J4|AMOL2_HUMAN	4	400	Q8NI17|IL31R_HUMAN	6
401	O96019|ACL6A_HUMAN	1	401	Q8N393|ZN786_HUMAN	2
402	C9JTQ0|ANR63_HUMAN	6	402	Q9BZZ2|SN_HUMAN	3
403	Q8TF76|HASP_HUMAN	10	403	P09086|PO2F2_HUMAN	3
404	Q07912|ACK1_HUMAN	7	404	Q9UPN3|MACF1_HUMAN	21
405	Q9H720|PG2IP_HUMAN	1	405	Q8N465|D2HDH_HUMAN	2
406	Q9NSY1|BMP2K_HUMAN	4	406	Q8N5C6|SRBD1_HUMAN	3
407	P12259|FA5_HUMAN	2	407	P29218|IMPA1_HUMAN	3

BAIT			CONTROL		
prot_hit_num	prot_acc	# peptides_all	prot_hit_num	prot_acc	# peptides_all
408	Q9H3H1|MOD5_HUMAN	2	408	Q14687|GSE1_HUMAN	2
409	Q8NI17|IL31R_HUMAN	6	409	Q8NHP7|EXD1_HUMAN	2
410	P80108|PHLD_HUMAN	5	410	O14776|TCRG1_HUMAN	6
411	Q9UPW5|CBPC1_HUMAN	4	411	Q99996|AKAP9_HUMAN	15
412	Q6ZTR5|CFA47_HUMAN	5	412	Q5SNV9|CA167_HUMAN	5
413	Q7Z7G8|VP13B_HUMAN	3	413	Q8IYD2|KLD8A_HUMAN	4
414	Q92997|DVL3_HUMAN	3	414	Q68DK2|ZFY26_HUMAN	7
415	Q96NW7|LRRC7_HUMAN	5	415	Q14168|MPP2_HUMAN	5
416	Q9BZA7|PC11X_HUMAN	4	416	Q8NCM8|DYHC2_HUMAN	10
417	Q5T4S7|UBR4_HUMAN	9	417	Q17RY0|CPEB4_HUMAN	2
418	O75970|MPDZ_HUMAN	5	418	Q14690|RRP5_HUMAN	5
419	Q9BZ23|PANK2_HUMAN	4	419	Q6IC83|CV042_HUMAN	2
420	Q96Q15|SMG1_HUMAN	3	420	Q58F21|BRDT_HUMAN	3
421	A2RRP1|NBAS_HUMAN	4	421	Q5XX13|FBW10_HUMAN	4
422	Q9UPS6|SET1B_HUMAN	4	422	P01023|A2MG_HUMAN	3
423	O94806|KPCD3_HUMAN	4	423	Q8NDZ2|SIMC1_HUMAN	3
424	P57081|WDR4_HUMAN	3	424	Q6P5Q4|LMOD2_HUMAN	2
425	Q86XJ1|GA2L3_HUMAN	2	425	Q9NRM1|ENAM_HUMAN	6
426	A4D2P6|GRD2I_HUMAN	7	426	P59045|NAL11_HUMAN	5
427	Q5U4N7|GDF5O_HUMAN	3	427	Q86X52|CHSS1_HUMAN	3
428	P0C626|OR5G3_HUMAN	1	428	Q70JA7|CHSS3_HUMAN	2
429	P59045|NAL11_HUMAN	2	429	Q9NXG0|CNTLN_HUMAN	6
430	Q70JA7|CHSS3_HUMAN	1	430	Q96HC4|PDLI5_HUMAN	2
431	Q86X52|CHSS1_HUMAN	1	431	Q9NVH2|INT7_HUMAN	7
432	Q96G01|BICD1_HUMAN	2	432	P36969|GPX4_HUMAN	3
433	Q9H0E3|SP130_HUMAN	6	433	O14917|PCD17_HUMAN	7
434	Q9Y566|SHAN1_HUMAN	4	434	Q8NE62|CHDH_HUMAN	2
435	Q9HCE0|EPG5_HUMAN	4	435	Q5BKX8|MURC_HUMAN	2
436	Q5T4T6|SYC2L_HUMAN	4	436	Q92187|SIA8D_HUMAN	3
437	Q7Z6K3|PTAR1_HUMAN	3	437	Q3B7T1|EDRF1_HUMAN	3
438	Q8NEG4|FA83F_HUMAN	3	438	Q9ULV5|HSF4_HUMAN	2
439	Q96MG8|PCMD1_HUMAN	3	439	O00763|ACACB_HUMAN	2
440	Q86TP1|PRUNE_HUMAN	1	440	P05305|EDN1_HUMAN	2
441	Q96EH5|RL39L_HUMAN	2	441	Q96L73|NSD1_HUMAN	6
442	Q6AHZ1|Z518A_HUMAN	3	442	Q7Z4L5|TT21B_HUMAN	8
443	P01011|AACT_HUMAN	4	443	Q9H3H1|MOD5_HUMAN	2
444	O00443|P3C2A_HUMAN	7	444	P02686|MBP_HUMAN	4
445	Q96ST2|IWS1_HUMAN	2	445	Q92673|SORL_HUMAN	7
446	Q5VU57|CBPC6_HUMAN	6	446	Q6P3S1|DEN1B_HUMAN	2
447	Q86UP2|KTN1_HUMAN	8	447	Q8IWZ8|SUGP1_HUMAN	5
448	P12821|ACE_HUMAN	5	448	A6NNM8|TTL13_HUMAN	4
449	O60749|SNX2_HUMAN	4	449	Q8IVE3|PKHH2_HUMAN	2
450	Q9NQ66|PLCB1_HUMAN	4	450	P56179|DLX6_HUMAN	3
451	O14948|TFEC_HUMAN	1	451	Q86WG3|ATCAY_HUMAN	3
452	O75762|TRPA1_HUMAN	3	452	P50851|LRBA_HUMAN	5
453	A7MBM2|DISP2_HUMAN	4	453	Q9BXF6|RFIP5_HUMAN	5
454	O95049|ZO3_HUMAN	4	454	Q92539|LPIN2_HUMAN	3
455	Q6P1S2|CC033_HUMAN	2	455	Q14693|LPIN1_HUMAN	3
456	Q9H9J4|UBP42_HUMAN	4	456	Q75VX8|GARE2_HUMAN	5
457	Q14159|SPIDR_HUMAN	3	457	Q8NI36|WDR36_HUMAN	2
458	Q9NSE7|ABCCD_HUMAN	2	458	Q96DE5|APC16_HUMAN	3

BAIT			CONTROL		
prot_hit_num	prot_acc	# peptides_all	prot_hit_num	prot_acc	# peptides_all
459	Q6I9Y2|THOC7_HUMAN	3	459	Q9UKN7|MYO15_HUMAN	10
460	Q7Z403|TMC6_HUMAN	4			
461	Q9UKJ3|GPTC8_HUMAN	7			
462	Q9P1Y6|PHRF1_HUMAN	3			
463	Q8NHP7|EXD1_HUMAN	2			
464	Q6PKC3|TXD11_HUMAN	2			
465	P51801|CLCKB_HUMAN	2			
466	Q13769|THOC5_HUMAN	3			
467	Q5TF21|SOGA3_HUMAN	9			
468	P63136|POK25_HUMAN	7			
469	Q9BXR3|POK6_HUMAN	7			
470	Q9HCE6|ARGAL_HUMAN	2			
471	P31269|HXA9_HUMAN	4			
472	Q8WXX7|AUTS2_HUMAN	3			
473	P49848|TAF6_HUMAN	2			
474	A8MVW0|F1712_HUMAN	2			
475	Q9Y4H2|IRS2_HUMAN	2			
476	Q93050|VPP1_HUMAN	2			
477	Q8IYD2|KLD8A_HUMAN	5			
478	Q5JV73|FRPD3_HUMAN	5			
479	Q9UPY3|DICER_HUMAN	24			
480	Q96EY7|PTCD3_HUMAN	4			
481	Q9NPF8|ADAP2_HUMAN	5			
482	Q9BQS8|FYCO1_HUMAN	4			
483	P24863|CCNC_HUMAN	1			
484	Q9UKA4|AKA11_HUMAN	2			
485	Q6P3S1|DEN1B_HUMAN	3			
486	P02786|TFR1_HUMAN	4			
487	Q92556|ELMO1_HUMAN	9			
488	O00763|ACACB_HUMAN	5			
489	Q92673|SORL_HUMAN	4			
490	Q6XYB7|LBX2_HUMAN	3			
491	Q9H0I2|ENKD1_HUMAN	2			
492	P11049|CD37_HUMAN	1			
493	Q96RS6|NUDC1_HUMAN	2			
494	Q9UKN7|MYO15_HUMAN	5			
495	Q8WWQ8|STAB2_HUMAN	10			
496	O43739|CYH3_HUMAN	4			

Table A.4: MaxQuant search parameters and identified protein interactors of NSMCE4a upon non-treated conditions (Figure 4.7)

A. MaxQuant search parameters used to identify peptides in the sample, LFQ intensities were used for quantitative measurements. **B.** Proteins identified in four biological replicates of TALON pull downs in control and bait cell lines by MaxQuant search, search results were filtered and proteins with peptides only identified by site, reverse and potential contaminants were excluded from the list, subunits of SMC5/6 complex are marked in yellow.

A

MaxQuant search parameters; experiment: NT 4 repeats

Parameter	**Value**
Version	1.6.3.3
User name	ab797
Machine name	GC04014987
Date of writing	11/18/2019 13:21
Include contaminants	TRUE
PSM FDR	0.01
PSM FDR Crosslink	0.01
Protein FDR	0.01
Site FDR	0.01
Use Normalized Ratios For Occupancy	TRUE
Min. peptide Length	7
Min. score for unmodified peptides	0
Min. score for modified peptides	40
Min. delta score for unmodified peptides	0
Min. delta score for modified peptides	6
Min. unique peptides	0
Min. razor peptides	1
Min. peptides	1
Use only unmodified peptides and	TRUE
Modifications included in protein quantification	Oxidation (M);Acetyl (Protein N-term)
Peptides used for protein quantification	Razor
Discard unmodified counterpart peptides	TRUE
Label min. ratio count	2
Use delta score	FALSE
iBAQ	FALSE
iBAQ log fit	FALSE
Match between runs	TRUE
Matching time window [min]	0.7
Alignment time window [min]	20
Find dependent peptides	FALSE
Fasta file	N:\Documents\Programmes\MaxQuant\Human_Swiss_Uniprot_20200_June2017.fasta
Decoy mode	revert
Include contaminants	TRUE
Advanced ratios	TRUE
Fixed andromeda index folder	
Temporary folder	
Combined folder location	
Second peptides	TRUE
Stabilize large LFQ ratios	TRUE
Separate LFQ in parameter groups	FALSE
Require MS/MS for LFQ comparisons	TRUE
Calculate peak properties	FALSE
Main search max. combinations	200

MaxQuant search parameters; experiment: NT 4 repeats

Parameter	Value
Advanced site intensities	TRUE
Write msScans table	FALSE
Write msmsScans table	TRUE
Write ms3Scans table	TRUE
Write allPeptides table	TRUE
Write mzRange table	TRUE
Write pasefMsmsScans table	TRUE
Write accumulatedPasefMsmsScans table	TRUE
Max. peptide mass [Da]	4600
Min. peptide length for unspecific search	8
Max. peptide length for unspecific search	25
Razor protein FDR	TRUE
Disable MD5	FALSE
Max mods in site table	3
Match unidentified features	FALSE
Epsilon score for mutations	
Evaluate variant peptides separately	TRUE
Variation mode	None
MS/MS tol. (FTMS)	20 ppm
Top MS/MS peaks per Da interval. (FTMS)	12
Da interval. (FTMS)	100
MS/MS deisotoping (FTMS)	TRUE
MS/MS deisotoping tolerance (FTMS)	7
MS/MS deisotoping tolerance unit (FTMS)	ppm
MS/MS higher charges (FTMS)	TRUE
MS/MS water loss (FTMS)	TRUE
MS/MS ammonia loss (FTMS)	TRUE
MS/MS dependent losses (FTMS)	TRUE
MS/MS recalibration (FTMS)	FALSE
MS/MS tol. (ITMS)	0.5 Da
Top MS/MS peaks per Da interval. (ITMS)	8
Da interval. (ITMS)	100
MS/MS deisotoping (ITMS)	FALSE
MS/MS deisotoping tolerance (ITMS)	0.15
MS/MS deisotoping tolerance unit (ITMS)	Da
MS/MS higher charges (ITMS)	TRUE
MS/MS water loss (ITMS)	TRUE
MS/MS ammonia loss (ITMS)	TRUE
MS/MS dependent losses (ITMS)	TRUE
MS/MS recalibration (ITMS)	FALSE
MS/MS tol. (TOF)	40 ppm
Top MS/MS peaks per Da interval. (TOF)	10
Da interval. (TOF)	100
MS/MS deisotoping (TOF)	TRUE
MS/MS deisotoping tolerance (TOF)	0.01

MaxQuant search parameters; experiment: NT 4 repeats

Parameter	**Value**
MS/MS deisotoping tolerance unit (TOF)	Da
MS/MS higher charges (TOF)	TRUE
MS/MS water loss (TOF)	TRUE
MS/MS ammonia loss (TOF)	TRUE
MS/MS dependent losses (TOF)	TRUE
MS/MS recalibration (TOF)	FALSE
MS/MS tol. (Unknown)	0.5 Da
Top MS/MS peaks per Da interval. (Unknown)	8
Da interval. (Unknown)	100
MS/MS deisotoping (Unknown)	FALSE
MS/MS deisotoping tolerance (Unknown)	0.15
MS/MS deisotoping tolerance unit (Unknown)	Da
MS/MS higher charges (Unknown)	TRUE
MS/MS water loss (Unknown)	TRUE
MS/MS ammonia loss (Unknown)	TRUE
MS/MS dependent losses (Unknown)	TRUE
MS/MS recalibration (Unknown)	FALSE
Site tables	Oxidation (M)Sites.txt

B

MaxQuant search_ NT 4 repeats

id	Protein name	Peptide counts (all)	LFQ intensity _Bait_1	LFQ intensity _Control_1	LFQ intensity_Bait_2	LFQ intensity_Control_2	LFQ intensity_Bait_3	LFQ intensity_Control_3	LFQ intensity_Bait_4	LFQ intensity
1	VWA8_HUMAN	3	0.00E+00	6.10E+06	0.00E+00	0.00E+00	0.00E+00	0.00E+00	0.00E+00	0.00E+00
2	CE051_HUMAN	2	0.00E+00	2.45E+06	0.00E+00	0.00E+00	0.00E+00	0.00E+00	0.00E+00	0.00E+00
3	CC85C_HUMAN	11	1.98E+07	2.15E+07	2.20E+07	2.96E+07	4.05E+07	3.89E+07	2.76E+07	3.46E+07
4	RGPD4_HUMAN;sp	1;1	0.00E+00	0.00E+00	0.00E+00	1.01E+07	0.00E+00	0.00E+00	0.00E+00	0.00E+00
5	BTBDB_HUMAN	3	1.21E+07	1.07E+07	0.00E+00	0.00E+00	0.00E+00	0.00E+00	0.00E+00	0.00E+00
6	RUXG_HUMAN;sp|	2;2	0.00E+00	0.00E+00	1.19E+07	0.00E+00	0.00E+00	0.00E+00	0.00E+00	0.00E+00
7	NUD19_HUMAN	10	2.56E+07	2.79E+07	3.15E+07	6.31E+07	0.00E+00	0.00E+00	2.40E+07	2.31E+07
8	MI4GD_HUMAN	1	0.00E+00	0.00E+00	0.00E+00	0.00E+00	0.00E+00	0.00E+00	0.00E+00	9.66E+06
9	MCRI1_HUMAN	6	4.14E+07	4.11E+07	7.07E+07	5.97E+07	1.70E+08	1.30E+08	5.31E+07	4.19E+07
10	SMAP_HUMAN	5	7.11E+06	1.46E+07	4.55E+07	0.00E+00	2.34E+08	8.18E+07	0.00E+00	0.00E+00
11	PSMD9_HUMAN	1	0.00E+00	2.42E+06	0.00E+00	0.00E+00	0.00E+00	0.00E+00	0.00E+00	0.00E+00
12	CBX4_HUMAN	3	7.84E+06	0.00E+00	0.00E+00	0.00E+00	0.00E+00	0.00E+00	0.00E+00	0.00E+00
13	PGRC1_HUMAN	1	0.00E+00	0.00E+00	0.00E+00	1.77E+07	0.00E+00	0.00E+00	0.00E+00	0.00E+00
14	EF2K_HUMAN	1	0.00E+00	0.00E+00	0.00E+00	0.00E+00	0.00E+00	0.00E+00	6.90E+05	0.00E+00
15	IF2B3_HUMAN	2	0.00E+00	0.00E+00	0.00E+00	0.00E+00	0.00E+00	0.00E+00	0.00E+00	3.33E+07
16	MEIS1_HUMAN;sp|	8;1;1	4.13E+07	3.56E+07	0.00E+00	2.87E+07	3.92E+07	0.00E+00	5.19E+07	4.73E+07
17	DDX3X_HUMAN;sp	4;2	0.00E+00	1.09E+07	0.00E+00	0.00E+00	0.00E+00	0.00E+00	0.00E+00	0.00E+00
18	NFIB_HUMAN	7	2.08E+07	2.91E+07	0.00E+00	0.00E+00	0.00E+00	0.00E+00	3.57E+07	2.99E+07
19	NDKM_HUMAN	9	5.48E+07	5.24E+07	5.29E+07	6.04E+07	2.07E+07	0.00E+00	7.59E+07	1.11E+08
20	ARI1A_HUMAN	6	1.24E+07	1.27E+07	2.83E+07	0.00E+00	0.00E+00	0.00E+00	0.00E+00	0.00E+00
21	CTRO_HUMAN	4	0.00E+00	0.00E+00	0.00E+00	0.00E+00	0.00E+00	0.00E+00	0.00E+00	2.34E+06
22	ABLM1_HUMAN	2	0.00E+00	0.00E+00	0.00E+00	0.00E+00	0.00E+00	0.00E+00	4.31E+06	0.00E+00
23	CHD1_HUMAN	3	0.00E+00	4.02E+06	0.00E+00	0.00E+00	0.00E+00	0.00E+00	0.00E+00	0.00E+00
24	IRS4_HUMAN	8	9.64E+06	1.32E+07	0.00E+00	0.00E+00	0.00E+00	0.00E+00	0.00E+00	0.00E+00
25	PDCD5_HUMAN	2	0.00E+00	0.00E+00	9.24E+06	0.00E+00	0.00E+00	0.00E+00	0.00E+00	0.00E+00
26	MEIS2_HUMAN	6	0.00E+00	0.00E+00	1.28E+07	0.00E+00	0.00E+00	0.00E+00	0.00E+00	1.10E+07
27	BCKD_HUMAN	9	2.08E+08	1.46E+08	8.09E+07	9.02E+07	8.05E+07	7.69E+07	1.83E+08	1.23E+08
28	AT2A1_HUMAN;sp|	1;1	0.00E+00	4.70E+06	0.00E+00	0.00E+00	0.00E+00	0.00E+00	0.00E+00	0.00E+00
29	ARHGA_HUMAN	7	0.00E+00	0.00E+00	0.00E+00	0.00E+00	0.00E+00	0.00E+00	4.48E+07	3.86E+07
30	ZN609_HUMAN	6	0.00E+00	1.09E+07	0.00E+00	0.00E+00	1.98E+07	0.00E+00	0.00E+00	0.00E+00
31	SC16A_HUMAN	11	6.51E+07	5.24E+07	7.06E+07	5.45E+07	1.12E+08	8.57E+07	9.94E+07	7.82E+07
32	SR140_HUMAN	51	9.91E+08	1.10E+09	7.89E+08	1.14E+09	6.90E+08	7.98E+08	6.16E+08	7.60E+08
33	AXIN1_HUMAN	4	0.00E+00	0.00E+00	0.00E+00	0.00E+00	6.10E+06	0.00E+00	0.00E+00	0.00E+00
34	NKRF_HUMAN	24	1.07E+08	8.43E+07	7.03E+07	6.35E+07	2.67E+07	0.00E+00	9.97E+07	1.05E+08
35	SURF4_HUMAN	1	0.00E+00	2.30E+06	0.00E+00	0.00E+00	0.00E+00	0.00E+00	0.00E+00	0.00E+00
36	TRI18_HUMAN;sp|	8;1	0.00E+00	0.00E+00	0.00E+00	0.00E+00	0.00E+00	0.00E+00	2.30E+07	3.68E+07
37	TYY2_HUMAN	5	9.32E+07	6.88E+07	4.31E+07	3.56E+07	1.14E+08	1.06E+08	0.00E+00	0.00E+00
38	COPT1_HUMAN	1	0.00E+00	3.77E+06	0.00E+00	0.00E+00	0.00E+00	0.00E+00	0.00E+00	0.00E+00
39	DHX15_HUMAN;sp	46;1;1	2.12E+09	2.10E+09	1.26E+09	1.54E+09	1.55E+09	1.73E+09	1.77E+09	1.80E+09
40	SNUT1_HUMAN	1	0.00E+00	0.00E+00	0.00E+00	0.00E+00	0.00E+00	0.00E+00	1.27E+06	0.00E+00
41	CTIF_HUMAN	4	0.00E+00	0.00E+00	0.00E+00	0.00E+00	0.00E+00	0.00E+00	1.38E+07	8.55E+06
42	RIPK2_HUMAN	2	0.00E+00	0.00E+00	0.00E+00	0.00E+00	0.00E+00	0.00E+00	0.00E+00	3.34E+06
43	ACTN4_HUMAN;sp	5;2	0.00E+00	0.00E+00	1.70E+07	2.07E+07	0.00E+00	0.00E+00	0.00E+00	0.00E+00
44	HTSF1_HUMAN	5	1.16E+07	1.46E+07	0.00E+00	0.00E+00	0.00E+00	0.00E+00	0.00E+00	0.00E+00
45	CPSF5_HUMAN	17	6.59E+08	6.03E+08	4.98E+08	4.60E+08	4.99E+08	4.93E+08	1.20E+09	8.52E+08
46	KPRB_HUMAN	7	1.85E+07	2.85E+07	0.00E+00	0.00E+00	0.00E+00	0.00E+00	2.53E+07	4.74E+07
47	OPA1_HUMAN	5	0.00E+00	1.36E+07	0.00E+00	1.70E+07	0.00E+00	0.00E+00	0.00E+00	0.00E+00
48	KDM1A_HUMAN	4	7.88E+06	0.00E+00	0.00E+00	0.00E+00	0.00E+00	0.00E+00	0.00E+00	0.00E+00
49	ACSL4_HUMAN;sp|	1;1	0.00E+00	4.49E+06	0.00E+00	0.00E+00	0.00E+00	0.00E+00	0.00E+00	0.00E+00
50	GMDS_HUMAN	1	0.00E+00	4.49E+06	0.00E+00	0.00E+00	0.00E+00	0.00E+00	0.00E+00	0.00E+00
51	CCNT1_HUMAN	25	3.16E+08	2.87E+08	2.10E+08	2.30E+08	2.94E+08	2.85E+08	0.00E+00	0.00E+00
52	CCNT2_HUMAN	6	1.66E+07	9.22E+06	0.00E+00	0.00E+00	0.00E+00	0.00E+00	0.00E+00	0.00E+00
53	DIAP1_HUMAN	5	0.00E+00	0.00E+00	0.00E+00	0.00E+00	0.00E+00	0.00E+00	1.02E+07	8.09E+06
54	H2B1L_HUMAN;sp|'	;7;7;7;7;7;7;(	2.74E+08	2.44E+08	1.19E+08	2.31E+08	1.22E+08	1.52E+08	9.18E+07	1.29E+08

id	Protein name	Peptide counts (all)	LFQ intensity _Bait_1	LFQ intensity _Control_1	LFQ intensity_Bait_2	LFQ intensity_Control_2	LFQ intensity_Bait_3	LFQ intensity_Control_3	LFQ intensity_Bait_4	LFQ intensity
55	DKC1_HUMAN	2	0.00E+00	0.00E+00	0.00E+00	0.00E+00	0.00E+00	0.00E+00	0.00E+00	2.21E+06
56	BRD4_HUMAN;sp|(	34;4;1;1	5.26E+08	4.86E+08	4.54E+08	3.88E+08	5.79E+08	5.91E+08	4.65E+08	5.16E+08
57	ABCB7_HUMAN	9	1.67E+07	2.43E+07	0.00E+00	6.19E+07	0.00E+00	0.00E+00	0.00E+00	0.00E+00
58	SRGP2_HUMAN;sp|	3;2;1;1	0.00E+00	0.00E+00	0.00E+00	0.00E+00	0.00E+00	0.00E+00	0.00E+00	8.13E+06
59	HIP1R_HUMAN	7	0.00E+00	0.00E+00	0.00E+00	0.00E+00	0.00E+00	0.00E+00	1.99E+07	2.39E+07
60	BRE1B_HUMAN	21	7.32E+07	7.65E+07	2.48E+07	2.58E+07	3.13E+07	2.34E+07	2.14E+07	1.88E+07
61	CNOT3_HUMAN	1	0.00E+00	0.00E+00	0.00E+00	0.00E+00	0.00E+00	0.00E+00	0.00E+00	2.95E+06
62	ANR17_HUMAN	1	0.00E+00	0.00E+00	0.00E+00	0.00E+00	0.00E+00	0.00E+00	0.00E+00	3.93E+06
63	NCOR1_HUMAN	3	0.00E+00	0.00E+00	0.00E+00	0.00E+00	0.00E+00	0.00E+00	4.16E+06	0.00E+00
64	NDUS6_HUMAN	3	0.00E+00	0.00E+00	0.00E+00	0.00E+00	3.06E+07	0.00E+00	0.00E+00	0.00E+00
65	SC22B_HUMAN	1	0.00E+00	0.00E+00	0.00E+00	4.09E+06	0.00E+00	0.00E+00	0.00E+00	0.00E+00
66	PR40A_HUMAN	21	1.11E+08	1.41E+08	6.31E+07	1.07E+08	5.27E+07	0.00E+00	1.17E+08	1.20E+08
67	SRS10_HUMAN;sp|	3;1	0.00E+00	8.74E+06	0.00E+00	0.00E+00	0.00E+00	0.00E+00	0.00E+00	0.00E+00
68	SF3B1_HUMAN	69	1.81E+09	2.02E+09	1.56E+09	2.29E+09	1.04E+09	1.23E+09	1.12E+09	1.26E+09
69	U520_HUMAN	5	0.00E+00	0.00E+00	8.05E+06	1.06E+07	0.00E+00	0.00E+00	0.00E+00	0.00E+00
70	CCNK_HUMAN	7	4.74E+07	6.68E+07	4.37E+07	4.91E+07	0.00E+00	3.24E+07	8.51E+07	8.74E+07
71	PIAS2_HUMAN;sp|(	1;1	0.00E+00	0.00E+00	0.00E+00	0.00E+00	0.00E+00	0.00E+00	0.00E+00	5.54E+06
72	DNJC8_HUMAN	17	1.91E+08	2.09E+08	3.53E+08	3.70E+08	3.15E+08	2.57E+08	1.23E+08	1.33E+08
73	SPF30_HUMAN	6	4.22E+07	5.32E+07	1.28E+08	9.91E+07	8.71E+07	6.30E+07	3.05E+07	2.56E+07
74	ATP5H_HUMAN	1	0.00E+00	3.94E+06	0.00E+00	0.00E+00	0.00E+00	0.00E+00	0.00E+00	0.00E+00
75	TRIO_HUMAN;sp|O	9;1	1.80E+07	1.18E+07	0.00E+00	0.00E+00	0.00E+00	0.00E+00	0.00E+00	0.00E+00
76	TOX4_HUMAN;sp|(	9;3;2	1.32E+08	1.18E+08	8.34E+07	9.57E+07	1.09E+08	1.43E+08	1.64E+07	9.78E+06
77	PRP6_HUMAN	4	0.00E+00	0.00E+00	0.00E+00	1.58E+07	0.00E+00	0.00E+00	0.00E+00	0.00E+00
78	PCF11_HUMAN	2	0.00E+00	0.00E+00	0.00E+00	6.53E+06	0.00E+00	0.00E+00	0.00E+00	0.00E+00
79	FBX21_HUMAN	5	2.75E+07	2.62E+07	1.92E+07	2.35E+07	2.27E+07	3.50E+07	1.50E+07	1.64E+07
80	SC31A_HUMAN;sp|	30;1	1.15E+08	1.51E+08	2.56E+07	6.52E+07	0.00E+00	1.31E+07	3.80E+08	4.32E+08
81	HEXI1_HUMAN;sp|	6;1	5.19E+07	4.91E+07	0.00E+00	5.56E+07	1.92E+08	1.33E+08	0.00E+00	0.00E+00
82	ELP1_HUMAN	22	3.60E+07	3.40E+07	0.00E+00	5.03E+07	0.00E+00	0.00E+00	9.53E+07	1.21E+08
83	MTMR5_HUMAN	4	0.00E+00	0.00E+00	0.00E+00	0.00E+00	0.00E+00	0.00E+00	8.15E+06	1.14E+07
84	SYFM_HUMAN	1	0.00E+00	0.00E+00	0.00E+00	0.00E+00	0.00E+00	0.00E+00	0.00E+00	4.84E+06
85	CD2B2_HUMAN	1	0.00E+00	0.00E+00	3.81E+06	0.00E+00	0.00E+00	0.00E+00	0.00E+00	0.00E+00
86	ZIC2_HUMAN;sp|Q	6;2;2	7.24E+07	6.29E+07	0.00E+00	0.00E+00	3.70E+07	0.00E+00	0.00E+00	0.00E+00
87	G6PE_HUMAN	11	0.00E+00	0.00E+00	0.00E+00	0.00E+00	0.00E+00	0.00E+00	6.94E+07	6.13E+07
88	SC24A_HUMAN	1	0.00E+00	0.00E+00	0.00E+00	0.00E+00	0.00E+00	0.00E+00	0.00E+00	6.28E+06
89	SC24B_HUMAN	9	1.64E+07	1.32E+07	0.00E+00	0.00E+00	0.00E+00	0.00E+00	4.72E+07	5.49E+07
90	CPSF4_HUMAN	3	1.13E+07	1.53E+07	0.00E+00	0.00E+00	0.00E+00	0.00E+00	0.00E+00	0.00E+00
91	BAG3_HUMAN	27	2.78E+08	3.12E+08	3.79E+08	2.80E+08	5.80E+08	4.53E+08	2.54E+08	2.30E+08
92	M4K4_HUMAN;sp|	8;3;3	2.07E+07	1.87E+07	0.00E+00	0.00E+00	0.00E+00	0.00E+00	1.72E+07	2.59E+07
93	ACL6A_HUMAN	8	3.40E+07	3.39E+07	0.00E+00	2.36E+07	0.00E+00	0.00E+00	4.49E+07	4.43E+07
94	NB5R3_HUMAN	1	0.00E+00	0.00E+00	0.00E+00	3.60E+06	0.00E+00	0.00E+00	0.00E+00	0.00E+00
95	LMNA_HUMAN	31	8.19E+07	6.67E+07	8.81E+07	3.10E+07	9.58E+07	6.71E+07	2.77E+08	2.01E+08
96	ALDOA_HUMAN	11	3.54E+07	3.02E+07	3.62E+07	0.00E+00	0.00E+00	0.00E+00	4.21E+07	4.49E+07
97	G3P_HUMAN;sp|O	24;1	2.61E+09	3.11E+09	6.17E+09	6.93E+09	1.49E+09	2.37E+09	5.10E+09	6.97E+09
98	RPN1_HUMAN	4	0.00E+00	0.00E+00	0.00E+00	2.23E+07	0.00E+00	0.00E+00	0.00E+00	0.00E+00
99	H2A1J_HUMAN;sp|I	;3;3;3;3;3;3;3	1.03E+08	9.79E+07	1.10E+08	1.48E+08	7.91E+07	1.09E+08	4.17E+07	4.78E+07
100	AT1A1_HUMAN;sp|	3;2;2;1	0.00E+00	0.00E+00	0.00E+00	7.22E+06	0.00E+00	0.00E+00	0.00E+00	0.00E+00
101	ADT2_HUMAN;sp|F	4;3;3;2	0.00E+00	0.00E+00	0.00E+00	2.26E+07	0.00E+00	0.00E+00	0.00E+00	7.16E+06
102	JUN_HUMAN	2	0.00E+00	6.30E+06	0.00E+00	0.00E+00	0.00E+00	0.00E+00	0.00E+00	0.00E+00
103	AP2A_HUMAN;sp|(	3;2;2	0.00E+00	0.00E+00	0.00E+00	0.00E+00	0.00E+00	0.00E+00	1.90E+07	0.00E+00
104	ATPB_HUMAN	12	5.24E+07	7.02E+07	0.00E+00	8.54E+07	0.00E+00	4.67E+07	0.00E+00	0.00E+00
105	NPM_HUMAN	1	0.00E+00	0.00E+00	0.00E+00	2.05E+06	0.00E+00	0.00E+00	0.00E+00	0.00E+00
106	H2B2E_HUMAN;sp|	6;6;6;6;5;2;2	0.00E+00	3.74E+06	0.00E+00	0.00E+00	0.00E+00	0.00E+00	0.00E+00	0.00E+00
107	TBB5_HUMAN;sp|A	18;5;4;4	5.32E+08	6.89E+08	4.77E+08	7.66E+08	2.74E+08	3.62E+08	5.02E+08	6.82E+08
108	HS90B_HUMAN;sp|	5;5;3;2;1;1	0.00E+00	2.06E+07	0.00E+00	0.00E+00	0.00E+00	0.00E+00	0.00E+00	0.00E+00
109	HNRPC_HUMAN;sp	8;2;2;2;2	2.16E+07	2.21E+07	4.51E+07	3.09E+07	5.93E+07	5.21E+07	0.00E+00	0.00E+00

id	Protein name	Peptide counts (all)	LFQ intensity _Bait_1	LFQ intensity _Control_1	LFQ intensity_Bait_2	LFQ intensity_Control_2	LFQ intensity_Bait_3	LFQ intensity_Control_3	LFQ intensity_Bait_4	LFQ intensity
110	PFKAM_HUMAN;sp	9;1	0.00E+00	0.00E+00	0.00E+00	2.49E+07	0.00E+00	0.00E+00	2.11E+07	2.25E+07
111	RU17_HUMAN	5	0.00E+00	1.88E+07	2.66E+07	2.43E+07	0.00E+00	0.00E+00	0.00E+00	0.00E+00
112	NFIC_HUMAN	5	2.60E+07	2.47E+07	0.00E+00	2.47E+07	0.00E+00	0.00E+00	1.86E+07	0.00E+00
113	HXC4_HUMAN	3	1.31E+07	1.07E+07	0.00E+00	0.00E+00	0.00E+00	0.00E+00	0.00E+00	0.00E+00
114	RU1C_HUMAN	2	0.00E+00	0.00E+00	0.00E+00	0.00E+00	0.00E+00	1.02E+07	0.00E+00	0.00E+00
115	ROA1_HUMAN;sp|(	7;4	0.00E+00	0.00E+00	3.04E+07	2.23E+07	3.53E+07	0.00E+00	0.00E+00	0.00E+00
116	PARP1_HUMAN	10	3.97E+07	3.32E+07	0.00E+00	0.00E+00	0.00E+00	0.00E+00	3.07E+07	2.77E+07
117	H2AV_HUMAN;sp|I	4;4	1.34E+08	9.85E+07	6.95E+07	9.72E+07	4.86E+07	4.69E+07	3.28E+07	4.20E+07
118	HS71B_HUMAN;sp|	32;32	2.40E+09	2.17E+09	1.21E+09	1.54E+09	1.05E+09	1.22E+09	2.26E+09	1.92E+09
119	U2AF1_HUMAN;sp|	5;5;2	3.93E+07	4.21E+07	4.23E+07	3.69E+07	2.39E+07	2.74E+07	3.65E+07	3.55E+07
120	CBS_HUMAN;sp|P0	5;5	0.00E+00	0.00E+00	0.00E+00	2.24E+07	0.00E+00	0.00E+00	0.00E+00	0.00E+00
121	CALM3_HUMAN;sp	6;6;6	4.05E+07	2.86E+07	4.53E+07	3.83E+07	6.05E+07	5.28E+07	0.00E+00	0.00E+00
122	CH60_HUMAN	17	6.05E+07	8.01E+07	2.01E+07	2.63E+07	1.86E+07	3.00E+07	6.19E+07	5.96E+07
123	GRP78_HUMAN	28	1.33E+08	1.94E+08	1.08E+08	1.64E+08	1.03E+08	8.97E+07	1.08E+08	1.48E+08
124	HSP7C_HUMAN;sp|	34;13	1.45E+09	1.53E+09	8.42E+08	1.39E+09	9.76E+08	1.05E+09	1.67E+09	1.80E+09
125	TOP1_HUMAN;sp|(	53;5	2.93E+09	2.71E+09	1.97E+09	1.47E+09	2.05E+09	1.51E+09	2.18E+09	1.86E+09
126	PRPS2_HUMAN	7	0.00E+00	0.00E+00	0.00E+00	0.00E+00	0.00E+00	0.00E+00	0.00E+00	2.00E+07
127	PABP1_HUMAN;sp|	21;8;4;2	3.80E+08	3.62E+08	2.14E+08	2.14E+08	2.76E+08	2.88E+08	2.48E+08	2.07E+08
128	TPR_HUMAN	11	1.39E+07	1.41E+07	1.64E+07	0.00E+00	0.00E+00	0.00E+00	0.00E+00	0.00E+00
129	KCRU_HUMAN;sp|F	13;2	2.11E+08	2.53E+08	1.67E+08	1.80E+08	5.87E+07	9.41E+07	6.46E+08	7.85E+08
130	SKI_HUMAN	2	0.00E+00	1.18E+07	0.00E+00	0.00E+00	0.00E+00	0.00E+00	0.00E+00	0.00E+00
131	COX41_HUMAN	1	0.00E+00	2.51E+06	0.00E+00	0.00E+00	0.00E+00	0.00E+00	0.00E+00	0.00E+00
132	RSMN_HUMAN;sp|	5;5	1.13E+07	9.57E+06	0.00E+00	0.00E+00	0.00E+00	0.00E+00	0.00E+00	0.00E+00
133	HNRPL_HUMAN	35	1.37E+10	1.21E+10	1.02E+10	9.80E+09	8.48E+09	8.81E+09	1.14E+10	1.02E+10
134	GLNA_HUMAN	7	2.10E+07	0.00E+00	7.33E+07	4.63E+07	0.00E+00	0.00E+00	7.21E+07	6.70E+07
135	NDKA_HUMAN	4	0.00E+00	0.00E+00	1.39E+07	1.54E+07	0.00E+00	0.00E+00	9.00E+06	1.12E+07
136	ITF2_HUMAN	2	0.00E+00	0.00E+00	0.00E+00	0.00E+00	0.00E+00	0.00E+00	0.00E+00	1.75E+06
137	TFE2_HUMAN	6	1.87E+07	2.14E+07	0.00E+00	0.00E+00	0.00E+00	0.00E+00	1.69E+07	1.82E+07
138	H2A1A_HUMAN;sp	3;3;2	3.76E+06	0.00E+00	0.00E+00	0.00E+00	0.00E+00	0.00E+00	0.00E+00	0.00E+00
139	HSP76_HUMAN;sp|	9;4	0.00E+00	0.00E+00	0.00E+00	0.00E+00	0.00E+00	0.00E+00	0.00E+00	1.09E+08
140	TCPA_HUMAN	23	1.36E+08	1.77E+08	1.40E+08	1.39E+08	0.00E+00	0.00E+00	3.51E+08	4.73E+08
141	NUCL_HUMAN	4	1.24E+07	0.00E+00	0.00E+00	0.00E+00	0.00E+00	0.00E+00	0.00E+00	0.00E+00
142	CSK22_HUMAN	7	4.22E+07	3.30E+07	0.00E+00	0.00E+00	0.00E+00	0.00E+00	1.60E+07	1.63E+07
143	TBP_HUMAN;sp|Q6	5;4	1.87E+07	1.95E+07	0.00E+00	0.00E+00	0.00E+00	1.50E+07	0.00E+00	0.00E+00
144	PO3F2_HUMAN;sp|	6;2;2;1;1	3.72E+07	4.26E+07	2.92E+07	3.09E+07	4.87E+07	3.59E+07	0.00E+00	0.00E+00
145	HXA5_HUMAN	3	8.70E+06	9.21E+06	1.19E+07	0.00E+00	1.17E+07	1.38E+07	9.36E+06	0.00E+00
146	CD11B_HUMAN;sp	6;5;1	4.59E+07	4.95E+07	0.00E+00	0.00E+00	0.00E+00	0.00E+00	0.00E+00	0.00E+00
147	FBRL_HUMAN	2	0.00E+00	5.24E+06	0.00E+00	0.00E+00	0.00E+00	0.00E+00	0.00E+00	0.00E+00
148	ROA2_HUMAN	3	0.00E+00	1.21E+07	0.00E+00	0.00E+00	0.00E+00	0.00E+00	0.00E+00	0.00E+00
149	CBL_HUMAN;sp|Q1	15;1	9.32E+07	8.27E+07	3.88E+07	4.55E+07	6.30E+07	6.92E+07	8.15E+07	8.26E+07
150	SFPQ_HUMAN	48	1.09E+10	9.28E+09	1.07E+10	6.79E+09	1.08E+10	8.83E+09	4.02E+09	3.85E+09
151	TBG1_HUMAN;sp|(	6;4	2.92E+07	3.73E+07	0.00E+00	3.74E+07	2.01E+07	0.00E+00	0.00E+00	0.00E+00
152	GATA3_HUMAN	1	0.00E+00	0.00E+00	0.00E+00	0.00E+00	5.07E+06	0.00E+00	0.00E+00	0.00E+00
153	EF1B_HUMAN	2	1.16E+07	0.00E+00	0.00E+00	0.00E+00	0.00E+00	0.00E+00	0.00E+00	0.00E+00
154	TYY1_HUMAN;sp|C	20;3	5.28E+08	4.41E+08	3.24E+08	2.48E+08	8.31E+08	5.45E+08	7.26E+06	0.00E+00
155	ATPA_HUMAN	5	0.00E+00	2.57E+07	1.76E+07	4.47E+07	0.00E+00	2.85E+07	0.00E+00	0.00E+00
156	DDX6_HUMAN	15	2.99E+08	3.10E+08	2.18E+08	2.54E+08	2.49E+08	3.78E+08	2.91E+08	2.62E+08
157	U2AF2_HUMAN	9	4.09E+07	4.95E+07	0.00E+00	0.00E+00	0.00E+00	0.00E+00	0.00E+00	0.00E+00
158	IVD_HUMAN	12	3.27E+07	4.91E+07	4.81E+07	4.43E+07	0.00E+00	1.43E+07	1.13E+08	1.32E+08
159	EF1G_HUMAN	2	0.00E+00	3.46E+06	0.00E+00	0.00E+00	0.00E+00	0.00E+00	0.00E+00	0.00E+00
160	1433T_HUMAN	4	0.00E+00	0.00E+00	0.00E+00	0.00E+00	0.00E+00	0.00E+00	0.00E+00	2.38E+06
161	PYR1_HUMAN	15	1.77E+07	3.91E+07	1.63E+07	5.51E+07	0.00E+00	0.00E+00	1.37E+07	3.53E+07
162	CALX_HUMAN	10	2.18E+07	3.25E+07	0.00E+00	3.53E+07	0.00E+00	3.06E+07	0.00E+00	0.00E+00
163	MK01_HUMAN	9	2.64E+07	2.69E+07	3.43E+07	3.71E+07	0.00E+00	0.00E+00	2.39E+07	2.64E+07
164	GRN_HUMAN	2	0.00E+00	1.71E+07	0.00E+00	0.00E+00	0.00E+00	0.00E+00	0.00E+00	0.00E+00

id	Protein name	Peptide counts (all)	LFQ intensity _Bait_1	LFQ intensity _Control_1	LFQ intensity_Bait_2	LFQ intensity_Control_2	LFQ intensity_Bait_3	LFQ intensity_Control_3	LFQ intensity_Bait_4	LFQ intensity
165	PRDX3_HUMAN	8	1.29E+08	2.03E+08	2.46E+08	2.01E+08	4.39E+07	4.51E+07	1.91E+08	2.10E+08
166	2AAA_HUMAN	3	0.00E+00	0.00E+00	0.00E+00	0.00E+00	0.00E+00	0.00E+00	2.03E+07	0.00E+00
167	AMRP_HUMAN	24	1.54E+08	1.83E+08	3.41E+08	2.73E+08	2.90E+08	2.91E+08	2.08E+08	2.50E+08
168	PUR8_HUMAN	10	1.26E+07	2.02E+07	4.91E+07	1.00E+08	0.00E+00	0.00E+00	4.97E+07	7.29E+07
169	RPB2_HUMAN	1	0.00E+00	2.36E+06	0.00E+00	0.00E+00	0.00E+00	0.00E+00	0.00E+00	0.00E+00
170	METK2_HUMAN;sp	7;1	2.19E+07	2.49E+07	7.39E+07	6.89E+07	0.00E+00	0.00E+00	5.83E+07	4.22E+07
171	HXA9_HUMAN	4	3.79E+07	3.03E+07	0.00E+00	0.00E+00	0.00E+00	0.00E+00	0.00E+00	0.00E+00
172	HXA13_HUMAN;sp	3;1	0.00E+00	0.00E+00	7.51E+06	8.56E+06	0.00E+00	0.00E+00	0.00E+00	7.84E+06
173	DNJA1_HUMAN	2	0.00E+00	3.79E+06	0.00E+00	0.00E+00	0.00E+00	0.00E+00	0.00E+00	0.00E+00
174	HNRH1_HUMAN;sp	6;3;2	4.18E+07	4.11E+07	3.61E+07	5.24E+07	1.89E+07	0.00E+00	3.29E+07	3.75E+07
175	1433B_HUMAN	5	0.00E+00	0.00E+00	0.00E+00	0.00E+00	0.00E+00	0.00E+00	0.00E+00	1.04E+06
176	CGL_HUMAN	12	1.33E+08	9.80E+07	4.49E+07	3.13E+07	3.33E+07	2.11E+07	2.20E+08	1.96E+08
177	CSTF2_HUMAN	8	2.78E+07	2.81E+07	3.86E+07	3.59E+07	4.44E+07	3.52E+07	2.44E+07	2.91E+07
178	DUT_HUMAN	1	0.00E+00	3.50E+06	0.00E+00	0.00E+00	0.00E+00	0.00E+00	0.00E+00	0.00E+00
179	GLYM_HUMAN;sp|	9;1	0.00E+00	0.00E+00	7.06E+07	6.22E+07	0.00E+00	0.00E+00	2.07E+07	2.74E+07
180	HSP74_HUMAN	1	0.00E+00	0.00E+00	0.00E+00	0.00E+00	0.00E+00	0.00E+00	0.00E+00	3.55E+06
181	BMI1_HUMAN	1	0.00E+00	4.28E+06	0.00E+00	0.00E+00	0.00E+00	0.00E+00	0.00E+00	0.00E+00
182	LONM_HUMAN	3	0.00E+00	1.24E+07	0.00E+00	0.00E+00	0.00E+00	0.00E+00	0.00E+00	0.00E+00
183	PP1G_HUMAN	6	4.98E+07	5.52E+07	0.00E+00	4.16E+07	0.00E+00	0.00E+00	1.88E+07	0.00E+00
184	RBMX_HUMAN;sp|	7;4;2;1	1.27E+07	1.36E+07	0.00E+00	0.00E+00	0.00E+00	0.00E+00	0.00E+00	0.00E+00
185	GRP75_HUMAN	24	1.46E+08	1.59E+08	1.51E+08	1.55E+08	9.88E+07	1.25E+08	1.73E+08	1.86E+08
186	IF4A3_HUMAN	2	0.00E+00	0.00E+00	0.00E+00	7.42E+06	0.00E+00	0.00E+00	0.00E+00	0.00E+00
187	TCPZ_HUMAN;sp|C	23;5	1.79E+08	2.63E+08	1.70E+08	2.01E+08	1.18E+07	5.38E+07	3.89E+08	6.72E+08
188	PBX1_HUMAN	4	1.76E+07	1.67E+07	0.00E+00	0.00E+00	0.00E+00	0.00E+00	1.35E+07	0.00E+00
189	PBX2_HUMAN;sp|C	7;1	1.96E+07	1.45E+07	1.42E+07	1.92E+07	1.75E+07	2.72E+07	3.23E+07	1.56E+07
190	PBX3_HUMAN	1	0.00E+00	0.00E+00	0.00E+00	2.79E+06	0.00E+00	0.00E+00	0.00E+00	0.00E+00
191	KPCI_HUMAN	3	0.00E+00	4.53E+06	0.00E+00	0.00E+00	0.00E+00	0.00E+00	0.00E+00	0.00E+00
192	LAP2B_HUMAN;sp|	4;3	0.00E+00	9.45E+06	0.00E+00	1.87E+07	0.00E+00	0.00E+00	0.00E+00	0.00E+00
193	SK2L2_HUMAN	2	5.22E+06	0.00E+00	0.00E+00	0.00E+00	0.00E+00	0.00E+00	0.00E+00	0.00E+00
194	HELZ_HUMAN	13	6.58E+07	8.07E+07	1.58E+07	2.76E+07	4.63E+07	0.00E+00	2.51E+07	2.44E+07
195	MATR3_HUMAN	16	5.33E+07	5.59E+07	6.56E+07	1.26E+08	0.00E+00	0.00E+00	4.38E+07	4.85E+07
196	RANG_HUMAN	3	0.00E+00	0.00E+00	0.00E+00	0.00E+00	1.23E+07	0.00E+00	0.00E+00	0.00E+00
197	BAG6_HUMAN	12	2.27E+07	3.54E+07	1.96E+07	2.97E+07	0.00E+00	0.00E+00	2.66E+07	3.17E+07
198	ID4_HUMAN	1	0.00E+00	0.00E+00	0.00E+00	0.00E+00	0.00E+00	0.00E+00	0.00E+00	1.39E+07
199	PP2BC_HUMAN	2	1.05E+06	0.00E+00	0.00E+00	0.00E+00	0.00E+00	0.00E+00	0.00E+00	0.00E+00
200	TCPE_HUMAN	25	1.96E+08	2.40E+08	1.48E+08	1.85E+08	8.79E+06	4.00E+07	4.18E+08	4.88E+08
201	LMAN1_HUMAN	18	4.19E+08	4.87E+08	2.43E+08	8.05E+08	1.28E+08	1.51E+08	1.21E+08	1.15E+08
202	FAS_HUMAN	2	0.00E+00	0.00E+00	0.00E+00	6.64E+06	0.00E+00	0.00E+00	0.00E+00	0.00E+00
203	TCPG_HUMAN	22	2.16E+08	2.98E+08	1.92E+08	2.39E+08	0.00E+00	0.00E+00	6.15E+08	7.72E+08
204	EFTU_HUMAN	13	1.14E+08	1.21E+08	2.24E+08	3.08E+08	1.09E+07	0.00E+00	1.88E+08	1.79E+08
205	SRP09_HUMAN	1	0.00E+00	0.00E+00	0.00E+00	0.00E+00	3.61E+06	0.00E+00	0.00E+00	0.00E+00
206	YLPM1_HUMAN	41	2.43E+08	2.26E+08	1.95E+08	2.00E+08	2.13E+08	1.85E+08	2.21E+08	2.19E+08
207	TMEDA_HUMAN	1	0.00E+00	0.00E+00	0.00E+00	6.68E+06	0.00E+00	0.00E+00	0.00E+00	0.00E+00
208	RBM25_HUMAN	16	6.77E+07	7.51E+07	2.15E+07	8.07E+07	0.00E+00	0.00E+00	7.14E+07	8.29E+07
209	CLK3_HUMAN	4	1.12E+07	1.01E+07	0.00E+00	0.00E+00	0.00E+00	0.00E+00	1.52E+07	9.45E+06
210	HINT1_HUMAN	2	0.00E+00	0.00E+00	4.41E+07	4.17E+07	0.00E+00	0.00E+00	0.00E+00	0.00E+00
211	RBP2_HUMAN	7	0.00E+00	1.02E+07	0.00E+00	1.51E+07	0.00E+00	0.00E+00	0.00E+00	0.00E+00
212	5NTC_HUMAN	5	0.00E+00	1.06E+07	0.00E+00	0.00E+00	0.00E+00	0.00E+00	3.00E+07	2.65E+07
213	MNX1_HUMAN	3	0.00E+00	7.50E+06	0.00E+00	0.00E+00	0.00E+00	0.00E+00	0.00E+00	0.00E+00
214	SERPH_HUMAN	7	0.00E+00	0.00E+00	1.87E+07	2.33E+07	0.00E+00	0.00E+00	1.37E+07	1.81E+07
215	CDK9_HUMAN;sp|(1;1;1;1;1;1;1;		1.46E+08	1.11E+08	8.66E+07	1.08E+08	1.24E+08	1.37E+08	2.56E+07	3.54E+07
216	TCPQ_HUMAN	30	2.60E+08	3.56E+08	2.61E+08	3.20E+08	1.67E+07	4.10E+07	7.34E+08	8.78E+08
217	TCPD_HUMAN	21	1.17E+08	1.57E+08	1.09E+08	1.06E+08	0.00E+00	1.92E+07	2.79E+08	3.83E+08
218	SMCA4_HUMAN;sp	17;7	3.60E+07	3.64E+07	3.41E+07	4.02E+07	0.00E+00	0.00E+00	3.25E+07	3.28E+07
219	MECP2_HUMAN	27	5.75E+08	4.96E+08	7.85E+08	5.13E+08	7.52E+08	5.71E+08	2.51E+08	2.32E+08

id	Protein name	Peptide counts (all)	LFQ intensity _Bait_1	LFQ intensity _Control_1	LFQ intensity_Bait_2	LFQ intensity_Control_2	LFQ intensity_Bait_3	LFQ intensity_Control_3	LFQ intensity_Bait_4	LFQ intensity
220	ROA3_HUMAN	4	0.00E+00	0.00E+00	2.44E+07	0.00E+00	1.21E+07	0.00E+00	0.00E+00	0.00E+00
221	HNRPM_HUMAN	3	7.12E+06	7.93E+06	0.00E+00	0.00E+00	0.00E+00	0.00E+00	0.00E+00	0.00E+00
222	IMA1_HUMAN	4	8.91E+06	9.75E+06	9.79E+06	0.00E+00	0.00E+00	1.01E+07	0.00E+00	9.60E+06
223	TF2AA_HUMAN	5	1.18E+08	1.03E+08	1.50E+08	1.09E+08	2.29E+08	1.59E+08	3.72E+07	4.61E+07
224	T2AG_HUMAN	1	0.00E+00	0.00E+00	0.00E+00	0.00E+00	0.00E+00	1.30E+07	0.00E+00	0.00E+00
225	ZN143_HUMAN	1	0.00E+00	0.00E+00	0.00E+00	0.00E+00	0.00E+00	0.00E+00	0.00E+00	5.95E+06
226	RBM5_HUMAN	3	0.00E+00	0.00E+00	0.00E+00	8.63E+06	0.00E+00	0.00E+00	0.00E+00	0.00E+00
227	CATC_HUMAN	5	0.00E+00	0.00E+00	1.22E+07	0.00E+00	0.00E+00	0.00E+00	1.92E+07	1.99E+07
228	TCP4_HUMAN	5	3.80E+07	2.49E+07	5.31E+07	2.54E+07	6.74E+07	9.01E+07	6.33E+07	4.07E+07
229	BLM_HUMAN	5	1.40E+07	0.00E+00	0.00E+00	0.00E+00	0.00E+00	0.00E+00	0.00E+00	0.00E+00
230	ATN1_HUMAN	11	8.75E+07	7.40E+07	5.01E+07	4.58E+07	1.02E+08	1.03E+08	0.00E+00	0.00E+00
231	P5CS_HUMAN	4	0.00E+00	0.00E+00	0.00E+00	0.00E+00	0.00E+00	0.00E+00	5.34E+06	7.84E+06
232	S12A2_HUMAN	11	5.17E+07	4.93E+07	1.06E+08	8.10E+07	6.98E+07	5.85E+07	5.77E+07	4.85E+07
233	XPO2_HUMAN	3	0.00E+00	0.00E+00	0.00E+00	3.69E+06	0.00E+00	0.00E+00	0.00E+00	0.00E+00
234	MFAP1_HUMAN	7	1.64E+07	1.25E+07	4.57E+07	3.70E+07	1.87E+07	2.97E+07	1.73E+07	1.67E+07
235	SEC13_HUMAN	6	6.08E+07	6.57E+07	0.00E+00	0.00E+00	0.00E+00	0.00E+00	9.40E+07	2.01E+08
236	DLX5_HUMAN;sp|C	3;3;1;1	0.00E+00	1.71E+07	2.90E+07	0.00E+00	3.88E+07	2.52E+07	0.00E+00	0.00E+00
237	MAZ_HUMAN;sp|Q	3;1;1	2.43E+07	2.33E+07	1.74E+07	0.00E+00	0.00E+00	0.00E+00	2.75E+07	1.78E+07
238	ACTG_HUMAN;sp|I	3;13;5;5;4;3;	5.51E+07	9.90E+07	4.95E+07	6.79E+07	3.81E+07	4.04E+07	5.13E+07	4.30E+07
239	PRPS1_HUMAN;sp|	7;3	2.22E+07	2.61E+07	1.55E+07	0.00E+00	0.00E+00	0.00E+00	2.99E+07	3.98E+07
240	MAX_HUMAN	4	0.00E+00	0.00E+00	8.78E+06	7.39E+06	1.02E+07	0.00E+00	8.71E+06	8.26E+06
241	PHS_HUMAN	3	0.00E+00	0.00E+00	2.48E+07	0.00E+00	0.00E+00	0.00E+00	0.00E+00	0.00E+00
242	DCAF7_HUMAN	8	1.98E+08	1.68E+08	7.92E+07	1.07E+08	7.14E+07	1.01E+08	8.96E+07	5.22E+07
243	WDR5_HUMAN	8	7.23E+07	7.40E+07	2.61E+07	1.94E+07	6.87E+07	4.98E+07	0.00E+00	0.00E+00
244	HNRPK_HUMAN	6	1.11E+07	9.86E+06	0.00E+00	0.00E+00	0.00E+00	0.00E+00	0.00E+00	0.00E+00
245	1433G_HUMAN	5	0.00E+00	0.00E+00	0.00E+00	0.00E+00	0.00E+00	0.00E+00	0.00E+00	2.13E+06
246	PP1A_HUMAN	7	5.90E+07	5.57E+07	2.19E+07	2.71E+07	3.29E+07	3.02E+07	2.95E+07	1.98E+07
247	PP1B_HUMAN	5	1.68E+07	1.66E+07	0.00E+00	0.00E+00	0.00E+00	0.00E+00	0.00E+00	0.00E+00
248	1433E_HUMAN;sp|	10;3	2.54E+07	2.48E+07	2.58E+07	3.31E+07	2.85E+07	1.96E+07	3.53E+07	3.95E+07
249	RUXE_HUMAN	2	8.45E+06	0.00E+00	0.00E+00	0.00E+00	0.00E+00	0.00E+00	0.00E+00	0.00E+00
250	RUXF_HUMAN	2	1.14E+07	1.82E+07	2.46E+07	2.54E+07	0.00E+00	0.00E+00	1.24E+07	0.00E+00
251	SMD1_HUMAN	2	2.52E+07	2.47E+07	0.00E+00	3.45E+07	0.00E+00	0.00E+00	0.00E+00	0.00E+00
252	SMD2_HUMAN	3	0.00E+00	0.00E+00	2.22E+07	2.29E+07	0.00E+00	0.00E+00	0.00E+00	0.00E+00
253	SMD3_HUMAN	3	0.00E+00	0.00E+00	4.82E+07	2.31E+07	0.00E+00	0.00E+00	1.83E+07	1.82E+07
254	PRS10_HUMAN	1	0.00E+00	3.55E+06	0.00E+00	0.00E+00	0.00E+00	0.00E+00	0.00E+00	0.00E+00
255	TBPL1_HUMAN	3	2.87E+07	2.80E+07	1.61E+07	1.31E+07	2.43E+07	2.26E+07	2.39E+07	2.78E+07
256	PP2AA_HUMAN;sp|	3;3	0.00E+00	0.00E+00	0.00E+00	0.00E+00	0.00E+00	0.00E+00	1.81E+07	1.55E+07
257	H4_HUMAN	7	3.20E+08	2.98E+08	2.07E+08	2.80E+08	1.55E+08	1.77E+08	1.62E+08	1.78E+08
258	RAB1B_HUMAN;sp	1;1;1	0.00E+00	0.00E+00	0.00E+00	5.80E+06	0.00E+00	0.00E+00	0.00E+00	0.00E+00
259	RS28_HUMAN	2	0.00E+00	0.00E+00	0.00E+00	0.00E+00	2.27E+07	0.00E+00	0.00E+00	0.00E+00
260	TRA2B_HUMAN	5	1.86E+07	2.58E+07	0.00E+00	3.12E+07	2.70E+07	3.24E+07	0.00E+00	0.00E+00
261	1433Z_HUMAN	5	0.00E+00	0.00E+00	0.00E+00	4.72E+06	0.00E+00	0.00E+00	0.00E+00	0.00E+00
262	DYL1_HUMAN;sp|C	4;1	0.00E+00	1.69E+07	0.00E+00	0.00E+00	0.00E+00	0.00E+00	0.00E+00	0.00E+00
263	SKP1_HUMAN	8	3.85E+07	4.75E+07	0.00E+00	4.25E+07	5.45E+07	5.41E+07	0.00E+00	3.58E+07
264	IF5A1_HUMAN;sp|(	5;2;1	1.66E+07	1.62E+07	2.49E+07	0.00E+00	0.00E+00	0.00E+00	0.00E+00	0.00E+00
265	CSK2B_HUMAN	4	3.33E+07	2.96E+07	2.40E+07	0.00E+00	1.87E+07	0.00E+00	0.00E+00	0.00E+00
266	ACTS_HUMAN;sp|P	9;9;8;8	3.17E+07	3.80E+07	0.00E+00	0.00E+00	0.00E+00	0.00E+00	0.00E+00	0.00E+00
267	EF1A3_HUMAN;sp|	7;7;4	6.99E+07	7.90E+07	3.70E+07	6.57E+07	4.04E+07	3.11E+07	6.96E+07	6.50E+07
268	TBA1B_HUMAN;sp|	;19;15;15;11	3.97E+08	5.26E+08	2.52E+08	5.15E+08	1.73E+08	3.09E+08	2.42E+08	3.20E+08
269	TBB4B_HUMAN;sp|	18;12;6	9.23E+07	8.94E+07	8.98E+07	1.16E+08	3.63E+07	0.00E+00	5.44E+07	5.88E+07
270	CSK21_HUMAN;sp|	15;13	1.40E+08	1.54E+08	4.09E+07	6.97E+07	5.01E+07	8.67E+07	6.74E+07	6.14E+07
271	H32_HUMAN;sp|Q	3;3;3;3;2	1.13E+08	1.17E+08	3.50E+07	7.70E+07	3.10E+07	3.13E+07	2.51E+07	1.54E+07
272	TCPB_HUMAN	28	2.02E+08	2.74E+08	1.88E+08	3.09E+08	0.00E+00	3.19E+07	4.51E+08	6.71E+08
273	RT35_HUMAN	1	0.00E+00	0.00E+00	0.00E+00	7.71E+06	0.00E+00	0.00E+00	0.00E+00	0.00E+00
274	RT09_HUMAN	1	0.00E+00	0.00E+00	0.00E+00	0.00E+00	0.00E+00	0.00E+00	2.40E+06	0.00E+00

id	Protein name	Peptide counts (all)	LFQ intensity _Bait_1	LFQ intensity _Control_1	LFQ intensity_Bait_2	LFQ intensity_Control_2	LFQ intensity_Bait_3	LFQ intensity_Control_3	LFQ intensity_Bait_4	LFQ intensity
275	ERH_HUMAN	6	8.63E+07	1.14E+08	2.43E+08	1.66E+08	1.26E+08	9.16E+07	4.91E+07	6.51E+07
276	SRSF3_HUMAN	5	2.85E+07	2.00E+07	6.96E+07	4.55E+07	2.37E+07	0.00E+00	0.00E+00	0.00E+00
277	RBM10_HUMAN	20	1.05E+08	7.29E+07	6.92E+07	9.79E+07	2.34E+07	2.78E+07	2.13E+07	2.64E+07
278	MPCP_HUMAN	1	0.00E+00	0.00E+00	0.00E+00	2.08E+07	0.00E+00	0.00E+00	0.00E+00	0.00E+00
279	HNRPU_HUMAN	6	1.67E+07	1.86E+07	0.00E+00	1.82E+07	2.03E+07	2.21E+07	0.00E+00	1.80E+07
280	AMPD2_HUMAN	2	3.02E+06	0.00E+00	0.00E+00	0.00E+00	0.00E+00	0.00E+00	0.00E+00	0.00E+00
281	TFAP4_HUMAN	1	0.00E+00	0.00E+00	0.00E+00	3.68E+06	0.00E+00	0.00E+00	0.00E+00	0.00E+00
282	OTUD4_HUMAN	2	0.00E+00	4.99E+06	0.00E+00	0.00E+00	0.00E+00	0.00E+00	0.00E+00	0.00E+00
283	PFKAP_HUMAN	4	0.00E+00	0.00E+00	0.00E+00	1.72E+07	0.00E+00	0.00E+00	0.00E+00	0.00E+00
284	SATB1_HUMAN	20	1.03E+08	9.41E+07	5.51E+07	7.38E+07	7.88E+07	5.28E+07	1.91E+08	1.88E+08
285	NUCB1_HUMAN	10	0.00E+00	1.30E+07	5.26E+07	3.12E+07	0.00E+00	0.00E+00	1.04E+07	1.55E+07
286	CREB5_HUMAN	3	9.72E+06	1.06E+07	0.00E+00	0.00E+00	0.00E+00	0.00E+00	0.00E+00	0.00E+00
287	NOTC2_HUMAN	3	0.00E+00	0.00E+00	1.57E+07	1.05E+07	1.25E+07	0.00E+00	0.00E+00	0.00E+00
288	TLE1_HUMAN;sp|Q	11;4;3	6.63E+07	5.92E+07	4.96E+07	0.00E+00	0.00E+00	5.70E+07	1.17E+08	9.27E+07
289	TLE3_HUMAN	18	2.28E+08	2.04E+08	1.76E+08	1.86E+08	2.11E+08	2.33E+08	4.42E+08	3.81E+08
290	PLP2_HUMAN	1	0.00E+00	0.00E+00	0.00E+00	3.26E+06	0.00E+00	0.00E+00	0.00E+00	0.00E+00
291	CSTF1_HUMAN	5	1.72E+07	1.65E+07	0.00E+00	0.00E+00	0.00E+00	0.00E+00	0.00E+00	0.00E+00
292	GFPT1_HUMAN	3	0.00E+00	0.00E+00	0.00E+00	1.44E+07	0.00E+00	0.00E+00	0.00E+00	0.00E+00
293	RING1_HUMAN	5	1.76E+07	1.68E+07	0.00E+00	0.00E+00	0.00E+00	0.00E+00	0.00E+00	0.00E+00
294	PRDX1_HUMAN;sp	4;1	2.35E+07	1.57E+07	0.00E+00	0.00E+00	0.00E+00	0.00E+00	0.00E+00	0.00E+00
295	C1QBP_HUMAN	5	1.77E+07	2.21E+07	3.23E+07	2.01E+07	3.06E+07	0.00E+00	2.57E+07	2.18E+07
296	CKAP4_HUMAN	25	1.80E+08	2.22E+08	8.87E+07	3.51E+08	0.00E+00	1.09E+07	0.00E+00	1.01E+07
297	ZO1_HUMAN	31	5.20E+07	5.72E+07	5.07E+07	5.43E+07	4.04E+07	0.00E+00	2.03E+08	1.63E+08
298	SRSF1_HUMAN	11	3.52E+07	3.87E+07	1.16E+08	6.66E+07	4.77E+07	4.31E+07	0.00E+00	0.00E+00
299	AES_HUMAN	3	3.65E+07	3.35E+07	0.00E+00	0.00E+00	3.43E+07	0.00E+00	9.36E+07	9.57E+07
300	SSRP1_HUMAN	1	2.84E+06	0.00E+00	0.00E+00	0.00E+00	0.00E+00	0.00E+00	0.00E+00	0.00E+00
301	RBBP4_HUMAN	7	0.00E+00	0.00E+00	0.00E+00	0.00E+00	0.00E+00	0.00E+00	0.00E+00	5.59E+06
302	CPSF1_HUMAN	30	9.37E+07	1.14E+08	0.00E+00	1.10E+08	1.86E+07	0.00E+00	3.59E+07	3.58E+07
303	NFIA_HUMAN	4	0.00E+00	0.00E+00	0.00E+00	0.00E+00	0.00E+00	0.00E+00	1.06E+07	1.52E+07
304	SF3A3_HUMAN	32	1.26E+09	1.27E+09	9.37E+08	1.08E+09	9.83E+08	9.86E+08	2.37E+09	2.19E+09
305	ILF3_HUMAN	4	0.00E+00	9.39E+06	0.00E+00	0.00E+00	0.00E+00	0.00E+00	0.00E+00	0.00E+00
306	TAF10_HUMAN	1	0.00E+00	2.58E+06	0.00E+00	0.00E+00	0.00E+00	0.00E+00	0.00E+00	0.00E+00
307	CSTF3_HUMAN	12	4.96E+07	4.16E+07	0.00E+00	3.53E+07	0.00E+00	0.00E+00	4.76E+07	5.22E+07
308	RED_HUMAN	8	0.00E+00	0.00E+00	2.07E+07	2.24E+07	0.00E+00	0.00E+00	1.04E+07	1.00E+07
309	AAPK1_HUMAN;sp|	2;1	0.00E+00	0.00E+00	0.00E+00	0.00E+00	0.00E+00	0.00E+00	0.00E+00	4.35E+06
310	LIPA1_HUMAN;sp|(	19;2;2;1	3.70E+07	3.09E+07	1.04E+07	3.65E+07	3.12E+07	0.00E+00	8.53E+07	1.03E+08
311	GPS2_HUMAN	2	0.00E+00	1.66E+06	0.00E+00	0.00E+00	0.00E+00	0.00E+00	0.00E+00	0.00E+00
312	NDK3_HUMAN	1	0.00E+00	0.00E+00	0.00E+00	0.00E+00	0.00E+00	0.00E+00	0.00E+00	1.72E+06
313	SRSF9_HUMAN	3	0.00E+00	0.00E+00	0.00E+00	1.66E+07	0.00E+00	0.00E+00	0.00E+00	0.00E+00
314	SRSF6_HUMAN;sp|	4;3;1	1.07E+07	0.00E+00	3.53E+07	2.18E+07	0.00E+00	0.00E+00	0.00E+00	0.00E+00
315	TIF1B_HUMAN	4	0.00E+00	1.31E+07	0.00E+00	0.00E+00	0.00E+00	0.00E+00	0.00E+00	0.00E+00
316	PABP4_HUMAN;sp|	20;2	9.55E+07	8.34E+07	6.24E+07	5.98E+07	5.69E+07	7.37E+07	5.56E+07	6.96E+07
317	CTBP1_HUMAN	7	1.25E+07	0.00E+00	1.59E+07	0.00E+00	0.00E+00	0.00E+00	3.72E+07	7.30E+07
318	S39A6_HUMAN	3	0.00E+00	1.26E+07	0.00E+00	1.51E+07	0.00E+00	0.00E+00	0.00E+00	0.00E+00
319	SF3B2_HUMAN	56	2.05E+09	2.11E+09	2.38E+09	2.56E+09	2.17E+09	1.97E+09	1.31E+09	1.35E+09
320	SMAD4_HUMAN	13	2.09E+08	1.94E+08	1.48E+07	8.75E+06	4.39E+07	5.59E+07	2.08E+08	1.29E+08
321	PRP4B_HUMAN	5	1.66E+07	1.72E+07	3.52E+07	2.36E+07	3.43E+07	3.71E+07	1.80E+07	0.00E+00
322	HDAC1_HUMAN;sp	8;1	1.86E+07	1.83E+07	0.00E+00	0.00E+00	0.00E+00	0.00E+00	2.45E+07	0.00E+00
323	SNW1_HUMAN	1	0.00E+00	0.00E+00	0.00E+00	7.07E+06	0.00E+00	0.00E+00	0.00E+00	0.00E+00
324	STIM1_HUMAN	21	5.53E+07	1.43E+08	2.99E+07	1.01E+08	1.11E+07	2.99E+07	2.33E+07	3.61E+07
325	TRA2A_HUMAN	2	1.08E+07	0.00E+00	0.00E+00	0.00E+00	0.00E+00	0.00E+00	0.00E+00	0.00E+00
326	ASPP2_HUMAN	1	2.09E+06	0.00E+00	0.00E+00	0.00E+00	0.00E+00	0.00E+00	0.00E+00	0.00E+00
327	DYR1A_HUMAN;sp	4;1	1.05E+07	1.27E+07	0.00E+00	0.00E+00	0.00E+00	0.00E+00	0.00E+00	0.00E+00
328	FHL1_HUMAN	2	0.00E+00	0.00E+00	3.84E+07	1.72E+07	0.00E+00	0.00E+00	0.00E+00	0.00E+00
329	TBB2B_HUMAN;sp|	14;14;6	0.00E+00	0.00E+00	0.00E+00	0.00E+00	0.00E+00	0.00E+00	0.00E+00	4.87E+06

id	Protein name	Peptide counts (all)	LFQ intensity _Bait_1	LFQ intensity _Control_1	LFQ intensity_Bait_2	LFQ intensity_Control_2	LFQ intensity_Bait_3	LFQ intensity_Control_3	LFQ intensity_Bait_4	LFQ intensity
330	HNRPD_HUMAN	1	0.00E+00	0.00E+00	0.00E+00	0.00E+00	0.00E+00	5.00E+06	0.00E+00	0.00E+00
331	VGLL4_HUMAN	2	0.00E+00	0.00E+00	0.00E+00	0.00E+00	7.54E+06	0.00E+00	0.00E+00	0.00E+00
332	SAFB2_HUMAN	24	4.15E+07	7.13E+07	3.94E+07	5.23E+07	7.77E+07	3.90E+07	1.54E+07	1.59E+07
333	ARHG7_HUMAN;sp	11;2	5.85E+07	7.37E+07	2.01E+07	7.80E+07	0.00E+00	1.73E+07	4.89E+07	4.92E+07
334	UBP2L_HUMAN	16	8.82E+07	9.73E+07	6.06E+07	4.62E+07	5.03E+07	7.26E+07	9.16E+07	1.10E+08
335	GIT2_HUMAN	4	0.00E+00	0.00E+00	0.00E+00	0.00E+00	0.00E+00	0.00E+00	0.00E+00	1.26E+07
336	ELOA1_HUMAN	14	9.37E+07	9.69E+07	1.19E+08	7.54E+07	1.36E+08	9.39E+07	1.08E+08	7.92E+07
337	MAP7_HUMAN	3	0.00E+00	1.00E+07	0.00E+00	0.00E+00	0.00E+00	0.00E+00	0.00E+00	0.00E+00
338	SRC8_HUMAN	24	1.05E+08	1.27E+08	3.09E+08	2.23E+08	2.54E+08	2.23E+08	1.43E+08	1.74E+08
339	RBM39_HUMAN	4	0.00E+00	1.17E+07	0.00E+00	2.69E+07	0.00E+00	0.00E+00	0.00E+00	0.00E+00
340	KPRA_HUMAN	3	0.00E+00	0.00E+00	0.00E+00	0.00E+00	0.00E+00	0.00E+00	0.00E+00	3.30E+06
341	PUM1_HUMAN	2	0.00E+00	0.00E+00	0.00E+00	0.00E+00	0.00E+00	0.00E+00	0.00E+00	4.89E+06
342	GSE1_HUMAN	5	1.46E+07	1.57E+07	1.09E+07	0.00E+00	1.08E+07	1.49E+07	0.00E+00	1.27E+07
343	NFIX_HUMAN	5	2.47E+07	2.88E+07	0.00E+00	0.00E+00	0.00E+00	0.00E+00	0.00E+00	0.00E+00
344	IMB1_HUMAN	4	6.57E+06	9.42E+06	0.00E+00	1.89E+07	0.00E+00	0.00E+00	0.00E+00	0.00E+00
345	FL2D_HUMAN	19	1.27E+08	1.23E+08	1.98E+08	1.81E+08	3.10E+08	2.85E+08	1.41E+08	1.09E+08
346	U5S1_HUMAN	13	1.96E+07	2.53E+07	3.15E+07	2.92E+07	0.00E+00	0.00E+00	0.00E+00	0.00E+00
347	S39AE_HUMAN	3	1.64E+07	2.67E+07	0.00E+00	3.98E+07	2.03E+07	2.26E+07	1.51E+07	2.29E+07
348	PA1B3_HUMAN	8	1.34E+07	1.97E+07	2.56E+07	0.00E+00	0.00E+00	0.00E+00	3.19E+07	3.14E+07
349	NONO_HUMAN;sp|	44;1	9.26E+09	8.39E+09	6.79E+09	6.22E+09	7.98E+09	6.82E+09	2.83E+09	2.60E+09
350	RNPS1_HUMAN	5	4.30E+07	4.82E+07	5.57E+07	0.00E+00	5.71E+07	0.00E+00	0.00E+00	0.00E+00
351	ELOC_HUMAN	4	2.99E+07	3.36E+07	0.00E+00	0.00E+00	0.00E+00	0.00E+00	1.89E+07	1.98E+07
352	ELOB_HUMAN	4	1.47E+07	1.50E+07	0.00E+00	0.00E+00	1.24E+07	0.00E+00	6.04E+06	0.00E+00
353	SF3B3_HUMAN	46	1.04E+09	1.10E+09	8.27E+08	1.11E+09	4.72E+08	5.94E+08	9.09E+08	1.08E+09
354	SAFB1_HUMAN	29	5.25E+08	4.99E+08	6.35E+08	5.82E+08	6.91E+08	6.75E+08	3.49E+08	2.79E+08
355	SF3B4_HUMAN	9	5.10E+08	4.62E+08	5.54E+08	4.82E+08	5.09E+08	7.63E+08	2.37E+08	2.12E+08
356	SF3A2_HUMAN	18	5.24E+08	5.22E+08	5.47E+08	4.93E+08	5.05E+08	5.64E+08	7.59E+08	7.05E+08
357	SC23A_HUMAN	5	0.00E+00	9.28E+06	0.00E+00	0.00E+00	0.00E+00	0.00E+00	0.00E+00	1.44E+07
358	SC23B_HUMAN	7	1.05E+07	1.47E+07	0.00E+00	0.00E+00	0.00E+00	0.00E+00	2.12E+07	1.42E+07
359	SF3A1_HUMAN	40	2.03E+09	1.85E+09	1.67E+09	1.62E+09	1.55E+09	1.50E+09	3.34E+09	3.22E+09
360	NHRF2_HUMAN	11	1.73E+07	3.03E+07	1.65E+08	5.40E+07	6.89E+07	3.09E+07	5.34E+07	4.09E+07
361	SF01_HUMAN;sp|B	20;1	1.39E+09	1.35E+09	1.66E+09	1.43E+09	1.98E+09	2.05E+09	1.71E+09	1.69E+09
362	MED1_HUMAN	2	0.00E+00	0.00E+00	0.00E+00	0.00E+00	0.00E+00	0.00E+00	0.00E+00	1.23E+06
363	JHD2C_HUMAN	6	1.13E+07	6.81E+06	0.00E+00	0.00E+00	2.14E+07	1.30E+07	0.00E+00	0.00E+00
364	PTN14_HUMAN	1	2.94E+06	0.00E+00	0.00E+00	0.00E+00	0.00E+00	0.00E+00	0.00E+00	0.00E+00
365	T22D1_HUMAN	7	7.10E+06	0.00E+00	0.00E+00	5.64E+06	0.00E+00	0.00E+00	0.00E+00	0.00E+00
366	ELAV1_HUMAN;sp|	9;1;1	9.87E+07	8.81E+07	1.27E+08	1.30E+08	0.00E+00	3.01E+07	1.42E+08	1.17E+08
367	DDB1_HUMAN	1	0.00E+00	0.00E+00	0.00E+00	0.00E+00	0.00E+00	0.00E+00	0.00E+00	3.02E+06
368	RBBP7_HUMAN	9	2.46E+07	3.16E+07	0.00E+00	0.00E+00	0.00E+00	0.00E+00	2.93E+07	2.80E+07
369	SRSF7_HUMAN	9	7.90E+07	9.37E+07	1.92E+08	1.66E+08	1.08E+08	9.05E+07	0.00E+00	2.97E+07
370	CPSF6_HUMAN	12	2.98E+08	2.99E+08	2.65E+08	2.43E+08	2.40E+08	2.49E+08	4.87E+08	4.51E+08
371	CPEB4_HUMAN	1	0.00E+00	0.00E+00	0.00E+00	0.00E+00	2.62E+06	0.00E+00	0.00E+00	0.00E+00
372	TYSD1_HUMAN	10	2.62E+07	3.26E+07	2.90E+07	2.86E+07	0.00E+00	0.00E+00	2.84E+07	2.97E+07
373	SMU1_HUMAN	9	2.61E+07	3.49E+07	3.37E+07	2.80E+07	0.00E+00	0.00E+00	2.48E+07	2.47E+07
374	LSM12_HUMAN	5	4.86E+07	4.62E+07	4.59E+07	3.96E+07	6.84E+07	9.81E+07	6.66E+07	5.16E+07
375	TIM50_HUMAN	5	0.00E+00	1.16E+07	0.00E+00	1.38E+07	0.00E+00	0.00E+00	0.00E+00	0.00E+00
376	LARP7_HUMAN	18	1.62E+08	1.59E+08	6.50E+07	8.10E+07	7.63E+07	1.16E+08	1.59E+08	1.49E+08
377	BCL7A_HUMAN;sp|	2;1;1	7.27E+06	0.00E+00	0.00E+00	0.00E+00	0.00E+00	0.00E+00	0.00E+00	0.00E+00
378	AMOT_HUMAN;sp|	37;3	8.49E+07	4.57E+08	7.45E+07	3.69E+08	6.38E+07	3.08E+08	0.00E+00	5.32E+07
379	CRTC2_HUMAN	4	2.21E+07	2.47E+07	2.58E+07	0.00E+00	0.00E+00	0.00E+00	0.00E+00	0.00E+00
380	P5CR3_HUMAN	7	9.36E+07	7.26E+07	4.20E+07	3.51E+07	6.11E+07	7.11E+07	5.90E+07	5.50E+07
381	SWAHC_HUMAN	3	0.00E+00	0.00E+00	0.00E+00	0.00E+00	0.00E+00	0.00E+00	2.56E+06	0.00E+00
382	ACTBL_HUMAN	3	0.00E+00	0.00E+00	0.00E+00	0.00E+00	0.00E+00	0.00E+00	3.08E+07	0.00E+00
383	RIPL1_HUMAN	2	0.00E+00	0.00E+00	0.00E+00	0.00E+00	0.00E+00	0.00E+00	0.00E+00	3.42E+06
384	FA76B_HUMAN	2	1.08E+07	0.00E+00	0.00E+00	0.00E+00	0.00E+00	0.00E+00	0.00E+00	0.00E+00

id	Protein name	Peptide counts (all)	LFQ intensity _Bait_1	LFQ intensity _Control_1	LFQ intensity_Bait_2	LFQ intensity_Control_2	LFQ intensity_Bait_3	LFQ intensity_Control_3	LFQ intensity_Bait_4	LFQ intensity
385	TJAP1_HUMAN	7	1.15E+07	1.54E+07	2.11E+07	2.29E+07	4.69E+07	2.60E+07	2.27E+07	2.22E+07
386	BRM1L_HUMAN	1	0.00E+00	0.00E+00	0.00E+00	0.00E+00	0.00E+00	5.84E+06	0.00E+00	0.00E+00
387	SYVM_HUMAN	9	0.00E+00	0.00E+00	0.00E+00	0.00E+00	0.00E+00	0.00E+00	9.60E+06	7.05E+06
388	CE170_HUMAN;sp|	48;2;2	2.24E+08	2.03E+08	1.91E+08	2.09E+08	2.85E+08	2.16E+08	3.00E+08	2.66E+08
389	FBP1L_HUMAN	11	1.45E+07	0.00E+00	1.41E+07	1.26E+07	6.69E+06	0.00E+00	8.26E+07	6.09E+07
390	ZC3HD_HUMAN	17	2.18E+07	3.96E+07	2.31E+07	2.46E+07	2.56E+07	0.00E+00	1.28E+07	1.34E+07
391	UBAP2_HUMAN	13	5.67E+07	6.67E+07	9.02E+07	7.15E+07	9.34E+07	1.14E+08	8.38E+07	8.55E+07
392	MRCKA_HUMAN	1	6.26E+06	0.00E+00	0.00E+00	0.00E+00	0.00E+00	0.00E+00	0.00E+00	0.00E+00
393	RPRD2_HUMAN	14	3.27E+07	3.61E+07	5.58E+07	4.41E+07	0.00E+00	3.55E+07	5.38E+07	4.43E+07
394	PR38B_HUMAN	1	0.00E+00	0.00E+00	0.00E+00	0.00E+00	0.00E+00	0.00E+00	0.00E+00	1.90E+06
395	BRE1A_HUMAN	21	4.68E+07	5.54E+07	2.95E+07	4.14E+07	4.89E+07	4.30E+07	2.50E+07	3.05E+07
396	ZN318_HUMAN	1	0.00E+00	0.00E+00	0.00E+00	0.00E+00	0.00E+00	0.00E+00	0.00E+00	4.16E+06
397	RSBN1_HUMAN	3	0.00E+00	0.00E+00	0.00E+00	0.00E+00	0.00E+00	0.00E+00	0.00E+00	3.32E+06
398	CP135_HUMAN	9	2.62E+07	2.71E+07	0.00E+00	0.00E+00	0.00E+00	0.00E+00	0.00E+00	0.00E+00
399	INT3_HUMAN	4	0.00E+00	1.32E+07	0.00E+00	0.00E+00	0.00E+00	0.00E+00	1.27E+07	0.00E+00
400	RHG17_HUMAN;sp	10;1	0.00E+00	0.00E+00	1.00E+07	8.33E+06	0.00E+00	0.00E+00	2.61E+07	3.51E+07
401	VIR_HUMAN	28	9.24E+07	9.97E+07	2.31E+07	6.61E+07	5.72E+07	6.54E+07	7.24E+07	7.02E+07
402	NADE_HUMAN	1	0.00E+00	0.00E+00	0.00E+00	0.00E+00	0.00E+00	0.00E+00	0.00E+00	2.49E+06
403	ELP2_HUMAN	1	0.00E+00	0.00E+00	0.00E+00	0.00E+00	0.00E+00	0.00E+00	0.00E+00	1.49E+06
404	GLYAT_HUMAN	1	4.17E+06	0.00E+00	0.00E+00	0.00E+00	0.00E+00	0.00E+00	0.00E+00	0.00E+00
405	NIPBL_HUMAN	16	2.41E+07	2.37E+07	2.30E+07	2.46E+07	0.00E+00	0.00E+00	3.79E+07	3.73E+07
406	HMBX1_HUMAN	3	9.05E+06	0.00E+00	0.00E+00	0.00E+00	0.00E+00	0.00E+00	0.00E+00	1.17E+07
407	ARMC6_HUMAN	6	0.00E+00	0.00E+00	0.00E+00	1.74E+07	0.00E+00	0.00E+00	0.00E+00	1.52E+07
408	CDC73_HUMAN	18	7.85E+07	8.39E+07	4.60E+07	3.83E+07	5.63E+07	5.50E+07	0.00E+00	7.43E+06
409	TAF2_HUMAN	1	0.00E+00	0.00E+00	0.00E+00	0.00E+00	0.00E+00	9.05E+06	0.00E+00	0.00E+00
410	CEP85_HUMAN	3	0.00E+00	0.00E+00	0.00E+00	0.00E+00	0.00E+00	0.00E+00	1.29E+07	1.40E+07
411	PRP8_HUMAN	13	0.00E+00	1.52E+07	2.43E+07	3.32E+07	0.00E+00	0.00E+00	0.00E+00	0.00E+00
412	ANR16_HUMAN	4	0.00E+00	0.00E+00	0.00E+00	0.00E+00	0.00E+00	0.00E+00	1.88E+07	1.88E+07
413	RSBNL_HUMAN	3	0.00E+00	0.00E+00	0.00E+00	0.00E+00	0.00E+00	0.00E+00	6.75E+06	0.00E+00
414	CTR9_HUMAN	8	5.12E+07	4.15E+07	0.00E+00	0.00E+00	3.77E+07	0.00E+00	0.00E+00	0.00E+00
415	SARM1_HUMAN	12	2.51E+07	2.93E+07	0.00E+00	0.00E+00	0.00E+00	0.00E+00	7.24E+07	6.72E+07
416	FIP1_HUMAN	13	1.86E+08	2.31E+08	2.72E+08	3.37E+08	2.66E+08	2.62E+08	1.83E+08	1.88E+08
417	CRTC3_HUMAN	1	0.00E+00	3.34E+06	0.00E+00	0.00E+00	0.00E+00	0.00E+00	0.00E+00	0.00E+00
418	WDR82_HUMAN	9	1.49E+08	1.13E+08	7.03E+06	1.62E+07	2.15E+07	1.51E+07	0.00E+00	1.00E+07
419	DPP8_HUMAN	1	0.00E+00	0.00E+00	0.00E+00	0.00E+00	0.00E+00	0.00E+00	3.16E+07	0.00E+00
420	QSOX2_HUMAN	4	0.00E+00	0.00E+00	5.60E+06	1.36E+07	0.00E+00	0.00E+00	0.00E+00	0.00E+00
421	SRCAP_HUMAN	2	0.00E+00	0.00E+00	0.00E+00	0.00E+00	0.00E+00	0.00E+00	0.00E+00	7.03E+06
422	PAXI1_HUMAN	2	0.00E+00	0.00E+00	0.00E+00	0.00E+00	0.00E+00	0.00E+00	5.23E+06	0.00E+00
423	UBP30_HUMAN	2	0.00E+00	0.00E+00	0.00E+00	8.04E+06	0.00E+00	0.00E+00	0.00E+00	0.00E+00
424	HAKAI_HUMAN	8	6.39E+07	5.70E+07	5.39E+07	5.21E+07	7.29E+07	6.89E+07	0.00E+00	0.00E+00
425	DHX30_HUMAN	14	1.74E+07	2.78E+07	0.00E+00	0.00E+00	0.00E+00	0.00E+00	0.00E+00	1.67E+07
426	MEPCE_HUMAN	18	1.53E+08	1.63E+08	6.01E+07	7.81E+07	8.03E+07	9.05E+07	7.32E+07	9.68E+07
427	CYFP1_HUMAN;sp|	20;8	2.67E+07	2.31E+07	8.51E+06	0.00E+00	0.00E+00	0.00E+00	1.51E+08	1.54E+08
428	TAOK1_HUMAN;sp	6;1;1	0.00E+00	0.00E+00	0.00E+00	0.00E+00	0.00E+00	0.00E+00	1.90E+07	1.47E+07
429	PHF5A_HUMAN	4	6.37E+07	6.81E+07	1.09E+08	9.64E+07	1.19E+08	9.51E+07	3.27E+07	4.43E+07
430	ATG9A_HUMAN	2	0.00E+00	0.00E+00	0.00E+00	9.38E+06	0.00E+00	0.00E+00	0.00E+00	0.00E+00
431	NUFP2_HUMAN	21	1.25E+08	1.40E+08	9.27E+07	1.33E+08	1.54E+08	1.81E+08	5.90E+07	5.20E+07
432	RAI1_HUMAN	3	0.00E+00	6.48E+06	0.00E+00	0.00E+00	0.00E+00	0.00E+00	0.00E+00	0.00E+00
433	I2BP2_HUMAN	12	7.99E+07	7.88E+07	9.91E+07	5.79E+07	5.60E+07	0.00E+00	8.03E+07	9.85E+07
434	PCGF5_HUMAN	2	1.07E+07	6.50E+06	0.00E+00	0.00E+00	8.48E+06	0.00E+00	0.00E+00	0.00E+00
435	PEG10_HUMAN	13	3.89E+08	3.06E+08	2.73E+08	2.60E+08	3.48E+08	3.39E+08	4.27E+08	3.75E+08
436	DPP9_HUMAN	30	3.22E+08	3.18E+08	1.57E+08	1.77E+08	1.49E+08	1.39E+08	4.88E+08	3.99E+08
437	NAA40_HUMAN	1	1.79E+06	0.00E+00	0.00E+00	0.00E+00	0.00E+00	0.00E+00	0.00E+00	0.00E+00
438	THOC4_HUMAN	5	0.00E+00	0.00E+00	2.74E+07	0.00E+00	4.85E+07	3.03E+07	0.00E+00	0.00E+00
439	NALP8_HUMAN	1	0.00E+00	0.00E+00	0.00E+00	0.00E+00	0.00E+00	0.00E+00	7.95E+06	0.00E+00

id	Protein name	Peptide counts (all)	LFQ intensity _Bait_1	LFQ intensity _Control_1	LFQ intensity_Bait_2	LFQ intensity_Control_2	LFQ intensity_Bait_3	LFQ intensity_Control_3	LFQ intensity_Bait_4	LFQ intensity
440	CARM1_HUMAN	21	3.19E+08	3.12E+08	1.80E+08	1.77E+08	1.60E+08	1.87E+08	8.06E+08	6.58E+08
441	DDX42_HUMAN	45	1.23E+09	1.05E+09	9.40E+08	7.87E+08	1.07E+09	1.13E+09	8.11E+08	5.73E+08
442	HOME1_HUMAN	8	0.00E+00	0.00E+00	0.00E+00	0.00E+00	0.00E+00	0.00E+00	4.38E+07	4.28E+07
443	I2BP1_HUMAN	3	0.00E+00	0.00E+00	0.00E+00	0.00E+00	0.00E+00	0.00E+00	0.00E+00	1.16E+07
444	RB6I2_HUMAN	1	0.00E+00	0.00E+00	0.00E+00	0.00E+00	0.00E+00	0.00E+00	0.00E+00	1.25E+06
445	RELL1_HUMAN	1	0.00E+00	2.58E+06	0.00E+00	0.00E+00	0.00E+00	0.00E+00	0.00E+00	0.00E+00
446	PLD3_HUMAN	6	4.14E+07	0.00E+00	4.08E+07	5.08E+07	3.19E+07	0.00E+00	9.97E+07	8.90E+07
447	CCD50_HUMAN	8	2.77E+07	3.22E+07	6.50E+07	4.08E+07	9.14E+07	7.49E+07	6.48E+07	6.75E+07
448	FABD_HUMAN	11	1.51E+08	1.14E+08	9.67E+07	5.98E+07	8.19E+07	6.78E+07	1.44E+08	1.17E+08
449	PHF6_HUMAN	1	0.00E+00	0.00E+00	0.00E+00	0.00E+00	0.00E+00	0.00E+00	0.00E+00	3.13E+06
450	CHERP_HUMAN	24	5.01E+08	4.89E+08	4.06E+08	4.91E+08	3.85E+08	3.90E+08	2.87E+08	3.07E+08
451	SUGP1_HUMAN	5	0.00E+00	1.00E+07	0.00E+00	0.00E+00	0.00E+00	0.00E+00	0.00E+00	0.00E+00
452	DHX40_HUMAN	4	0.00E+00	0.00E+00	0.00E+00	0.00E+00	0.00E+00	0.00E+00	1.44E+07	1.66E+07
453	DJC10_HUMAN	13	1.03E+08	1.08E+08	0.00E+00	5.66E+07	2.83E+07	6.06E+07	7.12E+07	7.79E+07
454	SMC5_HUMAN	14	6.63E+07	0.00E+00	2.81E+07	0.00E+00	1.89E+07	0.00E+00	5.30E+07	0.00E+00
455	RAVR1_HUMAN	5	2.81E+07	4.58E+07	0.00E+00	0.00E+00	0.00E+00	0.00E+00	0.00E+00	0.00E+00
456	P20D2_HUMAN	20	1.22E+09	1.16E+09	7.10E+08	6.53E+08	6.79E+08	8.18E+08	3.70E+08	4.28E+08
457	DCP1B_HUMAN	1	0.00E+00	0.00E+00	0.00E+00	0.00E+00	0.00E+00	0.00E+00	0.00E+00	1.10E+07
458	XRN1_HUMAN	9	1.37E+07	1.38E+07	0.00E+00	0.00E+00	0.00E+00	0.00E+00	1.43E+07	1.29E+07
459	ABI1_HUMAN;sp|Q	8;2	0.00E+00	0.00E+00	3.30E+07	0.00E+00	0.00E+00	0.00E+00	5.48E+07	4.44E+07
460	ZN444_HUMAN	3	1.70E+07	1.45E+07	0.00E+00	0.00E+00	0.00E+00	0.00E+00	0.00E+00	0.00E+00
461	CCAR2_HUMAN	27	2.49E+08	2.34E+08	1.23E+08	1.50E+08	9.38E+07	1.14E+08	1.62E+08	1.74E+08
462	NUP93_HUMAN	2	0.00E+00	1.15E+07	0.00E+00	0.00E+00	0.00E+00	0.00E+00	0.00E+00	0.00E+00
463	CMTR1_HUMAN	22	1.01E+08	8.21E+07	1.50E+07	1.56E+07	2.05E+07	1.09E+07	1.45E+08	9.02E+07
464	ASCC3_HUMAN	11	0.00E+00	0.00E+00	0.00E+00	0.00E+00	0.00E+00	0.00E+00	3.01E+07	2.14E+07
465	D2HDH_HUMAN	5	1.06E+07	9.40E+06	0.00E+00	0.00E+00	0.00E+00	0.00E+00	0.00E+00	0.00E+00
466	MMGT1_HUMAN	1	0.00E+00	0.00E+00	0.00E+00	7.95E+06	0.00E+00	0.00E+00	0.00E+00	0.00E+00
467	CPSF7_HUMAN	20	8.14E+08	6.14E+08	7.89E+08	5.90E+08	9.82E+08	6.91E+08	1.07E+09	9.20E+08
468	PAF1_HUMAN	18	1.21E+08	1.30E+08	7.48E+07	7.58E+07	1.35E+08	1.32E+08	1.70E+07	1.92E+07
469	GPT11_HUMAN	5	1.74E+07	0.00E+00	3.79E+07	2.36E+07	4.21E+07	3.42E+07	0.00E+00	0.00E+00
470	ASCC1_HUMAN	2	0.00E+00	0.00E+00	0.00E+00	0.00E+00	0.00E+00	0.00E+00	2.26E+07	1.95E+07
471	PR38A_HUMAN	3	0.00E+00	0.00E+00	0.00E+00	0.00E+00	0.00E+00	0.00E+00	1.34E+07	0.00E+00
472	XXLT1_HUMAN	2	5.04E+06	5.90E+06	0.00E+00	0.00E+00	0.00E+00	0.00E+00	0.00E+00	0.00E+00
473	PAIRB_HUMAN	4	0.00E+00	0.00E+00	1.20E+07	0.00E+00	0.00E+00	0.00E+00	0.00E+00	0.00E+00
474	FA98A_HUMAN	8	1.29E+08	1.33E+08	4.57E+07	5.73E+07	3.29E+07	5.68E+07	9.39E+07	1.03E+08
475	SMG8_HUMAN	4	0.00E+00	9.76E+06	0.00E+00	0.00E+00	0.00E+00	0.00E+00	0.00E+00	0.00E+00
476	RB15B_HUMAN	6	1.35E+07	1.34E+07	0.00E+00	0.00E+00	0.00E+00	0.00E+00	0.00E+00	0.00E+00
477	ARI1B_HUMAN	7	1.77E+07	1.59E+07	1.27E+07	1.36E+07	2.66E+07	0.00E+00	0.00E+00	0.00E+00
478	MCFD2_HUMAN	2	4.30E+07	7.85E+07	0.00E+00	1.77E+08	0.00E+00	0.00E+00	0.00E+00	0.00E+00
479	SNIP1_HUMAN	4	8.20E+06	0.00E+00	0.00E+00	0.00E+00	0.00E+00	0.00E+00	0.00E+00	0.00E+00
480	SMRC2_HUMAN	21	9.08E+07	8.68E+07	4.08E+07	6.98E+07	3.57E+07	3.99E+07	4.40E+07	6.74E+07
481	FA76A_HUMAN	2	0.00E+00	0.00E+00	0.00E+00	0.00E+00	0.00E+00	8.38E+06	0.00E+00	0.00E+00
482	SHKB1_HUMAN	9	2.40E+07	3.16E+07	0.00E+00	0.00E+00	0.00E+00	0.00E+00	4.29E+07	4.20E+07
483	TBC15_HUMAN	2	0.00E+00	0.00E+00	0.00E+00	4.87E+06	0.00E+00	0.00E+00	0.00E+00	0.00E+00
484	RPGF6_HUMAN;sp|	7;2	0.00E+00	0.00E+00	0.00E+00	0.00E+00	0.00E+00	0.00E+00	2.59E+07	2.34E+07
485	PARD3_HUMAN	4	0.00E+00	0.00E+00	0.00E+00	0.00E+00	0.00E+00	0.00E+00	0.00E+00	5.57E+06
486	PPIL4_HUMAN	20	1.62E+08	1.39E+08	1.60E+08	1.32E+08	1.47E+08	1.60E+08	2.26E+08	1.83E+08
487	BRK1_HUMAN	2	0.00E+00	7.15E+06	0.00E+00	0.00E+00	0.00E+00	0.00E+00	1.13E+07	1.04E+07
488	NSE1_HUMAN	4	1.80E+07	0.00E+00	0.00E+00	0.00E+00	0.00E+00	0.00E+00	0.00E+00	0.00E+00
489	LEO1_HUMAN	8	5.69E+07	5.71E+07	2.66E+07	3.85E+07	9.99E+07	5.41E+07	0.00E+00	0.00E+00
490	PCNP_HUMAN	8	7.58E+07	7.98E+07	1.38E+08	1.15E+08	1.09E+08	7.95E+07	3.00E+07	4.03E+07
491	ATX2L_HUMAN	38	6.17E+08	5.43E+08	7.37E+08	5.60E+08	1.01E+09	7.07E+08	7.63E+08	6.32E+08
492	PALLD_HUMAN	2	0.00E+00	0.00E+00	7.20E+06	0.00E+00	0.00E+00	0.00E+00	0.00E+00	0.00E+00
493	PSPC1_HUMAN	32	2.24E+09	1.94E+09	1.66E+09	1.41E+09	2.07E+09	1.67E+09	1.08E+09	1.05E+09
494	AUTS2_HUMAN	9	5.61E+07	3.91E+07	0.00E+00	0.00E+00	0.00E+00	0.00E+00	0.00E+00	0.00E+00

id	Protein name	Peptide counts (all)	LFQ intensity _Bait_1	LFQ intensity _Control_1	LFQ intensity_Bait_2	LFQ intensity_Control_2	LFQ intensity_Bait_3	LFQ intensity_Control_3	LFQ intensity_Bait_4	LFQ intensity
495	DGCR8_HUMAN	5	0.00E+00	0.00E+00	0.00E+00	0.00E+00	0.00E+00	0.00E+00	2.18E+07	2.84E+07
496	DDX1_HUMAN	30	3.14E+08	3.52E+08	1.58E+08	1.07E+08	1.86E+08	3.26E+08	2.81E+08	3.81E+08
497	S39A7_HUMAN	1	0.00E+00	0.00E+00	0.00E+00	1.99E+07	0.00E+00	0.00E+00	0.00E+00	0.00E+00
498	WASF1_HUMAN	4	0.00E+00	0.00E+00	0.00E+00	0.00E+00	0.00E+00	0.00E+00	1.12E+07	0.00E+00
499	PHF3_HUMAN	15	4.36E+07	3.60E+07	3.96E+07	3.16E+07	2.70E+07	0.00E+00	3.21E+07	3.73E+07
500	CNOT9_HUMAN	1	0.00E+00	0.00E+00	0.00E+00	0.00E+00	0.00E+00	0.00E+00	0.00E+00	2.00E+06
501	HDAC2_HUMAN	10	3.27E+07	4.81E+07	2.48E+07	3.77E+07	2.18E+07	0.00E+00	3.29E+07	3.79E+07
502	REQU_HUMAN	1	0.00E+00	4.70E+06	0.00E+00	0.00E+00	0.00E+00	0.00E+00	0.00E+00	0.00E+00
503	DDX17_HUMAN	4	8.85E+06	0.00E+00	0.00E+00	8.23E+06	0.00E+00	0.00E+00	0.00E+00	0.00E+00
504	GATA6_HUMAN;sp	5;1	3.97E+07	3.54E+07	3.48E+07	2.74E+07	0.00E+00	5.67E+07	0.00E+00	0.00E+00
505	SMRC1_HUMAN	18	2.81E+07	2.85E+07	0.00E+00	2.80E+07	0.00E+00	0.00E+00	2.63E+07	3.36E+07
506	SMRD2_HUMAN	5	1.68E+07	1.58E+07	0.00E+00	0.00E+00	0.00E+00	0.00E+00	0.00E+00	0.00E+00
507	DVL3_HUMAN;sp|(	5;2;1;1	1.22E+07	1.27E+07	0.00E+00	0.00E+00	0.00E+00	0.00E+00	1.73E+07	1.68E+07
508	USP9X_HUMAN;sp|	65;28	3.77E+08	4.72E+08	2.25E+08	2.91E+08	2.33E+08	1.88E+08	8.06E+08	7.28E+08
509	UBP7_HUMAN	33	1.16E+08	1.08E+08	9.04E+07	4.64E+07	3.26E+07	1.81E+07	3.08E+08	2.81E+08
510	SMCE1_HUMAN	7	2.93E+07	1.69E+07	1.81E+07	2.45E+07	2.59E+07	0.00E+00	1.65E+07	1.51E+07
511	ERGI1_HUMAN	4	0.00E+00	1.94E+07	0.00E+00	2.26E+07	0.00E+00	0.00E+00	0.00E+00	0.00E+00
512	LRC59_HUMAN	4	0.00E+00	0.00E+00	0.00E+00	2.69E+07	0.00E+00	1.40E+07	0.00E+00	0.00E+00
513	PBIP1_HUMAN	6	1.41E+07	0.00E+00	0.00E+00	2.79E+07	0.00E+00	0.00E+00	0.00E+00	0.00E+00
514	PINX1_HUMAN	4	0.00E+00	8.29E+06	0.00E+00	0.00E+00	0.00E+00	0.00E+00	0.00E+00	0.00E+00
515	SEH1_HUMAN	2	0.00E+00	5.39E+06	0.00E+00	0.00E+00	0.00E+00	0.00E+00	0.00E+00	0.00E+00
516	F120B_HUMAN	11	0.00E+00	1.73E+07	0.00E+00	0.00E+00	0.00E+00	0.00E+00	5.06E+07	3.91E+07
517	RBM33_HUMAN	23	2.88E+08	2.98E+08	1.72E+08	1.24E+08	3.82E+08	2.43E+08	1.86E+07	2.37E+07
518	CCD97_HUMAN	8	2.99E+07	3.66E+07	3.47E+07	2.47E+07	3.69E+07	5.05E+07	0.00E+00	2.67E+07
519	EDC3_HUMAN	13	4.14E+07	4.01E+07	2.38E+07	2.96E+07	0.00E+00	0.00E+00	5.15E+07	7.04E+07
520	BICD1_HUMAN	2	0.00E+00	0.00E+00	0.00E+00	0.00E+00	0.00E+00	0.00E+00	0.00E+00	1.08E+07
521	AURKB_HUMAN	3	1.64E+07	1.69E+07	0.00E+00	0.00E+00	0.00E+00	0.00E+00	0.00E+00	0.00E+00
522	SMRD1_HUMAN;sp	4;1	0.00E+00	0.00E+00	0.00E+00	0.00E+00	0.00E+00	0.00E+00	6.09E+06	4.54E+06
523	NAF1_HUMAN	1	0.00E+00	0.00E+00	0.00E+00	0.00E+00	0.00E+00	0.00E+00	4.08E+06	0.00E+00
524	DHTK1_HUMAN	6	0.00E+00	0.00E+00	0.00E+00	0.00E+00	0.00E+00	0.00E+00	2.29E+07	2.83E+07
525	SCLY_HUMAN	15	8.47E+07	9.43E+07	6.29E+07	4.76E+07	4.50E+07	5.22E+07	2.01E+08	2.02E+08
526	SPF45_HUMAN	20	2.91E+08	3.27E+08	2.74E+08	3.80E+08	3.19E+08	2.84E+08	1.56E+08	2.05E+08
527	ASPP1_HUMAN	2	0.00E+00	7.72E+06	0.00E+00	0.00E+00	0.00E+00	0.00E+00	0.00E+00	0.00E+00
528	NSE2_HUMAN	4	0.00E+00	0.00E+00	0.00E+00	0.00E+00	1.13E+07	0.00E+00	0.00E+00	0.00E+00
529	NSE3_HUMAN	11	3.41E+07	0.00E+00	4.41E+07	0.00E+00	4.57E+07	0.00E+00	2.80E+07	0.00E+00
530	DOCK7_HUMAN;sp	37;2;2	1.56E+08	1.52E+08	6.54E+07	9.06E+07	7.82E+07	6.61E+07	3.81E+07	4.38E+07
531	RPR1A_HUMAN	3	0.00E+00	0.00E+00	0.00E+00	1.74E+07	0.00E+00	0.00E+00	0.00E+00	0.00E+00
532	PP1RA_HUMAN	33	5.33E+08	2.65E+08	2.65E+08	2.21E+08	3.94E+08	4.83E+08	0.00E+00	1.53E+07
533	MAGI1_HUMAN	3	0.00E+00	0.00E+00	0.00E+00	0.00E+00	0.00E+00	0.00E+00	1.08E+07	0.00E+00
534	ERGI2_HUMAN	4	2.03E+07	2.32E+07	0.00E+00	3.05E+07	0.00E+00	0.00E+00	0.00E+00	2.46E+07
535	NUDC1_HUMAN	8	1.47E+07	0.00E+00	0.00E+00	0.00E+00	0.00E+00	0.00E+00	4.75E+07	0.00E+00
536	ERBIN_HUMAN	2	0.00E+00	4.49E+06	0.00E+00	0.00E+00	0.00E+00	0.00E+00	0.00E+00	0.00E+00
537	WRIP1_HUMAN	6	0.00E+00	0.00E+00	0.00E+00	0.00E+00	0.00E+00	0.00E+00	0.00E+00	2.22E+07
538	SMC6_HUMAN	24	1.16E+08	0.00E+00	7.15E+07	0.00E+00	4.49E+07	0.00E+00	6.78E+07	0.00E+00
539	SIN3A_HUMAN	24	1.86E+08	1.75E+08	1.92E+08	1.88E+08	1.66E+08	1.53E+08	1.85E+08	1.77E+08
540	OSBL9_HUMAN	5	1.28E+07	2.22E+07	0.00E+00	1.54E+07	0.00E+00	0.00E+00	8.81E+06	9.23E+06
541	INT14_HUMAN	3	0.00E+00	8.89E+06	0.00E+00	0.00E+00	0.00E+00	0.00E+00	0.00E+00	0.00E+00
542	ZIC5_HUMAN	3	0.00E+00	0.00E+00	0.00E+00	0.00E+00	0.00E+00	0.00E+00	0.00E+00	3.01E+06
543	RBM15_HUMAN	11	3.54E+07	3.64E+07	0.00E+00	0.00E+00	0.00E+00	0.00E+00	0.00E+00	0.00E+00
544	RUFY1_HUMAN	4	0.00E+00	0.00E+00	0.00E+00	0.00E+00	0.00E+00	0.00E+00	0.00E+00	1.11E+07
545	MINT_HUMAN	8	1.21E+07	0.00E+00	0.00E+00	0.00E+00	0.00E+00	0.00E+00	1.98E+07	2.64E+07
546	HTF4_HUMAN	4	0.00E+00	4.28E+06	0.00E+00	0.00E+00	0.00E+00	0.00E+00	0.00E+00	0.00E+00
547	MYCBP_HUMAN	2	0.00E+00	0.00E+00	0.00E+00	0.00E+00	0.00E+00	0.00E+00	0.00E+00	4.33E+06
548	NELL2_HUMAN	2	0.00E+00	5.03E+06	0.00E+00	0.00E+00	0.00E+00	0.00E+00	0.00E+00	0.00E+00
549	RING2_HUMAN	6	4.24E+07	4.03E+07	0.00E+00	0.00E+00	0.00E+00	0.00E+00	0.00E+00	0.00E+00

id	Protein name	Peptide counts (all)	LFQ intensity _Bait_1	LFQ intensity _Control_1	LFQ intensity_Bait_2	LFQ intensity_Control_2	LFQ intensity_Bait_3	LFQ intensity_Control_3	LFQ intensity_Bait_4	LFQ intensity
550	LGMN_HUMAN	3	1.92E+07	2.50E+07	2.57E+07	2.67E+07	2.62E+07	0.00E+00	3.14E+07	3.69E+07
551	MNT_HUMAN	4	0.00E+00	0.00E+00	0.00E+00	0.00E+00	0.00E+00	0.00E+00	6.86E+06	0.00E+00
552	CDX2_HUMAN;sp|F	2;1;1	1.07E+07	0.00E+00	0.00E+00	0.00E+00	2.10E+07	0.00E+00	0.00E+00	0.00E+00
553	ATX2_HUMAN	26	2.33E+08	2.61E+08	6.57E+07	9.60E+07	3.41E+08	2.97E+08	1.27E+07	3.51E+07
554	SMAD5_HUMAN	2	0.00E+00	6.68E+06	0.00E+00	0.00E+00	0.00E+00	0.00E+00	0.00E+00	0.00E+00
555	ROAA_HUMAN	1	0.00E+00	0.00E+00	0.00E+00	0.00E+00	0.00E+00	0.00E+00	1.10E+06	0.00E+00
556	TCPH_HUMAN	22	1.40E+08	2.17E+08	1.24E+08	9.89E+07	0.00E+00	0.00E+00	3.68E+08	4.98E+08
557	PKP2_HUMAN	4	0.00E+00	0.00E+00	0.00E+00	0.00E+00	0.00E+00	0.00E+00	7.23E+06	0.00E+00
558	CITE2_HUMAN	2	0.00E+00	0.00E+00	0.00E+00	0.00E+00	1.81E+07	0.00E+00	0.00E+00	0.00E+00
559	SOSB1_HUMAN	1	0.00E+00	0.00E+00	0.00E+00	0.00E+00	0.00E+00	0.00E+00	0.00E+00	3.01E+06
560	ADPGK_HUMAN	8	1.04E+08	1.12E+08	4.76E+07	1.11E+08	1.18E+07	2.73E+07	6.47E+07	6.81E+07
561	ERP44_HUMAN	17	2.33E+08	2.23E+08	1.10E+08	1.07E+08	1.21E+08	1.88E+08	1.40E+08	1.67E+08
562	TACO1_HUMAN	3	0.00E+00	0.00E+00	0.00E+00	0.00E+00	0.00E+00	0.00E+00	2.21E+07	1.90E+07
563	ESYT1_HUMAN	4	0.00E+00	1.28E+07	0.00E+00	2.05E+07	0.00E+00	0.00E+00	0.00E+00	0.00E+00
564	WAC_HUMAN	16	1.23E+08	1.25E+08	1.17E+08	1.01E+08	1.27E+08	9.62E+07	5.99E+07	5.30E+07
565	DIDO1_HUMAN	2	0.00E+00	0.00E+00	2.59E+07	0.00E+00	0.00E+00	0.00E+00	0.00E+00	0.00E+00
566	LRRC1_HUMAN	1	0.00E+00	0.00E+00	0.00E+00	0.00E+00	0.00E+00	0.00E+00	7.13E+06	0.00E+00
567	NDC1_HUMAN	3	0.00E+00	0.00E+00	0.00E+00	1.18E+07	0.00E+00	0.00E+00	0.00E+00	0.00E+00
568	MMTA2_HUMAN	4	1.29E+07	1.03E+07	3.40E+07	2.31E+07	0.00E+00	2.63E+07	0.00E+00	1.95E+07
569	MCRI2_HUMAN	4	0.00E+00	4.91E+06	0.00E+00	0.00E+00	0.00E+00	0.00E+00	0.00E+00	0.00E+00
570	SF3B5_HUMAN	6	1.07E+08	1.42E+08	1.16E+08	1.30E+08	6.18E+07	6.32E+07	6.20E+07	8.28E+07
571	NADAP_HUMAN	9	0.00E+00	0.00E+00	0.00E+00	9.51E+06	0.00E+00	0.00E+00	9.32E+06	1.14E+07
572	OSB11_HUMAN;sp|	5;1	1.47E+07	1.78E+07	0.00E+00	0.00E+00	0.00E+00	0.00E+00	0.00E+00	1.58E+07
573	RFIP5_HUMAN	4	9.64E+06	1.29E+07	0.00E+00	0.00E+00	0.00E+00	0.00E+00	0.00E+00	0.00E+00
574	SETD2_HUMAN	4	0.00E+00	0.00E+00	0.00E+00	0.00E+00	0.00E+00	0.00E+00	0.00E+00	1.22E+06
575	DOCK9_HUMAN	1	0.00E+00	0.00E+00	0.00E+00	0.00E+00	0.00E+00	0.00E+00	0.00E+00	2.37E+06
576	TBL1R_HUMAN;sp|	5;4;4	0.00E+00	0.00E+00	0.00E+00	0.00E+00	0.00E+00	0.00E+00	2.38E+07	2.35E+07
577	DPY30_HUMAN	2	3.77E+06	0.00E+00	0.00E+00	0.00E+00	0.00E+00	0.00E+00	0.00E+00	0.00E+00
578	UNK_HUMAN	1	0.00E+00	0.00E+00	0.00E+00	0.00E+00	0.00E+00	0.00E+00	0.00E+00	1.94E+06
579	WDR33_HUMAN	31	1.90E+08	1.71E+08	1.71E+08	1.91E+08	1.94E+08	1.18E+08	1.35E+08	1.22E+08
580	CT027_HUMAN	6	6.29E+08	6.28E+08	2.49E+08	2.64E+08	4.64E+08	3.11E+08	4.73E+08	3.30E+08
581	PITH1_HUMAN	7	2.33E+07	0.00E+00	0.00E+00	0.00E+00	0.00E+00	0.00E+00	0.00E+00	0.00E+00
582	WDR61_HUMAN	8	4.22E+07	5.12E+07	0.00E+00	3.69E+07	0.00E+00	0.00E+00	0.00E+00	0.00E+00
583	XRN2_HUMAN	31	2.07E+08	2.14E+08	1.35E+08	1.21E+08	5.11E+07	3.76E+07	1.76E+08	1.52E+08
584	NSRP1_HUMAN	26	1.19E+08	1.03E+08	1.83E+08	1.29E+08	3.56E+08	2.03E+08	1.40E+08	1.35E+08
585	CSTFT_HUMAN	7	0.00E+00	4.06E+06	0.00E+00	0.00E+00	0.00E+00	0.00E+00	0.00E+00	0.00E+00
586	SMG9_HUMAN	5	0.00E+00	1.00E+07	0.00E+00	0.00E+00	0.00E+00	0.00E+00	0.00E+00	0.00E+00
587	ASCC2_HUMAN	3	0.00E+00	0.00E+00	0.00E+00	0.00E+00	0.00E+00	0.00E+00	0.00E+00	8.31E+06
588	PININ_HUMAN	1	0.00E+00	0.00E+00	0.00E+00	9.46E+06	0.00E+00	0.00E+00	0.00E+00	0.00E+00
589	FOXP1_HUMAN	1	0.00E+00	0.00E+00	0.00E+00	0.00E+00	0.00E+00	0.00E+00	3.01E+06	0.00E+00
590	BACD3_HUMAN;sp	2;1;1	0.00E+00	0.00E+00	0.00E+00	0.00E+00	0.00E+00	0.00E+00	6.60E+06	0.00E+00
591	WDR26_HUMAN	2	0.00E+00	0.00E+00	0.00E+00	0.00E+00	0.00E+00	0.00E+00	0.00E+00	3.28E+06
592	SDS3_HUMAN	2	0.00E+00	0.00E+00	7.84E+06	0.00E+00	0.00E+00	0.00E+00	0.00E+00	0.00E+00
593	ZN703_HUMAN;sp|	7;1	2.04E+07	2.19E+07	0.00E+00	0.00E+00	0.00E+00	0.00E+00	4.30E+07	2.84E+07
594	NT5D2_HUMAN	17	6.54E+07	5.34E+07	2.70E+07	3.54E+07	1.85E+07	0.00E+00	1.43E+08	1.29E+08
595	ARP5_HUMAN	1	0.00E+00	3.22E+06	0.00E+00	0.00E+00	0.00E+00	0.00E+00	0.00E+00	0.00E+00
596	RM44_HUMAN	1	0.00E+00	0.00E+00	0.00E+00	0.00E+00	0.00E+00	0.00E+00	0.00E+00	8.87E+06
597	ELP3_HUMAN	3	0.00E+00	0.00E+00	0.00E+00	0.00E+00	0.00E+00	0.00E+00	0.00E+00	1.25E+07
598	SYCM_HUMAN	15	3.69E+07	3.23E+07	0.00E+00	1.71E+07	0.00E+00	0.00E+00	1.11E+08	1.32E+08
599	FBRS_HUMAN	6	6.60E+07	6.01E+07	0.00E+00	4.42E+07	0.00E+00	4.06E+07	0.00E+00	0.00E+00
600	SMUF2_HUMAN	2	1.73E+06	0.00E+00	0.00E+00	0.00E+00	0.00E+00	0.00E+00	0.00E+00	0.00E+00
601	GPBL1_HUMAN	3	8.27E+06	0.00E+00	0.00E+00	0.00E+00	0.00E+00	0.00E+00	0.00E+00	0.00E+00
602	SENP2_HUMAN	1	0.00E+00	7.35E+06	0.00E+00	0.00E+00	0.00E+00	0.00E+00	0.00E+00	0.00E+00
603	RAVR2_HUMAN	2	0.00E+00	9.04E+06	0.00E+00	0.00E+00	0.00E+00	0.00E+00	0.00E+00	0.00E+00
604	CHD8_HUMAN;sp|(	35;2;1	2.03E+08	3.11E+08	1.07E+07	1.70E+07	7.03E+07	1.58E+08	0.00E+00	0.00E+00

id	Protein name	Peptide counts (all)	LFQ intensity _Bait_1	LFQ intensity _Control_1	LFQ intensity_Bait_2	LFQ intensity_Control_2	LFQ intensity_Bait_3	LFQ intensity_Control_3	LFQ intensity_Bait_4	LFQ intensity
605	FBSL_HUMAN	5	2.35E+07	2.37E+07	0.00E+00	0.00E+00	0.00E+00	0.00E+00	0.00E+00	1.34E+07
606	SDF2L_HUMAN	7	2.65E+07	2.52E+07	4.52E+07	3.17E+07	0.00E+00	0.00E+00	3.18E+07	2.19E+07
607	GOPC_HUMAN	20	5.15E+07	5.84E+07	3.11E+07	1.11E+07	1.51E+07	2.71E+07	1.38E+08	1.74E+08
608	WDR6_HUMAN	1	0.00E+00	4.85E+06	0.00E+00	0.00E+00	0.00E+00	0.00E+00	0.00E+00	0.00E+00
609	DCP1A_HUMAN	5	1.09E+07	0.00E+00	0.00E+00	0.00E+00	0.00E+00	0.00E+00	0.00E+00	0.00E+00
610	TF7L2_HUMAN	5	0.00E+00	0.00E+00	0.00E+00	2.34E+06	0.00E+00	0.00E+00	0.00E+00	0.00E+00
611	PRD10_HUMAN	2	0.00E+00	3.36E+06	0.00E+00	0.00E+00	0.00E+00	0.00E+00	0.00E+00	0.00E+00
612	GEPH_HUMAN	13	5.18E+07	9.25E+07	2.99E+07	3.46E+07	1.77E+07	1.67E+07	7.10E+07	9.88E+07
613	4ET_HUMAN	1	0.00E+00	0.00E+00	0.00E+00	0.00E+00	0.00E+00	0.00E+00	0.00E+00	7.99E+06
614	AAAS_HUMAN	3	0.00E+00	0.00E+00	0.00E+00	1.24E+07	0.00E+00	0.00E+00	0.00E+00	0.00E+00
615	RNC_HUMAN	6	0.00E+00	0.00E+00	0.00E+00	0.00E+00	0.00E+00	0.00E+00	8.71E+06	9.34E+06
616	LANC2_HUMAN	2	0.00E+00	0.00E+00	0.00E+00	0.00E+00	0.00E+00	0.00E+00	0.00E+00	1.98E+07
617	BMP2K_HUMAN	7	1.39E+07	1.40E+07	0.00E+00	0.00E+00	2.41E+07	2.68E+07	0.00E+00	0.00E+00
618	MA2C1_HUMAN	2	0.00E+00	0.00E+00	0.00E+00	0.00E+00	0.00E+00	0.00E+00	0.00E+00	1.49E+06
619	CUTC_HUMAN	7	6.04E+07	4.40E+07	1.23E+08	4.80E+07	1.24E+08	8.91E+07	1.73E+08	1.39E+08
620	INT13_HUMAN	6	1.11E+07	0.00E+00	0.00E+00	0.00E+00	0.00E+00	0.00E+00	1.15E+07	1.35E+07
621	KLH11_HUMAN	3	0.00E+00	0.00E+00	0.00E+00	0.00E+00	0.00E+00	0.00E+00	0.00E+00	1.75E+07
622	SLTM_HUMAN	7	0.00E+00	0.00E+00	1.76E+07	9.93E+06	1.66E+07	0.00E+00	1.06E+07	1.29E+07
623	GID8_HUMAN	4	0.00E+00	0.00E+00	0.00E+00	1.18E+07	0.00E+00	0.00E+00	5.99E+06	0.00E+00
624	F120C_HUMAN	3	1.49E+07	1.25E+07	0.00E+00	0.00E+00	0.00E+00	0.00E+00	0.00E+00	0.00E+00
625	MIO_HUMAN	2	0.00E+00	0.00E+00	0.00E+00	0.00E+00	0.00E+00	0.00E+00	0.00E+00	6.44E+06
626	NSMA3_HUMAN	5	0.00E+00	0.00E+00	0.00E+00	1.38E+07	0.00E+00	0.00E+00	0.00E+00	0.00E+00
627	ANR10_HUMAN	2	0.00E+00	0.00E+00	0.00E+00	0.00E+00	0.00E+00	0.00E+00	2.00E+06	0.00E+00
628	DJB12_HUMAN	4	0.00E+00	1.22E+07	0.00E+00	0.00E+00	0.00E+00	0.00E+00	0.00E+00	0.00E+00
629	NSE4A_HUMAN;sp|	13;1	8.97E+07	0.00E+00	4.69E+07	0.00E+00	4.28E+07	0.00E+00	5.40E+07	0.00E+00
630	TE2IP_HUMAN	5	0.00E+00	0.00E+00	0.00E+00	0.00E+00	3.51E+07	4.53E+07	0.00E+00	0.00E+00
631	BCLF1_HUMAN	11	2.97E+07	3.58E+07	5.36E+07	5.22E+07	0.00E+00	0.00E+00	0.00E+00	0.00E+00
632	TAB2_HUMAN	3	0.00E+00	0.00E+00	0.00E+00	0.00E+00	0.00E+00	0.00E+00	1.16E+07	0.00E+00
633	CDK12_HUMAN	19	1.14E+08	8.21E+07	2.87E+07	3.45E+07	3.00E+07	0.00E+00	6.22E+07	4.98E+07
634	MAT2B_HUMAN	5	0.00E+00	0.00E+00	1.22E+07	0.00E+00	0.00E+00	0.00E+00	0.00E+00	1.92E+07
635	HACD3_HUMAN	2	0.00E+00	0.00E+00	0.00E+00	1.60E+07	0.00E+00	0.00E+00	0.00E+00	0.00E+00
636	PHRF1_HUMAN	1	0.00E+00	0.00E+00	0.00E+00	0.00E+00	0.00E+00	0.00E+00	0.00E+00	9.02E+06
637	STIM2_HUMAN	3	7.05E+06	8.93E+06	0.00E+00	6.76E+06	0.00E+00	0.00E+00	0.00E+00	0.00E+00
638	BCCIP_HUMAN	2	1.71E+07	0.00E+00	0.00E+00	0.00E+00	0.00E+00	0.00E+00	0.00E+00	0.00E+00
639	CHD7_HUMAN	12	1.32E+07	1.31E+07	1.37E+07	8.32E+06	2.79E+07	0.00E+00	8.68E+06	0.00E+00
640	CPSF2_HUMAN	19	2.79E+07	5.07E+07	0.00E+00	5.32E+07	0.00E+00	0.00E+00	2.50E+07	3.23E+07
641	RBM27_HUMAN	19	6.41E+07	7.78E+07	8.10E+07	6.85E+07	9.32E+07	3.81E+07	8.96E+07	6.83E+07
642	STAR9_HUMAN	3	0.00E+00	0.00E+00	0.00E+00	0.00E+00	0.00E+00	0.00E+00	0.00E+00	1.35E+07
643	RERE_HUMAN	9	1.41E+08	1.02E+08	6.00E+07	4.73E+07	1.94E+08	9.17E+07	0.00E+00	0.00E+00
644	ATX10_HUMAN	1	0.00E+00	0.00E+00	0.00E+00	0.00E+00	0.00E+00	0.00E+00	0.00E+00	2.80E+06
645	ORC3_HUMAN	1	0.00E+00	0.00E+00	0.00E+00	8.80E+05	0.00E+00	0.00E+00	0.00E+00	0.00E+00
646	HDC_HUMAN	2	0.00E+00	0.00E+00	0.00E+00	0.00E+00	0.00E+00	0.00E+00	0.00E+00	5.18E+06
647	DJB11_HUMAN	2	0.00E+00	0.00E+00	0.00E+00	1.12E+07	0.00E+00	0.00E+00	0.00E+00	0.00E+00
648	ZO2_HUMAN	2	0.00E+00	0.00E+00	0.00E+00	0.00E+00	0.00E+00	0.00E+00	0.00E+00	1.11E+07
649	LIMD1_HUMAN	2	0.00E+00	4.68E+06	0.00E+00	0.00E+00	0.00E+00	0.00E+00	0.00E+00	0.00E+00
650	TCF20_HUMAN	9	4.62E+07	4.82E+07	4.66E+07	2.61E+07	4.06E+07	0.00E+00	0.00E+00	0.00E+00
651	AFF4_HUMAN	12	3.86E+07	2.74E+07	2.51E+07	2.45E+07	4.83E+07	2.70E+07	2.66E+07	1.99E+07
652	BI2L1_HUMAN	9	1.56E+07	1.26E+07	0.00E+00	0.00E+00	1.28E+07	0.00E+00	3.88E+07	3.16E+07
653	S30BP_HUMAN	6	2.60E+07	2.52E+07	2.83E+07	0.00E+00	3.34E+07	3.11E+07	0.00E+00	2.22E+07
654	NRBP_HUMAN	2	7.29E+06	8.82E+06	0.00E+00	0.00E+00	0.00E+00	0.00E+00	0.00E+00	0.00E+00
655	ATIF1_HUMAN	5	4.20E+07	4.55E+07	1.00E+08	5.30E+07	7.94E+07	0.00E+00	4.65E+07	3.62E+07
656	LEF1_HUMAN;sp|P	6;3;2	2.21E+07	1.75E+07	0.00E+00	0.00E+00	2.30E+07	1.99E+07	1.65E+07	0.00E+00
657	CCNL1_HUMAN	2	0.00E+00	8.70E+06	0.00E+00	0.00E+00	0.00E+00	0.00E+00	0.00E+00	0.00E+00
658	CPSF3_HUMAN	11	4.81E+07	4.38E+07	0.00E+00	4.65E+07	0.00E+00	0.00E+00	2.92E+07	3.62E+07
659	GPTC8_HUMAN	14	2.88E+07	3.45E+07	4.33E+07	4.76E+07	6.44E+07	4.70E+07	1.53E+07	0.00E+00

id	Protein name	Peptide counts (all)	LFQ intensity _Bait_1	LFQ intensity _Control_1	LFQ intensity_Bait_2	LFQ intensity_Control_2	LFQ intensity_Bait_3	LFQ intensity_Control_3	LFQ intensity_Bait_4	LFQ intensity
660	RCOR1_HUMAN;sp	2;1	0.00E+00	0.00E+00	0.00E+00	0.00E+00	0.00E+00	0.00E+00	3.81E+06	0.00E+00
661	DNPEP_HUMAN	7	0.00E+00	0.00E+00	0.00E+00	0.00E+00	0.00E+00	0.00E+00	3.03E+07	2.92E+07
662	ZN608_HUMAN	2	0.00E+00	0.00E+00	0.00E+00	0.00E+00	8.00E+06	0.00E+00	0.00E+00	0.00E+00
663	S39AA_HUMAN	5	0.00E+00	6.94E+06	0.00E+00	0.00E+00	0.00E+00	0.00E+00	0.00E+00	0.00E+00
664	ZMIZ1_HUMAN	1	0.00E+00	0.00E+00	0.00E+00	0.00E+00	0.00E+00	0.00E+00	9.58E+06	0.00E+00
665	PRP19_HUMAN	4	0.00E+00	1.62E+07	0.00E+00	0.00E+00	0.00E+00	0.00E+00	0.00E+00	0.00E+00
666	G3BP2_HUMAN;sp	3;1	7.04E+06	9.24E+06	0.00E+00	0.00E+00	0.00E+00	0.00E+00	0.00E+00	0.00E+00
667	CHIP_HUMAN	14	1.35E+08	1.18E+08	1.56E+08	1.04E+08	1.13E+08	6.08E+07	1.60E+08	1.38E+08
668	TTF2_HUMAN	4	0.00E+00	0.00E+00	0.00E+00	0.00E+00	0.00E+00	0.00E+00	0.00E+00	6.24E+06
669	ZC3H4_HUMAN	9	1.64E+07	1.31E+07	3.07E+07	1.87E+07	3.08E+07	2.50E+07	0.00E+00	1.33E+07
670	UBP22_HUMAN;sp	3;2	0.00E+00	0.00E+00	0.00E+00	0.00E+00	0.00E+00	0.00E+00	1.30E+07	1.89E+07
671	FOXJ3_HUMAN	4	1.78E+07	1.65E+07	0.00E+00	0.00E+00	1.45E+07	0.00E+00	0.00E+00	0.00E+00
672	SATB2_HUMAN	11	5.10E+07	5.77E+07	3.42E+07	5.19E+07	3.90E+07	4.18E+07	5.36E+07	5.37E+07
673	SCML2_HUMAN	12	2.52E+07	2.71E+07	2.71E+07	2.90E+07	0.00E+00	0.00E+00	3.50E+07	3.12E+07
674	CN166_HUMAN	13	1.52E+08	2.07E+08	1.11E+08	8.53E+07	1.73E+08	1.29E+08	1.38E+08	1.76E+08
675	RUVB2_HUMAN	7	2.24E+07	2.13E+07	0.00E+00	1.41E+07	0.00E+00	0.00E+00	0.00E+00	1.23E+07
676	FOXA2_HUMAN	1	0.00E+00	0.00E+00	0.00E+00	0.00E+00	8.29E+06	0.00E+00	0.00E+00	0.00E+00
677	RUVB1_HUMAN	7	2.43E+07	2.18E+07	2.13E+07	2.65E+07	0.00E+00	0.00E+00	1.18E+07	0.00E+00
678	BCS1_HUMAN	13	4.54E+07	4.57E+07	3.70E+07	6.27E+07	0.00E+00	4.67E+07	2.90E+07	3.75E+07
679	ERGI3_HUMAN	3	0.00E+00	1.27E+07	0.00E+00	0.00E+00	0.00E+00	0.00E+00	0.00E+00	0.00E+00
680	NCKP1_HUMAN;sp	10;1	1.77E+07	2.27E+07	0.00E+00	1.04E+07	0.00E+00	0.00E+00	2.22E+07	6.27E+07
681	ZN652_HUMAN;sp|	2;1	5.55E+06	0.00E+00	0.00E+00	0.00E+00	0.00E+00	0.00E+00	0.00E+00	0.00E+00
682	LRCH1_HUMAN;sp|	6;1	2.03E+07	2.60E+07	1.69E+07	2.59E+07	2.23E+07	2.80E+07	0.00E+00	0.00E+00
683	PDIP2_HUMAN	4	0.00E+00	5.46E+06	0.00E+00	0.00E+00	0.00E+00	0.00E+00	0.00E+00	1.11E+07
684	TR150_HUMAN	11	2.23E+07	2.19E+07	2.64E+07	3.29E+07	0.00E+00	0.00E+00	0.00E+00	0.00E+00
685	GIT1_HUMAN	16	5.54E+07	7.48E+07	3.87E+07	7.07E+07	2.30E+07	2.94E+07	5.28E+07	6.09E+07
686	ZN281_HUMAN	4	1.46E+07	0.00E+00	0.00E+00	0.00E+00	0.00E+00	0.00E+00	0.00E+00	0.00E+00
687	ACOT9_HUMAN	13	3.77E+07	3.56E+07	0.00E+00	2.61E+07	0.00E+00	0.00E+00	7.54E+07	1.03E+08
688	LC7L2_HUMAN;sp|	5;2	1.42E+07	2.38E+07	4.03E+07	4.61E+07	0.00E+00	0.00E+00	1.42E+07	1.39E+07
689	SF3B6_HUMAN	7	1.82E+08	1.96E+08	1.99E+08	2.38E+08	1.70E+08	1.60E+08	1.98E+08	1.50E+08
690	RTCB_HUMAN	24	3.99E+08	4.29E+08	2.71E+08	2.90E+08	3.19E+08	3.76E+08	4.12E+08	4.27E+08
691	TCAF1_HUMAN	1	0.00E+00	0.00E+00	0.00E+00	0.00E+00	0.00E+00	0.00E+00	0.00E+00	3.02E+06
692	MARF1_HUMAN	2	0.00E+00	0.00E+00	0.00E+00	0.00E+00	0.00E+00	0.00E+00	7.54E+06	0.00E+00
693	IRS2_HUMAN	2	3.59E+06	0.00E+00	0.00E+00	0.00E+00	0.00E+00	0.00E+00	0.00E+00	0.00E+00
694	AMMR1_HUMAN	1	0.00E+00	0.00E+00	0.00E+00	0.00E+00	0.00E+00	0.00E+00	0.00E+00	4.94E+06
695	RBM7_HUMAN	2	0.00E+00	6.89E+06	0.00E+00	0.00E+00	0.00E+00	0.00E+00	0.00E+00	0.00E+00
696	KCTD3_HUMAN	8	0.00E+00	0.00E+00	0.00E+00	1.08E+07	0.00E+00	0.00E+00	1.04E+07	1.53E+07
697	RBM8A_HUMAN	1	0.00E+00	0.00E+00	0.00E+00	5.32E+06	0.00E+00	0.00E+00	0.00E+00	0.00E+00
698	NCOR2_HUMAN	10	0.00E+00	0.00E+00	0.00E+00	0.00E+00	0.00E+00	0.00E+00	1.19E+07	1.02E+07
699	CEPT1_HUMAN	1	0.00E+00	0.00E+00	0.00E+00	0.00E+00	0.00E+00	0.00E+00	0.00E+00	4.93E+06
700	IF2B2_HUMAN;sp|(	16;1	1.04E+08	9.36E+07	7.52E+07	7.00E+07	1.71E+07	3.17E+07	1.56E+08	1.84E+08
701	S4A7_HUMAN	2	0.00E+00	5.80E+06	0.00E+00	0.00E+00	0.00E+00	0.00E+00	0.00E+00	0.00E+00
702	WASF2_HUMAN	2	0.00E+00	0.00E+00	0.00E+00	0.00E+00	0.00E+00	0.00E+00	1.24E+07	1.02E+07
703	SCC4_HUMAN	4	0.00E+00	0.00E+00	0.00E+00	0.00E+00	0.00E+00	0.00E+00	1.91E+07	1.83E+07
704	NS1BP_HUMAN	6	0.00E+00	1.99E+07	0.00E+00	0.00E+00	0.00E+00	0.00E+00	2.34E+07	4.15E+07

Table A.5: Perseus statistical analysis of protein hits identified by MaxQuant search for non-treated conditions (Figure 4.7)

The LFQ intensities from of MaxQuant search of four independent replicate samples (bait and control) were subjected to processing in Perseus; samples were divided into two categorical groups named Bait and Control, the matrix rows were filtered to contain minimum of 3 valid LFQ intensity values in at least one group (Bait/Control), the missing LFQ intensities were replaced with values from normal distribution by imputation (Imputation parameters: Width: 0.3, Downshift:1.8); to calculate statistically significant hits, two-sample Student's T-test was used, to correct for false discovered interactors, the p-value of the analysed data set was adjusted by Benjamini-Hochberg false discovery rate (FDR = 0.05), '+' marks statistically significant hits enriched in the Bait cell line (T-test difference > 0), subunits of the SMC5/6 complex are marked in yellow.

Perseus non-treated student t-test - two sample (Benjamini-Hochberg)

Number	T: Protein IDs	C: Student's T-test Significant Bait_Control	N: -Log Student's T-test p-value Bait_Control	N: Student's T-test q-value Bait_Control	N: Student's T-test Difference Bait_Control	N: Student's T-test Test statistic Bait_Control
1	SMC6_HUMAN	+	6.564	0.0001	4.647	24.952
2	SMC5_HUMAN	+	6.155	0.0002	3.484	21.293
3	NSE3_HUMAN	+	4.440	0.005	3.268	10.852
4	NSE4A_HUMAN;sp|	+	4.147	0.008	4.174	9.641
5	NSE1_HUMAN	+	4.090	0.007	2.365	9.423
6	ERGI1_HUMAN		1.906	0.932	-0.835	-3.526
7	CRTC2_HUMAN		1.620	1.000	1.599	3.001
8	NSE2_HUMAN		1.596	1.000	1.118	2.957
9	AMOT_HUMAN;sp|Q8IY63|AM		1.392	1.000	-1.646	-2.602
10	PR38A_HUMAN		1.338	1.000	-1.367	-2.510
11	ELOA1_HUMAN		1.294	1.000	0.406	2.434
12	CPSF7_HUMAN		1.269	1.000	0.471	2.393
13	TBA1B_HUMAN;sp|Q9BQE3|TE		1.219	1.000	-0.587	-2.309
14	CHIP_HUMAN		1.216	1.000	0.436	2.303
15	ARMC6_HUMAN		1.208	1.000	-1.219	-2.290
16	STIM1_HUMAN		1.202	1.000	-0.772	-2.279
17	LONM_HUMAN		1.180	1.000	-0.419	-2.243
18	ESYT1_HUMAN		1.170	1.000	-1.009	-2.226
19	SDF2L_HUMAN		1.142	1.000	0.492	2.180
20	DJB12_HUMAN		1.127	1.000	-1.012	-2.155
21	ATIF1_HUMAN		1.120	1.000	0.636	2.142
22	ADT2_HUMAN;sp|P12236|ADT		1.117	1.000	-1.182	-2.138
23	MYCBP_HUMAN		1.037	1.000	-0.960	-2.004
24	BCS1_HUMAN		1.014	1.000	-0.486	-1.966
25	TIM50_HUMAN		1.014	1.000	-1.096	-1.966
26	CALX_HUMAN		0.997	1.000	-0.657	-1.938
27	SMRC2_HUMAN		0.946	1.000	-0.270	-1.853
28	CEP85_HUMAN		0.939	1.000	-0.975	-1.841
29	ATX2L_HUMAN		0.905	1.000	0.350	1.786
30	GRP78_HUMAN		0.889	1.000	-0.221	-1.759
31	S39AE_HUMAN		0.873	1.000	-0.461	-1.732
32	OSB11_HUMAN;sp|Q9BXB5|OS		0.866	1.000	-0.624	-1.721
33	GIT1_HUMAN		0.864	1.000	-0.407	-1.717
34	VIR_HUMAN		0.863	1.000	-0.183	-1.715
35	C1QBP_HUMAN		0.853	1.000	0.433	1.699
36	TOP1_HUMAN;sp|Q969P6|TOP		0.823	1.000	0.350	1.649
37	QSOX2_HUMAN		0.821	1.000	-0.565	-1.645
38	TBG1_HUMAN;sp|Q9NRH3|TB(		0.799	1.000	-0.274	-1.609
39	CSK2B_HUMAN		0.785	1.000	1.564	1.585
40	ERGI2_HUMAN		0.784	1.000	-0.404	-1.584
41	IMB1_HUMAN		0.775	1.000	-0.795	-1.568
42	LRC59_HUMAN		0.775	1.000	-0.786	-1.568
43	CPSF1_HUMAN		0.761	1.000	-0.411	-1.545

Number	T: Protein IDs	C: Student's T-test Significant Bait_Control	N: -Log Student's T-test p-value Bait_Control	N: Student's T-test q-value Bait_Control	N: Student's T-test Difference Bait_Control	N: Student's T-test Test statistic Bait_Control
44	SMRC1_HUMAN	0.750	1.000	-0.252	-1.526	
45	CPSF2_HUMAN	0.736	1.000	-0.506	-1.502	
46	ARI1A_HUMAN	0.726	1.000	0.503	1.486	
47	CLK3_HUMAN	0.724	1.000	0.312	1.483	
48	TCP4_HUMAN	0.721	1.000	0.720	1.477	
49	GID8_HUMAN	0.714	1.000	-0.366	-1.465	
50	LEF1_HUMAN;sp|P36402|TCF7	0.710	1.000	1.127	1.459	
51	CUTC_HUMAN	0.708	1.000	0.784	1.455	
52	CDX2_HUMAN;sp|P47902|CDX	0.704	1.000	0.833	1.449	
53	TCF20_HUMAN	0.702	1.000	0.407	1.445	
54	PEG10_HUMAN	0.699	1.000	0.265	1.441	
55	ATPB_HUMAN	0.697	1.000	-0.733	-1.436	
56	IMA1_HUMAN	0.690	1.000	-0.182	-1.425	
57	S39A6_HUMAN	0.664	1.000	-0.760	-1.381	
58	BAG6_HUMAN	0.661	1.000	-0.415	-1.374	
59	ATPA_HUMAN	0.658	1.000	-1.186	-1.370	
60	SYVM_HUMAN	0.644	1.000	0.262	1.346	
61	CREB5_HUMAN	0.635	1.000	-0.676	-1.331	
62	SATB2_HUMAN	0.632	1.000	-0.173	-1.326	
63	ZN444_HUMAN	0.628	1.000	0.391	1.318	
64	WRIP1_HUMAN	0.601	1.000	-0.465	-1.271	
65	WDR61_HUMAN	0.595	1.000	-0.198	-1.260	
66	ABCB7_HUMAN	0.594	1.000	-0.683	-1.260	
67	HS90B_HUMAN;sp|P07900|HS	0.589	1.000	-0.864	-1.251	
68	YLPM1_HUMAN	0.578	1.000	0.100	1.231	
69	RBM27_HUMAN	0.577	1.000	0.254	1.230	
70	NADAP_HUMAN	0.564	1.000	-0.176	-1.207	
71	NS1BP_HUMAN	0.561	1.000	-0.771	-1.202	
72	TBB5_HUMAN;sp|A6NNZ2|TBB	0.560	1.000	-0.420	-1.200	
73	ROA3_HUMAN	0.553	1.000	0.931	1.187	
74	PARP1_HUMAN	0.551	1.000	0.367	1.184	
75	HXA13_HUMAN;sp|P31276|HX	0.546	1.000	0.409	1.174	
76	OPA1_HUMAN	0.545	1.000	-0.622	-1.173	
77	ELP3_HUMAN	0.536	1.000	-0.499	-1.158	
78	SMG9_HUMAN	0.536	1.000	-0.672	-1.157	
79	BRD4_HUMAN;sp|Q15059|BRD	0.530	1.000	0.173	1.147	
80	SIN3A_HUMAN	0.527	1.000	0.061	1.141	
81	EF1B_HUMAN	0.526	1.000	-1.032	-1.139	
82	ROA1_HUMAN;sp|Q32P51|RA1	0.525	1.000	0.711	1.137	
83	NHRF2_HUMAN	0.523	1.000	0.529	1.135	
84	TFE2_HUMAN	0.522	1.000	0.150	1.132	
85	DDX42_HUMAN	0.519	1.000	0.305	1.128	
86	HNRPU_HUMAN	0.516	1.000	-0.173	-1.121	
87	BAG3_HUMAN	0.515	1.000	0.380	1.120	

Number	T: Protein IDs	C: Student's T-test Significant Bait_Control	N: -Log Student's T-test p-value Bait_Control	N: Student's T-test q-value Bait_Control	N: Student's T-test Difference Bait_Control	N: Student's T-test Test statistic Bait_Control
88	PRP4B_HUMAN	0.508	1.000	0.512	1.108	
89	DYR1A_HUMAN;sp|Q9Y463|DY	0.508	1.000	-0.436	-1.108	
90	CALM3_HUMAN;sp|P0DP24|CA	0.502	1.000	0.613	1.098	
91	NUP93_HUMAN	0.500	1.000	-0.676	-1.093	
92	NSRP1_HUMAN	0.499	1.000	0.464	1.092	
93	RBP2_HUMAN	0.497	1.000	-0.969	-1.088	
94	CPSF4_HUMAN	0.496	1.000	-0.298	-1.085	
95	HXA5_HUMAN	0.493	1.000	0.438	1.080	
96	NDUS6_HUMAN	0.492	1.000	0.866	1.079	
97	PCGF5_HUMAN	0.484	1.000	0.529	1.064	
98	MCRI2_HUMAN	0.483	1.000	0.337	1.062	
99	CKAP4_HUMAN	0.481	1.000	-0.912	-1.060	
100	SC23A_HUMAN	0.478	1.000	-0.521	-1.054	
101	FABD_HUMAN	0.470	1.000	0.374	1.038	
102	CHD7_HUMAN	0.461	1.000	0.353	1.023	
103	BCL7A_HUMAN;sp|Q9BQE9|BC	0.460	1.000	0.680	1.021	
104	NCKP1_HUMAN	0.444	1.000	-1.170	-0.992	
105	RBM25_HUMAN	0.443	1.000	-0.308	-0.989	
106	PITH1_HUMAN	0.442	1.000	1.294	0.988	
107	LRCH1_HUMAN;sp|Q5VUJ6|LR	0.438	1.000	-0.324	-0.980	
108	S39AA_HUMAN	0.437	1.000	-0.572	-0.979	
109	PA1B3_HUMAN	0.436	1.000	0.762	0.977	
110	GSE1_HUMAN	0.435	1.000	-0.202	-0.975	
111	ZC3HD_HUMAN	0.428	1.000	0.244	0.962	
112	SR140_HUMAN	0.427	1.000	-0.228	-0.961	
113	MCFD2_HUMAN	0.426	1.000	-1.619	-0.959	
114	WDR33_HUMAN	0.424	1.000	0.181	0.955	
115	NIPBL_HUMAN	0.423	1.000	0.460	0.953	
116	ADPGK_HUMAN	0.413	1.000	-0.372	-0.935	
117	PBIP1_HUMAN	0.411	1.000	-0.819	-0.930	
118	HNRPL_HUMAN	0.407	1.000	0.158	0.923	
119	RUVB1_HUMAN	0.403	1.000	-0.317	-0.915	
120	ALDOA_HUMAN	0.399	1.000	0.260	0.909	
121	SLTM_HUMAN	0.397	1.000	0.458	0.904	
122	PBX1_HUMAN	0.395	1.000	0.589	0.900	
123	SC16A_HUMAN	0.393	1.000	0.277	0.896	
124	RED_HUMAN	0.393	1.000	-0.636	-0.896	
125	RPGF6_HUMAN;sp|Q9Y4G8|RP	0.392	1.000	-0.817	-0.895	
126	CT027_HUMAN	0.390	1.000	0.375	0.891	
127	MINT_HUMAN	0.390	1.000	0.717	0.890	
128	DDX6_HUMAN	0.390	1.000	-0.169	-0.890	
129	CBS_HUMAN;sp|P0DN79|CBSL	0.388	1.000	-0.464	-0.888	
130	XRN1_HUMAN	0.384	1.000	-0.849	-0.878	
131	H2B1L_HUMAN;sp|Q99879|H2	0.382	1.000	-0.336	-0.875	

Number	T: Protein IDs	C: Student's T-test Significant Bait_Control	N: -Log Student's T-test p-value Bait_Control	N: Student's T-test q-value Bait_Control	N: Student's T-test Difference Bait_Control	N: Student's T-test Test statistic Bait_Control
132	MNX1_HUMAN	0.377	1.000	0.316	0.865	
133	DCP1A_HUMAN	0.372	1.000	0.346	0.857	
134	ARHG7_HUMAN;sp|Q15052|AI	0.370	1.000	-0.236	-0.853	
135	S4A7_HUMAN	0.370	1.000	-0.380	-0.852	
136	SMRD1_HUMAN;sp|Q6STE5|SM	0.366	1.000	0.080	0.845	
137	LMAN1_HUMAN	0.365	1.000	-0.459	-0.844	
138	BCKD_HUMAN	0.363	1.000	0.325	0.839	
139	CDK12_HUMAN	0.362	1.000	-0.240	-0.838	
140	SMCA4_HUMAN;sp|P51531|SM	0.360	1.000	-0.117	-0.833	
141	CPSF3_HUMAN	0.357	1.000	-0.375	-0.828	
142	FBX21_HUMAN	0.356	1.000	-0.213	-0.826	
143	DDX17_HUMAN	0.341	1.000	0.123	0.796	
144	SMG8_HUMAN	0.338	1.000	0.364	0.791	
145	INT3_HUMAN	0.336	1.000	-0.570	-0.786	
146	PABP4_HUMAN;sp|P0CB38|PA	0.335	1.000	-0.120	-0.785	
147	PSPC1_HUMAN	0.331	1.000	0.224	0.776	
148	KCTD3_HUMAN	0.329	1.000	-0.472	-0.773	
149	SF3B1_HUMAN	0.329	1.000	-0.232	-0.773	
150	CSTF1_HUMAN	0.328	1.000	-0.201	-0.771	
151	S12A2_HUMAN	0.327	1.000	0.191	0.769	
152	NFIA_HUMAN	0.323	1.000	-0.295	-0.761	
153	MEIS2_HUMAN	0.319	1.000	0.279	0.754	
154	THOC4_HUMAN	0.319	1.000	0.704	0.753	
155	MECP2_HUMAN	0.317	1.000	0.380	0.749	
156	RBM15_HUMAN	0.316	1.000	-0.642	-0.748	
157	I2BP2_HUMAN	0.312	1.000	0.222	0.740	
158	SFPQ_HUMAN	0.311	1.000	0.324	0.737	
159	CE170_HUMAN;sp|Q96L14|C17	0.308	1.000	0.142	0.731	
160	NUCL_HUMAN	0.306	1.000	0.445	0.728	
161	TRIO_HUMAN;sp|O60229|KALI	0.305	1.000	0.619	0.726	
162	ZN609_HUMAN	0.304	1.000	0.561	0.724	
163	SNIP1_HUMAN	0.302	1.000	0.176	0.720	
164	TBP_HUMAN;sp|Q6SJ96|TBPL2	0.302	1.000	-0.167	-0.719	
165	TCPB_HUMAN	0.299	1.000	-0.531	-0.713	
166	PPIL4_HUMAN	0.298	1.000	0.150	0.711	
167	CATC_HUMAN	0.297	1.000	0.456	0.710	
168	HSP7C_HUMAN;sp|P54652|HSI	0.297	1.000	-0.204	-0.709	
169	GLNA_HUMAN	0.297	1.000	0.811	0.709	
170	CMTR1_HUMAN	0.292	1.000	0.340	0.700	
171	SF3B3_HUMAN	0.291	1.000	-0.231	-0.698	
172	SMD2_HUMAN	0.286	1.000	-0.314	-0.687	
173	SAFB1_HUMAN	0.282	1.000	0.231	0.679	
174	CSK22_HUMAN	0.281	1.000	0.279	0.678	
175	LMNA_HUMAN	0.280	1.000	0.287	0.674	

Number	T: Protein IDs	C: Student's T-test Significant Bait_Control	N: -Log Student's T-test p-value Bait_Control	N: Student's T-test q-value Bait_Control	N: Student's T-test Difference Bait_Control	N: Student's T-test Test statistic Bait_Control
176	CHD8_HUMAN;sp|Q3L8U1|CHI	0.279	1.000	-0.986	-0.672	
177	MMTA2_HUMAN	0.276	1.000	0.155	0.667	
178	CP135_HUMAN	0.275	1.000	0.445	0.664	
179	HNRH1_HUMAN;sp|P55795|HN	0.271	1.000	-0.203	-0.656	
180	SMCE1_HUMAN	0.267	1.000	0.146	0.648	
181	TCPZ_HUMAN;sp|Q92526|TCP'	0.261	1.000	-0.540	-0.636	
182	MCRI1_HUMAN	0.258	1.000	0.352	0.629	
183	TRA2B_HUMAN	0.257	1.000	-0.329	-0.628	
184	CCAR2_HUMAN	0.257	1.000	-0.140	-0.628	
185	F120B_HUMAN	0.257	1.000	0.515	0.627	
186	MAZ_HUMAN;sp|Q14119|VEZF	0.256	1.000	0.427	0.626	
187	FBSL_HUMAN	0.256	1.000	0.140	0.625	
188	RAVR1_HUMAN	0.254	1.000	-0.446	-0.622	
189	BI2L1_HUMAN	0.253	1.000	0.398	0.619	
190	PABP1_HUMAN;sp|Q9H361|PA	0.253	1.000	0.138	0.619	
191	G3P_HUMAN;sp|O14556|G3PT	0.252	1.000	-0.376	-0.617	
192	PP1G_HUMAN	0.248	1.000	0.504	0.610	
193	G6PE_HUMAN	0.247	1.000	0.669	0.607	
194	AUTS2_HUMAN	0.247	1.000	0.896	0.607	
195	ELOB_HUMAN	0.246	1.000	-0.098	-0.606	
196	CPSF5_HUMAN	0.246	1.000	0.247	0.604	
197	SHKB1_HUMAN	0.239	1.000	-0.509	-0.589	
198	MEPCE_HUMAN	0.238	1.000	-0.144	-0.587	
199	CCD50_HUMAN	0.237	1.000	0.243	0.586	
200	DGCR8_HUMAN	0.237	1.000	0.467	0.585	
201	PRP19_HUMAN	0.233	1.000	-0.246	-0.577	
202	G3BP2_HUMAN;sp|Q13283|G3	0.233	1.000	0.223	0.576	
203	P5CR3_HUMAN	0.232	1.000	0.176	0.575	
204	DHX30_HUMAN	0.226	1.000	-0.479	-0.562	
205	M4K4_HUMAN;sp|Q8N4C8|MI	0.224	1.000	0.334	0.558	
206	S30BP_HUMAN	0.224	1.000	0.160	0.558	
207	RPRD2_HUMAN	0.223	1.000	0.064	0.556	
208	LSM12_HUMAN	0.221	1.000	0.177	0.552	
209	SF01_HUMAN;sp|B1AK53|ESPN	0.216	1.000	0.118	0.540	
210	AFF4_HUMAN	0.212	1.000	0.188	0.531	
211	AP2A_HUMAN;sp|Q6VUC0|AP2	0.212	1.000	0.281	0.531	
212	CD11B_HUMAN;sp|Q9UQ88|CI	0.208	1.000	-0.159	-0.524	
213	SF3A2_HUMAN	0.208	1.000	0.104	0.523	
214	H4_HUMAN	0.207	1.000	-0.178	-0.522	
215	HNRPC_HUMAN;sp|P0DMR1|H	0.205	1.000	0.295	0.517	
216	CCNK_HUMAN	0.203	1.000	-0.170	-0.513	
217	HDAC1_HUMAN;sp|O15379|HI	0.203	1.000	0.386	0.512	
218	NOTC2_HUMAN	0.203	1.000	0.227	0.512	
219	TBPL1_HUMAN	0.201	1.000	0.157	0.507	

Number	T: Protein IDs	C: Student's T-test Significant Bait_Control	N: -Log Student's T-test p-value Bait_Control	N: Student's T-test q-value Bait_Control	N: Student's T-test Difference Bait_Control	N: Student's T-test Test statistic Bait_Control
220	TPR_HUMAN	0.200	1.000	0.098	0.507	
221	SMD1_HUMAN	0.196	1.000	-0.380	-0.498	
222	LEO1_HUMAN	0.194	1.000	0.300	0.492	
223	SF3B5_HUMAN	0.193	1.000	-0.168	-0.491	
224	SRC8_HUMAN	0.193	1.000	0.181	0.491	
225	ELP1_HUMAN	0.193	1.000	-0.364	-0.490	
226	HOME1_HUMAN	0.192	1.000	0.333	0.489	
227	UBP2L_HUMAN	0.192	1.000	-0.120	-0.488	
228	CSK21_HUMAN;sp|Q8NEV1|CS	0.192	1.000	-0.145	-0.488	
229	ACTN4_HUMAN;sp|P12814|AC	0.191	1.000	-0.308	-0.487	
230	BRE1A_HUMAN	0.187	1.000	-0.093	-0.477	
231	FL2D_HUMAN	0.186	1.000	0.220	0.475	
232	FA98A_HUMAN	0.184	1.000	-0.174	-0.471	
233	RUVB2_HUMAN	0.184	1.000	-0.225	-0.469	
234	ACOT9_HUMAN	0.183	1.000	-0.280	-0.467	
235	P5CS_HUMAN	0.177	1.000	0.196	0.455	
236	CC85C_HUMAN	0.176	1.000	-0.146	-0.453	
237	NUFP2_HUMAN	0.175	1.000	-0.191	-0.450	
238	TCPE_HUMAN	0.175	1.000	-0.398	-0.449	
239	PR40A_HUMAN	0.173	1.000	-0.093	-0.447	
240	SRSF1_HUMAN	0.172	1.000	0.419	0.444	
241	DCAF7_HUMAN	0.170	1.000	-0.138	-0.440	
242	NT5D2_HUMAN	0.169	1.000	0.225	0.437	
243	CH60_HUMAN	0.169	1.000	-0.177	-0.436	
244	SCML2_HUMAN	0.168	1.000	0.398	0.435	
245	H2A1J_HUMAN;sp|Q96KK5|H2	0.168	1.000	-0.197	-0.434	
246	SKP1_HUMAN	0.167	1.000	-0.117	-0.433	
247	FIP1_HUMAN	0.166	1.000	-0.108	-0.429	
248	NCOR2_HUMAN	0.165	1.000	-0.077	-0.428	
249	RBM33_HUMAN	0.165	1.000	0.288	0.427	
250	TJAP1_HUMAN	0.165	1.000	0.215	0.427	
251	RBBP7_HUMAN	0.165	1.000	-0.105	-0.426	
252	GOPC_HUMAN	0.163	1.000	-0.187	-0.424	
253	CBL_HUMAN;sp|Q13191|CBLB_	0.163	1.000	0.116	0.422	
254	GRP75_HUMAN	0.162	1.000	-0.093	-0.421	
255	BCCIP_HUMAN	0.161	1.000	0.094	0.418	
256	TCPH_HUMAN	0.157	1.000	-0.330	-0.410	
257	WAC_HUMAN	0.157	1.000	0.127	0.408	
258	CPSF6_HUMAN	0.155	1.000	0.111	0.404	
259	GEPH_HUMAN	0.154	1.000	-0.116	-0.401	
260	ERP44_HUMAN	0.151	1.000	-0.105	-0.396	
261	DDX1_HUMAN	0.151	1.000	-0.107	-0.395	
262	EDC3_HUMAN	0.150	1.000	-0.169	-0.393	
263	RBM10_HUMAN	0.150	1.000	-0.178	-0.392	

Number	T: Protein IDs	C: Student's T-test Significant Bait_Control	N: -Log Student's T-test p-value Bait_Control	N: Student's T-test q-value Bait_Control	N: Student's T-test Difference Bait_Control	N: Student's T-test Test statistic Bait_Control
264	PFKAM_HUMAN;sp|P17858|PF	0.148	1.000	0.344	0.389	
265	TF2AA_HUMAN	0.148	1.000	0.259	0.387	
266	TACO1_HUMAN	0.147	1.000	0.305	0.386	
267	TCPQ_HUMAN	0.146	1.000	-0.321	-0.384	
268	PUR8_HUMAN	0.146	1.000	-0.409	-0.384	
269	DJC10_HUMAN	0.145	1.000	-0.089	-0.382	
270	PCF11_HUMAN	0.145	1.000	-0.181	-0.380	
271	SRSF3_HUMAN	0.143	1.000	0.302	0.377	
272	PDIP2_HUMAN	0.143	1.000	-0.156	-0.377	
273	T22D1_HUMAN	0.142	1.000	-0.436	-0.374	
274	RFIP5_HUMAN	0.141	1.000	-0.147	-0.371	
275	AES_HUMAN	0.138	1.000	0.279	0.366	
276	RTCB_HUMAN	0.138	1.000	-0.090	-0.365	
277	ATX2_HUMAN	0.136	1.000	0.209	0.361	
278	TCPD_HUMAN	0.136	1.000	-0.313	-0.361	
279	SARM1_HUMAN	0.136	1.000	-0.232	-0.361	
280	RING2_HUMAN	0.135	1.000	0.157	0.357	
281	HDAC2_HUMAN	0.135	1.000	-0.135	-0.357	
282	GLYM_HUMAN;sp|P34896|GLY	0.133	1.000	0.387	0.354	
283	NONO_HUMAN	0.130	1.000	0.183	0.345	
284	TLE3_HUMAN	0.130	1.000	0.139	0.345	
285	SRSF6_HUMAN;sp|Q08170|SRS	0.129	1.000	0.322	0.344	
286	ARHGA_HUMAN	0.129	1.000	-0.357	-0.342	
287	KPRB_HUMAN	0.128	1.000	-0.283	-0.342	
288	CHERP_HUMAN	0.128	1.000	-0.082	-0.341	
289	WDR5_HUMAN	0.126	1.000	0.340	0.336	
290	RING1_HUMAN	0.125	1.000	0.281	0.335	
291	CGL_HUMAN	0.125	1.000	0.217	0.334	
292	SPF45_HUMAN	0.125	1.000	-0.104	-0.333	
293	TCPG_HUMAN	0.125	1.000	-0.372	-0.333	
294	IRS4_HUMAN	0.123	1.000	-0.180	-0.329	
295	SF3A1_HUMAN	0.123	1.000	0.123	0.329	
296	SMU1_HUMAN	0.123	1.000	-0.182	-0.328	
297	ZIC2_HUMAN;sp|Q15915|ZIC1_	0.122	1.000	0.173	0.326	
298	SMAD4_HUMAN	0.121	1.000	0.170	0.324	
299	BTBDB_HUMAN	0.118	1.000	0.146	0.317	
300	ROA2_HUMAN	0.115	1.000	0.190	0.309	
301	U2AF1_HUMAN;sp|P0DN76|U2	0.114	1.000	0.069	0.307	
302	SDS3_HUMAN	0.111	1.000	0.120	0.299	
303	MEIS1_HUMAN;sp|A6NDR6|M	0.110	1.000	0.069	0.298	
304	DHTK1_HUMAN	0.110	1.000	0.207	0.298	
305	TBB4B_HUMAN;sp|P04350|TBI	0.109	1.000	-0.125	-0.296	
306	H32_HUMAN;sp|Q16695|H31T	0.109	1.000	-0.191	-0.295	
307	CSTF3_HUMAN	0.108	1.000	-0.158	-0.292	

Number	T: Protein IDs	C: Student's T-test Significant Bait_Control	N: -Log Student's T-test p-value Bait_Control	N: Student's T-test q-value Bait_Control	N: Student's T-test Difference Bait_Control	N: Student's T-test Test statistic Bait_Control
308	NFIC_HUMAN	0.106	1.000	0.136	0.287	
309	CTR9_HUMAN	0.104	1.000	0.368	0.282	
310	VGLL4_HUMAN	0.104	1.000	0.084	0.282	
311	PYR1_HUMAN	0.103	1.000	-0.369	-0.281	
312	HEXI1_HUMAN	0.102	1.000	0.293	0.278	
313	EF1A3_HUMAN;sp|P68104|EF1	0.101	1.000	-0.096	-0.276	
314	ZC3H4_HUMAN	0.098	1.000	0.127	0.268	
315	TRI18_HUMAN;sp|Q9UJV3|TRI	0.098	1.000	-0.274	-0.267	
316	RERE_HUMAN	0.097	1.000	0.240	0.264	
317	RUXF_HUMAN	0.094	1.000	-0.132	-0.258	
318	ASPP1_HUMAN	0.093	1.000	0.144	0.255	
319	RBMX_HUMAN;sp|Q96E39|RM	0.092	1.000	-0.177	-0.252	
320	5NTC_HUMAN	0.091	1.000	-0.139	-0.250	
321	ERH_HUMAN	0.091	1.000	0.138	0.249	
322	ZO1_HUMAN	0.089	1.000	0.098	0.244	
323	TYSD1_HUMAN	0.087	1.000	0.068	0.241	
324	PHS_HUMAN	0.087	1.000	-0.174	-0.240	
325	HMBX1_HUMAN	0.086	1.000	-0.133	-0.237	
326	IVD_HUMAN	0.084	1.000	-0.192	-0.232	
327	1433E_HUMAN;sp|P31947|143	0.084	1.000	0.061	0.231	
328	ACL6A_HUMAN	0.084	1.000	-0.107	-0.231	
329	ACTG_HUMAN;sp|P60709|ACT	0.082	1.000	0.082	0.227	
330	CN166_HUMAN	0.082	1.000	0.078	0.227	
331	CCNT1_HUMAN	0.082	1.000	0.219	0.226	
332	GPT11_HUMAN	0.082	1.000	-0.244	-0.226	
333	XXLT1_HUMAN	0.082	1.000	-0.066	-0.226	
334	PP1A_HUMAN	0.078	1.000	0.097	0.218	
335	DNJC8_HUMAN	0.078	1.000	0.116	0.217	
336	ARI1B_HUMAN	0.078	1.000	-0.228	-0.217	
337	PCNP_HUMAN	0.077	1.000	0.123	0.215	
338	CTBP1_HUMAN	0.077	1.000	0.234	0.213	
339	RU17_HUMAN	0.076	1.000	0.184	0.212	
340	PRPS2_HUMAN	0.075	1.000	-0.149	-0.208	
341	TAB2_HUMAN	0.074	1.000	-0.125	-0.207	
342	DDX3X_HUMAN;sp|O15523|DI	0.074	1.000	0.120	0.205	
343	BMP2K_HUMAN	0.074	1.000	0.230	0.205	
344	METK2_HUMAN	0.074	1.000	-0.256	-0.205	
345	PHF3_HUMAN	0.073	1.000	0.031	0.203	
346	TYY1_HUMAN;sp|Q96MM3|ZF	0.072	1.000	0.323	0.201	
347	TCPA_HUMAN	0.072	1.000	-0.275	-0.201	
348	SMAP_HUMAN	0.071	1.000	0.226	0.197	
349	LANC2_HUMAN	0.070	1.000	-0.124	-0.195	
350	PHF5A_HUMAN	0.069	1.000	0.093	0.193	
351	MATR3_HUMAN	0.069	1.000	-0.324	-0.193	

Number	T: Protein IDs	C: Student's T-test Significant Bait_Control	N: -Log Student's T-test p-value Bait_Control	N: Student's T-test q-value Bait_Control	N: Student's T-test Difference Bait_Control	N: Student's T-test Test statistic Bait_Control
352	SC24B_HUMAN	0.066	1.000	-0.085	-0.186	
353	LIPA1_HUMAN;sp|O75335|LIPA	0.066	1.000	-0.079	-0.185	
354	FHL1_HUMAN	0.065	1.000	-0.165	-0.183	
355	SPF30_HUMAN	0.064	1.000	0.100	0.181	
356	ZN281_HUMAN	0.063	1.000	-0.090	-0.179	
357	HAKAI_HUMAN	0.063	1.000	0.081	0.177	
358	TYY2_HUMAN	0.063	1.000	0.270	0.177	
359	PBX2_HUMAN	0.062	1.000	0.050	0.175	
360	TLE1_HUMAN;sp|Q04727|TLE4	0.062	1.000	0.055	0.174	
361	PRDX3_HUMAN	0.061	1.000	-0.132	-0.173	
362	BCLF1_HUMAN	0.061	1.000	-0.152	-0.171	
363	HELZ_HUMAN	0.057	1.000	-0.049	-0.162	
364	TR150_HUMAN	0.057	1.000	0.148	0.161	
365	SF3B6_HUMAN	0.056	1.000	-0.025	-0.159	
366	UBAP2_HUMAN	0.054	1.000	-0.045	-0.153	
367	SC23B_HUMAN	0.054	1.000	0.120	0.153	
368	DLX5_HUMAN;sp|Q07687|DLX	0.054	1.000	0.159	0.153	
369	NDKM_HUMAN	0.052	1.000	-0.084	-0.148	
370	SMRD2_HUMAN	0.051	1.000	0.061	0.146	
371	MAGI1_HUMAN	0.051	1.000	-0.097	-0.145	
372	DOCK7_HUMAN;sp|Q96HP0|D	0.049	1.000	-0.031	-0.141	
373	ZN703_HUMAN;sp|Q96F45|ZN	0.048	1.000	-0.044	-0.138	
374	JHD2C_HUMAN	0.048	1.000	0.069	0.137	
375	SF3B2_HUMAN	0.048	1.000	0.036	0.136	
376	U520_HUMAN	0.045	1.000	-0.085	-0.129	
377	DNPEP_HUMAN	0.044	1.000	-0.140	-0.127	
378	INT13_HUMAN	0.044	1.000	0.078	0.126	
379	LC7L2_HUMAN;sp|Q9NQ29|LU	0.044	1.000	-0.072	-0.125	
380	PP1RA_HUMAN	0.043	1.000	-0.131	-0.123	
381	IF5A1_HUMAN;sp|Q9GZV4|IF5	0.043	1.000	0.073	0.123	
382	ABI1_HUMAN;sp|Q9NYB9|ABI2	0.042	1.000	-0.113	-0.120	
383	ELOC_HUMAN	0.042	1.000	0.048	0.120	
384	NUCB1_HUMAN	0.040	1.000	-0.077	-0.115	
385	ATN1_HUMAN	0.040	1.000	0.196	0.114	
386	BRE1B_HUMAN	0.039	1.000	-0.020	-0.113	
387	SC31A_HUMAN;sp|Q9NQW1|S	0.038	1.000	-0.110	-0.111	
388	SYCM_HUMAN	0.038	1.000	-0.082	-0.111	
389	CSTF2_HUMAN	0.038	1.000	0.021	0.110	
390	USP9X_HUMAN;sp|O00507|US	0.038	1.000	-0.049	-0.110	
391	RHG17_HUMAN;sp|Q17R89|RH	0.038	1.000	-0.093	-0.109	
392	SEC13_HUMAN	0.037	1.000	0.197	0.108	
393	HNRPK_HUMAN	0.036	1.000	0.049	0.103	
394	XRN2_HUMAN	0.036	1.000	0.034	0.103	
395	UBP7_HUMAN	0.035	1.000	0.067	0.100	

Number	T: Protein IDs	C: Student's T-test Significant Bait_Control	N: -Log Student's T-test p-value Bait_Control	N: Student's T-test q-value Bait_Control	N: Student's T-test Difference Bait_Control	N: Student's T-test Test statistic Bait_Control
396	PO3F2_HUMAN;sp|Q03052|PO	0.034	1.000	-0.094	-0.098	
397	PRP8_HUMAN	0.034	1.000	-0.095	-0.098	
398	IF2B2_HUMAN;sp|Q9NZI8|IF2E	0.033	1.000	-0.056	-0.096	
399	DHX15_HUMAN;sp|O60231|DH	0.032	1.000	-0.016	-0.093	
400	NSMA3_HUMAN	0.031	1.000	0.039	0.091	
401	OSBL9_HUMAN	0.031	1.000	-0.073	-0.091	
402	TOX4_HUMAN;sp|O15405|TOX	0.030	1.000	-0.090	-0.088	
403	LGMN_HUMAN	0.029	1.000	-0.019	-0.086	
404	TBL1R_HUMAN;sp|Q9BQ87|TB	0.029	1.000	0.066	0.085	
405	MK01_HUMAN	0.029	1.000	-0.099	-0.084	
406	EFTU_HUMAN	0.028	1.000	-0.081	-0.083	
407	TAOK1_HUMAN;sp|Q9H2K8|TA	0.028	1.000	-0.042	-0.082	
408	NFIB_HUMAN	0.028	1.000	-0.049	-0.080	
409	KCRU_HUMAN;sp|P17540|KCR	0.027	1.000	-0.058	-0.080	
410	U5S1_HUMAN	0.027	1.000	0.063	0.080	
411	SATB1_HUMAN	0.027	1.000	0.037	0.080	
412	MAX_HUMAN	0.026	1.000	0.040	0.077	
413	U2AF2_HUMAN	0.026	1.000	0.018	0.075	
414	MAT2B_HUMAN	0.026	1.000	-0.037	-0.075	
415	PINX1_HUMAN	0.025	1.000	-0.051	-0.075	
416	FBRS_HUMAN	0.025	1.000	0.036	0.073	
417	PAF1_HUMAN	0.025	1.000	0.042	0.072	
418	CDC73_HUMAN	0.025	1.000	0.038	0.072	
419	H2AV_HUMAN;sp|P0C0S5|H2A	0.022	1.000	-0.033	-0.064	
420	LARP7_HUMAN	0.022	1.000	0.021	0.063	
421	FOXJ3_HUMAN	0.021	1.000	-0.044	-0.062	
422	HS71B_HUMAN;sp|P0DMV8|H	0.021	1.000	-0.021	-0.061	
423	TE2IP_HUMAN	0.020	1.000	-0.082	-0.060	
424	NUD19_HUMAN	0.020	1.000	0.088	0.059	
425	RNPS1_HUMAN	0.019	1.000	0.091	0.056	
426	RANG_HUMAN	0.019	1.000	0.046	0.056	
427	SCLY_HUMAN	0.018	1.000	0.030	0.054	
428	FBP1L_HUMAN	0.017	1.000	-0.036	-0.052	
429	SRSF7_HUMAN	0.017	1.000	0.037	0.051	
430	HIP1R_HUMAN	0.016	1.000	0.029	0.047	
431	ASCC3_HUMAN	0.012	1.000	-0.031	-0.036	
432	GPTC8_HUMAN	0.012	1.000	-0.021	-0.035	
433	CYFP1_HUMAN;sp|Q96F07|CYF	0.011	1.000	0.040	0.034	
434	DPP9_HUMAN	0.010	1.000	-0.012	-0.030	
435	MFAP1_HUMAN	0.010	1.000	0.012	0.029	
436	CDK9_HUMAN;sp|Q00535|CDK	0.010	1.000	-0.016	-0.028	
437	D2HDH_HUMAN	0.008	1.000	-0.019	-0.025	
438	WDR82_HUMAN	0.008	1.000	-0.031	-0.024	
439	CARM1_HUMAN	0.006	1.000	0.013	0.019	

Number	T: Protein IDs	C: Student's T-test Significant Bait_Control	N: -Log Student's T-test p-value Bait_Control	N: Student's T-test q-value Bait_Control	N: Student's T-test Difference Bait_Control	N: Student's T-test Test statistic Bait_Control
440	CCD97_HUMAN	0.006	1.000	-0.007	-0.018	
441	SAFB2_HUMAN	0.005	1.000	0.010	0.014	
442	GATA6_HUMAN;sp|Q9BWX5|G	0.005	1.000	0.019	0.014	
443	PLD3_HUMAN	0.003	1.000	0.005	0.010	
444	P20D2_HUMAN	0.003	1.000	0.004	0.010	
445	ELAV1_HUMAN;sp|Q12926|ELA	0.002	1.000	-0.005	-0.006	
446	AMRP_HUMAN	0.002	1.000	-0.002	-0.006	
447	NKRF_HUMAN	0.002	1.000	-0.002	-0.005	
448	SF3A3_HUMAN	0.002	1.000	-0.002	-0.005	
449	DVL3_HUMAN;sp|O14641|DVL	0.001	0.999	-0.001	-0.004	
450	SF3B4_HUMAN	0.000	0.999	0.000	0.001	

Table A.6: MaxQuant search parameters and identified protein interactors of NSMCE4a after 2h and 24h of hydroxyurea treatment (Figure 4.10 and 4.11)
A. MaxQuant search parameters used to identify peptides in the sample, LFQ intensities were used for quantitative measurements. **B.** Proteins identified in nine biological replicates (NT/2h HU/24h HU) of TALON pull downs in control and bait cell lines by MaxQuant search; displayed are LFQ intensities of 2h and 24h HU treated samples, search results were filtered and proteins with peptides only identified by site, reverse and potential contaminants were excluded from the list, subunits of SMC5/6 complex are marked in yellow.

2h HU and 24h HU MQ search parameters

Parameter	**Value**
Version	1.6.3.3
User name	ab797
Machine name	GC04014987
Date of writing	11/27/2019 22:14:16
Include contaminants	TRUE
PSM FDR	0.01
PSM FDR Crosslink	0.01
Protein FDR	0.01
Site FDR	0.01
Use Normalized Ratios For Occupancy	TRUE
Min. peptide Length	7
Min. score for unmodified peptides	0
Min. score for modified peptides	40
Min. delta score for unmodified peptides	0
Min. delta score for modified peptides	6
Min. unique peptides	0
Min. razor peptides	1
Min. peptides	1
Use only unmodified peptides and	TRUE
Modifications included in protein quantification	Oxidation (M);Acetyl (Protein N-term)
Peptides used for protein quantification	Razor
Discard unmodified counterpart peptides	TRUE
Label min. ratio count	2
Use delta score	FALSE
iBAQ	FALSE
iBAQ log fit	FALSE
Match between runs	TRUE
Matching time window [min]	0.7
Alignment time window [min]	20
Find dependent peptides	FALSE
Fasta file	N:\Documents\Programmes\MaxQuant\Human_Swiss_Uniprot_20200_June2017.fasta
Decoy mode	revert
Include contaminants	TRUE
Advanced ratios	TRUE
Fixed andromeda index folder	
Temporary folder	
Combined folder location	Z:\jo_murray_lab\ab797\Data\Mass spec data_raw data\MaxQuant_191127
Second peptides	TRUE
Stabilize large LFQ ratios	TRUE
Separate LFQ in parameter groups	FALSE
Require MS/MS for LFQ comparisons	TRUE
Calculate peak properties	FALSE
Main search max. combinations	200
Advanced site intensities	TRUE
Write msScans table	FALSE
Write msmsScans table	TRUE
Write ms3Scans table	TRUE
Write allPeptides table	TRUE
Write mzRange table	TRUE
Write pasefMsmsScans table	TRUE
Write accumulatedPasefMsmsScans table	TRUE
Max. peptide mass [Da]	4600
Min. peptide length for unspecific search	8
Max. peptide length for unspecific search	25
Razor protein FDR	TRUE
Disable MD5	FALSE
Max mods in site table	3
Match unidentified features	FALSE
Epsilon score for mutations	Z:\jo_murray_lab\ab797\Data\Mass spec data_raw data\MaxQuant_191127
Evaluate variant peptides separately	TRUE
Variation mode	None
MS/MS tol. (FTMS)	20 ppm
Top MS/MS peaks per Da interval. (FTMS)	12
Da interval. (FTMS)	100
MS/MS deisotoping (FTMS)	TRUE

Parameter	Value
MS/MS deisotoping tolerance (FTMS)	7
MS/MS deisotoping tolerance unit (FTMS)	ppm
MS/MS higher charges (FTMS)	TRUE
MS/MS water loss (FTMS)	TRUE
MS/MS ammonia loss (FTMS)	TRUE
MS/MS dependent losses (FTMS)	TRUE
MS/MS recalibration (FTMS)	FALSE
MS/MS tol. (ITMS)	0.5 Da
Top MS/MS peaks per Da interval. (ITMS)	8
Da interval. (ITMS)	100
MS/MS deisotoping (ITMS)	FALSE
MS/MS deisotoping tolerance (ITMS)	0.15
MS/MS deisotoping tolerance unit (ITMS)	Da
MS/MS higher charges (ITMS)	TRUE
MS/MS water loss (ITMS)	TRUE
MS/MS ammonia loss (ITMS)	TRUE
MS/MS dependent losses (ITMS)	TRUE
MS/MS recalibration (ITMS)	FALSE
MS/MS tol. (TOF)	40 ppm
Top MS/MS peaks per Da interval. (TOF)	10
Da interval. (TOF)	100
MS/MS deisotoping (TOF)	TRUE
MS/MS deisotoping tolerance (TOF)	0.01
MS/MS deisotoping tolerance unit (TOF)	Da
MS/MS higher charges (TOF)	TRUE
MS/MS water loss (TOF)	TRUE
MS/MS ammonia loss (TOF)	TRUE
MS/MS dependent losses (TOF)	TRUE
MS/MS recalibration (TOF)	FALSE
MS/MS tol. (Unknown)	0.5 Da
Top MS/MS peaks per Da interval. (Unknown)	8
Da interval. (Unknown)	100
MS/MS deisotoping (Unknown)	FALSE
MS/MS deisotoping tolerance (Unknown)	0.15
MS/MS deisotoping tolerance unit (Unknown)	Da
MS/MS higher charges (Unknown)	TRUE
MS/MS water loss (Unknown)	TRUE
MS/MS ammonia loss (Unknown)	TRUE
MS/MS dependent losses (Unknown)	TRUE
MS/MS recalibration (Unknown)	FALSE
Site tables	Oxidation (M)Sites.txt

MaxQuant search; experiment: 2h and 24h HU treatment

id	Gene names	Unique peptides	LFQ intensity Bait 2h_1	LFQ intensity Control 2h_1	LFQ intensity Bait 2h_2	LFQ intensity Control 2h_2	LFQ intensity Bait 2h_3	LFQ intensity Control 2h_3	LFQ intensity Bait 24h_1	LFQ intensity Control_24h_1	LFQ intensity Bait 24h_2	LFQ intensity Control_24h_2	LFQ intensity 2_Bait 24h_3	LFQ intensity
1	MED19	1	0.00E+00	0.00E+00	0.00E+00	0.00E+00	0.00E+00	0.00E+00	0.00E+00	0.00E+00	0.00E+00	0.00E+00	0.00E+00	0.00E+00
2	VWA8	3	3.23E+06	2.94E+06	1.70E+06	0.00E+00	0.00E+00	0.00E+00	2.13E+06	3.01E+06	1.79E+06	0.00E+00	0.00E+00	0.00E+00
3	C5orf51	2	3.71E+06	0.00E+00	0.00E+00	0.00E+00	0.00E+00	0.00E+00	0.00E+00	0.00E+00	0.00E+00	0.00E+00	0.00E+00	0.00E+00
4	CCDC85C	10	1.18E+07	1.57E+07	1.05E+07	1.18E+07	1.31E+07	1.70E+07	1.08E+07	1.26E+07	8.91E+06	1.10E+07	1.00E+07	1.25E+07
5	RGPD4;RGI	1	0.00E+00	0.00E+00	0.00E+00	0.00E+00	0.00E+00	0.00E+00	0.00E+00	0.00E+00	0.00E+00	0.00E+00	0.00E+00	0.00E+00
6	BTBD11	1	0.00E+00	2.18E+05	0.00E+00	0.00E+00	0.00E+00	0.00E+00	0.00E+00	0.00E+00	0.00E+00	0.00E+00	0.00E+00	0.00E+00
7	MYH7B;MY	2	6.21E+06	0.00E+00	1.24E+07	0.00E+00	1.12E+07	1.26E+07	6.55E+06	0.00E+00	0.00E+00	1.07E+07	0.00E+00	1.21E+07
8	SNRPG;SNI	3	3.09E+06	2.27E+06	5.86E+06	6.10E+06	3.04E+06	2.76E+06	2.27E+06	0.00E+00	4.35E+06	3.06E+06	4.23E+06	2.82E+06
9	NUDT19	10	1.21E+07	1.22E+07	2.96E+07	2.27E+07	7.18E+06	0.00E+00	1.54E+07	1.32E+07	2.90E+07	2.16E+07	6.10E+06	6.56E+06
10	MIF4GD	3	0.00E+00	3.40E+06	0.00E+00	0.00E+00	0.00E+00	0.00E+00	3.77E+06	4.17E+06	0.00E+00	0.00E+00	0.00E+00	0.00E+00
11	FAM195B	5	1.96E+07	1.88E+07	2.09E+07	3.22E+07	4.35E+07	7.07E+07	2.40E+07	2.43E+07	1.60E+07	2.70E+07	3.88E+07	6.29E+07
12	MYO1C	2	0.00E+00	0.00E+00	0.00E+00	0.00E+00	0.00E+00	0.00E+00	0.00E+00	0.00E+00	4.03E+06	0.00E+00	0.00E+00	0.00E+00
13	SMAP	7	2.30E+07	1.51E+07	1.48E+07	1.37E+07	4.19E+07	5.58E+07	2.89E+07	3.25E+07	5.20E+07	5.19E+07	6.64E+07	8.93E+07
14	PGRMC1	2	0.00E+00	0.00E+00	0.00E+00	0.00E+00	0.00E+00	0.00E+00	0.00E+00	0.00E+00	0.00E+00	0.00E+00	0.00E+00	0.00E+00
15	EEF2K	1	0.00E+00	0.00E+00	0.00E+00	0.00E+00	0.00E+00	0.00E+00	0.00E+00	0.00E+00	0.00E+00	0.00E+00	0.00E+00	0.00E+00
16	IGF2BP3	1	0.00E+00	0.00E+00	0.00E+00	0.00E+00	0.00E+00	0.00E+00	0.00E+00	0.00E+00	0.00E+00	0.00E+00	0.00E+00	0.00E+00
17	MEIS1	4	1.47E+07	1.48E+07	1.26E+07	1.09E+07	1.45E+07	1.20E+07	1.51E+07	1.85E+07	1.21E+07	8.89E+06	9.96E+06	1.63E+07
18	KPNA3	2	0.00E+00	0.00E+00	0.00E+00	0.00E+00	0.00E+00	0.00E+00	1.42E+06	2.48E+06	0.00E+00	0.00E+00	0.00E+00	0.00E+00
19	DDX3X;DD	3	2.81E+06	0.00E+00	2.99E+06	2.29E+06	1.99E+06	0.00E+00	0.00E+00	0.00E+00	2.43E+06	0.00E+00	0.00E+00	0.00E+00
20	NFIB	5	5.00E+06	6.78E+06	0.00E+00	0.00E+00	0.00E+00	0.00E+00	6.98E+06	8.05E+06	4.15E+06	5.53E+06	0.00E+00	0.00E+00
21	NME4	11	4.01E+07	4.61E+07	2.13E+07	1.83E+07	1.38E+07	1.08E+07	3.50E+07	4.60E+07	1.93E+07	2.24E+07	1.03E+07	1.11E+07
22	ARID1A	12	9.43E+06	8.50E+06	1.14E+07	1.06E+07	4.62E+06	0.00E+00	8.55E+06	7.87E+06	6.64E+06	7.24E+06	7.91E+06	5.10E+06
23	CIT	6	4.66E+06	3.96E+06	0.00E+00	0.00E+00	0.00E+00	0.00E+00	4.13E+06	4.22E+06	0.00E+00	0.00E+00	0.00E+00	0.00E+00
24	ABLIM1	3	1.23E+06	1.50E+06	1.87E+06	1.92E+06	0.00E+00	0.00E+00	1.92E+06	1.69E+06	1.73E+06	0.00E+00	0.00E+00	0.00E+00
25	IRS4	4	2.06E+06	1.91E+06	3.67E+06	1.83E+06	2.35E+06	0.00E+00	1.24E+06	1.48E+06	2.97E+06	2.49E+06	2.31E+06	0.00E+00
26	PDCD5	3	2.32E+06	2.56E+06	6.79E+06	4.04E+06	0.00E+00	2.21E+06	2.43E+06	0.00E+00	3.25E+06	0.00E+00	0.00E+00	0.00E+00
27	MEIS2	3	7.39E+06	5.03E+06	0.00E+00	3.54E+06	5.11E+06	0.00E+00	6.93E+06	5.42E+06	4.76E+06	2.03E+06	3.61E+06	4.09E+06
28	BCKDK	11	7.41E+07	4.95E+07	3.98E+07	3.08E+07	3.86E+07	2.69E+07	6.74E+07	4.87E+07	2.95E+07	1.96E+07	3.15E+07	1.90E+07
29	ARHGEF10	7	2.12E+07	1.57E+07	3.97E+06	0.00E+00	0.00E+00	0.00E+00	1.68E+07	1.45E+07	2.53E+06	0.00E+00	0.00E+00	0.00E+00
30	ZNF609	3	0.00E+00	1.63E+06	0.00E+00	0.00E+00	2.06E+06	0.00E+00	0.00E+00	1.64E+06	0.00E+00	0.00E+00	0.00E+00	0.00E+00
31	SEC16A	13	3.46E+07	4.96E+07	3.56E+07	3.08E+07	3.48E+07	4.28E+07	3.97E+07	3.96E+07	3.71E+07	3.41E+07	4.09E+07	4.01E+07
32	U2SURP	48	2.11E+08	1.96E+08	3.21E+08	2.98E+08	3.04E+08	2.85E+08	2.01E+08	1.98E+08	3.01E+08	3.07E+08	3.78E+08	3.28E+08
33	AXIN1	3	0.00E+00	0.00E+00	0.00E+00	1.09E+06	2.21E+06	1.63E+06	0.00E+00	0.00E+00	0.00E+00	1.23E+06	1.24E+06	0.00E+00
34	NKRF	24	2.76E+07	3.42E+07	3.50E+07	4.26E+07	1.70E+07	1.43E+07	3.42E+07	4.25E+07	2.63E+07	3.50E+07	1.87E+07	1.72E+07
35	SURF4	2	0.00E+00	0.00E+00	1.96E+06	0.00E+00	0.00E+00	0.00E+00	0.00E+00	0.00E+00	0.00E+00	0.00E+00	0.00E+00	0.00E+00
36	MID1	9	1.10E+07	1.21E+07	2.64E+06	0.00E+00	0.00E+00	0.00E+00	1.66E+07	1.11E+07	4.34E+06	0.00E+00	0.00E+00	0.00E+00
37	YY2	2	0.00E+00	0.00E+00	1.40E+07	1.87E+07	2.74E+07	3.39E+07	0.00E+00	0.00E+00	2.00E+07	2.47E+07	3.23E+07	3.34E+07
38	DHX15	45	6.63E+08	6.41E+08	4.43E+08	3.69E+08	7.92E+08	6.15E+08	8.25E+08	8.14E+08	6.06E+08	6.89E+08	8.66E+08	7.10E+08
39	SART1	3	0.00E+00	1.16E+06	2.12E+06	3.74E+06	0.00E+00	0.00E+00	0.00E+00	0.00E+00	3.83E+06	1.76E+06	0.00E+00	0.00E+00
40	CTIF	5	2.68E+06	3.19E+06	0.00E+00	0.00E+00	0.00E+00	1.57E+06	3.55E+06	4.36E+06	2.32E+06	2.08E+06	3.89E+06	2.48E+06
41	RIPK2	5	0.00E+00	5.69E+06	0.00E+00	0.00E+00	5.23E+06	0.00E+00	6.20E+06	0.00E+00	0.00E+00	0.00E+00	0.00E+00	0.00E+00
42	EMC8	1	0.00E+00	0.00E+00	0.00E+00	0.00E+00	0.00E+00	0.00E+00	0.00E+00	0.00E+00	0.00E+00	0.00E+00	0.00E+00	0.00E+00
43	ZNF207	1	0.00E+00	0.00E+00	1.42E+06	2.86E+06	0.00E+00	0.00E+00	0.00E+00	0.00E+00	1.45E+06	1.17E+06	0.00E+00	0.00E+00
44	ACTN4	6	4.92E+06	3.82E+06	8.38E+06	5.58E+06	0.00E+00	0.00E+00	4.29E+06	3.01E+06	6.57E+06	4.89E+06	2.38E+06	0.00E+00
45	HTATSF1	3	0.00E+00	0.00E+00	0.00E+00	0.00E+00	0.00E+00	0.00E+00	0.00E+00	0.00E+00	0.00E+00	0.00E+00	0.00E+00	0.00E+00
46	NUDT21	18	5.10E+08	4.29E+08	1.62E+08	1.42E+08	1.69E+08	1.34E+08	5.19E+08	4.94E+08	1.93E+08	1.88E+08	2.45E+08	1.69E+08
47	PRPSAP2	6	8.08E+06	8.39E+06	5.21E+06	4.38E+06	0.00E+00	0.00E+00	5.03E+06	6.48E+06	2.77E+06	2.74E+06	0.00E+00	0.00E+00
48	OPA1	5	2.53E+06	2.85E+06	4.94E+06	3.63E+06	0.00E+00	0.00E+00	2.62E+06	2.66E+06	3.98E+06	0.00E+00	0.00E+00	0.00E+00
49	KDM1A	3	4.16E+06	5.15E+06	0.00E+00	0.00E+00	0.00E+00	0.00E+00	0.00E+00	3.53E+06	0.00E+00	0.00E+00	0.00E+00	0.00E+00
50	SYNCRIP	1	0.00E+00	0.00E+00	0.00E+00	0.00E+00	0.00E+00	0.00E+00	3.27E+05	0.00E+00	0.00E+00	0.00E+00	0.00E+00	0.00E+00
51	CCNT1	21	8.78E+06	1.18E+07	6.54E+07	5.26E+07	1.48E+08	1.27E+08	1.89E+06	5.41E+06	7.35E+07	8.13E+07	1.25E+08	9.61E+07
52	CCNT2	2	0.00E+00	0.00E+00	0.00E+00	2.05E+06	2.26E+06	2.59E+06	0.00E+00	0.00E+00	2.73E+06	2.56E+06	0.00E+00	2.01E+06
53	DIAPH1	9	6.84E+06	7.82E+06	0.00E+00	0.00E+00	0.00E+00	0.00E+00	7.40E+06	6.70E+06	0.00E+00	0.00E+00	0.00E+00	0.00E+00
54	HIST1H2BL	2	3.48E+07	3.44E+07	6.59E+07	4.58E+07	7.20E+07	4.16E+07	2.87E+07	3.24E+07	3.91E+07	3.47E+07	4.41E+07	5.12E+07
55	PQBP1	2	0.00E+00	0.00E+00	4.84E+06	8.43E+06	0.00E+00	0.00E+00	0.00E+00	0.00E+00	0.00E+00	0.00E+00	0.00E+00	0.00E+00
56	DKC1	1	0.00E+00	0.00E+00	0.00E+00	0.00E+00	0.00E+00	0.00E+00	0.00E+00	0.00E+00	0.00E+00	0.00E+00	0.00E+00	0.00E+00
57	BRD4	38	1.46E+08	1.68E+08	1.32E+08	1.72E+08	1.61E+08	2.48E+08	1.42E+08	1.75E+08	1.63E+08	1.96E+08	2.03E+08	2.16E+08
58	ABCB7	6	7.17E+06	3.77E+06	7.93E+06	4.25E+06	5.22E+06	0.00E+00	0.00E+00	3.28E+06	4.71E+06	4.50E+06	4.62E+06	7.56E+06
59	SRGAP2;SR	3	2.40E+06	2.03E+06	1.64E+06	0.00E+00	0.00E+00	0.00E+00	2.44E+06	1.90E+06	0.00E+00	0.00E+00	0.00E+00	0.00E+00
60	HIP1R	12	1.35E+07	8.96E+06	3.78E+06	3.82E+06	1.59E+06	1.71E+06	1.09E+07	1.41E+07	5.79E+06	4.08E+06	2.92E+06	3.08E+06
61	RNF40	13	1.30E+07	1.12E+07	1.61E+07	1.72E+07	1.98E+07	2.42E+07	1.28E+07	1.36E+07	1.24E+07	1.62E+07	1.80E+07	2.45E+07
62	CNOT3	1	0.00E+00	0.00E+00	0.00E+00	0.00E+00	0.00E+00	0.00E+00	0.00E+00	0.00E+00	0.00E+00	0.00E+00	0.00E+00	0.00E+00
63	ANKRD17	1	0.00E+00	0.00E+00	0.00E+00	0.00E+00	0.00E+00	0.00E+00	0.00E+00	0.00E+00	0.00E+00	0.00E+00	0.00E+00	0.00E+00
64	NCOR1	2	1.10E+06	1.15E+06	0.00E+00	0.00E+00	0.00E+00	0.00E+00	0.00E+00	9.28E+05	0.00E+00	0.00E+00	0.00E+00	0.00E+00
65	NDUFS6	3	0.00E+00	0.00E+00	2.76E+06	2.65E+06	2.44E+06	2.77E+06	0.00E+00	0.00E+00	3.16E+06	2.65E+06	2.35E+06	0.00E+00
66	SEC22B	2	0.00E+00	0.00E+00	0.00E+00	0.00E+00	0.00E+00	0.00E+00	0.00E+00	0.00E+00	0.00E+00	0.00E+00	0.00E+00	0.00E+00

id	Gene names	Unique peptides	LFQ intensity Bait 2h_1	LFQ intensity Control 2h_1	LFQ intensity Bait 2h_2	LFQ intensity Control 2h_2	LFQ intensity Bait 2h_3	LFQ intensity Control 2h_3	LFQ intensity Bait 24h_1	LFQ intensity Control_24h_1	LFQ intensity Bait 24h_2	LFQ intensity Control_24h_2	LFQ intensity 2_Bait 24h_3	LFQ intensity
67	PRPF40A	21	4.70E+07	5.25E+07	4.34E+07	4.40E+07	3.29E+07	2.90E+07	4.53E+07	4.88E+07	3.26E+07	2.66E+07	2.99E+07	3.62E+07
68	SRSF10	2	0.00E+00	0.00E+00	0.00E+00	4.53E+06	0.00E+00	2.20E+06	0.00E+00	0.00E+00	0.00E+00	0.00E+00	0.00E+00	0.00E+00
69	HSBP1	1	0.00E+00	0.00E+00	0.00E+00	0.00E+00	0.00E+00	0.00E+00	0.00E+00	0.00E+00	0.00E+00	0.00E+00	0.00E+00	0.00E+00
70	SF3B1	69	4.26E+08	4.75E+08	7.75E+08	8.98E+08	4.66E+08	6.26E+08	4.82E+08	4.11E+08	6.50E+08	6.68E+08	7.21E+08	5.33E+08
71	ERAL1	1	0.00E+00	0.00E+00	0.00E+00	0.00E+00	0.00E+00	0.00E+00	0.00E+00	0.00E+00	0.00E+00	0.00E+00	0.00E+00	0.00E+00
72	SNRNP200	5	2.36E+06	1.44E+06	6.08E+06	3.15E+06	2.19E+06	0.00E+00	1.32E+06	1.24E+06	7.44E+06	2.98E+06	0.00E+00	0.00E+00
73	CCNK	7	3.07E+07	4.29E+07	1.79E+07	2.25E+07	1.65E+07	1.85E+07	3.45E+07	3.33E+07	2.08E+07	2.15E+07	1.67E+07	1.92E+07
74	PIAS1;PIAS	2	2.83E+06	2.07E+06	0.00E+00	0.00E+00	0.00E+00	0.00E+00	0.00E+00	0.00E+00	0.00E+00	0.00E+00	0.00E+00	0.00E+00
75	BCAS2	1	0.00E+00	0.00E+00	0.00E+00	0.00E+00	0.00E+00	0.00E+00	0.00E+00	0.00E+00	0.00E+00	0.00E+00	0.00E+00	0.00E+00
76	DNAJC8	15	4.31E+07	3.62E+07	1.27E+08	1.65E+08	8.01E+07	1.06E+08	4.06E+07	3.75E+07	8.64E+07	7.99E+07	8.14E+07	8.18E+07
77	SMNDC1	6	1.24E+07	1.54E+07	5.08E+07	6.20E+07	2.92E+07	3.26E+07	1.68E+07	1.55E+07	3.30E+07	2.77E+07	3.44E+07	4.05E+07
78	TRIO	14	1.05E+07	6.87E+06	7.19E+06	5.82E+06	1.04E+07	3.86E+06	1.05E+07	8.92E+06	9.18E+06	5.12E+06	7.93E+06	5.76E+06
79	TOX4	7	5.10E+06	4.86E+06	3.13E+07	3.99E+07	4.82E+07	5.72E+07	5.54E+06	8.03E+06	2.83E+07	4.13E+07	3.21E+07	6.78E+07
80	PRPF6	6	0.00E+00	0.00E+00	5.64E+06	4.25E+06	0.00E+00	2.96E+06	2.34E+06	0.00E+00	4.57E+06	3.15E+06	0.00E+00	2.39E+06
81	PCF11	2	1.32E+06	1.26E+06	1.46E+06	0.00E+00	0.00E+00	0.00E+00	1.25E+06	1.25E+06	1.74E+06	0.00E+00	0.00E+00	0.00E+00
82	FBXO21	4	6.36E+06	5.27E+06	4.93E+06	5.21E+06	1.18E+07	9.85E+06	5.54E+06	0.00E+00	5.42E+06	3.24E+06	5.16E+06	0.00E+00
83	SEC31A	35	1.40E+08	1.54E+08	4.27E+07	4.00E+07	2.78E+07	2.81E+07	1.65E+08	1.92E+08	3.79E+07	4.06E+07	3.78E+07	3.32E+07
84	HEXIM1	6	5.10E+06	0.00E+00	1.85E+07	1.92E+07	8.54E+07	4.85E+07	3.76E+06	4.85E+06	2.72E+07	2.49E+07	4.64E+07	7.07E+07
85	IKBKAP	22	5.66E+07	6.21E+07	1.83E+07	1.28E+07	2.04E+07	1.32E+07	6.36E+07	7.02E+07	1.46E+07	1.72E+07	1.41E+07	1.59E+07
86	SBF1	4	2.98E+06	3.43E+06	1.76E+06	0.00E+00	0.00E+00	0.00E+00	2.31E+06	2.67E+06	0.00E+00	0.00E+00	0.00E+00	0.00E+00
87	PAPSS2	2	1.97E+06	1.87E+06	0.00E+00	0.00E+00	0.00E+00	0.00E+00	2.32E+06	1.70E+06	0.00E+00	0.00E+00	0.00E+00	0.00E+00
88	FARS2	2	0.00E+00	0.00E+00	0.00E+00	0.00E+00	0.00E+00	0.00E+00	0.00E+00	0.00E+00	0.00E+00	0.00E+00	0.00E+00	0.00E+00
89	ZIC2	2	2.30E+06	2.17E+06	4.37E+06	5.08E+06	1.18E+07	1.41E+07	0.00E+00	0.00E+00	3.13E+06	3.94E+06	3.12E+06	3.43E+06
90	H6PD	15	2.45E+07	2.06E+07	4.81E+06	2.67E+06	2.46E+06	0.00E+00	4.86E+07	4.75E+07	8.92E+06	5.90E+06	7.90E+06	1.67E+06
91	SEC24A	1	0.00E+00	0.00E+00	0.00E+00	0.00E+00	0.00E+00	0.00E+00	0.00E+00	0.00E+00	0.00E+00	0.00E+00	0.00E+00	0.00E+00
92	SEC24B	13	1.95E+07	2.04E+07	9.97E+06	6.02E+06	1.01E+07	8.04E+06	1.87E+07	2.69E+07	9.10E+06	9.02E+06	8.81E+06	1.00E+07
93	CPSF4	3	6.51E+06	6.20E+06	5.81E+06	4.86E+06	4.52E+06	4.22E+06	5.73E+06	7.46E+06	0.00E+00	0.00E+00	5.23E+06	5.12E+06
94	NFATC1	2	0.00E+00	4.89E+06	0.00E+00	0.00E+00	0.00E+00	0.00E+00	3.07E+06	3.01E+06	0.00E+00	0.00E+00	0.00E+00	0.00E+00
95	BAG3	30	1.05E+08	1.11E+08	1.23E+08	1.42E+08	1.39E+08	1.77E+08	1.04E+08	8.97E+07	1.49E+08	1.36E+08	1.33E+08	1.44E+08
96	MAP4K4	10	9.08E+06	7.38E+06	3.78E+06	4.24E+06	3.75E+06	5.01E+06	7.74E+06	1.03E+07	6.82E+06	4.29E+06	3.20E+06	5.00E+06
97	SYF2	1	0.00E+00	0.00E+00	0.00E+00	0.00E+00	0.00E+00	0.00E+00	0.00E+00	0.00E+00	0.00E+00	0.00E+00	0.00E+00	0.00E+00
98	ACTL6A	9	2.80E+07	3.14E+07	1.83E+07	1.26E+07	1.02E+07	1.17E+07	1.93E+07	2.95E+07	8.67E+06	1.31E+07	1.02E+07	1.01E+07
99	LMNA	30	6.24E+07	6.53E+07	4.52E+07	5.55E+07	3.03E+07	4.63E+07	4.56E+07	4.64E+07	1.84E+07	2.40E+07	2.03E+07	2.89E+07
100	ALDOA	10	1.84E+07	1.64E+07	1.29E+07	1.19E+07	8.69E+06	7.45E+06	2.09E+07	1.37E+07	1.60E+07	1.58E+07	1.21E+07	8.78E+06
101	CSTB	1	0.00E+00	0.00E+00	0.00E+00	0.00E+00	0.00E+00	0.00E+00	0.00E+00	0.00E+00	0.00E+00	0.00E+00	0.00E+00	0.00E+00
102	GAPDH	25	2.38E+09	2.58E+09	2.29E+09	2.07E+09	7.29E+08	6.11E+08	2.42E+09	2.31E+09	2.04E+09	2.13E+09	7.80E+08	6.47E+08
103	RPN1	5	0.00E+00	0.00E+00	4.55E+06	0.00E+00	0.00E+00	0.00E+00	0.00E+00	0.00E+00	0.00E+00	0.00E+00	0.00E+00	0.00E+00
104	HIST1H2AJ	1	2.69E+07	2.24E+07	8.77E+07	6.56E+07	7.37E+07	5.03E+07	2.12E+07	2.01E+07	6.77E+07	6.54E+07	6.31E+07	5.86E+07
105	SLC4A2	2	0.00E+00	0.00E+00	0.00E+00	0.00E+00	0.00E+00	2.09E+06	0.00E+00	0.00E+00	0.00E+00	0.00E+00	0.00E+00	0.00E+00
106	ATP1A1;AT	4	0.00E+00	0.00E+00	3.87E+06	0.00E+00	2.74E+06	0.00E+00	0.00E+00	0.00E+00	0.00E+00	0.00E+00	0.00E+00	0.00E+00
107	SLC25A5;SI	3	2.30E+06	2.29E+06	2.85E+06	0.00E+00	0.00E+00	0.00E+00	1.89E+06	1.79E+06	0.00E+00	0.00E+00	0.00E+00	0.00E+00
108	RPLP1	1	0.00E+00	0.00E+00	0.00E+00	0.00E+00	0.00E+00	0.00E+00	0.00E+00	0.00E+00	0.00E+00	0.00E+00	0.00E+00	0.00E+00
109	JUN	1	0.00E+00	0.00E+00	0.00E+00	0.00E+00	0.00E+00	0.00E+00	0.00E+00	0.00E+00	0.00E+00	0.00E+00	0.00E+00	0.00E+00
110	TFAP2A;TF	3	3.76E+06	4.49E+06	0.00E+00	0.00E+00	0.00E+00	0.00E+00	3.26E+06	0.00E+00	3.41E+06	0.00E+00	0.00E+00	0.00E+00
111	ATP5B	8	3.90E+06	4.85E+06	1.60E+07	1.18E+07	1.28E+07	9.66E+06	5.18E+06	3.64E+06	7.30E+06	1.28E+07	1.28E+07	9.57E+06
112	ENO1	2	0.00E+00	0.00E+00	0.00E+00	0.00E+00	0.00E+00	0.00E+00	2.66E+06	0.00E+00	0.00E+00	3.98E+06	2.49E+06	0.00E+00
113	NPM1	3	1.92E+06	0.00E+00	2.16E+06	2.23E+06	0.00E+00	0.00E+00	0.00E+00	1.35E+06	2.43E+06	0.00E+00	3.18E+06	1.93E+06
114	TUBB	4	1.69E+08	1.81E+08	2.49E+08	1.42E+08	1.49E+08	8.89E+07	1.78E+08	1.41E+08	1.26E+08	1.20E+08	1.12E+08	1.16E+08
115	PSAP	1	0.00E+00	0.00E+00	0.00E+00	0.00E+00	0.00E+00	0.00E+00	0.00E+00	0.00E+00	0.00E+00	0.00E+00	0.00E+00	0.00E+00
116	HSP90AA1;	3	2.12E+06	2.82E+06	0.00E+00	0.00E+00	0.00E+00	0.00E+00	2.90E+06	2.13E+06	0.00E+00	3.98E+06	0.00E+00	0.00E+00
117	HNRNPC	8	4.82E+06	6.09E+06	1.85E+07	2.08E+07	1.48E+07	1.88E+07	5.76E+06	4.48E+06	1.64E+07	2.30E+07	1.48E+07	2.05E+07
118	PFKM	8	9.81E+06	1.17E+07	1.20E+07	8.31E+06	8.80E+06	0.00E+00	1.10E+07	6.62E+06	1.35E+07	1.22E+07	5.36E+06	5.77E+06
119	SNRNP70	6	2.53E+06	1.64E+06	1.11E+07	9.73E+06	0.00E+00	2.52E+06	1.78E+06	2.19E+06	7.07E+06	3.35E+06	2.42E+06	0.00E+00
120	NFIC	5	9.06E+06	1.47E+07	6.68E+06	8.75E+06	4.45E+06	3.21E+06	1.33E+07	1.49E+07	9.48E+06	8.92E+06	7.75E+06	4.85E+06
121	RPSA	2	0.00E+00	0.00E+00	0.00E+00	0.00E+00	0.00E+00	0.00E+00	0.00E+00	0.00E+00	0.00E+00	0.00E+00	0.00E+00	0.00E+00
122	SNRPA	2	0.00E+00	0.00E+00	1.71E+06	0.00E+00	0.00E+00	0.00E+00	0.00E+00	0.00E+00	0.00E+00	0.00E+00	0.00E+00	0.00E+00
123	SNRPC	2	0.00E+00	0.00E+00	0.00E+00	0.00E+00	0.00E+00	0.00E+00	0.00E+00	0.00E+00	0.00E+00	0.00E+00	0.00E+00	0.00E+00
124	HNRNPA1	7	2.41E+06	2.58E+06	1.07E+07	1.07E+07	1.70E+07	9.76E+06	3.89E+06	2.87E+06	1.79E+07	1.50E+07	1.46E+07	1.01E+07
125	SNRPA1	3	0.00E+00	0.00E+00	2.68E+06	1.87E+06	1.53E+06	2.14E+06	1.47E+06	1.18E+06	2.80E+06	2.91E+06	3.46E+06	1.88E+06
126	PARP1	5	4.09E+06	4.20E+06	4.69E+06	4.70E+06	4.66E+06	6.81E+06	4.11E+06	3.95E+06	8.62E+06	7.87E+06	5.28E+06	7.97E+06
127	UBA52;RPS	1	0.00E+00	0.00E+00	0.00E+00	0.00E+00	0.00E+00	0.00E+00	0.00E+00	0.00E+00	0.00E+00	0.00E+00	0.00E+00	0.00E+00
128	SET;SETSIP	2	0.00E+00	0.00E+00	0.00E+00	0.00E+00	0.00E+00	0.00E+00	0.00E+00	1.17E+06	0.00E+00	0.00E+00	0.00E+00	0.00E+00
129	HSPA1B;HS	17	7.27E+08	6.46E+08	5.52E+08	3.93E+08	4.87E+08	3.73E+08	7.00E+08	5.98E+08	5.98E+08	5.17E+08	5.54E+08	4.08E+08
130	U2AF1	5	6.40E+06	9.08E+06	1.47E+07	1.20E+07	6.83E+06	7.45E+06	7.77E+06	6.56E+06	1.13E+07	1.59E+07	7.03E+06	8.03E+06
131	CBS	6	3.56E+06	4.37E+06	7.29E+06	5.56E+06	5.07E+06	0.00E+00	3.92E+06	3.34E+06	8.03E+06	6.29E+06	4.47E+06	0.00E+00
132	HSPD1	12	1.14E+07	1.32E+07	1.10E+07	1.18E+07	9.15E+06	1.17E+07	2.81E+07	8.37E+06	9.52E+06	1.13E+07	1.99E+07	1.73E+07
133	HSPA5	23	5.87E+07	5.78E+07	6.22E+07	4.75E+07	5.44E+07	4.42E+07	5.52E+07	5.63E+07	6.29E+07	6.02E+07	4.44E+07	4.72E+07

id	Gene names	Unique peptides	LFQ intensity Bait 2h_1	LFQ intensity Control 2h_1	LFQ intensity Bait 2h_2	LFQ intensity Control 2h_2	LFQ intensity Bait 2h_3	LFQ intensity Control 2h_3	LFQ intensity Bait 24h_1	LFQ intensity Control_24h_1	LFQ intensity Bait 24h_2	LFQ intensity Control_24h_2	LFQ intensity 2_Bait 24h_3	LFQ intensity
134	HSPA8	28	5.05E+08	5.69E+08	3.64E+08	3.25E+08	3.83E+08	3.37E+08	5.24E+08	5.50E+08	3.28E+08	3.71E+08	4.01E+08	4.02E+08
135	TOP1	46	5.52E+08	6.59E+08	6.02E+08	7.55E+08	7.04E+08	6.82E+08	6.50E+08	7.35E+08	6.35E+08	7.61E+08	7.58E+08	7.53E+08
136	UBL4A	4	0.00E+00	0.00E+00	5.21E+06	2.95E+06	3.24E+06	2.86E+06	2.23E+06	0.00E+00	3.18E+06	0.00E+00	0.00E+00	3.20E+06
137	PRPS2	2	3.42E+06	3.18E+06	0.00E+00	0.00E+00	0.00E+00	0.00E+00	2.59E+06	2.94E+06	0.00E+00	0.00E+00	0.00E+00	0.00E+00
138	PABPC1	13	1.10E+08	9.16E+07	9.01E+07	6.86E+07	1.42E+08	1.12E+08	1.29E+08	1.21E+08	1.29E+08	1.28E+08	1.73E+08	1.50E+08
139	TPR	13	7.05E+06	7.52E+06	9.22E+06	1.19E+07	6.57E+06	6.19E+06	6.21E+06	4.43E+06	8.07E+06	7.14E+06	1.02E+07	7.82E+06
140	CKMT1A	15	2.38E+08	2.67E+08	1.07E+08	1.19E+08	6.43E+07	6.51E+07	3.22E+08	3.77E+08	1.83E+08	1.60E+08	7.78E+07	8.71E+07
141	PRKCSH	2	0.00E+00	0.00E+00	0.00E+00	0.00E+00	0.00E+00	0.00E+00	0.00E+00	0.00E+00	0.00E+00	0.00E+00	0.00E+00	0.00E+00
142	PKM	2	0.00E+00	0.00E+00	0.00E+00	2.65E+06	0.00E+00	0.00E+00	0.00E+00	0.00E+00	0.00E+00	0.00E+00	0.00E+00	0.00E+00
143	SNRPN;SNI	3	0.00E+00	0.00E+00	7.64E+06	5.91E+06	0.00E+00	0.00E+00	0.00E+00	0.00E+00	3.94E+06	3.46E+06	3.29E+06	0.00E+00
144	IDE	1	0.00E+00	0.00E+00	0.00E+00	0.00E+00	0.00E+00	0.00E+00	0.00E+00	0.00E+00	0.00E+00	0.00E+00	0.00E+00	0.00E+00
145	HNRNPL	34	2.97E+09	3.43E+09	2.79E+09	3.20E+09	3.32E+09	3.88E+09	3.75E+09	4.25E+09	3.44E+09	4.91E+09	4.12E+09	4.29E+09
146	GLUL	7	2.26E+07	2.98E+07	3.38E+07	2.05E+07	3.28E+06	0.00E+00	3.25E+07	2.92E+07	4.04E+07	2.93E+07	7.81E+06	3.93E+06
147	NME1	2	4.22E+06	3.87E+06	6.34E+06	4.37E+06	0.00E+00	0.00E+00	3.95E+06	3.63E+06	5.02E+06	5.48E+06	3.21E+06	0.00E+00
148	TCF4	1	0.00E+00	0.00E+00	0.00E+00	0.00E+00	0.00E+00	0.00E+00	0.00E+00	0.00E+00	0.00E+00	0.00E+00	0.00E+00	0.00E+00
149	TCF3	7	8.63E+06	7.22E+06	8.71E+06	7.38E+06	8.15E+06	8.78E+06	5.15E+06	7.04E+06	5.97E+06	8.39E+06	7.47E+06	6.37E+06
150	HSPA6	1	0.00E+00	0.00E+00	0.00E+00	0.00E+00	0.00E+00	0.00E+00	0.00E+00	0.00E+00	0.00E+00	0.00E+00	0.00E+00	0.00E+00
151	TCP1	24	1.41E+08	1.78E+08	5.41E+07	3.75E+07	1.12E+07	4.30E+06	1.46E+08	1.14E+08	4.17E+07	3.45E+07	1.04E+07	6.51E+06
152	NCL	3	0.00E+00	0.00E+00	0.00E+00	0.00E+00	0.00E+00	0.00E+00	0.00E+00	0.00E+00	0.00E+00	0.00E+00	0.00E+00	4.20E+06
153	CSNK2A2	6	9.84E+06	9.07E+06	6.78E+06	6.44E+06	9.02E+06	6.85E+06	7.62E+06	6.27E+06	8.91E+06	7.24E+06	8.92E+06	5.25E+06
154	TBP;TBPL2	3	4.17E+06	4.50E+06	3.60E+06	3.02E+06	5.33E+06	3.54E+06	4.52E+06	4.45E+06	4.01E+06	4.06E+06	4.20E+06	3.45E+06
155	POU3F2;PC	4	0.00E+00	0.00E+00	1.43E+07	1.25E+07	2.16E+07	1.91E+07	0.00E+00	0.00E+00	1.19E+07	1.71E+07	1.27E+07	1.98E+07
156	HOXA5	3	3.93E+06	3.29E+06	4.05E+06	4.46E+06	2.75E+06	5.82E+06	2.86E+06	2.85E+06	3.15E+06	4.22E+06	0.00E+00	4.61E+06
157	CDK11B;CI	8	9.91E+06	0.00E+00	1.43E+07	1.35E+07	1.09E+07	1.06E+07	9.52E+06	1.02E+07	1.84E+07	1.31E+07	1.43E+07	1.25E+07
158	NF1	1	0.00E+00	0.00E+00	0.00E+00	0.00E+00	0.00E+00	0.00E+00	0.00E+00	0.00E+00	0.00E+00	0.00E+00	0.00E+00	0.00E+00
159	GART	2	1.98E+06	2.64E+06	3.46E+06	2.12E+06	1.76E+06	0.00E+00	0.00E+00	1.50E+06	2.22E+06	0.00E+00	0.00E+00	1.50E+06
160	HNRNPA2E	3	0.00E+00	0.00E+00	0.00E+00	0.00E+00	0.00E+00	0.00E+00	0.00E+00	0.00E+00	0.00E+00	4.19E+06	0.00E+00	0.00E+00
161	CBL	21	3.92E+07	4.02E+07	2.93E+07	2.70E+07	3.51E+07	3.56E+07	5.29E+07	5.30E+07	3.61E+07	4.13E+07	5.45E+07	3.58E+07
162	SFPQ	52	1.35E+09	1.59E+09	2.79E+09	3.91E+09	4.05E+09	4.09E+09	1.49E+09	1.64E+09	2.60E+09	4.67E+09	3.78E+09	5.23E+09
163	TUBG1;TUI	6	8.59E+06	8.82E+06	1.45E+07	1.07E+07	1.23E+07	8.37E+06	1.23E+07	9.64E+06	1.24E+07	1.09E+07	1.16E+07	8.14E+06
164	GATA3	2	0.00E+00	0.00E+00	0.00E+00	0.00E+00	0.00E+00	1.99E+06	0.00E+00	0.00E+00	0.00E+00	0.00E+00	0.00E+00	0.00E+00
165	EEF1B2	1	0.00E+00	0.00E+00	0.00E+00	0.00E+00	0.00E+00	0.00E+00	0.00E+00	0.00E+00	0.00E+00	0.00E+00	0.00E+00	0.00E+00
166	RPS12	1	0.00E+00	0.00E+00	0.00E+00	0.00E+00	0.00E+00	0.00E+00	1.24E+05	0.00E+00	0.00E+00	0.00E+00	0.00E+00	0.00E+00
167	YY1	18	7.09E+06	1.01E+07	1.10E+08	1.49E+08	2.61E+08	2.38E+08	1.05E+07	8.78E+06	1.58E+08	1.59E+08	2.44E+08	2.74E+08
168	ATP5A1	5	3.26E+06	3.29E+06	1.76E+07	8.94E+06	1.15E+07	8.40E+06	3.57E+06	0.00E+00	9.02E+06	9.03E+06	8.83E+06	1.13E+07
169	DDX6	17	1.01E+08	9.44E+07	1.05E+08	9.38E+07	1.53E+08	1.21E+08	1.51E+08	1.45E+08	1.06E+08	1.33E+08	1.57E+08	1.71E+08
170	U2AF2	6	5.86E+06	5.76E+06	1.31E+07	8.68E+06	7.12E+06	5.94E+06	5.63E+06	6.15E+06	1.37E+07	1.02E+07	5.82E+06	6.01E+06
171	IVD	15	5.68E+07	6.83E+07	2.03E+07	1.40E+07	1.29E+07	2.79E+06	6.17E+07	6.26E+07	2.64E+07	1.52E+07	1.30E+07	7.73E+06
172	EEF1G	2	0.00E+00	3.33E+06	2.39E+06	0.00E+00	2.49E+06	0.00E+00	5.08E+06	0.00E+00	0.00E+00	0.00E+00	0.00E+00	0.00E+00
173	YWHAQ;SF	1	0.00E+00	0.00E+00	0.00E+00	0.00E+00	0.00E+00	0.00E+00	0.00E+00	0.00E+00	0.00E+00	0.00E+00	0.00E+00	0.00E+00
174	CAD	17	1.70E+07	2.02E+07	2.08E+07	1.01E+07	4.39E+06	0.00E+00	1.93E+07	1.23E+07	1.39E+07	7.68E+06	6.09E+06	0.00E+00
175	CANX	8	4.37E+06	4.86E+06	2.41E+07	1.11E+07	1.32E+07	7.10E+06	4.95E+06	5.18E+06	1.23E+07	1.16E+07	1.66E+07	1.18E+07
176	MAPK1	9	6.44E+06	1.15E+07	1.51E+07	1.31E+07	6.20E+06	7.26E+06	9.96E+06	1.17E+07	8.42E+06	1.21E+07	4.34E+06	6.17E+06
177	PRDX3	8	4.76E+07	5.54E+07	5.88E+07	5.17E+07	1.22E+07	1.16E+07	5.61E+07	5.34E+07	8.04E+07	6.19E+07	2.14E+07	2.04E+07
178	ATP5D	1	0.00E+00	0.00E+00	0.00E+00	0.00E+00	0.00E+00	0.00E+00	0.00E+00	0.00E+00	0.00E+00	0.00E+00	0.00E+00	0.00E+00
179	PPP2R1A	4	9.98E+06	1.32E+07	6.49E+06	0.00E+00	0.00E+00	0.00E+00	8.80E+06	7.71E+06	6.04E+06	0.00E+00	0.00E+00	0.00E+00
180	LRPAP1	23	7.47E+07	1.15E+08	9.41E+07	1.43E+08	6.89E+07	1.23E+08	5.66E+07	7.17E+07	6.53E+07	7.88E+07	4.88E+07	7.29E+07
181	ADSL	12	2.80E+07	3.42E+07	2.59E+07	1.87E+07	4.23E+06	3.91E+06	3.08E+07	3.52E+07	2.46E+07	1.96E+07	6.78E+06	5.22E+06
182	MAT2A	6	1.57E+07	1.90E+07	1.90E+07	1.81E+07	0.00E+00	0.00E+00	1.71E+07	1.26E+07	1.68E+07	1.16E+07	0.00E+00	0.00E+00
183	HOXA9	2	0.00E+00	0.00E+00	0.00E+00	0.00E+00	4.06E+06	3.40E+06	0.00E+00	0.00E+00	0.00E+00	0.00E+00	0.00E+00	0.00E+00
184	HOXA13	3	2.54E+06	3.80E+06	4.12E+06	2.21E+06	1.73E+06	1.53E+06	1.41E+06	1.64E+06	2.25E+06	0.00E+00	0.00E+00	0.00E+00
185	DNAJA1	2	0.00E+00	0.00E+00	0.00E+00	0.00E+00	0.00E+00	0.00E+00	0.00E+00	0.00E+00	0.00E+00	0.00E+00	0.00E+00	0.00E+00
186	HNRNPH1;	5	1.34E+07	1.40E+07	1.60E+07	1.32E+07	1.07E+07	6.85E+06	1.35E+07	1.47E+07	1.47E+07	1.46E+07	1.23E+07	1.10E+07
187	YWHAB	2	0.00E+00	1.71E+06	0.00E+00	0.00E+00	0.00E+00	0.00E+00	1.87E+06	1.63E+06	0.00E+00	0.00E+00	0.00E+00	0.00E+00
188	CTH	12	6.73E+07	6.11E+07	2.54E+07	1.79E+07	3.34E+07	1.97E+07	8.63E+07	1.01E+08	3.86E+07	2.87E+07	4.31E+07	2.80E+07
189	CSTF2	5	1.56E+07	1.45E+07	2.06E+07	2.68E+07	1.83E+07	2.13E+07	1.75E+07	1.75E+07	2.22E+07	1.27E+07	2.76E+07	2.35E+07
190	SHMT2	12	7.63E+06	9.29E+06	3.62E+07	2.31E+07	5.94E+06	0.00E+00	1.39E+07	2.03E+07	3.34E+07	2.63E+07	6.00E+06	8.15E+06
191	HSPA4	4	2.81E+06	2.68E+06	0.00E+00	0.00E+00	0.00E+00	0.00E+00	3.62E+06	2.47E+06	0.00E+00	0.00E+00	0.00E+00	0.00E+00
192	LONP1	1	0.00E+00	0.00E+00	0.00E+00	0.00E+00	0.00E+00	0.00E+00	0.00E+00	0.00E+00	0.00E+00	0.00E+00	0.00E+00	0.00E+00
193	PPP1CC	3	3.59E+06	4.57E+06	6.75E+06	8.65E+06	1.88E+07	1.44E+07	4.17E+06	5.11E+06	6.42E+06	1.34E+07	1.48E+07	1.40E+07
194	RBMX;RBM	7	2.84E+06	2.64E+06	1.30E+07	8.82E+06	1.27E+07	6.01E+06	3.29E+06	3.08E+06	8.35E+06	6.50E+06	6.45E+06	8.55E+06
195	HSPA9	26	6.37E+07	6.39E+07	7.41E+07	6.17E+07	4.98E+07	4.35E+07	6.16E+07	6.73E+07	5.37E+07	5.69E+07	5.35E+07	5.02E+07
196	EIF4A3	2	0.00E+00	1.11E+06	0.00E+00	0.00E+00	0.00E+00	0.00E+00	0.00E+00	0.00E+00	0.00E+00	0.00E+00	0.00E+00	0.00E+00
197	CCT6A	24	1.76E+08	1.91E+08	7.91E+07	5.57E+07	2.27E+07	1.25E+07	1.64E+08	1.51E+08	6.30E+07	4.91E+07	2.50E+07	1.95E+07
198	PBX1	3	4.20E+06	3.20E+06	3.90E+06	3.36E+06	5.06E+06	0.00E+00	4.37E+06	4.43E+06	3.55E+06	3.23E+06	3.97E+06	6.56E+06
199	PBX2	6	1.12E+07	7.95E+06	5.53E+06	8.01E+06	9.98E+06	7.99E+06	1.10E+07	1.29E+07	7.34E+06	5.26E+06	7.61E+06	1.15E+07
200	PBX3	1	0.00E+00	0.00E+00	0.00E+00	0.00E+00	0.00E+00	0.00E+00	0.00E+00	0.00E+00	0.00E+00	0.00E+00	0.00E+00	0.00E+00

id	Gene names	Unique peptides	LFQ intensity Bait 2h_1	LFQ intensity Control 2h_1	LFQ intensity Bait 2h_2	LFQ intensity Control 2h_2	LFQ intensity Bait 2h_3	LFQ intensity Control 2h_3	LFQ intensity Bait 24h_1	LFQ intensity Control_24h_1	LFQ intensity Bait 24h_2	LFQ intensity Control_24h_2	LFQ intensity 2_Bait 24h_3	LFQ intensity
201	PRKCI	4	4.43E+06	5.72E+06	0.00E+00	0.00E+00	0.00E+00	0.00E+00	3.57E+06	5.49E+06	3.91E+06	0.00E+00	0.00E+00	0.00E+00
202	TMPO	3	0.00E+00	0.00E+00	3.59E+06	3.02E+06	0.00E+00	0.00E+00	0.00E+00	0.00E+00	0.00E+00	0.00E+00	2.47E+06	0.00E+00
203	HELZ	11	1.16E+07	1.07E+07	1.85E+07	1.12E+07	2.18E+07	1.96E+07	8.85E+06	7.03E+06	1.72E+07	1.39E+07	1.48E+07	1.43E+07
204	MATR3	14	1.46E+07	2.03E+07	2.89E+07	2.07E+07	3.88E+06	0.00E+00	1.59E+07	1.58E+07	1.52E+07	1.25E+07	3.95E+06	6.16E+06
205	RANBP1	3	2.85E+06	0.00E+00	4.48E+06	4.70E+06	3.84E+06	7.52E+06	3.61E+06	2.69E+06	6.85E+06	6.48E+06	5.73E+06	7.68E+06
206	BAG6	10	1.56E+07	1.22E+07	1.15E+07	5.46E+06	7.21E+06	5.43E+06	8.39E+06	9.20E+06	7.74E+06	4.26E+06	6.18E+06	4.81E+06
207	ID4	1	0.00E+00	0.00E+00	0.00E+00	0.00E+00	0.00E+00	0.00E+00	0.00E+00	0.00E+00	0.00E+00	0.00E+00	0.00E+00	0.00E+00
208	ATP5O	1	0.00E+00	0.00E+00	0.00E+00	0.00E+00	0.00E+00	0.00E+00	0.00E+00	0.00E+00	0.00E+00	0.00E+00	0.00E+00	0.00E+00
209	PPP3CC	1	0.00E+00	0.00E+00	0.00E+00	0.00E+00	0.00E+00	0.00E+00	0.00E+00	0.00E+00	0.00E+00	0.00E+00	0.00E+00	0.00E+00
210	CCT5	25	1.69E+08	1.61E+08	6.65E+07	5.59E+07	1.84E+07	1.76E+07	1.58E+08	1.32E+08	5.90E+07	5.15E+07	1.64E+07	2.13E+07
211	LMAN1	19	7.37E+07	8.04E+07	2.12E+08	1.44E+08	1.37E+08	9.76E+07	8.29E+07	6.09E+07	6.47E+07	1.02E+08	1.63E+08	1.53E+08
212	FASN	2	0.00E+00	0.00E+00	0.00E+00	0.00E+00	0.00E+00	0.00E+00	6.71E+05	0.00E+00	8.60E+05	0.00E+00	0.00E+00	0.00E+00
213	CCT3	25	2.32E+08	2.27E+08	8.44E+07	6.14E+07	1.85E+07	1.18E+07	2.31E+08	1.76E+08	6.18E+07	5.36E+07	1.82E+07	1.58E+07
214	TUFM	13	4.92E+07	6.09E+07	9.55E+07	5.34E+07	1.39E+07	6.91E+06	4.16E+07	4.12E+07	3.48E+07	3.30E+07	1.02E+07	1.14E+07
215	SRP9	1	0.00E+00	0.00E+00	0.00E+00	0.00E+00	0.00E+00	0.00E+00	0.00E+00	0.00E+00	0.00E+00	0.00E+00	0.00E+00	0.00E+00
216	YLPM1	32	8.36E+07	9.11E+07	6.77E+07	7.81E+07	9.22E+07	8.51E+07	9.47E+07	1.00E+08	7.58E+07	7.47E+07	1.00E+08	8.44E+07
217	TMED10	1	0.00E+00	0.00E+00	0.00E+00	0.00E+00	0.00E+00	0.00E+00	0.00E+00	0.00E+00	0.00E+00	0.00E+00	0.00E+00	0.00E+00
218	RBM25	14	3.16E+07	2.88E+07	2.78E+07	2.50E+07	1.51E+07	2.10E+07	2.37E+07	2.91E+07	1.93E+07	1.25E+07	1.98E+07	2.04E+07
219	CLK3	7	8.12E+06	6.92E+06	3.84E+06	4.82E+06	7.54E+06	5.19E+06	1.09E+07	7.49E+06	6.58E+06	5.15E+06	4.20E+06	7.50E+06
220	HINT1	4	0.00E+00	0.00E+00	1.63E+07	2.29E+07	0.00E+00	0.00E+00	3.57E+06	0.00E+00	1.23E+07	1.16E+07	5.02E+06	3.12E+06
221	RANBP2	6	7.04E+06	6.89E+06	5.61E+06	4.94E+06	0.00E+00	0.00E+00	6.42E+06	6.08E+06	0.00E+00	0.00E+00	0.00E+00	0.00E+00
222	NT5C2	12	1.37E+07	2.66E+07	3.43E+06	2.54E+06	0.00E+00	0.00E+00	9.71E+06	1.70E+07	3.17E+06	0.00E+00	0.00E+00	0.00E+00
223	MNX1	4	7.93E+06	8.71E+06	5.76E+06	7.68E+06	5.36E+06	5.41E+06	7.87E+06	8.84E+06	6.64E+06	6.91E+06	4.98E+06	4.61E+06
224	SERPINH1	7	9.62E+06	6.52E+06	1.13E+07	6.47E+06	6.45E+06	0.00E+00	8.15E+06	6.38E+06	6.14E+06	5.42E+06	0.00E+00	5.03E+06
225	CDK9	8	9.82E+06	1.01E+07	3.04E+07	2.37E+07	5.76E+07	4.09E+07	9.45E+06	8.74E+06	3.75E+07	4.32E+07	5.67E+07	4.56E+07
226	CCT8	31	2.56E+08	2.83E+08	9.56E+07	8.04E+07	3.25E+07	2.64E+07	2.48E+08	2.26E+08	7.21E+07	7.71E+07	3.51E+07	2.94E+07
227	CCT4	21	1.45E+08	1.52E+08	5.69E+07	4.30E+07	1.69E+07	1.11E+07	1.33E+08	1.44E+08	4.58E+07	4.57E+07	2.12E+07	1.48E+07
228	DAP3	2	0.00E+00	0.00E+00	0.00E+00	0.00E+00	0.00E+00	0.00E+00	0.00E+00	0.00E+00	0.00E+00	0.00E+00	0.00E+00	0.00E+00
229	DNA2	2	0.00E+00	0.00E+00	0.00E+00	0.00E+00	0.00E+00	0.00E+00	0.00E+00	0.00E+00	0.00E+00	0.00E+00	0.00E+00	0.00E+00
230	SMARCA4	9	1.61E+07	1.50E+07	2.20E+07	1.80E+07	1.77E+07	1.14E+07	1.55E+07	1.46E+07	1.69E+07	1.46E+07	1.64E+07	1.27E+07
231	GALK1	2	0.00E+00	0.00E+00	2.14E+06	1.73E+06	0.00E+00	0.00E+00	1.44E+06	1.21E+06	5.96E+06	5.65E+06	0.00E+00	0.00E+00
232	MECP2	28	6.97E+07	9.58E+07	2.16E+08	2.89E+08	1.82E+08	2.34E+08	9.56E+07	1.15E+08	2.40E+08	2.68E+08	2.46E+08	3.07E+08
233	HNRNPA3	3	0.00E+00	1.91E+06	3.70E+06	3.40E+06	3.87E+06	3.33E+06	1.96E+06	1.56E+06	3.66E+06	7.06E+06	3.32E+06	4.87E+06
234	HNRNPM	2	0.00E+00	0.00E+00	0.00E+00	0.00E+00	0.00E+00	0.00E+00	0.00E+00	0.00E+00	0.00E+00	0.00E+00	0.00E+00	0.00E+00
235	KPNA2	5	5.07E+06	4.54E+06	5.61E+06	5.20E+06	4.78E+06	5.34E+06	3.07E+06	3.93E+06	5.47E+06	4.40E+06	2.79E+06	3.88E+06
236	GTF2A1	4	1.04E+07	1.16E+07	4.41E+07	5.48E+07	6.67E+07	6.70E+07	1.68E+07	1.60E+07	5.15E+07	4.55E+07	6.07E+07	7.78E+07
237	GTF2A2	1	0.00E+00	0.00E+00	0.00E+00	0.00E+00	0.00E+00	0.00E+00	0.00E+00	0.00E+00	0.00E+00	0.00E+00	0.00E+00	0.00E+00
238	ZNF143;ZN	2	0.00E+00	0.00E+00	0.00E+00	0.00E+00	0.00E+00	0.00E+00	0.00E+00	0.00E+00	0.00E+00	4.70E+06	0.00E+00	0.00E+00
239	RBM5	2	0.00E+00	0.00E+00	3.47E+06	2.72E+06	0.00E+00	0.00E+00	0.00E+00	1.98E+06	0.00E+00	0.00E+00	0.00E+00	0.00E+00
240	CTSC	5	9.37E+06	1.32E+07	4.16E+06	3.52E+06	0.00E+00	0.00E+00	9.80E+06	1.05E+07	3.48E+06	1.88E+06	0.00E+00	0.00E+00
241	SUB1	5	1.68E+07	2.09E+07	1.97E+07	3.53E+07	3.02E+07	2.51E+07	2.56E+07	2.25E+07	2.15E+07	2.63E+07	2.30E+07	3.93E+07
242	ATN1	10	0.00E+00	0.00E+00	2.11E+07	3.32E+07	4.91E+07	5.26E+07	0.00E+00	0.00E+00	2.13E+07	2.05E+07	2.67E+07	2.97E+07
243	ALDH18A1	5	4.52E+06	2.60E+06	4.89E+06	0.00E+00	0.00E+00	0.00E+00	2.56E+06	2.38E+06	2.90E+06	0.00E+00	0.00E+00	0.00E+00
244	SLC12A2	10	2.03E+07	2.64E+07	3.60E+07	4.05E+07	1.85E+07	2.18E+07	1.32E+07	1.63E+07	1.88E+07	1.76E+07	1.39E+07	1.62E+07
245	CSE1L	4	0.00E+00	0.00E+00	2.09E+07	0.00E+00	3.04E+07	1.31E+07	0.00E+00	0.00E+00	1.23E+07	0.00E+00	1.54E+07	0.00E+00
246	MFAP1	4	6.66E+06	7.18E+06	1.78E+07	2.03E+07	6.89E+06	9.01E+06	5.73E+06	4.93E+06	9.59E+06	7.19E+06	6.03E+06	8.00E+06
247	LAMB2	1	0.00E+00	0.00E+00	0.00E+00	0.00E+00	0.00E+00	0.00E+00	0.00E+00	0.00E+00	0.00E+00	0.00E+00	0.00E+00	0.00E+00
248	FOXA1	1	0.00E+00	0.00E+00	0.00E+00	0.00E+00	0.00E+00	0.00E+00	0.00E+00	0.00E+00	0.00E+00	0.00E+00	0.00E+00	0.00E+00
249	SEC13	7	5.87E+07	5.70E+07	9.41E+06	0.00E+00	9.72E+06	0.00E+00	5.51E+07	7.60E+07	6.16E+06	8.62E+06	1.03E+07	9.08E+06
250	DLX5;DLX2	3	0.00E+00	0.00E+00	6.63E+06	1.15E+07	1.57E+07	1.09E+07	0.00E+00	0.00E+00	1.14E+07	9.38E+06	5.32E+06	1.33E+07
251	MAZ	2	4.74E+06	3.62E+06	3.56E+06	4.22E+06	0.00E+00	2.37E+06	4.25E+06	3.14E+06	3.59E+06	2.87E+06	0.00E+00	3.06E+06
252	CTBP2	1	0.00E+00	0.00E+00	0.00E+00	0.00E+00	0.00E+00	0.00E+00	0.00E+00	0.00E+00	0.00E+00	0.00E+00	0.00E+00	0.00E+00
253	ACTG1;ACT	5	2.38E+07	2.86E+07	3.08E+07	2.56E+07	2.22E+07	1.85E+07	3.00E+07	2.41E+07	2.46E+07	4.18E+07	3.14E+07	1.92E+07
254	PRPS1;PRP	2	1.06E+07	1.38E+07	1.02E+07	8.27E+06	5.89E+06	0.00E+00	8.99E+06	9.54E+06	5.51E+06	6.30E+06	0.00E+00	0.00E+00
255	MAX	4	3.28E+06	3.28E+06	3.35E+06	5.70E+06	3.97E+06	5.04E+06	3.63E+06	3.66E+06	2.60E+06	2.87E+06	3.67E+06	3.89E+06
256	PCBD1	3	2.08E+06	1.96E+06	4.83E+06	6.39E+06	0.00E+00	0.00E+00	1.77E+06	1.61E+06	8.57E+06	3.49E+06	0.00E+00	0.00E+00
257	DCAF7	7	2.75E+07	3.10E+07	2.91E+07	1.78E+07	4.48E+07	2.18E+07	1.95E+07	1.75E+07	1.55E+07	2.00E+07	2.46E+07	2.70E+07
258	WDR5	6	0.00E+00	2.67E+06	7.44E+06	7.20E+06	1.35E+07	1.46E+07	2.96E+06	0.00E+00	7.87E+06	8.56E+06	1.33E+07	1.07E+07
259	HNRNPK	7	5.53E+06	6.71E+06	7.98E+06	7.30E+06	0.00E+00	0.00E+00	8.39E+06	7.86E+06	7.19E+06	1.21E+07	6.02E+06	4.28E+06
260	YWHAG	1	0.00E+00	0.00E+00	0.00E+00	0.00E+00	0.00E+00	0.00E+00	0.00E+00	0.00E+00	0.00E+00	0.00E+00	0.00E+00	0.00E+00
261	PPP1CA	4	6.42E+06	6.05E+06	7.07E+06	1.07E+07	1.33E+07	1.79E+07	8.64E+06	7.89E+06	1.05E+07	1.42E+07	1.04E+07	1.75E+07
262	PPP1CB	2	0.00E+00	0.00E+00	0.00E+00	0.00E+00	0.00E+00	0.00E+00	1.21E+06	0.00E+00	0.00E+00	0.00E+00	0.00E+00	0.00E+00
263	YWHAE	7	1.52E+07	1.88E+07	1.30E+07	9.64E+06	1.09E+07	9.38E+06	2.10E+07	1.72E+07	1.52E+07	1.49E+07	1.40E+07	1.07E+07
264	SNRPE	1	0.00E+00	0.00E+00	0.00E+00	0.00E+00	0.00E+00	0.00E+00	0.00E+00	0.00E+00	0.00E+00	0.00E+00	0.00E+00	0.00E+00
265	SNRPF	2	5.05E+06	4.97E+06	1.04E+07	9.64E+06	4.66E+06	3.64E+06	4.23E+06	4.03E+06	6.16E+06	5.67E+06	5.78E+06	4.36E+06
266	SNRPD1	2	2.32E+06	1.30E+06	5.09E+06	2.66E+06	1.93E+06	0.00E+00	2.04E+06	0.00E+00	0.00E+00	2.66E+06	0.00E+00	0.00E+00
267	SNRPD2	5	2.95E+06	2.20E+06	1.41E+07	1.37E+07	4.24E+06	4.10E+06	2.23E+06	2.58E+06	6.35E+06	4.28E+06	5.08E+06	4.08E+06

id	Gene names	Unique peptides	LFQ intensity Bait 2h_1	LFQ intensity Control 2h_1	LFQ intensity Bait 2h_2	LFQ intensity Control 2h_2	LFQ intensity Bait 2h_3	LFQ intensity Control 2h_3	LFQ intensity Bait 24h_1	LFQ intensity Control_24h_1	LFQ intensity Bait 24h_2	LFQ intensity Control_24h_2	LFQ intensity 2_Bait 24h_3	LFQ intensity
268	SNRPD3	3	5.35E+06	3.26E+06	1.12E+07	1.32E+07	5.69E+06	0.00E+00	6.48E+06	3.80E+06	0.00E+00	0.00E+00	0.00E+00	0.00E+00
269	TBPL1	2	8.45E+06	7.18E+06	7.04E+06	5.62E+06	1.26E+07	8.78E+06	7.14E+06	9.40E+06	8.55E+06	6.53E+06	9.80E+06	6.91E+06
270	RAB11A;RA	2	0.00E+00	0.00E+00	2.54E+06	0.00E+00	1.81E+06	0.00E+00	0.00E+00	0.00E+00	0.00E+00	0.00E+00	0.00E+00	0.00E+00
271	PPP2CA;PP	3	8.28E+06	7.25E+06	4.13E+06	0.00E+00	0.00E+00	0.00E+00	7.21E+06	6.82E+06	0.00E+00	0.00E+00	0.00E+00	0.00E+00
272	ACTG2;ACT	1	0.00E+00	0.00E+00	0.00E+00	0.00E+00	0.00E+00	0.00E+00	0.00E+00	0.00E+00	0.00E+00	0.00E+00	0.00E+00	0.00E+00
273	HIST1H4A	6	4.67E+07	4.49E+07	8.77E+07	5.50E+07	7.92E+07	4.78E+07	4.28E+07	4.17E+07	5.58E+07	5.63E+07	7.35E+07	6.70E+07
274	RAB1B;RAE	1	0.00E+00	0.00E+00	0.00E+00	0.00E+00	0.00E+00	0.00E+00	0.00E+00	0.00E+00	0.00E+00	0.00E+00	0.00E+00	0.00E+00
275	RAN	2	1.40E+06	0.00E+00	1.75E+06	0.00E+00	0.00E+00	0.00E+00	1.53E+06	0.00E+00	1.47E+06	0.00E+00	1.88E+06	1.27E+06
276	RPS28	2	0.00E+00	0.00E+00	0.00E+00	4.35E+06	0.00E+00	6.16E+06	0.00E+00	0.00E+00	0.00E+00	0.00E+00	0.00E+00	4.36E+06
277	PPIA	1	0.00E+00	0.00E+00	0.00E+00	0.00E+00	0.00E+00	0.00E+00	0.00E+00	0.00E+00	0.00E+00	0.00E+00	0.00E+00	0.00E+00
278	TRA2B	3	2.89E+06	3.67E+06	1.24E+07	9.95E+06	1.01E+07	1.05E+07	2.88E+06	2.47E+06	1.27E+07	7.71E+06	4.74E+06	9.74E+06
279	PPP3R1	3	1.92E+06	0.00E+00	0.00E+00	0.00E+00	0.00E+00	0.00E+00	0.00E+00	0.00E+00	0.00E+00	0.00E+00	0.00E+00	0.00E+00
280	YWHAZ	2	0.00E+00	0.00E+00	0.00E+00	0.00E+00	0.00E+00	0.00E+00	0.00E+00	0.00E+00	0.00E+00	2.22E+06	2.47E+06	0.00E+00
281	DYNLL2;DY	1	0.00E+00	0.00E+00	0.00E+00	0.00E+00	0.00E+00	0.00E+00	0.00E+00	0.00E+00	0.00E+00	0.00E+00	0.00E+00	0.00E+00
282	SKP1	6	1.15E+07	7.68E+06	7.44E+06	6.77E+06	1.97E+07	1.15E+07	5.15E+06	7.68E+06	9.56E+06	1.09E+07	1.00E+07	9.10E+06
283	EIF5A	6	6.27E+06	3.85E+06	1.29E+07	1.46E+07	9.76E+06	5.41E+06	8.02E+06	4.60E+06	1.75E+07	1.36E+07	1.15E+07	8.96E+06
284	CSNK2B	3	6.85E+06	0.00E+00	5.87E+06	4.12E+06	5.29E+06	5.63E+06	4.83E+06	5.22E+06	6.22E+06	7.55E+06	7.21E+06	4.31E+06
285	EEF1A1P5;	7	2.72E+07	2.25E+07	3.00E+07	1.39E+07	1.54E+07	8.00E+06	2.37E+07	2.19E+07	1.37E+07	1.59E+07	1.37E+07	1.34E+07
286	TUBA1C;TU	15	1.15E+08	1.22E+08	1.69E+08	1.03E+08	1.22E+08	6.68E+07	1.18E+08	9.55E+07	8.59E+07	8.38E+07	1.03E+08	9.95E+07
287	TUBB4B;TU	3	2.79E+07	2.49E+07	5.30E+07	2.47E+07	2.80E+07	1.37E+07	2.20E+07	1.07E+07	2.06E+07	1.62E+07	1.46E+07	1.98E+07
288	CSNK2A1;C	12	3.32E+07	2.74E+07	2.93E+07	2.71E+07	4.59E+07	3.99E+07	2.48E+07	2.31E+07	3.18E+07	2.50E+07	2.99E+07	3.19E+07
289	HIST2H3A;I	3	7.61E+06	8.97E+06	1.86E+07	8.51E+06	1.29E+07	8.33E+06	6.36E+06	6.79E+06	1.06E+07	1.30E+07	1.38E+07	1.40E+07
290	CCT2	30	2.22E+08	2.47E+08	1.18E+08	9.06E+07	3.06E+07	2.26E+07	2.27E+08	1.84E+08	8.63E+07	6.98E+07	2.75E+07	3.10E+07
291	MRPS35	1	0.00E+00	0.00E+00	0.00E+00	0.00E+00	0.00E+00	0.00E+00	0.00E+00	0.00E+00	0.00E+00	0.00E+00	0.00E+00	0.00E+00
292	MRPS9	2	3.06E+06	2.91E+06	0.00E+00	1.32E+06	0.00E+00	0.00E+00	0.00E+00	0.00E+00	0.00E+00	0.00E+00	0.00E+00	0.00E+00
293	ERH	6	2.15E+07	2.21E+07	8.52E+07	7.34E+07	3.41E+07	3.26E+07	2.28E+07	1.75E+07	8.65E+07	5.08E+07	4.80E+07	3.80E+07
294	SRSF3	4	0.00E+00	2.63E+06	1.23E+07	1.61E+07	9.06E+06	0.00E+00	0.00E+00	0.00E+00	1.52E+07	1.39E+07	1.08E+07	6.74E+06
295	RBM10	15	1.34E+07	1.41E+07	3.40E+07	3.84E+07	1.79E+07	1.19E+07	1.82E+07	1.25E+07	3.63E+07	3.20E+07	2.64E+07	2.30E+07
296	SLC25A3	1	0.00E+00	0.00E+00	0.00E+00	0.00E+00	0.00E+00	0.00E+00	0.00E+00	0.00E+00	0.00E+00	0.00E+00	0.00E+00	0.00E+00
297	HNRNPU	5	7.17E+06	9.40E+06	1.43E+07	6.96E+06	1.27E+07	1.07E+07	8.24E+06	5.71E+06	1.48E+07	1.53E+07	1.10E+07	1.06E+07
298	SRSF2	1	0.00E+00	4.80E+05	0.00E+00	0.00E+00	0.00E+00	0.00E+00	0.00E+00	0.00E+00	0.00E+00	0.00E+00	0.00E+00	0.00E+00
299	AMPD2	3	3.43E+06	4.17E+06	0.00E+00	0.00E+00	0.00E+00	0.00E+00	3.79E+06	3.59E+06	0.00E+00	0.00E+00	0.00E+00	0.00E+00
300	TFAP4	1	0.00E+00	0.00E+00	0.00E+00	0.00E+00	0.00E+00	0.00E+00	0.00E+00	0.00E+00	0.00E+00	0.00E+00	0.00E+00	0.00E+00
301	OTUD4	4	2.88E+06	3.50E+06	2.28E+06	2.32E+06	2.66E+06	3.22E+06	2.59E+06	3.30E+06	0.00E+00	2.31E+06	0.00E+00	2.65E+06
302	PFKP	4	1.33E+06	1.69E+06	3.04E+06	1.87E+06	0.00E+00	0.00E+00	0.00E+00	0.00E+00	2.14E+06	0.00E+00	0.00E+00	0.00E+00
303	SATB1	17	6.66E+07	5.43E+07	3.44E+07	2.64E+07	3.55E+07	2.98E+07	5.71E+07	5.51E+07	2.37E+07	2.59E+07	4.07E+07	2.57E+07
304	ALDH6A1	4	6.27E+06	4.51E+06	0.00E+00	0.00E+00	0.00E+00	0.00E+00	5.59E+06	4.04E+06	0.00E+00	3.27E+06	0.00E+00	0.00E+00
305	NUCB1	11	7.67E+06	1.27E+07	1.54E+07	1.36E+07	2.23E+06	3.06E+06	2.93E+06	2.08E+06	7.17E+06	0.00E+00	0.00E+00	0.00E+00
306	CREB5	1	0.00E+00	0.00E+00	0.00E+00	0.00E+00	0.00E+00	0.00E+00	0.00E+00	0.00E+00	0.00E+00	0.00E+00	0.00E+00	0.00E+00
307	NOTCH2	3	5.75E+06	4.97E+06	4.09E+06	4.33E+06	4.22E+06	4.33E+06	3.77E+06	4.52E+06	2.59E+06	2.21E+06	0.00E+00	4.07E+06
308	TLE1	6	3.73E+07	3.37E+07	2.18E+07	2.00E+07	2.77E+07	2.13E+07	3.46E+07	4.08E+07	1.96E+07	1.91E+07	2.44E+07	2.37E+07
309	TLE3	16	1.71E+08	1.53E+08	6.34E+07	6.50E+07	8.48E+07	8.27E+07	1.80E+08	1.93E+08	5.99E+07	7.56E+07	9.22E+07	9.13E+07
310	PLP2	1	0.00E+00	0.00E+00	0.00E+00	0.00E+00	0.00E+00	0.00E+00	3.16E+05	0.00E+00	0.00E+00	0.00E+00	0.00E+00	0.00E+00
311	CSTF1	9	1.37E+07	1.59E+07	4.96E+06	5.22E+06	0.00E+00	0.00E+00	2.00E+07	2.24E+07	5.52E+06	5.05E+06	6.50E+06	5.21E+06
312	GFPT1	3	0.00E+00	0.00E+00	2.56E+06	2.22E+06	0.00E+00	0.00E+00	0.00E+00	0.00E+00	0.00E+00	0.00E+00	0.00E+00	0.00E+00
313	RING1	3	3.75E+06	0.00E+00	4.20E+06	3.63E+06	5.73E+06	4.13E+06	0.00E+00	2.67E+06	4.13E+06	4.39E+06	5.10E+06	5.47E+06
314	PRDX1	3	0.00E+00	0.00E+00	5.01E+06	4.90E+06	0.00E+00	0.00E+00	8.63E+06	0.00E+00	0.00E+00	4.78E+06	4.54E+06	0.00E+00
315	C1QBP	3	8.16E+06	5.66E+06	9.32E+06	9.70E+06	7.97E+06	6.04E+06	8.56E+06	7.95E+06	9.33E+06	8.16E+06	1.04E+07	5.22E+06
316	CKAP4	23	1.38E+07	1.45E+07	7.87E+07	6.22E+07	4.55E+07	3.28E+07	8.98E+06	6.56E+06	7.07E+06	1.23E+07	2.80E+07	4.24E+07
317	TJP1	34	7.70E+07	7.73E+07	4.39E+07	4.91E+07	2.59E+07	3.52E+07	7.18E+07	7.57E+07	4.03E+07	4.21E+07	2.66E+07	2.93E+07
318	SOS1	1	0.00E+00	0.00E+00	0.00E+00	0.00E+00	0.00E+00	0.00E+00	0.00E+00	0.00E+00	0.00E+00	0.00E+00	0.00E+00	0.00E+00
319	SRSF1	11	4.02E+06	2.13E+06	4.24E+07	4.50E+07	7.90E+06	7.82E+06	3.91E+06	1.94E+06	2.85E+07	2.46E+07	1.38E+07	9.87E+06
320	AES	3	3.13E+07	2.93E+07	8.81E+06	7.78E+06	1.02E+07	1.02E+07	2.72E+07	3.27E+07	7.41E+06	7.28E+06	1.01E+07	7.95E+06
321	RBBP4	1	0.00E+00	0.00E+00	0.00E+00	0.00E+00	0.00E+00	0.00E+00	0.00E+00	0.00E+00	0.00E+00	0.00E+00	0.00E+00	0.00E+00
322	CPSF1	24	3.40E+07	2.98E+07	3.19E+07	2.27E+07	2.50E+07	1.83E+07	2.81E+07	2.69E+07	2.43E+07	1.56E+07	3.03E+07	1.82E+07
323	NFIA	4	7.59E+06	1.19E+07	6.21E+06	6.06E+06	4.67E+06	4.09E+06	7.26E+06	1.03E+07	6.73E+06	7.55E+06	3.58E+06	3.89E+06
324	SF3A3	33	8.76E+08	8.83E+08	3.56E+08	3.65E+08	3.01E+08	3.68E+08	8.08E+08	9.14E+08	3.35E+08	3.13E+08	4.50E+08	3.79E+08
325	ILF3	1	0.00E+00	0.00E+00	0.00E+00	0.00E+00	0.00E+00	0.00E+00	0.00E+00	0.00E+00	0.00E+00	0.00E+00	0.00E+00	0.00E+00
326	TRAP1	1	0.00E+00	0.00E+00	0.00E+00	0.00E+00	0.00E+00	0.00E+00	0.00E+00	0.00E+00	0.00E+00	0.00E+00	0.00E+00	0.00E+00
327	NFATC3	2	1.27E+06	1.28E+06	0.00E+00	0.00E+00	0.00E+00	0.00E+00	1.26E+06	1.46E+06	0.00E+00	0.00E+00	0.00E+00	0.00E+00
328	CSTF3	15	2.65E+07	2.36E+07	1.44E+07	1.21E+07	1.93E+07	1.03E+07	3.04E+07	3.29E+07	1.26E+07	1.12E+07	1.23E+07	9.09E+06
329	IK	5	5.51E+06	3.80E+06	1.49E+07	1.28E+07	3.44E+06	4.07E+06	3.13E+06	3.40E+06	5.79E+06	4.73E+06	3.32E+06	3.88E+06
330	PRKAA1;PF	2	0.00E+00	1.83E+06	0.00E+00	0.00E+00	0.00E+00	0.00E+00	0.00E+00	0.00E+00	0.00E+00	0.00E+00	0.00E+00	0.00E+00
331	PPFIA1	24	3.14E+07	3.31E+07	1.95E+07	1.79E+07	1.43E+07	1.42E+07	3.04E+07	3.18E+07	1.72E+07	1.78E+07	1.53E+07	1.41E+07
332	GPS2	2	1.54E+06	1.79E+06	1.83E+06	0.00E+00	0.00E+00	0.00E+00	2.04E+06	2.04E+06	0.00E+00	0.00E+00	0.00E+00	0.00E+00
333	NME3	3	1.46E+06	0.00E+00	0.00E+00	0.00E+00	0.00E+00	0.00E+00	0.00E+00	0.00E+00	0.00E+00	0.00E+00	0.00E+00	0.00E+00
334	SRSF9	3	0.00E+00	0.00E+00	5.58E+06	3.85E+06	3.26E+06	0.00E+00	0.00E+00	0.00E+00	0.00E+00	3.27E+06	2.71E+06	3.85E+06

id	Gene names	Unique peptides	LFQ intensity Bait 2h_1	LFQ intensity Control 2h_1	LFQ intensity Bait 2h_2	LFQ intensity Control 2h_2	LFQ intensity Bait 2h_3	LFQ intensity Control 2h_3	LFQ intensity Bait 24h_1	LFQ intensity Control_24h_1	LFQ intensity Bait 24h_2	LFQ intensity Control_24h_2	LFQ intensity 2_Bait 24h_3	LFQ intensity
335	SRSF6;SRSF	4	1.24E+06	0.00E+00	1.03E+07	1.05E+07	1.77E+06	2.46E+06	0.00E+00	0.00E+00	5.77E+06	2.97E+06	2.21E+06	0.00E+00
336	TRIM28	1	0.00E+00	0.00E+00	0.00E+00	0.00E+00	0.00E+00	0.00E+00	0.00E+00	0.00E+00	0.00E+00	0.00E+00	0.00E+00	0.00E+00
337	G3BP1	2	0.00E+00	0.00E+00	0.00E+00	0.00E+00	0.00E+00	0.00E+00	0.00E+00	0.00E+00	0.00E+00	0.00E+00	0.00E+00	0.00E+00
338	PABPC4	11	2.74E+07	2.34E+07	2.77E+07	2.33E+07	4.11E+07	3.00E+07	4.24E+07	3.81E+07	4.78E+07	4.13E+07	4.63E+07	3.99E+07
339	CTBP1	8	3.46E+07	4.03E+07	9.70E+06	7.52E+06	4.55E+06	0.00E+00	3.32E+07	4.32E+07	8.78E+06	1.12E+07	4.74E+06	3.04E+06
340	SLC39A6	3	0.00E+00	0.00E+00	4.00E+06	4.33E+06	5.46E+06	5.44E+06	0.00E+00	0.00E+00	3.06E+06	4.28E+06	4.48E+06	8.35E+06
341	SF3B2	62	4.31E+08	4.26E+08	7.77E+08	9.66E+08	5.90E+08	8.43E+08	4.58E+08	4.54E+08	6.21E+08	6.83E+08	7.78E+08	8.52E+08
342	SMAD4	11	4.83E+07	6.60E+07	2.37E+07	2.16E+07	4.79E+07	4.03E+07	7.42E+07	7.53E+07	3.49E+07	4.08E+07	3.67E+07	4.43E+07
343	PRPF4B	5	9.83E+06	8.96E+06	1.14E+07	1.40E+07	8.98E+06	8.09E+06	9.12E+06	1.03E+07	1.38E+07	9.91E+06	1.08E+07	7.65E+06
344	HDAC1	4	9.31E+06	6.81E+06	6.13E+06	3.73E+06	0.00E+00	0.00E+00	7.22E+06	5.72E+06	6.46E+06	0.00E+00	5.80E+06	0.00E+00
345	SNW1	1	0.00E+00	0.00E+00	0.00E+00	0.00E+00	0.00E+00	0.00E+00	0.00E+00	0.00E+00	0.00E+00	0.00E+00	0.00E+00	0.00E+00
346	STIM1	14	1.11E+07	1.87E+07	2.55E+07	1.60E+07	1.36E+07	1.31E+07	1.08E+07	1.61E+07	1.15E+07	1.67E+07	1.21E+07	2.43E+07
347	TRA2A	2	3.64E+06	0.00E+00	6.06E+06	3.54E+06	3.80E+06	3.53E+06	3.35E+06	0.00E+00	3.72E+06	0.00E+00	0.00E+00	3.84E+06
348	DYRK1A	4	2.31E+06	2.28E+06	3.06E+06	0.00E+00	3.32E+06	0.00E+00	0.00E+00	0.00E+00	2.46E+06	2.33E+06	3.86E+06	5.86E+06
349	FHL1	2	5.48E+06	5.45E+06	5.52E+06	9.14E+06	2.34E+06	0.00E+00	4.39E+06	5.38E+06	5.01E+06	6.98E+06	3.63E+06	0.00E+00
350	HNRNPD	1	0.00E+00	0.00E+00	0.00E+00	0.00E+00	0.00E+00	0.00E+00	0.00E+00	0.00E+00	0.00E+00	0.00E+00	0.00E+00	0.00E+00
351	VGLL4	2	0.00E+00	0.00E+00	1.95E+06	2.33E+06	1.64E+06	2.16E+06	0.00E+00	0.00E+00	1.90E+06	0.00E+00	0.00E+00	0.00E+00
352	SAFB2	10	4.98E+06	7.48E+06	1.44E+07	2.04E+07	1.85E+07	1.96E+07	6.90E+06	6.86E+06	9.86E+06	1.19E+07	2.20E+07	2.18E+07
353	ARHGEF7	11	2.76E+07	2.92E+07	2.12E+07	1.87E+07	1.70E+07	1.49E+07	2.24E+07	2.06E+07	1.58E+07	1.52E+07	1.73E+07	1.52E+07
354	UBAP2L	18	5.07E+07	6.12E+07	4.61E+07	4.74E+07	3.68E+07	4.55E+07	7.19E+07	7.33E+07	4.31E+07	5.38E+07	4.05E+07	4.99E+07
355	GIT2	5	5.16E+06	4.06E+06	3.67E+06	3.35E+06	3.61E+06	0.00E+00	3.61E+06	3.62E+06	4.36E+06	0.00E+00	0.00E+00	0.00E+00
356	TCEB3	14	4.27E+07	3.60E+07	3.27E+07	3.74E+07	4.02E+07	3.72E+07	4.16E+07	4.02E+07	4.10E+07	3.34E+07	4.18E+07	3.39E+07
357	MAP7	1	0.00E+00	0.00E+00	0.00E+00	0.00E+00	0.00E+00	0.00E+00	0.00E+00	0.00E+00	0.00E+00	0.00E+00	0.00E+00	0.00E+00
358	CTTN	23	6.24E+07	8.03E+07	1.15E+08	1.20E+08	6.88E+07	7.88E+07	5.53E+07	6.14E+07	9.50E+07	1.03E+08	6.15E+07	7.62E+07
359	RBM39	3	0.00E+00	2.11E+06	4.55E+06	3.27E+06	0.00E+00	0.00E+00	0.00E+00	0.00E+00	3.22E+06	0.00E+00	0.00E+00	0.00E+00
360	PRPSAP1	2	0.00E+00	5.59E+05	0.00E+00	0.00E+00	0.00E+00	0.00E+00	0.00E+00	0.00E+00	0.00E+00	0.00E+00	0.00E+00	0.00E+00
361	PUM1	4	2.67E+06	4.13E+06	0.00E+00	0.00E+00	0.00E+00	0.00E+00	2.82E+06	2.67E+06	0.00E+00	0.00E+00	0.00E+00	0.00E+00
362	GSE1	5	8.47E+06	9.41E+06	7.02E+06	6.95E+06	6.03E+06	8.70E+06	4.43E+06	3.61E+06	5.29E+06	6.50E+06	5.24E+06	4.34E+06
363	NFIX	2	0.00E+00	0.00E+00	0.00E+00	0.00E+00	0.00E+00	0.00E+00	2.33E+06	2.66E+06	0.00E+00	0.00E+00	0.00E+00	0.00E+00
364	KPNB1	5	2.22E+06	1.72E+06	8.92E+06	3.28E+06	5.56E+06	2.73E+06	1.95E+06	1.50E+06	2.24E+06	3.34E+06	4.99E+06	6.17E+06
365	NOLC1	1	0.00E+00	0.00E+00	0.00E+00	0.00E+00	0.00E+00	0.00E+00	0.00E+00	0.00E+00	0.00E+00	0.00E+00	0.00E+00	0.00E+00
366	WTAP	17	4.54E+07	4.16E+07	5.85E+07	6.96E+07	9.11E+07	1.07E+08	3.90E+07	3.98E+07	6.25E+07	5.64E+07	7.90E+07	1.02E+08
367	EFTUD2	12	4.01E+06	3.11E+06	1.65E+07	8.82E+06	5.31E+06	2.93E+06	3.03E+06	0.00E+00	1.29E+07	5.16E+06	3.18E+06	3.29E+06
368	SLC39A14	3	6.08E+06	6.73E+06	1.12E+07	7.88E+06	1.25E+07	9.81E+06	5.10E+06	4.03E+06	7.11E+06	7.39E+06	8.69E+06	1.02E+07
369	PAFAH1B3	7	1.30E+07	1.39E+07	1.01E+07	8.74E+06	0.00E+00	4.07E+06	1.43E+07	1.73E+07	1.09E+07	7.72E+06	0.00E+00	0.00E+00
370	NONO	45	8.53E+08	1.00E+09	2.14E+09	2.63E+09	3.91E+09	3.54E+09	9.80E+08	1.09E+09	2.12E+09	3.23E+09	3.31E+09	3.62E+09
371	RNPS1	5	1.46E+07	1.07E+07	2.26E+07	1.71E+07	1.71E+07	1.53E+07	1.52E+07	1.18E+07	2.15E+07	2.27E+07	1.96E+07	1.90E+07
372	TCEB1	3	5.64E+06	6.83E+06	4.59E+06	4.99E+06	0.00E+00	0.00E+00	4.23E+06	4.66E+06	0.00E+00	0.00E+00	0.00E+00	5.12E+06
373	TCEB2	3	4.33E+06	6.03E+06	6.45E+06	5.00E+06	7.47E+06	4.30E+06	4.01E+06	6.23E+06	5.38E+06	5.08E+06	6.50E+06	5.35E+06
374	SF3B3	44	3.63E+08	3.13E+08	3.39E+08	2.88E+08	2.10E+08	1.84E+08	3.15E+08	2.87E+08	1.99E+08	2.08E+08	2.45E+08	1.69E+08
375	SAFB	16	1.03E+08	1.21E+08	1.77E+08	2.41E+08	1.78E+08	2.26E+08	1.37E+08	1.44E+08	1.51E+08	1.16E+08	2.11E+08	2.22E+08
376	SF3B4	8	1.28E+08	7.61E+07	1.29E+08	2.31E+08	2.03E+08	2.70E+08	1.07E+08	8.20E+07	2.03E+08	1.38E+08	1.37E+08	1.97E+08
377	SF3A2	19	2.85E+08	2.46E+08	1.69E+08	2.06E+08	1.72E+08	2.37E+08	3.08E+08	2.81E+08	1.58E+08	1.88E+08	2.30E+08	2.39E+08
378	SEC23A	8	5.24E+06	7.23E+06	3.99E+06	0.00E+00	0.00E+00	0.00E+00	7.40E+06	1.09E+07	3.63E+06	6.50E+06	0.00E+00	0.00E+00
379	SEC23B	9	1.22E+07	1.50E+07	9.10E+06	6.05E+06	6.42E+06	6.35E+06	1.74E+07	2.60E+07	1.24E+07	1.05E+07	6.46E+06	6.01E+06
380	SF3A1	41	1.21E+09	1.21E+09	5.46E+08	6.81E+08	4.52E+08	7.02E+08	1.19E+09	1.35E+09	5.31E+08	5.29E+08	7.66E+08	5.22E+08
381	TERF2	3	0.00E+00	0.00E+00	1.74E+06	0.00E+00	3.70E+06	4.84E+06	0.00E+00	0.00E+00	3.70E+06	8.04E+06	2.98E+06	8.33E+06
382	SLC9A3R2	11	2.49E+07	2.48E+07	3.76E+07	3.64E+07	2.39E+07	2.00E+07	2.34E+07	2.21E+07	3.86E+07	2.81E+07	2.04E+07	1.64E+07
383	SF1	22	5.48E+08	6.16E+08	5.29E+08	7.62E+08	6.84E+08	8.45E+08	6.23E+08	7.02E+08	4.22E+08	6.37E+08	5.63E+08	8.55E+08
384	MED1	2	0.00E+00	7.96E+05	0.00E+00	0.00E+00	0.00E+00	0.00E+00	0.00E+00	9.45E+05	9.07E+05	0.00E+00	0.00E+00	0.00E+00
385	JMJD1C	7	3.79E+06	3.27E+06	4.84E+06	5.14E+06	1.10E+07	1.19E+07	2.40E+06	2.79E+06	3.31E+06	5.28E+06	4.80E+06	7.40E+06
386	PTPN14	2	0.00E+00	0.00E+00	0.00E+00	0.00E+00	0.00E+00	0.00E+00	0.00E+00	0.00E+00	0.00E+00	0.00E+00	0.00E+00	0.00E+00
387	TSC22D1	5	0.00E+00	0.00E+00	4.19E+06	6.11E+06	9.06E+06	9.79E+06	4.91E+06	0.00E+00	6.62E+06	7.88E+06	8.21E+06	9.03E+06
388	ELAVL1	11	5.07E+07	5.33E+07	4.28E+07	4.47E+07	1.51E+07	1.17E+07	4.93E+07	4.94E+07	4.91E+07	5.51E+07	1.49E+07	1.91E+07
389	SLC1A5	1	0.00E+00	0.00E+00	0.00E+00	0.00E+00	0.00E+00	0.00E+00	0.00E+00	0.00E+00	0.00E+00	0.00E+00	0.00E+00	0.00E+00
390	CCDC6	4	1.56E+06	2.62E+06	3.04E+06	3.98E+06	0.00E+00	0.00E+00	3.02E+06	2.63E+06	2.85E+06	2.72E+06	2.09E+06	0.00E+00
391	DDB1	2	3.10E+06	2.29E+06	2.20E+06	0.00E+00	0.00E+00	0.00E+00	2.15E+06	1.96E+06	0.00E+00	0.00E+00	0.00E+00	0.00E+00
392	RBBP7	3	1.03E+07	1.07E+07	6.54E+06	8.07E+06	9.88E+06	7.94E+06	9.09E+06	7.66E+06	7.80E+06	9.86E+06	1.06E+07	6.98E+06
393	SRSF7	8	1.20E+07	9.98E+06	6.72E+07	6.03E+07	2.83E+07	2.57E+07	1.24E+07	1.07E+07	5.14E+07	4.59E+07	3.49E+07	3.41E+07
394	CPSF6	12	1.57E+08	1.83E+08	1.12E+08	1.12E+08	8.55E+07	9.26E+07	2.10E+08	2.20E+08	1.15E+08	9.39E+07	9.99E+07	1.22E+08
395	CDO1	2	3.62E+06	4.28E+06	0.00E+00	0.00E+00	0.00E+00	0.00E+00	3.25E+06	4.38E+06	1.77E+06	0.00E+00	0.00E+00	0.00E+00
396	UGT8	4	2.46E+06	2.48E+06	2.70E+06	2.25E+06	0.00E+00	0.00E+00	1.73E+06	2.31E+06	0.00E+00	0.00E+00	0.00E+00	0.00E+00
397	CPEB4	1	0.00E+00	0.00E+00	0.00E+00	0.00E+00	0.00E+00	0.00E+00	0.00E+00	0.00E+00	0.00E+00	0.00E+00	0.00E+00	0.00E+00
398	CLEC16A	1	0.00E+00	0.00E+00	0.00E+00	0.00E+00	0.00E+00	0.00E+00	0.00E+00	0.00E+00	0.00E+00	0.00E+00	0.00E+00	0.00E+00
399	TYSND1	9	1.35E+07	1.06E+07	1.06E+07	1.05E+07	8.25E+06	9.73E+06	1.15E+07	1.27E+07	1.59E+07	1.45E+07	1.60E+07	1.10E+07
400	SMU1	9	1.23E+07	1.40E+07	1.60E+07	1.06E+07	5.37E+06	4.59E+06	9.24E+06	1.25E+07	8.96E+06	6.09E+06	5.07E+06	0.00E+00
401	LEPRE1	1	0.00E+00	3.69E+05	0.00E+00	0.00E+00	0.00E+00	0.00E+00	0.00E+00	0.00E+00	0.00E+00	0.00E+00	0.00E+00	0.00E+00

id	Gene names	Unique peptides	LFQ intensity Bait 2h_1	LFQ intensity Control 2h_1	LFQ intensity Bait 2h_2	LFQ intensity Control 2h_2	LFQ intensity Bait 2h_3	LFQ intensity Control 2h_3	LFQ intensity Bait 24h_1	LFQ intensity Control_24h_1	LFQ intensity Bait 24h_2	LFQ intensity Control_24h_2	LFQ intensity 2_Bait 24h_3	LFQ intensity
402	LSM12	4	2.82E+07	2.31E+07	2.03E+07	1.80E+07	4.46E+07	3.13E+07	3.69E+07	3.88E+07	1.67E+07	2.03E+07	3.90E+07	5.87E+07
403	TIMM50	5	0.00E+00	0.00E+00	2.26E+06	2.04E+06	1.70E+06	0.00E+00	1.35E+06	0.00E+00	1.80E+06	0.00E+00	1.81E+06	1.87E+06
404	LARP7	18	6.21E+07	6.01E+07	3.52E+07	3.10E+07	4.47E+07	3.87E+07	6.71E+07	7.63E+07	3.98E+07	4.59E+07	6.32E+07	5.25E+07
405	BCL7A;BCL	2	0.00E+00	0.00E+00	0.00E+00	5.28E+06	2.14E+06	0.00E+00	2.12E+06	1.60E+06	0.00E+00	0.00E+00	2.02E+06	0.00E+00
406	AMOT	34	1.08E+06	4.29E+07	3.40E+07	1.57E+08	3.10E+07	1.42E+08	3.90E+06	3.47E+07	3.82E+07	1.65E+08	2.44E+07	1.44E+08
407	CRTC2	4	0.00E+00	0.00E+00	0.00E+00	0.00E+00	4.07E+06	0.00E+00	0.00E+00	0.00E+00	1.18E+07	0.00E+00	4.31E+06	4.76E+06
408	PYCRL	6	1.53E+07	1.24E+07	1.62E+07	1.36E+07	2.90E+07	1.79E+07	1.47E+07	1.69E+07	1.48E+07	1.93E+07	3.13E+07	2.09E+07
409	SOWAHC	4	1.33E+06	0.00E+00	0.00E+00	0.00E+00	0.00E+00	0.00E+00	1.60E+06	2.20E+06	0.00E+00	0.00E+00	0.00E+00	0.00E+00
410	RILPL1	4	2.25E+06	2.49E+06	0.00E+00	0.00E+00	0.00E+00	0.00E+00	2.68E+06	2.37E+06	0.00E+00	0.00E+00	0.00E+00	0.00E+00
411	FAM76B	3	0.00E+00	0.00E+00	0.00E+00	0.00E+00	0.00E+00	0.00E+00	0.00E+00	0.00E+00	0.00E+00	0.00E+00	0.00E+00	2.81E+06
412	TJAP1	7	8.93E+06	9.51E+06	7.91E+06	8.86E+06	1.06E+07	1.08E+07	9.50E+06	9.97E+06	9.86E+06	1.08E+07	1.11E+07	1.13E+07
413	BRMS1L	1	0.00E+00	0.00E+00	0.00E+00	0.00E+00	0.00E+00	0.00E+00	0.00E+00	0.00E+00	0.00E+00	0.00E+00	0.00E+00	0.00E+00
414	NUP188	1	8.31E+05	4.25E+05	9.17E+05	0.00E+00	1.12E+06	0.00E+00	7.32E+05	0.00E+00	0.00E+00	0.00E+00	0.00E+00	0.00E+00
415	VARS2	12	9.12E+06	1.12E+07	1.34E+07	1.12E+07	1.34E+07	1.37E+07	1.41E+07	1.26E+07	1.68E+07	1.63E+07	1.93E+07	1.67E+07
416	CEP170	48	1.22E+08	1.24E+08	9.28E+07	1.01E+08	1.04E+08	1.20E+08	1.10E+08	1.14E+08	9.53E+07	9.89E+07	1.04E+08	1.12E+08
417	FNBP1L	16	3.30E+07	3.16E+07	1.52E+07	1.22E+07	1.21E+07	1.13E+07	3.48E+07	4.03E+07	1.30E+07	2.21E+07	1.39E+07	1.38E+07
418	ZC3H13	16	1.01E+07	8.48E+06	1.52E+07	1.71E+07	1.88E+07	2.10E+07	8.67E+06	8.84E+06	1.68E+07	1.82E+07	1.70E+07	2.18E+07
419	ABCC10	1	0.00E+00	0.00E+00	0.00E+00	0.00E+00	0.00E+00	0.00E+00	0.00E+00	5.38E+05	0.00E+00	0.00E+00	0.00E+00	0.00E+00
420	UBAP2	15	4.22E+07	5.02E+07	3.90E+07	4.38E+07	4.65E+07	6.20E+07	4.91E+07	5.13E+07	3.57E+07	4.78E+07	5.56E+07	5.63E+07
421	RPRD2	14	2.48E+07	2.67E+07	2.62E+07	2.46E+07	2.15E+07	2.01E+07	3.05E+07	2.70E+07	1.94E+07	2.39E+07	1.87E+07	2.11E+07
422	PRPF38B	2	0.00E+00	1.27E+06	0.00E+00	0.00E+00	0.00E+00	0.00E+00	0.00E+00	0.00E+00	0.00E+00	0.00E+00	0.00E+00	0.00E+00
423	RNF20	18	1.39E+07	1.42E+07	1.97E+07	2.22E+07	2.51E+07	2.71E+07	1.67E+07	1.47E+07	1.96E+07	2.30E+07	3.15E+07	2.94E+07
424	ZNF318	1	0.00E+00	0.00E+00	0.00E+00	0.00E+00	0.00E+00	0.00E+00	0.00E+00	0.00E+00	0.00E+00	0.00E+00	0.00E+00	0.00E+00
425	LRCH2	1	0.00E+00	0.00E+00	0.00E+00	0.00E+00	0.00E+00	0.00E+00	0.00E+00	0.00E+00	0.00E+00	0.00E+00	0.00E+00	0.00E+00
426	RSBN1	2	1.79E+06	2.05E+06	1.95E+06	0.00E+00	0.00E+00	0.00E+00	2.00E+06	1.71E+06	0.00E+00	1.94E+06	1.98E+06	0.00E+00
427	CEP135	3	0.00E+00	1.87E+06	2.31E+06	2.06E+06	2.43E+06	4.21E+06	0.00E+00	1.53E+06	0.00E+00	0.00E+00	0.00E+00	1.99E+06
428	KAZN	2	0.00E+00	0.00E+00	0.00E+00	1.60E+06	0.00E+00	0.00E+00	0.00E+00	0.00E+00	0.00E+00	0.00E+00	0.00E+00	0.00E+00
429	INTS3	5	8.89E+06	8.07E+06	4.58E+06	3.14E+06	0.00E+00	0.00E+00	8.56E+06	5.66E+06	5.20E+06	0.00E+00	3.79E+06	0.00E+00
430	ARHGAP17	17	3.42E+07	1.86E+07	1.02E+07	7.05E+06	2.00E+06	2.65E+06	4.83E+07	3.67E+07	9.64E+06	7.57E+06	3.57E+06	5.43E+06
431	KIAA1429	24	3.32E+07	2.60E+07	2.45E+07	2.13E+07	4.10E+07	2.66E+07	2.72E+07	2.90E+07	3.09E+07	3.04E+07	3.59E+07	3.11E+07
432	NADSYN1	4	4.74E+06	5.16E+06	0.00E+00	0.00E+00	0.00E+00	0.00E+00	4.55E+06	4.51E+06	0.00E+00	0.00E+00	0.00E+00	0.00E+00
433	ELP2	2	1.16E+06	1.11E+06	0.00E+00	0.00E+00	0.00E+00	0.00E+00	0.00E+00	1.47E+06	0.00E+00	0.00E+00	0.00E+00	0.00E+00
434	NIPBL	17	1.58E+07	1.51E+07	1.41E+07	1.15E+07	1.07E+07	1.11E+07	1.49E+07	1.68E+07	1.04E+07	1.02E+07	7.39E+06	1.01E+07
435	HMBOX1	2	4.58E+06	4.94E+06	3.85E+06	0.00E+00	2.59E+06	2.87E+06	3.43E+06	3.86E+06	0.00E+00	0.00E+00	0.00E+00	2.34E+06
436	ARMC6	6	9.29E+06	7.25E+06	5.46E+06	0.00E+00	4.37E+06	0.00E+00	6.58E+06	6.26E+06	4.24E+06	2.65E+06	2.60E+06	4.17E+06
437	MZT2A;MZ	1	0.00E+00	0.00E+00	0.00E+00	0.00E+00	0.00E+00	0.00E+00	0.00E+00	0.00E+00	0.00E+00	0.00E+00	0.00E+00	0.00E+00
438	CDC73	14	6.85E+06	6.99E+06	2.29E+07	1.95E+07	3.85E+07	3.74E+07	9.63E+06	7.07E+06	2.38E+07	2.66E+07	3.08E+07	3.48E+07
439	CEP85	4	3.43E+06	4.45E+06	3.61E+06	3.60E+06	3.26E+06	0.00E+00	3.58E+06	3.46E+06	3.73E+06	2.93E+06	2.93E+06	2.98E+06
440	PRMT9	1	0.00E+00	0.00E+00	0.00E+00	0.00E+00	0.00E+00	0.00E+00	0.00E+00	0.00E+00	0.00E+00	0.00E+00	0.00E+00	0.00E+00
441	PRPF8	14	7.65E+06	8.14E+06	1.96E+07	1.61E+07	5.87E+06	4.81E+06	4.60E+06	3.96E+06	1.84E+07	7.23E+06	5.22E+06	0.00E+00
442	ANKRD16	5	4.62E+06	6.41E+06	1.28E+06	2.07E+06	2.47E+06	0.00E+00	5.45E+06	8.55E+06	2.68E+06	2.80E+06	2.41E+06	1.89E+06
443	RSBN1L	3	2.15E+06	2.95E+06	0.00E+00	0.00E+00	0.00E+00	0.00E+00	0.00E+00	2.10E+06	0.00E+00	0.00E+00	0.00E+00	0.00E+00
444	CTR9	9	7.56E+06	7.80E+06	1.58E+07	1.24E+07	2.68E+07	2.23E+07	1.04E+07	0.00E+00	1.62E+07	1.50E+07	1.76E+07	1.75E+07
445	TTC33	3	0.00E+00	2.36E+06	0.00E+00	0.00E+00	0.00E+00	0.00E+00	0.00E+00	0.00E+00	4.24E+06	0.00E+00	0.00E+00	0.00E+00
446	SARM1	13	3.12E+07	3.29E+07	8.75E+06	5.40E+06	8.41E+06	3.50E+06	3.84E+07	3.96E+07	1.52E+07	5.35E+06	1.07E+07	9.66E+06
447	FIP1L1	13	8.64E+07	7.09E+07	1.08E+08	1.24E+08	9.71E+07	1.05E+08	7.20E+07	7.59E+07	9.82E+07	6.44E+07	1.03E+08	1.25E+08
448	WDR82	3	2.90E+06	2.86E+06	6.07E+06	5.06E+06	1.51E+07	1.30E+07	3.75E+06	3.81E+06	5.89E+06	1.32E+07	9.15E+06	1.16E+07
449	DPP8	1	0.00E+00	0.00E+00	0.00E+00	0.00E+00	0.00E+00	0.00E+00	0.00E+00	0.00E+00	0.00E+00	0.00E+00	0.00E+00	0.00E+00
450	QSOX2	2	3.57E+06	3.53E+06	2.82E+06	1.13E+06	1.26E+06	0.00E+00	1.76E+06	1.44E+06	0.00E+00	0.00E+00	0.00E+00	0.00E+00
451	SRCAP	2	0.00E+00	2.18E+06	3.17E+06	0.00E+00	2.56E+06	0.00E+00	2.35E+06	2.04E+06	2.81E+06	0.00E+00	2.39E+06	2.32E+06
452	PAXIP1	4	1.98E+06	1.97E+06	1.29E+06	0.00E+00	0.00E+00	0.00E+00	2.67E+06	3.72E+06	1.78E+06	1.95E+06	0.00E+00	0.00E+00
453	USP34	1	0.00E+00	0.00E+00	0.00E+00	0.00E+00	0.00E+00	0.00E+00	0.00E+00	0.00E+00	0.00E+00	0.00E+00	0.00E+00	0.00E+00
454	USP30	1	0.00E+00	0.00E+00	0.00E+00	0.00E+00	0.00E+00	0.00E+00	0.00E+00	0.00E+00	0.00E+00	0.00E+00	0.00E+00	0.00E+00
455	CBLL1	4	9.60E+06	9.95E+06	1.46E+07	1.60E+07	2.22E+07	2.57E+07	9.54E+06	7.81E+06	1.69E+07	1.91E+07	2.46E+07	2.47E+07
456	DHX30	10	8.70E+06	8.19E+06	8.52E+06	8.21E+06	7.98E+06	0.00E+00	7.61E+06	6.10E+06	7.06E+06	5.17E+06	0.00E+00	0.00E+00
457	MEPCE	14	3.00E+07	3.47E+07	2.98E+07	2.84E+07	3.97E+07	3.95E+07	3.56E+07	4.51E+07	3.52E+07	3.85E+07	4.11E+07	3.79E+07
458	CYFIP1	12	6.23E+07	5.55E+07	1.18E+07	1.06E+07	3.66E+06	0.00E+00	6.36E+07	5.58E+07	1.17E+07	6.69E+06	3.70E+06	1.81E+06
459	TAOK1	9	6.56E+06	7.70E+06	4.20E+06	4.79E+06	0.00E+00	0.00E+00	7.00E+06	6.75E+06	4.21E+06	3.90E+06	0.00E+00	0.00E+00
460	PHF5A	3	1.06E+07	1.08E+07	2.70E+07	4.25E+07	2.58E+07	3.02E+07	1.22E+07	1.05E+07	2.05E+07	2.62E+07	3.29E+07	2.73E+07
461	ATG9A	2	0.00E+00	0.00E+00	2.39E+06	0.00E+00	0.00E+00	0.00E+00	0.00E+00	0.00E+00	0.00E+00	0.00E+00	0.00E+00	0.00E+00
462	NUFIP2	21	3.07E+07	3.02E+07	9.02E+07	4.58E+07	8.98E+07	4.31E+07	3.64E+07	4.22E+07	3.23E+07	3.36E+07	8.82E+07	9.53E+07
463	RAI1	3	1.78E+06	1.83E+06	3.08E+06	1.99E+06	2.62E+06	2.10E+06	1.50E+06	1.90E+06	2.20E+06	2.24E+06	0.00E+00	2.51E+06
464	IRF2BP2	15	4.45E+07	5.04E+07	3.58E+07	3.67E+07	2.03E+07	2.95E+07	3.63E+07	3.35E+07	2.95E+07	2.15E+07	1.75E+07	1.76E+07
465	ADCK2	1	0.00E+00	0.00E+00	0.00E+00	0.00E+00	0.00E+00	0.00E+00	0.00E+00	0.00E+00	0.00E+00	0.00E+00	0.00E+00	0.00E+00
466	TAF8	2	0.00E+00	0.00E+00	1.83E+06	0.00E+00	2.52E+06	2.25E+06	0.00E+00	0.00E+00	0.00E+00	2.15E+06	2.16E+06	2.79E+06
467	PCGF5	2	2.22E+06	1.52E+06	2.22E+06	1.94E+06	0.00E+00	2.71E+06	1.72E+06	1.76E+06	2.58E+06	2.70E+06	3.25E+06	2.31E+06
468	PEG10	12	1.49E+08	1.40E+08	9.77E+07	8.59E+07	1.23E+08	1.52E+08	8.22E+07	8.75E+07	7.60E+07	7.39E+07	7.58E+07	7.15E+07

id	Gene names	Unique peptides	LFQ intensity Bait 2h_1	LFQ intensity Control 2h_1	LFQ intensity Bait 2h_2	LFQ intensity Control 2h_2	LFQ intensity Bait 2h_3	LFQ intensity Control 2h_3	LFQ intensity Bait 24h_1	LFQ intensity Control_24h_1	LFQ intensity Bait 24h_2	LFQ intensity Control_24h_2	LFQ intensity 2_Bait 24h_3	LFQ intensity
469	DPP9	30	1.86E+08	1.94E+08	7.49E+07	7.16E+07	1.08E+08	1.04E+08	2.12E+08	2.27E+08	9.98E+07	1.01E+08	1.26E+08	9.66E+07
470	NAA40	1	0.00E+00	0.00E+00	0.00E+00	0.00E+00	0.00E+00	0.00E+00	0.00E+00	0.00E+00	0.00E+00	0.00E+00	0.00E+00	0.00E+00
471	ALYREF	8	3.39E+06	3.59E+06	1.18E+07	1.08E+07	1.32E+07	1.58E+07	0.00E+00	3.93E+06	1.41E+07	1.86E+07	2.93E+07	2.27E+07
472	NLRP8	1	0.00E+00	2.24E+06	0.00E+00	0.00E+00	0.00E+00	0.00E+00	0.00E+00	0.00E+00	0.00E+00	0.00E+00	0.00E+00	0.00E+00
473	CARM1	21	2.85E+08	2.77E+08	7.80E+07	6.36E+07	8.18E+07	5.73E+07	3.17E+08	3.31E+08	9.23E+07	8.18E+07	8.98E+07	6.14E+07
474	DDX42	45	1.72E+08	1.98E+08	3.08E+08	3.23E+08	5.24E+08	6.26E+08	3.09E+08	3.53E+08	4.47E+08	5.55E+08	5.71E+08	6.67E+08
475	HOMER1	11	1.95E+07	1.58E+07	6.80E+06	7.24E+06	6.19E+06	5.68E+06	2.03E+07	1.70E+07	5.40E+06	1.12E+07	7.85E+06	7.56E+06
476	IRF2BP1	3	2.95E+06	2.75E+06	0.00E+00	0.00E+00	0.00E+00	0.00E+00	2.51E+06	2.25E+06	0.00E+00	0.00E+00	0.00E+00	0.00E+00
477	ERC1	1	0.00E+00	0.00E+00	0.00E+00	0.00E+00	0.00E+00	0.00E+00	0.00E+00	0.00E+00	0.00E+00	0.00E+00	0.00E+00	0.00E+00
478	PLD3	7	4.32E+07	4.83E+07	1.81E+07	1.51E+07	1.54E+07	1.01E+07	2.07E+07	1.88E+07	9.21E+06	5.80E+06	4.83E+06	3.30E+06
479	CCDC50	10	2.83E+07	3.49E+07	2.54E+07	3.06E+07	3.11E+07	4.90E+07	4.06E+07	4.75E+07	2.31E+07	3.51E+07	3.40E+07	4.80E+07
480	MCAT	10	4.06E+07	4.73E+07	2.42E+07	2.29E+07	3.95E+07	2.25E+07	6.05E+07	6.00E+07	3.21E+07	3.76E+07	3.39E+07	2.24E+07
481	PHF6	1	0.00E+00	0.00E+00	0.00E+00	0.00E+00	0.00E+00	0.00E+00	0.00E+00	0.00E+00	0.00E+00	0.00E+00	0.00E+00	0.00E+00
482	CHERP	27	1.14E+08	1.24E+08	1.76E+08	1.52E+08	1.66E+08	1.67E+08	9.75E+07	1.19E+08	1.65E+08	1.82E+08	2.06E+08	1.93E+08
483	SUGP1	4	2.79E+06	0.00E+00	0.00E+00	0.00E+00	0.00E+00	0.00E+00	0.00E+00	0.00E+00	0.00E+00	0.00E+00	0.00E+00	0.00E+00
484	DHX40	7	1.29E+07	1.18E+07	0.00E+00	0.00E+00	0.00E+00	0.00E+00	1.12E+07	7.78E+06	0.00E+00	0.00E+00	0.00E+00	0.00E+00
485	DNAJC10	13	3.68E+07	3.08E+07	2.13E+07	2.11E+07	3.69E+07	2.82E+07	2.75E+07	2.79E+07	2.26E+07	2.39E+07	3.02E+07	2.57E+07
486	SMC5	17	2.05E+07	0.00E+00	1.93E+07	0.00E+00	1.73E+07	0.00E+00	2.24E+07	0.00E+00	1.87E+07	0.00E+00	2.42E+07	0.00E+00
487	AMOTL1	3	0.00E+00	0.00E+00	0.00E+00	0.00E+00	0.00E+00	0.00E+00	1.77E+06	0.00E+00	0.00E+00	0.00E+00	0.00E+00	0.00E+00
488	RAVER1	2	2.38E+06	2.88E+06	0.00E+00	0.00E+00	0.00E+00	0.00E+00	1.95E+06	2.73E+06	0.00E+00	0.00E+00	0.00E+00	0.00E+00
489	PM20D2	17	1.11E+08	1.06E+08	2.08E+08	1.87E+08	3.28E+08	2.19E+08	1.28E+08	1.49E+08	4.07E+08	4.29E+08	4.78E+08	2.92E+08
490	DCP1B	1	0.00E+00	0.00E+00	0.00E+00	0.00E+00	0.00E+00	0.00E+00	0.00E+00	0.00E+00	0.00E+00	0.00E+00	0.00E+00	0.00E+00
491	XRN1	9	1.45E+07	1.31E+07	7.71E+06	5.81E+06	5.73E+06	5.78E+06	1.63E+07	2.24E+07	5.67E+06	8.46E+06	5.62E+06	6.06E+06
492	ABI1	9	1.99E+07	1.59E+07	1.40E+07	7.29E+06	6.84E+06	6.71E+06	2.22E+07	2.00E+07	1.49E+07	1.02E+07	6.33E+06	8.01E+06
493	ZNF444	3	3.99E+06	3.31E+06	3.65E+06	0.00E+00	5.18E+06	0.00E+00	2.32E+06	2.35E+06	2.55E+06	2.27E+06	0.00E+00	0.00E+00
494	CCAR2	24	6.93E+07	6.83E+07	5.82E+07	5.39E+07	5.64E+07	5.77E+07	7.65E+07	8.60E+07	8.12E+07	1.04E+08	7.18E+07	7.84E+07
495	NUP93	2	3.46E+06	2.52E+06	2.55E+06	0.00E+00	2.25E+06	0.00E+00	2.35E+06	2.17E+06	0.00E+00	0.00E+00	0.00E+00	0.00E+00
496	CMTR1	19	3.19E+07	2.82E+07	1.96E+07	1.78E+07	1.46E+07	7.01E+06	4.24E+07	4.23E+07	1.70E+07	2.04E+07	1.74E+07	1.20E+07
497	ASCC3	14	1.16E+07	1.16E+07	3.21E+06	0.00E+00	0.00E+00	0.00E+00	1.09E+07	1.20E+07	3.47E+06	3.58E+06	0.00E+00	0.00E+00
498	MICALL1	5	0.00E+00	0.00E+00	0.00E+00	0.00E+00	0.00E+00	0.00E+00	3.31E+06	2.91E+06	0.00E+00	0.00E+00	0.00E+00	2.68E+06
499	D2HGDH	8	1.09E+07	8.72E+06	4.57E+06	5.37E+06	4.98E+06	0.00E+00	1.36E+07	1.56E+07	9.24E+06	8.39E+06	1.04E+07	5.75E+06
500	HDDC3	3	0.00E+00	0.00E+00	4.68E+06	0.00E+00	0.00E+00	0.00E+00	1.29E+06	0.00E+00	1.90E+06	0.00E+00	0.00E+00	0.00E+00
501	CPSF7	20	3.50E+08	3.06E+08	2.17E+08	2.46E+08	2.90E+08	2.69E+08	4.14E+08	3.94E+08	2.38E+08	2.54E+08	2.88E+08	2.82E+08
502	PAF1	18	1.25E+07	1.33E+07	3.86E+07	3.11E+07	5.47E+07	6.59E+07	1.40E+07	1.36E+07	3.83E+07	4.26E+07	5.29E+07	5.58E+07
503	GPATCH11	4	3.14E+06	3.23E+06	1.21E+07	2.04E+07	1.11E+07	1.02E+07	3.15E+06	2.99E+06	5.96E+06	5.58E+06	5.31E+06	1.31E+07
504	ASCC1	3	8.43E+06	1.07E+07	7.15E+06	0.00E+00	0.00E+00	0.00E+00	1.08E+07	9.14E+06	4.08E+06	0.00E+00	0.00E+00	0.00E+00
505	PRPF38A	3	6.02E+06	2.61E+06	0.00E+00	0.00E+00	0.00E+00	0.00E+00	0.00E+00	3.22E+06	0.00E+00	0.00E+00	0.00E+00	0.00E+00
506	SERBP1	5	1.26E+06	2.12E+06	9.23E+06	8.12E+06	0.00E+00	2.09E+06	2.04E+06	1.71E+06	4.84E+06	3.03E+06	2.43E+06	1.72E+06
507	FAM98A	8	2.85E+07	3.77E+07	1.93E+07	2.40E+07	3.13E+07	2.13E+07	2.88E+07	3.31E+07	2.68E+07	2.57E+07	2.51E+07	2.67E+07
508	SMG8	4	3.03E+06	3.73E+06	0.00E+00	2.46E+06	0.00E+00	0.00E+00	2.11E+06	1.91E+06	2.24E+06	0.00E+00	0.00E+00	0.00E+00
509	RBM15B	2	0.00E+00	0.00E+00	0.00E+00	0.00E+00	0.00E+00	0.00E+00	0.00E+00	0.00E+00	0.00E+00	0.00E+00	0.00E+00	2.81E+06
510	ARID1B	7	0.00E+00	0.00E+00	6.80E+06	5.39E+06	1.07E+07	9.87E+06	0.00E+00	5.13E+06	5.75E+06	5.83E+06	1.22E+07	1.19E+07
511	KBTBD8	1	5.83E+05	0.00E+00	0.00E+00	0.00E+00	0.00E+00	0.00E+00	0.00E+00	0.00E+00	0.00E+00	0.00E+00	0.00E+00	0.00E+00
512	MCFD2	2	1.58E+07	1.72E+07	1.42E+07	2.28E+07	1.56E+07	0.00E+00	1.26E+07	1.64E+07	1.44E+07	1.57E+07	1.56E+07	1.75E+07
513	SNIP1	3	1.44E+06	1.65E+06	1.65E+06	0.00E+00	0.00E+00	0.00E+00	1.39E+06	1.32E+06	1.77E+06	0.00E+00	0.00E+00	0.00E+00
514	SMARCC2	13	3.21E+07	3.41E+07	3.56E+07	2.92E+07	3.02E+07	2.39E+07	3.38E+07	2.90E+07	2.63E+07	2.46E+07	2.88E+07	2.63E+07
515	FAM76A	2	0.00E+00	0.00E+00	2.87E+06	1.85E+06	4.13E+06	2.90E+06	0.00E+00	0.00E+00	2.26E+06	2.61E+06	2.78E+06	3.21E+06
516	SHKBP1	9	2.39E+07	3.09E+07	7.41E+06	7.19E+06	5.84E+06	0.00E+00	1.05E+07	1.28E+07	0.00E+00	5.47E+06	0.00E+00	0.00E+00
517	PIP4K2C	1	0.00E+00	0.00E+00	0.00E+00	0.00E+00	0.00E+00	0.00E+00	0.00E+00	0.00E+00	0.00E+00	0.00E+00	0.00E+00	0.00E+00
518	TBC1D15	3	2.45E+06	3.74E+06	3.05E+06	0.00E+00	2.39E+06	0.00E+00	2.90E+06	2.86E+06	0.00E+00	0.00E+00	0.00E+00	2.27E+06
519	RAPGEF6	7	7.35E+06	7.49E+06	3.33E+06	3.15E+06	3.41E+06	2.72E+06	8.90E+06	8.10E+06	2.49E+06	4.17E+06	2.79E+06	1.97E+06
520	PARD3	6	3.28E+06	3.92E+06	0.00E+00	0.00E+00	0.00E+00	0.00E+00	3.08E+06	3.59E+06	3.14E+06	0.00E+00	0.00E+00	0.00E+00
521	PPIL4	18	7.14E+07	6.16E+07	4.43E+07	4.51E+07	5.30E+07	5.66E+07	7.98E+07	8.58E+07	4.95E+07	5.06E+07	6.33E+07	7.25E+07
522	BRK1	5	6.28E+06	6.21E+06	0.00E+00	0.00E+00	0.00E+00	0.00E+00	5.62E+06	6.44E+06	0.00E+00	0.00E+00	0.00E+00	0.00E+00
523	NSMCE1	4	6.64E+06	0.00E+00	3.88E+06	0.00E+00	4.49E+06	0.00E+00	9.42E+06	0.00E+00	5.12E+06	0.00E+00	4.56E+06	0.00E+00
524	LEO1	12	9.18E+06	6.96E+06	2.91E+07	3.20E+07	5.75E+07	5.67E+07	1.27E+07	1.42E+07	3.58E+07	4.12E+07	2.86E+07	5.87E+07
525	HNRNPLL	2	0.00E+00	1.97E+06	0.00E+00	0.00E+00	0.00E+00	0.00E+00	0.00E+00	0.00E+00	0.00E+00	0.00E+00	0.00E+00	0.00E+00
526	PCNP	8	1.17E+07	1.28E+07	4.10E+07	5.77E+07	2.31E+07	3.03E+07	1.09E+07	1.36E+07	3.69E+07	2.92E+07	3.54E+07	2.55E+07
527	ATXN2L	37	2.59E+08	2.37E+08	2.35E+08	2.32E+08	3.19E+08	3.08E+08	3.24E+08	3.33E+08	2.48E+08	2.55E+08	3.73E+08	3.47E+08
528	PALLD	2	1.80E+06	2.31E+06	3.99E+06	2.42E+06	1.36E+06	0.00E+00	1.84E+06	0.00E+00	0.00E+00	2.20E+06	1.42E+06	0.00E+00
529	PSPC1	31	3.18E+08	3.70E+08	5.34E+08	6.19E+08	8.24E+08	9.50E+08	4.52E+08	5.03E+08	6.98E+08	9.17E+08	9.55E+08	1.06E+09
530	AUTS2	4	0.00E+00	0.00E+00	4.75E+06	0.00E+00	1.42E+07	9.01E+06	0.00E+00	0.00E+00	5.61E+06	0.00E+00	8.01E+06	9.42E+06
531	DGCR8	9	1.87E+07	1.27E+07	4.05E+06	0.00E+00	5.85E+06	5.33E+06	9.79E+06	1.16E+07	4.54E+06	4.08E+06	4.25E+06	4.63E+06
532	DDX1	29	1.22E+08	1.14E+08	8.05E+07	1.01E+08	1.47E+08	1.08E+08	9.43E+07	1.06E+08	1.36E+08	1.62E+08	1.05E+08	1.09E+08
533	SLC39A7	1	0.00E+00	0.00E+00	0.00E+00	0.00E+00	0.00E+00	0.00E+00	0.00E+00	0.00E+00	0.00E+00	0.00E+00	0.00E+00	0.00E+00
534	WASF1	7	1.28E+07	9.73E+06	4.04E+06	3.58E+06	0.00E+00	0.00E+00	1.28E+07	7.95E+06	6.00E+06	5.32E+06	2.32E+06	0.00E+00
535	PHF3	9	1.18E+07	1.50E+07	1.38E+07	1.50E+07	1.43E+07	1.50E+07	1.32E+07	1.43E+07	1.03E+07	1.03E+07	1.18E+07	1.26E+07

id	Gene names	Unique peptides	LFQ intensity Bait 2h_1	LFQ intensity Control 2h_1	LFQ intensity Bait 2h_2	LFQ intensity Control 2h_2	LFQ intensity Bait 2h_3	LFQ intensity Control 2h_3	LFQ intensity Bait 24h_1	LFQ intensity Control_24h_1	LFQ intensity Bait 24h_2	LFQ intensity Control_24h_2	LFQ intensity 2_Bait 24h_3	LFQ intensity
536	RQCD1	1	0.00E+00	0.00E+00	0.00E+00	0.00E+00	0.00E+00	0.00E+00	0.00E+00	0.00E+00	0.00E+00	0.00E+00	0.00E+00	0.00E+00
537	ANKS1A	2	0.00E+00	0.00E+00	0.00E+00	0.00E+00	0.00E+00	0.00E+00	1.84E+06	0.00E+00	0.00E+00	0.00E+00	0.00E+00	0.00E+00
538	HDAC2	6	1.57E+07	1.40E+07	9.72E+06	8.17E+06	9.48E+06	1.08E+07	1.15E+07	1.01E+07	6.62E+06	6.58E+06	1.19E+07	9.20E+06
539	DPF2	1	0.00E+00	0.00E+00	0.00E+00	0.00E+00	0.00E+00	0.00E+00	0.00E+00	0.00E+00	0.00E+00	0.00E+00	0.00E+00	0.00E+00
540	DDX17	4	6.22E+06	5.31E+06	8.08E+06	6.67E+06	6.15E+06	4.99E+06	4.92E+06	4.99E+06	8.04E+06	7.38E+06	6.85E+06	6.17E+06
541	GATA6	3	0.00E+00	0.00E+00	8.42E+06	6.91E+06	1.32E+07	1.20E+07	0.00E+00	0.00E+00	6.66E+06	5.47E+06	8.04E+06	8.21E+06
542	SMARCC1	9	1.29E+07	1.08E+07	8.62E+06	9.69E+06	1.05E+07	9.29E+06	9.09E+06	8.37E+06	7.01E+06	7.09E+06	9.51E+06	9.05E+06
543	SMARCD2	2	0.00E+00	0.00E+00	0.00E+00	0.00E+00	0.00E+00	0.00E+00	0.00E+00	0.00E+00	0.00E+00	0.00E+00	0.00E+00	0.00E+00
544	DVL3	5	8.25E+06	7.22E+06	3.37E+06	3.91E+06	3.27E+06	4.30E+06	6.30E+06	6.16E+06	3.34E+06	4.16E+06	3.45E+06	2.86E+06
545	USP9X	65	3.06E+08	2.98E+08	1.26E+08	9.98E+07	1.26E+08	1.09E+08	2.76E+08	2.70E+08	1.23E+08	1.21E+08	1.25E+08	9.90E+07
546	USP7	37	1.42E+08	1.06E+08	4.17E+07	3.50E+07	3.13E+07	1.99E+07	1.06E+08	9.82E+07	4.76E+07	3.20E+07	2.50E+07	1.82E+07
547	PHKB	2	1.32E+06	1.41E+06	0.00E+00	0.00E+00	0.00E+00	0.00E+00	2.15E+06	1.24E+06	0.00E+00	0.00E+00	0.00E+00	0.00E+00
548	SMARCE1	9	1.36E+07	1.37E+07	1.84E+07	2.22E+07	1.24E+07	1.28E+07	1.27E+07	1.14E+07	1.26E+07	1.32E+07	1.66E+07	1.37E+07
549	ERGIC1	3	2.24E+06	2.44E+06	5.78E+06	3.34E+06	7.42E+06	2.90E+06	2.95E+06	2.87E+06	6.31E+06	3.85E+06	5.89E+06	4.48E+06
550	LRRC59	4	0.00E+00	1.99E+06	1.03E+07	2.78E+06	7.86E+06	2.15E+06	0.00E+00	0.00E+00	3.34E+06	2.66E+06	3.30E+06	5.15E+06
551	PBXIP1	8	0.00E+00	0.00E+00	6.48E+06	6.56E+06	8.68E+06	6.57E+06	0.00E+00	0.00E+00	3.38E+06	3.48E+06	3.71E+06	3.97E+06
552	PINX1	3	2.09E+06	2.55E+06	0.00E+00	3.36E+06	3.29E+06	0.00E+00	0.00E+00	0.00E+00	0.00E+00	2.45E+06	0.00E+00	0.00E+00
553	PYCR2	3	2.74E+06	2.39E+06	3.41E+06	0.00E+00	0.00E+00	0.00E+00	2.41E+06	1.75E+06	4.09E+06	2.68E+06	0.00E+00	0.00E+00
554	SEH1L	3	4.21E+06	3.18E+06	0.00E+00	0.00E+00	0.00E+00	0.00E+00	4.19E+06	2.95E+06	0.00E+00	0.00E+00	0.00E+00	0.00E+00
555	FAM120B	10	1.97E+07	1.90E+07	3.70E+06	3.94E+06	4.41E+06	3.93E+06	1.30E+07	2.35E+07	3.64E+06	3.57E+06	3.67E+06	3.71E+06
556	RBM33	21	2.26E+07	2.01E+07	7.41E+07	8.27E+07	1.42E+08	1.22E+08	2.61E+07	2.16E+07	8.49E+07	1.05E+08	1.20E+08	1.58E+08
557	CYFIP2	2	2.11E+06	2.08E+06	0.00E+00	0.00E+00	0.00E+00	0.00E+00	1.89E+06	1.69E+06	0.00E+00	0.00E+00	0.00E+00	0.00E+00
558	CCDC97	8	1.88E+07	1.97E+07	2.15E+07	2.58E+07	2.26E+07	2.88E+07	2.10E+07	1.40E+07	2.15E+07	1.53E+07	1.95E+07	2.69E+07
559	EDC3	13	2.80E+07	3.25E+07	1.79E+07	1.53E+07	1.51E+07	6.99E+06	2.72E+07	2.76E+07	1.58E+07	1.36E+07	1.03E+07	7.48E+06
560	BICD1	3	3.08E+06	2.18E+06	0.00E+00	0.00E+00	0.00E+00	0.00E+00	2.32E+06	0.00E+00	0.00E+00	0.00E+00	0.00E+00	0.00E+00
561	AURKB	1	0.00E+00	0.00E+00	0.00E+00	0.00E+00	0.00E+00	0.00E+00	0.00E+00	0.00E+00	0.00E+00	0.00E+00	0.00E+00	0.00E+00
562	SMARCD1	5	4.36E+06	4.62E+06	3.23E+06	4.07E+06	0.00E+00	2.38E+06	3.35E+06	3.26E+06	3.07E+06	2.34E+06	0.00E+00	0.00E+00
563	NAF1	2	2.00E+06	2.62E+06	1.96E+06	0.00E+00	0.00E+00	0.00E+00	1.75E+06	1.79E+06	0.00E+00	0.00E+00	0.00E+00	0.00E+00
564	DHTKD1	9	9.02E+06	1.10E+07	4.75E+06	3.88E+06	0.00E+00	0.00E+00	8.14E+06	8.50E+06	4.75E+06	6.16E+06	0.00E+00	0.00E+00
565	SCLY	14	8.36E+07	7.25E+07	3.05E+07	3.11E+07	2.87E+07	3.14E+07	7.29E+07	9.26E+07	3.70E+07	3.91E+07	3.94E+07	3.34E+07
566	RBM17	18	4.89E+07	6.01E+07	9.51E+07	1.01E+08	9.44E+07	9.61E+07	5.22E+07	4.96E+07	1.04E+08	1.13E+08	1.29E+08	1.16E+08
567	NSMCE2	4	5.43E+06	0.00E+00	3.74E+06	0.00E+00	4.23E+06	0.00E+00	4.83E+06	0.00E+00	4.75E+06	0.00E+00	5.71E+06	0.00E+00
568	NDNL2	10	9.52E+06	0.00E+00	1.22E+07	0.00E+00	1.48E+07	0.00E+00	1.18E+07	0.00E+00	1.47E+07	0.00E+00	2.02E+07	0.00E+00
569	DOCK7	24	2.67E+07	2.41E+07	3.85E+07	2.32E+07	4.36E+07	3.31E+07	3.08E+07	2.44E+07	3.63E+07	3.97E+07	4.20E+07	3.57E+07
570	RPRD1A	3	4.89E+06	3.29E+06	4.56E+06	0.00E+00	0.00E+00	0.00E+00	0.00E+00	3.89E+06	5.72E+06	4.48E+06	3.41E+06	0.00E+00
571	PLEKHG4B	1	0.00E+00	0.00E+00	0.00E+00	0.00E+00	0.00E+00	0.00E+00	0.00E+00	0.00E+00	0.00E+00	0.00E+00	0.00E+00	0.00E+00
572	PPP1R10	32	9.09E+06	1.33E+07	9.60E+07	1.17E+08	1.65E+08	2.14E+08	1.40E+07	1.79E+07	1.10E+08	1.33E+08	1.32E+08	2.07E+08
573	MAGI1	6	5.21E+06	4.84E+06	3.47E+06	3.83E+06	3.07E+06	5.93E+06	3.49E+06	4.77E+06	3.69E+06	4.18E+06	2.31E+06	2.79E+06
574	ERGIC2	3	7.55E+06	6.83E+06	7.41E+06	3.85E+06	5.89E+06	3.93E+06	9.90E+06	8.52E+06	6.28E+06	4.03E+06	7.21E+06	6.23E+06
575	NUDCD1	9	8.44E+06	1.27E+07	3.66E+06	0.00E+00	0.00E+00	0.00E+00	1.50E+07	2.58E+07	4.30E+06	0.00E+00	5.31E+06	0.00E+00
576	WDR24	1	0.00E+00	0.00E+00	0.00E+00	0.00E+00	0.00E+00	0.00E+00	0.00E+00	0.00E+00	0.00E+00	0.00E+00	0.00E+00	0.00E+00
577	WRNIP1	6	3.73E+06	4.00E+06	0.00E+00	0.00E+00	0.00E+00	0.00E+00	2.78E+06	2.82E+06	0.00E+00	0.00E+00	0.00E+00	0.00E+00
578	SMC6	20	3.74E+07	0.00E+00	3.78E+07	0.00E+00	3.80E+07	0.00E+00	4.15E+07	0.00E+00	4.01E+07	0.00E+00	5.65E+07	0.00E+00
579	SIN3A	21	7.39E+07	6.44E+07	6.89E+07	8.44E+07	6.86E+07	6.39E+07	5.69E+07	5.66E+07	7.24E+07	5.14E+07	6.21E+07	5.39E+07
580	OSBPL9	4	0.00E+00	1.44E+06	3.04E+06	2.31E+06	0.00E+00	0.00E+00	2.02E+06	1.32E+06	4.34E+06	1.48E+06	0.00E+00	1.74E+06
581	VWA9	3	2.36E+06	3.00E+06	0.00E+00	1.82E+06	0.00E+00	0.00E+00	2.39E+06	2.30E+06	0.00E+00	0.00E+00	1.68E+06	1.76E+06
582	ZIC5	1	1.77E+06	1.94E+06	1.70E+06	1.71E+06	2.02E+06	1.74E+06	1.94E+06	1.66E+06	1.60E+06	0.00E+00	0.00E+00	2.13E+06
583	RBM15	6	0.00E+00	5.02E+06	1.37E+07	7.51E+06	1.17E+07	9.68E+06	0.00E+00	5.26E+06	1.72E+07	1.37E+07	8.34E+06	1.43E+07
584	RUFY1	4	3.34E+06	3.05E+06	2.23E+06	0.00E+00	0.00E+00	0.00E+00	4.04E+06	2.91E+06	1.43E+06	1.37E+06	0.00E+00	0.00E+00
585	SPEN	9	1.53E+07	1.63E+07	6.38E+06	6.04E+06	3.78E+06	0.00E+00	1.09E+07	1.14E+07	6.23E+06	4.72E+06	0.00E+00	0.00E+00
586	TCF12	3	1.77E+06	2.00E+06	0.00E+00	0.00E+00	0.00E+00	0.00E+00	0.00E+00	0.00E+00	0.00E+00	0.00E+00	0.00E+00	0.00E+00
587	MYCBP	2	0.00E+00	0.00E+00	0.00E+00	0.00E+00	0.00E+00	0.00E+00	0.00E+00	0.00E+00	0.00E+00	0.00E+00	0.00E+00	0.00E+00
588	CDC5L	2	0.00E+00	0.00E+00	2.17E+06	0.00E+00	0.00E+00	0.00E+00	0.00E+00	0.00E+00	1.90E+06	0.00E+00	0.00E+00	0.00E+00
589	RNF2	2	1.64E+06	0.00E+00	0.00E+00	0.00E+00	0.00E+00	0.00E+00	0.00E+00	0.00E+00	0.00E+00	0.00E+00	0.00E+00	0.00E+00
590	LGMN	4	1.15E+07	1.54E+07	1.31E+07	8.60E+06	7.87E+06	5.98E+06	1.14E+07	6.16E+06	5.62E+06	0.00E+00	6.55E+06	4.48E+06
591	MNT	5	5.08E+06	5.32E+06	4.56E+06	4.20E+06	3.87E+06	4.23E+06	5.30E+06	5.58E+06	4.34E+06	3.83E+06	3.93E+06	3.78E+06
592	CDX2;CDX1	2	0.00E+00	0.00E+00	2.76E+06	2.77E+06	3.15E+06	3.66E+06	0.00E+00	0.00E+00	2.69E+06	2.48E+06	3.13E+06	3.30E+06
593	ATXN2	25	2.36E+07	3.05E+07	5.14E+07	7.48E+07	1.11E+08	1.54E+08	2.96E+07	3.63E+07	6.85E+07	1.01E+08	1.14E+08	1.57E+08
594	SMAD5;SM	2	0.00E+00	0.00E+00	0.00E+00	0.00E+00	0.00E+00	0.00E+00	0.00E+00	0.00E+00	0.00E+00	0.00E+00	0.00E+00	0.00E+00
595	HNRNPAB	2	0.00E+00	0.00E+00	1.30E+06	1.25E+06	1.16E+06	0.00E+00	0.00E+00	0.00E+00	3.49E+06	1.33E+06	1.27E+06	1.22E+06
596	CCT7	24	1.56E+08	1.38E+08	5.92E+07	4.69E+07	2.27E+07	1.67E+07	1.55E+08	1.05E+08	5.14E+07	4.01E+07	1.62E+07	1.92E+07
597	PKP2	5	2.55E+06	3.52E+06	2.83E+06	3.32E+06	2.71E+06	0.00E+00	2.06E+06	2.46E+06	3.07E+06	4.25E+06	0.00E+00	2.30E+06
598	CITED2	2	0.00E+00	0.00E+00	0.00E+00	2.02E+06	3.31E+06	3.39E+06	0.00E+00	0.00E+00	0.00E+00	0.00E+00	0.00E+00	0.00E+00
599	NABP2	1	0.00E+00	0.00E+00	0.00E+00	0.00E+00	0.00E+00	0.00E+00	0.00E+00	0.00E+00	0.00E+00	0.00E+00	0.00E+00	0.00E+00
600	ADPGK	8	2.59E+07	2.34E+07	2.87E+07	1.67E+07	2.20E+07	1.14E+07	2.45E+07	2.27E+07	1.60E+07	1.56E+07	1.61E+07	2.02E+07
601	ERP44	15	5.69E+07	5.11E+07	5.15E+07	4.35E+07	8.67E+07	4.69E+07	4.66E+07	5.84E+07	5.54E+07	6.07E+07	5.83E+07	5.38E+07
602	TACO1	3	1.50E+07	1.29E+07	0.00E+00	0.00E+00	6.55E+06	0.00E+00	8.11E+06	1.05E+07	9.86E+06	0.00E+00	0.00E+00	6.74E+06

id	Gene names	Unique peptides	LFQ intensity Bait 2h_1	LFQ intensity Control 2h_1	LFQ intensity Bait 2h_2	LFQ intensity Control 2h_2	LFQ intensity Bait 2h_3	LFQ intensity Control 2h_3	LFQ intensity Bait 24h_1	LFQ intensity Control_24h_1	LFQ intensity Bait 24h_2	LFQ intensity Control_24h_2	LFQ intensity 2_Bait 24h_3	LFQ intensity
603	ESYT1	5	1.78E+06	3.86E+06	7.01E+06	2.00E+06	0.00E+00	0.00E+00	1.70E+06	1.57E+06	2.23E+06	0.00E+00	0.00E+00	0.00E+00
604	WAC	14	2.13E+07	2.16E+07	4.07E+07	3.99E+07	4.34E+07	4.84E+07	2.32E+07	2.23E+07	4.42E+07	4.07E+07	4.99E+07	4.77E+07
605	NDC1	2	7.73E+05	0.00E+00	1.67E+06	1.11E+06	0.00E+00	0.00E+00	0.00E+00	0.00E+00	1.35E+06	1.03E+06	0.00E+00	1.07E+06
606	MMTAG2	5	8.18E+06	6.09E+06	1.17E+07	8.97E+06	9.77E+06	7.21E+06	8.93E+06	6.48E+06	1.38E+07	1.13E+07	1.10E+07	1.19E+07
607	FAM195A	3	2.08E+06	1.47E+06	2.61E+06	3.45E+06	8.01E+06	6.57E+06	2.48E+06	3.19E+06	2.14E+06	3.26E+06	2.68E+06	9.11E+06
608	TUBB2B;TL	4	0.00E+00	0.00E+00	1.91E+07	1.61E+07	0.00E+00	0.00E+00	0.00E+00	0.00E+00	0.00E+00	0.00E+00	0.00E+00	0.00E+00
609	SF3B5	6	2.88E+07	3.51E+07	3.61E+07	4.80E+07	2.74E+07	3.13E+07	2.27E+07	2.28E+07	2.34E+07	1.95E+07	2.85E+07	2.42E+07
610	SLC4A1AP	9	1.77E+07	1.39E+07	8.70E+06	1.29E+07	6.34E+06	7.11E+06	1.11E+07	1.16E+07	5.90E+06	7.52E+06	6.27E+06	5.03E+06
611	OSBPL11	3	1.93E+06	2.39E+06	3.69E+06	2.54E+06	2.16E+06	0.00E+00	2.87E+06	1.58E+06	2.11E+06	1.77E+06	0.00E+00	2.46E+06
612	CECR2	1	0.00E+00	0.00E+00	0.00E+00	0.00E+00	0.00E+00	0.00E+00	0.00E+00	3.80E+05	0.00E+00	0.00E+00	0.00E+00	0.00E+00
613	RAB11FIP5	5	5.58E+06	5.73E+06	5.84E+06	5.59E+06	3.43E+06	4.87E+06	5.09E+06	6.47E+06	5.57E+06	6.80E+06	4.07E+06	3.66E+06
614	PARD6B	2	0.00E+00	0.00E+00	0.00E+00	0.00E+00	0.00E+00	0.00E+00	0.00E+00	2.17E+06	0.00E+00	0.00E+00	0.00E+00	0.00E+00
615	SETD2	4	1.20E+06	1.26E+06	0.00E+00	0.00E+00	0.00E+00	0.00E+00	0.00E+00	1.21E+06	0.00E+00	0.00E+00	0.00E+00	0.00E+00
616	DOCK9	2	2.48E+06	2.22E+06	0.00E+00	0.00E+00	0.00E+00	0.00E+00	0.00E+00	2.11E+06	0.00E+00	0.00E+00	0.00E+00	0.00E+00
617	TBL1XR1	9	1.14E+07	1.30E+07	6.68E+06	5.37E+06	3.31E+06	0.00E+00	1.37E+07	1.25E+07	5.13E+06	5.89E+06	6.41E+06	0.00E+00
618	SHCBP1L	2	0.00E+00	0.00E+00	3.37E+06	0.00E+00	4.57E+06	7.12E+06	0.00E+00	0.00E+00	0.00E+00	0.00E+00	3.26E+06	0.00E+00
619	DPY30	2	0.00E+00	0.00E+00	0.00E+00	0.00E+00	0.00E+00	0.00E+00	0.00E+00	0.00E+00	0.00E+00	0.00E+00	0.00E+00	0.00E+00
620	UNK	5	4.33E+06	6.02E+06	3.52E+06	2.96E+06	2.78E+06	0.00E+00	4.48E+06	6.20E+06	4.92E+06	4.11E+06	4.16E+06	3.47E+06
621	WDR33	27	5.04E+07	5.51E+07	4.93E+07	6.30E+07	5.45E+07	6.60E+07	4.90E+07	5.14E+07	5.25E+07	4.41E+07	6.77E+07	6.02E+07
622	C20orf27	6	1.47E+08	1.73E+08	7.19E+07	8.73E+07	1.35E+08	1.27E+08	1.60E+08	1.84E+08	1.21E+08	1.31E+08	1.52E+08	1.21E+08
623	PITHD1	6	2.98E+06	0.00E+00	1.21E+07	1.07E+07	1.06E+07	6.55E+06	6.14E+06	4.07E+06	2.06E+07	1.78E+07	1.52E+07	1.01E+07
624	WDR61	5	8.32E+06	7.49E+06	1.14E+07	7.41E+06	1.66E+07	1.23E+07	8.04E+06	7.10E+06	9.62E+06	8.32E+06	1.37E+07	1.06E+07
625	XRN2	27	5.29E+07	5.31E+07	5.11E+07	5.63E+07	3.06E+07	2.32E+07	5.79E+07	6.84E+07	3.66E+07	5.37E+07	3.47E+07	3.73E+07
626	NSRP1	26	4.90E+07	5.08E+07	5.89E+07	7.99E+07	7.62E+07	1.04E+08	7.25E+07	8.51E+07	7.42E+07	7.84E+07	9.99E+07	1.38E+08
627	CSTF2T	3	0.00E+00	0.00E+00	4.04E+06	7.74E+06	2.91E+06	3.46E+06	0.00E+00	0.00E+00	2.89E+06	0.00E+00	4.66E+06	3.13E+06
628	SMG9	4	4.18E+06	1.85E+06	0.00E+00	0.00E+00	0.00E+00	0.00E+00	1.61E+06	1.52E+06	1.42E+06	0.00E+00	0.00E+00	0.00E+00
629	ASCC2	4	2.41E+06	1.87E+06	0.00E+00	0.00E+00	0.00E+00	0.00E+00	3.29E+06	2.27E+06	0.00E+00	0.00E+00	0.00E+00	0.00E+00
630	VPS16	2	0.00E+00	0.00E+00	0.00E+00	0.00E+00	0.00E+00	0.00E+00	0.00E+00	0.00E+00	0.00E+00	0.00E+00	0.00E+00	0.00E+00
631	PNN	2	0.00E+00	0.00E+00	3.18E+06	0.00E+00	0.00E+00	0.00E+00	0.00E+00	0.00E+00	0.00E+00	0.00E+00	0.00E+00	0.00E+00
632	FOXP1	1	0.00E+00	0.00E+00	0.00E+00	0.00E+00	0.00E+00	0.00E+00	0.00E+00	0.00E+00	0.00E+00	0.00E+00	0.00E+00	0.00E+00
633	KCTD10	5	6.81E+06	5.47E+06	0.00E+00	0.00E+00	1.83E+06	0.00E+00	3.69E+06	3.64E+06	0.00E+00	0.00E+00	0.00E+00	0.00E+00
634	WDR26	1	0.00E+00	0.00E+00	0.00E+00	0.00E+00	0.00E+00	0.00E+00	0.00E+00	0.00E+00	0.00E+00	0.00E+00	0.00E+00	0.00E+00
635	SUDS3	2	2.87E+06	2.65E+06	3.56E+06	3.73E+06	3.53E+06	3.99E+06	0.00E+00	0.00E+00	2.67E+06	0.00E+00	3.65E+06	0.00E+00
636	ZNF703	6	1.52E+07	1.72E+07	5.33E+06	4.87E+06	4.45E+06	6.21E+06	4.41E+06	5.43E+06	3.82E+06	3.26E+06	3.64E+06	3.10E+06
637	NT5DC2	18	6.22E+07	5.05E+07	1.92E+07	1.58E+07	2.16E+07	1.02E+07	5.18E+07	5.24E+07	1.67E+07	1.57E+07	1.57E+07	1.25E+07
638	PSTPIP2	1	0.00E+00	0.00E+00	0.00E+00	0.00E+00	0.00E+00	0.00E+00	0.00E+00	0.00E+00	0.00E+00	0.00E+00	0.00E+00	0.00E+00
639	QTRTD1	2	2.29E+06	2.18E+06	0.00E+00	0.00E+00	0.00E+00	0.00E+00	3.15E+06	3.74E+06	0.00E+00	0.00E+00	0.00E+00	0.00E+00
640	MRPL44	1	0.00E+00	0.00E+00	0.00E+00	0.00E+00	0.00E+00	0.00E+00	0.00E+00	0.00E+00	0.00E+00	0.00E+00	0.00E+00	0.00E+00
641	ELP3	6	5.42E+06	6.23E+06	2.74E+06	0.00E+00	0.00E+00	0.00E+00	8.14E+06	5.95E+06	3.01E+06	0.00E+00	2.17E+06	0.00E+00
642	CARS2	17	6.82E+07	6.12E+07	1.94E+07	1.87E+07	1.05E+07	9.11E+06	5.18E+07	5.12E+07	1.63E+07	1.90E+07	9.88E+06	1.04E+07
643	FBRS	5	8.14E+06	8.39E+06	1.31E+07	1.05E+07	2.23E+07	1.74E+07	0.00E+00	7.54E+06	1.63E+07	1.37E+07	1.95E+07	1.25E+07
644	GPBP1L1	1	0.00E+00	0.00E+00	0.00E+00	0.00E+00	0.00E+00	0.00E+00	0.00E+00	0.00E+00	0.00E+00	0.00E+00	0.00E+00	0.00E+00
645	CHD8	18	2.80E+06	6.16E+06	2.80E+07	3.31E+07	7.85E+07	5.83E+07	6.95E+06	5.71E+06	2.24E+07	4.04E+07	2.68E+07	6.80E+07
646	FBRSL1	4	3.13E+06	3.77E+06	3.67E+06	3.20E+06	4.14E+06	3.65E+06	0.00E+00	0.00E+00	4.34E+06	4.62E+06	3.45E+06	0.00E+00
647	SDF2L1	8	3.10E+07	3.88E+07	2.01E+07	2.58E+07	1.24E+07	1.36E+07	2.85E+07	2.56E+07	1.72E+07	1.83E+07	1.11E+07	1.24E+07
648	GOPC	22	4.43E+07	4.87E+07	2.26E+07	1.68E+07	1.22E+07	1.53E+07	3.15E+07	4.07E+07	1.47E+07	1.82E+07	1.22E+07	1.65E+07
649	DCP1A	7	5.36E+06	5.89E+06	5.72E+06	3.90E+06	5.66E+06	3.04E+06	6.89E+06	5.64E+06	6.40E+06	4.47E+06	0.00E+00	0.00E+00
650	LUC7L	2	0.00E+00	0.00E+00	1.82E+06	1.41E+06	0.00E+00	0.00E+00	0.00E+00	0.00E+00	0.00E+00	0.00E+00	0.00E+00	0.00E+00
651	TCF7L2	2	0.00E+00	1.70E+06	0.00E+00	0.00E+00	0.00E+00	0.00E+00	0.00E+00	0.00E+00	0.00E+00	0.00E+00	0.00E+00	0.00E+00
652	PRDM10	1	0.00E+00	0.00E+00	0.00E+00	0.00E+00	0.00E+00	0.00E+00	0.00E+00	0.00E+00	0.00E+00	0.00E+00	0.00E+00	0.00E+00
653	GPHN	12	3.76E+07	3.17E+07	2.53E+07	2.41E+07	1.60E+07	1.71E+07	3.59E+07	4.29E+07	2.22E+07	1.58E+07	2.93E+07	2.26E+07
654	EIF4ENIF1	3	4.60E+06	3.94E+06	5.49E+06	0.00E+00	0.00E+00	4.47E+06	0.00E+00	0.00E+00	4.96E+06	0.00E+00	0.00E+00	4.33E+06
655	AAAS	3	2.32E+06	0.00E+00	3.98E+06	0.00E+00	0.00E+00	0.00E+00	0.00E+00	0.00E+00	0.00E+00	0.00E+00	0.00E+00	0.00E+00
656	DROSHA	7	6.86E+06	4.86E+06	3.48E+06	0.00E+00	3.04E+06	0.00E+00	4.76E+06	3.83E+06	2.71E+06	0.00E+00	2.85E+06	3.20E+06
657	INIP	2	0.00E+00	1.45E+06	0.00E+00	0.00E+00	0.00E+00	0.00E+00	0.00E+00	1.36E+06	0.00E+00	0.00E+00	0.00E+00	0.00E+00
658	LANCL2	2	6.37E+06	8.72E+06	0.00E+00	3.28E+06	0.00E+00	0.00E+00	5.85E+06	7.57E+06	0.00E+00	3.77E+06	0.00E+00	0.00E+00
659	BMP2K	8	2.37E+06	0.00E+00	3.47E+06	3.24E+06	1.83E+07	1.47E+07	0.00E+00	0.00E+00	1.11E+07	7.83E+06	1.94E+07	1.80E+07
660	MAN2C1	3	9.99E+05	1.12E+06	0.00E+00	0.00E+00	0.00E+00	0.00E+00	9.21E+05	1.24E+06	0.00E+00	0.00E+00	0.00E+00	0.00E+00
661	CUTC	9	5.40E+07	5.04E+07	3.47E+07	3.54E+07	3.07E+07	4.40E+07	4.83E+07	4.28E+07	4.96E+07	2.54E+07	2.88E+07	3.40E+07
662	ASUN	6	5.08E+06	4.36E+06	2.91E+06	3.03E+06	3.91E+06	2.91E+06	4.86E+06	5.14E+06	3.68E+06	0.00E+00	3.98E+06	0.00E+00
663	KLHL11	3	4.53E+06	3.86E+06	0.00E+00	0.00E+00	0.00E+00	0.00E+00	2.60E+06	2.34E+06	0.00E+00	0.00E+00	0.00E+00	0.00E+00
664	SLTM	8	5.37E+06	5.50E+06	8.90E+06	8.81E+06	5.98E+06	7.21E+06	5.10E+06	5.52E+06	5.58E+06	7.25E+06	5.43E+06	6.58E+06
665	GID8	4	3.39E+06	4.33E+06	4.88E+06	5.26E+06	7.09E+06	4.36E+06	2.28E+06	2.61E+06	3.59E+06	0.00E+00	3.93E+06	5.73E+06
666	FAM120C	3	0.00E+00	0.00E+00	0.00E+00	0.00E+00	3.57E+06	0.00E+00	0.00E+00	2.39E+06	0.00E+00	4.71E+06	0.00E+00	3.02E+06
667	MIOS	3	3.26E+06	3.12E+06	0.00E+00	0.00E+00	0.00E+00	0.00E+00	3.12E+06	5.53E+06	0.00E+00	0.00E+00	3.11E+06	0.00E+00
668	SMPD4	5	2.43E+06	2.19E+06	3.07E+06	2.60E+06	2.86E+06	2.38E+06	2.00E+06	1.86E+06	2.45E+06	0.00E+00	3.01E+06	2.80E+06
669	ANKRD10	3	0.00E+00	0.00E+00	0.00E+00	0.00E+00	0.00E+00	0.00E+00	0.00E+00	0.00E+00	0.00E+00	0.00E+00	0.00E+00	0.00E+00

id	Gene names	Unique peptides	LFQ intensity Bait 2h_1	LFQ intensity Control 2h_1	LFQ intensity Bait 2h_2	LFQ intensity Control 2h_2	LFQ intensity Bait 2h_3	LFQ intensity Control 2h_3	LFQ intensity Bait 24h_1	LFQ intensity Control_24h_1	LFQ intensity Bait 24h_2	LFQ intensity Control_24h_2	LFQ intensity 2_Bait 24h_3	LFQ intensity
670	DNAJB12	3	3.32E+06	2.53E+06	1.99E+06	1.92E+06	1.99E+06	2.53E+06	0.00E+00	1.58E+06	0.00E+00	1.54E+06	0.00E+00	1.91E+06
671	NSMCE4A	16	2.51E+07	0.00E+00	2.29E+07	0.00E+00	2.57E+07	0.00E+00	3.00E+07	0.00E+00	3.70E+07	0.00E+00	4.57E+07	0.00E+00
672	TERF2IP	8	0.00E+00	0.00E+00	6.07E+06	3.70E+06	1.29E+07	1.66E+07	0.00E+00	2.22E+06	8.81E+06	1.57E+07	7.57E+06	2.30E+07
673	FAM53C	1	0.00E+00	0.00E+00	0.00E+00	0.00E+00	0.00E+00	0.00E+00	0.00E+00	0.00E+00	0.00E+00	0.00E+00	0.00E+00	0.00E+00
674	BCLAF1	6	3.20E+06	2.32E+06	1.70E+07	1.67E+07	3.93E+06	3.33E+06	2.50E+06	2.51E+06	1.19E+07	5.30E+06	4.22E+06	3.82E+06
675	TAB2	4	2.76E+06	2.62E+06	2.30E+06	0.00E+00	2.15E+06	3.43E+06	2.24E+06	2.40E+06	2.42E+06	2.43E+06	0.00E+00	2.90E+06
676	CDK12	21	3.66E+07	4.17E+07	1.76E+07	2.00E+07	1.57E+07	2.07E+07	4.16E+07	4.63E+07	1.81E+07	1.62E+07	1.71E+07	1.56E+07
677	MAT2B	5	4.74E+06	6.19E+06	5.76E+06	4.06E+06	0.00E+00	0.00E+00	4.61E+06	4.77E+06	5.22E+06	3.16E+06	0.00E+00	0.00E+00
678	CWC15	2	0.00E+00	0.00E+00	0.00E+00	4.59E+06	0.00E+00	0.00E+00	0.00E+00	0.00E+00	0.00E+00	0.00E+00	0.00E+00	0.00E+00
679	HACD3	3	0.00E+00	0.00E+00	4.53E+06	4.85E+06	3.65E+06	0.00E+00	0.00E+00	0.00E+00	0.00E+00	0.00E+00	0.00E+00	0.00E+00
680	STIM2	1	0.00E+00	0.00E+00	0.00E+00	0.00E+00	0.00E+00	0.00E+00	0.00E+00	0.00E+00	0.00E+00	0.00E+00	0.00E+00	0.00E+00
681	CHD7	9	5.82E+06	4.19E+06	4.08E+06	6.69E+06	7.23E+06	1.01E+07	3.74E+06	3.30E+06	4.93E+06	3.83E+06	5.83E+06	5.12E+06
682	CPSF2	10	1.15E+07	1.19E+07	9.60E+06	6.54E+06	8.83E+06	6.60E+06	9.10E+06	1.21E+07	7.17E+06	3.95E+06	8.83E+06	7.99E+06
683	RBM27	17	3.83E+07	3.28E+07	3.51E+07	3.72E+07	3.70E+07	4.29E+07	3.70E+07	4.17E+07	3.92E+07	4.07E+07	3.62E+07	4.44E+07
684	KLHL13;KLI	2	0.00E+00	0.00E+00	0.00E+00	0.00E+00	0.00E+00	0.00E+00	0.00E+00	0.00E+00	0.00E+00	0.00E+00	0.00E+00	0.00E+00
685	STARD9	3	1.59E+07	1.52E+07	0.00E+00	0.00E+00	0.00E+00	0.00E+00	1.66E+07	1.55E+07	0.00E+00	0.00E+00	0.00E+00	0.00E+00
686	RERE	7	4.71E+06	3.31E+06	1.98E+07	1.93E+07	3.89E+07	3.68E+07	3.12E+06	2.26E+06	1.54E+07	2.06E+07	2.90E+07	3.20E+07
687	ATXN10	1	0.00E+00	0.00E+00	0.00E+00	0.00E+00	0.00E+00	0.00E+00	0.00E+00	0.00E+00	0.00E+00	0.00E+00	0.00E+00	0.00E+00
688	ORC3	1	0.00E+00	0.00E+00	0.00E+00	0.00E+00	0.00E+00	0.00E+00	0.00E+00	0.00E+00	0.00E+00	0.00E+00	0.00E+00	0.00E+00
689	HECA	3	3.11E+06	3.56E+06	0.00E+00	0.00E+00	0.00E+00	0.00E+00	2.98E+06	3.05E+06	0.00E+00	0.00E+00	0.00E+00	0.00E+00
690	DNAJB11	1	0.00E+00	0.00E+00	0.00E+00	0.00E+00	0.00E+00	0.00E+00	0.00E+00	0.00E+00	0.00E+00	0.00E+00	0.00E+00	0.00E+00
691	TJP2	6	3.48E+06	4.23E+06	0.00E+00	2.61E+06	0.00E+00	0.00E+00	4.11E+06	5.09E+06	0.00E+00	0.00E+00	0.00E+00	0.00E+00
692	MALT1	2	0.00E+00	0.00E+00	0.00E+00	0.00E+00	0.00E+00	0.00E+00	0.00E+00	0.00E+00	0.00E+00	0.00E+00	0.00E+00	0.00E+00
693	LIMD1	4	2.05E+06	2.46E+06	1.70E+06	2.02E+06	0.00E+00	0.00E+00	1.98E+06	2.88E+06	2.37E+06	0.00E+00	0.00E+00	1.77E+06
694	TCF20	8	8.46E+06	8.18E+06	1.32E+07	1.70E+07	1.16E+07	1.49E+07	8.63E+06	1.11E+07	1.51E+07	1.59E+07	9.77E+06	1.41E+07
695	AFF4	13	8.12E+06	1.02E+07	1.30E+07	1.49E+07	1.74E+07	2.90E+07	1.09E+07	9.21E+06	1.36E+07	1.76E+07	1.86E+07	2.75E+07
696	TBK1	2	2.26E+06	0.00E+00	0.00E+00	0.00E+00	0.00E+00	0.00E+00	0.00E+00	0.00E+00	0.00E+00	0.00E+00	0.00E+00	0.00E+00
697	BAIAP2L1	8	7.60E+06	8.94E+06	4.38E+06	4.46E+06	3.48E+06	5.06E+06	7.41E+06	8.61E+06	4.99E+06	5.14E+06	3.73E+06	0.00E+00
698	SAP30BP	5	5.07E+06	5.63E+06	8.26E+06	1.47E+07	7.41E+06	9.64E+06	7.10E+06	6.18E+06	1.45E+07	1.02E+07	1.17E+07	1.16E+07
699	ATPIF1	6	2.06E+07	2.38E+07	2.06E+07	2.78E+07	1.36E+07	2.26E+07	2.24E+07	1.75E+07	2.63E+07	2.43E+07	1.77E+07	1.92E+07
700	LEF1	4	4.85E+06	4.22E+06	5.03E+06	7.40E+06	6.11E+06	9.30E+06	2.77E+06	3.48E+06	4.98E+06	3.95E+06	0.00E+00	4.20E+06
701	CCNL1	2	0.00E+00	0.00E+00	0.00E+00	0.00E+00	2.69E+06	2.95E+06	0.00E+00	0.00E+00	0.00E+00	0.00E+00	3.55E+06	0.00E+00
702	CPSF3	8	1.43E+07	1.07E+07	1.04E+07	4.77E+06	6.01E+06	5.38E+06	1.15E+07	1.03E+07	4.22E+06	4.26E+06	7.14E+06	0.00E+00
703	GPATCH8	11	6.29E+06	5.31E+06	1.70E+07	1.46E+07	2.50E+07	2.24E+07	6.00E+06	5.31E+06	2.30E+07	2.50E+07	2.73E+07	2.82E+07
704	RCOR1	3	1.72E+06	0.00E+00	0.00E+00	0.00E+00	0.00E+00	0.00E+00	0.00E+00	1.68E+06	0.00E+00	0.00E+00	0.00E+00	0.00E+00
705	DNPEP	6	6.54E+06	4.53E+06	0.00E+00	2.81E+06	0.00E+00	0.00E+00	4.89E+06	4.89E+06	3.81E+06	3.25E+06	0.00E+00	0.00E+00
706	ZNF608	2	0.00E+00	0.00E+00	0.00E+00	1.49E+06	1.60E+06	2.36E+06	0.00E+00	0.00E+00	0.00E+00	0.00E+00	1.76E+06	1.68E+06
707	SLC39A10	5	0.00E+00	0.00E+00	3.73E+06	6.59E+06	5.59E+06	7.99E+06	0.00E+00	0.00E+00	4.16E+06	6.22E+06	5.26E+06	7.51E+06
708	ZMIZ1	2	3.32E+06	4.04E+06	0.00E+00	0.00E+00	0.00E+00	0.00E+00	4.82E+06	4.24E+06	0.00E+00	0.00E+00	0.00E+00	0.00E+00
709	PRPF19	4	4.00E+06	3.08E+06	6.52E+06	3.17E+06	0.00E+00	0.00E+00	2.55E+06	1.89E+06	2.89E+06	0.00E+00	0.00E+00	0.00E+00
710	G3BP2	2	0.00E+00	0.00E+00	2.05E+06	1.88E+06	3.52E+06	1.63E+06	0.00E+00	0.00E+00	2.00E+06	0.00E+00	3.33E+06	2.55E+06
711	STUB1	14	6.43E+07	5.55E+07	4.83E+07	3.96E+07	3.04E+07	3.01E+07	5.52E+07	3.97E+07	5.56E+07	3.77E+07	4.02E+07	2.80E+07
712	TTF2	6	3.15E+06	3.36E+06	0.00E+00	0.00E+00	0.00E+00	0.00E+00	3.56E+06	4.16E+06	2.93E+06	0.00E+00	0.00E+00	0.00E+00
713	FZD1	1	0.00E+00	0.00E+00	0.00E+00	0.00E+00	0.00E+00	0.00E+00	0.00E+00	0.00E+00	0.00E+00	0.00E+00	0.00E+00	0.00E+00
714	ZC3H4	11	8.33E+06	8.60E+06	1.55E+07	1.87E+07	1.21E+07	2.72E+07	1.03E+07	1.10E+07	1.90E+07	2.23E+07	1.78E+07	2.87E+07
715	USP22;USF	4	8.26E+06	8.27E+06	0.00E+00	0.00E+00	0.00E+00	0.00E+00	4.48E+06	4.50E+06	0.00E+00	0.00E+00	0.00E+00	0.00E+00
716	FOXJ3	5	0.00E+00	0.00E+00	6.41E+06	5.44E+06	1.40E+07	1.07E+07	0.00E+00	0.00E+00	5.25E+06	6.96E+06	6.17E+06	1.12E+07
717	SATB2	9	1.95E+07	2.17E+07	1.77E+07	1.16E+07	1.64E+07	1.58E+07	1.49E+07	1.59E+07	1.11E+07	1.33E+07	1.37E+07	1.79E+07
718	WASF3	1	0.00E+00	0.00E+00	0.00E+00	0.00E+00	0.00E+00	0.00E+00	0.00E+00	0.00E+00	0.00E+00	0.00E+00	0.00E+00	0.00E+00
719	SCML2	12	1.68E+07	1.85E+07	2.16E+07	1.47E+07	4.79E+06	6.18E+06	1.03E+07	9.54E+06	9.91E+06	9.51E+06	0.00E+00	4.80E+06
720	C14orf166	13	6.10E+07	5.93E+07	4.04E+07	5.33E+07	7.13E+07	5.63E+07	4.84E+07	5.35E+07	6.66E+07	6.49E+07	6.08E+07	8.71E+07
721	RUVBL2	8	3.70E+06	6.04E+06	1.01E+07	5.29E+06	6.02E+06	5.93E+06	4.63E+06	4.19E+06	4.67E+06	0.00E+00	5.94E+06	0.00E+00
722	FOXA2	1	0.00E+00	0.00E+00	0.00E+00	0.00E+00	0.00E+00	2.85E+06	0.00E+00	0.00E+00	0.00E+00	0.00E+00	0.00E+00	0.00E+00
723	RUVBL1	4	4.63E+06	3.39E+06	6.82E+06	5.99E+06	5.49E+06	5.51E+06	4.62E+06	5.00E+06	4.97E+06	5.29E+06	5.56E+06	5.08E+06
724	BCS1L	12	1.89E+07	1.67E+07	2.20E+07	1.69E+07	2.32E+07	1.33E+07	1.97E+07	1.83E+07	1.80E+07	1.59E+07	1.73E+07	2.21E+07
725	ERGIC3	3	2.73E+06	1.92E+06	1.95E+06	1.64E+06	2.74E+06	2.01E+06	2.36E+06	2.61E+06	2.26E+06	2.05E+06	0.00E+00	2.53E+06
726	NCKAP1	14	2.11E+07	2.45E+07	7.48E+06	3.61E+06	0.00E+00	0.00E+00	2.07E+07	1.98E+07	6.27E+06	4.96E+06	0.00E+00	0.00E+00
727	LRCH1	4	2.90E+06	2.66E+06	8.47E+06	3.99E+06	9.43E+06	8.54E+06	2.25E+06	0.00E+00	6.57E+06	7.13E+06	1.18E+07	7.77E+06
728	POLDIP2	3	5.78E+06	6.66E+06	4.02E+06	4.94E+06	0.00E+00	0.00E+00	4.04E+06	3.72E+06	5.24E+06	0.00E+00	0.00E+00	0.00E+00
729	THRAP3	8	0.00E+00	0.00E+00	1.40E+07	8.30E+06	4.03E+06	3.83E+06	4.23E+06	3.96E+06	1.36E+07	8.75E+06	5.72E+06	5.10E+06
730	GIT1	14	3.27E+07	2.49E+07	2.36E+07	2.32E+07	2.93E+07	1.76E+07	2.79E+07	2.14E+07	2.22E+07	1.57E+07	3.09E+07	1.88E+07
731	ZNF281	1	0.00E+00	0.00E+00	0.00E+00	0.00E+00	0.00E+00	0.00E+00	0.00E+00	0.00E+00	0.00E+00	0.00E+00	0.00E+00	0.00E+00
732	ACOT9	15	3.40E+07	4.25E+07	1.55E+07	1.06E+07	1.34E+07	9.35E+06	3.94E+07	4.38E+07	1.51E+07	1.88E+07	1.25E+07	1.03E+07
733	LUC7L2	2	5.09E+06	5.70E+06	1.26E+07	1.18E+07	3.08E+06	3.42E+06	4.59E+06	4.67E+06	6.94E+06	5.16E+06	3.13E+06	3.01E+06
734	MRPS2	2	1.08E+06	1.15E+06	0.00E+00	0.00E+00	0.00E+00	0.00E+00	0.00E+00	0.00E+00	0.00E+00	0.00E+00	0.00E+00	0.00E+00
735	SF3B6	7	5.85E+07	5.69E+07	8.58E+07	8.54E+07	6.53E+07	6.15E+07	4.82E+07	4.53E+07	6.83E+07	5.87E+07	6.78E+07	6.78E+07
736	MRPS23	2	0.00E+00	0.00E+00	0.00E+00	0.00E+00	0.00E+00	0.00E+00	0.00E+00	0.00E+00	0.00E+00	0.00E+00	0.00E+00	0.00E+00

id	Gene names	Unique peptides	LFQ intensity Bait 2h_1	LFQ intensity Control 2h_1	LFQ intensity Bait 2h_2	LFQ intensity Control 2h_2	LFQ intensity Bait 2h_3	LFQ intensity Control 2h_3	LFQ intensity Bait 24h_1	LFQ intensity Control_24h_1	LFQ intensity Bait 24h_2	LFQ intensity Control_24h_2	LFQ intensity 2_Bait 24h_3	LFQ intensity
737	RTCB	24	1.43E+08	1.36E+08	9.50E+07	1.14E+08	1.52E+08	1.04E+08	1.38E+08	1.28E+08	1.14E+08	1.58E+08	1.30E+08	1.13E+08
738	KIAA0430	2	0.00E+00	2.47E+06	0.00E+00	0.00E+00	0.00E+00	0.00E+00	0.00E+00	2.62E+06	0.00E+00	0.00E+00	0.00E+00	0.00E+00
739	AMMECR1	1	0.00E+00	0.00E+00	0.00E+00	0.00E+00	0.00E+00	0.00E+00	0.00E+00	0.00E+00	0.00E+00	0.00E+00	0.00E+00	0.00E+00
740	RBM7	3	8.49E+05	0.00E+00	0.00E+00	0.00E+00	1.72E+06	0.00E+00	0.00E+00	0.00E+00	0.00E+00	0.00E+00	0.00E+00	0.00E+00
741	KCTD3	8	6.96E+06	7.62E+06	3.43E+06	3.33E+06	2.89E+06	0.00E+00	3.49E+06	4.71E+06	0.00E+00	0.00E+00	0.00E+00	0.00E+00
742	PAXBP1	1	0.00E+00	0.00E+00	0.00E+00	0.00E+00	0.00E+00	0.00E+00	0.00E+00	0.00E+00	0.00E+00	0.00E+00	0.00E+00	0.00E+00
743	RBM8A	1	0.00E+00	3.12E+05	0.00E+00	0.00E+00	0.00E+00	0.00E+00	0.00E+00	0.00E+00	0.00E+00	0.00E+00	0.00E+00	0.00E+00
744	NCOR2	8	4.40E+06	4.50E+06	5.45E+06	4.24E+06	5.54E+06	6.44E+06	3.97E+06	4.24E+06	5.15E+06	4.34E+06	7.47E+06	4.62E+06
745	CEPT1	1	0.00E+00	0.00E+00	0.00E+00	0.00E+00	0.00E+00	0.00E+00	0.00E+00	0.00E+00	0.00E+00	0.00E+00	0.00E+00	0.00E+00
746	IGF2BP2	16	6.63E+07	6.28E+07	3.59E+07	2.52E+07	2.15E+07	1.89E+07	5.73E+07	5.81E+07	5.71E+07	4.66E+07	2.11E+07	2.04E+07
747	SLC4A7	2	0.00E+00	0.00E+00	0.00E+00	0.00E+00	0.00E+00	0.00E+00	0.00E+00	0.00E+00	0.00E+00	0.00E+00	0.00E+00	0.00E+00
748	WASF2	2	5.48E+06	3.94E+06	1.74E+06	2.07E+06	0.00E+00	0.00E+00	3.21E+06	3.18E+06	2.78E+06	0.00E+00	0.00E+00	0.00E+00
749	MAU2	4	7.30E+06	7.68E+06	0.00E+00	0.00E+00	0.00E+00	0.00E+00	4.58E+06	5.62E+06	0.00E+00	0.00E+00	0.00E+00	0.00E+00
750	IVNS1ABP	7	1.32E+07	1.61E+07	3.12E+06	3.08E+06	4.86E+06	4.75E+06	3.31E+06	7.47E+06	0.00E+00	0.00E+00	0.00E+00	0.00E+00

Table A.7: Perseus statistical analysis of protein hits identified by MaxQuant search for 2h HU treatment (Figure 4.10)

The LFQ intensities from of MaxQuant search of three independent replicates of bait and control cell lines were subjected to processing in Perseus; samples were divided into two categorical groups named Bait and Control, the matrix rows were filtered to contain minimum of 2 valid LFQ intensity values in at least one group (Bait/Control), the missing LFQ intensities were replaced with values from normal distribution by imputation (Imputation parameters: Width: 0.3, Downshift:1.8); to calculate statistically significant hits, two-sample Student's T-test was used, to correct for false discovered interactors, the p-value of the analysed data set was adjusted by Benjamini-Hochberg false discovery rate (FDR = 0.05), '+' marks statistically significant hits enriched in the Bait cell line (T-test difference > 0), subunits of the SMC5/6 complex are marked in yellow.

Perseus 2h HU student t-test - two sample (Benjamini-Hochberg)

number	Gene names	Student's T-test Significant Bait 2hHU_Control 2hHU	-Log Student's T-test p-value Bait 2hHU_Control 2hHU	Student's T-test q-value Bait 2hHU_Control 2hHU	Student's T-test Difference Bait 2hHU_Control 2hHU	Student's T-test Test statistic Bait 2hHU_Control 2hHU
1	SMC6	+	5.502	0.002	5.483	37.121
2	SMC5	+	3.742	0.046	4.195	13.369
3	NDNL2		3.447	0.060	3.112	11.234
4	NSMCE4A		2.760	0.219	4.903	7.445
5	NSMCE2		2.583	0.263	1.769	6.680
6	NSMCE1		2.569	0.227	2.314	6.620
7	LRPAP1		1.874	0.963	-0.692	-4.230
8	BCS1L		1.481	1.000	0.453	3.195
9	G3BP2		1.378	1.000	0.733	2.953
10	WDR33		1.320	1.000	-0.252	-2.819
11	DYRK1A		1.289	1.000	0.890	2.750
12	TRIO		1.199	1.000	0.780	2.552
13	PCF11		1.187	1.000	0.890	2.525
14	ZNF444		1.149	1.000	1.196	2.444
15	LRRC59		1.082	1.000	1.399	2.302
16	ERGIC3		1.019	1.000	0.404	2.171
17	DDX3X;DDX3Y		1.019	1.000	1.009	2.170
18	PHF3		0.994	1.000	-0.179	-2.119
19	RAN		0.979	1.000	0.616	2.090
20	ATPIF1		0.977	1.000	-0.455	-2.084
21	ABCB7		0.967	1.000	1.377	2.064
22	ALDH18A1		0.940	1.000	1.442	2.011
23	BRD4		0.937	1.000	-0.401	-2.003
24	ADPGK		0.908	1.000	0.625	1.945
25	HSPD1		0.901	1.000	-0.219	-1.930
26	HNRNPL		0.892	1.000	-0.209	-1.913
27	ERGIC2		0.884	1.000	0.557	1.897
28	MMTAG2		0.882	1.000	0.416	1.893
29	SF1		0.876	1.000	-0.334	-1.882
30	CCDC50		0.870	1.000	-0.409	-1.869
31	GIT1		0.868	1.000	0.384	1.865
32	AMOT		0.864	1.000	-3.238	-1.858
33	HSPA5		0.857	1.000	0.237	1.845
34	TUBB4B;TUBB4A		0.846	1.000	0.764	1.821
35	ERP44		0.829	1.000	0.429	1.789
36	PBX1		0.823	1.000	0.916	1.776
37	RPS28		0.821	1.000	-1.909	-1.772
38	SMPD4		0.813	1.000	0.217	1.757
39	CCDC6		0.813	1.000	-1.087	-1.757
40	SERPINH1		0.804	1.000	0.924	1.740
41	CCDC85C		0.799	1.000	-0.319	-1.729
42	GPS2		0.785	1.000	0.887	1.701
43	UBAP2		0.779	1.000	-0.276	-1.690

number	Gene names	Student's T-test Significant Bait 2hHU_Control 2hHU	-Log Student's T-test p-value Bait 2hHU_Control 2hHU	Student's T-test q-value Bait 2hHU_Control 2hHU	Student's T-test Difference Bait 2hHU_Control 2hHU	Student's T-test Test statistic Bait 2hHU_Control 2hHU
44	ARMC6		0.761	1.000	1.776	1.654
45	KIAA1429		0.758	1.000	0.394	1.649
46	HIST1H4A		0.756	1.000	0.486	1.645
47	DCAF7		0.748	1.000	0.525	1.629
48	TUBA1C;TUBA1B;TUBA1		0.737	1.000	0.500	1.607
49	CSNK2B		0.735	1.000	0.733	1.604
50	DOCK7		0.725	1.000	0.424	1.585
51	DCP1A		0.717	1.000	0.438	1.568
52	CPSF1		0.706	1.000	0.379	1.546
53	MYH7B;MYH7;MYH8;M'		0.704	1.000	1.995	1.543
54	SNRPD1		0.701	1.000	0.993	1.537
55	TOP1		0.686	1.000	-0.179	-1.508
56	DDX17		0.674	1.000	0.269	1.485
57	EEF1A1P5;EEF1A1;EEF1A		0.672	1.000	0.778	1.480
58	NUP93		0.669	1.000	1.123	1.475
59	SMARCA4		0.663	1.000	0.342	1.464
60	KPNB1		0.661	1.000	0.950	1.460
61	TRA2A		0.656	1.000	0.831	1.450
62	MAX		0.648	1.000	-0.370	-1.434
63	SNRNP200		0.633	1.000	1.133	1.405
64	TCF3		0.621	1.000	0.130	1.381
65	PABPC4		0.619	1.000	0.313	1.377
66	IRS4		0.613	1.000	0.374	1.366
67	HIST2H3A;HIST3H3;H3F3		0.606	1.000	0.507	1.352
68	SF3B5		0.596	1.000	-0.295	-1.332
69	DROSHA		0.592	1.000	0.867	1.325
70	TUBG1;TUBG2		0.580	1.000	0.321	1.302
71	TUBB		0.575	1.000	0.484	1.291
72	HIST1H2BL;HIST1H2BM;		0.561	1.000	0.444	1.264
73	PYCRL		0.559	1.000	0.422	1.260
74	GIT2		0.558	1.000	0.511	1.259
75	SMG8		0.555	1.000	-0.922	-1.253
76	NUFIP2		0.554	1.000	0.688	1.250
77	RAI1		0.551	1.000	0.303	1.245
78	AXIN1		0.550	1.000	0.595	1.242
79	ERGIC1		0.549	1.000	0.675	1.242
80	CCDC97		0.547	1.000	-0.224	-1.236
81	ZNF608		0.543	1.000	-0.922	-1.229
82	RNPS1		0.536	1.000	0.335	1.216
83	BAG6		0.535	1.000	0.613	1.214
84	SRGAP2;SRGAP1		0.534	1.000	0.761	1.211
85	BCKDK		0.532	1.000	0.490	1.207
86	PYCR2		0.531	1.000	0.736	1.206
87	PABPC1		0.526	1.000	0.334	1.196

number	Gene names	Student's T-test Significant Bait 2hHU_Control 2hHU	-Log Student's T-test p-value Bait 2hHU_Control 2hHU	Student's T-test q-value Bait 2hHU_Control 2hHU	Student's T-test Difference Bait 2hHU_Control 2hHU	Student's T-test Test statistic Bait 2hHU_Control 2hHU
88	RING1		0.526	1.000	1.184	1.195
89	TBPL1		0.510	1.000	0.361	1.164
90	HNRNPAB		0.503	1.000	0.262	1.150
91	GSE1		0.502	1.000	-0.222	-1.148
92	HSPA1B;HSPA1A		0.500	1.000	0.349	1.144
93	C1QBP		0.494	1.000	0.289	1.133
94	MAGI1		0.489	1.000	-0.330	-1.123
95	AUTS2		0.478	1.000	1.949	1.102
96	CPSF3		0.475	1.000	0.565	1.095
97	SMARCC2		0.470	1.000	0.178	1.086
98	HOXA5		0.470	1.000	-0.323	-1.084
99	SKP1		0.465	1.000	0.502	1.076
100	UBAP2L		0.464	1.000	-0.206	-1.074
101	WDR61		0.462	1.000	0.403	1.069
102	MEIS1		0.457	1.000	0.157	1.059
103	TBP;TBPL2		0.449	1.000	0.246	1.044
104	VWA9		0.449	1.000	-0.495	-1.043
105	SEC13		0.445	1.000	2.227	1.036
106	DHX30		0.444	1.000	1.040	1.033
107	RUFY1		0.440	1.000	0.837	1.025
108	PFKM		0.437	1.000	1.094	1.020
109	CPSF2		0.429	1.000	0.309	1.004
110	SAP30BP		0.428	1.000	-0.455	-1.002
111	SEC16A		0.426	1.000	-0.203	-0.997
112	CSTF3		0.421	1.000	0.440	0.988
113	LMNA		0.413	1.000	-0.324	-0.971
114	CBS		0.412	1.000	0.734	0.970
115	AAAS		0.411	1.000	0.898	0.967
116	SLC25A5;SLC25A6;SLC25		0.411	1.000	0.528	0.967
117	OSBPL9		0.410	1.000	-0.726	-0.966
118	CEP135		0.398	1.000	-0.553	-0.941
119	BAG3		0.395	1.000	-0.213	-0.935
120	OTUD4		0.394	1.000	-0.193	-0.933
121	CDK11B;CDK11A		0.393	1.000	0.919	0.931
122	TBC1D15		0.384	1.000	0.495	0.913
123	LEF1		0.380	1.000	-0.321	-0.905
124	RPRD1A		0.377	1.000	0.817	0.899
125	DDX6		0.376	1.000	0.202	0.897
126	PARP1		0.376	1.000	-0.197	-0.896
127	ZC3H4		0.374	1.000	-0.494	-0.892
128	NSRP1		0.372	1.000	-0.313	-0.887
129	CSNK2A2		0.371	1.000	0.197	0.885
130	SUB1		0.367	1.000	-0.295	-0.878
131	EFTUD2		0.366	1.000	0.708	0.876

number	Gene names	Student's T-test Significant Bait 2hHU_Control 2hHU	-Log Student's T-test p-value Bait 2hHU_Control 2hHU	Student's T-test q-value Bait 2hHU_Control 2hHU	Student's T-test Difference Bait 2hHU_Control 2hHU	Student's T-test Test statistic Bait 2hHU_Control 2hHU
132	CSTF2T		0.366	1.000	-0.606	-0.875
133	SNRPD3		0.358	1.000	0.928	0.860
134	HMBOX1		0.355	1.000	0.788	0.853
135	HELZ		0.350	1.000	0.330	0.844
136	TCEB2		0.346	1.000	0.229	0.835
137	SRSF10		0.343	1.000	-0.542	-0.829
138	SRSF9		0.343	1.000	1.135	0.829
139	HNRNPU		0.341	1.000	0.296	0.824
140	SAFB		0.339	1.000	-0.339	-0.821
141	ESYT1		0.337	1.000	0.679	0.816
142	LSM12		0.332	1.000	0.323	0.805
143	CEP170		0.327	1.000	-0.118	-0.795
144	SMARCD1		0.325	1.000	-0.583	-0.792
145	AFF4		0.320	1.000	-0.424	-0.781
146	CANX		0.317	1.000	0.620	0.775
147	GART		0.315	1.000	0.450	0.769
148	HNRNPH1;HNRNPH2		0.314	1.000	0.286	0.769
149	PAXIP1		0.312	1.000	-0.473	-0.764
150	D2HGDH		0.308	1.000	0.723	0.755
151	CSNK2A1;CSNK2A3		0.305	1.000	0.199	0.750
152	OSBPL11		0.303	1.000	0.310	0.745
153	MCFD2		0.301	1.000	1.110	0.741
154	PRPS1;PRPS1L1		0.300	1.000	1.004	0.738
155	U2AF2		0.300	1.000	0.293	0.738
156	SEC23A		0.299	1.000	0.843	0.737
157	TACO1		0.289	1.000	1.259	0.716
158	ABI1		0.289	1.000	0.431	0.715
159	DGCR8		0.284	1.000	0.878	0.705
160	SF3B1		0.284	1.000	-0.267	-0.704
161	DNAJC10		0.284	1.000	0.219	0.704
162	CCNK		0.284	1.000	-0.325	-0.704
163	EIF5A		0.282	1.000	0.456	0.700
164	FAM76A		0.281	1.000	0.675	0.699
165	MNX1		0.281	1.000	-0.188	-0.699
166	RUVBL1		0.281	1.000	0.211	0.697
167	ARID1A		0.281	1.000	0.780	0.697
168	SF3A2		0.280	1.000	-0.180	-0.696
169	SATB1		0.280	1.000	0.310	0.695
170	CITED2		0.279	1.000	-0.570	-0.694
171	PRPF19		0.277	1.000	0.667	0.690
172	CMTR1		0.273	1.000	0.460	0.682
173	EIF4ENIF1		0.269	1.000	0.676	0.672
174	CAD		0.266	1.000	1.007	0.665
175	TLE1		0.264	1.000	0.216	0.661

number	Gene names	Student's T-test Significant Bait 2hHU_Control 2hHU	-Log Student's T-test p-value Bait 2hHU_Control 2hHU	Student's T-test q-value Bait 2hHU_Control 2hHU	Student's T-test Difference Bait 2hHU_Control 2hHU	Student's T-test Test statistic Bait 2hHU_Control 2hHU
176	SLC12A2		0.264	1.000	-0.264	-0.661
177	CTH		0.264	1.000	0.466	0.660
178	ASUN		0.264	1.000	0.196	0.660
179	SLC39A14		0.262	1.000	0.236	0.657
180	NUDT19		0.262	1.000	0.859	0.656
181	RBMX;RBMXL1		0.260	1.000	0.581	0.654
182	CEP85		0.260	1.000	0.432	0.653
183	NPM1		0.258	1.000	0.261	0.648
184	CPSF4		0.255	1.000	0.144	0.641
185	SATB2		0.254	1.000	0.174	0.641
186	NT5DC2		0.254	1.000	0.560	0.640
187	DHX15		0.252	1.000	0.226	0.635
188	FAM195B		0.251	1.000	-0.422	-0.634
189	TJAP1		0.249	1.000	-0.093	-0.628
190	RAB11FIP5		0.248	1.000	-0.160	-0.627
191	HSPA9		0.247	1.000	0.152	0.625
192	SF3B3		0.246	1.000	0.213	0.622
193	SF3A1		0.245	1.000	-0.318	-0.620
194	IRF2BP2		0.245	1.000	-0.251	-0.619
195	CTTN		0.244	1.000	-0.208	-0.618
196	SF3B2		0.243	1.000	-0.271	-0.615
197	LRCH1		0.242	1.000	0.451	0.614
198	CTIF		0.242	1.000	-0.445	-0.613
199	PALLD		0.239	1.000	0.465	0.606
200	LMAN1		0.238	1.000	0.306	0.605
201	TCF20		0.235	1.000	-0.224	-0.597
202	CSTF2		0.231	1.000	-0.167	-0.589
203	BAIAP2L1		0.230	1.000	-0.267	-0.587
204	MECP2		0.230	1.000	-0.414	-0.587
205	SHMT2		0.229	1.000	0.866	0.584
206	PITHD1		0.229	1.000	0.626	0.584
207	TCEB1		0.229	1.000	-0.531	-0.584
208	HIST1H2AJ;HIST1H2AH;H		0.228	1.000	0.411	0.582
209	MAPK1		0.226	1.000	-0.284	-0.577
210	PKP2		0.222	1.000	0.456	0.569
211	IVD		0.219	1.000	0.829	0.563
212	PPP1CA		0.219	1.000	-0.314	-0.562
213	ABLIM1		0.219	1.000	-0.310	-0.562
214	HACD3		0.216	1.000	0.581	0.555
215	KCTD10		0.215	1.000	0.694	0.554
216	MEIS2		0.215	1.000	0.472	0.554
217	CHD7		0.213	1.000	-0.240	-0.548
218	ATP5A1		0.212	1.000	0.474	0.546
219	EDC3		0.209	1.000	0.375	0.541

number	Gene names	Student's T-test Significant Bait 2hHU_Control 2hHU	-Log Student's T-test p-value Bait 2hHU_Control 2hHU	Student's T-test q-value Bait 2hHU_Control 2hHU	Student's T-test Difference Bait 2hHU_Control 2hHU	Student's T-test Test statistic Bait 2hHU_Control 2hHU
220	LANCL2		0.209	1.000	-0.684	-0.539
221	ASCC1		0.208	1.000	0.708	0.538
222	SARM1		0.208	1.000	0.627	0.537
223	SEC24B		0.204	1.000	0.329	0.529
224	MCAT		0.203	1.000	0.225	0.525
225	SAFB2		0.202	1.000	-0.392	-0.524
226	PFKP		0.202	1.000	-0.283	-0.524
227	PPP2R1A		0.200	1.000	0.789	0.519
228	INTS3		0.200	1.000	0.646	0.518
229	CUTC		0.199	1.000	-0.150	-0.518
230	HEXIM1		0.198	1.000	1.076	0.515
231	SMARCC1		0.196	1.000	0.092	0.511
232	VGLL4		0.195	1.000	-0.413	-0.507
233	RTCB		0.191	1.000	0.121	0.498
234	CDK12		0.191	1.000	-0.257	-0.498
235	ATXN2		0.189	1.000	-0.462	-0.495
236	YLPM1		0.188	1.000	-0.072	-0.491
237	ATP1A1;ATP1A3;ATP1A2		0.187	1.000	0.508	0.490
238	PAFAH1B3		0.187	1.000	-0.623	-0.489
239	WDR5		0.186	1.000	-0.766	-0.487
240	SLC39A10		0.186	1.000	-0.611	-0.486
241	RBM7		0.184	1.000	0.227	0.483
242	PM20D2		0.184	1.000	0.268	0.482
243	ACTN4		0.177	1.000	0.426	0.467
244	SDF2L1		0.177	1.000	-0.271	-0.466
245	SHKBP1		0.176	1.000	0.721	0.465
246	TCEB3		0.176	1.000	0.055	0.463
247	CDX2;CDX1;CDX4		0.175	1.000	-0.460	-0.463
248	CSE1L		0.175	1.000	1.030	0.462
249	NIPBL		0.174	1.000	0.099	0.459
250	USP7		0.172	1.000	0.442	0.454
251	NDUFS6		0.168	1.000	-0.184	-0.446
252	PRPF6		0.167	1.000	-0.498	-0.444
253	SNIP1		0.166	1.000	-0.320	-0.442
254	CTBP1		0.164	1.000	0.761	0.435
255	LGMN		0.159	1.000	0.192	0.424
256	UNK		0.159	1.000	0.276	0.423
257	TJP2		0.158	1.000	-0.412	-0.422
258	STUB1		0.158	1.000	0.171	0.422
259	HDAC1		0.157	1.000	0.412	0.419
260	MATR3		0.155	1.000	0.726	0.415
261	MID1		0.154	1.000	0.517	0.413
262	PCNP		0.154	1.000	-0.337	-0.411
263	PHF5A		0.153	1.000	-0.302	-0.409

number	Gene names	Student's T-test Significant Bait 2hHU_Control 2hHU	-Log Student's T-test p-value Bait 2hHU_Control 2hHU	Student's T-test q-value Bait 2hHU_Control 2hHU	Student's T-test Difference Bait 2hHU_Control 2hHU	Student's T-test Test statistic Bait 2hHU_Control 2hHU
264	ARHGEF10		0.152	1.000	0.737	0.408
265	FBRS		0.152	1.000	0.213	0.407
266	LARP7		0.148	1.000	0.146	0.398
267	TUFM		0.147	1.000	0.514	0.394
268	MAZ		0.147	1.000	-0.245	-0.394
269	TPR		0.146	1.000	-0.124	-0.392
270	RBM39		0.145	1.000	-0.411	-0.390
271	GLUL		0.144	1.000	0.748	0.389
272	CLK3		0.143	1.000	0.147	0.386
273	BMP2K		0.143	1.000	0.554	0.385
274	SFPQ		0.143	1.000	-0.247	-0.384
275	U2SURP		0.141	1.000	0.103	0.381
276	SPEN		0.141	1.000	0.440	0.380
277	PSPC1		0.140	1.000	-0.212	-0.379
278	ALDOA		0.139	1.000	0.172	0.376
279	ACTG1;ACTB		0.138	1.000	0.088	0.374
280	KPNA2		0.137	1.000	0.037	0.372
281	IKBKAP		0.136	1.000	0.337	0.369
282	IGF2BP2		0.136	1.000	0.259	0.369
283	RANBP1		0.135	1.000	-0.207	-0.366
284	TSC22D1		0.133	1.000	-0.338	-0.361
285	TJP1		0.133	1.000	-0.202	-0.361
286	LIMD1		0.133	1.000	-0.169	-0.361
287	SMARCE1		0.130	1.000	-0.109	-0.355
288	MFAP1		0.130	1.000	-0.230	-0.354
289	TAOK1		0.128	1.000	-0.460	-0.349
290	RBM17		0.128	1.000	-0.139	-0.348
291	PINX1		0.126	1.000	-0.147	-0.345
292	HNRNPC		0.126	1.000	-0.284	-0.344
293	ELP3		0.125	1.000	0.259	0.342
294	PPP2CA;PPP2CB		0.125	1.000	0.494	0.341
295	ATXN2L		0.125	1.000	0.063	0.341
296	NUDT21		0.124	1.000	0.261	0.339
297	GATA6		0.120	1.000	0.614	0.328
298	C20orf27		0.119	1.000	-0.142	-0.328
299	SLTM		0.119	1.000	-0.097	-0.327
300	SNRPG;SNRPGP15		0.118	1.000	0.174	0.325
301	RBM15		0.118	1.000	-0.412	-0.325
302	XRN1		0.118	1.000	0.181	0.325
303	SLC9A3R2		0.115	1.000	0.104	0.317
304	HOXA13		0.115	1.000	0.167	0.316
305	H6PD		0.114	1.000	0.453	0.314
306	SMU1		0.113	1.000	0.211	0.312
307	FBXO21		0.113	1.000	0.149	0.311

number	Gene names	Student's T-test Significant Bait 2hHU_Control 2hHU	-Log Student's T-test p-value Bait 2hHU_Control 2hHU	Student's T-test q-value Bait 2hHU_Control 2hHU	Student's T-test Difference Bait 2hHU_Control 2hHU	Student's T-test Test statistic Bait 2hHU_Control 2hHU
308	PCGF5		0.112	1.000	-0.109	-0.310
309	NUCB1		0.112	1.000	-0.333	-0.310
310	MRPS9		0.112	1.000	0.249	0.308
311	YWHAE		0.112	1.000	0.110	0.308
312	SMNDC1		0.111	1.000	-0.255	-0.308
313	ACOT9		0.111	1.000	0.249	0.305
314	KCTD3		0.110	1.000	0.223	0.303
315	QSOX2		0.110	1.000	0.199	0.303
316	SRCAP		0.109	1.000	-0.298	-0.301
317	TAF8		0.109	1.000	0.210	0.301
318	CPSF6		0.108	1.000	-0.116	-0.300
319	USP9X		0.107	1.000	0.197	0.298
320	SNRPF		0.107	1.000	0.165	0.298
321	CYFIP1		0.107	1.000	0.576	0.296
322	ARID1B		0.107	1.000	0.491	0.296
323	CARM1		0.106	1.000	0.282	0.295
324	PBX2		0.106	1.000	0.092	0.293
325	NFIC		0.105	1.000	-0.207	-0.291
326	PLD3		0.105	1.000	0.239	0.291
327	CCT6A		0.105	1.000	0.415	0.291
328	RNF20		0.104	1.000	-0.107	-0.290
329	HNRNPA3		0.103	1.000	-0.200	-0.287
330	NFIA		0.103	1.000	-0.142	-0.286
331	TAB2		0.103	1.000	0.140	0.286
332	CDK9		0.102	1.000	0.270	0.285
333	NUP188		0.100	1.000	0.146	0.278
334	PCBD1		0.099	1.000	-0.300	-0.277
335	TCP1		0.099	1.000	0.522	0.276
336	CTR9		0.099	1.000	0.190	0.276
337	DDX1		0.099	1.000	0.072	0.275
338	CTSC		0.098	1.000	-0.322	-0.274
339	NAF1		0.098	1.000	0.153	0.274
340	DNPEP		0.098	1.000	-0.255	-0.274
341	ARHGEF7		0.097	1.000	0.095	0.272
342	FBRSL1		0.097	1.000	0.037	0.271
343	SF3B4		0.096	1.000	-0.166	-0.269
344	DVL3		0.096	1.000	-0.139	-0.268
345	CCT7		0.095	1.000	0.316	0.265
346	DDX42		0.094	1.000	-0.176	-0.263
347	U2AF1		0.093	1.000	-0.113	-0.262
348	CKAP4		0.092	1.000	0.247	0.257
349	THRAP3		0.090	1.000	-0.320	-0.254
350	CBLL1		0.089	1.000	-0.133	-0.251
351	ZIC5		0.089	1.000	0.024	0.249

number	Gene names	Student's T-test Significant Bait 2hHU_Control 2hHU	-Log Student's T-test p-value Bait 2hHU_Control 2hHU	Student's T-test q-value Bait 2hHU_Control 2hHU	Student's T-test Difference Bait 2hHU_Control 2hHU	Student's T-test Test statistic Bait 2hHU_Control 2hHU
352	SRSF6;SRSF4		0.088	1.000	-0.308	-0.248
353	GID8		0.088	1.000	0.079	0.248
354	CCAR2		0.088	1.000	0.034	0.247
355	WASF2		0.088	1.000	0.138	0.246
356	GPATCH8		0.086	1.000	0.208	0.243
357	FNBP1L		0.086	1.000	0.158	0.243
358	WTAP		0.085	1.000	-0.118	-0.241
359	NDC1		0.085	1.000	0.088	0.240
360	CCNT2		0.085	1.000	0.227	0.239
361	SLC4A1AP		0.085	1.000	-0.128	-0.239
362	PDCD5		0.084	1.000	-0.205	-0.238
363	ATP5B		0.084	1.000	0.175	0.236
364	SBF1		0.083	1.000	0.176	0.235
365	CCT3		0.083	1.000	0.380	0.233
366	MEPCE		0.082	1.000	-0.045	-0.232
367	ARHGAP17		0.082	1.000	0.333	0.231
368	HDAC2		0.081	1.000	0.075	0.229
369	ASCC3		0.081	1.000	-0.357	-0.229
370	PPP1R10		0.081	1.000	-0.404	-0.228
371	ZNF703		0.080	1.000	-0.178	-0.226
372	GPATCH11		0.079	1.000	-0.223	-0.223
373	DNAJC8		0.079	1.000	-0.177	-0.223
374	CCT4		0.078	1.000	0.314	0.222
375	HNRNPA1		0.078	1.000	0.239	0.221
376	PRPF8		0.077	1.000	0.160	0.218
377	SNRNP70		0.075	1.000	0.228	0.213
378	RAPGEF6		0.074	1.000	0.124	0.211
379	BCLAF1		0.073	1.000	0.242	0.209
380	RBM27		0.073	1.000	-0.025	-0.209
381	SUDS3		0.072	1.000	-0.043	-0.205
382	RSBN1		0.071	1.000	0.130	0.203
383	IK		0.071	1.000	0.171	0.202
384	RUVBL2		0.070	1.000	0.085	0.200
385	NKRF		0.069	1.000	-0.113	-0.199
386	SEC23B		0.069	1.000	0.100	0.198
387	MAP4K4		0.069	1.000	-0.095	-0.196
388	HSPA8		0.069	1.000	0.059	0.196
389	CPSF7		0.066	1.000	0.042	0.190
390	NOTCH2		0.065	1.000	0.032	0.188
391	SART1		0.065	1.000	0.170	0.188
392	TYSND1		0.065	1.000	0.039	0.187
393	CHD8		0.064	1.000	-0.317	-0.184
394	RBM25		0.063	1.000	-0.064	-0.181
395	SERBP1		0.063	1.000	-0.196	-0.181

number	Gene names	Student's T-test Significant Bait 2hHU_Control 2hHU	-Log Student's T-test p-value Bait 2hHU_Control 2hHU	Student's T-test q-value Bait 2hHU_Control 2hHU	Student's T-test Difference Bait 2hHU_Control 2hHU	Student's T-test Test statistic Bait 2hHU_Control 2hHU
396	NCOR2		0.062	1.000	0.039	0.180
397	SF3B6		0.062	1.000	0.044	0.179
398	SRSF7		0.062	1.000	0.186	0.179
399	CSTF1		0.062	1.000	0.283	0.178
400	WDR82		0.061	1.000	0.166	0.177
401	SF3A3		0.061	1.000	-0.112	-0.175
402	SRSF1		0.060	1.000	0.283	0.174
403	RBM10		0.060	1.000	0.114	0.173
404	XRN2		0.060	1.000	0.084	0.173
405	TBL1XR1		0.060	1.000	0.145	0.173
406	TIMM50		0.059	1.000	0.066	0.171
407	RPRD2		0.059	1.000	0.025	0.171
408	SNRPD2		0.058	1.000	0.174	0.168
409	GPHN		0.058	1.000	0.074	0.167
410	NME4		0.058	1.000	0.126	0.167
411	CCT2		0.057	1.000	0.217	0.166
412	HOMER1		0.057	1.000	0.114	0.164
413	FAM98A		0.056	1.000	-0.053	-0.162
414	MNT		0.055	1.000	-0.026	-0.160
415	OPA1		0.055	1.000	0.121	0.159
416			0.055	1.000	-0.059	-0.158
417	EEF1G		0.053	1.000	0.118	0.153
418	WASF1		0.052	1.000	0.214	0.152
419	RNF40		0.052	1.000	-0.056	-0.152
420	RERE		0.052	1.000	0.209	0.152
421	NONO		0.052	1.000	-0.127	-0.150
422	HNRNPK		0.052	1.000	-0.153	-0.150
423	DLX5;DLX2		0.052	1.000	-0.304	-0.150
424	FAM195A		0.051	1.000	0.128	0.147
425	NUDCD1		0.051	1.000	-0.224	-0.147
426	SHCBP1L		0.050	1.000	-0.185	-0.145
427	GTF2A1		0.049	1.000	-0.163	-0.143
428	CKMT1A		0.048	1.000	-0.113	-0.141
429	HIP1R		0.047	1.000	0.157	0.139
430	DHTKD1		0.046	1.000	0.182	0.135
431	PRPSAP2		0.046	1.000	-0.158	-0.134
432	SMAP		0.045	1.000	0.103	0.131
433	YY1		0.043	1.000	-0.268	-0.127
434	UBL4A		0.043	1.000	0.110	0.126
435	PPP1CC		0.043	1.000	-0.106	-0.126
436	DDB1		0.043	1.000	0.104	0.125
437	PPIL4		0.043	1.000	0.030	0.125
438	DNAJB12		0.042	1.000	0.035	0.124
439	ZIC2		0.042	1.000	-0.129	-0.124

number	Gene names	Student's T-test Significant Bait 2hHU_Control 2hHU	-Log Student's T-test p-value Bait 2hHU_Control 2hHU	Student's T-test q-value Bait 2hHU_Control 2hHU	Student's T-test Difference Bait 2hHU_Control 2hHU	Student's T-test Test statistic Bait 2hHU_Control 2hHU
440	ATN1		0.042	1.000	-0.339	-0.123
441	CARS2		0.041	1.000	0.136	0.121
442	TOX4		0.040	1.000	-0.175	-0.117
443	CHERP		0.040	1.000	0.027	0.117
444	VARS2		0.039	1.000	-0.024	-0.114
445	FOXJ3		0.039	1.000	-0.198	-0.113
446	AES		0.038	1.000	0.093	0.113
447	GAPDH		0.038	1.000	0.095	0.111
448	CBL		0.037	1.000	0.023	0.108
449	MAT2B		0.036	1.000	0.144	0.105
450	CCT8		0.035	1.000	0.134	0.103
451	ERH		0.035	1.000	0.080	0.103
452	WAC		0.034	1.000	-0.049	-0.102
453	CCT5		0.033	1.000	0.129	0.099
454	RAB11A;RAB11B		0.033	1.000	0.066	0.099
455	LUC7L2		0.032	1.000	-0.075	-0.095
456	TLE3		0.032	1.000	0.053	0.094
457	NT5C2		0.031	1.000	0.171	0.093
458	ACTL6A		0.031	1.000	0.057	0.091
459	TERF2		0.030	1.000	0.078	0.089
460	ELAVL1		0.030	1.000	0.078	0.088
461	IVNS1ABP		0.028	1.000	-0.078	-0.083
462	SLC39A6		0.027	1.000	-0.096	-0.082
463	CDC73		0.027	1.000	0.083	0.081
464	VWA8		0.027	1.000	0.051	0.081
465	ALYREF		0.027	1.000	-0.071	-0.079
466	LEO1		0.026	1.000	0.093	0.078
467	ADSL		0.025	1.000	0.097	0.075
468	UGT8		0.025	1.000	-0.048	-0.075
469	RBM33		0.023	1.000	0.076	0.069
470	PBXIP1		0.022	1.000	-0.077	-0.067
471	ANKRD16		0.022	1.000	0.062	0.065
472	RBBP7		0.022	1.000	-0.016	-0.064
473	ZC3H13		0.016	1.000	-0.023	-0.048
474	POLDIP2		0.015	1.000	0.050	0.045
475	NME1		0.014	1.000	-0.040	-0.043
476	NCKAP1		0.014	1.000	0.082	0.041
477	SMAD4		0.013	1.000	-0.023	-0.040
478	FAM120B		0.013	1.000	0.043	0.040
479	PPFIA1		0.013	1.000	0.019	0.038
480	DPP9		0.012	1.000	0.020	0.035
481	FIP1L1		0.011	1.000	-0.008	-0.032
482	TRA2B		0.008	1.000	-0.021	-0.025
483	STIM1		0.008	1.000	-0.010	-0.025

number	Gene names	Student's T-test Significant Bait 2hHU_Control 2hHU	-Log Student's T-test p-value Bait 2hHU_Control 2hHU	Student's T-test q-value Bait 2hHU_Control 2hHU	Student's T-test Difference Bait 2hHU_Control 2hHU	Student's T-test Test statistic Bait 2hHU_Control 2hHU
484	SCLY		0.008	1.000	0.016	0.025
485	SNRPA1		0.008	1.000	0.018	0.025
486	CCNT1		0.008	1.000	0.037	0.023
487	RANBP2		0.007	1.000	0.028	0.022
488	SCML2		0.007	1.000	0.019	0.022
489	PRPF4B		0.007	1.000	-0.006	-0.022
490	C14orf166		0.007	1.000	-0.005	-0.021
491	SIN3A		0.007	1.000	0.003	0.020
492	PAF1		0.006	1.000	-0.017	-0.018
493	SEC31A		0.006	1.000	-0.018	-0.018
494	PEG10		0.005	1.000	-0.005	-0.017
495	GOPC		0.005	1.000	-0.012	-0.016
496	POU3F2;POU3F3		0.005	1.000	0.031	0.015
497	PRDX3		0.004	1.000	0.013	0.012
498	SRSF3		0.004	1.000	-0.020	-0.012
499	MAT2A		0.004	1.000	0.022	0.012
500	FHL1		0.004	0.999	-0.010	-0.011
501	JMJD1C		0.003	1.000	0.006	0.008
502	PRPF40A		0.001	1.000	0.001	0.003
503	TERF2IP		0.001	1.000	0.004	0.002
504	YY2		0.001	0.999	-0.004	-0.002

Table A.8: Perseus statistical analysis of protein hits identified by MaxQuant search for 24h HU treatment (Figure 4.11)

The LFQ intensities from of MaxQuant search of three independent replicates of bait and control cell lines were subjected to processing in Perseus; samples were divided into two categorical groups named Bait and Control, the matrix rows were filtered to contain minimum of 2 valid LFQ intensity values in at least one group (Bait/Control), the missing LFQ intensities were replaced with values from normal distribution by imputation (Imputation parameters: Width: 0.3, Downshift:1.8); to calculate statistically significant hits, two-sample Student's T-test was used, to correct for false discovered interactors, the p-value of the analysed data set was adjusted by Benjamini-Hochberg false discovery rate (FDR = 0.05), '+' marks statistically significant hits enriched in the Bait cell line (T-test difference > 0), subunits of the SMC5/6 complex are marked in yellow.

Perseus 24h HU student t-test - two sample (Benjamini-Hochberg)

Number	Gene names	Student's T-test Significant Bait_24hHU_Control_24hHU	-Log Student's T-test p-value Bait_24hHU_Control_24hHU	Student's T-test q-value Bait_24hHU_Control_24hHU	Student's T-test Difference Bait_24hHU_Control_24hHU	Student's T-test Test statistic Bait_24hHU_Control_24hHU
1	SMC6	+	5.144	0.003	5.642	30.182
2	NSMCE4A	+	4.146	0.017	4.603	16.929
3	SMC5	+	4.126	0.012	3.541	16.725
4	NDNL2	+	3.756	0.021	4.245	13.475
5	NSMCE2		2.977	0.103	1.820	8.493
6	NSMCE1		2.187	0.528	2.149	5.203
7	CEP135		2.101	0.551	-1.079	-4.922
8	STIM1		1.645	1.000	-0.708	-3.605
9	RBM27		1.572	1.000	-0.174	-3.421
10	FAM120C		1.543	1.000	-1.408	-3.348
11	FBXO21		1.475	1.000	1.913	3.181
12	PABPC4		1.455	1.000	0.194	3.133
13	LRPAP1		1.435	1.000	-0.397	-3.086
14	CSNK2A2		1.365	1.000	0.449	2.921
15	SMARCA4		1.345	1.000	0.221	2.877
16	TUBG1;TUBG2		1.329	1.000	0.352	2.840
17	GIT1		1.302	1.000	0.533	2.779
18	CCDC85C		1.275	1.000	-0.284	-2.717
19	TCEB3		1.169	1.000	0.215	2.486
20	HNRNPL		1.169	1.000	-0.251	-2.486
21	OSBPL9		1.157	1.000	0.873	2.461
22	STUB1		1.112	1.000	0.521	2.365
23	RUVBL2		1.110	1.000	1.602	2.361
24	MCFD2		1.078	1.000	-0.227	-2.294
25	SUDS3		1.065	1.000	1.806	2.266
26	SF1		1.023	1.000	-0.457	-2.179
27	PDCD5		1.014	1.000	1.301	2.161
28	SIN3A		1.010	1.000	0.235	2.152
29	TFAP2A;TFAP2E;TFAP2B		1.008	1.000	1.724	2.148
30	SLTM		0.991	1.000	-0.256	-2.113
31	AMOT		0.989	1.000	-2.608	-2.109
32	HDAC1		0.919	1.000	1.280	1.967
33	C1QBP		0.895	1.000	0.429	1.920
34	TRIO		0.883	1.000	0.511	1.895
35	CPSF1		0.882	1.000	0.479	1.894
36	G3BP2		0.855	1.000	0.856	1.839
37	FAM195A		0.831	1.000	-0.911	-1.792
38	NDC1		0.820	1.000	0.404	1.770
39	TOP1		0.816	1.000	-0.143	-1.763
40	CSE1L		0.815	1.000	2.637	1.761
41	LGMN		0.805	1.000	0.913	1.741

Number	Gene names	Student's T-test Significant Bait_24hHU_Control_24hHU	-Log Student's T-test p-value Bait_24hHU_Control_24hHU	Student's T-test q-value Bait_24hHU_Control_24hHU	Student's T-test Difference Bait_24hHU_Control_24hHU	Student's T-test Test statistic Bait_24hHU_Control_24hHU
42	ESYT1		0.785	1.000	0.785	1.702
43	CCAR2		0.772	1.000	-0.217	-1.676
44	TAB2		0.763	1.000	-0.291	-1.659
45	GART		0.755	1.000	0.660	1.643
46	SRCAP		0.729	1.000	0.512	1.593
47	ASUN		0.729	1.000	1.299	1.591
48	CCDC50		0.715	1.000	-0.443	-1.564
49	HSPA1B;HSPA1A		0.707	1.000	0.293	1.550
50	INTS3		0.707	1.000	1.169	1.548
51	HOXA5		0.704	1.000	-0.855	-1.543
52	PYCR2		0.701	1.000	1.048	1.538
53	HMBOX1		0.670	1.000	-0.832	-1.477
54	RAI1		0.666	1.000	-0.749	-1.468
55	TIMM50		0.634	1.000	0.647	1.407
56	SATB2		0.619	1.000	-0.247	-1.378
57	OTUD4		0.619	1.000	-0.754	-1.377
58	OPA1		0.611	1.000	0.754	1.363
59	CSTF2T		0.587	1.000	1.175	1.315
60	SNRPG;SNRPGP15		0.555	1.000	0.797	1.252
61	BRD4		0.551	1.000	-0.216	-1.246
62	RAN		0.548	1.000	0.333	1.238
63	SRSF9		0.541	1.000	-0.677	-1.225
64	TCF3		0.536	1.000	-0.236	-1.215
65	PRPF4B		0.535	1.000	0.267	1.214
66	SF3B5		0.524	1.000	0.165	1.192
67	SMARCD1		0.516	1.000	0.644	1.176
68	SUB1		0.515	1.000	-0.295	-1.174
69	PKP2		0.515	1.000	-0.722	-1.174
70	SMARCC2		0.515	1.000	0.150	1.173
71	PALLD		0.511	1.000	0.530	1.167
72	WASF2		0.490	1.000	0.724	1.125
73	CAD		0.489	1.000	1.477	1.124
74	TCF20		0.489	1.000	-0.324	-1.123
75	PRPF19		0.486	1.000	0.833	1.116
76	ABLIM1		0.485	1.000	0.499	1.115
77	SMG8		0.483	1.000	0.344	1.111
78	MEPCE		0.479	1.000	-0.119	-1.102
79	CBS		0.474	1.000	1.039	1.092
80	SMPD4		0.473	1.000	0.754	1.091
81	CSTF2		0.471	1.000	0.346	1.088
82	TPR		0.461	1.000	0.349	1.067
83	ALDOA		0.458	1.000	0.363	1.061

Number	Gene names	Student's T-test Significant Bait_24hHU_Control_24hHU	-Log Student's T-test p-value Bait_24hHU_Control_24hHU	Student's T-test q-value Bait_24hHU_Control_24hHU	Student's T-test Difference Bait_24hHU_Control_24hHU	Student's T-test Test statistic Bait_24hHU_Control_24hHU
84	NCOR2		0.455	1.000	0.282	1.056
85	ERP44		0.444	1.000	-0.114	-1.034
86	HSPD1		0.443	1.000	0.571	1.032
87	ERGIC3		0.440	1.000	-0.171	-1.025
88	PRDX1		0.439	1.000	1.242	1.023
89	BCKDK		0.435	1.000	0.597	1.016
90	SERBP1		0.433	1.000	0.476	1.013
91	RNF40		0.431	1.000	-0.306	-1.008
92	JMJD1C		0.430	1.000	-0.506	-1.005
93	PPP1CA		0.426	1.000	-0.355	-0.998
94	TUBB4B;TUBB4A		0.422	1.000	0.314	0.989
95	LEF1		0.421	1.000	-0.536	-0.988
96	BAG6		0.420	1.000	0.364	0.985
97	PRPF8		0.417	1.000	0.696	0.980
98	ERGIC2		0.410	1.000	0.356	0.965
99	CPSF3		0.409	1.000	1.200	0.962
100	ERGIC1		0.406	1.000	0.381	0.958
101	MAGI1		0.404	1.000	-0.302	-0.954
102	ARID1A		0.401	1.000	0.209	0.947
103	ABCB7		0.398	1.000	-0.698	-0.942
104	CEP85		0.396	1.000	0.125	0.937
105	CCDC6		0.394	1.000	0.662	0.932
106	MEIS2		0.393	1.000	0.467	0.931
107	CHD7		0.391	1.000	0.244	0.926
108	EIF5A		0.383	1.000	0.510	0.911
109	ACTN4		0.380	1.000	0.701	0.904
110	CUTC		0.377	1.000	0.301	0.899
111	WDR61		0.377	1.000	0.254	0.898
112	NOTCH2		0.376	1.000	-0.393	-0.896
113	TYSND1		0.374	1.000	0.175	0.893
114	SNRPF		0.370	1.000	0.198	0.883
115	YWHAE		0.369	1.000	0.240	0.883
116	NSRP1		0.367	1.000	-0.259	-0.879
117	MAPK1		0.365	1.000	-0.422	-0.873
118	SNRPN;SNRPB		0.364	1.000	0.940	0.871
119	SLC12A2		0.363	1.000	-0.143	-0.870
120	ZIC5		0.363	1.000	0.318	0.869
121	CTR9		0.362	1.000	1.301	0.868
122	TUBA1C;TUBA1B;TUBA1A;		0.360	1.000	0.132	0.864
123	RBBP7		0.360	1.000	0.169	0.863
124	FAM195B		0.359	1.000	-0.492	-0.862
125	XRN2		0.359	1.000	-0.298	-0.861

Number	Gene names	Student's T-test Significant Bait_24hHU_Control_24hHU	-Log Student's T-test p-value Bait_24hHU_Control_24hHU	Student's T-test q-value Bait_24hHU_Control_24hHU	Student's T-test Difference Bait_24hHU_Control_24hHU	Student's T-test Test statistic Bait_24hHU_Control_24hHU
126	BCL7A;BCL7B;BCL7C		0.357	1.000	0.356	0.857
127	C14orf166		0.353	1.000	-0.208	-0.850
128	TJAP1		0.350	1.000	-0.073	-0.843
129	LIMD1		0.344	1.000	-0.313	-0.831
130	TTF2		0.344	1.000	0.571	0.830
131	UBAP2		0.340	1.000	-0.166	-0.821
132	IRS4		0.338	1.000	0.474	0.819
133	CEP170		0.336	1.000	-0.072	-0.814
134	TBP;TBPL2		0.335	1.000	0.097	0.812
135	HNRNPAB		0.330	1.000	0.651	0.802
136	RSBN1		0.329	1.000	-0.379	-0.799
137	HINT1		0.328	1.000	0.994	0.797
138	NDUFS6		0.327	1.000	0.822	0.795
139	SMARCE1		0.327	1.000	0.122	0.794
140	SLC9A3R2		0.326	1.000	0.284	0.793
141	ARID1B		0.326	1.000	-1.233	-0.793
142	TBPL1		0.322	1.000	0.165	0.785
143	SF3B1		0.320	1.000	0.209	0.781
144	ELP3		0.320	1.000	0.694	0.781
145	TERF2IP		0.318	1.000	-1.059	-0.777
146	EFTUD2		0.318	1.000	0.607	0.776
147	PPP2R1A		0.317	1.000	0.985	0.774
148	DROSHA		0.314	1.000	0.460	0.768
149	SLC39A6		0.313	1.000	-1.020	-0.766
150	POLDIP2		0.312	1.000	0.899	0.765
151	WDR82		0.305	1.000	-0.509	-0.749
152	RBM15		0.305	1.000	-1.073	-0.748
153	SMU1		0.301	1.000	0.847	0.742
154	VARS2		0.299	1.000	0.135	0.737
155	SFPQ		0.298	1.000	-0.485	-0.735
156	PBXIP1		0.296	1.000	-0.631	-0.730
157	TBC1D15		0.293	1.000	-0.390	-0.723
158	SNRPA1		0.291	1.000	0.380	0.719
159	NUCB1		0.285	1.000	0.560	0.706
160	UBAP2L		0.279	1.000	-0.217	-0.693
161	SNIP1		0.278	1.000	0.266	0.692
162	SF3B3		0.277	1.000	0.202	0.688
163	ERH		0.275	1.000	0.495	0.686
164	PCF11		0.272	1.000	0.227	0.679
165	ZC3H4		0.272	1.000	-0.339	-0.679
166	ACTL6A		0.272	1.000	-0.396	-0.678
167	CCDC97		0.270	1.000	0.201	0.675

Number	Gene names	Student's T-test Significant Bait_24hHU_Control_24hHU	-Log Student's T-test p-value Bait_24hHU_Control_24hHU	Student's T-test q-value Bait_24hHU_Control_24hHU	Student's T-test Difference Bait_24hHU_Control_24hHU	Student's T-test Test statistic Bait_24hHU_Control_24hHU
168	LRRC59		0.270	1.000	-0.661	-0.673
169	NME1		0.267	1.000	0.426	0.669
170	SNRNP70		0.267	1.000	0.451	0.667
171	CSNK2A1;CSNK2A3		0.266	1.000	0.118	0.665
172	PBX1		0.263	1.000	-0.203	-0.658
173	GID8		0.262	1.000	0.700	0.657
174	NUDCD1		0.262	1.000	1.031	0.657
175	CDK11B;CDK11A		0.258	1.000	0.193	0.649
176	DDX42		0.257	1.000	-0.243	-0.646
177	PABPC1		0.252	1.000	0.107	0.635
178	DDX1		0.250	1.000	-0.158	-0.630
179	GOPC		0.248	1.000	-0.369	-0.627
180	MMTAG2		0.247	1.000	0.209	0.624
181	PARD3		0.247	1.000	0.541	0.623
182	RBM10		0.246	1.000	0.305	0.622
183	FAM98A		0.246	1.000	-0.079	-0.622
184	RING1		0.244	1.000	-0.440	-0.619
185	SKP1		0.242	1.000	-0.210	-0.614
186	PCBD1		0.241	1.000	0.517	0.612
187	LEO1		0.241	1.000	-0.467	-0.610
188	WDR33		0.240	1.000	0.117	0.610
189	DDX6		0.240	1.000	-0.127	-0.608
190	LMNA		0.240	1.000	-0.305	-0.608
191	ASCC1		0.238	1.000	0.861	0.605
192	ZNF444		0.237	1.000	-0.401	-0.603
193	DYRK1A		0.237	1.000	-0.563	-0.601
194	TBL1XR1		0.236	1.000	0.521	0.600
195	ENO1		0.235	1.000	0.585	0.598
196	CTTN		0.235	1.000	-0.192	-0.597
197	SEC16A		0.234	1.000	0.051	0.595
198	BCLAF1		0.234	1.000	0.436	0.595
199	PPP1CC		0.232	1.000	-0.423	-0.590
200	D2HGDH		0.231	1.000	0.266	0.590
201	ARHGEF7		0.230	1.000	0.124	0.587
202	DOCK7		0.230	1.000	0.146	0.586
203	H6PD		0.228	1.000	0.958	0.583
204	SAP30BP		0.228	1.000	0.239	0.581
205	SCML2		0.228	1.000	-0.641	-0.581
206	TOX4		0.227	1.000	-0.719	-0.581
207	TERF2		0.226	1.000	-0.795	-0.579
208	PITHD1		0.224	1.000	0.465	0.574
209	HDAC2		0.222	1.000	0.190	0.569

Number	Gene names	Student's T-test Significant Bait_24hHU_Control_24hHU	-Log Student's T-test p-value Bait_24hHU_Control_24hHU	Student's T-test q-value Bait_24hHU_Control_24hHU	Student's T-test Difference Bait_24hHU_Control_24hHU	Student's T-test Test statistic Bait_24hHU_Control_24hHU
210	DCP1A		0.218	1.000	0.708	0.561
211	KPNA2		0.216	1.000	-0.171	-0.555
212	GPATCH11		0.215	1.000	-0.377	-0.554
213	MYH7B;MYH7;MYH8;MYH		0.214	1.000	-0.945	-0.552
214	HNRNPA3		0.213	1.000	-0.391	-0.549
215	MID1		0.213	1.000	0.836	0.548
216	CBL		0.211	1.000	0.137	0.544
217	WASF1		0.210	1.000	0.584	0.542
218	TUBB		0.208	1.000	0.118	0.538
219	ATPIF1		0.206	1.000	0.116	0.533
220	LSM12		0.205	1.000	-0.316	-0.530
221	NIPBL		0.204	1.000	-0.200	-0.528
222	SARM1		0.203	1.000	0.536	0.527
223	MAT2A		0.203	1.000	0.945	0.526
224	ATXN2		0.201	1.000	-0.440	-0.521
225	HELZ		0.200	1.000	0.231	0.519
226	PSPC1		0.199	1.000	-0.235	-0.517
227	CHD8		0.196	1.000	-0.638	-0.511
228	RAB11FIP5		0.194	1.000	-0.160	-0.505
229	ATP5A1		0.194	1.000	0.711	0.505
230	XRN1		0.192	1.000	-0.381	-0.500
231	BAIAP2L1		0.191	1.000	0.441	0.500
232	FBRS		0.191	1.000	-0.736	-0.499
233	FNBP1L		0.191	1.000	-0.319	-0.498
234			0.191	1.000	0.260	0.498
235	NFIA		0.190	1.000	-0.260	-0.496
236	MEIS1		0.190	1.000	-0.183	-0.496
237	TSC22D1		0.189	1.000	0.411	0.494
238	THRAP3		0.189	1.000	0.300	0.494
239	PAXIP1		0.187	1.000	-0.426	-0.489
240	ALYREF		0.187	1.000	-0.937	-0.488
241	PFKM		0.184	1.000	0.252	0.482
242	PLD3		0.180	1.000	0.452	0.474
243	DNPEP		0.179	1.000	-0.441	-0.470
244	IVD		0.176	1.000	0.510	0.464
245	WDR5		0.175	1.000	0.577	0.461
246	AFF4		0.173	1.000	-0.232	-0.456
247	LRCH1		0.170	1.000	0.530	0.450
248	IRF2BP2		0.170	1.000	0.187	0.449
249	GLUL		0.166	1.000	0.537	0.441
250	SNRPD2		0.164	1.000	0.225	0.437
251	CTIF		0.164	1.000	0.172	0.435

Number	Gene names	Student's T-test Significant Bait_24hHU_Control_24hHU	-Log Student's T-test p-value Bait_24hHU_Control_24hHU	Student's T-test q-value Bait_24hHU_Control_24hHU	Student's T-test Difference Bait_24hHU_Control_24hHU	Student's T-test Test statistic Bait_24hHU_Control_24hHU
252	SF3B6		0.164	1.000	0.103	0.435
253	TAOK1		0.162	1.000	0.390	0.432
254	NKRF		0.162	1.000	-0.202	-0.430
255	DCAF7		0.161	1.000	-0.114	-0.429
256	GPHN		0.161	1.000	0.200	0.429
257	HSP90AA1;HSP90AB2P;HS		0.160	1.000	-0.298	-0.427
258	SHKBP1		0.159	1.000	-0.689	-0.424
259	ALDH18A1		0.157	1.000	0.249	0.419
260	SRSF1		0.157	1.000	0.569	0.418
261	CRTC2		0.155	1.000	0.537	0.413
262	TCEB2		0.154	1.000	-0.091	-0.412
263	SERPINH1		0.153	1.000	-0.250	-0.409
264	HNRNPA1		0.152	1.000	0.405	0.407
265	MIOS		0.152	1.000	0.424	0.407
266	ARHGEF10		0.152	1.000	0.653	0.406
267	CPSF2		0.152	1.000	0.197	0.406
268	USP7		0.151	1.000	0.378	0.405
269	PHF3		0.151	1.000	-0.069	-0.404
270	FOXJ3		0.149	1.000	-0.509	-0.400
271	CSNK2B		0.149	1.000	0.117	0.400
272	RPRD2		0.149	1.000	-0.099	-0.399
273	PCGF5		0.148	1.000	0.129	0.398
274	FHL1		0.148	1.000	0.347	0.398
275	MECP2		0.148	1.000	-0.250	-0.397
276	NONO		0.145	1.000	-0.294	-0.390
277	SMAD4		0.144	1.000	-0.174	-0.389
278	NFIC		0.142	1.000	0.199	0.382
279	MAX		0.142	1.000	-0.081	-0.382
280	CTH		0.141	1.000	0.272	0.382
281	KIAA1429		0.141	1.000	0.046	0.380
282	HOMER1		0.140	1.000	-0.251	-0.379
283	SEC24B		0.140	1.000	-0.232	-0.378
284	SATB1		0.138	1.000	0.194	0.374
285	LUC7L2		0.138	1.000	0.153	0.374
286	PPIL4		0.137	1.000	-0.111	-0.371
287	SMG9		0.136	1.000	0.232	0.370
288	HNRNPU		0.136	1.000	0.178	0.369
289	CYFIP1		0.133	1.000	0.674	0.360
290	PRPF6		0.132	1.000	0.210	0.358
291	SMAP		0.131	1.000	-0.197	-0.357
292	YLPM1		0.131	1.000	0.062	0.355
293	RNPS1		0.129	1.000	0.112	0.351

Number	Gene names	Student's T-test Significant Bait_24hHU_Control_24hHU	-Log Student's T-test p-value Bait_24hHU_Control_24hHU	Student's T-test q-value Bait_24hHU_Control_24hHU	Student's T-test Difference Bait_24hHU_Control_24hHU	Student's T-test Test statistic Bait_24hHU_Control_24hHU
294	HOXA13		0.129	1.000	0.092	0.351
295	DLX5;DLX2		0.125	1.000	-0.443	-0.343
296	GSE1		0.124	1.000	0.090	0.339
297	U2AF1		0.124	1.000	-0.148	-0.338
298	SMARCC1		0.123	1.000	0.058	0.338
299	ALDH6A1		0.121	1.000	-0.390	-0.331
300	DNAJC10		0.120	1.000	0.046	0.330
301	NUDT21		0.120	1.000	0.215	0.329
302	ZC3H13		0.119	1.000	-0.168	-0.328
303	EDC3		0.118	1.000	0.220	0.324
304	DDX17		0.115	1.000	0.084	0.318
305	GIT2		0.115	1.000	0.335	0.316
306	HSPA8		0.114	1.000	-0.082	-0.314
307	CKAP4		0.114	1.000	-0.314	-0.314
308	NME4		0.114	1.000	-0.245	-0.313
309	GALK1		0.112	1.000	0.443	0.308
310	DHX30		0.111	1.000	0.323	0.308
311	SF3B4		0.111	1.000	0.139	0.306
312	RTCB		0.111	1.000	-0.050	-0.306
313	YY2		0.109	1.000	-0.686	-0.301
314	RUVBL1		0.108	1.000	-0.024	-0.300
315	PARP1		0.106	1.000	-0.135	-0.294
316	BAG3		0.106	1.000	0.077	0.294
317	ATN1		0.104	1.000	0.629	0.290
318	HIST2H3A;HIST3H3;H3F3A		0.103	1.000	-0.133	-0.286
319	PPP1R10		0.102	1.000	-0.427	-0.284
320	CHERP		0.102	1.000	-0.110	-0.283
321	HSPA9		0.102	1.000	-0.039	-0.283
322	FAM76A		0.102	1.000	-0.321	-0.283
323	NPM1		0.099	1.000	0.199	0.277
324	TCP1		0.096	1.000	0.435	0.267
325	HIST1H2BL;HIST1H2BM;HI		0.095	1.000	-0.073	-0.265
326	CTSC		0.094	1.000	0.358	0.263
327	PBX2		0.093	1.000	-0.116	-0.260
328	TRA2A		0.092	1.000	0.244	0.259
329	FAM120B		0.092	1.000	-0.281	-0.258
330	RBM25		0.092	1.000	0.094	0.257
331	ZIC2		0.091	1.000	-0.242	-0.256
332	CANX		0.091	1.000	0.168	0.256
333	ASCC3		0.091	1.000	0.432	0.255
334	MCAT		0.091	1.000	0.128	0.254
335	FIP1L1		0.089	1.000	0.083	0.250

Number	Gene names	Student's T-test Significant Bait_24hHU_Control_24hHU	-Log Student's T-test p-value Bait_24hHU_Control_24hHU	Student's T-test q-value Bait_24hHU_Control_24hHU	Student's T-test Difference Bait_24hHU_Control_24hHU	Student's T-test Test statistic Bait_24hHU_Control_24hHU
336	PCNP		0.088	1.000	0.165	0.247
337	SF3B2		0.088	1.000	-0.085	-0.247
338	ACTG1;ACTB		0.087	1.000	0.085	0.245
339	MNT		0.086	1.000	0.054	0.243
340	NT5C2		0.086	1.000	0.463	0.243
341	DHTKD1		0.086	1.000	-0.267	-0.243
342	SHMT2		0.086	1.000	-0.213	-0.242
343	PRPS1;PRPS1L1		0.086	1.000	0.241	0.242
344	UBL4A		0.086	1.000	-0.127	-0.242
345	CCT6A		0.086	1.000	0.280	0.242
346	MICALL1		0.085	1.000	-0.196	-0.241
347	MFAP1		0.085	1.000	0.076	0.239
348	LANCL2		0.084	1.000	-0.323	-0.238
349	SAFB		0.084	1.000	0.079	0.238
350	ELAVL1		0.083	1.000	-0.177	-0.236
351	ADPGK		0.082	1.000	-0.060	-0.232
352	CSTF3		0.082	1.000	0.166	0.231
353	MAP4K4		0.081	1.000	-0.128	-0.229
354	CARM1		0.080	1.000	0.218	0.227
355	DHX15		0.080	1.000	0.040	0.227
356	PRDX3		0.080	1.000	0.172	0.227
357	TLE3		0.080	1.000	-0.141	-0.227
358	KPNB1		0.080	1.000	-0.164	-0.226
359	TCEB1		0.080	1.000	-0.317	-0.226
360	CDO1		0.079	1.000	0.183	0.223
361	HNRNPC		0.079	1.000	-0.201	-0.223
362	SF3A1		0.079	1.000	0.126	0.223
363	USP9X		0.077	1.000	0.129	0.220
364	SRSF3		0.077	1.000	0.371	0.220
365	NUDT19		0.077	1.000	0.179	0.218
366	CCNT2		0.072	1.000	-0.142	-0.205
367	OSBPL11		0.071	1.000	0.077	0.204
368	SNRNP200		0.070	1.000	0.185	0.200
369	ZNF703		0.070	1.000	0.054	0.199
370	NUFIP2		0.069	1.000	-0.127	-0.197
371	CCT7		0.068	1.000	0.229	0.194
372	FASN		0.067	1.000	-0.115	-0.193
373	U2SURP		0.067	1.000	0.067	0.191
374	RUFY1		0.066	1.000	-0.177	-0.190
375	IKBKAP		0.064	1.000	-0.184	-0.185
376	PM20D2		0.064	1.000	0.137	0.184
377	CCNT1		0.064	1.000	-0.427	-0.183

Number	Gene names	Student's T-test Significant Bait_24hHU_Control_24hHU	-Log Student's T-test p-value Bait_24hHU_Control_24hHU	Student's T-test q-value Bait_24hHU_Control_24hHU	Student's T-test Difference Bait_24hHU_Control_24hHU	Student's T-test Test statistic Bait_24hHU_Control_24hHU
378	CCT3		0.063	1.000	0.267	0.183
379	SEC13		0.063	1.000	-0.254	-0.181
380	HEXIM1		0.062	1.000	-0.282	-0.179
381	DPP9		0.062	1.000	0.091	0.178
382	HIST1H4A		0.061	1.000	0.053	0.177
383	ABI1		0.061	1.000	0.117	0.176
384	NFIB		0.061	1.000	0.209	0.176
385	AUTS2		0.060	1.000	0.271	0.172
386	SF3A2		0.060	1.000	-0.056	-0.172
387	U2AF2		0.059	1.000	0.084	0.171
388	WAC		0.058	1.000	0.081	0.169
389	WTAP		0.057	1.000	-0.082	-0.165
390	CCNK		0.057	1.000	-0.065	-0.164
391	IGF2BP2		0.056	1.000	0.108	0.162
392	ADSL		0.056	1.000	0.171	0.161
393	TJP1		0.055	1.000	-0.093	-0.161
394	ANKRD16		0.055	1.000	-0.120	-0.161
395	SRSF7		0.053	1.000	0.137	0.155
396	NT5DC2		0.053	1.000	0.131	0.154
397	SLC39A10		0.053	1.000	-0.197	-0.153
398	PRPSAP2		0.052	1.000	0.157	0.152
399	MATR3		0.052	1.000	-0.117	-0.151
400	BCS1L		0.050	1.000	-0.022	-0.147
401	DNAJB12		0.050	1.000	-0.061	-0.145
402	DNAJC8		0.049	1.000	0.072	0.142
403	CMTR1		0.046	1.000	0.092	0.135
404	RBM33		0.045	1.000	-0.144	-0.131
405	PEG10		0.043	1.000	0.012	0.127
406	CCT2		0.043	1.000	0.146	0.127
407	TLE1		0.043	1.000	-0.051	-0.126
408	LARP7		0.043	1.000	-0.041	-0.125
409	HNRNPK		0.041	1.000	-0.056	-0.122
410	SAFB2		0.041	1.000	-0.083	-0.121
411	DGCR8		0.040	1.000	-0.071	-0.117
412	GAPDH		0.040	1.000	0.091	0.116
413	SCLY		0.039	1.000	-0.064	-0.115
414	MNX1		0.038	1.000	-0.038	-0.112
415	CCT4		0.037	1.000	0.134	0.110
416	SEC23B		0.035	1.000	-0.077	-0.104
417	HSPA5		0.035	1.000	-0.019	-0.103
418	CSTF1		0.035	1.000	0.094	0.102
419	HIST1H2AJ;HIST1H2AH;H2		0.034	1.000	0.077	0.100

Number	Gene names	Student's T-test Significant Bait_24hHU_Control_24hHU	-Log Student's T-test p-value Bait_24hHU_Control_24hHU	Student's T-test q-value Bait_24hHU_Control_24hHU	Student's T-test Difference Bait_24hHU_Control_24hHU	Student's T-test Test statistic Bait_24hHU_Control_24hHU
420	HNRNPH1;HNRNPH2		0.034	1.000	0.015	0.100
421	PRPF40A		0.033	1.000	-0.031	-0.099
422	NCKAP1		0.033	1.000	0.170	0.097
423	CARS2		0.032	1.000	-0.093	-0.096
424	VWA8		0.032	1.000	-0.051	-0.096
425	SF3A3		0.030	1.000	0.054	0.090
426	SRSF6;SRSF4		0.029	1.000	0.104	0.087
427	ACOT9		0.028	1.000	-0.066	-0.083
428	SMNDC1		0.028	1.000	0.043	0.082
429	CCT8		0.027	1.000	0.097	0.082
430	RPRD1A		0.027	1.000	-0.101	-0.079
431	HDDC3		0.026	1.000	0.060	0.078
432	LMAN1		0.026	1.000	-0.043	-0.077
433	CKMT1A		0.025	1.000	-0.065	-0.076
434	PAF1		0.025	1.000	-0.064	-0.076
435	BMP2K		0.024	1.000	-0.121	-0.071
436	PHF5A		0.024	1.000	0.043	0.071
437	UNK		0.024	1.000	0.018	0.071
438	POU3F2;POU3F3		0.024	1.000	-0.130	-0.070
439	RBM17		0.023	1.000	0.039	0.070
440	CDK12		0.023	1.000	0.046	0.070
441	SLC4A1AP		0.023	1.000	-0.031	-0.068
442	CDK9		0.022	1.000	0.073	0.066
443	ATP5B		0.021	1.000	0.043	0.064
444	FBRSL1		0.021	1.000	-0.082	-0.063
445	EEF1A1P5;EEF1A1;EEF1A2		0.020	1.000	-0.021	-0.061
446	MAZ		0.020	1.000	-0.024	-0.059
447	SDF2L1		0.019	1.000	-0.029	-0.058
448	CBLL1		0.019	1.000	0.037	0.058
449	IK		0.019	1.000	-0.018	-0.056
450	CPSF4		0.018	1.000	-0.067	-0.054
451	RANBP1		0.016	1.000	0.026	0.049
452	MAT2B		0.015	1.000	0.026	0.045
453	CLK3		0.014	1.000	0.019	0.043
454	TAF8		0.014	1.000	0.035	0.043
455	CPSF6		0.014	1.000	-0.021	-0.042
456	CDC73		0.014	1.000	0.037	0.042
457	RNF20		0.014	1.000	0.017	0.042
458	RAPGEF6		0.014	1.000	-0.035	-0.042
459	GTF2A1		0.014	1.000	-0.037	-0.041
460	ARMC6		0.014	1.000	0.022	0.041
461	ATXN2L		0.013	1.000	0.009	0.040

Number	Gene names	Student's T-test Significant Bait_24hHU_Control_24hHU	-Log Student's T-test p-value Bait_24hHU_Control_24hHU	Student's T-test q-value Bait_24hHU_Control_24hHU	Student's T-test Difference Bait_24hHU_Control_24hHU	Student's T-test Test statistic Bait_24hHU_Control_24hHU
462	SEC31A		0.013	1.000	-0.043	-0.040
463	AES		0.013	1.000	0.035	0.039
464	TRA2B		0.012	1.000	-0.033	-0.037
465	ARHGAP17		0.011	1.000	0.047	0.034
466	SLC39A14		0.011	1.000	0.015	0.033
467	TUFM		0.010	1.000	-0.027	-0.031
468	SPEN		0.010	1.000	0.049	0.030
469	HIP1R		0.009	1.000	0.023	0.027
470	RBMX;RBMXL1		0.009	1.000	0.016	0.027
471	CCT5		0.008	1.000	0.029	0.024
472	GATA6		0.008	1.000	0.038	0.024
473	PAFAH1B3		0.008	1.000	-0.040	-0.023
474	CTBP1		0.007	1.000	-0.029	-0.021
475	C20orf27		0.007	1.000	0.005	0.020
476	RERE		0.007	1.000	-0.031	-0.020
477	YY1		0.004	1.000	0.027	0.013
478	DVL3		0.003	1.000	-0.004	-0.010
479	VWA9		0.002	1.000	-0.002	-0.005
480	SEC23A		0.001	1.000	0.005	0.004
481	TACO1		0.001	1.000	-0.003	-0.002
482	PRKCI		0.001	1.000	0.002	0.002
483	PYCRL		0.001	1.000	0.001	0.002
484	GPATCH8		0.001	1.000	0.002	0.002
485	CPSF7		0.001	1.000	0.001	0.002
486	CDX2;CDX1;CDX4		0.000	1.000	-0.001	-0.001
487	PPFIA1		0.000	0.999	0.000	0.001

Table A.9: MaxQuant search results for initial SILAC experiment
Proteins identified by MaxQuant search performed by mass spectrometry facility at the University of Oxford; for each condition (NT/2h HU/24h HU) two elution fractions from TALON IMAC pull downs were subjected to liquid chromatography coupled with mass spectrometry analysis, table shows intensities of light (L) and heavy (H) peptides detected in each sample, light labeled is the Bait cell line, heavy labeled is the Control cell line; search results were filtered and proteins with peptides only identified by site, reverse and potential contaminants were excluded from the list, subunits of the SMC5/6 complex are marked in yellow.

MQ search SILAC data

hit number	Gene names	Number of proteins	Peptides	Intensity L 2%SDS_24hHU	Intensity H 2%SDS_24hHU	Intensity L 2%SDS_2hHU	Intensity H 2%SDS_2hHU	Intensity L 2%SDS_NT	Intensity H 2%SDS_NT	Intensity L el150_24hHU	Intensity H el150_24hHU	Intensity L el150_2hHU	Intensity H el150_2hHU	Intensity L el150_NT	Intensity H el150_NT
1	NONO	2	51	1.49E+11	6.46E+10	8.74E+10	5.16E+10	1.62E+11	7.45E+10	4.61E+10	1.93E+10	5.27E+10	2.31E+10	2.84E+10	1.53E+10
2	SFPQ	2	50	1.47E+11	3.44E+10	8.34E+10	3.06E+10	1.12E+11	3.83E+10	6.63E+10	1.79E+10	5.45E+10	1.91E+10	6.14E+10	1.90E+10
3	HNRNPL	5	35	4.02E+10	5.72E+09	1.97E+10	3.80E+09	3.16E+10	5.75E+09	1.65E+10	2.35E+09	1.10E+10	2.36E+09	2.06E+10	3.08E+09
4	DHX15	3	53	3.48E+10	1.01E+10	1.37E+10	6.50E+09	2.46E+10	9.43E+09	1.13E+10	3.90E+09	8.18E+09	3.73E+09	9.87E+09	3.88E+09
5	TOP1	1	66	3.52E+10	3.57E+09	1.91E+10	2.84E+09	3.05E+10	4.41E+09	1.30E+10	8.14E+08	9.45E+09	1.34E+09	1.37E+10	1.52E+09
6	HSPA1A;HS	3	37	2.08E+10	7.82E+09	9.70E+09	5.36E+09	1.47E+10	8.23E+09	7.99E+09	3.11E+09	6.08E+09	3.78E+09	7.44E+09	4.22E+09
7	SF3B3	3	57	1.69E+10	5.69E+09	7.39E+09	4.40E+09	1.06E+10	5.42E+09	5.28E+09	2.05E+09	3.94E+09	2.05E+09	6.06E+09	2.83E+09
8	PSPC1	2	35	1.68E+10	4.74E+09	5.76E+09	2.66E+09	1.52E+10	5.51E+09	6.43E+09	2.12E+09	4.94E+09	2.18E+09	4.03E+09	9.97E+08
9	DDX42	1	51	1.63E+10	5.15E+09	6.21E+09	2.88E+09	9.57E+09	4.01E+09	6.90E+09	2.16E+09	4.04E+09	1.76E+09	4.23E+09	1.96E+09
10	SF3B2	1	52	1.69E+10	4.28E+09	7.04E+09	2.20E+09	9.46E+09	2.80E+09	5.51E+09	1.18E+09	2.79E+09	9.88E+08	6.12E+09	2.13E+09
11	HOMER1	15	18	1.17E+10	9.09E+09	6.52E+09	7.02E+09	7.94E+09	7.67E+09	4.84E+09	3.72E+09	4.23E+09	4.13E+09	1.89E+09	1.61E+09
12	SF3B1	2	66	1.31E+10	2.60E+09	6.35E+09	1.84E+09	8.18E+09	2.83E+09	4.05E+09	8.13E+08	2.90E+09	9.30E+08	3.66E+09	1.04E+09
13	MAZ	7	19	1.04E+10	2.41E+09	2.41E+09	1.70E+08	8.53E+09	2.50E+09	9.95E+08	3.19E+08	6.79E+08	2.57E+08	7.83E+08	3.04E+08
14	CKAP4	1	37	7.76E+09	3.53E+09	3.51E+09	1.83E+09	5.93E+09	2.48E+09	1.36E+09	4.88E+08	1.74E+09	1.09E+09	1.10E+09	5.04E+08
15	HIST1H2BL	11	8	8.84E+09	9.71E+08	2.84E+09	5.30E+08	5.18E+09	9.49E+08	3.98E+08	8.02E+07	3.53E+08	1.04E+08	3.30E+08	9.07E+07
16	TUBA1B;TU	5	21	7.12E+09	2.46E+09	3.58E+09	1.88E+09	6.98E+09	3.07E+09	9.89E+08	3.47E+08	1.13E+09	4.91E+08	1.78E+09	6.41E+08
17	NUFIP2	2	34	8.34E+09	8.65E+08	3.53E+09	5.07E+08	6.43E+09	1.06E+09	7.32E+08	6.40E+07	4.69E+08	9.16E+07	3.86E+08	4.45E+07
18	HSPA8	3	36	6.68E+09	1.95E+09	3.48E+09	1.34E+09	4.55E+09	1.83E+09	2.47E+09	8.80E+08	1.72E+09	8.70E+08	1.96E+09	9.40E+08
19	TUBB	3	21	5.39E+09	2.74E+09	2.54E+09	1.76E+09	4.75E+09	3.60E+09	8.88E+08	4.55E+08	8.08E+08	5.73E+08	1.06E+09	6.30E+08
20	DDX1	3	43	6.00E+09	1.65E+09	3.12E+09	8.24E+08	5.03E+09	1.31E+09	1.48E+09	1.92E+08	1.02E+09	1.95E+08	1.96E+09	2.81E+08
21	KRT1	3	54	7.58E+09	0.00E+00	8.37E+09	0.00E+00	5.34E+09	0.00E+00	7.17E+09	0.00E+00	2.49E+10	1.32E+07	6.96E+09	0.00E+00
22	HNRNPU	2	35	6.13E+09	1.42E+09	3.57E+09	1.12E+09	3.23E+09	1.07E+09	1.86E+08	5.28E+07	2.85E+08	8.68E+07	5.52E+08	1.55E+08
23	SAFB	4	39	5.89E+09	1.66E+09	2.53E+09	8.50E+08	2.24E+09	6.57E+08	1.19E+09	3.27E+08	7.43E+08	1.96E+08	1.41E+09	3.61E+08
24	MEPCE	2	35	5.93E+09	1.45E+09	2.20E+09	7.60E+08	5.91E+09	1.84E+09	4.28E+08	1.26E+08	4.22E+08	1.66E+08	4.60E+08	1.52E+08
25	CPSF7	3	21	5.38E+09	1.81E+09	3.41E+09	1.16E+09	4.12E+09	1.66E+09	4.66E+09	1.25E+09	1.77E+09	8.06E+08	3.41E+09	1.53E+09
26	CPSF1	1	66	4.73E+09	2.34E+09	2.39E+09	1.64E+09	3.36E+09	2.08E+09	6.94E+08	2.96E+08	4.52E+08	2.97E+08	9.01E+08	5.79E+08
27	U2SURP	3	50	6.13E+09	9.30E+08	2.20E+09	6.00E+08	3.29E+09	1.12E+09	1.65E+09	2.60E+08	1.43E+09	3.13E+08	1.42E+09	2.82E+08
28	H3F3A;HIS	5	6	4.71E+09	2.24E+09	1.14E+09	1.20E+09	2.23E+09	1.35E+09	4.60E+08	2.34E+08	2.73E+08	2.70E+08	3.03E+08	1.80E+08
29	EEF1A1;EEI	4	21	5.94E+09	9.07E+08	3.32E+09	6.64E+08	3.50E+09	6.82E+08	6.26E+08	1.07E+08	1.32E+09	2.11E+08	4.73E+08	1.15E+08
30	LARP7	3	30	5.40E+09	1.10E+09	1.78E+09	4.03E+08	4.33E+09	1.27E+09	8.05E+08	1.74E+08	5.04E+08	1.40E+08	6.03E+08	1.50E+08
31	ATXN2L	9	41	5.72E+09	7.22E+08	2.82E+09	3.45E+08	4.28E+09	7.16E+08	9.86E+08	1.46E+08	6.83E+08	1.66E+08	5.61E+08	1.73E+08
32	PPP1R10	1	44	5.38E+09	8.47E+08	2.57E+09	5.00E+08	3.59E+09	1.02E+09	2.67E+09	5.45E+08	1.51E+09	4.13E+08	8.72E+08	2.70E+08
33	DDX6	1	27	4.54E+09	1.64E+09	2.06E+09	1.20E+09	4.61E+09	2.17E+09	1.03E+09	4.12E+08	8.78E+08	4.32E+08	9.96E+08	5.07E+08
34	NCL	1	29	4.70E+09	8.20E+08	1.54E+09	3.90E+08	2.63E+09	4.98E+08	3.00E+08	7.30E+07	1.99E+08	6.54E+07	3.02E+08	7.91E+07
35	YY1	2	26	4.33E+09	1.15E+09	2.71E+09	7.47E+08	5.04E+09	1.06E+09	1.80E+09	5.82E+08	1.57E+09	4.63E+08	1.66E+09	3.41E+08
36	PPIL4	1	28	3.96E+09	1.05E+09	2.13E+09	6.43E+08	2.05E+09	6.72E+08	1.98E+09	5.35E+08	9.92E+08	3.95E+08	2.38E+09	8.18E+08
37	RPS4X	3	16	4.05E+09	9.03E+08	1.97E+09	8.96E+08	5.79E+09	1.74E+09	1.05E+08	4.25E+07	1.41E+08	6.25E+07	2.14E+08	1.01E+08
38	RPS3	2	19	3.79E+09	1.16E+09	1.41E+09	5.56E+08	3.11E+09	1.37E+09	1.48E+08	3.63E+07	9.64E+07	4.90E+07	1.11E+08	5.87E+07
39	PRPF8	1	94	3.82E+09	1.08E+09	1.74E+09	7.59E+08	2.67E+09	8.94E+08	3.76E+08	9.27E+07	3.49E+08	1.34E+08	6.48E+08	2.10E+08
40	FBL	1	17	3.96E+09	7.57E+08	1.47E+09	3.37E+08	2.78E+09	6.16E+08	5.00E+08	6.81E+07	1.75E+08	5.83E+07	2.74E+08	3.98E+07
41	CCNT1	2	25	3.88E+09	8.17E+08	1.63E+09	3.53E+08	6.81E+09	1.41E+09	7.26E+08	6.04E+07	5.96E+08	1.01E+08	5.21E+08	9.14E+07
42	SNRNP200	2	84	3.58E+09	1.09E+09	1.49E+09	8.20E+08	2.18E+09	1.07E+09	3.94E+08	1.47E+08	2.64E+08	1.54E+08	5.11E+08	2.57E+08
43	CHERP	1	32	3.91E+09	7.03E+08	1.77E+09	5.03E+08	2.72E+09	5.50E+08	1.56E+09	2.11E+08	8.29E+08	1.75E+08	2.26E+09	3.45E+08
44	RTCB	1	27	3.97E+09	6.24E+08	2.63E+09	5.17E+08	4.61E+09	9.50E+08	1.08E+09	1.44E+08	8.79E+08	1.89E+08	1.27E+09	1.49E+08
45	BRD4	9	42	3.59E+09	9.10E+08	1.97E+09	6.34E+08	1.77E+09	6.98E+08	1.97E+09	4.92E+08	1.37E+09	6.44E+08	2.67E+09	8.64E+08
46	SLC30A7	1	9	3.01E+09	1.47E+09	1.84E+09	1.39E+09	2.53E+09	1.65E+09	4.47E+08	2.45E+08	3.46E+08	2.58E+08	5.54E+08	3.58E+08
47	KRT9	2	43	4.47E+09	1.08E+07	5.74E+09	0.00E+00	3.03E+09	0.00E+00	4.30E+09	1.28E+06	2.09E+10	1.23E+07	4.31E+09	2.27E+06
48	WDR82	1	20	3.89E+09	4.87E+08	1.56E+09	3.24E+08	2.02E+09	4.96E+08	8.25E+08	5.86E+07	6.84E+08	1.32E+08	4.69E+08	1.19E+08
49	FIP1L1	3	22	3.53E+09	8.18E+08	1.73E+09	4.63E+08	3.22E+09	8.63E+08	1.04E+09	2.33E+08	5.23E+08	1.84E+08	1.34E+09	3.59E+08
50	SART1	1	42	3.09E+09	1.20E+09	1.16E+09	6.42E+08	1.68E+09	9.86E+08	8.90E+08	3.31E+08	4.91E+08	3.03E+08	5.07E+08	3.07E+08
51	PRPF4B	1	31	3.53E+09	6.57E+08	1.97E+09	5.29E+08	1.67E+09	5.09E+08	1.20E+09	1.65E+08	6.00E+08	1.44E+08	7.94E+08	1.30E+08
52	SF3A1	2	38	3.44E+09	6.84E+08	1.65E+09	3.93E+08	2.33E+09	5.98E+08	1.64E+09	2.23E+08	1.23E+09	2.80E+08	1.79E+09	4.64E+08
53	DOCK7	7	87	3.17E+09	9.34E+08	1.23E+09	6.05E+08	2.40E+09	9.68E+08	1.16E+09	3.81E+08	6.06E+08	2.72E+08	1.42E+09	5.49E+08
54	CPSF2	1	42	3.00E+09	1.04E+09	1.45E+09	7.52E+08	1.99E+09	1.04E+09	6.14E+08	2.47E+08	2.86E+08	1.60E+08	5.44E+08	2.45E+08
55	CDK12	5	48	3.44E+09	5.53E+08	1.77E+09	4.89E+08	1.57E+09	5.44E+08	1.33E+09	1.69E+08	8.01E+08	1.95E+08	1.23E+09	2.67E+08
56	PABPC1	7	25	2.94E+09	9.23E+08	7.01E+08	4.76E+08	2.15E+09	9.46E+08	2.75E+08	1.09E+08	1.79E+08	1.23E+08	3.54E+08	1.70E+08
57	CMTR1	1	45	2.49E+09	1.12E+09	9.58E+08	6.74E+08	1.75E+09	1.16E+09	1.30E+09	6.37E+08	7.42E+08	5.92E+08	1.64E+09	9.59E+08
58	HSPA6;HSP	2	10	2.07E+09	1.49E+09	5.21E+08	1.03E+09	1.49E+09	1.43E+09	9.11E+08	6.05E+08	7.40E+08	7.08E+08	8.04E+08	8.15E+08
59	CHD8	4	87	2.58E+09	9.78E+08	2.33E+09	1.18E+09	3.90E+09	1.39E+09	7.66E+08	2.58E+08	1.06E+09	5.15E+08	1.36E+09	5.34E+08
60	NSRP1	1	28	3.00E+09	4.15E+08	1.12E+09	1.06E+08	1.30E+09	2.07E+08	1.46E+09	2.23E+08	7.52E+08	1.28E+08	1.42E+09	2.42E+08
61	RBMX;RBM	7	19	2.43E+09	9.37E+08	7.31E+08	6.06E+08	1.09E+09	5.56E+08	4.44E+07	1.87E+07	3.84E+07	1.74E+07	2.93E+07	2.87E+07
62	CDK9	23	21	2.53E+09	8.28E+08	1.47E+09	8.34E+08	3.73E+09	1.68E+09	3.51E+08	1.78E+08	4.09E+08	2.56E+08	4.23E+08	1.76E+08
63	RPS8	1	9	2.09E+09	1.20E+09	9.61E+08	5.49E+08	2.44E+09	1.20E+09	3.43E+07	1.06E+07	1.12E+07	1.20E+07	1.89E+07	1.19E+07
64	SF3B4	1	10	2.81E+09	3.72E+08	1.57E+09	2.04E+08	1.26E+09	2.42E+08	2.05E+09	1.53E+08	7.89E+08	1.27E+08	1.03E+09	1.21E+08
65	HIST1H2AJ	15	5	2.04E+09	1.08E+09	5.88E+08	4.69E+08	8.77E+08	5.23E+08	1.76E+08	1.26E+08	1.75E+08	1.80E+08	1.17E+08	7.05E+07
66	CPSF6	3	18	2.85E+09	2.42E+08	9.99E+08	3.03E+08	8.37E+08	2.41E+08	1.92E+09	5.09E+08	1.07E+09	3.24E+08	2.79E+09	8.72E+08
67	CPSF3	1	32	2.20E+09	7.58E+08	9.29E+08	6.16E+08	1.39E+09	7.60E+08	3.23E+08	1.05E+08	2.82E+08	1.67E+08	3.46E+08	1.94E+08
68	FAM98A	3	13	2.04E+09	9.05E+08	7.64E+08	4.70E+08	1.63E+09	9.53E+08	4.55E+08	1.73E+08	5.01E+08	2.48E+08	4.68E+08	3.32E+08
69	RPL4	1	19	2.41E+09	4.99E+08	8.50E+08	3.15E+08	2.15E+09	9.15E+08	7.25E+07	1.49E+07	2.68E+07	1.19E+07	5.70E+07	1.55E+07
70	SUPT16H	1	35	2.22E+09	5.57E+08	5.50E+08	2.20E+08	1.09E+09	3.52E+08	4.93E+07	2.59E+07	1.22E+07	9.87E+06	5.08E+07	2.57E+07
71	SF3A2	1	17	2.16E+09	5.37E+08	8.74E+08	2.80E+08	8.00E+08	3.46E+08	1.22E+09	3.40E+08	3.49E+08	1.32E+08	1.72E+09	3.78E+08
72	XRN2	2	43	1.93E+09	7.07E+08	8.19E+08	3.90E+08	2.12E+09	9.40E+08	4.98E+08	1.52E+08	3.46E+08	1.71E+08	8.70E+08	3.17E+08
73	MECP2	2	21	2.37E+09	2.22E+08	7.32E+08	1.76E+08	1.28E+09	2.13E+08	3.29E+08	5.02E+07	1.47E+08	3.37E+07	1.76E+08	3.88E+07
74	RPL6	1	15	1.93E+09	5.64E+08	6.02E+08	1.87E+08	2.00E+09	5.74E+08	1.60E+07	6.12E+06	4.53E+06	3.45E+06	1.33E+07	9.96E+06
75	PARP1	1	46	2.07E+09	4.00E+08	7.12E+08	1.40E+08	3.21E+09	5.81E+08	1.79E+08	9.17E+06	1.30E+08	1.79E+06	5.31E+08	1.07E+08
76	RBM15B	2	33	1.88E+09	5.27E+08	7.09E+08	3.39E+08	1.71E+09	7.37E+08	2.55E+08	5.06E+07	1.52E+08	7.51E+07	1.31E+08	2.41E+07
77	RPL3	2	16	2.04E+09	3.77E+08	7.07E+08	2.64E+08	1.25E+09	6.56E+08	4.62E+07	0.00E+00	9.10E+06	0.00E+00	3.39E+07	0.00E+00
78	DYRK1A	10	28	1.86E+09	4.94E+08	6.27E+08	2.56E+08	2.06E+09	7.01E+08	3.87E+08	9.30E+07	2.11E+08	5.63E+07	1.66E+08	4.75E+07
79	SF3A3	1	27	1.81E+09	5.27E+08	9.92E+08	2.95E+08	1.40E+09	5.32E+08	7.32E+08	1.76E+08	5.71E+08	1.92E+08	1.24E+09	4.74E+08
80	RPL15	2	14	1.54E+09	7.99E+08	5.65E+08	2.52E+08	1.74E+09	7.53E+08	1.62E+07	8.17E+06	4.52E+06	0.00E+00	5.66E+06	6.62E+06
81	EFTUD2	3	38	1.65E+09	6.72E+08	9.12E+08	3.43E+08	1.38E+09	6.13E+08	2.03E+08	7.76E+07	2.21E+08	8.92E+07	4.18E+08	1.85E+08
82	RBM33	2	28	1.85E+09	4.58E+08	8.78E+08	2.69E+08	1.69E+09	3.16E+08	6.32E+08	1.32E+08	4.13E+08	1.37E+08	4.71E+08	1.50E+08

MQ search SILAC data

hit number	Gene names	Number of proteins	Peptides	Intensity L 2%SDS_24hHU	Intensity H 2%SDS_24hHU	Intensity L 2%SDS_2hHU	Intensity H 2%SDS_2hHU	Intensity L 2%SDS_NT	Intensity H 2%SDS_NT	Intensity L el150_24hHU	Intensity H el150_24hHU	Intensity L el150_2hHU	Intensity H el150_2hHU	Intensity L el150_NT	Intensity H el150_NT
83	RPS6	1	9	1.94E+09	3.33E+08	7.24E+08	2.58E+08	1.73E+09	4.27E+08	4.24E+07	0.00E+00	3.63E+07	6.48E+06	4.40E+07	9.30E+06
84	KRT16	4	37	2.25E+09	2.97E+06	6.12E+08	0.00E+00	2.59E+08	0.00E+00	1.12E+09	0.00E+00	1.10E+09	0.00E+00	6.42E+08	0.00E+00
85	PPP1CA	3	21	1.66E+09	5.42E+08	7.15E+08	5.53E+08	2.16E+09	1.24E+09	5.31E+08	3.30E+08	6.02E+08	3.99E+08	3.38E+08	2.63E+08
86	DDX3X	6	26	1.39E+09	7.99E+08	6.60E+08	3.96E+08	5.40E+08	3.55E+08	4.41E+07	1.59E+07	5.30E+07	3.80E+07	4.23E+07	3.03E+07
87	MCAT	2	19	1.80E+09	3.82E+08	9.69E+08	3.24E+08	1.76E+09	6.24E+08	4.21E+08	5.97E+07	4.00E+08	1.22E+08	3.97E+08	1.13E+08
88	HIST1H4A	1	7	1.44E+09	6.75E+08	5.72E+08	3.03E+08	8.26E+08	4.02E+08	1.31E+08	8.15E+07	2.61E+08	1.50E+08	7.27E+07	6.01E+07
89	RPLP0;RPLI	3	10	2.12E+09	1.58E+06	6.04E+08	0.00E+00	1.68E+09	1.18E+08	7.07E+07	4.12E+06	3.46E+07	3.71E+06	3.55E+07	0.00E+00
90	ATXN2	4	34	1.91E+09	2.10E+08	6.83E+08	2.66E+08	1.09E+09	3.00E+08	6.25E+08	1.47E+08	3.59E+08	1.41E+08	4.16E+08	1.12E+08
91	KRT10	36	37	2.11E+09	4.69E+06	3.47E+09	0.00E+00	2.62E+09	0.00E+00	1.62E+09	0.00E+00	6.67E+09	0.00E+00	3.38E+09	0.00E+00
92	MMTAG2	4	11	1.39E+09	7.04E+08	5.09E+08	3.21E+08	9.28E+08	7.59E+08	1.17E+08	4.60E+07	3.56E+07	3.25E+07	1.05E+08	7.45E+07
93	RPS9	1	13	1.43E+09	6.68E+08	5.68E+08	3.28E+08	1.02E+09	5.69E+08	3.15E+07	2.09E+07	5.76E+07	3.30E+07	2.15E+07	1.24E+07
94	WDR33	3	41	1.88E+09	1.96E+08	9.27E+08	2.17E+08	1.49E+09	2.84E+08	3.66E+08	4.78E+07	2.62E+08	4.96E+07	3.16E+08	5.36E+07
95	RPS3A	1	17	1.36E+09	7.08E+08	7.20E+08	3.86E+08	1.42E+09	8.36E+08	3.91E+07	1.27E+07	2.69E+07	1.53E+07	4.13E+07	3.27E+07
96	RBM17	1	20	1.90E+09	1.53E+08	7.44E+08	1.80E+08	1.05E+09	1.43E+08	4.62E+08	3.51E+07	3.61E+08	3.74E+07	4.39E+08	4.33E+07
97	RPS14	1	7	1.42E+09	5.81E+08	5.30E+08	2.93E+08	9.67E+08	4.27E+08	3.25E+07	8.77E+06	3.31E+07	2.30E+07	1.03E+07	0.00E+00
98	LSM12	2	6	1.62E+09	3.67E+08	9.38E+08	2.64E+08	1.60E+09	4.78E+08	2.65E+08	7.42E+07	2.41E+08	7.71E+07	3.08E+08	9.86E+07
99	KIAA1429	4	61	1.41E+09	5.64E+08	6.51E+08	2.93E+08	1.03E+09	4.43E+08	8.10E+08	3.21E+08	4.47E+08	2.32E+08	8.06E+08	3.59E+08
100	PKP2	2	40	1.35E+09	6.12E+08	6.33E+08	4.02E+08	1.80E+09	9.03E+08	4.29E+08	1.78E+08	1.84E+08	1.22E+08	4.13E+08	2.29E+08
101	RPL8	1	8	1.77E+09	1.82E+08	5.80E+08	7.50E+07	1.75E+09	3.08E+08	2.44E+07	0.00E+00	0.00E+00	0.00E+00	1.36E+07	0.00E+00
102	TOX4	10	16	1.63E+09	3.09E+08	9.70E+08	6.36E+07	1.39E+09	3.69E+08	8.04E+08	1.23E+08	5.77E+08	1.28E+08	3.36E+08	1.19E+08
103	SLC25A6	1	14	1.31E+09	5.94E+08	7.52E+08	5.14E+08	5.86E+08	4.41E+08	1.47E+08	6.66E+07	1.94E+08	1.36E+08	1.07E+08	7.78E+07
104	SF1	6	19	1.60E+09	2.89E+08	7.98E+08	2.39E+08	8.92E+08	2.31E+08	6.15E+08	1.10E+08	4.03E+08	1.53E+08	4.48E+08	1.14E+08
105	TCEB3	1	30	1.70E+09	1.74E+08	7.90E+08	9.12E+07	9.04E+08	1.55E+08	7.13E+08	5.01E+07	4.08E+08	5.54E+07	4.61E+08	9.19E+07
106	RPS23	1	7	1.65E+09	2.02E+08	5.01E+08	9.37E+07	2.05E+09	2.55E+08	1.79E+07	3.72E+06	1.43E+07	0.00E+00	5.86E+07	6.45E+06
107	DCAF7	2	13	1.52E+09	3.36E+08	1.23E+09	7.93E+08	2.67E+09	1.38E+09	4.06E+08	2.07E+08	3.94E+08	2.55E+08	4.80E+08	2.81E+08
108	RPL27A	1	5	1.33E+09	5.05E+08	4.62E+08	2.60E+08	1.21E+09	5.79E+08	4.30E+07	1.98E+07	1.11E+07	1.08E+07	1.95E+07	2.24E+07
109	SLC39A7	1	6	1.81E+09	2.00E+07	9.00E+08	0.00E+00	1.52E+09	3.68E+07	1.09E+08	1.25E+06	5.51E+07	9.74E+06	1.27E+08	0.00E+00
110	PBXIP1	3	25	1.17E+09	6.57E+08	7.89E+08	4.53E+08	1.50E+09	9.27E+08	2.01E+08	7.66E+07	2.22E+08	1.50E+08	2.98E+08	1.67E+08
111	NPM1	3	9	1.32E+09	4.51E+08	2.93E+08	2.26E+08	3.04E+08	1.73E+08	1.14E+08	5.78E+07	7.69E+07	6.71E+07	4.33E+07	2.22E+07
112	MATR3	2	25	1.42E+09	2.86E+08	6.62E+08	1.96E+08	1.23E+09	3.67E+08	1.25E+08	3.95E+07	1.34E+08	3.36E+07	6.57E+07	2.51E+07
113	NKRF	2	34	1.28E+09	3.95E+08	8.08E+08	3.18E+08	1.46E+09	7.68E+08	5.41E+08	1.16E+08	3.68E+08	1.74E+08	5.67E+08	2.10E+08
114	TRIM28	2	23	1.40E+09	2.76E+08	4.70E+08	1.98E+08	1.12E+09	3.31E+08	2.78E+08	3.71E+07	1.73E+08	4.10E+07	2.49E+08	7.63E+07
115	CCNK	4	18	1.38E+09	2.27E+08	8.39E+08	2.06E+08	1.03E+09	1.03E+08	6.66E+08	1.13E+08	5.00E+08	1.24E+08	6.70E+08	1.36E+08
116	KRT6C	2	34	1.59E+09	0.00E+00	2.97E+08	0.00E+00	2.38E+08	0.00E+00	7.81E+08	8.72E+05	6.14E+08	0.00E+00	4.75E+08	0.00E+00
117	RPL18	2	9	1.28E+09	3.05E+08	2.11E+08	1.22E+08	1.24E+09	4.75E+08	2.22E+07	0.00E+00	0.00E+00	0.00E+00	2.29E+07	0.00E+00
118	SSRP1	1	22	1.16E+09	3.91E+08	3.34E+08	2.06E+08	7.02E+08	4.06E+08	5.98E+07	2.89E+07	1.47E+07	1.91E+07	6.20E+07	2.36E+07
119	HNRNPH1	1	16	1.21E+09	3.42E+08	5.93E+08	2.76E+08	8.24E+08	3.93E+08	1.04E+08	2.48E+07	1.40E+08	4.79E+07	1.71E+08	4.66E+07
120	EWSR1	6	8	1.52E+09	1.09E+07	6.19E+08	1.81E+08	1.48E+09	1.39E+08	2.07E+07	3.34E+06	8.96E+06	0.00E+00	5.35E+06	0.00E+00
121	RPL7	1	13	1.05E+09	4.72E+08	2.74E+08	2.44E+08	6.06E+08	5.71E+08	9.03E+06	5.26E+06	0.00E+00	0.00E+00	0.00E+00	0.00E+00
122	TAF2	1	45	1.18E+09	3.35E+08	1.10E+09	3.62E+08	2.14E+09	5.49E+08	1.81E+08	4.43E+07	2.66E+08	6.60E+07	1.07E+08	5.23E+07
123	RUVBL1	2	26	1.33E+09	1.76E+08	9.06E+08	1.86E+08	1.16E+09	2.32E+08	2.36E+08	3.37E+07	2.21E+08	5.44E+07	2.57E+08	4.72E+07
124	VIM	21	24	1.09E+09	3.95E+08	2.76E+08	1.26E+08	0.00E+00	0.00E+00	6.24E+07	1.74E+07	9.56E+07	3.92E+07	0.00E+00	0.00E+00
125	HSPD1	2	28	1.19E+09	2.64E+08	4.78E+08	1.37E+08	9.13E+08	1.88E+08	2.11E+08	4.00E+07	2.72E+08	6.65E+07	2.25E+08	6.89E+07
126	CDK11B;CD	13	32	1.03E+09	4.20E+08	4.49E+08	2.47E+08	1.51E+09	7.84E+08	3.02E+08	9.97E+07	1.30E+08	7.07E+07	7.61E+08	3.62E+08
127	ALYREF	1	8	9.92E+08	4.45E+08	3.94E+08	3.27E+08	1.15E+08	1.34E+08	6.30E+07	4.71E+07	7.69E+07	5.53E+07	1.98E+07	2.94E+07
128	FBLL1	1	3	8.76E+08	5.00E+08	3.80E+08	2.55E+08	5.52E+08	3.38E+08	1.02E+08	6.09E+07	6.37E+07	0.00E+00	9.70E+07	3.77E+07
129	CEP170	7	46	1.02E+09	3.51E+08	4.52E+08	1.69E+08	9.09E+08	3.36E+08	4.13E+08	8.96E+07	2.13E+08	9.50E+07	6.66E+08	1.67E+08
130	NUDT21	1	14	1.20E+09	1.58E+08	4.69E+08	1.23E+08	6.56E+08	2.00E+08	5.07E+08	8.76E+07	2.97E+08	1.21E+08	2.91E+08	7.83E+07
131	RBM27	6	24	1.09E+09	2.50E+08	3.18E+08	1.17E+08	7.36E+08	2.38E+08	2.73E+08	6.73E+07	1.28E+08	3.75E+07	3.40E+08	5.39E+07
132	IRS4	1	35	7.99E+08	4.99E+08	4.49E+08	3.49E+08	1.78E+09	9.87E+08	6.98E+07	4.96E+07	3.67E+07	3.47E+07	2.84E+08	9.15E+07
133	H2AFY	3	12	1.24E+09	5.72E+07	1.68E+08	3.96E+07	2.66E+08	3.04E+07	1.59E+07	5.66E+06	0.00E+00	5.05E+06	0.00E+00	0.00E+00
134	YTHDC2	1	38	8.73E+08	4.19E+08	1.61E+08	9.40E+07	5.68E+08	2.71E+08	5.86E+07	1.40E+07	2.00E+07	9.16E+06	9.05E+07	2.84E+07
135	TUFM	1	21	1.10E+09	1.94E+08	3.58E+08	1.47E+08	7.65E+08	2.85E+08	1.39E+08	2.70E+07	1.49E+08	5.26E+07	9.31E+07	2.46E+07
136	HACD3	2	11	1.08E+09	2.08E+08	4.92E+08	2.69E+08	9.94E+08	4.13E+08	8.96E+07	6.95E+06	7.09E+07	3.36E+07	1.27E+08	5.05E+07
137	RPL10	2	9	1.00E+09	2.41E+08	1.43E+08	2.15E+07	8.45E+08	3.89E+08	1.70E+07	8.52E+06	0.00E+00	0.00E+00	0.00E+00	0.00E+00
138	DDX23	1	28	1.00E+09	2.34E+08	4.29E+08	1.67E+08	6.94E+08	2.83E+08	8.35E+07	1.22E+07	3.75E+07	5.10E+06	1.45E+08	3.50E+07
139	RPL13	2	7	8.39E+08	3.86E+08	1.74E+08	1.19E+08	4.95E+08	3.33E+08	1.67E+07	9.51E+06	5.44E+06	3.65E+06	6.14E+06	5.38E+06
140	DDX21	2	23	1.02E+09	1.74E+08	2.73E+08	8.19E+07	7.96E+08	1.10E+08	1.41E+07	4.03E+06	2.30E+06	0.00E+00	4.61E+06	2.49E+06
141	FAM120C	2	28	1.02E+09	1.65E+08	3.77E+08	1.07E+08	8.23E+08	2.14E+08	2.70E+08	4.37E+07	1.45E+08	6.28E+07	2.45E+08	6.47E+07
142	RPS15A	1	7	7.83E+08	3.94E+08	3.05E+08	2.10E+08	8.92E+08	6.37E+08	1.65E+07	1.34E+07	2.74E+07	2.30E+07	1.66E+07	3.01E+06
143	ILF3	9	25	9.33E+08	2.35E+08	4.66E+08	1.54E+08	3.04E+08	1.20E+08	8.99E+07	2.40E+07	8.75E+07	7.27E+07	4.87E+07	1.92E+07
144	DDX5	2	23	8.68E+08	2.96E+08	4.43E+08	2.21E+08	5.88E+08	2.17E+08	4.45E+07	1.61E+07	4.29E+07	3.01E+07	2.27E+07	1.87E+07
145	ACTG1;ACT	8	17	8.61E+08	2.85E+08	6.23E+08	4.00E+08	4.99E+08	2.55E+08	2.14E+08	5.47E+07	7.78E+08	4.60E+08	2.14E+08	7.59E+07
146	WTAP	2	19	8.61E+08	2.72E+08	3.38E+08	1.87E+08	6.71E+08	2.70E+08	2.80E+08	1.31E+08	2.05E+08	1.12E+08	2.90E+08	1.77E+08
147	PABPC4	4	24	1.04E+09	8.90E+07	2.35E+08	4.56E+07	6.17E+08	8.77E+07	1.41E+08	1.26E+07	8.64E+07	1.04E+07	9.14E+07	1.91E+07
148	DHX9	2	31	9.07E+08	2.16E+08	3.74E+08	1.88E+08	6.36E+08	2.30E+08	2.27E+07	9.10E+06	2.88E+07	1.62E+07	1.79E+07	1.66E+07
149	RPS16	1	9	7.52E+08	3.64E+08	3.41E+08	1.15E+08	7.57E+08	4.26E+08	2.62E+07	6.16E+06	3.64E+07	1.22E+07	2.57E+07	9.56E+06
150	RBM25	4	29	9.67E+08	1.42E+08	5.62E+08	1.97E+08	4.26E+08	1.72E+08	3.39E+08	5.25E+07	2.38E+08	2.44E+07	3.84E+08	1.49E+08
151	TUBB4B;TU	3	20	8.96E+08	2.01E+08	4.35E+08	1.51E+08	9.95E+08	3.61E+08	1.23E+08	3.60E+07	1.30E+08	5.31E+07	2.33E+08	1.18E+08
152	AFF4	3	30	8.68E+08	2.15E+08	5.97E+08	1.53E+08	1.11E+09	1.89E+08	2.30E+08	8.68E+07	2.04E+08	9.43E+07	4.41E+08	9.66E+07
153	RPS11	1	10	8.26E+08	2.54E+08	5.05E+08	1.34E+08	1.35E+09	5.07E+07	9.53E+06	7.52E+06	8.85E+06	9.01E+06	1.73E+07	1.18E+07
154	PHF5A	1	7	6.43E+08	4.19E+08	4.71E+08	3.61E+08	4.65E+08	3.60E+08	1.84E+08	8.93E+07	1.24E+08	8.53E+07	2.42E+08	1.60E+08
155	RSBN1	2	23	8.21E+08	2.36E+08	4.06E+08	2.18E+08	1.03E+09	3.17E+08	8.05E+07	2.53E+07	5.19E+07	2.59E+07	1.61E+08	6.82E+07
156	WDR5	2	16	9.14E+08	1.42E+08	4.48E+08	4.45E+07	6.22E+08	8.19E+07	5.01E+08	7.23E+07	2.90E+08	5.55E+07	6.58E+08	7.39E+07
157	RUVBL2	2	19	7.42E+08	3.09E+08	5.01E+08	2.80E+08	5.88E+08	2.93E+08	1.13E+08	7.64E+07	1.40E+08	8.83E+07	1.44E+08	5.11E+07
158	HSP90AA1	4	26	8.13E+08	2.21E+08	6.11E+08	2.92E+08	4.58E+08	2.80E+08	1.28E+08	5.20E+07	6.01E+08	2.43E+08	8.93E+07	5.10E+07
159	SAFB2	2	36	8.26E+08	1.96E+08	4.89E+08	2.26E+08	2.05E+08	1.10E+08	3.28E+08	1.13E+08	1.34E+08	3.96E+07	9.20E+07	4.36E+07
160	VDAC1	1	13	8.62E+08	1.59E+08	4.36E+08	1.00E+08	1.78E+08	1.08E+07	6.70E+07	0.00E+00	2.55E+07	0.00E+00	2.27E+07	0.00E+00
161	PRPF6	2	27	7.69E+08	2.47E+08	3.29E+08	1.65E+08	8.14E+08	4.10E+08	7.26E+07	4.16E+07	5.41E+07	3.82E+07	1.38E+08	1.16E+08
162	HEXIM1	2	6	6.90E+08	3.18E+08	2.86E+08	2.27E+08	8.00E+08	6.34E+08	7.00E+07	3.63E+07	4.04E+07	3.15E+07	7.80E+07	5.99E+07
163	HNRNPM	2	26	6.76E+08	3.26E+08	2.70E+08	1.72E+08	3.66E+08	2.16E+08	4.58E+07	1.46E+07	3.03E+07	1.99E+07	4.80E+06	0.00E+00
164	RPL9	1	7	9.69E+08	1.40E+07	9.04E+07	6.63E+06	3.94E+08	1.58E+07	0.00E+00	0.00E+00	1.45E+07	0.00E+00	1.05E+07	0.00E+00

MQ search SILAC data

hit number	Gene names	Number of proteins	Peptides	Intensity L 2%SDS_24hHU	Intensity H 2%SDS_24hHU	Intensity L 2%SDS_2hHU	Intensity H 2%SDS_2hHU	Intensity L 2%SDS_NT	Intensity H 2%SDS_NT	Intensity L el150_24hHU	Intensity H el150_24hHU	Intensity L el150_2hHU	Intensity H el150_2hHU	Intensity L el150_NT	Intensity H el150_NT
165	HSPA5	1	24	8.49E+08	1.34E+08	3.28E+08	1.37E+08	7.13E+08	1.32E+08	3.64E+08	7.08E+07	2.82E+08	8.91E+07	3.78E+08	1.06E+08
166	FAM120B	3	30	6.71E+08	2.87E+08	5.03E+08	2.29E+08	7.45E+08	3.15E+08	2.39E+08	4.08E+07	2.14E+08	1.04E+08	3.23E+08	1.31E+08
167	RPL18A	1	7	6.79E+08	2.74E+08	1.84E+08	1.22E+08	8.11E+08	4.02E+08	3.00E+06	0.00E+00	2.50E+06	0.00E+00	0.00E+00	0.00E+00
168	HSPA9	1	27	6.99E+08	2.41E+08	2.34E+08	1.42E+08	7.77E+08	3.58E+08	2.55E+08	9.86E+07	2.60E+08	1.35E+08	4.30E+08	1.72E+08
169	RPS20	2	3	6.52E+08	2.86E+08	1.78E+08	7.29E+07	5.13E+08	2.35E+08	3.09E+07	4.89E+06	2.71E+07	7.61E+06	2.11E+07	5.50E+06
170	ATP5A1	3	15	6.98E+08	2.35E+08	2.55E+08	1.60E+08	8.94E+08	5.86E+08	3.58E+07	2.10E+07	6.23E+07	4.07E+07	6.95E+07	2.70E+07
171	RPL5	1	13	7.68E+08	1.65E+08	3.27E+08	1.13E+08	8.65E+08	3.06E+08	2.55E+07	8.39E+06	7.03E+06	0.00E+00	9.47E+06	0.00E+00
172	SNIP1	1	15	6.60E+08	2.61E+08	2.51E+08	1.80E+08	3.37E+08	2.63E+08	1.72E+08	9.79E+07	1.29E+08	7.74E+07	1.74E+08	6.96E+07
173	ATP5B	1	21	6.69E+08	2.46E+08	3.51E+08	2.22E+08	1.21E+09	5.94E+08	6.09E+07	2.88E+07	9.80E+07	7.59E+07	1.37E+08	5.87E+07
174	RPS27A;UB	4	5	6.49E+08	2.63E+08	5.69E+08	5.74E+07	6.08E+08	3.32E+08	1.27E+08	0.00E+00	2.88E+08	7.71E+07	0.00E+00	0.00E+00
175	FUS	2	9	8.37E+08	7.11E+07	6.65E+08	1.07E+08	1.19E+08	0.00E+00	5.06E+07	0.00E+00	9.58E+07	0.00E+00	1.57E+07	0.00E+00
176	HIST2H2BE	7	8	9.06E+08	0.00E+00	2.61E+08	0.00E+00	2.87E+08	0.00E+00	4.80E+07	0.00E+00	9.52E+06	0.00E+00	4.42E+07	0.00E+00
177	HNRNPR	2	17	6.96E+08	1.95E+08	4.64E+08	1.84E+08	5.55E+08	2.03E+08	1.46E+07	1.53E+06	1.38E+07	1.55E+07	2.10E+07	1.26E+07
178	PRPF40A	3	23	7.56E+08	1.23E+08	2.57E+08	4.99E+07	2.46E+08	7.62E+07	2.04E+08	4.50E+07	1.80E+08	2.58E+07	3.46E+08	2.15E+07
179	ZNF281	2	26	7.59E+08	1.20E+08	6.59E+08	1.82E+08	1.31E+09	2.21E+08	1.40E+08	1.17E+07	1.03E+08	3.54E+07	1.14E+08	0.00E+00
180	HNRNPC	8	10	6.65E+08	2.11E+08	3.15E+08	1.22E+08	1.03E+09	3.21E+08	5.45E+07	1.21E+07	5.51E+07	1.93E+07	5.18E+07	2.01E+07
181	SRSF7	4	7	6.54E+08	2.02E+08	2.13E+08	7.40E+07	2.48E+08	6.80E+07	5.69E+07	7.21E+06	2.56E+07	0.00E+00	4.31E+07	6.84E+06
182	RAVER1	3	25	6.85E+08	1.62E+08	2.20E+08	8.25E+07	1.71E+09	3.82E+08	1.08E+08	2.83E+07	6.71E+07	2.89E+07	1.27E+08	1.05E+07
183	PWP1	2	13	6.77E+08	1.61E+08	1.06E+08	4.33E+07	2.64E+08	8.65E+07	6.63E+06	6.53E+06	3.11E+06	4.46E+06	7.78E+06	7.11E+06
184	TCEB1	2	6	7.21E+08	1.16E+08	3.93E+08	7.19E+07	6.26E+08	1.62E+08	2.34E+08	3.32E+07	1.17E+08	2.63E+07	2.71E+08	6.11E+07
185	KRT14	10	29	8.36E+08	0.00E+00	3.86E+08	0.00E+00	1.96E+08	0.00E+00	4.85E+08	0.00E+00	5.98E+08	0.00E+00	2.37E+08	0.00E+00
186	DNAJC10	3	19	6.15E+08	2.10E+08	4.14E+08	2.08E+08	4.16E+08	2.41E+08	8.51E+07	5.59E+07	1.16E+08	7.12E+07	5.54E+07	5.00E+07
187	RPS2	1	12	7.23E+08	9.51E+07	3.38E+08	6.10E+07	8.21E+08	8.89E+07	4.72E+07	4.24E+06	3.66E+07	3.83E+06	4.03E+07	3.77E+06
188	EIF5A;EIF5/	4	11	6.75E+08	1.41E+08	3.45E+08	1.05E+08	5.70E+08	1.41E+08	3.30E+08	5.99E+07	1.74E+08	1.23E+07	2.62E+08	6.73E+07
189	RPLP2	1	6	7.61E+08	4.19E+07	5.87E+07	2.07E+07	3.19E+08	4.77E+07	0.00E+00	0.00E+00	0.00E+00	0.00E+00	0.00E+00	0.00E+00
190	RPL7A	1	9	7.55E+08	4.35E+07	1.32E+08	0.00E+00	3.63E+08	3.99E+07	6.71E+06	3.04E+06	1.11E+07	2.50E+06	1.23E+07	2.03E+06
191	ILF2	1	12	6.95E+08	1.03E+08	3.67E+08	5.18E+07	4.47E+08	7.28E+07	8.15E+07	1.00E+07	6.02E+07	1.69E+07	6.82E+07	7.90E+06
192	PELO	1	18	5.70E+08	2.22E+08	3.02E+08	1.82E+08	9.47E+08	5.22E+08	7.83E+07	1.83E+07	3.10E+07	2.03E+07	2.07E+08	1.49E+08
193	HELZ	2	46	5.72E+08	1.95E+08	2.30E+08	6.49E+07	7.63E+08	2.22E+08	1.28E+08	3.56E+07	1.05E+08	3.14E+07	3.86E+08	1.43E+08
194	NOLC1	1	11	6.02E+08	1.27E+08	2.16E+08	8.66E+07	3.13E+08	4.58E+07	3.13E+07	1.07E+07	1.78E+07	4.88E+06	5.06E+07	1.93E+07
195	MAP7	8	23	4.68E+08	2.49E+08	2.64E+08	2.15E+08	8.64E+08	5.47E+08	3.41E+07	1.40E+07	1.89E+07	1.92E+07	6.61E+07	2.89E+07
196	KRT5	2	35	7.16E+08	0.00E+00	4.46E+08	0.00E+00	2.30E+08	0.00E+00	4.75E+08	0.00E+00	1.30E+09	0.00E+00	4.87E+08	0.00E+00
197	HNRNPK	3	17	6.15E+08	9.99E+07	1.80E+08	2.56E+07	1.45E+08	1.28E+07	4.16E+07	3.23E+06	1.17E+08	3.65E+07	3.50E+07	0.00E+00
198	C20orf27	2	9	7.15E+08	0.00E+00	2.69E+08	1.53E+07	1.12E+09	2.34E+07	4.26E+08	2.16E+07	2.43E+08	2.23E+07	5.68E+08	2.50E+07
199	RPL22	1	4	4.09E+08	3.04E+08	1.97E+08	1.23E+08	4.30E+08	4.27E+08	2.51E+07	6.27E+06	2.69E+07	1.68E+07	2.70E+07	2.10E+07
200	PHF3	2	44	6.22E+08	8.96E+07	4.62E+08	6.23E+07	8.36E+08	2.05E+08	2.13E+08	5.00E+07	1.95E+08	5.62E+07	4.38E+08	1.11E+08
201	DROSHA	4	35	5.97E+08	1.09E+08	2.58E+08	1.28E+08	3.15E+08	1.07E+08	2.55E+08	4.29E+07	1.83E+08	5.66E+07	4.68E+08	1.35E+08
202	SLC25A3	2	13	4.87E+08	2.06E+08	2.69E+08	1.37E+08	4.53E+08	2.05E+08	8.43E+07	6.40E+07	2.80E+07	3.18E+07	1.29E+08	4.17E+07
203	RPL27	1	5	4.72E+08	2.20E+08	9.57E+07	4.29E+07	4.29E+08	2.33E+08	0.00E+00	0.00E+00	0.00E+00	0.00E+00	0.00E+00	0.00E+00
204	RING1	2	10	4.94E+08	1.89E+08	2.43E+08	7.93E+07	4.79E+08	2.08E+08	1.06E+08	2.84E+07	5.56E+07	3.77E+07	1.16E+08	4.88E+07
205	CPSF4	4	12	6.08E+08	7.38E+07	3.01E+08	4.99E+07	4.99E+08	8.82E+07	8.60E+07	9.95E+06	8.00E+07	7.41E+06	9.03E+07	8.62E+06
206	CBX4	2	16	5.20E+08	1.59E+08	1.28E+08	7.62E+07	3.82E+08	1.79E+08	2.56E+07	1.39E+07	2.52E+07	1.30E+07	0.00E+00	0.00E+00
207	HIST1H1E;H	6	9	6.77E+08	0.00E+00	3.01E+08	0.00E+00	9.80E+08	0.00E+00	1.46E+07	0.00E+00	3.97E+07	0.00E+00	3.61E+07	0.00E+00
208	CBL	4	27	4.77E+08	1.97E+08	3.00E+08	1.10E+08	5.22E+08	1.19E+08	1.61E+08	7.07E+07	2.00E+08	8.30E+07	4.15E+08	1.69E+08
209	XRN1	3	40	4.98E+08	1.75E+08	2.23E+08	1.52E+08	7.43E+08	3.00E+08	1.20E+08	5.40E+07	4.87E+07	3.60E+07	2.29E+08	1.18E+08
210	DHX30	3	28	4.88E+08	1.75E+08	2.16E+08	9.26E+07	4.69E+08	1.73E+08	2.92E+06	1.41E+06	1.04E+07	3.48E+06	1.77E+06	1.38E+06
211	ARHGEF7	6	29	5.53E+08	1.03E+08	3.62E+08	1.08E+08	2.34E+08	6.72E+07	2.95E+08	5.55E+07	2.05E+08	8.10E+07	2.47E+08	8.74E+07
212	RPL28	5	5	5.40E+08	1.15E+08	1.25E+08	3.61E+07	4.33E+08	1.31E+08	3.98E+06	2.97E+06	0.00E+00	2.81E+06	0.00E+00	0.00E+00
213	WAC	4	14	6.29E+08	2.00E+07	3.23E+08	9.83E+06	7.97E+08	7.08E+07	1.11E+08	4.99E+06	8.00E+07	4.24E+06	1.69E+08	0.00E+00
214	RNPS1	3	6	5.89E+08	5.98E+07	1.87E+08	2.66E+07	3.11E+08	6.31E+07	8.51E+07	2.31E+06	4.69E+07	0.00E+00	2.06E+08	3.09E+06
215	G3BP2	3	10	5.90E+08	5.36E+07	2.19E+08	3.94E+07	5.51E+08	9.35E+07	3.16E+06	1.57E+06	3.62E+06	2.12E+06	1.13E+07	2.19E+06
216	RPS24	4	4	5.85E+08	5.86E+07	2.15E+08	3.01E+07	5.99E+08	7.80E+07	2.62E+06	1.74E+06	1.26E+07	2.86E+06	7.50E+06	1.23E+06
217	SLC25A5	2	12	5.58E+08	8.45E+07	2.77E+08	4.15E+07	1.79E+08	3.94E+07	3.90E+07	1.36E+07	3.78E+07	1.44E+07	7.42E+07	9.92E+06
218	FOXJ3	2	8	5.20E+08	1.18E+08	3.00E+08	9.60E+07	3.96E+08	1.23E+08	9.33E+07	1.25E+07	6.18E+07	9.41E+06	1.02E+08	2.69E+07
219	SLC4A7	22	33	4.89E+08	1.48E+08	1.90E+08	1.14E+08	5.84E+08	1.64E+08	9.57E+07	3.13E+07	4.81E+07	3.66E+07	3.84E+08	6.61E+07
220	BCLAF1	3	9	5.47E+08	8.90E+07	1.25E+08	2.88E+07	1.67E+08	3.63E+07	2.83E+07	2.37E+06	5.50E+06	0.00E+00	8.62E+06	0.00E+00
221	LRRC8A	2	22	4.58E+08	1.73E+08	3.13E+08	2.00E+08	2.17E+08	1.50E+08	7.60E+07	3.81E+07	5.42E+07	4.76E+07	1.10E+08	5.84E+07
222	LRCH1	3	19	5.00E+08	1.28E+08	2.00E+08	9.98E+07	4.50E+08	1.71E+08	1.76E+08	4.77E+07	1.36E+08	6.33E+07	2.25E+08	9.13E+07
223	HDAC1	1	12	4.63E+08	1.62E+08	2.56E+08	1.04E+08	5.90E+08	4.08E+08	9.74E+07	4.32E+07	9.69E+07	3.28E+07	1.25E+08	1.42E+07
224	ZIC2	9	9	4.58E+08	1.60E+08	3.10E+08	8.98E+07	6.13E+08	2.14E+08	1.16E+08	4.54E+07	7.06E+07	5.68E+07	9.91E+07	6.65E+07
225	RPLP1	1	3	6.16E+08	0.00E+00	1.72E+08	0.00E+00	6.21E+08	0.00E+00	1.97E+07	0.00E+00	1.42E+07	0.00E+00	1.67E+07	0.00E+00
226	TMA16	1	6	4.78E+08	1.32E+08	2.00E+08	1.05E+08	4.48E+08	1.92E+08	1.31E+08	3.30E+07	6.24E+07	3.75E+07	2.12E+08	9.22E+07
227	CBX5	1	4	5.90E+08	0.00E+00	0.00E+00	0.00E+00	0.00E+00	0.00E+00	0.00E+00	0.00E+00	0.00E+00	0.00E+00	0.00E+00	0.00E+00
228	RPS5	1	8	4.80E+08	1.09E+08	2.12E+08	6.06E+07	4.36E+08	1.06E+08	1.42E+07	0.00E+00	8.15E+06	0.00E+00	1.76E+07	0.00E+00
229	C14orf166	1	13	4.87E+08	1.02E+08	3.37E+08	8.08E+07	3.79E+08	1.90E+08	7.64E+07	1.21E+07	2.72E+07	7.03E+06	2.63E+07	1.45E+07
230	POU3F2	7	10	5.35E+08	5.34E+07	2.37E+08	1.09E+07	6.48E+08	4.53E+07	1.26E+08	0.00E+00	1.40E+08	1.88E+07	1.65E+08	0.00E+00
231	SNRNP40	2	12	3.44E+08	2.43E+08	1.46E+08	1.18E+08	5.82E+08	2.16E+08	2.86E+07	1.01E+07	3.53E+07	2.65E+07	3.90E+07	4.10E+07
232	RPL24	1	4	5.04E+08	8.15E+07	1.17E+08	4.07E+07	1.37E+08	1.10E+08	1.07E+07	0.00E+00	0.00E+00	0.00E+00	0.00E+00	0.00E+00
233	CBLL1	2	10	4.71E+08	1.10E+08	1.01E+08	8.25E+07	1.22E+08	1.07E+08	2.17E+08	3.46E+07	9.41E+07	6.64E+07	2.21E+08	1.24E+08
234	TBPL1	1	8	4.54E+08	1.17E+08	2.47E+08	9.57E+07	2.24E+08	1.42E+08	1.00E+08	0.00E+00	1.73E+08	5.36E+07	3.18E+08	4.85E+07
235	RPL11	2	10	5.63E+08	5.46E+06	1.30E+08	0.00E+00	3.07E+08	4.81E+07	1.91E+07	0.00E+00	1.36E+07	0.00E+00	1.66E+07	0.00E+00
236	PTDSS1	3	10	3.92E+08	1.76E+08	2.77E+08	1.96E+08	5.04E+08	3.38E+08	2.97E+07	2.19E+07	2.49E+07	2.35E+07	6.86E+07	5.26E+07
237	EPHX1	1	5	3.12E+08	2.51E+08	9.56E+06	5.95E+06	3.21E+08	3.09E+08	0.00E+00	0.00E+00	0.00E+00	0.00E+00	0.00E+00	0.00E+00
238	RPL17	3	5	5.03E+08	5.50E+07	2.23E+08	2.53E+07	4.20E+08	7.86E+07	1.73E+07	2.20E+06	5.84E+06	0.00E+00	2.01E+07	0.00E+00
239	RPL19	1	6	3.81E+08	1.72E+08	1.45E+08	5.76E+07	4.53E+08	2.58E+08	1.70E+07	1.02E+07	1.14E+07	1.10E+07	7.15E+06	1.43E+07
240	GIT1	3	26	4.27E+08	1.23E+08	2.10E+08	1.26E+08	2.42E+08	1.17E+08	2.74E+08	1.09E+08	2.42E+08	1.22E+08	3.01E+08	1.04E+08
241	TUBB8	1	9	5.50E+08	0.00E+00	1.55E+08	0.00E+00	1.98E+08	0.00E+00	3.91E+07	0.00E+00	4.37E+07	0.00E+00	1.08E+08	0.00E+00
242	RPL21	1	6	4.76E+08	7.03E+07	5.45E+07	1.58E+07	3.95E+08	6.95E+07	0.00E+00	0.00E+00	0.00E+00	0.00E+00	0.00E+00	0.00E+00
243	BTBD11	5	26	4.12E+08	1.32E+08	7.84E+07	6.66E+07	3.12E+08	1.38E+08	1.95E+08	6.63E+07	7.21E+07	3.81E+07	1.73E+08	6.61E+07
244	RSBN1L	2	17	4.11E+08	1.32E+08	1.68E+08	6.84E+07	3.97E+08	1.72E+08	2.10E+07	0.00E+00	3.31E+06	0.00E+00	5.65E+07	2.92E+07
245	PHF6	5	14	4.49E+08	9.00E+07	1.64E+08	5.61E+07	2.22E+08	9.28E+07	1.66E+08	4.72E+07	1.05E+08	4.92E+07	8.38E+07	5.69E+06
246	PHGDH	1	13	3.36E+08	2.02E+08	1.24E+08	1.26E+08	3.85E+08	2.57E+08	1.13E+07	1.01E+07	3.00E+07	4.35E+07	5.21E+07	4.27E+07

MQ search SILAC data

hit number	Gene names	Number of proteins	Peptides	Intensity L 2%SDS_24hHU	Intensity H 2%SDS_24hHU	Intensity L 2%SDS_2hHU	Intensity H 2%SDS_2hHU	Intensity L 2%SDS_NT	Intensity H 2%SDS_NT	Intensity L el150_24hHU	Intensity H el150_24hHU	Intensity L el150_2hHU	Intensity H el150_2hHU	Intensity L el150_NT	Intensity H el150_NT
247	RPL13A	2	8	4.43E+08	7.91E+07	9.64E+07	1.66E+07	3.36E+08	6.61E+07	0.00E+00	0.00E+00	0.00E+00	0.00E+00	0.00E+00	0.00E+00
248	RPL12	2	5	4.68E+08	4.82E+07	1.74E+08	5.85E+07	3.91E+08	9.39E+07	1.75E+07	0.00E+00	6.85E+06	0.00E+00	1.30E+07	0.00E+00
249	NUDCD1	3	24	5.07E+08	0.00E+00	1.52E+08	3.27E+07	3.50E+08	1.19E+08	3.99E+08	9.55E+07	1.56E+08	5.58E+07	3.91E+08	9.07E+07
250	PPP2R1A	6	16	3.98E+08	1.02E+08	2.18E+08	3.31E+07	2.93E+08	4.08E+07	1.09E+08	1.77E+07	1.22E+08	2.82E+07	5.46E+07	2.73E+07
251	SIN3A	2	27	3.44E+08	1.51E+08	1.97E+08	1.06E+08	3.22E+08	1.65E+08	1.22E+08	4.08E+07	6.60E+07	4.63E+07	1.50E+08	8.33E+07
252	RPS26;RPS:	2	4	3.70E+08	1.25E+08	1.37E+08	7.16E+07	2.89E+08	1.22E+08	0.00E+00	0.00E+00	3.94E+06	4.26E+06	1.36E+07	0.00E+00
253	SRSF9	1	9	3.56E+08	1.35E+08	1.15E+08	6.19E+07	1.54E+08	7.58E+07	0.00E+00	0.00E+00	0.00E+00	0.00E+00	0.00E+00	0.00E+00
254	RPL37A	2	4	4.91E+08	0.00E+00	1.86E+08	0.00E+00	4.29E+08	0.00E+00	0.00E+00	0.00E+00	4.29E+06	0.00E+00	6.17E+06	0.00E+00
255	METTL17	3	16	3.43E+08	1.47E+08	1.85E+08	8.00E+07	9.97E+08	3.93E+08	2.46E+07	1.00E+07	2.09E+07	7.41E+06	6.49E+06	4.21E+06
256	RPL10A	1	7	3.90E+08	9.88E+07	9.24E+07	0.00E+00	4.41E+08	1.18E+08	5.75E+06	0.00E+00	1.73E+06	0.00E+00	0.00E+00	0.00E+00
257	ACTL6A	3	15	3.88E+08	9.18E+07	2.39E+08	7.00E+07	4.09E+08	9.25E+07	8.59E+07	1.76E+07	8.93E+07	2.06E+07	1.40E+08	3.50E+07
258	PRPF19	1	14	4.06E+08	7.03E+07	1.92E+08	8.33E+07	3.98E+08	1.26E+08	1.97E+07	6.71E+06	2.47E+07	1.15E+07	3.55E+07	5.28E+06
259	ACIN1	4	14	3.45E+08	1.22E+08	1.17E+08	6.18E+07	1.02E+08	2.60E+07	7.05E+06	5.61E+06	2.55E+06	2.46E+06	1.82E+07	1.03E+07
260	SMAD4	2	16	3.63E+08	1.03E+08	3.16E+08	1.22E+08	4.47E+08	1.51E+08	4.29E+08	8.63E+07	2.55E+08	1.37E+08	1.63E+09	1.64E+08
261	SAP30BP	2	10	2.77E+08	1.87E+08	1.23E+08	8.55E+07	4.47E+08	3.14E+08	7.56E+07	5.33E+07	1.64E+07	3.38E+07	2.13E+08	1.39E+08
262	KPNA2	1	14	3.21E+08	1.42E+08	3.07E+08	1.99E+08	3.78E+08	2.31E+08	7.69E+07	3.97E+07	1.04E+08	7.27E+07	8.89E+07	4.22E+07
263	SRSF10	6	6	3.37E+08	1.21E+08	1.32E+08	7.74E+07	9.69E+07	8.12E+07	1.79E+07	9.68E+06	6.58E+06	5.55E+06	2.77E+06	1.38E+06
264	RPSA	1	10	2.98E+08	1.58E+08	1.53E+08	1.11E+08	3.72E+08	1.63E+08	5.60E+07	2.93E+07	5.67E+07	3.74E+07	4.43E+07	2.53E+07
265	SMU1	2	14	3.91E+08	5.80E+07	2.18E+08	3.81E+07	3.38E+08	1.51E+08	7.66E+07	2.88E+07	6.79E+07	2.71E+07	1.15E+08	4.89E+07
266	AMOT	2	20	9.30E+07	3.55E+08	2.80E+07	2.77E+08	4.57E+08	7.16E+08	1.22E+07	1.02E+08	2.68E+07	1.37E+08	1.01E+08	1.87E+08
267	VDAC2	3	8	4.44E+08	0.00E+00	1.61E+08	0.00E+00	6.03E+07	0.00E+00	1.62E+07	0.00E+00	1.72E+07	0.00E+00	0.00E+00	0.00E+00
268	CSNK2A1;C	3	17	3.92E+08	4.51E+07	2.11E+08	1.01E+08	3.36E+08	9.34E+07	8.37E+07	3.20E+07	1.52E+08	6.38E+07	1.41E+08	4.60E+07
269	PPP1CC	2	18	3.64E+08	7.02E+07	3.92E+08	3.65E+08	4.35E+08	7.89E+07	1.30E+08	7.73E+07	9.62E+07	3.46E+07	9.73E+07	1.59E+07
270	ZNF146	3	14	3.06E+08	1.28E+08	5.73E+08	2.69E+08	8.94E+08	3.07E+08	3.43E+07	2.77E+07	5.34E+07	5.60E+07	7.05E+07	4.71E+07
271	BMP2K	5	20	3.47E+08	8.46E+07	9.68E+07	6.01E+07	1.76E+08	2.45E+07	1.59E+08	3.56E+07	1.15E+08	4.44E+07	1.18E+08	4.38E+07
272	PRPF4	2	10	2.72E+08	1.59E+08	1.52E+08	8.40E+07	1.51E+08	5.96E+07	2.52E+07	1.24E+07	2.34E+07	1.49E+07	4.37E+07	3.43E+07
273	DDX17	4	20	3.23E+08	1.07E+08	1.89E+08	7.22E+07	2.31E+08	1.00E+08	2.36E+07	1.07E+07	2.42E+07	2.41E+07	1.49E+07	6.65E+06
274	PTBP1	10	12	3.53E+08	7.72E+07	1.03E+08	1.59E+07	4.39E+07	1.08E+07	4.34E+06	0.00E+00	9.01E+06	3.61E+06	0.00E+00	0.00E+00
275	PEG10	2	9	3.35E+08	9.50E+07	2.08E+08	7.17E+07	8.23E+08	2.83E+08	5.74E+07	3.15E+07	1.10E+08	7.20E+07	9.33E+07	6.20E+07
276	WDR6	1	24	2.97E+08	1.30E+08	3.41E+08	2.04E+08	6.83E+08	3.91E+08	1.45E+07	1.19E+07	1.91E+07	2.03E+07	8.38E+07	3.19E+07
277	WARS2	2	17	3.96E+08	2.72E+07	2.02E+08	1.79E+07	6.60E+08	9.96E+07	9.93E+07	1.41E+07	7.03E+07	2.29E+07	1.95E+08	2.87E+07
278	DDX39B;DI	5	9	2.94E+08	1.21E+08	8.52E+07	7.46E+07	1.19E+08	7.64E+07	2.23E+07	1.35E+07	3.02E+07	2.37E+07	4.09E+06	4.63E+06
279	CCT2	2	20	3.01E+08	1.13E+08	1.34E+08	5.05E+07	1.04E+08	4.17E+07	3.96E+07	8.79E+06	8.23E+07	3.09E+07	5.81E+07	1.50E+07
280	RBM15	4	19	2.98E+08	1.11E+08	8.71E+07	2.23E+07	3.48E+08	1.71E+08	0.00E+00	0.00E+00	2.79E+06	1.77E+06	2.42E+06	2.71E+06
281	CSE1L	4	25	3.83E+08	2.34E+07	1.70E+08	5.66E+07	5.85E+08	1.29E+08	3.11E+07	5.60E+06	1.94E+07	1.61E+07	7.19E+07	3.95E+07
282	RPL29	1	2	4.06E+08	0.00E+00	1.14E+08	0.00E+00	3.61E+08	0.00E+00	0.00E+00	0.00E+00	0.00E+00	0.00E+00	0.00E+00	0.00E+00
283	SF3B5	1	4	3.49E+08	5.66E+07	2.07E+08	5.82E+07	3.00E+08	8.35E+07	5.96E+07	2.15E+07	9.15E+07	1.42E+07	7.21E+07	2.53E+07
284	CTIF	2	21	2.74E+08	1.31E+08	5.95E+07	5.65E+07	2.08E+08	9.70E+07	2.23E+08	1.11E+08	5.70E+07	4.01E+07	1.69E+08	9.43E+07
285	USP39	3	13	3.48E+08	5.67E+07	1.05E+08	4.81E+07	3.82E+08	1.04E+08	5.18E+07	5.58E+06	3.33E+07	2.22E+07	6.72E+07	2.18E+07
286	RPS15	1	6	2.88E+08	1.12E+08	3.73E+07	0.00E+00	1.46E+08	4.46E+07	0.00E+00	0.00E+00	0.00E+00	0.00E+00	0.00E+00	0.00E+00
287	KIAA0430	5	28	3.30E+08	6.55E+07	1.35E+08	7.49E+07	2.34E+08	1.49E+08	1.85E+08	2.56E+07	8.21E+07	3.68E+07	1.59E+08	5.10E+07
288	SLC39A10	2	13	2.11E+08	1.83E+08	1.93E+08	2.60E+08	6.49E+08	2.34E+08	4.62E+07	3.68E+07	5.64E+07	9.26E+07	9.75E+07	5.97E+07
289	PIAS1	3	15	2.78E+08	1.16E+08	2.23E+08	1.25E+08	5.22E+08	2.13E+08	3.25E+07	8.77E+06	7.33E+07	3.32E+07	1.50E+08	8.16E+07
290	RERE	2	18	3.28E+08	6.62E+07	1.34E+08	3.59E+07	2.91E+08	6.21E+07	1.01E+08	5.46E+07	9.41E+07	2.18E+07	2.15E+08	1.13E+08
291	TRMT2A	2	16	2.73E+08	1.18E+08	3.84E+07	2.14E+07	2.15E+08	1.03E+08	3.28E+07	1.11E+07	2.36E+07	1.32E+07	6.60E+07	4.64E+07
292	TAF5	2	16	3.41E+08	4.99E+07	1.27E+08	4.70E+07	1.47E+08	3.52E+07	1.87E+07	8.46E+06	2.21E+07	8.62E+06	2.66E+07	8.44E+06
293	CPEB4	13	15	3.07E+08	8.14E+07	7.52E+07	6.10E+07	1.71E+08	7.10E+07	4.30E+07	7.62E+06	1.55E+07	0.00E+00	1.82E+07	5.31E+06
294	GPATCH8	2	22	3.69E+08	1.75E+07	8.21E+07	1.05E+07	3.72E+08	4.70E+07	7.38E+07	1.08E+07	4.93E+07	1.02E+07	1.66E+08	1.32E+07
295	USP34	3	40	3.08E+08	7.11E+07	1.12E+08	2.85E+07	1.83E+08	4.53E+07	5.64E+07	7.40E+06	3.76E+07	1.70E+07	1.56E+08	4.71E+07
296	THRAP3	1	11	2.81E+08	9.55E+07	5.49E+07	3.85E+07	8.17E+07	0.00E+00	0.00E+00	0.00E+00	0.00E+00	0.00E+00	0.00E+00	0.00E+00
297	PIP5K1A;PI	9	14	2.33E+08	1.43E+08	3.61E+08	2.03E+08	5.84E+08	4.20E+08	2.53E+07	1.47E+07	3.48E+07	2.06E+07	5.62E+07	2.97E+07
298	RPL23	1	4	3.76E+08	0.00E+00	9.88E+07	0.00E+00	3.03E+08	1.68E+07	2.74E+07	0.00E+00	5.14E+06	0.00E+00	6.66E+06	0.00E+00
299	RPL31	3	4	2.10E+08	1.64E+08	1.10E+08	1.13E+08	3.10E+08	1.06E+08	0.00E+00	0.00E+00	0.00E+00	0.00E+00	0.00E+00	0.00E+00
300	RBM10	7	16	2.90E+08	8.18E+07	1.14E+08	3.27E+07	2.63E+08	1.24E+08	5.49E+07	9.67E+06	2.51E+07	1.17E+07	4.90E+07	2.49E+07
301	KPNA3	1	13	2.86E+08	8.55E+07	1.04E+08	5.73E+07	1.50E+08	5.47E+07	1.05E+08	3.59E+07	8.40E+07	7.19E+06	9.43E+07	4.68E+07
302	USP30	1	15	3.00E+08	7.10E+07	1.84E+08	9.03E+07	1.78E+08	7.99E+07	4.23E+07	2.42E+07	3.26E+07	5.90E+06	4.28E+07	1.16E+07
303	RPS12	1	5	2.78E+08	9.23E+07	1.78E+08	5.39E+07	5.80E+08	1.13E+08	5.77E+06	5.30E+06	4.14E+06	6.21E+06	5.56E+06	5.91E+06
304	RPS28	1	3	2.14E+08	1.56E+08	9.66E+07	9.84E+07	1.19E+08	1.12E+08	5.81E+06	0.00E+00	0.00E+00	6.00E+06	1.13E+07	7.97E+06
305	RPN1	1	14	2.52E+08	1.19E+08	1.06E+08	8.04E+07	3.90E+08	2.92E+08	5.85E+06	4.68E+06	1.40E+07	1.60E+07	2.14E+07	1.44E+07
306	SMARCC2	3	18	2.53E+08	1.16E+08	8.31E+07	1.11E+08	1.46E+08	5.45E+07	5.25E+07	1.61E+07	2.71E+07	2.02E+07	3.62E+07	2.74E+07
307	RNF20	1	24	2.81E+08	8.61E+07	1.18E+08	3.37E+07	4.74E+08	1.88E+08	3.00E+07	3.02E+06	1.21E+07	1.05E+07	7.28E+07	2.74E+07
308	HSP90AB1	4	26	3.41E+08	2.35E+07	2.37E+08	1.74E+08	9.10E+07	2.57E+07	4.78E+07	2.10E+06	1.85E+08	5.04E+07	5.25E+07	1.79E+07
309	CCT4	2	17	2.30E+08	1.31E+08	7.92E+07	8.90E+07	5.08E+08	2.26E+08	6.07E+06	8.90E+06	4.96E+07	4.22E+07	8.08E+07	4.41E+07
310	RPL14	1	5	2.42E+08	1.18E+08	4.50E+07	3.03E+07	1.88E+08	1.47E+08	8.19E+06	5.58E+06	4.53E+06	4.57E+06	6.10E+06	8.51E+06
311	LRRC8C	1	20	2.72E+08	8.54E+07	1.06E+08	8.77E+07	9.36E+07	2.85E+07	3.49E+07	1.94E+07	3.08E+07	1.12E+07	2.66E+07	2.06E+07
312	FAM76B	3	10	2.82E+08	7.50E+07	2.54E+08	7.70E+07	5.96E+08	1.60E+08	7.23E+07	1.67E+07	5.47E+07	2.87E+07	0.00E+00	0.00E+00
313	RPN2	2	14	3.12E+08	3.60E+07	1.41E+08	4.95E+07	3.40E+08	1.03E+08	2.65E+06	1.72E+06	6.47E+06	4.76E+06	1.65E+07	6.21E+06
314	TCEB2	2	8	2.78E+08	6.91E+07	1.23E+08	6.39E+07	2.06E+08	1.07E+08	4.30E+07	9.42E+06	2.67E+07	9.85E+06	1.18E+07	2.58E+07
315	HNRNPA0	1	7	2.39E+08	1.06E+08	1.53E+08	1.41E+08	2.33E+08	6.98E+07	1.11E+07	4.95E+06	4.21E+06	5.12E+06	1.15E+07	5.14E+06
316	LANCL2	1	8	3.11E+08	3.46E+07	3.07E+07	1.32E+06	5.24E+07	3.23E+07	1.09E+08	9.86E+06	1.12E+07	8.15E+06	2.86E+07	1.67E+07
317	PPP1CB	1	18	2.13E+08	1.30E+08	3.64E+07	2.56E+07	1.79E+08	1.10E+08	5.89E+07	3.34E+07	4.73E+07	4.06E+07	6.06E+07	4.40E+07
318	SUB1	1	6	3.42E+08	0.00E+00	1.93E+07	0.00E+00	4.59E+08	0.00E+00	1.24E+08	0.00E+00	1.93E+08	0.00E+00	3.99E+08	0.00E+00
319	CCT8	3	20	2.61E+08	7.86E+07	1.78E+08	9.44E+07	3.38E+08	1.12E+08	8.21E+07	1.88E+07	1.14E+08	5.37E+07	8.71E+07	5.94E+07
320	SLTM	2	16	2.95E+08	4.47E+07	9.78E+07	7.67E+07	2.19E+08	1.10E+08	2.23E+07	8.77E+06	7.30E+06	5.98E+06	1.91E+07	1.00E+07
321	TMPO	2	11	2.19E+08	1.20E+08	8.34E+07	4.85E+07	1.45E+08	6.97E+07	1.59E+07	2.89E+06	2.00E+07	9.90E+06	1.31E+07	3.30E+06
322	SMARCA4	7	22	2.29E+08	1.07E+08	1.49E+08	1.15E+08	1.95E+08	1.18E+08	1.02E+08	4.33E+07	6.83E+07	5.68E+07	1.51E+08	1.09E+08
323	TRA2B	2	6	1.91E+08	1.44E+08	1.60E+08	1.04E+08	1.49E+08	1.01E+08	3.26E+07	1.19E+07	1.93E+07	1.49E+07	2.22E+07	1.96E+07
324	HNRNPF	1	12	2.62E+08	7.19E+07	7.50E+07	3.79E+07	2.21E+08	5.03E+07	4.37E+07	7.41E+06	4.42E+07	1.38E+07	5.51E+07	1.04E+07
325	SETD1B	3	17	2.97E+08	3.65E+07	1.17E+08	3.14E+07	2.83E+08	6.49E+07	8.00E+06	0.00E+00	4.56E+06	3.47E+06	2.14E+07	0.00E+00
326	HNRNPA1;I	4	12	2.72E+08	6.02E+07	1.57E+08	8.24E+07	2.03E+08	9.12E+07	1.05E+07	0.00E+00	1.64E+08	5.54E+07	2.86E+07	1.04E+07
327	IQSEC1	6	17	2.77E+08	5.35E+07	1.48E+08	8.39E+07	6.07E+08	1.88E+08	3.22E+07	1.82E+07	3.38E+07	1.19E+07	2.30E+07	7.68E+06
328	DGCR8	3	28	3.02E+08	2.46E+07	1.89E+08	4.55E+07	1.78E+08	1.49E+07	2.10E+08	4.40E+07	1.14E+08	2.84E+07	1.36E+08	3.27E+07

MQ search SILAC data

hit number	Gene names	Number of proteins	Peptides	Intensity L 2%SDS_24hHU	Intensity H 2%SDS_24hHU	Intensity L 2%SDS_2hHU	Intensity H 2%SDS_2hHU	Intensity L 2%SDS_NT	Intensity H 2%SDS_NT	Intensity L el150_24hHU	Intensity H el150_24hHU	Intensity L el150_2hHU	Intensity H el150_2hHU	Intensity L el150_NT	Intensity H el150_NT
329	PRPF3	2	12	2.63E+08	6.14E+07	3.00E+07	1.82E+07	4.92E+07	4.14E+07	0.00E+00	0.00E+00	0.00E+00	0.00E+00	0.00E+00	0.00E+00
330	PRKDC	2	41	2.71E+08	5.24E+07	7.80E+07	3.83E+07	1.19E+08	8.04E+06	1.36E+07	2.40E+06	3.59E+07	7.74E+06	6.39E+07	1.55E+07
331	PHB	2	11	2.11E+08	1.13E+08	1.30E+08	1.12E+08	1.49E+08	7.61E+07	0.00E+00	0.00E+00	5.35E+06	4.27E+06	0.00E+00	0.00E+00
332	TRA2A	4	6	2.09E+08	1.12E+08	6.53E+07	4.72E+07	7.56E+07	6.44E+07	1.24E+07	8.20E+06	9.35E+06	8.15E+06	1.82E+07	1.70E+07
333	RPL30	1	5	2.55E+08	6.54E+07	2.20E+07	0.00E+00	3.11E+08	5.48E+07	0.00E+00	0.00E+00	0.00E+00	0.00E+00	9.54E+06	2.12E+06
334	CANX	3	12	2.87E+08	3.27E+07	1.27E+08	3.30E+07	4.09E+08	3.43E+07	1.48E+07	3.95E+06	1.32E+07	6.58E+06	1.21E+07	6.81E+06
335	SLC4A1AP	1	22	2.65E+08	5.50E+07	2.37E+08	4.92E+07	8.69E+07	0.00E+00	2.25E+08	6.04E+07	1.83E+08	3.53E+07	3.13E+08	9.00E+07
336	DCAF13	2	15	2.15E+08	1.05E+08	3.16E+08	1.61E+08	9.41E+08	3.29E+08	2.27E+06	0.00E+00	2.67E+07	1.01E+07	6.04E+07	1.13E+07
337	CSNK2A2	1	13	2.45E+08	7.36E+07	1.73E+08	8.79E+07	2.48E+08	9.02E+07	1.05E+08	3.16E+07	6.15E+07	2.82E+07	7.66E+07	3.22E+07
338	CHD7	4	49	2.41E+08	7.61E+07	1.46E+08	4.41E+07	4.05E+08	1.12E+08	5.92E+07	8.15E+06	4.99E+07	8.42E+06	1.69E+08	5.27E+07
339	ZC3H13	2	23	2.23E+08	9.28E+07	1.41E+08	1.46E+08	2.07E+08	1.84E+08	1.29E+08	6.52E+07	2.91E+07	1.89E+07	1.77E+08	7.91E+07
340	PYCRL	2	9	2.43E+08	7.15E+07	9.05E+07	3.86E+07	8.86E+07	4.89E+07	1.57E+08	5.40E+07	3.84E+07	3.82E+07	3.15E+08	1.73E+08
341	NAP1L1	5	7	2.47E+08	6.70E+07	8.63E+07	2.72E+07	4.70E+07	1.66E+07	1.97E+07	0.00E+00	3.19E+07	6.18E+06	0.00E+00	0.00E+00
342	GMDS	2	16	2.75E+08	3.87E+07	1.56E+08	6.05E+07	3.47E+08	1.53E+08	8.11E+07	3.19E+07	2.10E+07	1.29E+07	6.67E+07	3.99E+07
343	YWHAQ	4	9	2.14E+08	9.76E+07	1.11E+08	8.21E+07	1.46E+08	7.91E+07	5.94E+07	2.53E+07	7.82E+07	7.29E+07	2.73E+07	1.65E+07
344	MYBBP1A	2	24	2.39E+08	6.93E+07	8.59E+07	3.01E+07	3.77E+08	1.36E+08	5.02E+06	9.49E+05	5.05E+06	0.00E+00	3.03E+06	0.00E+00
345	MIOS	2	19	2.51E+08	5.51E+07	7.63E+07	5.91E+07	1.48E+08	4.61E+07	5.01E+07	1.98E+07	1.16E+07	7.36E+06	1.09E+08	5.09E+07
346	CLK3	3	9	1.52E+08	1.53E+08	5.29E+07	7.24E+07	1.27E+08	1.07E+08	2.34E+07	1.37E+07	1.44E+07	2.83E+07	3.01E+07	4.72E+07
347	TRAP1	2	12	2.30E+08	7.41E+07	7.98E+07	3.03E+07	5.43E+07	2.61E+07	1.19E+07	9.89E+05	1.77E+07	4.81E+06	0.00E+00	0.00E+00
348	GATA6	4	10	2.37E+08	6.44E+07	2.81E+08	1.25E+08	8.08E+08	1.87E+08	5.86E+07	2.34E+07	1.31E+08	7.76E+07	5.57E+07	4.16E+07
349	TAF8	3	4	4.75E+07	2.54E+08	2.55E+07	5.10E+06	5.39E+07	1.00E+07	0.00E+00	0.00E+00	0.00E+00	0.00E+00	0.00E+00	0.00E+00
350	DLX6	4	5	2.58E+08	4.24E+07	1.07E+08	7.25E+06	4.75E+08	1.90E+08	3.96E+07	0.00E+00	2.83E+07	0.00E+00	2.37E+07	0.00E+00
351	NFX1	3	9	2.54E+08	4.60E+07	5.81E+07	3.21E+07	1.70E+08	7.21E+07	2.38E+07	1.20E+07	5.14E+06	4.58E+06	2.78E+07	3.73E+06
352	ARID1B	4	11	2.39E+08	5.91E+07	2.75E+07	2.36E+07	2.85E+08	3.70E+07	1.97E+07	6.01E+06	8.59E+06	1.72E+07	2.57E+07	1.57E+07
353	TFIP11	2	17	2.13E+08	8.47E+07	1.45E+08	7.37E+07	2.68E+08	1.20E+08	1.53E+07	3.62E+06	7.01E+06	6.81E+06	3.39E+07	2.68E+07
354	SURF4	3	5	1.67E+08	1.30E+08	4.03E+07	4.33E+07	1.84E+08	1.73E+08	5.82E+06	4.94E+06	1.08E+07	1.19E+07	2.32E+07	2.16E+07
355	RBM39	3	12	2.32E+08	6.44E+07	8.89E+07	4.49E+07	2.74E+08	8.09E+07	1.41E+07	3.97E+06	1.47E+07	0.00E+00	1.22E+07	0.00E+00
356	CSNK2B	1	9	2.24E+08	6.39E+07	1.73E+08	5.28E+07	2.53E+08	1.25E+08	1.14E+08	2.21E+07	1.66E+08	3.85E+07	2.39E+08	7.18E+06
357	HNRNPA2B	2	13	2.00E+08	8.45E+07	1.03E+08	7.22E+07	6.02E+07	5.30E+07	0.00E+00	0.00E+00	7.26E+07	8.62E+07	1.46E+07	0.00E+00
358	RBBP7	2	11	1.96E+08	8.85E+07	6.15E+07	6.64E+07	4.34E+08	1.71E+08	2.41E+07	2.07E+07	4.17E+07	4.25E+07	1.26E+08	5.44E+07
359	INO80	1	19	1.70E+08	1.12E+08	1.59E+08	1.45E+08	9.23E+07	6.22E+07	2.84E+07	2.20E+07	2.65E+07	2.93E+07	1.62E+07	2.08E+07
360	NSMCE4A	3	10	2.78E+08	1.12E+06	6.40E+07	0.00E+00	1.99E+08	1.24E+06	8.88E+07	0.00E+00	1.85E+07	0.00E+00	7.94E+07	0.00E+00
361	RPL26;RPL2	2	7	2.37E+08	3.94E+07	5.18E+07	1.01E+07	2.49E+08	9.37E+07	0.00E+00	0.00E+00	0.00E+00	0.00E+00	0.00E+00	0.00E+00
362	TIMM50	3	7	2.23E+08	5.25E+07	1.06E+08	2.53E+07	2.59E+08	1.09E+08	1.74E+07	4.54E+06	1.87E+07	4.38E+06	3.30E+07	8.71E+06
363	KHSRP	4	11	2.07E+08	6.10E+07	1.03E+08	4.18E+07	5.23E+07	3.45E+07	1.97E+07	5.91E+06	2.37E+07	6.43E+06	4.67E+06	3.87E+06
364	YY2	1	9	2.66E+08	0.00E+00	1.95E+08	0.00E+00	4.22E+08	0.00E+00	5.77E+07	0.00E+00	4.40E+07	0.00E+00	6.90E+07	0.00E+00
365	RSL1D1	2	8	2.18E+08	4.35E+07	3.22E+07	1.93E+07	9.26E+07	3.37E+07	2.25E+06	0.00E+00	0.00E+00	0.00E+00	0.00E+00	0.00E+00
366	U2AF2	2	7	2.46E+08	1.36E+07	5.41E+07	6.40E+06	9.78E+07	3.59E+06	2.71E+07	2.07E+06	2.36E+07	3.62E+06	3.54E+07	5.33E+06
367	DDOST	3	14	1.87E+08	7.15E+07	1.51E+08	9.51E+07	4.41E+08	1.70E+08	5.34E+06	7.12E+06	3.23E+07	1.57E+07	3.30E+07	1.61E+07
368	BMS1	1	17	2.23E+08	3.11E+07	5.16E+07	3.15E+07	4.19E+08	1.72E+08	0.00E+00	0.00E+00	0.00E+00	0.00E+00	0.00E+00	0.00E+00
369	TECR	2	9	1.75E+08	7.92E+07	8.95E+07	4.04E+07	2.21E+08	6.84E+07	4.38E+06	0.00E+00	9.27E+06	8.77E+06	0.00E+00	0.00E+00
370	CCAR2	2	13	2.29E+08	2.32E+07	2.67E+07	9.39E+06	2.25E+08	5.32E+07	3.61E+07	7.19E+06	2.33E+07	4.98E+06	9.11E+07	1.88E+07
371	EEF1G	2	15	2.21E+08	2.92E+07	7.95E+07	3.74E+07	1.91E+07	0.00E+00	2.53E+07	1.41E+06	5.10E+07	3.31E+07	1.74E+07	8.76E+06
372	MFAP1	4	7	2.03E+08	4.59E+07	2.79E+07	0.00E+00	1.66E+08	2.85E+07	1.98E+07	2.05E+06	0.00E+00	0.00E+00	1.16E+07	2.28E+06
373	CKAP2	4	10	2.27E+08	2.01E+07	8.14E+07	3.03E+07	2.65E+08	5.16E+07	3.15E+07	5.97E+06	0.00E+00	0.00E+00	4.48E+07	1.36E+07
374	HNRNPA3	2	9	1.79E+08	6.77E+07	6.34E+07	4.89E+07	1.85E+08	5.90E+07	0.00E+00	0.00E+00	3.85E+07	2.48E+07	3.33E+07	8.03E+06
375	EIF4A3	1	12	1.96E+08	5.05E+07	8.09E+07	1.61E+07	9.00E+07	3.90E+06	0.00E+00	0.00E+00	0.00E+00	0.00E+00	0.00E+00	0.00E+00
376	LRRC59	1	9	2.18E+08	2.81E+07	1.03E+08	0.00E+00	5.72E+08	7.71E+07	0.00E+00	0.00E+00	0.00E+00	0.00E+00	9.99E+06	0.00E+00
377	TAF6	4	16	1.84E+08	6.15E+07	1.61E+08	7.24E+07	2.24E+08	5.97E+07	1.89E+07	6.35E+06	2.15E+07	1.60E+07	1.41E+07	7.67E+06
378	IPO5	4	16	2.14E+08	3.00E+07	9.86E+07	6.12E+06	1.95E+08	1.79E+07	1.95E+07	4.58E+06	2.43E+07	1.14E+07	4.05E+07	9.76E+06
379	SMURF2	1	19	1.92E+08	5.14E+07	1.14E+08	8.19E+07	2.41E+08	1.51E+08	7.77E+07	5.50E+07	4.21E+07	1.58E+07	2.50E+07	1.27E+07
380	RAB11FIP5	1	12	1.50E+08	9.18E+07	3.33E+07	3.60E+07	2.10E+08	1.47E+08	2.84E+07	1.72E+07	8.29E+06	9.99E+06	5.44E+07	4.13E+07
381	RAB6A;RAE	6	1	1.35E+08	1.07E+08	5.00E+07	5.55E+07	1.25E+08	1.15E+08	9.32E+06	5.93E+06	1.27E+07	1.24E+07	1.41E+07	1.39E+07
382	LMNB1	2	12	1.82E+08	5.92E+07	5.54E+07	1.34E+07	2.24E+07	0.00E+00	2.96E+07	0.00E+00	4.55E+06	0.00E+00	4.01E+06	0.00E+00
383	RPS27L;RPS	2	2	1.90E+08	5.01E+07	7.45E+07	3.13E+07	2.17E+08	7.28E+07	4.78E+06	0.00E+00	0.00E+00	0.00E+00	5.63E+06	0.00E+00
384	SLC9A3R2	3	10	1.87E+08	5.29E+07	1.97E+07	6.14E+06	6.84E+07	2.83E+07	2.82E+06	0.00E+00	0.00E+00	7.37E+06	3.60E+06	0.00E+00
385	PINX1	3	10	2.19E+08	2.07E+07	1.37E+08	1.16E+07	1.89E+08	1.40E+07	4.69E+07	0.00E+00	2.29E+07	0.00E+00	2.75E+07	0.00E+00
386	CAPN1	1	14	2.20E+08	1.90E+07	6.52E+07	8.83E+06	1.07E+08	2.33E+07	8.71E+06	3.19E+06	1.63E+06	0.00E+00	0.00E+00	0.00E+00
387	EEF2	1	22	1.92E+08	4.66E+07	1.07E+08	6.71E+07	2.66E+07	1.48E+07	1.98E+07	3.92E+06	2.21E+08	6.29E+07	2.79E+07	1.40E+07
388	PRPF31	4	8	1.97E+08	3.84E+07	6.09E+07	7.47E+06	8.77E+07	3.31E+07	1.93E+07	4.54E+06	1.57E+07	1.07E+06	2.48E+07	0.00E+00
389	HOXA5	14	5	1.53E+08	8.24E+07	5.19E+07	4.01E+07	1.93E+08	1.47E+08	0.00E+00	0.00E+00	0.00E+00	0.00E+00	0.00E+00	0.00E+00
390	PRDX1	1	10	2.16E+08	1.84E+07	1.11E+08	2.18E+07	9.22E+07	1.53E+07	4.73E+07	4.66E+06	1.75E+08	6.08E+07	1.37E+08	2.85E+07
391	CXXC1	2	7	1.43E+08	8.64E+07	7.05E+07	3.96E+07	9.68E+07	4.22E+07	5.17E+06	3.46E+06	3.69E+06	2.24E+06	2.66E+07	6.35E+06
392	S100A8	1	4	2.29E+08	0.00E+00	0.00E+00	0.00E+00	0.00E+00	0.00E+00	0.00E+00	0.00E+00	0.00E+00	0.00E+00	0.00E+00	0.00E+00
393	SPAG17	1	2	2.27E+08	0.00E+00	0.00E+00	0.00E+00	0.00E+00	0.00E+00	0.00E+00	0.00E+00	0.00E+00	0.00E+00	2.15E+07	0.00E+00
394	MTCL1	4	20	1.61E+08	6.56E+07	5.36E+07	2.11E+07	1.68E+08	8.95E+07	1.92E+07	1.19E+07	1.39E+07	9.88E+06	2.86E+07	1.43E+07
395	DVL3	7	9	1.60E+08	6.62E+07	2.58E+07	2.77E+07	5.81E+07	5.01E+07	5.97E+07	2.77E+07	2.40E+07	1.44E+07	3.73E+07	1.82E+07
396	SYNCRIP	5	10	2.25E+08	0.00E+00	7.99E+07	0.00E+00	9.94E+07	2.59E+07	2.21E+06	0.00E+00	1.23E+07	0.00E+00	2.69E+06	0.00E+00
397	SEH1L	2	12	1.85E+08	3.71E+07	7.12E+07	2.01E+07	1.68E+08	6.38E+07	4.74E+07	3.07E+07	4.11E+07	6.82E+06	1.93E+08	5.56E+07
398	SRPK2	6	13	1.66E+08	5.49E+07	6.19E+07	4.94E+07	1.12E+08	4.62E+07	1.74E+07	7.07E+06	4.82E+06	0.00E+00	2.29E+07	1.10E+07
399	GLUD1;GLU	4	15	1.31E+08	8.96E+07	7.17E+07	4.43E+07	3.48E+07	2.86E+07	1.18E+08	3.90E+07	8.64E+07	4.52E+07	1.32E+08	4.82E+07
400	MZB1	1	1	1.67E+08	5.07E+07	0.00E+00	0.00E+00	0.00E+00	0.00E+00	0.00E+00	0.00E+00	0.00E+00	0.00E+00	0.00E+00	0.00E+00
401	DKC1	2	14	2.03E+08	1.34E+07	5.31E+07	7.18E+06	1.57E+08	1.10E+07	2.29E+07	3.60E+06	1.69E+07	2.47E+06	9.09E+07	1.36E+07
402	HSD17B12	2	10	1.74E+08	4.08E+07	5.40E+07	1.70E+07	1.47E+08	4.96E+07	0.00E+00	0.00E+00	3.09E+06	4.51E+06	1.23E+07	8.02E+06
403	AKAP17A	3	11	1.73E+08	4.04E+07	6.05E+07	1.52E+07	3.58E+07	1.14E+07	3.68E+07	8.88E+06	1.14E+07	1.44E+06	3.63E+07	1.84E+06
404	JUN	2	6	1.59E+08	5.19E+07	1.50E+07	0.00E+00	4.97E+07	2.36E+07	1.04E+07	0.00E+00	4.27E+06	4.91E+06	0.00E+00	0.00E+00
405	SMC6	2	23	2.11E+08	0.00E+00	5.31E+07	2.75E+05	9.94E+07	4.17E+05	9.75E+07	0.00E+00	5.57E+07	5.65E+05	1.97E+08	2.55E+05
406	LMAN2	1	7	1.75E+08	3.61E+07	7.32E+07	3.07E+07	1.89E+08	7.38E+07	0.00E+00	0.00E+00	0.00E+00	0.00E+00	1.20E+07	2.22E+06
407	GNL3	2	14	1.72E+08	3.75E+07	1.00E+08	2.45E+07	3.41E+08	1.02E+08	7.43E+06	2.01E+06	0.00E+00	0.00E+00	1.09E+07	2.24E+06
408	SNRNP70	4	6	1.52E+08	5.58E+07	6.94E+07	3.89E+07	9.27E+07	4.72E+07	6.45E+06	0.00E+00	3.46E+06	8.03E+06	1.10E+07	4.17E+06
409	NFRKB	3	19	1.63E+08	4.37E+07	6.72E+07	3.18E+07	9.32E+07	2.89E+07	2.07E+07	4.83E+07	2.30E+07	3.50E+06	2.03E+07	7.78E+06
410	PM20D2	1	9	1.48E+08	5.68E+07	4.86E+07	1.36E+07	4.10E+07	1.80E+07	5.31E+07	1.31E+07	2.65E+07	1.42E+07	9.14E+07	3.88E+07

MQ search SILAC data

hit number	Gene names	Number of proteins	Peptides	Intensity L 2%SDS_24hHU	Intensity H 2%SDS_24hHU	Intensity L 2%SDS_2hHU	Intensity H 2%SDS_2hHU	Intensity L 2%SDS_NT	Intensity H 2%SDS_NT	Intensity L el150_24hHU	Intensity H el150_24hHU	Intensity L el150_2hHU	Intensity H el150_2hHU	Intensity L el150_NT	Intensity H el150_NT
411	GALNT2	4	9	1.76E+08	2.70E+07	3.73E+07	3.24E+07	2.54E+08	1.16E+08	1.87E+06	0.00E+00	1.51E+06	0.00E+00	0.00E+00	0.00E+00
412	SLC1A5	3	9	1.12E+08	9.08E+07	5.75E+07	7.99E+07	1.76E+08	1.56E+08	1.31E+07	8.69E+06	1.60E+07	1.70E+07	4.60E+07	4.51E+07
413	ATP2A2	15	15	1.73E+08	2.92E+07	4.10E+07	3.20E+07	1.55E+08	2.01E+07	4.03E+06	0.00E+00	1.39E+07	6.56E+06	1.83E+07	4.99E+06
414	DPP9	3	19	1.49E+08	5.22E+07	4.56E+07	3.16E+07	9.65E+07	5.47E+07	1.69E+08	2.52E+07	8.88E+07	4.99E+06	2.18E+08	6.73E+07
415	ZNF444	1	9	1.90E+08	1.17E+07	1.02E+08	1.21E+07	3.25E+08	2.18E+07	0.00E+00	0.00E+00	0.00E+00	0.00E+00	0.00E+00	0.00E+00
416	CREB5	8	8	1.78E+08	2.39E+07	8.09E+07	1.24E+07	3.66E+08	0.00E+00	6.38E+07	4.72E+06	0.00E+00	0.00E+00	2.41E+07	0.00E+00
417	CCNT2	2	14	1.47E+08	5.32E+07	6.89E+07	0.00E+00	1.73E+08	0.00E+00	1.90E+07	0.00E+00	2.93E+07	0.00E+00	3.96E+07	5.97E+06
418	RPL35A	1	4	1.44E+08	5.66E+07	6.57E+06	1.08E+07	2.47E+07	0.00E+00	0.00E+00	0.00E+00	0.00E+00	0.00E+00	0.00E+00	0.00E+00
419	EGLN3;EGL	4	2	2.08E+07	1.79E+08	0.00E+00	0.00E+00	0.00E+00	0.00E+00	0.00E+00	0.00E+00	0.00E+00	0.00E+00	1.14E+07	1.56E+07
420	KTN1	4	12	1.99E+08	0.00E+00	1.25E+08	4.24E+07	1.36E+07	0.00E+00	0.00E+00	0.00E+00	0.00E+00	0.00E+00	0.00E+00	0.00E+00
421	HDAC2	2	11	1.64E+08	3.25E+07	1.97E+08	7.15E+07	3.49E+08	4.77E+07	7.01E+07	1.13E+07	7.53E+07	8.35E+06	1.68E+08	2.85E+07
422	RPS17	1	4	1.96E+08	0.00E+00	4.05E+07	0.00E+00	1.68E+08	0.00E+00	9.05E+06	0.00E+00	7.18E+06	0.00E+00	4.29E+06	0.00E+00
423	H2AFV;H2A	6	4	1.95E+08	0.00E+00	0.00E+00	0.00E+00	0.00E+00	0.00E+00	6.89E+06	0.00E+00	7.25E+06	0.00E+00	0.00E+00	0.00E+00
424	TSR1	1	9	1.32E+08	6.34E+07	4.68E+07	3.56E+07	1.12E+08	5.17E+07	8.28E+06	2.88E+06	2.34E+06	2.59E+06	8.43E+05	1.08E+06
425	PCBP2	13	8	1.55E+08	4.01E+07	5.31E+07	4.87E+07	9.05E+07	3.79E+07	7.78E+06	4.05E+06	1.77E+07	1.39E+07	0.00E+00	0.00E+00
426	SMARCA5	3	11	1.30E+08	6.38E+07	1.74E+07	1.69E+07	1.21E+08	6.61E+07	2.17E+06	2.89E+06	0.00E+00	0.00E+00	8.23E+05	2.17E+06
427	KPNB1	2	14	1.27E+08	6.64E+07	1.12E+08	5.48E+07	2.63E+08	1.18E+08	3.17E+07	1.09E+07	3.11E+07	2.51E+07	1.68E+07	1.66E+07
428	RPL36	1	3	1.31E+08	6.13E+07	2.06E+07	1.72E+07	7.50E+07	4.61E+07	6.96E+06	0.00E+00	0.00E+00	0.00E+00	0.00E+00	0.00E+00
429	RPS13	1	4	8.51E+07	1.07E+08	4.01E+07	3.66E+07	1.46E+08	5.84E+07	0.00E+00	0.00E+00	1.16E+07	3.91E+06	0.00E+00	0.00E+00
430	PITHD1	2	6	1.64E+08	2.77E+07	4.11E+07	5.19E+06	8.23E+07	2.12E+07	7.42E+07	1.73E+07	2.91E+07	1.32E+07	7.77E+07	0.00E+00
431	PPP2CA;PP	3	6	1.53E+08	3.70E+07	6.48E+07	3.35E+07	9.34E+07	5.30E+07	3.69E+07	5.40E+06	3.06E+07	1.14E+07	2.89E+07	1.39E+07
432	IGF2BP2	7	10	1.25E+08	6.38E+07	4.13E+07	1.90E+07	2.25E+08	1.01E+08	3.83E+06	1.54E+06	0.00E+00	0.00E+00	4.41E+06	0.00E+00
433	USP7	2	22	1.76E+08	1.28E+07	4.18E+07	1.25E+07	9.07E+07	5.19E+06	5.17E+07	8.77E+06	2.67E+07	4.52E+06	2.35E+07	4.36E+06
434	RBM5	5	15	1.17E+08	7.06E+07	8.00E+07	6.62E+07	7.84E+07	5.36E+07	1.54E+07	1.18E+07	2.04E+07	1.79E+07	1.05E+07	0.00E+00
435	ELAVL1	2	5	1.33E+08	5.44E+07	4.54E+07	2.61E+07	4.20E+07	3.67E+07	1.06E+07	6.57E+06	1.33E+07	9.85E+06	1.25E+07	8.04E+06
436	CNIH4	1	1	1.07E+08	8.05E+07	7.38E+07	0.00E+00	8.16E+07	0.00E+00	0.00E+00	0.00E+00	1.70E+07	1.89E+07	0.00E+00	0.00E+00
437	BSG	4	4	1.33E+08	5.36E+07	4.58E+07	2.61E+07	2.15E+08	6.83E+07	0.00E+00	0.00E+00	9.03E+06	1.23E+07	1.77E+07	8.77E+06
438	PAXBP1	4	14	1.69E+08	1.71E+07	5.70E+07	1.20E+07	1.82E+08	2.02E+07	7.53E+06	2.89E+06	2.73E+06	0.00E+00	2.04E+07	7.51E+06
439	DNAJA1	2	6	1.31E+08	5.26E+07	3.79E+07	0.00E+00	8.77E+06	8.18E+06	0.00E+00	0.00E+00	0.00E+00	0.00E+00	0.00E+00	0.00E+00
440	S100A9	1	3	1.82E+08	0.00E+00	0.00E+00	0.00E+00	0.00E+00	0.00E+00	0.00E+00	0.00E+00	0.00E+00	0.00E+00	0.00E+00	0.00E+00
441	RBM8A	2	3	1.79E+08	0.00E+00	0.00E+00	0.00E+00	1.92E+07	1.08E+07	0.00E+00	0.00E+00	0.00E+00	0.00E+00	0.00E+00	0.00E+00
442	TFAP2A;TF	7	7	1.19E+08	5.88E+07	7.61E+07	6.17E+07	3.24E+08	1.62E+08	7.56E+06	4.81E+06	3.86E+07	4.05E+07	8.40E+07	4.77E+07
443	SNRPD1	1	4	1.78E+08	0.00E+00	2.95E+07	0.00E+00	0.00E+00	0.00E+00	0.00E+00	0.00E+00	0.00E+00	0.00E+00	7.16E+06	5.97E+06
444	EIF3A	2	8	1.43E+08	3.40E+07	4.67E+07	1.74E+07	2.65E+07	1.14E+07	1.36E+06	0.00E+00	5.45E+06	0.00E+00	0.00E+00	0.00E+00
445	SRPK1	3	10	1.32E+08	4.46E+07	6.56E+07	3.10E+07	1.88E+08	7.65E+07	1.82E+07	5.38E+06	1.80E+07	1.57E+07	3.44E+07	7.09E+06
446	SNRPD3	2	2	1.18E+08	5.81E+07	6.05E+07	3.63E+07	8.02E+07	5.16E+07	5.86E+06	0.00E+00	1.96E+07	1.16E+07	1.75E+07	2.57E+07
447	POP1	1	17	1.67E+08	7.61E+06	6.71E+07	5.89E+06	3.54E+08	3.89E+07	0.00E+00	0.00E+00	0.00E+00	0.00E+00	0.00E+00	0.00E+00
448	ASH2L	3	5	1.74E+08	0.00E+00	9.19E+07	0.00E+00	1.40E+08	0.00E+00	5.30E+06	0.00E+00	9.44E+06	0.00E+00	1.75E+07	0.00E+00
449	NRBP1	1	9	1.73E+08	0.00E+00	5.55E+07	0.00E+00	2.13E+08	0.00E+00	1.20E+08	7.50E+06	9.45E+07	1.11E+07	1.06E+08	1.22E+07
450	LSM14A	3	5	1.52E+08	1.97E+07	2.03E+07	0.00E+00	0.00E+00	0.00E+00	0.00E+00	0.00E+00	0.00E+00	0.00E+00	0.00E+00	0.00E+00
451	ZIC5	1	5	9.02E+07	8.10E+07	4.96E+07	5.19E+07	1.12E+08	1.06E+08	0.00E+00	0.00E+00	2.89E+06	0.00E+00	4.52E+07	3.77E+07
452	TEX10	2	9	1.55E+08	1.66E+07	3.56E+06	0.00E+00	3.42E+07	1.72E+07	0.00E+00	0.00E+00	0.00E+00	0.00E+00	0.00E+00	0.00E+00
453	NFIC;NFIA	10	6	1.05E+08	6.56E+07	6.41E+06	4.16E+06	1.86E+08	7.18E+07	2.84E+07	2.13E+07	1.48E+07	1.08E+07	6.43E+07	3.98E+07
454	SATB2	4	14	1.39E+08	3.02E+07	8.33E+07	2.23E+07	5.95E+07	3.99E+07	7.09E+07	3.09E+07	5.05E+07	2.69E+07	9.71E+07	4.52E+07
455	RBBP5	2	10	1.50E+08	1.88E+07	7.45E+07	3.50E+07	1.64E+08	1.93E+07	2.07E+06	1.63E+06	2.16E+06	2.27E+06	1.47E+07	0.00E+00
456	H2AFY2	1	6	1.34E+08	3.42E+07	0.00E+00	0.00E+00	3.62E+07	0.00E+00	0.00E+00	0.00E+00	0.00E+00	0.00E+00	0.00E+00	0.00E+00
457	PPP2R2A	14	11	1.55E+08	1.32E+07	6.17E+07	1.64E+07	6.66E+07	1.67E+07	4.56E+07	1.32E+07	3.29E+07	1.07E+07	2.10E+07	8.00E+06
458	CTR9	1	12	9.62E+07	7.13E+07	2.07E+07	4.59E+06	1.58E+08	1.06E+08	6.23E+06	3.90E+06	0.00E+00	0.00E+00	3.16E+07	1.12E+07
459	IK	1	6	1.40E+08	2.74E+07	7.09E+07	4.11E+06	1.12E+08	2.60E+07	1.09E+07	0.00E+00	8.36E+06	3.83E+06	2.10E+07	5.44E+06
460	RPS21	1	3	1.14E+08	5.26E+07	5.93E+07	3.56E+07	8.34E+07	5.52E+07	1.32E+07	9.58E+06	8.79E+06	8.90E+06	2.61E+07	1.85E+07
461	PAF1	3	12	8.33E+07	8.34E+07	2.37E+07	5.01E+07	1.33E+08	1.23E+08	1.18E+07	4.89E+06	8.24E+06	3.70E+07	3.98E+07	4.23E+07
462	ACTR5	1	11	1.13E+08	5.29E+07	1.22E+08	5.36E+07	1.29E+08	5.87E+07	1.77E+07	6.51E+06	2.16E+07	1.38E+07	1.63E+07	7.83E+06
463	RPS18	1	7	9.71E+07	6.85E+07	6.68E+07	3.71E+07	8.99E+07	5.28E+07	0.00E+00	0.00E+00	6.56E+06	5.49E+06	0.00E+00	0.00E+00
464	CSTF1	1	7	8.54E+07	7.92E+07	2.41E+07	1.19E+07	7.48E+07	9.52E+07	1.90E+07	7.10E+06	9.48E+06	4.75E+06	3.18E+07	1.66E+07
465	TBL1XR1	2	12	1.27E+08	3.76E+07	2.68E+07	1.64E+07	1.42E+08	6.56E+07	5.46E+07	1.38E+07	1.31E+07	4.21E+06	9.59E+07	3.01E+07
466	DDX54	2	2	9.93E+07	6.50E+07	5.53E+07	4.42E+07	1.18E+08	9.19E+07	5.90E+07	3.87E+07	5.31E+07	4.37E+07	2.85E+07	1.96E+07
467	VEZF1	1	12	1.64E+08	0.00E+00	1.11E+08	0.00E+00	3.99E+08	0.00E+00	1.47E+07	0.00E+00	1.66E+07	0.00E+00	1.43E+07	0.00E+00
468	KBTBD4	2	8	1.23E+08	4.07E+07	7.13E+07	3.20E+07	1.28E+08	6.51E+07	2.14E+07	8.18E+06	1.29E+07	9.51E+06	4.88E+07	2.88E+07
469	TCF20	2	15	1.50E+08	1.11E+07	4.30E+07	0.00E+00	3.69E+08	4.60E+07	1.52E+07	0.00E+00	0.00E+00	0.00E+00	1.25E+07	0.00E+00
470	DLX2;DLX5	4	3	1.60E+08	0.00E+00	5.65E+07	4.88E+07	2.95E+08	9.39E+07	4.70E+07	3.15E+07	3.42E+07	0.00E+00	5.34E+07	1.58E+07
471	CPVL	1	10	1.41E+08	1.68E+07	7.71E+07	7.80E+06	2.04E+08	1.21E+07	3.23E+07	2.25E+06	5.37E+06	0.00E+00	3.54E+07	3.13E+06
472	HDGFRP2	5	7	1.42E+08	1.42E+07	0.00E+00	0.00E+00	0.00E+00	0.00E+00	4.65E+06	0.00E+00	0.00E+00	0.00E+00	0.00E+00	0.00E+00
473	LCLAT1	3	6	1.21E+08	3.49E+07	3.36E+07	9.84E+06	2.60E+08	1.34E+08	0.00E+00	0.00E+00	0.00E+00	0.00E+00	0.00E+00	0.00E+00
474	CSTF3	3	11	9.10E+07	6.48E+07	3.94E+07	1.89E+07	8.11E+07	3.76E+07	9.81E+06	4.21E+06	9.81E+06	6.81E+06	1.94E+07	1.29E+07
475	RNF40	3	17	1.38E+08	1.74E+07	4.83E+07	1.45E+07	2.59E+08	6.43E+07	9.77E+06	3.75E+06	2.55E+07	1.73E+06	8.95E+06	6.73E+06
476	EIF3B	2	8	1.12E+08	4.25E+07	6.35E+07	4.31E+07	0.00E+00	0.00E+00	0.00E+00	0.00E+00	3.56E+06	3.47E+06	0.00E+00	0.00E+00
477	POLDIP3	2	7	1.22E+08	3.17E+07	2.36E+07	0.00E+00	8.49E+07	2.81E+07	0.00E+00	0.00E+00	0.00E+00	0.00E+00	0.00E+00	0.00E+00
478	MED23	5	2	8.82E+07	6.52E+07	0.00E+00	0.00E+00	7.55E+07	7.40E+07	0.00E+00	0.00E+00	0.00E+00	0.00E+00	0.00E+00	0.00E+00
479	RPS25	1	4	1.11E+08	4.24E+07	3.79E+07	2.38E+07	4.07E+07	6.16E+07	4.68E+06	0.00E+00	4.28E+06	0.00E+00	7.14E+06	0.00E+00
480	RPS7	1	6	1.32E+08	2.10E+07	2.85E+07	9.82E+06	6.07E+07	2.12E+07	4.95E+06	0.00E+00	1.07E+07	2.52E+06	3.50E+06	0.00E+00
481	KHDRBS1	4	4	1.25E+08	2.75E+07	3.60E+07	0.00E+00	4.34E+07	0.00E+00	8.36E+06	0.00E+00	7.04E+06	0.00E+00	4.80E+06	0.00E+00
482	GTPBP4	3	11	1.41E+08	1.11E+07	3.89E+07	1.16E+07	1.07E+08	2.94E+07	0.00E+00	0.00E+00	0.00E+00	0.00E+00	1.95E+06	1.39E+06
483	LARP1	8	21	7.56E+07	7.33E+07	1.16E+08	6.23E+07	6.55E+08	2.63E+08	1.83E+06	0.00E+00	4.21E+06	5.71E+06	5.74E+07	1.58E+07
484	SMC5	1	24	1.49E+08	0.00E+00	6.66E+07	0.00E+00	2.31E+08	0.00E+00	8.87E+07	0.00E+00	2.86E+07	0.00E+00	1.92E+08	5.71E+06
485	RAD51	3	1	7.53E+07	7.21E+07	4.20E+07	5.09E+07	4.71E+07	5.97E+07	0.00E+00	0.00E+00	2.16E+07	2.30E+07	3.78E+07	4.48E+07
486	FAM76A	5	6	1.06E+08	4.07E+07	5.83E+07	3.45E+07	1.94E+08	7.06E+07	1.60E+07	9.73E+06	1.88E+07	7.10E+06	5.67E+06	0.00E+00
487	LBR	1	3	9.28E+07	5.41E+07	5.20E+07	5.66E+07	2.24E+07	1.51E+07	2.97E+06	0.00E+00	5.26E+06	5.60E+06	3.28E+06	2.11E+06
488	SPATS2L	4	7	1.00E+08	4.46E+07	1.98E+07	1.22E+07	1.19E+08	3.43E+07	3.94E+06	3.29E+06	3.74E+06	3.20E+06	0.00E+00	0.00E+00
489	CYB5R3	3	5	9.28E+07	5.11E+07	3.23E+07	3.18E+07	1.53E+08	1.09E+08	0.00E+00	0.00E+00	0.00E+00	0.00E+00	4.04E+06	1.89E+06
490	PELP1	1	10	1.04E+08	3.84E+07	1.72E+07	5.36E+06	1.20E+08	5.83E+07	0.00E+00	0.00E+00	0.00E+00	0.00E+00	0.00E+00	0.00E+00
491	GTPBP2	4	8	8.39E+07	5.77E+07	4.00E+06	1.18E+07	8.41E+07	3.17E+07	1.50E+07	8.60E+06	0.00E+00	0.00E+00	1.35E+07	4.55E+06
492	WWP2	4	10	1.06E+08	3.57E+07	3.09E+07	2.39E+07	8.02E+07	5.27E+07	7.18E+06	5.57E+06	5.97E+06	6.65E+06	1.47E+07	5.80E+06

MQ search SILAC data

hit number	Gene names	Number of proteins	Peptides	Intensity L 2%SDS_24hHU	Intensity H 2%SDS_24hHU	Intensity L 2%SDS_2hHU	Intensity H 2%SDS_2hHU	Intensity L 2%SDS_NT	Intensity H 2%SDS_NT	Intensity L el150_24hHU	Intensity H el150_24hHU	Intensity L el150_2hHU	Intensity H el150_2hHU	Intensity L el150_NT	Intensity H el150_NT
493	EBNA1BP2	1	4	1.16E+08	2.41E+07	1.81E+07	7.20E+06	9.28E+07	2.17E+07	0.00E+00	0.00E+00	0.00E+00	0.00E+00	0.00E+00	0.00E+00
494	WDR61	1	10	1.40E+08	0.00E+00	9.89E+07	0.00E+00	2.22E+08	2.00E+07	1.44E+07	0.00E+00	3.08E+07	0.00E+00	9.09E+07	1.30E+07
495	TMED2	1	7	1.07E+08	3.27E+07	3.32E+07	3.06E+07	1.31E+08	8.10E+07	0.00E+00	0.00E+00	0.00E+00	3.89E+06	0.00E+00	0.00E+00
496	ZC3H18	2	5	1.19E+08	1.99E+07	1.50E+07	0.00E+00	2.12E+07	0.00E+00	0.00E+00	0.00E+00	0.00E+00	0.00E+00	0.00E+00	2.87E+06
497	EIF3CL;EIF3	3	9	8.48E+07	5.34E+07	4.42E+07	2.83E+07	1.37E+07	8.24E+06	2.67E+06	1.71E+06	3.59E+06	3.61E+06	0.00E+00	0.00E+00
498	PGAM5	2	3	8.25E+07	5.52E+07	3.96E+07	3.68E+07	1.37E+07	9.83E+06	0.00E+00	0.00E+00	0.00E+00	0.00E+00	0.00E+00	0.00E+00
499	RCC2	1	10	9.92E+07	3.70E+07	2.24E+07	2.27E+07	3.54E+07	3.58E+07	1.40E+07	1.03E+07	1.30E+07	1.13E+07	1.78E+07	1.30E+07
500	RRP12	3	15	9.95E+07	3.67E+07	5.95E+07	4.72E+07	1.00E+08	4.30E+07	0.00E+00	0.00E+00	9.78E+05	6.15E+05	0.00E+00	0.00E+00
501	PRPF38A	1	8	1.17E+08	1.87E+07	4.89E+07	1.51E+07	9.78E+07	4.12E+07	2.51E+07	5.78E+06	1.29E+06	0.00E+00	4.08E+07	1.30E+07
502	NOP56	1	6	9.08E+07	4.51E+07	2.27E+07	2.84E+07	2.22E+07	1.26E+07	0.00E+00	0.00E+00	0.00E+00	0.00E+00	0.00E+00	0.00E+00
503	CLPTM1L	2	8	1.25E+08	1.01E+07	4.06E+07	2.90E+07	1.54E+08	8.35E+07	6.40E+06	3.45E+06	5.37E+06	4.62E+06	1.63E+07	8.06E+06
504	ATP1A1	9	11	1.08E+08	2.63E+07	4.23E+07	2.08E+07	1.11E+08	8.16E+07	7.08E+06	1.74E+06	2.05E+07	1.43E+07	2.67E+07	1.77E+07
505	LEO1	2	6	1.22E+08	1.17E+07	2.05E+07	4.28E+06	7.23E+07	2.74E+07	2.80E+07	1.79E+06	0.00E+00	0.00E+00	7.73E+07	1.63E+07
506	SLC39A6	2	12	8.82E+07	4.40E+07	1.18E+08	8.80E+07	3.25E+08	2.46E+08	1.14E+07	0.00E+00	7.46E+06	1.59E+07	3.67E+07	1.32E+07
507	CAND1	3	14	1.18E+08	1.29E+07	2.92E+07	4.88E+06	1.26E+08	3.92E+07	0.00E+00	0.00E+00	7.30E+06	8.33E+06	3.20E+07	3.73E+06
508	TUBB2B;TU	2	18	7.86E+07	5.23E+07	5.59E+06	9.61E+06	2.97E+07	1.53E+07	0.00E+00	0.00E+00	0.00E+00	0.00E+00	1.07E+07	4.54E+06
509	THOC2	1	11	9.18E+07	3.86E+07	2.56E+07	0.00E+00	2.75E+07	0.00E+00	1.66E+06	0.00E+00	0.00E+00	0.00E+00	9.69E+06	0.00E+00
510	LMNA	6	12	1.05E+08	2.54E+07	4.03E+07	1.37E+07	0.00E+00	0.00E+00	6.15E+07	1.76E+07	2.26E+07	1.33E+07	4.12E+07	1.73E+07
511	CCT6A	2	8	1.27E+08	0.00E+00	5.52E+07	9.25E+06	3.02E+08	1.40E+07	0.00E+00	0.00E+00	2.68E+07	0.00E+00	1.64E+07	0.00E+00
512	HNRNPR	2	17	1.26E+08	0.00E+00	5.72E+07	0.00E+00	7.58E+07	0.00E+00	0.00E+00	0.00E+00	0.00E+00	0.00E+00	0.00E+00	0.00E+00
513	ERH	1	2	1.25E+08	0.00E+00	0.00E+00	0.00E+00	5.12E+07	0.00E+00	0.00E+00	0.00E+00	0.00E+00	0.00E+00	0.00E+00	0.00E+00
514	PLRG1	2	9	1.02E+08	2.31E+07	4.58E+07	4.27E+06	4.91E+07	2.55E+07	2.67E+07	8.02E+06	7.77E+06	6.54E+06	3.15E+07	1.03E+07
515	IQCD	3	1	1.24E+08	0.00E+00	0.00E+00	0.00E+00	0.00E+00	0.00E+00	0.00E+00	0.00E+00	6.42E+07	0.00E+00	0.00E+00	0.00E+00
516	PATL1	4	13	7.74E+07	4.66E+07	3.14E+07	2.16E+07	1.70E+08	7.28E+07	4.63E+07	2.02E+07	2.19E+07	1.97E+07	7.71E+07	4.76E+07
517	POLRMT	1	9	7.05E+07	5.34E+07	8.45E+06	7.87E+06	8.17E+07	5.64E+07	0.00E+00	0.00E+00	0.00E+00	0.00E+00	1.69E+06	1.47E+06
518	SNRPB;SNR	5	5	9.13E+07	3.18E+07	5.37E+07	2.52E+07	2.29E+07	2.40E+07	3.35E+06	3.31E+06	4.93E+06	5.42E+06	1.04E+07	3.94E+06
519	KNOP1	1	7	1.22E+08	0.00E+00	2.80E+07	1.99E+07	3.51E+07	0.00E+00	0.00E+00	0.00E+00	0.00E+00	0.00E+00	0.00E+00	0.00E+00
520	MID1	4	13	8.92E+07	3.22E+07	1.43E+07	0.00E+00	7.33E+07	1.54E+07	6.14E+07	2.95E+07	1.98E+07	1.71E+07	1.20E+08	7.15E+07
521	SMAP	1	4	1.05E+08	1.66E+07	1.73E+07	0.00E+00	2.63E+07	0.00E+00	6.90E+07	9.79E+06	1.18E+07	5.41E+06	2.88E+07	0.00E+00
522	SAP18	2	6	1.21E+08	0.00E+00	4.42E+07	0.00E+00	7.99E+07	2.36E+07	1.60E+06	0.00E+00	0.00E+00	0.00E+00	5.88E+06	0.00E+00
523	BRIX1	1	9	1.11E+08	9.09E+06	4.49E+07	0.00E+00	1.91E+08	4.44E+07	0.00E+00	0.00E+00	0.00E+00	0.00E+00	0.00E+00	0.00E+00
524	TOP2A;TOP	6	9	9.61E+07	2.41E+07	1.42E+07	0.00E+00	1.94E+07	4.17E+06	4.64E+06	0.00E+00	0.00E+00	0.00E+00	9.75E+05	6.11E+05
525	KRT17	6	23	1.20E+08	0.00E+00	3.14E+07	0.00E+00	2.08E+07	0.00E+00	1.45E+08	2.81E+07	6.01E+07	0.00E+00	8.27E+07	3.36E+06
526	MLLT1	1	10	1.19E+08	0.00E+00	1.19E+08	3.19E+07	1.91E+08	3.93E+07	1.77E+07	0.00E+00	6.56E+07	1.93E+07	9.50E+07	5.88E+07
527	NOP58	1	6	9.09E+07	2.75E+07	1.59E+07	0.00E+00	1.11E+07	3.51E+06	1.91E+06	0.00E+00	0.00E+00	0.00E+00	0.00E+00	0.00E+00
528	ZFP64	10	4	5.00E+07	6.82E+07	5.56E+06	0.00E+00	0.00E+00	0.00E+00	1.42E+07	5.61E+06	0.00E+00	0.00E+00	6.81E+06	8.19E+06
529	HTATSF1	1	6	8.73E+07	3.08E+07	4.31E+07	0.00E+00	3.82E+07	2.88E+07	3.60E+07	7.58E+06	1.91E+07	0.00E+00	3.63E+07	1.53E+07
530	NCOA5	1	5	1.03E+08	1.48E+07	2.88E+07	1.92E+07	2.53E+07	8.29E+06	0.00E+00	0.00E+00	0.00E+00	0.00E+00	0.00E+00	0.00E+00
531	SERBP1	4	3	1.17E+08	0.00E+00	3.18E+07	0.00E+00	2.35E+07	0.00E+00	3.20E+06	0.00E+00	3.21E+06	0.00E+00	1.79E+06	0.00E+00
532	CCDC97	1	5	7.98E+07	3.48E+07	5.65E+07	3.30E+07	0.00E+00	0.00E+00	1.77E+07	1.09E+07	6.96E+06	3.95E+06	0.00E+00	0.00E+00
533	TACO1	1	7	1.14E+08	0.00E+00	1.80E+07	0.00E+00	5.83E+07	1.28E+07	2.83E+07	1.20E+07	2.12E+07	1.77E+07	1.54E+07	1.55E+07
534	SMNDC1	1	6	1.12E+08	0.00E+00	5.93E+07	0.00E+00	9.53E+07	0.00E+00	4.74E+07	0.00E+00	3.48E+07	0.00E+00	8.16E+06	0.00E+00
535	GPATCH11	2	4	1.11E+08	0.00E+00	8.40E+07	5.73E+06	2.36E+07	0.00E+00	9.00E+06	0.00E+00	1.08E+07	3.31E+06	5.47E+06	0.00E+00
536	AMMECR1	3	2	1.10E+08	0.00E+00	6.41E+07	0.00E+00	0.00E+00	0.00E+00	0.00E+00	0.00E+00	0.00E+00	0.00E+00	7.74E+06	0.00E+00
537	RNF2	2	9	9.06E+07	1.91E+07	4.83E+07	2.84E+07	8.01E+07	3.49E+07	5.20E+06	0.00E+00	2.39E+07	8.70E+06	1.37E+07	0.00E+00
538	STT3A	2	5	7.97E+07	2.93E+07	2.45E+07	1.86E+07	7.07E+07	4.44E+07	0.00E+00	0.00E+00	0.00E+00	0.00E+00	0.00E+00	0.00E+00
539	TOMM40	2	5	1.07E+08	0.00E+00	1.31E+07	1.20E+07	0.00E+00	0.00E+00	0.00E+00	0.00E+00	0.00E+00	0.00E+00	0.00E+00	0.00E+00
540	TARDBP	2	5	7.82E+07	2.91E+07	3.82E+07	1.83E+07	1.29E+08	4.37E+07	2.05E+06	0.00E+00	4.35E+06	0.00E+00	2.35E+06	0.00E+00
541	NCBP1	1	5	8.89E+07	1.82E+07	1.66E+07	0.00E+00	1.20E+07	2.98E+06	0.00E+00	0.00E+00	0.00E+00	0.00E+00	0.00E+00	0.00E+00
542	TSC22D1	2	3	8.91E+07	1.78E+07	4.73E+07	1.55E+07	6.68E+07	0.00E+00	6.77E+07	1.90E+07	4.53E+07	9.29E+06	6.78E+07	1.43E+07
543	ZGPAT	4	9	5.95E+07	4.66E+07	6.87E+06	7.65E+06	3.42E+07	1.70E+07	2.47E+07	1.37E+07	8.80E+06	6.08E+06	5.11E+06	1.82E+06
544	RBBP4	4	8	1.06E+08	0.00E+00	7.65E+07	0.00E+00	1.89E+08	0.00E+00	1.40E+07	0.00E+00	8.05E+06	0.00E+00	1.08E+07	0.00E+00
545	LUC7L2	4	7	1.05E+08	0.00E+00	9.27E+07	2.14E+07	1.95E+08	2.19E+07	7.79E+07	1.08E+07	5.88E+07	1.06E+07	1.90E+08	5.00E+07
546	EMD	1	3	6.73E+07	3.73E+07	3.59E+07	2.81E+07	5.94E+07	4.82E+07	0.00E+00	0.00E+00	0.00E+00	0.00E+00	0.00E+00	0.00E+00
547	CAPNS1	2	5	8.76E+07	1.66E+07	9.76E+06	1.77E+07	1.68E+07	9.82E+06	0.00E+00	0.00E+00	1.37E+06	1.44E+06	0.00E+00	0.00E+00
548	TPX2	2	13	1.04E+08	0.00E+00	3.92E+06	0.00E+00	8.97E+07	0.00E+00	0.00E+00	0.00E+00	0.00E+00	0.00E+00	5.46E+07	1.61E+07
549	CSNK1D	2	8	5.36E+07	5.04E+07	4.39E+07	4.20E+07	3.82E+08	9.02E+07	1.06E+07	3.47E+06	1.60E+07	1.76E+07	2.66E+07	4.88E+06
550	RBMX2	1	5	6.64E+07	3.65E+07	3.19E+07	3.18E+07	1.65E+08	9.07E+07	0.00E+00	0.00E+00	2.13E+06	3.07E+06	5.70E+06	4.97E+06
551	TP53	9	6	8.01E+07	2.19E+07	2.03E+07	5.44E+06	1.10E+07	6.20E+06	2.42E+07	1.22E+07	4.77E+06	0.00E+00	3.57E+07	9.24E+06
552	SIGMAR1	3	1	6.06E+07	4.04E+07	1.34E+07	1.61E+07	2.76E+07	3.82E+07	0.00E+00	0.00E+00	0.00E+00	0.00E+00	0.00E+00	0.00E+00
553	SF3B6	1	6	1.01E+08	0.00E+00	8.04E+07	0.00E+00	8.66E+07	0.00E+00	0.00E+00	0.00E+00	1.65E+07	8.14E+06	2.10E+07	0.00E+00
554	RPL37	1	2	1.01E+08	0.00E+00	0.00E+00	0.00E+00	0.00E+00	0.00E+00	0.00E+00	0.00E+00	0.00E+00	0.00E+00	0.00E+00	0.00E+00
555	LRRC8E	1	10	6.33E+07	3.65E+07	6.96E+07	6.00E+07	4.57E+07	3.64E+07	1.36E+07	5.29E+06	1.50E+07	4.83E+06	1.77E+07	1.00E+07
556	G3BP1	1	7	6.29E+07	3.59E+07	1.51E+07	0.00E+00	4.69E+07	2.79E+07	1.91E+06	0.00E+00	3.27E+06	0.00E+00	0.00E+00	0.00E+00
557	VDAC3	2	2	7.83E+07	1.94E+07	1.56E+07	0.00E+00	1.36E+07	0.00E+00	0.00E+00	0.00E+00	0.00E+00	0.00E+00	3.24E+06	0.00E+00
558	SYMPK	2	8	8.11E+07	1.60E+07	1.64E+07	6.49E+06	5.09E+07	9.70E+06	7.00E+06	1.82E+06	4.60E+06	2.21E+06	1.99E+06	1.42E+06
559	TBP;TBPL2	3	5	6.71E+07	2.87E+07	2.15E+07	2.49E+07	9.22E+07	2.70E+07	3.26E+07	4.83E+06	2.67E+07	1.17E+07	2.33E+07	1.10E+07
560	XPO1	1	11	7.84E+07	1.73E+07	2.70E+07	0.00E+00	9.95E+07	2.82E+07	4.25E+06	0.00E+00	5.06E+06	1.37E+06	1.70E+07	1.55E+06
561	VARS2	4	14	8.86E+07	6.93E+06	2.36E+07	4.24E+06	1.69E+08	3.22E+07	1.78E+07	2.74E+06	2.03E+07	3.44E+06	9.34E+07	8.60E+06
562	SRRT	5	4	7.48E+07	1.92E+07	8.39E+06	0.00E+00	0.00E+00	0.00E+00	0.00E+00	0.00E+00	0.00E+00	0.00E+00	0.00E+00	0.00E+00
563	DDX42	1	49	5.90E+07	3.44E+07	2.43E+07	2.18E+07	3.81E+07	3.54E+07	3.44E+07	2.55E+07	1.76E+07	1.74E+07	2.58E+07	2.07E+07
564	SFXN1	1	4	6.65E+07	2.68E+07	5.74E+06	0.00E+00	4.94E+07	1.15E+07	0.00E+00	0.00E+00	0.00E+00	0.00E+00	0.00E+00	0.00E+00
565	YLPM1	3	7	7.66E+07	1.67E+07	6.30E+07	1.88E+07	6.48E+07	9.89E+06	8.30E+06	0.00E+00	8.83E+06	0.00E+00	0.00E+00	0.00E+00
566	SEC22B	1	5	6.55E+07	2.78E+07	2.03E+07	2.25E+07	8.15E+07	7.50E+07	0.00E+00	0.00E+00	0.00E+00	0.00E+00	0.00E+00	0.00E+00
567	ATN1	1	8	7.80E+07	1.48E+07	1.04E+08	3.84E+07	1.04E+08	3.14E+07	2.85E+07	7.00E+06	5.76E+07	1.78E+07	8.29E+07	1.92E+07
568	PBX2	2	7	6.16E+07	2.92E+07	1.02E+07	1.28E+07	1.81E+07	1.53E+07	5.71E+07	2.08E+07	2.53E+07	1.46E+07	5.36E+07	1.92E+07
569	ERAL1	2	10	8.98E+07	0.00E+00	9.48E+07	0.00E+00	2.84E+08	3.73E+07	1.93E+07	0.00E+00	3.45E+07	6.27E+06	3.01E+07	2.97E+06
570	GTF2A2	1	3	6.18E+07	2.76E+07	5.28E+07	4.55E+07	6.75E+07	3.53E+07	2.75E+07	2.43E+07	1.05E+07	1.51E+07	3.08E+07	2.93E+07
571	USP9X	4	19	7.61E+07	1.26E+07	2.28E+07	1.70E+07	5.97E+07	1.90E+07	1.76E+07	5.53E+06	3.43E+06	1.41E+06	1.16E+08	3.71E+07
572	NOP2	4	5	6.06E+07	2.77E+07	1.52E+07	5.55E+06	2.22E+07	1.91E+07	1.64E+06	9.38E+05	0.00E+00	0.00E+00	0.00E+00	0.00E+00
573	ASUN	2	9	6.59E+07	2.22E+07	3.02E+07	9.86E+06	9.10E+07	4.92E+07	1.29E+07	4.17E+06	2.66E+06	4.21E+06	3.86E+07	2.23E+07
574	SLC30A5	4	3	6.96E+07	1.78E+07	3.01E+07	0.00E+00	1.42E+07	0.00E+00	3.98E+06	3.01E+06	4.77E+06	0.00E+00	0.00E+00	0.00E+00

MQ search SILAC data

hit number	Gene names	Number of proteins	Peptides	Intensity L 2%SDS_24hHU	Intensity H 2%SDS_24hHU	Intensity L 2%SDS_2hHU	Intensity H 2%SDS_2hHU	Intensity L 2%SDS_NT	Intensity H 2%SDS_NT	Intensity L el150_24hHU	Intensity H el150_24hHU	Intensity L el150_2hHU	Intensity H el150_2hHU	Intensity L el150_NT	Intensity H el150_NT
575	ZNF771	4	7	7.29E+07	1.40E+07	3.56E+07	1.09E+07	2.08E+08	1.38E+08	0.00E+00	0.00E+00	0.00E+00	0.00E+00	0.00E+00	0.00E+00
576	BMI1	2	3	5.07E+07	3.62E+07	2.63E+07	1.58E+07	5.46E+07	3.34E+07	4.19E+06	2.53E+06	0.00E+00	0.00E+00	0.00E+00	0.00E+00
577	YTHDC1	2	7	5.72E+07	2.90E+07	7.86E+06	1.83E+06	0.00E+00	1.47E+07	0.00E+00	0.00E+00	0.00E+00	0.00E+00	0.00E+00	0.00E+00
578	SKIV2L2	1	9	7.43E+07	1.14E+07	5.76E+07	1.37E+07	4.64E+07	1.31E+07	2.34E+07	1.69E+06	2.27E+07	0.00E+00	3.63E+07	3.47E+06
579	SUPT6H	3	8	8.37E+07	1.86E+06	0.00E+00	0.00E+00	0.00E+00	0.00E+00	0.00E+00	0.00E+00	0.00E+00	0.00E+00	0.00E+00	0.00E+00
580	TUBAL3	2	3	4.76E+07	3.79E+07	2.40E+07	2.46E+07	4.74E+07	4.16E+07	5.30E+06	4.82E+06	9.52E+06	8.22E+06	1.27E+07	1.10E+07
581	ACTR8	3	7	5.92E+07	2.61E+07	4.15E+07	3.04E+07	5.89E+07	2.44E+07	2.74E+06	0.00E+00	3.31E+06	0.00E+00	2.23E+06	0.00E+00
582	ALKBH2	2	5	6.55E+07	1.95E+07	1.30E+07	1.43E+07	1.20E+08	9.54E+07	7.59E+06	8.42E+06	0.00E+00	7.07E+06	2.12E+07	8.27E+06
583	FGB	1	2	8.48E+07	0.00E+00	7.92E+07	0.00E+00	8.84E+07	0.00E+00	7.35E+07	0.00E+00	7.20E+07	0.00E+00	7.04E+07	0.00E+00
584	CCNL1	4	7	5.20E+07	3.25E+07	1.56E+07	1.32E+07	1.48E+08	8.72E+07	4.34E+07	7.62E+06	2.72E+07	1.80E+07	5.26E+07	4.43E+07
585	TAF1;TAF1I	13	10	7.08E+07	1.36E+07	2.98E+07	1.46E+07	2.21E+07	1.21E+07	0.00E+00	0.00E+00	0.00E+00	0.00E+00	0.00E+00	0.00E+00
586	ALB	4	10	8.40E+07	0.00E+00	2.08E+07	0.00E+00	3.04E+07	0.00E+00	2.07E+07	0.00E+00	9.50E+07	0.00E+00	1.07E+08	0.00E+00
587	GIT2	11	16	5.73E+07	2.59E+07	2.30E+07	1.35E+07	3.58E+07	1.51E+07	5.59E+07	1.50E+07	4.12E+07	1.31E+07	5.11E+07	2.16E+07
588	GRWD1	1	3	5.65E+07	2.65E+07	8.06E+06	6.29E+06	1.22E+07	0.00E+00	0.00E+00	0.00E+00	0.00E+00	0.00E+00	0.00E+00	0.00E+00
589	MEIS1	2	7	6.84E+07	1.41E+07	2.30E+07	0.00E+00	5.41E+07	1.40E+07	3.04E+07	1.10E+07	3.59E+07	1.15E+07	4.09E+07	3.09E+07
590	ZNF273;ZN	46	2	2.88E+07	5.36E+07	0.00E+00	4.44E+07	2.97E+07	9.03E+07	0.00E+00	0.00E+00	0.00E+00	1.64E+07	0.00E+00	8.18E+06
591	HADHA	1	11	6.51E+07	1.72E+07	1.32E+07	1.33E+07	1.37E+08	2.31E+07	0.00E+00	0.00E+00	0.00E+00	0.00E+00	4.19E+06	1.30E+06
592	SNRPD2	2	6	6.44E+07	1.72E+07	3.09E+07	0.00E+00	1.90E+07	0.00E+00	6.14E+06	0.00E+00	5.09E+06	0.00E+00	8.61E+06	3.57E+06
593	PAPD7	2	9	5.08E+07	3.03E+07	4.89E+07	1.13E+07	1.23E+08	8.16E+07	3.50E+06	1.29E+06	5.96E+06	6.03E+06	3.60E+07	1.13E+07
594	XRCC6	2	13	8.03E+07	0.00E+00	3.99E+07	8.72E+06	3.88E+07	0.00E+00	2.00E+07	3.42E+06	2.55E+07	8.76E+06	4.45E+06	3.52E+06
595	ZNF768	1	4	2.65E+07	5.38E+07	2.13E+07	1.34E+07	5.88E+07	9.05E+07	3.15E+06	2.48E+06	0.00E+00	0.00E+00	3.12E+06	4.48E+06
596	DNAJA2	1	9	7.97E+07	0.00E+00	0.00E+00	0.00E+00	7.86E+07	0.00E+00	5.47E+06	0.00E+00	4.23E+06	0.00E+00	2.86E+06	4.04E+06
597	RAN	1	7	7.97E+07	0.00E+00	3.88E+07	6.64E+06	4.60E+07	0.00E+00	9.67E+06	0.00E+00	4.86E+07	4.02E+06	1.03E+07	3.14E+06
598	EBP	1	2	4.20E+07	3.75E+07	2.24E+07	3.03E+07	0.00E+00	0.00E+00	0.00E+00	0.00E+00	0.00E+00	0.00E+00	0.00E+00	0.00E+00
599	PHB2	2	7	3.45E+07	4.46E+07	3.06E+07	3.74E+07	3.24E+06	2.38E+06	0.00E+00	0.00E+00	5.95E+06	6.94E+06	0.00E+00	0.00E+00
600	DDB1	2	11	4.71E+07	3.14E+07	2.63E+07	1.31E+07	2.91E+07	6.80E+06	2.79E+06	9.99E+05	6.22E+06	4.95E+06	6.68E+06	1.99E+06
601	GAPDH	3	12	6.13E+07	1.71E+07	1.02E+08	6.11E+07	3.92E+07	7.49E+06	2.97E+07	3.24E+06	3.31E+08	1.08E+08	5.05E+07	1.49E+07
602	RAB7A	1	7	7.83E+07	0.00E+00	3.74E+07	0.00E+00	1.39E+08	0.00E+00	0.00E+00	0.00E+00	0.00E+00	0.00E+00	0.00E+00	0.00E+00
603	NFIX	7	5	6.42E+07	1.32E+07	2.18E+07	6.77E+06	2.39E+07	2.22E+07	5.74E+06	0.00E+00	4.44E+06	4.30E+06	2.14E+07	0.00E+00
604	DDX50	1	9	5.32E+07	2.42E+07	9.26E+06	6.32E+06	5.01E+07	3.81E+07	5.87E+05	3.53E+05	0.00E+00	0.00E+00	0.00E+00	0.00E+00
605	EIF3D	3	4	5.13E+07	2.56E+07	6.00E+06	1.82E+07	5.04E+06	5.06E+06	0.00E+00	0.00E+00	7.04E+06	2.95E+06	0.00E+00	0.00E+00
606	CHD1	2	12	7.49E+07	1.64E+06	1.49E+07	0.00E+00	1.33E+08	3.10E+07	5.77E+06	0.00E+00	3.42E+06	0.00E+00	0.00E+00	0.00E+00
607	CLK1	4	6	5.82E+07	1.81E+07	0.00E+00	0.00E+00	7.87E+07	1.93E+07	4.27E+06	0.00E+00	0.00E+00	0.00E+00	0.00E+00	0.00E+00
608	UGT8	1	12	7.00E+07	5.86E+06	2.65E+08	1.08E+08	4.28E+08	9.86E+07	7.02E+06	0.00E+00	6.23E+07	1.54E+07	3.56E+07	1.73E+06
609	TLE1	4	23	6.03E+07	1.49E+07	6.06E+07	1.88E+07	4.84E+07	0.00E+00	1.41E+08	2.99E+07	6.54E+07	2.74E+07	2.22E+08	6.61E+07
610	ZNF326	3	6	4.18E+07	3.23E+07	3.70E+07	1.68E+07	3.20E+07	1.34E+07	0.00E+00	0.00E+00	0.00E+00	0.00E+00	0.00E+00	0.00E+00
611	EPPK1	10	4	5.84E+07	1.55E+07	7.61E+06	4.11E+06	0.00E+00	0.00E+00	0.00E+00	0.00E+00	0.00E+00	0.00E+00	0.00E+00	0.00E+00
612	RBBP6	3	7	7.38E+07	0.00E+00	2.29E+07	0.00E+00	1.88E+07	4.80E+06	9.84E+06	0.00E+00	1.22E+07	0.00E+00	1.32E+07	1.92E+06
613	SEC61A1	2	5	5.93E+07	1.42E+07	2.94E+07	1.30E+07	2.90E+07	0.00E+00	0.00E+00	0.00E+00	1.49E+06	0.00E+00	0.00E+00	0.00E+00
614	PPIA	8	5	5.54E+07	1.80E+07	7.00E+07	2.60E+07	3.01E+07	1.97E+07	1.70E+07	6.26E+06	1.36E+08	4.23E+07	3.24E+07	8.19E+06
615	CCT7	4	9	7.27E+07	0.00E+00	5.12E+07	2.06E+07	1.57E+08	6.62E+07	9.54E+06	0.00E+00	2.27E+07	1.48E+07	3.83E+07	1.99E+07
616	RCL1	2	6	6.65E+07	5.98E+06	0.00E+00	0.00E+00	9.59E+07	1.48E+07	0.00E+00	0.00E+00	0.00E+00	0.00E+00	0.00E+00	0.00E+00
617	COPA	2	10	7.24E+07	0.00E+00	1.89E+07	6.43E+06	7.61E+07	1.51E+07	0.00E+00	0.00E+00	8.88E+06	4.38E+06	8.00E+06	3.59E+06
618	STIM1	2	5	5.87E+07	1.36E+07	2.69E+07	1.45E+07	9.42E+07	6.52E+07	8.65E+06	2.56E+06	6.26E+06	2.76E+06	1.08E+07	3.98E+06
619	SMARCB1	2	6	4.41E+07	2.74E+07	5.64E+07	3.96E+07	5.37E+07	2.03E+07	2.28E+07	5.60E+06	1.94E+07	8.56E+06	1.91E+07	1.32E+07
620	PPIH	2	4	5.67E+07	1.43E+07	9.20E+06	0.00E+00	1.67E+07	1.15E+07	4.11E+06	3.30E+06	0.00E+00	5.19E+06	3.53E+06	2.98E+06
621	RFC5	2	5	4.64E+07	2.41E+07	3.41E+07	1.69E+07	5.32E+06	5.35E+06	0.00E+00	0.00E+00	0.00E+00	0.00E+00	2.60E+06	2.29E+06
622	WDR60	1	13	6.24E+07	7.69E+06	4.42E+06	0.00E+00	1.10E+08	2.79E+07	1.38E+07	3.06E+06	0.00E+00	0.00E+00	7.90E+07	1.86E+07
623	TMEM43	1	2	3.47E+07	3.46E+07	2.75E+06	1.95E+06	3.70E+06	2.18E+06	0.00E+00	0.00E+00	0.00E+00	0.00E+00	0.00E+00	0.00E+00
624	RAB1A	6	6	6.89E+07	0.00E+00	3.79E+07	0.00E+00	1.57E+08	3.18E+07	3.85E+06	0.00E+00	0.00E+00	0.00E+00	6.87E+06	0.00E+00
625	TMED10	1	4	5.43E+07	1.31E+07	3.18E+07	1.14E+07	6.44E+07	2.09E+07	2.68E+06	0.00E+00	3.95E+06	0.00E+00	0.00E+00	0.00E+00
626	CAAP1	2	3	6.69E+07	0.00E+00	1.86E+07	0.00E+00	3.92E+07	0.00E+00	6.50E+06	0.00E+00	8.01E+06	0.00E+00	5.51E+06	0.00E+00
627	RPL36AL;Rl	2	1	4.92E+07	1.74E+07	2.75E+07	2.09E+07	7.36E+07	1.17E+08	0.00E+00	0.00E+00	0.00E+00	0.00E+00	0.00E+00	0.00E+00
628	PFKP	3	5	4.89E+07	1.76E+07	1.11E+07	1.12E+07	1.06E+08	3.82E+07	0.00E+00	0.00E+00	7.71E+06	0.00E+00	1.93E+07	4.32E+06
629	SENP1	2	5	5.63E+07	1.01E+07	0.00E+00	0.00E+00	7.37E+07	2.49E+07	3.06E+06	0.00E+00	0.00E+00	0.00E+00	0.00E+00	0.00E+00
630	HP1BP3	4	4	4.43E+07	2.15E+07	9.40E+06	9.65E+06	5.03E+07	3.08E+07	0.00E+00	0.00E+00	0.00E+00	0.00E+00	0.00E+00	0.00E+00
631	WDR48	5	11	3.46E+07	3.09E+07	4.49E+06	8.60E+06	1.01E+08	2.39E+07	9.11E+06	0.00E+00	2.25E+06	0.00E+00	4.08E+07	8.27E+06
632	PKM	5	17	6.51E+07	0.00E+00	1.14E+08	2.62E+07	1.93E+07	2.32E+07	6.41E+06	0.00E+00	2.15E+08	7.55E+07	1.80E+06	1.38E+06
633	PGRMC1	2	4	5.74E+07	7.37E+06	2.81E+07	2.61E+07	8.18E+07	4.19E+07	0.00E+00	0.00E+00	0.00E+00	0.00E+00	0.00E+00	0.00E+00
634	LNP	4	3	6.47E+07	0.00E+00	1.08E+07	0.00E+00	1.19E+07	1.04E+07	0.00E+00	0.00E+00	0.00E+00	0.00E+00	4.05E+06	0.00E+00
635	PCBP1	1	4	4.27E+07	2.17E+07	0.00E+00	0.00E+00	0.00E+00	0.00E+00	0.00E+00	0.00E+00	9.00E+05	0.00E+00	0.00E+00	0.00E+00
636	IWS1	3	5	6.41E+07	0.00E+00	4.71E+06	0.00E+00	0.00E+00	0.00E+00	0.00E+00	0.00E+00	0.00E+00	0.00E+00	0.00E+00	0.00E+00
637	LSM2	1	2	3.76E+07	2.53E+07	2.14E+07	2.00E+07	4.47E+07	3.08E+07	0.00E+00	0.00E+00	0.00E+00	0.00E+00	0.00E+00	0.00E+00
638	DPF2	2	3	4.08E+07	2.20E+07	3.41E+07	0.00E+00	3.72E+07	2.23E+07	8.36E+06	4.35E+06	6.43E+06	6.91E+06	6.94E+06	5.91E+06
639	EIF3G	1	2	4.44E+07	1.80E+07	8.99E+06	7.81E+06	1.07E+07	8.37E+06	0.00E+00	0.00E+00	0.00E+00	0.00E+00	0.00E+00	0.00E+00
640	YWHAZ	2	7	4.95E+07	1.27E+07	5.14E+06	0.00E+00	1.68E+07	0.00E+00	1.40E+07	3.45E+06	3.65E+07	9.96E+06	1.30E+07	3.93E+06
641	EBF3;EBF2;	8	6	4.45E+07	1.76E+07	2.27E+07	3.26E+07	8.64E+07	3.35E+07	1.41E+07	4.31E+06	0.00E+00	0.00E+00	2.40E+07	1.88E+07
642	RAB2A;RAE	3	4	5.18E+07	1.03E+07	2.39E+07	2.76E+07	1.46E+07	2.56E+07	0.00E+00	0.00E+00	0.00E+00	0.00E+00	0.00E+00	0.00E+00
643	SNW1	1	3	4.47E+07	1.70E+07	1.23E+07	1.15E+07	0.00E+00	0.00E+00	0.00E+00	0.00E+00	0.00E+00	0.00E+00	0.00E+00	0.00E+00
644	HNRNPH2	1	8	5.00E+07	1.14E+07	1.22E+07	8.71E+06	1.63E+07	1.25E+07	2.93E+06	0.00E+00	3.51E+06	0.00E+00	3.12E+06	2.13E+06
645	ASCC3	2	11	5.72E+07	4.01E+06	1.68E+07	2.93E+06	3.93E+07	6.67E+06	3.09E+06	0.00E+00	1.02E+06	0.00E+00	1.11E+07	1.36E+07
646	INO80E	2	4	6.11E+07	0.00E+00	2.82E+07	5.43E+06	2.17E+07	0.00E+00	7.13E+06	2.29E+06	0.00E+00	0.00E+00	2.99E+06	3.40E+06
647	VAPA	2	4	6.10E+07	0.00E+00	4.40E+07	0.00E+00	8.47E+07	1.51E+07	0.00E+00	0.00E+00	0.00E+00	0.00E+00	0.00E+00	0.00E+00
648	DOCK9	5	13	5.19E+07	8.84E+06	8.82E+06	3.59E+06	1.84E+07	5.51E+06	1.35E+07	3.60E+06	2.88E+06	0.00E+00	6.89E+07	1.64E+07
649	SEC13	4	2	3.59E+07	2.47E+07	1.19E+07	1.48E+07	3.00E+07	2.91E+07	0.00E+00	0.00E+00	0.00E+00	0.00E+00	7.34E+06	5.08E+06
650	ARF1;ARF3	5	5	6.00E+07	0.00E+00	2.19E+07	0.00E+00	1.94E+07	0.00E+00	0.00E+00	0.00E+00	4.56E+06	3.57E+06	0.00E+00	0.00E+00
651	HSPA4	2	7	5.40E+07	4.62E+06	2.48E+07	1.11E+07	2.31E+07	1.84E+07	1.45E+07	3.59E+06	2.01E+07	7.20E+06	4.70E+07	3.08E+07
652	NOL9	1	4	5.61E+07	2.29E+06	2.80E+06	0.00E+00	8.83E+06	2.53E+06	0.00E+00	0.00E+00	0.00E+00	0.00E+00	0.00E+00	0.00E+00
653	LYAR	1	3	4.53E+07	1.26E+07	1.18E+07	0.00E+00	6.81E+06	0.00E+00	0.00E+00	0.00E+00	0.00E+00	0.00E+00	0.00E+00	0.00E+00
654	PNN	1	4	4.48E+07	1.25E+07	5.38E+06	0.00E+00	6.60E+06	0.00E+00	0.00E+00	0.00E+00	0.00E+00	0.00E+00	0.00E+00	0.00E+00
655	WDR18	1	4	5.25E+07	4.76E+06	1.32E+07	0.00E+00	2.61E+07	0.00E+00	0.00E+00	0.00E+00	0.00E+00	0.00E+00	0.00E+00	0.00E+00
656	RPL32	1	6	5.72E+07	0.00E+00	7.63E+07	0.00E+00	9.60E+07	4.58E+07	0.00E+00	0.00E+00	0.00E+00	0.00E+00	0.00E+00	0.00E+00

MQ search SILAC data

hit number	Gene names	Number of proteins	Peptides	Intensity L 2%SDS_24hHU	Intensity H 2%SDS_24hHU	Intensity L 2%SDS_2hHU	Intensity H 2%SDS_2hHU	Intensity L 2%SDS_NT	Intensity H 2%SDS_NT	Intensity L el150_24hHU	Intensity H el150_24hHU	Intensity L el150_2hHU	Intensity H el150_2hHU	Intensity L el150_NT	Intensity H el150_NT
657	ZNF646	2	2	3.34E+07	2.38E+07	5.29E+06	3.99E+06	0.00E+00	0.00E+00	4.96E+06	3.55E+06	0.00E+00	0.00E+00	0.00E+00	0.00E+00
658	SLC3A2	4	5	4.92E+07	7.90E+06	1.86E+07	1.17E+07	5.28E+07	1.97E+07	6.07E+06	1.68E+06	3.35E+06	1.86E+06	6.50E+06	3.48E+06
659	SCAMP3	2	4	4.90E+07	7.97E+06	1.55E+07	1.03E+07	3.07E+07	1.63E+07	0.00E+00	0.00E+00	0.00E+00	0.00E+00	0.00E+00	0.00E+00
660	RAP1B;RAF	6	4	3.48E+07	2.22E+07	1.44E+07	1.60E+07	6.81E+07	2.54E+07	2.11E+06	1.27E+06	1.43E+06	0.00E+00	0.00E+00	3.20E+06
661	SMAD5	1	13	3.36E+07	2.15E+07	2.13E+08	7.84E+07	3.15E+08	1.42E+08	4.40E+07	0.00E+00	7.46E+07	2.43E+06	9.07E+07	2.46E+07
662	IPO7	1	7	4.65E+07	8.42E+06	4.06E+07	1.94E+07	2.75E+07	4.30E+06	7.89E+06	1.51E+06	5.51E+06	1.86E+06	3.43E+06	1.72E+06
663	DIAPH3	7	10	2.44E+07	3.00E+07	2.15E+06	2.00E+06	1.07E+07	7.27E+06	6.03E+06	0.00E+00	0.00E+00	0.00E+00	2.95E+07	1.21E+07
664	BRSK1	9	5	5.43E+07	0.00E+00	0.00E+00	0.00E+00	4.11E+07	0.00E+00	2.00E+07	0.00E+00	0.00E+00	0.00E+00	2.49E+07	0.00E+00
665	DOCK11	1	18	2.87E+07	2.53E+07	1.18E+07	4.86E+06	9.83E+06	0.00E+00	1.32E+07	0.00E+00	0.00E+00	0.00E+00	7.82E+07	4.19E+07
666	AXIN1	2	6	4.06E+07	1.28E+07	1.81E+07	1.69E+07	3.82E+07	2.72E+07	0.00E+00	0.00E+00	0.00E+00	0.00E+00	1.15E+07	6.74E+06
667	ZNF740	1	6	5.34E+07	0.00E+00	3.33E+07	1.33E+07	4.86E+07	1.34E+07	0.00E+00	0.00E+00	0.00E+00	0.00E+00	8.01E+06	0.00E+00
668	UTS2	2	1	3.56E+07	1.77E+07	1.24E+07	1.15E+07	2.41E+07	0.00E+00	1.11E+07	0.00E+00	0.00E+00	0.00E+00	7.43E+06	0.00E+00
669	YWHAE	2	9	5.30E+07	0.00E+00	1.88E+07	0.00E+00	3.04E+07	0.00E+00	1.66E+07	0.00E+00	5.44E+07	0.00E+00	9.79E+06	0.00E+00
670	BAIAP2L1	1	5	4.64E+07	6.49E+06	1.53E+07	0.00E+00	9.52E+06	3.89E+06	8.79E+06	3.01E+06	3.52E+06	0.00E+00	1.89E+07	6.65E+06
671	KRT2	2	47	5.29E+07	0.00E+00	4.81E+07	0.00E+00	6.90E+07	0.00E+00	2.71E+07	0.00E+00	1.46E+08	0.00E+00	8.94E+07	0.00E+00
672	FBRS	2	9	5.29E+07	0.00E+00	4.34E+07	1.29E+07	2.99E+07	5.93E+06	7.33E+07	2.38E+06	8.01E+07	6.12E+06	7.48E+07	2.42E+07
673	THAP11	1	3	3.54E+07	1.68E+07	2.75E+07	1.97E+07	1.17E+08	8.12E+07	5.05E+06	4.35E+06	9.92E+06	5.89E+06	8.36E+06	5.05E+06
674	ZNF652	3	3	5.21E+07	0.00E+00	2.65E+07	0.00E+00	2.44E+07	0.00E+00	5.73E+06	0.00E+00	0.00E+00	0.00E+00	6.64E+06	0.00E+00
675	DDX28	1	8	4.45E+07	7.25E+06	3.25E+07	2.97E+06	1.44E+08	1.43E+07	0.00E+00	0.00E+00	0.00E+00	0.00E+00	0.00E+00	0.00E+00
676	MIF4GD	3	6	2.09E+07	3.07E+07	1.65E+07	4.36E+06	2.45E+07	6.34E+06	2.44E+07	1.41E+07	1.88E+07	3.89E+06	2.58E+06	2.10E+06
677	UCHL5	4	4	4.31E+07	8.49E+06	2.74E+07	2.85E+07	3.37E+07	4.00E+07	3.56E+06	3.20E+06	1.43E+07	1.15E+07	1.45E+07	9.71E+06
678	DDX47	2	7	2.98E+07	2.17E+07	2.29E+07	2.08E+07	5.35E+07	3.40E+07	4.45E+06	1.79E+06	3.09E+07	2.54E+07	3.43E+07	2.07E+07
679	PHC2	8	6	3.49E+07	1.63E+07	2.13E+07	9.07E+06	1.38E+08	4.16E+07	5.13E+06	0.00E+00	3.86E+06	0.00E+00	5.10E+06	0.00E+00
680	RFC2	2	4	4.51E+07	5.95E+06	2.70E+07	1.39E+07	8.33E+07	3.25E+07	8.27E+05	0.00E+00	1.17E+06	1.23E+06	6.22E+06	5.59E+06
681	ZNF358	1	6	4.47E+07	6.06E+06	1.48E+07	1.13E+07	5.90E+07	5.39E+07	0.00E+00	0.00E+00	0.00E+00	0.00E+00	0.00E+00	0.00E+00
682	GRB10	4	7	3.25E+07	1.80E+07	1.26E+07	1.16E+07	3.99E+07	3.46E+07	2.23E+07	8.03E+06	3.79E+06	3.65E+06	2.07E+07	2.17E+07
683	TUBG1;TUI	2	9	3.25E+07	1.77E+07	9.92E+06	7.09E+06	7.69E+07	3.75E+07	0.00E+00	0.00E+00	0.00E+00	0.00E+00	7.47E+07	4.01E+07
684	SLC25A11	2	5	3.45E+07	1.55E+07	1.56E+07	2.36E+07	1.47E+07	7.92E+06	2.14E+06	0.00E+00	2.07E+06	2.12E+06	2.73E+06	1.53E+06
685	SLC16A1	2	2	3.99E+07	1.00E+07	2.76E+07	3.05E+07	8.04E+07	4.74E+07	0.00E+00	0.00E+00	0.00E+00	4.03E+06	5.22E+06	4.30E+06
686	TUBA1A;TU	6	21	4.98E+07	0.00E+00	0.00E+00	0.00E+00	6.23E+07	0.00E+00	1.46E+07	2.08E+06	9.04E+05	1.56E+06	1.95E+06	2.64E+06
687	SRSF1	3	1	3.23E+07	1.71E+07	1.10E+07	9.32E+06	1.26E+07	1.07E+07	3.93E+06	2.92E+06	7.45E+06	8.88E+06	8.31E+06	6.91E+06
688	FAU	1	1	4.90E+07	0.00E+00	0.00E+00	0.00E+00	0.00E+00	0.00E+00	0.00E+00	0.00E+00	0.00E+00	0.00E+00	0.00E+00	0.00E+00
689	ATP5C1	2	4	2.73E+07	2.12E+07	2.08E+07	2.92E+06	1.48E+08	2.89E+07	0.00E+00	0.00E+00	4.73E+06	0.00E+00	0.00E+00	0.00E+00
690	NHP2L1	1	1	2.73E+07	2.05E+07	1.65E+07	1.74E+07	0.00E+00	0.00E+00	0.00E+00	0.00E+00	0.00E+00	0.00E+00	0.00E+00	0.00E+00
691	SRSF6	6	5	4.37E+07	3.78E+06	1.10E+07	2.11E+07	0.00E+00	0.00E+00	0.00E+00	0.00E+00	1.38E+07	7.01E+06	8.47E+06	5.29E+06
692	RSRC1	2	2	4.65E+07	0.00E+00	0.00E+00	0.00E+00	3.41E+07	0.00E+00	0.00E+00	0.00E+00	0.00E+00	0.00E+00	1.55E+07	0.00E+00
693	NAF1	2	3	4.43E+07	2.00E+06	3.27E+07	1.42E+06	6.16E+07	2.38E+06	1.50E+06	7.00E+05	0.00E+00	0.00E+00	2.05E+07	1.26E+06
694	DAD1	1	1	2.78E+07	1.80E+07	1.19E+07	1.09E+07	2.36E+07	1.85E+07	0.00E+00	0.00E+00	0.00E+00	0.00E+00	0.00E+00	0.00E+00
695	LMAN1	1	5	3.69E+07	8.88E+06	9.77E+07	2.82E+07	1.72E+08	1.27E+07	0.00E+00	0.00E+00	0.00E+00	0.00E+00	0.00E+00	0.00E+00
696	GNL3L	1	10	3.26E+07	1.25E+07	1.01E+08	1.92E+07	2.53E+08	3.64E+07	0.00E+00	0.00E+00	9.97E+06	5.84E+06	2.03E+07	5.68E+06
697	RPUSD3	3	5	3.68E+07	8.34E+06	0.00E+00	7.14E+06	1.24E+08	1.75E+07	4.82E+06	0.00E+00	0.00E+00	0.00E+00	5.14E+06	0.00E+00
698	SNRPF	1	1	2.47E+07	2.04E+07	1.77E+07	1.52E+07	0.00E+00	1.31E+07	0.00E+00	0.00E+00	0.00E+00	0.00E+00	0.00E+00	0.00E+00
699	BCL7A;BCL	7	2	2.45E+07	2.03E+07	0.00E+00	0.00E+00	0.00E+00	0.00E+00	0.00E+00	0.00E+00	0.00E+00	0.00E+00	5.78E+06	0.00E+00
700	FTSJ3	1	3	4.47E+07	0.00E+00	9.84E+06	0.00E+00	0.00E+00	0.00E+00	0.00E+00	0.00E+00	0.00E+00	0.00E+00	0.00E+00	0.00E+00
701	HNRNPAB	4	3	3.26E+07	1.20E+07	2.91E+06	0.00E+00	2.63E+07	1.92E+07	0.00E+00	0.00E+00	7.68E+06	7.65E+06	5.38E+06	3.25E+06
702	THOC1	2	3	3.27E+07	1.17E+07	7.70E+06	0.00E+00	0.00E+00	0.00E+00	0.00E+00	0.00E+00	0.00E+00	0.00E+00	0.00E+00	0.00E+00
703	HRNR	2	19	4.42E+07	0.00E+00	4.75E+07	0.00E+00	1.24E+08	0.00E+00	1.63E+08	0.00E+00	6.56E+08	0.00E+00	1.12E+08	0.00E+00
704	CLTC	4	12	2.55E+07	1.86E+07	1.40E+07	1.39E+07	1.19E+07	7.24E+06	2.79E+06	9.48E+05	2.15E+07	2.06E+07	6.96E+06	2.70E+06
705	TCP1	1	8	2.14E+07	2.22E+07	1.87E+07	1.80E+07	9.28E+07	7.90E+07	3.60E+06	2.29E+06	1.81E+07	8.14E+06	2.36E+07	1.92E+07
706	USP6NL	2	6	3.52E+07	8.40E+06	8.51E+06	0.00E+00	2.74E+07	5.87E+06	1.45E+06	0.00E+00	6.57E+06	0.00E+00	0.00E+00	0.00E+00
707	RRP1B	2	5	4.34E+07	0.00E+00	0.00E+00	0.00E+00	9.57E+06	0.00E+00	0.00E+00	0.00E+00	0.00E+00	0.00E+00	0.00E+00	0.00E+00
708	FAM195A	2	2	4.33E+07	0.00E+00	2.04E+07	0.00E+00	0.00E+00	0.00E+00	0.00E+00	0.00E+00	0.00E+00	0.00E+00	2.94E+07	8.93E+06
709	SURF2	1	1	4.31E+07	0.00E+00	1.76E+07	0.00E+00	2.19E+07	0.00E+00	0.00E+00	0.00E+00	0.00E+00	0.00E+00	0.00E+00	0.00E+00
710	RBM12B	1	3	2.12E+07	2.18E+07	7.12E+06	6.22E+06	2.05E+06	9.61E+05	0.00E+00	0.00E+00	0.00E+00	0.00E+00	0.00E+00	0.00E+00
711	M6PR	1	2	3.39E+07	8.80E+06	0.00E+00	4.34E+06	5.42E+07	4.14E+07	0.00E+00	0.00E+00	0.00E+00	0.00E+00	0.00E+00	0.00E+00
712	BRMS1L	2	6	4.27E+07	0.00E+00	3.45E+06	6.92E+06	1.88E+07	0.00E+00	3.68E+06	0.00E+00	0.00E+00	0.00E+00	1.85E+07	9.25E+06
713	FAM160A1	1	1	2.26E+07	1.98E+07	1.44E+07	1.60E+07	2.59E+07	2.61E+07	3.23E+06	2.83E+06	3.18E+06	3.45E+06	5.68E+06	6.40E+06
714	PHF14	2	7	2.18E+07	2.06E+07	1.55E+07	1.44E+07	7.87E+07	9.19E+07	0.00E+00	0.00E+00	0.00E+00	2.42E+06	6.20E+06	1.57E+07
715	SNRPE	1	1	2.56E+07	1.67E+07	1.81E+07	1.86E+07	2.19E+07	1.96E+07	5.34E+06	3.95E+06	1.02E+07	8.68E+06	0.00E+00	0.00E+00
716	XRCC5	1	8	3.15E+07	1.06E+07	0.00E+00	0.00E+00	0.00E+00	0.00E+00	2.11E+07	3.02E+06	2.79E+07	7.35E+06	9.28E+06	3.87E+06
717	ATP5J2	4	2	2.67E+07	1.52E+07	1.90E+07	1.70E+07	3.76E+07	3.28E+07	0.00E+00	0.00E+00	1.64E+06	1.76E+06	0.00E+00	0.00E+00
718	TNPO1	3	4	2.71E+07	1.46E+07	7.80E+06	1.49E+07	2.83E+07	1.36E+07	2.32E+06	1.96E+06	3.18E+06	3.95E+06	4.56E+06	4.15E+06
719	STIM2	3	2	2.40E+07	1.73E+07	0.00E+00	1.15E+07	2.81E+07	3.06E+07	0.00E+00	0.00E+00	0.00E+00	0.00E+00	0.00E+00	0.00E+00
720	TRIM3	4	8	4.10E+07	0.00E+00	0.00E+00	0.00E+00	5.42E+06	0.00E+00	1.24E+07	6.38E+06	4.30E+06	3.18E+06	2.26E+07	5.49E+06
721	HNRNPDL	3	3	4.10E+07	0.00E+00	2.04E+07	0.00E+00	1.97E+07	0.00E+00	0.00E+00	0.00E+00	1.18E+07	0.00E+00	1.50E+06	0.00E+00
722	AUTS2	3	4	4.07E+07	0.00E+00	1.80E+07	0.00E+00	2.46E+07	0.00E+00	1.75E+07	0.00E+00	0.00E+00	0.00E+00	0.00E+00	0.00E+00
723	KIF2A	5	6	2.40E+07	1.67E+07	9.43E+06	8.44E+06	1.87E+07	1.61E+07	8.55E+06	8.11E+06	4.90E+06	4.56E+06	1.62E+07	1.10E+07
724	RAB10	4	4	2.18E+07	1.88E+07	5.34E+06	1.60E+07	3.16E+07	2.73E+07	7.78E+05	0.00E+00	1.05E+06	1.04E+06	7.49E+05	7.58E+05
725	TAF15	2	4	2.49E+07	1.54E+07	2.10E+07	2.85E+07	0.00E+00	0.00E+00	0.00E+00	0.00E+00	0.00E+00	0.00E+00	0.00E+00	0.00E+00
726	IGF2BP3	1	4	3.47E+07	5.39E+06	1.70E+07	2.78E+06	4.09E+07	8.04E+06	2.52E+06	0.00E+00	3.42E+06	0.00E+00	3.18E+06	0.00E+00
727	INO80B	1	2	2.27E+07	1.73E+07	1.94E+07	2.03E+07	3.74E+07	2.96E+07	7.93E+06	5.23E+06	8.63E+06	6.46E+06	0.00E+00	0.00E+00
728	GNB1;GNB	7	2	2.58E+07	1.42E+07	1.35E+07	1.43E+07	7.51E+07	7.68E+07	0.00E+00	0.00E+00	2.88E+06	2.75E+06	4.24E+06	0.00E+00
729	CDC5L	1	6	3.45E+07	5.43E+06	5.37E+06	7.16E+06	4.44E+07	1.46E+07	0.00E+00	0.00E+00	0.00E+00	0.00E+00	0.00E+00	0.00E+00
730	USMG5	1	1	3.99E+07	0.00E+00	0.00E+00	0.00E+00	0.00E+00	0.00E+00	0.00E+00	0.00E+00	3.65E+06	0.00E+00	0.00E+00	0.00E+00
731	TEX30	2	7	2.46E+07	1.52E+07	9.53E+07	5.64E+07	2.39E+08	1.11E+08	3.27E+06	3.41E+06	3.89E+07	4.92E+07	3.14E+07	3.56E+07
732	USP22	3	9	2.18E+07	1.79E+07	2.91E+07	2.30E+07	1.12E+08	4.67E+07	1.99E+06	4.36E+06	0.00E+00	0.00E+00	8.35E+06	5.49E+06
733	FOXG1	1	5	3.95E+07	0.00E+00	7.24E+07	0.00E+00	8.00E+07	4.62E+07	4.17E+06	0.00E+00	0.00E+00	0.00E+00	0.00E+00	0.00E+00
734	LRRC8D	1	7	3.94E+07	0.00E+00	1.05E+07	0.00E+00	3.29E+06	0.00E+00	1.44E+07	0.00E+00	3.71E+06	0.00E+00	1.06E+07	0.00E+00
735	PRMT5	5	6	3.91E+07	0.00E+00	6.31E+06	0.00E+00	6.39E+06	0.00E+00	6.96E+06	0.00E+00	7.17E+06	0.00E+00	0.00E+00	0.00E+00
736	ABCB7	3	4	3.41E+07	4.47E+06	0.00E+00	0.00E+00	1.15E+07	7.96E+06	0.00E+00	0.00E+00	0.00E+00	0.00E+00	4.68E+06	1.74E+06
737	DYNLL1	2	3	3.81E+07	0.00E+00	1.85E+07	0.00E+00	9.29E+07	0.00E+00	6.26E+06	0.00E+00	8.32E+06	0.00E+00	2.82E+07	0.00E+00
738	PPP6R2	6	2	3.34E+07	4.72E+06	0.00E+00	0.00E+00	0.00E+00	0.00E+00	1.73E+07	0.00E+00	1.88E+07	0.00E+00	0.00E+00	0.00E+00

MQ search SILAC data

hit number	Gene names	Number of proteins	Peptides	Intensity L 2%SDS_24hHU	Intensity H 2%SDS_24hHU	Intensity L 2%SDS_2hHU	Intensity H 2%SDS_2hHU	Intensity L 2%SDS_NT	Intensity H 2%SDS_NT	Intensity L el150_24hHU	Intensity H el150_24hHU	Intensity L el150_2hHU	Intensity H el150_2hHU	Intensity L el150_NT	Intensity H el150_NT
739	ADAR	5	6	2.75E+07	1.01E+07	1.64E+07	1.59E+07	1.66E+07	1.33E+07	0.00E+00	0.00E+00	4.23E+06	3.78E+06	0.00E+00	0.00E+00
740	MED19	2	1	3.75E+07	0.00E+00	0.00E+00	0.00E+00	0.00E+00	0.00E+00	4.75E+06	0.00E+00	0.00E+00	0.00E+00	0.00E+00	0.00E+00
741	KRT8	12	11	2.72E+07	1.03E+07	0.00E+00	1.03E+07	0.00E+00	0.00E+00	0.00E+00	0.00E+00	0.00E+00	3.46E+06	0.00E+00	0.00E+00
742	LYZ	1	1	3.73E+07	0.00E+00	0.00E+00	0.00E+00	0.00E+00	0.00E+00	0.00E+00	0.00E+00	0.00E+00	0.00E+00	0.00E+00	0.00E+00
743	SCAMP2	1	1	2.08E+07	1.63E+07	0.00E+00	0.00E+00	2.57E+07	2.93E+07	0.00E+00	0.00E+00	0.00E+00	0.00E+00	0.00E+00	0.00E+00
744	PRMT1;PRI	6	2	2.72E+07	9.64E+06	0.00E+00	0.00E+00	0.00E+00	0.00E+00	3.75E+06	0.00E+00	8.52E+06	0.00E+00	3.86E+06	0.00E+00
745	ZNF691	2	1	3.68E+07	0.00E+00	0.00E+00	0.00E+00	0.00E+00	0.00E+00	1.25E+07	0.00E+00	0.00E+00	0.00E+00	1.15E+07	0.00E+00
746	SLC30A6	4	5	2.01E+07	1.64E+07	5.36E+07	2.65E+07	2.73E+06	1.56E+06	0.00E+00	0.00E+00	0.00E+00	0.00E+00	0.00E+00	0.00E+00
747	SNRPG;SNF	2	2	2.19E+07	1.46E+07	1.59E+07	1.38E+07	4.08E+07	3.88E+07	3.02E+06	2.64E+06	1.07E+07	9.83E+06	1.05E+07	9.52E+06
748	SPATS2	1	2	2.82E+07	8.24E+06	4.26E+06	4.88E+06	1.06E+07	8.75E+06	0.00E+00	0.00E+00	0.00E+00	0.00E+00	0.00E+00	0.00E+00
749	RFC4	2	3	2.96E+07	6.74E+06	2.31E+07	8.82E+06	7.62E+07	3.45E+07	0.00E+00	0.00E+00	0.00E+00	1.50E+06	0.00E+00	0.00E+00
750	RPS10;RPS:	2	2	2.14E+07	1.49E+07	0.00E+00	0.00E+00	1.02E+07	0.00E+00	0.00E+00	0.00E+00	0.00E+00	0.00E+00	0.00E+00	0.00E+00
751	TMED9	1	2	3.60E+07	0.00E+00	1.58E+07	0.00E+00	2.40E+07	0.00E+00	0.00E+00	0.00E+00	0.00E+00	0.00E+00	0.00E+00	0.00E+00
752	NSUN2	3	5	2.98E+07	6.17E+06	1.06E+07	8.16E+06	2.01E+07	6.39E+06	0.00E+00	0.00E+00	5.11E+06	1.43E+06	0.00E+00	0.00E+00
753	RBM14	1	1	2.27E+07	1.32E+07	0.00E+00	0.00E+00	2.76E+07	2.06E+07	0.00E+00	0.00E+00	0.00E+00	0.00E+00	0.00E+00	0.00E+00
754	COPB2	2	5	2.12E+07	1.45E+07	1.33E+07	0.00E+00	2.06E+07	0.00E+00	0.00E+00	0.00E+00	0.00E+00	0.00E+00	0.00E+00	0.00E+00
755	CTTN	3	3	3.56E+07	0.00E+00	0.00E+00	0.00E+00	0.00E+00	0.00E+00	0.00E+00	0.00E+00	3.08E+06	0.00E+00	1.47E+07	0.00E+00
756	SND1-IT1	1	1	0.00E+00	3.56E+07	0.00E+00	3.20E+07	0.00E+00	4.07E+07	0.00E+00	0.00E+00	0.00E+00	1.99E+07	0.00E+00	1.58E+07
757	LRCH2	2	15	3.54E+07	0.00E+00	2.08E+07	0.00E+00	7.36E+07	0.00E+00	3.58E+07	8.05E+05	9.49E+06	7.81E+06	8.18E+07	1.88E+07
758	PCID2	4	2	3.52E+07	0.00E+00	0.00E+00	0.00E+00	3.85E+07	0.00E+00	0.00E+00	0.00E+00	0.00E+00	0.00E+00	0.00E+00	0.00E+00
759	TMPO	2	9	2.88E+07	6.28E+06	8.33E+06	5.33E+06	1.60E+07	7.90E+06	0.00E+00	0.00E+00	0.00E+00	0.00E+00	0.00E+00	0.00E+00
760	SAR1A	3	4	3.50E+07	0.00E+00	1.21E+07	0.00E+00	1.21E+08	4.21E+06	0.00E+00	0.00E+00	0.00E+00	0.00E+00	0.00E+00	0.00E+00
761	CCT5	2	13	1.96E+07	1.53E+07	1.86E+07	1.04E+07	1.17E+08	7.18E+07	1.69E+06	1.32E+06	3.73E+07	1.72E+07	3.06E+07	1.91E+07
762	EIF3E	1	5	2.58E+07	8.78E+06	1.13E+07	4.26E+06	7.25E+06	4.96E+06	0.00E+00	0.00E+00	0.00E+00	0.00E+00	0.00E+00	0.00E+00
763	NME2;NMI	3	6	2.98E+07	4.60E+06	1.60E+07	5.38E+06	0.00E+00	0.00E+00	5.11E+06	0.00E+00	5.75E+07	1.08E+07	4.77E+06	0.00E+00
764	LSG1	1	5	2.57E+07	8.62E+06	2.64E+07	1.46E+07	3.81E+07	1.40E+07	6.80E+06	0.00E+00	4.31E+06	4.01E+06	6.53E+06	5.70E+06
765	CCT3	2	14	3.40E+07	0.00E+00	1.22E+07	1.18E+07	1.88E+08	6.42E+07	3.22E+06	0.00E+00	2.92E+07	1.22E+07	3.73E+07	1.86E+07
766	NFIB	4	4	2.01E+07	1.38E+07	8.85E+06	8.26E+06	1.29E+07	2.79E+07	4.42E+06	3.72E+06	0.00E+00	0.00E+00	1.33E+07	6.25E+06
767	LAS1L	4	3	2.55E+07	8.40E+06	1.12E+07	5.76E+06	4.22E+07	1.92E+07	0.00E+00	0.00E+00	0.00E+00	0.00E+00	0.00E+00	0.00E+00
768	PAICS	2	4	2.32E+07	1.05E+07	1.36E+07	9.23E+06	1.14E+07	9.67E+06	0.00E+00	0.00E+00	1.13E+07	5.85E+06	0.00E+00	0.00E+00
769	IQGAP1	1	2	1.76E+07	1.60E+07	1.22E+07	1.02E+07	1.55E+07	1.60E+07	3.97E+06	4.24E+06	3.53E+06	4.57E+06	6.72E+06	6.20E+06
770	TM9SF4	1	2	2.40E+07	9.49E+06	0.00E+00	0.00E+00	1.31E+07	0.00E+00	0.00E+00	0.00E+00	0.00E+00	0.00E+00	0.00E+00	0.00E+00
771	SLC39A13	2	1	0.00E+00	3.33E+07	1.88E+07	2.44E+07	3.44E+07	3.68E+07	0.00E+00	0.00E+00	0.00E+00	0.00E+00	0.00E+00	0.00E+00
772	APMAP	2	5	3.33E+07	0.00E+00	0.00E+00	0.00E+00	5.36E+07	0.00E+00	0.00E+00	0.00E+00	0.00E+00	0.00E+00	0.00E+00	0.00E+00
773	RFC3	2	5	1.65E+07	1.68E+07	2.79E+07	2.11E+07	7.77E+07	7.88E+07	3.42E+06	1.79E+06	4.42E+06	5.62E+06	4.32E+06	3.78E+06
774	WDR36	1	4	3.32E+07	0.00E+00	0.00E+00	0.00E+00	9.74E+06	0.00E+00	0.00E+00	0.00E+00	0.00E+00	0.00E+00	0.00E+00	0.00E+00
775	TIMM44	1	4	3.31E+07	0.00E+00	2.21E+07	0.00E+00	1.20E+07	1.14E+07	1.10E+06	0.00E+00	0.00E+00	0.00E+00	0.00E+00	0.00E+00
776	DNAJA3	3	4	3.27E+07	0.00E+00	7.08E+06	0.00E+00	1.36E+08	1.23E+07	1.84E+06	7.54E+05	0.00E+00	0.00E+00	2.70E+06	0.00E+00
777	CAD	1	7	1.83E+07	1.43E+07	6.53E+06	2.35E+06	3.68E+07	1.97E+07	3.90E+06	7.59E+05	6.75E+06	5.09E+06	1.24E+07	3.81E+06
778	KDELR1;KD	4	2	1.72E+07	1.52E+07	1.51E+06	0.00E+00	0.00E+00	0.00E+00	0.00E+00	0.00E+00	0.00E+00	0.00E+00	0.00E+00	0.00E+00
779	LTF	2	1	3.24E+07	0.00E+00	0.00E+00	0.00E+00	0.00E+00	0.00E+00	0.00E+00	0.00E+00	0.00E+00	0.00E+00	0.00E+00	0.00E+00
780	COX15	2	2	2.12E+07	1.11E+07	1.99E+07	7.58E+06	3.47E+07	9.31E+06	0.00E+00	0.00E+00	0.00E+00	0.00E+00	0.00E+00	0.00E+00
781	FBXO21	2	12	2.55E+07	6.79E+06	1.89E+08	2.72E+07	4.74E+08	3.17E+07	1.53E+06	1.66E+06	7.93E+07	3.69E+07	1.50E+08	1.88E+07
782	GCN1L1	1	11	2.81E+07	3.91E+06	7.02E+06	2.23E+06	2.82E+07	7.01E+06	0.00E+00	0.00E+00	0.00E+00	0.00E+00	2.01E+06	0.00E+00
783	AAAS	2	3	2.47E+07	7.16E+06	6.36E+06	0.00E+00	2.49E+07	0.00E+00	0.00E+00	0.00E+00	0.00E+00	0.00E+00	2.54E+06	0.00E+00
784	TROAP	3	6	1.64E+07	1.55E+07	2.91E+07	8.77E+06	8.71E+07	1.89E+07	2.50E+06	2.85E+06	2.58E+06	2.92E+06	2.72E+06	2.47E+06
785	RBM7	1	3	2.00E+07	1.18E+07	0.00E+00	0.00E+00	2.49E+07	1.71E+07	0.00E+00	0.00E+00	0.00E+00	0.00E+00	2.85E+06	2.37E+06
786	P4HB	1	9	3.15E+07	0.00E+00	4.27E+07	1.46E+07	0.00E+00	0.00E+00	5.24E+06	0.00E+00	3.77E+07	1.09E+07	3.84E+06	0.00E+00
787	ATAD3A;AT	7	5	2.21E+07	9.32E+06	7.80E+06	8.56E+06	1.75E+07	1.14E+07	0.00E+00	0.00E+00	0.00E+00	0.00E+00	0.00E+00	0.00E+00
788	ZC3H4	1	3	3.14E+07	0.00E+00	3.08E+06	0.00E+00	1.03E+07	0.00E+00	9.33E+05	0.00E+00	0.00E+00	0.00E+00	0.00E+00	0.00E+00
789	ELL	1	4	3.10E+07	0.00E+00	3.35E+06	1.09E+07	7.12E+06	0.00E+00	2.25E+06	0.00E+00	0.00E+00	0.00E+00	0.00E+00	0.00E+00
790	COPB1	1	5	2.20E+07	8.84E+06	7.94E+06	6.78E+06	2.69E+07	3.96E+06	2.33E+06	4.26E+05	2.91E+06	2.15E+06	3.27E+06	1.02E+06
791	POU3F3;PC	2	6	3.06E+07	0.00E+00	1.11E+07	0.00E+00	2.67E+07	0.00E+00	7.41E+06	0.00E+00	4.90E+06	0.00E+00	6.76E+06	0.00E+00
792	SSR4	1	4	3.06E+07	0.00E+00	3.27E+07	2.61E+07	1.13E+08	6.38E+07	0.00E+00	0.00E+00	0.00E+00	0.00E+00	3.85E+06	0.00E+00
793	ESYT1	2	4	2.48E+07	5.48E+06	6.20E+06	3.46E+06	2.64E+07	1.34E+07	0.00E+00	0.00E+00	0.00E+00	0.00E+00	0.00E+00	0.00E+00
794	RFC1	2	3	2.14E+07	8.59E+06	1.07E+07	5.43E+06	3.09E+07	1.99E+07	1.84E+06	7.81E+05	1.03E+06	0.00E+00	5.49E+06	3.04E+06
795	ARCN1	2	2	2.17E+07	8.08E+06	5.16E+06	6.41E+06	2.09E+07	9.03E+06	0.00E+00	0.00E+00	0.00E+00	0.00E+00	0.00E+00	0.00E+00
796	CACHD1	2	6	2.13E+07	8.45E+06	3.48E+07	7.29E+06	3.68E+07	1.19E+07	4.44E+06	0.00E+00	3.99E+06	3.05E+06	4.05E+06	3.48E+06
797	AES	2	1	1.63E+07	1.35E+07	1.06E+07	8.97E+06	0.00E+00	0.00E+00	3.98E+06	3.29E+06	0.00E+00	0.00E+00	0.00E+00	0.00E+00
798	KAT8	2	3	2.03E+07	9.13E+06	1.23E+07	0.00E+00	0.00E+00	0.00E+00	3.43E+06	0.00E+00	0.00E+00	0.00E+00	1.68E+06	0.00E+00
799	TUBB6	1	11	2.16E+07	7.66E+06	0.00E+00	0.00E+00	6.14E+06	7.35E+06	7.46E+06	0.00E+00	5.97E+06	0.00E+00	0.00E+00	0.00E+00
800	EAF1	1	2	2.93E+07	0.00E+00	9.27E+06	0.00E+00	2.53E+07	0.00E+00	4.98E+06	0.00E+00	0.00E+00	0.00E+00	3.88E+06	0.00E+00
801	SACM1L	2	2	1.80E+07	1.13E+07	3.50E+06	0.00E+00	1.97E+07	1.13E+07	0.00E+00	0.00E+00	0.00E+00	0.00E+00	0.00E+00	0.00E+00
802	RNH1	1	1	1.63E+07	1.30E+07	7.68E+06	0.00E+00	0.00E+00	0.00E+00	7.32E+06	0.00E+00	0.00E+00	0.00E+00	0.00E+00	0.00E+00
803	POLR2B	1	5	2.58E+07	3.18E+06	0.00E+00	0.00E+00	2.02E+07	1.78E+07	0.00E+00	0.00E+00	0.00E+00	0.00E+00	0.00E+00	0.00E+00
804	CAPZA1	1	3	2.90E+07	0.00E+00	2.13E+07	0.00E+00	3.02E+07	0.00E+00	0.00E+00	0.00E+00	8.78E+06	0.00E+00	0.00E+00	0.00E+00
805	PAPD5	5	8	1.46E+07	1.43E+07	1.82E+07	7.30E+05	1.38E+08	1.19E+07	0.00E+00	0.00E+00	1.01E+07	0.00E+00	7.50E+06	8.36E+05
806	KPNA4	1	10	2.25E+07	6.09E+06	1.93E+07	0.00E+00	8.45E+06	0.00E+00	0.00E+00	0.00E+00	4.93E+06	7.71E+06	6.55E+06	0.00E+00
807	XPOT	1	7	2.86E+07	0.00E+00	2.33E+06	2.21E+06	3.27E+07	1.16E+07	0.00E+00	0.00E+00	1.62E+06	2.57E+06	3.13E+06	2.34E+06
808	MSH6	4	3	2.85E+07	0.00E+00	2.36E+06	0.00E+00	6.96E+06	0.00E+00	0.00E+00	0.00E+00	0.00E+00	0.00E+00	7.29E+05	0.00E+00
809	NSUN5	4	5	1.27E+07	1.59E+07	2.86E+06	0.00E+00	3.46E+07	2.84E+07	0.00E+00	0.00E+00	0.00E+00	0.00E+00	0.00E+00	0.00E+00
810	RSRC2	2	1	2.83E+07	0.00E+00	1.25E+07	0.00E+00	0.00E+00	0.00E+00	0.00E+00	0.00E+00	0.00E+00	0.00E+00	0.00E+00	0.00E+00
811	CDC73	1	7	2.83E+07	0.00E+00	6.64E+06	0.00E+00	2.34E+07	1.43E+07	0.00E+00	0.00E+00	0.00E+00	0.00E+00	0.00E+00	0.00E+00
812	SUPT5H	2	2	2.04E+07	7.77E+06	0.00E+00	0.00E+00	0.00E+00	0.00E+00	0.00E+00	0.00E+00	0.00E+00	0.00E+00	0.00E+00	0.00E+00
813	ATXN10	2	3	2.80E+07	0.00E+00	1.80E+07	2.82E+06	1.06E+07	4.99E+06	5.18E+06	0.00E+00	3.94E+06	0.00E+00	3.71E+06	1.77E+06
814	FNDC3B	2	7	2.73E+07	0.00E+00	1.85E+07	1.19E+07	7.94E+07	0.00E+00	0.00E+00	0.00E+00	3.43E+06	0.00E+00	1.53E+06	1.59E+06
815	AGK	1	3	2.71E+07	0.00E+00	2.16E+07	0.00E+00	1.79E+07	0.00E+00	0.00E+00	0.00E+00	0.00E+00	0.00E+00	0.00E+00	0.00E+00
816	CD81	1	1	2.71E+07	0.00E+00	1.17E+07	0.00E+00	0.00E+00	0.00E+00	0.00E+00	0.00E+00	0.00E+00	0.00E+00	0.00E+00	0.00E+00
817	DSEL	1	2	0.00E+00	2.71E+07	0.00E+00	2.24E+07	0.00E+00	0.00E+00	0.00E+00	0.00E+00	0.00E+00	0.00E+00	3.60E+07	0.00E+00
818	P4HA1	3	4	2.69E+07	0.00E+00	4.03E+07	1.28E+07	0.00E+00	0.00E+00	0.00E+00	0.00E+00	4.15E+06	0.00E+00	0.00E+00	0.00E+00
819	FAM53C	1	4	2.69E+07	0.00E+00	1.71E+07	0.00E+00	4.49E+07	0.00E+00	7.52E+06	0.00E+00	0.00E+00	0.00E+00	0.00E+00	0.00E+00
820	PRPF38B	2	6	2.19E+07	4.81E+06	0.00E+00	0.00E+00	3.92E+06	3.03E+06	4.18E+06	0.00E+00	5.83E+06	0.00E+00	1.73E+07	4.88E+06

MQ search SILAC data

hit number	Gene names	Number of proteins	Peptides	Intensity L 2%SDS_24hHU	Intensity H 2%SDS_24hHU	Intensity L 2%SDS_2hHU	Intensity H 2%SDS_2hHU	Intensity L 2%SDS_NT	Intensity H 2%SDS_NT	Intensity L el150_24hHU	Intensity H el150_24hHU	Intensity L el150_2hHU	Intensity H el150_2hHU	Intensity L el150_NT	Intensity H el150_NT
821	PCGF5	1	4	2.64E+07	0.00E+00	3.32E+07	0.00E+00	5.44E+07	0.00E+00	1.83E+07	0.00E+00	0.00E+00	0.00E+00	3.60E+07	1.65E+06
822	GEN1	1	3	2.62E+07	0.00E+00	0.00E+00	0.00E+00	0.00E+00	0.00E+00	0.00E+00	0.00E+00	0.00E+00	0.00E+00	0.00E+00	0.00E+00
823	QSOX2	1	7	1.89E+07	7.34E+06	2.30E+07	1.84E+07	7.62E+07	1.29E+07	1.96E+07	1.18E+07	0.00E+00	0.00E+00	1.39E+07	1.16E+07
824	PTPN14	2	15	1.34E+07	1.28E+07	5.48E+06	1.19E+07	1.73E+08	3.82E+07	0.00E+00	0.00E+00	0.00E+00	0.00E+00	3.13E+07	1.58E+07
825	HOMER2	2	8	2.61E+07	0.00E+00	1.43E+07	0.00E+00	4.80E+07	4.47E+07	4.85E+06	0.00E+00	4.30E+06	0.00E+00	1.55E+07	0.00E+00
826	BUB3	2	3	2.59E+07	0.00E+00	0.00E+00	0.00E+00	1.99E+07	0.00E+00	1.99E+06	2.42E+06	0.00E+00	0.00E+00	0.00E+00	0.00E+00
827	SRSF3	2	3	2.00E+07	5.87E+06	2.74E+07	3.81E+07	2.46E+07	0.00E+00	1.19E+07	0.00E+00	1.14E+07	1.13E+07	0.00E+00	0.00E+00
828	PRR3	2	1	2.20E+07	3.83E+06	1.73E+07	3.71E+06	4.22E+07	6.82E+06	0.00E+00	0.00E+00	0.00E+00	0.00E+00	0.00E+00	0.00E+00
829	PCNP	3	2	2.57E+07	0.00E+00	1.46E+07	0.00E+00	3.09E+07	0.00E+00	5.58E+06	0.00E+00	0.00E+00	0.00E+00	0.00E+00	0.00E+00
830	NHP2	1	1	1.58E+07	9.80E+06	0.00E+00	0.00E+00	1.76E+07	9.67E+06	4.52E+06	0.00E+00	0.00E+00	0.00E+00	0.00E+00	0.00E+00
831	HSPH1	5	8	2.55E+07	0.00E+00	1.93E+07	2.65E+07	0.00E+00	0.00E+00	5.86E+06	5.57E+06	2.36E+07	6.99E+06	9.07E+06	1.66E+07
832	NARF	4	1	0.00E+00	2.52E+07	1.42E+07	1.71E+07	0.00E+00	7.94E+07	0.00E+00	0.00E+00	0.00E+00	6.58E+06	0.00E+00	0.00E+00
833	ZSCAN26	3	5	2.50E+07	0.00E+00	2.08E+07	1.33E+07	7.74E+07	2.43E+07	0.00E+00	0.00E+00	0.00E+00	0.00E+00	0.00E+00	0.00E+00
834	MCM3	2	4	2.08E+07	4.14E+06	2.75E+06	3.18E+06	0.00E+00	0.00E+00	0.00E+00	0.00E+00	6.14E+06	1.76E+06	1.58E+06	0.00E+00
835	ZNF8	2	9	2.46E+07	0.00E+00	3.51E+07	2.07E+06	6.69E+07	2.19E+07	4.74E+06	0.00E+00	4.22E+06	0.00E+00	1.20E+07	0.00E+00
836	VMP1	2	1	1.48E+07	9.55E+06	7.09E+06	6.26E+06	3.17E+07	3.21E+07	0.00E+00	0.00E+00	0.00E+00	0.00E+00	0.00E+00	0.00E+00
837	FOXF2;FOX	3	4	1.44E+07	1.00E+07	1.07E+07	9.85E+06	4.94E+07	3.81E+07	6.24E+06	3.84E+06	2.02E+06	2.13E+06	8.11E+06	9.18E+06
838	PSMC6	1	2	1.65E+07	7.70E+06	5.10E+06	3.35E+06	1.18E+07	1.14E+07	0.00E+00	0.00E+00	0.00E+00	0.00E+00	0.00E+00	0.00E+00
839	ATP1B3	2	3	1.31E+07	1.11E+07	8.22E+06	1.48E+07	1.31E+07	0.00E+00	0.00E+00	0.00E+00	0.00E+00	0.00E+00	0.00E+00	0.00E+00
840	DARS	2	2	2.42E+07	0.00E+00	5.41E+06	1.47E+06	2.73E+07	0.00E+00	0.00E+00	0.00E+00	0.00E+00	0.00E+00	0.00E+00	0.00E+00
841	NOLC1	2	11	2.41E+07	0.00E+00	0.00E+00	0.00E+00	1.77E+07	0.00E+00	3.80E+06	0.00E+00	0.00E+00	0.00E+00	0.00E+00	0.00E+00
842	RELL1	1	3	1.24E+07	1.15E+07	1.99E+07	9.27E+06	6.14E+07	2.24E+07	0.00E+00	0.00E+00	0.00E+00	0.00E+00	0.00E+00	0.00E+00
843	LUZP1	3	4	2.38E+07	0.00E+00	0.00E+00	0.00E+00	0.00E+00	0.00E+00	0.00E+00	4.40E+06	5.43E+06	4.66E+06	3.35E+07	1.07E+07
844	CDC37	1	1	2.36E+07	0.00E+00	1.55E+07	0.00E+00	1.46E+07	0.00E+00	0.00E+00	0.00E+00	0.00E+00	0.00E+00	0.00E+00	0.00E+00
845	CDX2	1	2	2.36E+07	0.00E+00	1.18E+07	0.00E+00	2.32E+07	0.00E+00	6.99E+06	0.00E+00	1.08E+06	1.65E+06	4.56E+06	0.00E+00
846	SMARCE1	6	5	2.36E+07	0.00E+00	3.62E+07	2.35E+07	3.77E+07	2.20E+07	1.00E+07	6.93E+06	6.84E+06	6.44E+06	1.02E+07	1.48E+07
847	CWC25	2	12	4.33E+06	1.93E+07	5.45E+07	3.14E+07	1.95E+08	7.23E+07	3.00E+07	6.81E+06	1.94E+07	7.24E+06	5.36E+07	1.40E+07
848	TMEM33	1	3	2.35E+07	0.00E+00	3.86E+07	0.00E+00	6.91E+07	8.55E+06	0.00E+00	0.00E+00	0.00E+00	0.00E+00	0.00E+00	0.00E+00
849	PFN1	1	4	1.45E+07	8.87E+06	1.64E+07	1.28E+07	0.00E+00	0.00E+00	4.46E+06	1.84E+06	4.51E+07	2.30E+07	0.00E+00	0.00E+00
850	TAF4	2	4	2.33E+07	0.00E+00	4.21E+07	7.72E+06	0.00E+00	0.00E+00	3.41E+06	0.00E+00	0.00E+00	0.00E+00	0.00E+00	0.00E+00
851	CKB	1	11	1.87E+07	4.40E+06	3.24E+07	1.60E+07	0.00E+00	0.00E+00	9.38E+06	1.77E+06	2.75E+08	1.58E+08	8.28E+06	2.37E+06
852	ZCCHC14	2	4	1.60E+07	7.09E+06	0.00E+00	0.00E+00	0.00E+00	0.00E+00	1.24E+07	3.84E+06	7.66E+06	0.00E+00	1.69E+07	0.00E+00
853	MED1	2	10	1.95E+07	3.38E+06	3.16E+07	3.02E+06	5.91E+07	6.72E+06	2.16E+07	7.09E+05	1.52E+06	9.75E+05	4.19E+07	2.78E+06
854	PTRH2	1	2	2.25E+07	0.00E+00	6.77E+06	0.00E+00	2.78E+07	0.00E+00	0.00E+00	0.00E+00	0.00E+00	0.00E+00	0.00E+00	0.00E+00
855	LSM4	1	3	2.23E+07	0.00E+00	0.00E+00	0.00E+00	1.34E+07	0.00E+00	0.00E+00	0.00E+00	0.00E+00	0.00E+00	1.40E+07	0.00E+00
856	EIF4G2	2	3	1.84E+07	3.94E+06	5.79E+06	3.24E+06	5.95E+06	3.06E+06	0.00E+00	0.00E+00	0.00E+00	0.00E+00	0.00E+00	0.00E+00
857	U2AF1	4	3	2.20E+07	0.00E+00	0.00E+00	0.00E+00	1.72E+07	1.79E+07	4.18E+06	0.00E+00	6.46E+06	0.00E+00	0.00E+00	0.00E+00
858	WDR24	1	6	1.89E+07	3.15E+06	8.98E+06	0.00E+00	1.93E+07	0.00E+00	3.29E+06	5.36E+05	9.73E+05	5.84E+05	1.46E+07	3.38E+06
859	ALDH3A2	2	2	1.59E+07	6.05E+06	0.00E+00	0.00E+00	1.72E+07	0.00E+00	0.00E+00	0.00E+00	0.00E+00	0.00E+00	2.53E+06	0.00E+00
860	CTSG	1	2	2.19E+07	0.00E+00	0.00E+00	0.00E+00	0.00E+00	0.00E+00	0.00E+00	0.00E+00	0.00E+00	0.00E+00	0.00E+00	0.00E+00
861	TAF3	1	2	2.15E+07	0.00E+00	6.36E+06	0.00E+00	1.10E+07	0.00E+00	2.58E+06	0.00E+00	1.87E+06	0.00E+00	4.33E+06	0.00E+00
862	SMARCD2;I	5	2	1.04E+07	1.10E+07	0.00E+00	0.00E+00	1.10E+07	0.00E+00	4.10E+06	0.00E+00	4.30E+06	4.56E+06	5.84E+06	2.47E+06
863	OTUD4	3	2	2.14E+07	0.00E+00	0.00E+00	0.00E+00	0.00E+00	0.00E+00	1.66E+06	0.00E+00	0.00E+00	0.00E+00	0.00E+00	0.00E+00
864	BMP7	1	3	1.12E+07	9.88E+06	3.22E+07	2.42E+07	3.10E+07	2.78E+07	0.00E+00	0.00E+00	1.75E+07	6.26E+06	1.42E+07	1.23E+07
865	TXN	2	4	2.09E+07	0.00E+00	1.23E+07	0.00E+00	2.93E+07	0.00E+00	2.18E+07	0.00E+00	3.18E+07	0.00E+00	6.09E+07	0.00E+00
866	INTS10	1	7	2.08E+07	0.00E+00	1.58E+07	0.00E+00	4.72E+07	2.73E+07	5.91E+05	4.86E+05	0.00E+00	0.00E+00	1.18E+07	9.57E+05
867	ZNF425	1	1	2.06E+07	0.00E+00	6.71E+06	0.00E+00	5.24E+07	0.00E+00	0.00E+00	0.00E+00	0.00E+00	0.00E+00	0.00E+00	0.00E+00
868	NSMCE2	1	5	2.05E+07	0.00E+00	4.38E+07	0.00E+00	2.46E+07	0.00E+00	1.64E+07	0.00E+00	8.08E+06	0.00E+00	5.95E+07	0.00E+00
869	ZNF608	2	1	1.25E+07	8.00E+06	9.76E+06	8.42E+06	9.90E+06	0.00E+00	0.00E+00	0.00E+00	0.00E+00	0.00E+00	0.00E+00	0.00E+00
870	ABCF2	2	1	1.44E+07	5.77E+06	7.00E+06	4.01E+06	0.00E+00	0.00E+00	0.00E+00	0.00E+00	0.00E+00	0.00E+00	0.00E+00	0.00E+00
871	SON	9	2	1.23E+07	7.87E+06	8.42E+06	6.62E+06	0.00E+00	0.00E+00	3.02E+06	2.30E+06	6.71E+06	6.53E+06	5.24E+06	4.92E+06
872	SNX8	1	4	2.00E+07	0.00E+00	1.02E+06	0.00E+00	4.68E+06	0.00E+00	7.78E+06	0.00E+00	0.00E+00	0.00E+00	0.00E+00	0.00E+00
873	NELL2	4	4	1.99E+07	0.00E+00	2.99E+07	0.00E+00	1.34E+08	0.00E+00	0.00E+00	0.00E+00	0.00E+00	0.00E+00	1.12E+07	0.00E+00
874	CD2BP2	1	8	1.98E+07	0.00E+00	2.84E+07	7.60E+06	1.69E+08	7.36E+07	3.01E+06	0.00E+00	3.33E+06	0.00E+00	2.26E+07	0.00E+00
875	RBM22	2	1	1.97E+07	0.00E+00	0.00E+00	0.00E+00	0.00E+00	0.00E+00	0.00E+00	0.00E+00	0.00E+00	0.00E+00	0.00E+00	0.00E+00
876	OSTC	2	1	1.97E+07	0.00E+00	0.00E+00	0.00E+00	0.00E+00	0.00E+00	0.00E+00	0.00E+00	0.00E+00	0.00E+00	0.00E+00	0.00E+00
877	DUSP11	2	5	1.97E+07	0.00E+00	3.30E+07	6.33E+06	1.17E+08	2.70E+07	0.00E+00	0.00E+00	0.00E+00	0.00E+00	0.00E+00	0.00E+00
878	RWDD2B	1	3	1.96E+07	0.00E+00	0.00E+00	0.00E+00	5.06E+07	0.00E+00	0.00E+00	0.00E+00	0.00E+00	0.00E+00	4.15E+06	0.00E+00
879	YBX1	1	1	1.96E+07	0.00E+00	0.00E+00	0.00E+00	1.58E+07	0.00E+00	0.00E+00	0.00E+00	0.00E+00	0.00E+00	0.00E+00	0.00E+00
880	PDCD6	3	3	1.67E+07	2.82E+06	5.65E+06	0.00E+00	9.81E+06	0.00E+00	0.00E+00	0.00E+00	0.00E+00	0.00E+00	1.35E+06	1.66E+06
881	TAF10	1	2	1.95E+07	0.00E+00	0.00E+00	0.00E+00	1.05E+07	0.00E+00	0.00E+00	0.00E+00	3.51E+06	0.00E+00	0.00E+00	0.00E+00
882	RPP30	2	2	1.94E+07	0.00E+00	4.12E+06	0.00E+00	2.47E+07	2.04E+07	4.81E+06	3.83E+06	0.00E+00	0.00E+00	0.00E+00	0.00E+00
883	DOCK6	1	9	1.26E+07	6.72E+06	0.00E+00	0.00E+00	5.66E+06	0.00E+00	1.76E+06	1.39E+06	1.52E+06	2.21E+06	5.54E+06	4.29E+06
884	SMARCC1	1	13	1.93E+07	0.00E+00	6.51E+06	0.00E+00	2.50E+07	0.00E+00	8.72E+06	7.58E+05	3.22E+06	0.00E+00	2.73E+06	0.00E+00
885	TFRC	1	3	1.91E+07	0.00E+00	8.30E+06	5.79E+06	3.51E+07	1.04E+07	0.00E+00	0.00E+00	0.00E+00	0.00E+00	3.98E+06	0.00E+00
886	ZNF609	1	4	1.89E+07	0.00E+00	0.00E+00	0.00E+00	0.00E+00	0.00E+00	4.82E+06	0.00E+00	0.00E+00	0.00E+00	8.19E+06	3.31E+06
887	RAB11A;RA	4	4	1.88E+07	0.00E+00	1.97E+07	0.00E+00	6.64E+07	0.00E+00	0.00E+00	0.00E+00	0.00E+00	0.00E+00	0.00E+00	0.00E+00
888	HLA-H;HLA	24	3	1.87E+07	0.00E+00	0.00E+00	0.00E+00	7.84E+07	4.79E+06	0.00E+00	0.00E+00	0.00E+00	0.00E+00	7.71E+06	0.00E+00
889	MRPS9	1	2	1.20E+07	6.56E+06	3.20E+06	0.00E+00	7.20E+06	0.00E+00	0.00E+00	0.00E+00	1.25E+06	0.00E+00	0.00E+00	0.00E+00
890	HSP90AB2I	1	4	1.85E+07	0.00E+00	0.00E+00	0.00E+00	0.00E+00	0.00E+00	0.00E+00	0.00E+00	0.00E+00	0.00E+00	0.00E+00	0.00E+00
891	RAB5C	6	4	1.84E+07	0.00E+00	0.00E+00	0.00E+00	1.60E+07	1.99E+07	0.00E+00	0.00E+00	0.00E+00	0.00E+00	8.42E+06	0.00E+00
892	ELOVL5	3	1	1.84E+07	0.00E+00	1.32E+07	0.00E+00	0.00E+00	0.00E+00	0.00E+00	0.00E+00	0.00E+00	0.00E+00	2.12E+06	0.00E+00
893	C1QBP	1	3	1.82E+07	0.00E+00	1.38E+07	0.00E+00	2.21E+07	0.00E+00	1.44E+07	0.00E+00	3.73E+07	8.42E+06	2.08E+07	0.00E+00
894	LUC7L3	2	2	1.80E+07	0.00E+00	1.06E+07	0.00E+00	0.00E+00	0.00E+00	0.00E+00	0.00E+00	0.00E+00	0.00E+00	4.99E+06	0.00E+00
895	CSNK1A1	4	5	1.80E+07	0.00E+00	1.16E+07	0.00E+00	1.03E+08	3.51E+07	1.60E+06	0.00E+00	2.25E+06	0.00E+00	7.06E+06	4.55E+06
896	VWA9	3	6	1.79E+07	0.00E+00	6.31E+06	0.00E+00	3.37E+07	0.00E+00	4.88E+06	0.00E+00	1.73E+06	0.00E+00	1.30E+07	0.00E+00
897	ZNF629	1	1	1.24E+07	5.41E+06	0.00E+00	0.00E+00	8.27E+06	5.34E+06	0.00E+00	0.00E+00	0.00E+00	0.00E+00	0.00E+00	0.00E+00
898	TAF7	1	4	1.76E+07	0.00E+00	1.42E+07	0.00E+00	1.85E+07	0.00E+00	0.00E+00	0.00E+00	0.00E+00	0.00E+00	0.00E+00	0.00E+00
899	MRTO4	1	1	1.76E+07	0.00E+00	0.00E+00	0.00E+00	0.00E+00	0.00E+00	0.00E+00	0.00E+00	0.00E+00	0.00E+00	0.00E+00	0.00E+00
900	NDUFS2	2	1	1.12E+07	6.30E+06	5.58E+06	5.66E+06	1.39E+07	1.02E+07	0.00E+00	0.00E+00	0.00E+00	0.00E+00	0.00E+00	0.00E+00
901	NDC1	6	1	1.52E+07	2.20E+06	8.85E+06	2.14E+06	1.17E+07	4.76E+06	0.00E+00	0.00E+00	0.00E+00	0.00E+00	0.00E+00	0.00E+00
902	UQCRFS1	1	1	1.16E+07	5.70E+06	0.00E+00	0.00E+00	8.11E+06	4.53E+06	0.00E+00	0.00E+00	0.00E+00	0.00E+00	0.00E+00	0.00E+00

MQ search SILAC data

hit number	Gene names	Number of proteins	Peptides	Intensity L 2%SDS_24hHU	Intensity H 2%SDS_24hHU	Intensity L 2%SDS_2hHU	Intensity H 2%SDS_2hHU	Intensity L 2%SDS_NT	Intensity H 2%SDS_NT	Intensity L el150_24hHU	Intensity H el150_24hHU	Intensity L el150_2hHU	Intensity H el150_2hHU	Intensity L el150_NT	Intensity H el150_NT
903	MAP4K4;TI	14	5	1.72E+07	0.00E+00	0.00E+00	0.00E+00	0.00E+00	0.00E+00	1.81E+07	5.55E+06	2.53E+06	0.00E+00	0.00E+00	1.64E+06
904	PWP2	1	3	1.32E+07	3.93E+06	0.00E+00	0.00E+00	1.64E+07	4.48E+06	9.88E+05	0.00E+00	9.74E+05	0.00E+00	1.96E+06	5.05E+05
905	ACAT1	2	2	1.70E+07	0.00E+00	0.00E+00	0.00E+00	2.63E+07	0.00E+00	0.00E+00	0.00E+00	0.00E+00	0.00E+00	0.00E+00	0.00E+00
906	EIF3M	2	2	1.68E+07	0.00E+00	1.32E+07	3.41E+06	3.05E+06	0.00E+00	0.00E+00	0.00E+00	0.00E+00	0.00E+00	0.00E+00	0.00E+00
907	SMEK1	7	4	1.25E+07	4.21E+06	2.97E+06	0.00E+00	0.00E+00	0.00E+00	7.58E+06	0.00E+00	1.14E+07	2.94E+06	5.18E+06	1.32E+06
908	DDX24	2	3	1.05E+07	6.03E+06	0.00E+00	0.00E+00	1.47E+07	0.00E+00	0.00E+00	0.00E+00	0.00E+00	0.00E+00	0.00E+00	0.00E+00
909	PSMC3	1	3	1.14E+07	5.00E+06	6.43E+06	3.88E+06	1.48E+07	5.63E+06	0.00E+00	0.00E+00	2.18E+06	2.13E+06	0.00E+00	0.00E+00
910	GTF2A1	2	3	1.64E+07	0.00E+00	0.00E+00	0.00E+00	0.00E+00	3.84E+07	0.00E+00	0.00E+00	0.00E+00	1.11E+07	0.00E+00	9.15E+06
911	SYPL1	2	1	0.00E+00	1.63E+07	0.00E+00	9.88E+06	0.00E+00	0.00E+00	0.00E+00	0.00E+00	0.00E+00	0.00E+00	0.00E+00	0.00E+00
912	SLC39A14	3	3	1.08E+07	5.44E+06	5.18E+06	5.45E+06	1.02E+07	8.52E+06	1.31E+07	0.00E+00	1.06E+07	0.00E+00	1.15E+07	3.74E+06
913	TMED7	3	2	1.62E+07	0.00E+00	5.60E+06	2.73E+06	1.93E+07	0.00E+00	0.00E+00	0.00E+00	0.00E+00	0.00E+00	0.00E+00	0.00E+00
914	EIF3L	2	3	9.51E+06	6.73E+06	1.46E+07	1.62E+07	0.00E+00	0.00E+00	0.00E+00	0.00E+00	5.67E+06	6.00E+06	0.00E+00	0.00E+00
915	MEIS2;MEI	13	4	1.62E+07	0.00E+00	6.14E+06	0.00E+00	0.00E+00	0.00E+00	1.30E+07	7.41E+06	6.21E+06	4.62E+06	9.16E+06	6.54E+06
916	NIFK	1	2	1.62E+07	0.00E+00	0.00E+00	0.00E+00	0.00E+00	0.00E+00	0.00E+00	0.00E+00	0.00E+00	0.00E+00	0.00E+00	0.00E+00
917	SRP14	1	1	1.05E+07	5.55E+06	6.37E+06	6.78E+06	1.17E+07	1.29E+07	1.18E+06	9.60E+05	1.96E+06	2.35E+06	0.00E+00	0.00E+00
918	TNKS	2	6	1.60E+07	0.00E+00	2.86E+07	4.11E+07	2.73E+07	2.62E+07	9.76E+06	6.08E+06	8.42E+06	5.41E+06	3.06E+06	4.71E+06
919	KPNA6;KPN	3	5	1.59E+07	0.00E+00	0.00E+00	0.00E+00	1.31E+07	0.00E+00	7.19E+06	3.01E+06	0.00E+00	0.00E+00	0.00E+00	0.00E+00
920	MARS	2	4	1.59E+07	0.00E+00	0.00E+00	0.00E+00	1.01E+07	8.06E+06	0.00E+00	0.00E+00	2.07E+06	1.60E+06	0.00E+00	0.00E+00
921	ZNFX1	2	2	1.58E+07	0.00E+00	0.00E+00	0.00E+00	0.00E+00	0.00E+00	0.00E+00	0.00E+00	0.00E+00	0.00E+00	1.03E+06	8.10E+05
922	HNRNPUL1	4	1	1.01E+07	5.69E+06	7.15E+06	4.76E+06	1.10E+07	6.70E+06	0.00E+00	0.00E+00	1.98E+06	1.64E+06	0.00E+00	0.00E+00
923	USP46;USP	5	2	9.28E+06	6.43E+06	2.13E+07	9.38E+06	1.47E+07	1.15E+07	1.11E+07	2.18E+06	0.00E+00	0.00E+00	8.40E+06	5.02E+06
924	HOXA1	1	1	1.57E+07	0.00E+00	0.00E+00	0.00E+00	1.12E+07	0.00E+00	0.00E+00	0.00E+00	0.00E+00	0.00E+00	0.00E+00	0.00E+00
925	WDR3	1	1	1.56E+07	0.00E+00	0.00E+00	0.00E+00	0.00E+00	0.00E+00	0.00E+00	0.00E+00	0.00E+00	0.00E+00	0.00E+00	0.00E+00
926	NDNL2	1	5	1.56E+07	0.00E+00	3.08E+06	0.00E+00	5.14E+07	0.00E+00	1.01E+07	0.00E+00	5.83E+06	0.00E+00	2.41E+07	5.35E+05
927	HNRNPUL2	1	2	1.56E+07	0.00E+00	3.33E+06	1.60E+06	6.35E+06	0.00E+00	0.00E+00	0.00E+00	0.00E+00	0.00E+00	0.00E+00	0.00E+00
928	TNPO3	4	4	1.23E+07	3.26E+06	8.76E+06	2.35E+06	1.60E+07	4.20E+06	0.00E+00	0.00E+00	1.32E+06	5.37E+05	0.00E+00	0.00E+00
929	KAT7	5	2	1.17E+07	3.80E+06	6.71E+06	0.00E+00	1.81E+07	0.00E+00	0.00E+00	0.00E+00	0.00E+00	0.00E+00	2.25E+06	2.13E+06
930	TLN2	1	2	1.55E+07	0.00E+00	1.34E+07	0.00E+00	2.95E+07	0.00E+00	0.00E+00	0.00E+00	0.00E+00	0.00E+00	5.02E+06	0.00E+00
931	XPO5	1	5	1.35E+07	1.83E+06	1.05E+07	4.29E+06	1.58E+07	1.26E+07	0.00E+00	0.00E+00	0.00E+00	0.00E+00	3.56E+06	0.00E+00
932	RAB1B;RAE	2	6	1.53E+07	0.00E+00	9.22E+06	0.00E+00	1.58E+07	0.00E+00	0.00E+00	0.00E+00	0.00E+00	0.00E+00	0.00E+00	0.00E+00
933	VAT1	1	1	1.53E+07	0.00E+00	6.48E+06	3.41E+06	0.00E+00	0.00E+00	2.87E+06	0.00E+00	0.00E+00	0.00E+00	0.00E+00	0.00E+00
934	FBXO44	2	3	1.53E+07	0.00E+00	1.44E+07	0.00E+00	1.14E+07	0.00E+00	6.97E+06	1.73E+06	5.70E+06	1.11E+06	8.94E+06	0.00E+00
935	NUP93	2	4	1.39E+07	1.33E+06	0.00E+00	0.00E+00	2.82E+07	8.83E+06	0.00E+00	0.00E+00	0.00E+00	0.00E+00	0.00E+00	0.00E+00
936	SDHB	1	2	1.52E+07	0.00E+00	1.44E+07	6.99E+06	0.00E+00	0.00E+00	0.00E+00	0.00E+00	0.00E+00	0.00E+00	0.00E+00	0.00E+00
937	GATA3	2	3	1.52E+07	0.00E+00	0.00E+00	0.00E+00	4.45E+07	2.75E+07	0.00E+00	0.00E+00	0.00E+00	0.00E+00	0.00E+00	0.00E+00
938	NLK	1	4	1.52E+07	0.00E+00	1.97E+07	0.00E+00	5.95E+07	2.68E+07	0.00E+00	0.00E+00	0.00E+00	0.00E+00	0.00E+00	0.00E+00
939	SLC25A10	2	2	9.37E+06	5.77E+06	6.30E+06	6.73E+06	0.00E+00	0.00E+00	0.00E+00	0.00E+00	1.38E+06	1.51E+06	0.00E+00	0.00E+00
940	NTHL1	3	2	1.49E+07	0.00E+00	5.06E+06	0.00E+00	1.23E+07	0.00E+00	0.00E+00	0.00E+00	0.00E+00	0.00E+00	5.78E+06	0.00E+00
941	ZNF711	3	9	0.00E+00	1.48E+07	0.00E+00	2.33E+07	3.41E+08	9.60E+07	0.00E+00	0.00E+00	0.00E+00	0.00E+00	0.00E+00	0.00E+00
942	TLE4	4	22	1.47E+07	0.00E+00	0.00E+00	0.00E+00	4.49E+06	0.00E+00	2.50E+07	0.00E+00	2.98E+06	0.00E+00	1.57E+07	2.39E+06
943	WDR77	2	2	1.47E+07	0.00E+00	0.00E+00	0.00E+00	1.00E+07	0.00E+00	3.41E+06	0.00E+00	4.36E+06	0.00E+00	0.00E+00	0.00E+00
944	PPP3CA;PP	11	1	1.44E+07	0.00E+00	8.64E+06	0.00E+00	1.62E+07	1.63E+07	7.72E+06	6.48E+06	5.67E+06	7.13E+06	8.96E+06	1.01E+07
945	PECR	1	2	1.44E+07	0.00E+00	8.21E+06	0.00E+00	1.74E+07	0.00E+00	6.21E+06	0.00E+00	0.00E+00	0.00E+00	9.94E+06	0.00E+00
946	IGF2BP1	2	8	1.44E+07	0.00E+00	5.40E+06	0.00E+00	2.03E+08	5.58E+07	0.00E+00	0.00E+00	0.00E+00	0.00E+00	0.00E+00	0.00E+00
947	ZDHHC13	3	1	1.44E+07	0.00E+00	0.00E+00	0.00E+00	0.00E+00	0.00E+00	0.00E+00	0.00E+00	0.00E+00	0.00E+00	0.00E+00	0.00E+00
948	MSL1	3	2	1.43E+07	0.00E+00	0.00E+00	0.00E+00	0.00E+00	0.00E+00	0.00E+00	0.00E+00	0.00E+00	0.00E+00	2.80E+06	1.34E+06
949	TFCP2	4	2	1.25E+07	1.82E+06	0.00E+00	0.00E+00	0.00E+00	0.00E+00	0.00E+00	0.00E+00	0.00E+00	0.00E+00	0.00E+00	0.00E+00
950	DYNLT1	1	1	1.43E+07	0.00E+00	0.00E+00	0.00E+00	1.85E+07	0.00E+00	2.98E+06	0.00E+00	2.67E+06	0.00E+00	6.78E+06	0.00E+00
951	LDHB	1	8	1.43E+07	0.00E+00	1.65E+07	0.00E+00	7.50E+06	0.00E+00	3.48E+06	0.00E+00	1.02E+08	1.29E+07	5.45E+06	0.00E+00
952	LRPPRC	1	6	1.42E+07	0.00E+00	6.44E+06	1.16E+06	9.71E+06	4.21E+06	0.00E+00	0.00E+00	6.07E+06	5.68E+06	0.00E+00	0.00E+00
953	FUBP3	1	5	0.00E+00	1.41E+07	0.00E+00	0.00E+00	2.75E+07	0.00E+00	0.00E+00	0.00E+00	0.00E+00	0.00E+00	0.00E+00	0.00E+00
954	ITCH	3	1	1.41E+07	0.00E+00	0.00E+00	0.00E+00	0.00E+00	0.00E+00	0.00E+00	0.00E+00	0.00E+00	0.00E+00	0.00E+00	0.00E+00
955	NSDHL	1	2	9.06E+06	5.00E+06	4.10E+06	3.54E+06	2.28E+07	1.85E+07	0.00E+00	0.00E+00	0.00E+00	0.00E+00	0.00E+00	0.00E+00
956	SPCS2	1	3	7.52E+06	6.46E+06	1.24E+07	1.52E+07	1.64E+07	1.40E+07	0.00E+00	0.00E+00	0.00E+00	0.00E+00	0.00E+00	0.00E+00
957	AIFM1	6	4	1.38E+07	0.00E+00	5.72E+06	0.00E+00	3.69E+07	2.51E+07	0.00E+00	0.00E+00	5.55E+06	4.60E+06	3.60E+06	0.00E+00
958	METTL9	2	3	7.34E+06	6.28E+06	0.00E+00	0.00E+00	5.00E+07	1.68E+07	0.00E+00	0.00E+00	0.00E+00	0.00E+00	0.00E+00	0.00E+00
959	LAMP1	2	4	1.35E+07	0.00E+00	1.56E+07	8.16E+06	1.53E+07	0.00E+00	0.00E+00	0.00E+00	0.00E+00	0.00E+00	0.00E+00	0.00E+00
960	TMCO1	3	2	9.65E+06	3.79E+06	7.09E+06	5.39E+06	1.39E+07	1.62E+07	0.00E+00	0.00E+00	1.12E+06	1.11E+06	0.00E+00	0.00E+00
961	ASCC2	1	2	1.04E+07	2.98E+06	2.56E+06	1.54E+06	7.93E+06	2.98E+06	0.00E+00	0.00E+00	0.00E+00	0.00E+00	0.00E+00	0.00E+00
962	PCNA	1	4	1.34E+07	0.00E+00	1.38E+07	0.00E+00	0.00E+00	0.00E+00	0.00E+00	0.00E+00	2.19E+07	0.00E+00	0.00E+00	0.00E+00
963	ZNF316	1	2	7.60E+06	5.72E+06	2.96E+06	1.27E+06	6.31E+06	0.00E+00	0.00E+00	0.00E+00	0.00E+00	0.00E+00	2.65E+06	8.36E+05
964	BAZ1B	2	4	1.33E+07	0.00E+00	6.58E+06	1.05E+06	1.44E+07	0.00E+00	0.00E+00	0.00E+00	0.00E+00	0.00E+00	0.00E+00	0.00E+00
965	NDUFA4	1	1	1.33E+07	0.00E+00	6.67E+06	0.00E+00	0.00E+00	0.00E+00	0.00E+00	0.00E+00	0.00E+00	0.00E+00	0.00E+00	0.00E+00
966	RABL3	1	1	1.33E+07	0.00E+00	0.00E+00	0.00E+00	0.00E+00	0.00E+00	0.00E+00	0.00E+00	0.00E+00	0.00E+00	0.00E+00	0.00E+00
967	OGT	4	10	1.33E+07	0.00E+00	3.67E+07	2.16E+06	8.74E+07	4.13E+06	0.00E+00	0.00E+00	1.48E+07	3.17E+06	5.18E+06	0.00E+00
968	MPO	3	2	1.31E+07	0.00E+00	0.00E+00	0.00E+00	0.00E+00	0.00E+00	0.00E+00	0.00E+00	0.00E+00	0.00E+00	0.00E+00	0.00E+00
969	SLC25A13	2	4	9.50E+06	3.57E+06	1.54E+07	6.53E+06	4.12E+06	0.00E+00	0.00E+00	0.00E+00	2.11E+06	0.00E+00	0.00E+00	0.00E+00
970	TRMT10C	1	3	9.12E+06	3.92E+06	8.06E+06	5.74E+06	0.00E+00	0.00E+00	0.00E+00	0.00E+00	0.00E+00	0.00E+00	0.00E+00	0.00E+00
971	APOBEC3C	1	1	1.29E+07	0.00E+00	5.03E+06	0.00E+00	0.00E+00	0.00E+00	0.00E+00	0.00E+00	0.00E+00	0.00E+00	0.00E+00	0.00E+00
972	MTHFD1	1	2	1.29E+07	0.00E+00	8.47E+06	0.00E+00	2.15E+06	0.00E+00	0.00E+00	0.00E+00	0.00E+00	0.00E+00	0.00E+00	0.00E+00
973	DDX18	1	1	1.29E+07	0.00E+00	0.00E+00	0.00E+00	0.00E+00	0.00E+00	0.00E+00	0.00E+00	0.00E+00	0.00E+00	0.00E+00	0.00E+00
974	SLC25A4	1	10	6.77E+06	6.05E+06	0.00E+00	0.00E+00	0.00E+00	0.00E+00	0.00E+00	0.00E+00	0.00E+00	0.00E+00	0.00E+00	0.00E+00
975	C9orf114	1	1	1.28E+07	0.00E+00	0.00E+00	0.00E+00	0.00E+00	0.00E+00	0.00E+00	0.00E+00	0.00E+00	0.00E+00	0.00E+00	0.00E+00
976	TRMT1L	2	2	9.87E+06	2.89E+06	0.00E+00	0.00E+00	5.57E+06	5.12E+06	0.00E+00	0.00E+00	0.00E+00	0.00E+00	1.50E+06	0.00E+00
977	FKBP8	3	2	1.26E+07	0.00E+00	6.63E+06	5.76E+06	0.00E+00	0.00E+00	0.00E+00	0.00E+00	0.00E+00	0.00E+00	0.00E+00	0.00E+00
978	LONP1	3	2	8.12E+06	4.40E+06	4.09E+06	2.45E+06	6.41E+06	2.63E+06	1.24E+06	0.00E+00	0.00E+00	0.00E+00	0.00E+00	0.00E+00
979	SUGP2	3	3	1.25E+07	0.00E+00	2.32E+06	0.00E+00	8.61E+06	0.00E+00	0.00E+00	0.00E+00	0.00E+00	0.00E+00	0.00E+00	0.00E+00
980	MRPL9	1	1	6.89E+06	5.51E+06	6.11E+06	5.73E+06	9.91E+06	8.16E+06	0.00E+00	0.00E+00	0.00E+00	0.00E+00	0.00E+00	0.00E+00
981	DDX52	1	3	8.81E+06	3.51E+06	1.47E+07	4.01E+06	3.73E+07	9.34E+06	0.00E+00	0.00E+00	0.00E+00	0.00E+00	0.00E+00	0.00E+00
982	NOMO2;N(	5	2	6.69E+06	5.55E+06	0.00E+00	0.00E+00	9.68E+06	5.57E+06	0.00E+00	0.00E+00	0.00E+00	0.00E+00	0.00E+00	0.00E+00
983	HSD17B4	3	2	1.01E+07	2.10E+06	0.00E+00	0.00E+00	0.00E+00	0.00E+00	0.00E+00	0.00E+00	0.00E+00	0.00E+00	0.00E+00	0.00E+00
984	CBX3	1	2	1.20E+07	0.00E+00	0.00E+00	0.00E+00	0.00E+00	0.00E+00	0.00E+00	0.00E+00	0.00E+00	0.00E+00	0.00E+00	0.00E+00

MQ search SILAC data

hit number	Gene names	Number of proteins	Peptides	Intensity L 2%SDS_24hHU	Intensity H 2%SDS_24hHU	Intensity L 2%SDS_2hHU	Intensity H 2%SDS_2hHU	Intensity L 2%SDS_NT	Intensity H 2%SDS_NT	Intensity L el150_24hHU	Intensity H el150_24hHU	Intensity L el150_2hHU	Intensity H el150_2hHU	Intensity L el150_NT	Intensity H el150_NT
985	UBAP2L	5	2	1.19E+07	0.00E+00	1.96E+07	0.00E+00	1.03E+07	0.00E+00	0.00E+00	0.00E+00	0.00E+00	0.00E+00	0.00E+00	0.00E+00
986	MGST3	1	1	6.03E+06	5.72E+06	2.62E+06	3.37E+06	0.00E+00	0.00E+00	0.00E+00	0.00E+00	0.00E+00	0.00E+00	0.00E+00	0.00E+00
987	CEP135	2	4	7.05E+06	4.66E+06	8.20E+06	4.34E+06	0.00E+00	0.00E+00	0.00E+00	0.00E+00	2.36E+06	0.00E+00	0.00E+00	0.00E+00
988	IGHG1	1	1	1.16E+07	0.00E+00	0.00E+00	0.00E+00	0.00E+00	0.00E+00	0.00E+00	0.00E+00	0.00E+00	0.00E+00	0.00E+00	0.00E+00
989	CLK4	1	4	1.14E+07	0.00E+00	0.00E+00	0.00E+00	1.08E+07	0.00E+00	0.00E+00	0.00E+00	0.00E+00	0.00E+00	0.00E+00	0.00E+00
990	LTV1	1	1	1.13E+07	0.00E+00	0.00E+00	0.00E+00	2.21E+07	0.00E+00	0.00E+00	0.00E+00	0.00E+00	0.00E+00	0.00E+00	0.00E+00
991	TTC1	1	2	1.13E+07	0.00E+00	0.00E+00	0.00E+00	2.56E+07	0.00E+00	0.00E+00	0.00E+00	0.00E+00	0.00E+00	0.00E+00	0.00E+00
992	CTBP2	3	1	5.84E+06	5.41E+06	3.72E+06	4.96E+06	7.91E+06	9.20E+06	1.90E+06	1.81E+06	0.00E+00	0.00E+00	0.00E+00	0.00E+00
993	TTC37	1	3	8.13E+06	3.11E+06	0.00E+00	0.00E+00	3.61E+06	3.18E+06	0.00E+00	0.00E+00	0.00E+00	0.00E+00	0.00E+00	0.00E+00
994	DHX40	4	5	1.12E+07	0.00E+00	6.71E+06	0.00E+00	8.68E+06	0.00E+00	4.32E+06	6.41E+05	4.14E+06	0.00E+00	2.08E+07	1.02E+06
995	CHD2	2	6	1.11E+07	0.00E+00	0.00E+00	0.00E+00	2.31E+06	1.20E+07	0.00E+00	0.00E+00	0.00E+00	0.00E+00	0.00E+00	0.00E+00
996	DIAPH1	3	9	9.84E+06	1.24E+06	0.00E+00	0.00E+00	0.00E+00	0.00E+00	0.00E+00	0.00E+00	0.00E+00	0.00E+00	3.15E+07	1.05E+07
997	RNFT2	5	2	6.59E+06	4.49E+06	0.00E+00	0.00E+00	2.67E+07	5.60E+06	0.00E+00	0.00E+00	0.00E+00	0.00E+00	0.00E+00	0.00E+00
998	SMAD9	8	9	1.11E+07	0.00E+00	1.82E+07	4.06E+06	4.64E+07	0.00E+00	0.00E+00	0.00E+00	3.17E+06	1.80E+06	1.13E+07	3.42E+06
999	SORT1	1	1	7.68E+06	3.26E+06	0.00E+00	0.00E+00	9.22E+06	4.86E+06	0.00E+00	0.00E+00	0.00E+00	0.00E+00	0.00E+00	0.00E+00
1000	SRP72	2	3	1.08E+07	0.00E+00	4.26E+06	0.00E+00	2.39E+07	0.00E+00	0.00E+00	0.00E+00	0.00E+00	0.00E+00	0.00E+00	0.00E+00
1001	ZMPSTE24	1	4	1.08E+07	0.00E+00	1.60E+07	0.00E+00	1.04E+07	0.00E+00	0.00E+00	0.00E+00	0.00E+00	0.00E+00	0.00E+00	0.00E+00
1002	DDX56	2	16	1.07E+07	0.00E+00	1.21E+08	7.37E+07	4.47E+08	1.93E+08	0.00E+00	0.00E+00	5.93E+06	2.79E+06	6.27E+06	2.77E+06
1003	HAT1	2	1	1.07E+07	0.00E+00	6.45E+06	0.00E+00	0.00E+00	0.00E+00	0.00E+00	0.00E+00	2.47E+06	0.00E+00	0.00E+00	0.00E+00
1004	GOLT1B	1	1	6.24E+06	4.37E+06	3.26E+06	2.93E+06	8.25E+06	5.48E+06	0.00E+00	0.00E+00	0.00E+00	0.00E+00	1.21E+06	7.97E+05
1005	ABCD3	2	2	6.28E+06	4.30E+06	1.09E+07	4.18E+06	6.30E+06	5.75E+06	0.00E+00	0.00E+00	9.43E+05	0.00E+00	0.00E+00	0.00E+00
1006	GSK3B	3	5	1.06E+07	0.00E+00	2.50E+07	0.00E+00	7.54E+07	1.60E+07	0.00E+00	0.00E+00	0.00E+00	0.00E+00	0.00E+00	0.00E+00
1007	AKAP8L	2	1	5.04E+06	5.43E+06	3.38E+06	4.32E+06	5.81E+06	5.82E+06	0.00E+00	0.00E+00	0.00E+00	0.00E+00	9.97E+05	1.01E+06
1008	YAF2	3	1	1.04E+07	0.00E+00	0.00E+00	0.00E+00	0.00E+00	0.00E+00	8.17E+06	0.00E+00	0.00E+00	0.00E+00	0.00E+00	0.00E+00
1009	TRIP13	1	2	0.00E+00	1.04E+07	5.73E+06	0.00E+00	1.26E+07	8.24E+06	0.00E+00	0.00E+00	0.00E+00	0.00E+00	0.00E+00	0.00E+00
1010	GART	2	3	1.03E+07	0.00E+00	0.00E+00	0.00E+00	0.00E+00	0.00E+00	8.94E+05	0.00E+00	6.33E+06	0.00E+00	1.70E+06	0.00E+00
1011	GALNT14	4	3	1.02E+07	0.00E+00	4.82E+06	0.00E+00	2.27E+07	8.15E+06	0.00E+00	0.00E+00	0.00E+00	0.00E+00	0.00E+00	0.00E+00
1012	IRS1	1	3	5.31E+06	4.80E+06	1.87E+06	2.57E+06	3.71E+06	4.80E+06	0.00E+00	0.00E+00	0.00E+00	0.00E+00	7.30E+06	2.89E+06
1013	POLR2A	1	2	5.98E+06	4.13E+06	0.00E+00	0.00E+00	6.06E+06	3.55E+06	0.00E+00	0.00E+00	0.00E+00	0.00E+00	0.00E+00	0.00E+00
1014	JMJD6	3	2	7.31E+06	2.76E+06	2.29E+06	2.42E+06	0.00E+00	0.00E+00	5.38E+06	3.21E+06	1.63E+06	1.80E+06	3.94E+06	3.61E+06
1015	GPBP1	4	1	1.00E+07	0.00E+00	0.00E+00	0.00E+00	1.67E+07	0.00E+00	0.00E+00	0.00E+00	0.00E+00	0.00E+00	0.00E+00	0.00E+00
1016	STAU1	3	3	9.96E+06	0.00E+00	1.30E+07	4.54E+06	2.88E+07	1.52E+07	0.00E+00	0.00E+00	0.00E+00	0.00E+00	0.00E+00	0.00E+00
1017	ACSL3	3	3	9.92E+06	0.00E+00	6.15E+06	0.00E+00	0.00E+00	0.00E+00	0.00E+00	0.00E+00	0.00E+00	0.00E+00	0.00E+00	0.00E+00
1018	VAPB	2	5	9.90E+06	0.00E+00	1.42E+07	0.00E+00	7.08E+07	0.00E+00	0.00E+00	0.00E+00	0.00E+00	0.00E+00	0.00E+00	0.00E+00
1019	SEC23A;SE(	3	2	9.84E+06	0.00E+00	4.48E+06	3.73E+06	8.31E+06	4.86E+06	0.00E+00	0.00E+00	0.00E+00	1.58E+06	0.00E+00	1.42E+06
1020	MRPS27	2	3	9.81E+06	0.00E+00	1.91E+07	4.87E+06	1.58E+07	6.16E+06	0.00E+00	0.00E+00	0.00E+00	0.00E+00	1.73E+06	0.00E+00
1021	RBM23	5	5	9.77E+06	0.00E+00	6.04E+06	0.00E+00	5.42E+07	9.43E+06	0.00E+00	0.00E+00	0.00E+00	0.00E+00	3.46E+06	0.00E+00
1022	ZNF483	2	3	9.56E+06	0.00E+00	1.10E+07	0.00E+00	2.49E+07	0.00E+00	0.00E+00	0.00E+00	0.00E+00	0.00E+00	0.00E+00	0.00E+00
1023	ZC3HAV1	2	1	9.37E+06	0.00E+00	0.00E+00	0.00E+00	0.00E+00	0.00E+00	0.00E+00	0.00E+00	0.00E+00	0.00E+00	0.00E+00	0.00E+00
1024	RYBP	1	1	5.80E+06	3.57E+06	2.31E+06	2.05E+06	4.07E+06	3.18E+06	1.91E+06	1.09E+06	1.11E+06	1.03E+06	2.55E+06	2.10E+06
1025	DNM1L	8	2	5.70E+06	3.55E+06	3.24E+06	3.20E+06	0.00E+00	0.00E+00	0.00E+00	0.00E+00	0.00E+00	0.00E+00	0.00E+00	0.00E+00
1026	EED	3	7	9.17E+06	0.00E+00	2.24E+07	1.04E+07	3.49E+07	0.00E+00	2.98E+06	0.00E+00	0.00E+00	0.00E+00	5.69E+06	1.50E+07
1027	ABHD12	3	2	6.31E+06	2.69E+06	0.00E+00	0.00E+00	9.25E+06	5.83E+06	0.00E+00	0.00E+00	0.00E+00	0.00E+00	0.00E+00	0.00E+00
1028	ILVBL	1	2	5.63E+06	3.33E+06	7.68E+06	5.76E+06	4.98E+06	3.97E+06	0.00E+00	0.00E+00	0.00E+00	0.00E+00	0.00E+00	0.00E+00
1029	BOP1	2	1	8.90E+06	0.00E+00	3.30E+06	3.39E+06	0.00E+00	0.00E+00	0.00E+00	0.00E+00	0.00E+00	0.00E+00	0.00E+00	0.00E+00
1030	ERLIN2	1	1	5.90E+06	2.99E+06	0.00E+00	0.00E+00	0.00E+00	3.61E+06	0.00E+00	0.00E+00	0.00E+00	0.00E+00	0.00E+00	0.00E+00
1031	DNAJB11	1	1	8.83E+06	0.00E+00	5.21E+06	4.78E+06	0.00E+00	0.00E+00	0.00E+00	0.00E+00	0.00E+00	0.00E+00	0.00E+00	0.00E+00
1032	PLAGL2	1	1	8.75E+06	0.00E+00	1.02E+07	0.00E+00	1.72E+07	0.00E+00	0.00E+00	0.00E+00	0.00E+00	0.00E+00	0.00E+00	0.00E+00
1033	RAB18	3	3	8.71E+06	0.00E+00	2.68E+07	8.12E+06	1.07E+07	0.00E+00	0.00E+00	0.00E+00	0.00E+00	0.00E+00	0.00E+00	0.00E+00
1034	TUBGCP2	3	4	6.45E+06	2.22E+06	0.00E+00	0.00E+00	4.27E+06	0.00E+00	0.00E+00	0.00E+00	0.00E+00	0.00E+00	5.46E+06	1.18E+06
1035	NUP205	1	2	7.07E+06	1.60E+06	0.00E+00	0.00E+00	0.00E+00	0.00E+00	0.00E+00	0.00E+00	0.00E+00	6.84E+05	0.00E+00	0.00E+00
1036	RCOR3;RC(	5	1	8.61E+06	0.00E+00	0.00E+00	0.00E+00	9.83E+06	0.00E+00	0.00E+00	0.00E+00	1.99E+06	0.00E+00	4.61E+06	0.00E+00
1037	NUSAP1	7	8	8.59E+06	0.00E+00	1.94E+07	1.36E+07	2.49E+08	1.20E+08	0.00E+00	0.00E+00	0.00E+00	0.00E+00	5.48E+06	0.00E+00
1038	ALG3	2	1	4.61E+06	3.90E+06	0.00E+00	0.00E+00	0.00E+00	0.00E+00	0.00E+00	0.00E+00	0.00E+00	0.00E+00	0.00E+00	0.00E+00
1039	HDAC3	2	1	4.81E+06	3.69E+06	4.12E+06	3.69E+06	9.21E+06	7.40E+06	1.37E+06	1.57E+06	1.66E+06	1.06E+06	2.88E+06	2.56E+06
1040	ATAD5	2	6	8.47E+06	0.00E+00	1.88E+07	7.51E+06	1.55E+07	0.00E+00	0.00E+00	0.00E+00	0.00E+00	0.00E+00	2.49E+06	0.00E+00
1041	MUS81	1	3	8.46E+06	0.00E+00	5.56E+06	6.64E+06	4.28E+07	2.21E+07	0.00E+00	0.00E+00	0.00E+00	0.00E+00	1.93E+06	1.62E+06
1042	ASNA1	1	3	8.43E+06	0.00E+00	0.00E+00	0.00E+00	1.69E+07	6.23E+06	0.00E+00	0.00E+00	0.00E+00	0.00E+00	0.00E+00	0.00E+00
1043	ELL2	1	1	8.38E+06	0.00E+00	5.05E+06	0.00E+00	1.07E+07	0.00E+00	0.00E+00	0.00E+00	1.75E+06	0.00E+00	0.00E+00	0.00E+00
1044	XPO7	1	2	5.22E+06	3.10E+06	0.00E+00	0.00E+00	6.29E+06	5.22E+06	0.00E+00	0.00E+00	0.00E+00	0.00E+00	1.76E+06	0.00E+00
1045	SEC61G	1	1	4.97E+06	3.33E+06	2.51E+06	2.61E+06	4.81E+06	4.15E+06	0.00E+00	0.00E+00	0.00E+00	0.00E+00	6.65E+05	7.39E+05
1046	RRS1	1	1	5.30E+06	3.00E+06	1.96E+06	0.00E+00	0.00E+00	0.00E+00	0.00E+00	0.00E+00	0.00E+00	0.00E+00	0.00E+00	0.00E+00
1047	MOGS	2	2	4.66E+06	3.61E+06	2.35E+06	2.93E+06	5.40E+06	1.81E+07	0.00E+00	0.00E+00	0.00E+00	0.00E+00	0.00E+00	0.00E+00
1048	PDCD11	1	2	7.57E+06	6.42E+05	0.00E+00	0.00E+00	0.00E+00	0.00E+00	0.00E+00	0.00E+00	0.00E+00	0.00E+00	0.00E+00	0.00E+00
1049	CSTF2;CSTF	3	2	6.38E+06	1.69E+06	0.00E+00	0.00E+00	0.00E+00	0.00E+00	0.00E+00	0.00E+00	0.00E+00	0.00E+00	0.00E+00	0.00E+00
1050	BAZ1A	2	3	2.53E+06	5.48E+06	2.92E+06	2.16E+06	1.77E+07	6.47E+06	1.02E+06	3.89E+05	1.32E+06	6.56E+05	0.00E+00	0.00E+00
1051	GLCCI1	1	1	8.01E+06	0.00E+00	4.91E+06	0.00E+00	1.10E+07	0.00E+00	3.47E+06	0.00E+00	0.00E+00	0.00E+00	0.00E+00	0.00E+00
1052	CTPS1	2	2	5.24E+06	2.75E+06	1.92E+06	1.19E+06	6.24E+06	2.13E+06	0.00E+00	0.00E+00	1.01E+06	9.61E+05	0.00E+00	0.00E+00
1053	EIF3K	2	2	7.95E+06	0.00E+00	4.72E+06	0.00E+00	6.20E+06	0.00E+00	0.00E+00	0.00E+00	5.63E+06	0.00E+00	0.00E+00	0.00E+00
1054	MAU2	3	2	4.08E+06	3.80E+06	6.95E+06	0.00E+00	6.41E+06	8.91E+06	4.40E+06	0.00E+00	1.14E+06	1.30E+06	1.01E+07	2.25E+06
1055	AGPS	1	2	7.78E+06	0.00E+00	0.00E+00	0.00E+00	3.81E+06	3.27E+06	0.00E+00	0.00E+00	0.00E+00	0.00E+00	0.00E+00	0.00E+00
1056	CORO1C	3	2	7.75E+06	0.00E+00	0.00E+00	0.00E+00	0.00E+00	0.00E+00	0.00E+00	0.00E+00	0.00E+00	0.00E+00	4.60E+06	0.00E+00
1057	EPRS	1	3	7.65E+06	0.00E+00	3.74E+06	0.00E+00	4.06E+06	0.00E+00	0.00E+00	0.00E+00	0.00E+00	0.00E+00	4.45E+06	0.00E+00
1058	KIAA0020	1	2	7.62E+06	0.00E+00	0.00E+00	0.00E+00	0.00E+00	0.00E+00	0.00E+00	0.00E+00	0.00E+00	0.00E+00	0.00E+00	0.00E+00
1059	NOC3L	1	1	7.61E+06	0.00E+00	0.00E+00	0.00E+00	0.00E+00	0.00E+00	0.00E+00	0.00E+00	0.00E+00	0.00E+00	0.00E+00	0.00E+00
1060	MPDU1	2	2	7.57E+06	0.00E+00	4.55E+06	0.00E+00	2.24E+07	0.00E+00	0.00E+00	0.00E+00	1.92E+06	0.00E+00	0.00E+00	0.00E+00
1061	DOCK4	3	2	7.56E+06	0.00E+00	0.00E+00	0.00E+00	0.00E+00	0.00E+00	0.00E+00	0.00E+00	0.00E+00	0.00E+00	0.00E+00	0.00E+00
1062	NIPBL	3	6	5.04E+06	2.50E+06	9.75E+06	5.20E+06	4.15E+06	0.00E+00	0.00E+00	0.00E+00	0.00E+00	0.00E+00	1.73E+07	8.37E+06
1063	KCTD15	4	5	7.52E+06	0.00E+00	8.14E+06	0.00E+00	3.82E+07	6.22E+06	3.02E+06	0.00E+00	9.25E+06	0.00E+00	4.65E+06	0.00E+00
1064	ADPGK	4	2	7.43E+06	0.00E+00	3.67E+06	0.00E+00	9.72E+06	0.00E+00	0.00E+00	0.00E+00	0.00E+00	0.00E+00	0.00E+00	0.00E+00
1065	BZW2	2	2	7.40E+06	0.00E+00	1.01E+07	3.77E+06	1.51E+07	0.00E+00	0.00E+00	0.00E+00	0.00E+00	0.00E+00	2.69E+06	0.00E+00
1066	LARP4	6	1	4.21E+06	3.10E+06	2.68E+06	2.00E+06	3.93E+06	2.63E+06	0.00E+00	0.00E+00	0.00E+00	0.00E+00	0.00E+00	0.00E+00

MQ search SILAC data

hit number	Gene names	Number of proteins	Peptides	Intensity L 2%SDS_24hHU	Intensity H 2%SDS_24hHU	Intensity L 2%SDS_2hHU	Intensity H 2%SDS_2hHU	Intensity L 2%SDS_NT	Intensity H 2%SDS_NT	Intensity L el150_24hHU	Intensity H el150_24hHU	Intensity L el150_2hHU	Intensity H el150_2hHU	Intensity L el150_NT	Intensity H el150_NT
1067	DNAAF5	3	4	4.59E+06	2.69E+06	8.41E+06	2.44E+06	1.19E+07	4.19E+06	0.00E+00	0.00E+00	0.00E+00	0.00E+00	0.00E+00	0.00E+00
1068	ARHGEF2	3	2	6.14E+06	1.08E+06	9.01E+05	6.20E+05	8.89E+06	1.31E+06	0.00E+00	0.00E+00	0.00E+00	0.00E+00	0.00E+00	0.00E+00
1069	PSIP1	3	2	7.22E+06	0.00E+00	0.00E+00	0.00E+00	3.55E+06	0.00E+00	0.00E+00	0.00E+00	0.00E+00	0.00E+00	0.00E+00	0.00E+00
1070	EIF4G1	8	4	7.15E+06	0.00E+00	7.49E+06	0.00E+00	2.76E+06	2.82E+06	0.00E+00	0.00E+00	6.38E+05	9.98E+05	0.00E+00	0.00E+00
1071	ARL1	2	1	7.08E+06	0.00E+00	6.38E+06	0.00E+00	1.41E+07	0.00E+00	0.00E+00	0.00E+00	0.00E+00	0.00E+00	0.00E+00	0.00E+00
1072	ZCCHC3	1	2	6.48E+06	5.82E+05	0.00E+00	0.00E+00	0.00E+00	0.00E+00	0.00E+00	0.00E+00	0.00E+00	0.00E+00	0.00E+00	0.00E+00
1073	ENO1	5	16	4.98E+06	2.07E+06	3.97E+07	2.28E+07	0.00E+00	0.00E+00	2.06E+07	1.05E+06	3.43E+08	1.41E+07	3.66E+07	1.66E+06
1074	CHD4;CHD:	5	1	7.04E+06	0.00E+00	2.90E+06	1.98E+06	7.00E+06	4.68E+06	0.00E+00	0.00E+00	0.00E+00	0.00E+00	0.00E+00	0.00E+00
1075	FASN	1	14	6.99E+06	0.00E+00	1.84E+07	7.40E+06	0.00E+00	0.00E+00	0.00E+00	0.00E+00	6.22E+07	2.22E+07	0.00E+00	0.00E+00
1076	EMC1	4	3	6.94E+06	0.00E+00	1.56E+06	0.00E+00	1.17E+07	0.00E+00	0.00E+00	0.00E+00	0.00E+00	0.00E+00	0.00E+00	0.00E+00
1077	ALKBH5	3	2	6.94E+06	0.00E+00	0.00E+00	0.00E+00	0.00E+00	0.00E+00	0.00E+00	0.00E+00	0.00E+00	0.00E+00	0.00E+00	0.00E+00
1078	TRIO	4	2	5.04E+06	1.90E+06	1.33E+06	1.67E+06	2.07E+06	1.46E+06	5.99E+05	5.71E+05	0.00E+00	0.00E+00	9.13E+05	9.36E+05
1079	ADRM1	1	1	6.92E+06	0.00E+00	2.75E+06	3.64E+06	8.91E+06	8.23E+06	0.00E+00	0.00E+00	0.00E+00	0.00E+00	0.00E+00	0.00E+00
1080	LDHA	5	5	6.88E+06	0.00E+00	1.19E+07	0.00E+00	4.45E+06	0.00E+00	1.65E+06	0.00E+00	2.86E+07	2.20E+07	4.35E+06	0.00E+00
1081	DNAJB1	2	1	4.00E+06	2.88E+06	3.50E+06	2.64E+06	0.00E+00	0.00E+00	0.00E+00	0.00E+00	0.00E+00	0.00E+00	0.00E+00	0.00E+00
1082	CFAP20	1	1	4.28E+06	2.59E+06	1.55E+06	2.00E+06	2.29E+06	2.72E+06	0.00E+00	0.00E+00	0.00E+00	0.00E+00	0.00E+00	0.00E+00
1083	ORC5	2	3	0.00E+00	6.86E+06	9.74E+06	9.79E+06	2.74E+07	1.59E+07	8.81E+05	1.27E+06	0.00E+00	0.00E+00	3.35E+06	2.45E+06
1084	FARP1	2	1	4.64E+06	2.19E+06	0.00E+00	0.00E+00	0.00E+00	0.00E+00	1.63E+06	0.00E+00	0.00E+00	0.00E+00	0.00E+00	1.65E+06
1085	TMEM65	1	1	6.81E+06	0.00E+00	0.00E+00	0.00E+00	0.00E+00	0.00E+00	0.00E+00	0.00E+00	0.00E+00	0.00E+00	0.00E+00	0.00E+00
1086	MKI67	2	3	6.68E+06	0.00E+00	0.00E+00	0.00E+00	3.91E+06	0.00E+00	0.00E+00	0.00E+00	0.00E+00	0.00E+00	0.00E+00	0.00E+00
1087	EIF4A1	4	9	6.67E+06	0.00E+00	2.68E+06	4.44E+06	0.00E+00	0.00E+00	0.00E+00	0.00E+00	5.40E+07	2.88E+07	0.00E+00	0.00E+00
1088	NDUFS1	5	1	6.64E+06	0.00E+00	0.00E+00	0.00E+00	0.00E+00	0.00E+00	0.00E+00	0.00E+00	0.00E+00	0.00E+00	0.00E+00	0.00E+00
1089	EEF1B2	1	1	6.57E+06	0.00E+00	0.00E+00	0.00E+00	0.00E+00	0.00E+00	0.00E+00	0.00E+00	3.74E+06	0.00E+00	0.00E+00	0.00E+00
1090	SENP2	2	3	6.54E+06	0.00E+00	0.00E+00	0.00E+00	6.12E+07	0.00E+00	0.00E+00	0.00E+00	0.00E+00	0.00E+00	7.34E+06	0.00E+00
1091	LARS	3	2	6.52E+06	0.00E+00	4.40E+06	0.00E+00	6.96E+06	0.00E+00	0.00E+00	0.00E+00	0.00E+00	0.00E+00	0.00E+00	0.00E+00
1092	DSP	3	33	6.43E+06	0.00E+00	1.63E+07	0.00E+00	2.97E+06	0.00E+00	3.39E+07	0.00E+00	3.67E+08	1.50E+07	9.26E+06	0.00E+00
1093	LAMP2	3	2	2.71E+06	3.67E+06	6.17E+06	6.96E+06	3.02E+06	2.85E+06	0.00E+00	0.00E+00	0.00E+00	0.00E+00	0.00E+00	0.00E+00
1094	CKAP5	3	2	6.36E+06	0.00E+00	0.00E+00	0.00E+00	0.00E+00	0.00E+00	0.00E+00	0.00E+00	9.86E+05	0.00E+00	0.00E+00	0.00E+00
1095	GTF3C5	3	1	5.45E+06	9.10E+05	0.00E+00	0.00E+00	0.00E+00	0.00E+00	0.00E+00	0.00E+00	0.00E+00	0.00E+00	0.00E+00	0.00E+00
1096	INO80D	1	1	6.34E+06	0.00E+00	4.88E+06	0.00E+00	5.77E+06	0.00E+00	0.00E+00	0.00E+00	0.00E+00	0.00E+00	0.00E+00	0.00E+00
1097	PARP14	5	6	6.30E+06	0.00E+00	5.53E+06	0.00E+00	1.04E+07	0.00E+00	0.00E+00	0.00E+00	0.00E+00	0.00E+00	1.03E+07	1.70E+06
1098	YWHAG	1	3	6.29E+06	0.00E+00	0.00E+00	0.00E+00	0.00E+00	0.00E+00	0.00E+00	0.00E+00	0.00E+00	0.00E+00	0.00E+00	0.00E+00
1099	BANF1	1	2	6.23E+06	0.00E+00	7.77E+06	0.00E+00	2.81E+07	0.00E+00	0.00E+00	0.00E+00	0.00E+00	0.00E+00	0.00E+00	0.00E+00
1100	FARSA	2	1	3.93E+06	2.20E+06	0.00E+00	0.00E+00	0.00E+00	0.00E+00	0.00E+00	0.00E+00	0.00E+00	0.00E+00	0.00E+00	0.00E+00
1101	STOML2	2	1	3.83E+06	2.29E+06	1.93E+06	1.57E+06	3.30E+06	1.90E+06	0.00E+00	0.00E+00	0.00E+00	0.00E+00	0.00E+00	0.00E+00
1102	FIZ1	1	1	6.04E+06	0.00E+00	0.00E+00	0.00E+00	0.00E+00	0.00E+00	0.00E+00	0.00E+00	0.00E+00	0.00E+00	0.00E+00	0.00E+00
1103	PSMD2	3	5	6.04E+06	0.00E+00	3.87E+06	5.34E+06	1.23E+07	8.14E+06	0.00E+00	0.00E+00	5.02E+06	6.88E+05	0.00E+00	0.00E+00
1104	AP3D1	4	2	6.01E+06	0.00E+00	2.56E+06	0.00E+00	3.88E+06	0.00E+00	0.00E+00	0.00E+00	0.00E+00	0.00E+00	0.00E+00	0.00E+00
1105	JUP	2	12	5.45E+06	5.21E+05	3.95E+06	0.00E+00	5.07E+06	8.41E+05	2.58E+07	0.00E+00	1.26E+08	6.02E+06	1.76E+07	0.00E+00
1106	POGZ	6	1	5.95E+06	0.00E+00	2.27E+06	0.00E+00	0.00E+00	0.00E+00	0.00E+00	0.00E+00	0.00E+00	0.00E+00	0.00E+00	0.00E+00
1107	LRCH3	4	6	5.94E+06	0.00E+00	4.00E+06	0.00E+00	4.34E+06	2.66E+06	1.88E+06	8.83E+05	9.68E+06	6.44E+06	1.31E+07	5.20E+06
1108	NAT10	2	2	5.90E+06	0.00E+00	0.00E+00	0.00E+00	1.58E+06	7.59E+05	0.00E+00	0.00E+00	0.00E+00	0.00E+00	0.00E+00	0.00E+00
1109	COPG1;COI	3	2	5.67E+06	0.00E+00	3.08E+06	0.00E+00	4.18E+06	0.00E+00	0.00E+00	0.00E+00	4.03E+06	1.62E+06	1.48E+06	0.00E+00
1110	TMEM70	2	1	5.65E+06	0.00E+00	3.63E+06	1.87E+06	9.20E+06	0.00E+00	0.00E+00	0.00E+00	0.00E+00	0.00E+00	0.00E+00	0.00E+00
1111	MRPL10	2	3	5.61E+06	0.00E+00	1.88E+06	1.59E+06	2.36E+07	0.00E+00	1.85E+06	0.00E+00	0.00E+00	8.35E+06	0.00E+00	0.00E+00
1112	PTGES3	2	1	5.58E+06	0.00E+00	4.45E+06	0.00E+00	0.00E+00	0.00E+00	2.58E+06	0.00E+00	7.18E+06	0.00E+00	2.76E+06	0.00E+00
1113	PSMC2	2	2	2.98E+06	2.56E+06	2.62E+06	0.00E+00	4.63E+06	3.96E+06	0.00E+00	0.00E+00	0.00E+00	0.00E+00	2.11E+06	9.01E+05
1114	SGPL1	1	2	5.44E+06	0.00E+00	0.00E+00	0.00E+00	0.00E+00	3.07E+06	0.00E+00	0.00E+00	0.00E+00	0.00E+00	0.00E+00	0.00E+00
1115	WDR34	1	4	5.43E+06	0.00E+00	7.21E+06	0.00E+00	7.88E+06	0.00E+00	1.89E+06	0.00E+00	0.00E+00	0.00E+00	1.78E+07	0.00E+00
1116	DDX31	3	5	2.48E+06	2.91E+06	0.00E+00	0.00E+00	5.65E+07	1.30E+07	0.00E+00	0.00E+00	0.00E+00	0.00E+00	0.00E+00	0.00E+00
1117	TRIP12	4	3	3.88E+06	1.42E+06	3.37E+06	1.60E+06	7.72E+06	3.03E+06	0.00E+00	0.00E+00	0.00E+00	0.00E+00	0.00E+00	0.00E+00
1118	NOB1	1	3	5.30E+06	0.00E+00	3.41E+06	2.32E+06	3.88E+07	1.67E+07	0.00E+00	0.00E+00	0.00E+00	0.00E+00	0.00E+00	0.00E+00
1119	PDCD2L	1	1	5.21E+06	0.00E+00	3.28E+06	0.00E+00	4.21E+06	0.00E+00	0.00E+00	0.00E+00	0.00E+00	0.00E+00	0.00E+00	0.00E+00
1120	KCTD1;KCT	2	2	5.21E+06	0.00E+00	1.11E+07	0.00E+00	6.42E+06	0.00E+00	0.00E+00	0.00E+00	0.00E+00	0.00E+00	2.94E+06	0.00E+00
1121	NUP62	1	1	5.21E+06	0.00E+00	0.00E+00	0.00E+00	0.00E+00	0.00E+00	0.00E+00	0.00E+00	0.00E+00	0.00E+00	0.00E+00	0.00E+00
1122	CREBBP;EP	3	2	5.18E+06	0.00E+00	3.38E+06	0.00E+00	1.88E+07	0.00E+00	0.00E+00	0.00E+00	0.00E+00	0.00E+00	2.73E+06	0.00E+00
1123	NPM3	1	1	3.00E+06	2.17E+06	1.28E+06	1.45E+06	1.56E+06	1.60E+06	0.00E+00	0.00E+00	0.00E+00	0.00E+00	0.00E+00	0.00E+00
1124	TTF2	2	5	5.16E+06	0.00E+00	0.00E+00	0.00E+00	0.00E+00	0.00E+00	9.95E+06	5.05E+06	3.42E+06	2.96E+06	1.96E+07	6.51E+06
1125	VAMP7	3	2	5.11E+06	0.00E+00	0.00E+00	0.00E+00	1.05E+07	0.00E+00	0.00E+00	0.00E+00	0.00E+00	0.00E+00	0.00E+00	0.00E+00
1126	EPT1	1	2	5.08E+06	0.00E+00	0.00E+00	0.00E+00	9.89E+06	0.00E+00	0.00E+00	0.00E+00	0.00E+00	0.00E+00	0.00E+00	0.00E+00
1127	DNAJC7	2	2	5.08E+06	0.00E+00	6.22E+06	0.00E+00	6.87E+06	0.00E+00	0.00E+00	0.00E+00	0.00E+00	0.00E+00	0.00E+00	0.00E+00
1128	SMPD4	10	3	5.05E+06	0.00E+00	0.00E+00	0.00E+00	1.68E+07	7.43E+06	0.00E+00	0.00E+00	0.00E+00	0.00E+00	1.80E+06	1.80E+06
1129	SDHA	3	3	5.03E+06	0.00E+00	9.92E+06	1.36E+06	4.20E+07	3.31E+06	0.00E+00	0.00E+00	0.00E+00	0.00E+00	0.00E+00	0.00E+00
1130	ACTN4;ACT	9	4	3.11E+06	1.90E+06	4.26E+06	5.27E+06	0.00E+00	0.00E+00	0.00E+00	0.00E+00	1.21E+07	1.51E+07	0.00E+00	0.00E+00
1131	MYH9	7	4	2.95E+06	1.96E+06	1.92E+06	2.17E+06	0.00E+00	0.00E+00	0.00E+00	0.00E+00	9.86E+06	6.53E+06	0.00E+00	0.00E+00
1132	NR2F2;NR2	4	2	2.98E+06	1.87E+06	0.00E+00	2.61E+06	7.87E+06	6.64E+06	0.00E+00	0.00E+00	0.00E+00	0.00E+00	0.00E+00	1.19E+06
1133	BYSL	1	3	4.74E+06	0.00E+00	5.24E+06	1.26E+07	8.64E+06	2.18E+07	0.00E+00	0.00E+00	0.00E+00	0.00E+00	0.00E+00	0.00E+00
1134	TERF2IP	1	1	4.68E+06	0.00E+00	0.00E+00	0.00E+00	2.67E+06	0.00E+00	0.00E+00	0.00E+00	0.00E+00	0.00E+00	0.00E+00	0.00E+00
1135	KCTD12	1	1	4.64E+06	0.00E+00	3.03E+06	0.00E+00	4.01E+06	0.00E+00	9.30E+05	4.72E+05	1.90E+06	0.00E+00	0.00E+00	0.00E+00
1136	RSF1	2	1	4.51E+06	0.00E+00	0.00E+00	0.00E+00	0.00E+00	0.00E+00	0.00E+00	0.00E+00	0.00E+00	0.00E+00	0.00E+00	0.00E+00
1137	UHRF1	2	2	4.48E+06	0.00E+00	2.30E+06	0.00E+00	6.16E+06	4.88E+06	0.00E+00	0.00E+00	0.00E+00	0.00E+00	0.00E+00	0.00E+00
1138	DHRS7B	1	2	4.46E+06	0.00E+00	0.00E+00	0.00E+00	0.00E+00	0.00E+00	0.00E+00	0.00E+00	0.00E+00	0.00E+00	0.00E+00	0.00E+00
1139	HEATR1	1	2	2.77E+06	1.68E+06	4.78E+06	4.54E+06	0.00E+00	0.00E+00	0.00E+00	0.00E+00	0.00E+00	0.00E+00	0.00E+00	0.00E+00
1140	CDIPT	2	1	4.30E+06	0.00E+00	0.00E+00	0.00E+00	5.12E+06	0.00E+00	0.00E+00	0.00E+00	0.00E+00	0.00E+00	0.00E+00	0.00E+00
1141	TMEM41A	1	1	2.62E+06	1.63E+06	0.00E+00	0.00E+00	0.00E+00	0.00E+00	0.00E+00	0.00E+00	0.00E+00	0.00E+00	0.00E+00	0.00E+00
1142	CADM1	5	3	4.25E+06	0.00E+00	7.23E+06	1.18E+07	1.71E+07	0.00E+00	0.00E+00	0.00E+00	0.00E+00	0.00E+00	0.00E+00	0.00E+00
1143	DHX36	3	1	4.24E+06	0.00E+00	0.00E+00	0.00E+00	0.00E+00	0.00E+00	0.00E+00	0.00E+00	0.00E+00	0.00E+00	0.00E+00	0.00E+00
1144	KIF23	3	2	4.12E+06	0.00E+00	0.00E+00	0.00E+00	0.00E+00	0.00E+00	0.00E+00	0.00E+00	0.00E+00	0.00E+00	0.00E+00	0.00E+00
1145	ANXA2	3	3	4.09E+06	0.00E+00	0.00E+00	0.00E+00	0.00E+00	0.00E+00	0.00E+00	0.00E+00	9.22E+06	0.00E+00	0.00E+00	0.00E+00
1146	GPI	3	3	4.08E+06	0.00E+00	7.59E+06	1.56E+06	0.00E+00	0.00E+00	0.00E+00	0.00E+00	1.69E+07	0.00E+00	0.00E+00	0.00E+00
1147	UNC45A	2	1	2.55E+06	1.50E+06	0.00E+00	0.00E+00	3.01E+06	2.97E+06	0.00E+00	0.00E+00	0.00E+00	0.00E+00	0.00E+00	0.00E+00
1148	SRP54	2	2	3.99E+06	0.00E+00	0.00E+00	0.00E+00	1.71E+07	0.00E+00	0.00E+00	0.00E+00	0.00E+00	0.00E+00	0.00E+00	0.00E+00

MQ search SILAC data

hit number	Gene names	Number of proteins	Peptides	Intensity L 2%SDS_24hHU	Intensity H 2%SDS_24hHU	Intensity L 2%SDS_2hHU	Intensity H 2%SDS_2hHU	Intensity L 2%SDS_NT	Intensity H 2%SDS_NT	Intensity L el150_24hHU	Intensity H el150_24hHU	Intensity L el150_2hHU	Intensity H el150_2hHU	Intensity L el150_NT	Intensity H el150_NT
1149	NOP9	2	2	2.09E+06	1.85E+06	0.00E+00	0.00E+00	9.10E+06	6.66E+06	0.00E+00	0.00E+00	0.00E+00	0.00E+00	0.00E+00	1.67E+07
1150	AP2M1	2	2	3.79E+06	0.00E+00	4.03E+06	0.00E+00	1.59E+07	7.30E+06	0.00E+00	0.00E+00	0.00E+00	0.00E+00	3.32E+06	0.00E+00
1151	MTA1	3	1	3.70E+06	0.00E+00	1.54E+06	0.00E+00	3.54E+06	0.00E+00	0.00E+00	0.00E+00	0.00E+00	0.00E+00	0.00E+00	0.00E+00
1152	FMR1	11	1	2.33E+06	1.33E+06	0.00E+00	0.00E+00	0.00E+00	0.00E+00	0.00E+00	0.00E+00	0.00E+00	0.00E+00	0.00E+00	0.00E+00
1153	SCMH1	6	1	1.99E+06	1.66E+06	0.00E+00	0.00E+00	2.45E+06	1.74E+06	0.00E+00	0.00E+00	0.00E+00	0.00E+00	0.00E+00	0.00E+00
1154	LTN1	3	1	1.83E+06	1.77E+06	2.12E+06	1.40E+06	2.50E+06	1.88E+06	0.00E+00	0.00E+00	0.00E+00	0.00E+00	0.00E+00	0.00E+00
1155	NXN	3	2	3.54E+06	0.00E+00	0.00E+00	0.00E+00	0.00E+00	0.00E+00	8.40E+05	0.00E+00	0.00E+00	0.00E+00	0.00E+00	0.00E+00
1156	INTS3	4	2	1.89E+06	1.61E+06	0.00E+00	0.00E+00	2.84E+06	1.45E+06	0.00E+00	0.00E+00	0.00E+00	0.00E+00	0.00E+00	0.00E+00
1157	VCP	1	6	3.29E+06	0.00E+00	3.79E+06	0.00E+00	3.45E+06	0.00E+00	0.00E+00	0.00E+00	9.72E+06	5.60E+06	9.47E+05	0.00E+00
1158	PIGU	2	1	2.06E+06	1.09E+06	0.00E+00	0.00E+00	3.64E+06	2.49E+06	0.00E+00	0.00E+00	0.00E+00	0.00E+00	0.00E+00	0.00E+00
1159	EXOSC10	2	2	0.00E+00	3.15E+06	0.00E+00	0.00E+00	5.08E+06	0.00E+00	0.00E+00	0.00E+00	0.00E+00	0.00E+00	0.00E+00	0.00E+00
1160	LPCAT1	1	1	3.12E+06	0.00E+00	2.09E+06	0.00E+00	4.18E+06	0.00E+00	0.00E+00	0.00E+00	0.00E+00	0.00E+00	0.00E+00	0.00E+00
1161	ARID1A	3	3	1.71E+06	1.35E+06	0.00E+00	0.00E+00	0.00E+00	0.00E+00	0.00E+00	0.00E+00	0.00E+00	0.00E+00	3.17E+06	2.22E+06
1162	SKIV2L	1	2	2.93E+06	0.00E+00	0.00E+00	0.00E+00	2.76E+06	0.00E+00	0.00E+00	0.00E+00	0.00E+00	0.00E+00	0.00E+00	0.00E+00
1163	ANAPC1	1	1	1.96E+06	8.03E+05	1.60E+06	7.12E+05	3.65E+06	1.96E+06	0.00E+00	0.00E+00	0.00E+00	0.00E+00	0.00E+00	0.00E+00
1164	FAR1	1	2	2.75E+06	0.00E+00	0.00E+00	0.00E+00	2.15E+07	0.00E+00	0.00E+00	0.00E+00	0.00E+00	0.00E+00	0.00E+00	0.00E+00
1165	EXOSC2	2	1	0.00E+00	2.69E+06	0.00E+00	0.00E+00	0.00E+00	3.66E+06	0.00E+00	0.00E+00	0.00E+00	0.00E+00	0.00E+00	0.00E+00
1166	AP2A1	2	1	2.00E+06	6.93E+05	2.09E+06	9.51E+05	2.80E+06	0.00E+00	0.00E+00	0.00E+00	0.00E+00	0.00E+00	0.00E+00	0.00E+00
1167	ANXA1	1	1	2.42E+06	0.00E+00	0.00E+00	0.00E+00	0.00E+00	0.00E+00	0.00E+00	0.00E+00	0.00E+00	0.00E+00	0.00E+00	0.00E+00
1168	TMEM161A	2	1	1.40E+06	9.68E+05	8.64E+05	7.68E+05	2.67E+06	1.92E+06	0.00E+00	0.00E+00	0.00E+00	0.00E+00	0.00E+00	0.00E+00
1169	HEATR3	3	2	2.28E+06	0.00E+00	2.29E+06	1.49E+06	6.09E+06	2.31E+06	0.00E+00	0.00E+00	0.00E+00	0.00E+00	0.00E+00	0.00E+00
1170	TBC1D15	3	2	1.34E+06	8.62E+05	0.00E+00	0.00E+00	4.49E+06	1.44E+06	0.00E+00	0.00E+00	0.00E+00	0.00E+00	0.00E+00	0.00E+00
1171	ATL2	5	2	2.18E+06	0.00E+00	2.20E+06	0.00E+00	7.83E+06	0.00E+00	0.00E+00	0.00E+00	0.00E+00	0.00E+00	0.00E+00	0.00E+00
1172	TAMM41	3	1	0.00E+00	2.15E+06	0.00E+00	0.00E+00	2.17E+06	3.11E+06	0.00E+00	0.00E+00	0.00E+00	0.00E+00	0.00E+00	0.00E+00
1173	EXD2	2	2	2.12E+06	0.00E+00	0.00E+00	0.00E+00	4.06E+06	1.77E+06	0.00E+00	0.00E+00	0.00E+00	0.00E+00	0.00E+00	0.00E+00
1174	MFSD10	1	1	1.38E+06	6.98E+05	0.00E+00	0.00E+00	1.84E+06	1.14E+06	0.00E+00	0.00E+00	0.00E+00	0.00E+00	0.00E+00	0.00E+00
1175	AIMP2	2	1	2.06E+06	0.00E+00	2.82E+06	0.00E+00	3.74E+06	0.00E+00	0.00E+00	0.00E+00	0.00E+00	0.00E+00	0.00E+00	0.00E+00
1176	SLC12A2	2	2	2.01E+06	0.00E+00	0.00E+00	0.00E+00	6.83E+06	0.00E+00	0.00E+00	0.00E+00	0.00E+00	0.00E+00	0.00E+00	0.00E+00
1177	ORC4	4	1	1.99E+06	0.00E+00	0.00E+00	0.00E+00	2.10E+06	0.00E+00	0.00E+00	0.00E+00	0.00E+00	0.00E+00	0.00E+00	0.00E+00
1178	DEPDC1B	2	1	1.98E+06	0.00E+00	0.00E+00	0.00E+00	4.76E+06	0.00E+00	0.00E+00	0.00E+00	0.00E+00	0.00E+00	0.00E+00	0.00E+00
1179	UPF1	2	2	1.86E+06	0.00E+00	2.62E+06	0.00E+00	0.00E+00	0.00E+00	0.00E+00	0.00E+00	0.00E+00	0.00E+00	0.00E+00	0.00E+00
1180	SRPR	2	3	1.58E+06	0.00E+00	0.00E+00	0.00E+00	1.00E+07	7.18E+06	0.00E+00	0.00E+00	0.00E+00	0.00E+00	0.00E+00	0.00E+00
1181	NCOR2	4	9	0.00E+00	1.49E+06	0.00E+00	0.00E+00	2.77E+06	0.00E+00	0.00E+00	1.35E+07	2.31E+06	8.74E+06	6.28E+06	1.11E+07	6.86E+06
1182	DHX37	1	2	8.43E+05	6.14E+05	0.00E+00	0.00E+00	0.00E+00	0.00E+00	0.00E+00	1.44E+07	0.00E+00	0.00E+00	0.00E+00	0.00E+00
1183	TPBG	1	2	9.00E+05	5.25E+05	0.00E+00	0.00E+00	2.70E+06	2.30E+06	0.00E+00	0.00E+00	0.00E+00	0.00E+00	0.00E+00	0.00E+00
1184	TTYH3	4	1	0.00E+00	1.29E+06	0.00E+00	0.00E+00	0.00E+00	1.70E+06	0.00E+00	0.00E+00	0.00E+00	0.00E+00	0.00E+00	0.00E+00
1185	CYFIP2;CYF	4	2	9.06E+05	0.00E+00	1.40E+07	1.71E+07	0.00E+00	0.00E+00	3.02E+06	2.64E+06	5.72E+06	5.24E+06	0.00E+00	0.00E+00
1186	CNOT1	4	1	0.00E+00	0.00E+00	0.00E+00	0.00E+00	1.45E+06	0.00E+00	0.00E+00	0.00E+00	0.00E+00	0.00E+00	0.00E+00	0.00E+00
1187	ARGFX	1	1	0.00E+00	0.00E+00	0.00E+00	0.00E+00	0.00E+00	0.00E+00	0.00E+00	0.00E+00	0.00E+00	0.00E+00	0.00E+00	0.00E+00
1188	KRT13	5	8	0.00E+00	0.00E+00	0.00E+00	0.00E+00	0.00E+00	0.00E+00	8.75E+06	0.00E+00	0.00E+00	0.00E+00	0.00E+00	0.00E+00
1189	KRT6A	5	33	0.00E+00	0.00E+00	3.07E+07	0.00E+00	2.22E+07	0.00E+00	6.85E+07	0.00E+00	7.38E+07	0.00E+00	3.58E+07	0.00E+00
1190	PRSS1;PRSS	4	2	0.00E+00	0.00E+00	0.00E+00	0.00E+00	0.00E+00	0.00E+00	0.00E+00	0.00E+00	0.00E+00	0.00E+00	1.47E+07	0.00E+00
1191	VTN	2	1	0.00E+00	0.00E+00	1.28E+07	7.21E+05	1.10E+07	0.00E+00	1.33E+06	0.00E+00	3.49E+06	0.00E+00	2.01E+06	0.00E+00
1192	FLG2	2	4	0.00E+00	0.00E+00	2.43E+07	0.00E+00	0.00E+00	0.00E+00	2.14E+06	0.00E+00	1.84E+07	0.00E+00	1.90E+06	0.00E+00
1193	KRT73	4	5	0.00E+00	0.00E+00	0.00E+00	0.00E+00	0.00E+00	0.00E+00	9.33E+06	0.00E+00	0.00E+00	0.00E+00	0.00E+00	0.00E+00
1194	KRT78	4	6	0.00E+00	0.00E+00	0.00E+00	0.00E+00	0.00E+00	0.00E+00	5.47E+06	0.00E+00	2.18E+07	0.00E+00	6.46E+06	0.00E+00
1195	KRT77	2	5	0.00E+00	0.00E+00	0.00E+00	0.00E+00	0.00E+00	0.00E+00	0.00E+00	0.00E+00	5.28E+06	0.00E+00	0.00E+00	0.00E+00
1196	KRT82	2	1	0.00E+00	0.00E+00	0.00E+00	0.00E+00	0.00E+00	0.00E+00	0.00E+00	0.00E+00	0.00E+00	0.00E+00	0.00E+00	0.00E+00
1197	NACA;NAC	4	2	0.00E+00	0.00E+00	0.00E+00	0.00E+00	0.00E+00	0.00E+00	0.00E+00	0.00E+00	1.38E+07	0.00E+00	0.00E+00	0.00E+00
1198	TOR1A	1	1	0.00E+00	0.00E+00	0.00E+00	0.00E+00	5.10E+06	5.66E+06	0.00E+00	0.00E+00	0.00E+00	0.00E+00	0.00E+00	0.00E+00
1199	TIMM23;TI	2	2	0.00E+00	0.00E+00	1.81E+07	0.00E+00	0.00E+00	0.00E+00	0.00E+00	0.00E+00	0.00E+00	0.00E+00	0.00E+00	0.00E+00
1200	KIAA0391	4	1	0.00E+00	0.00E+00	0.00E+00	0.00E+00	2.39E+06	0.00E+00	0.00E+00	0.00E+00	0.00E+00	0.00E+00	0.00E+00	0.00E+00
1201	MSI1;MSI2	4	2	0.00E+00	0.00E+00	0.00E+00	0.00E+00	2.03E+07	0.00E+00	0.00E+00	0.00E+00	0.00E+00	0.00E+00	0.00E+00	0.00E+00
1202	TBX1	3	5	0.00E+00	0.00E+00	6.20E+06	0.00E+00	1.06E+08	0.00E+00	0.00E+00	0.00E+00	0.00E+00	0.00E+00	0.00E+00	0.00E+00
1203	ZBTB14	1	2	0.00E+00	0.00E+00	2.90E+06	0.00E+00	0.00E+00	0.00E+00	0.00E+00	0.00E+00	0.00E+00	0.00E+00	0.00E+00	0.00E+00
1204	KDM1A	2	2	0.00E+00	0.00E+00	0.00E+00	8.20E+06	0.00E+00	0.00E+00	0.00E+00	0.00E+00	0.00E+00	0.00E+00	2.31E+06	0.00E+00
1205	STX10	2	1	0.00E+00	0.00E+00	0.00E+00	0.00E+00	0.00E+00	0.00E+00	0.00E+00	0.00E+00	0.00E+00	0.00E+00	0.00E+00	0.00E+00
1206	DPM1	1	2	0.00E+00	0.00E+00	8.72E+06	0.00E+00	3.42E+07	1.02E+07	0.00E+00	0.00E+00	0.00E+00	0.00E+00	0.00E+00	0.00E+00
1207	CPNE8;CPN	14	1	0.00E+00	0.00E+00	1.40E+06	1.22E+06	2.16E+06	1.62E+06	0.00E+00	0.00E+00	1.55E+06	0.00E+00	0.00E+00	0.00E+00
1208	ARL6IP5	1	1	0.00E+00	0.00E+00	0.00E+00	0.00E+00	1.45E+07	7.70E+06	0.00E+00	0.00E+00	0.00E+00	0.00E+00	0.00E+00	0.00E+00
1209	FARP2	1	1	0.00E+00	0.00E+00	0.00E+00	0.00E+00	2.82E+06	2.71E+06	0.00E+00	0.00E+00	0.00E+00	0.00E+00	0.00E+00	0.00E+00
1210	PCF11	1	2	0.00E+00	0.00E+00	0.00E+00	0.00E+00	0.00E+00	0.00E+00	2.61E+06	0.00E+00	0.00E+00	0.00E+00	0.00E+00	0.00E+00
1211	DUSP14	1	2	0.00E+00	0.00E+00	3.67E+06	4.85E+06	6.67E+06	6.80E+06	0.00E+00	0.00E+00	1.27E+06	1.84E+06	0.00E+00	0.00E+00
1212	ZRANB2	2	2	0.00E+00	0.00E+00	0.00E+00	0.00E+00	0.00E+00	0.00E+00	1.15E+07	7.65E+06	0.00E+00	0.00E+00	0.00E+00	0.00E+00
1213	NSA2	1	3	0.00E+00	0.00E+00	3.16E+06	0.00E+00	5.63E+07	1.92E+07	0.00E+00	0.00E+00	0.00E+00	0.00E+00	0.00E+00	0.00E+00
1214	FADS2	2	1	0.00E+00	0.00E+00	0.00E+00	0.00E+00	0.00E+00	1.44E+07	0.00E+00	0.00E+00	0.00E+00	0.00E+00	0.00E+00	0.00E+00
1215	ONECUT2;(	3	3	0.00E+00	0.00E+00	0.00E+00	0.00E+00	1.40E+07	4.14E+06	6.03E+06	0.00E+00	3.36E+06	3.19E+06	0.00E+00	0.00E+00
1216	SOD1	1	4	0.00E+00	0.00E+00	0.00E+00	0.00E+00	0.00E+00	0.00E+00	0.00E+00	0.00E+00	5.63E+07	5.49E+06	0.00E+00	0.00E+00
1217	PNP	1	1	0.00E+00	0.00E+00	0.00E+00	0.00E+00	0.00E+00	0.00E+00	0.00E+00	0.00E+00	5.59E+06	3.03E+06	0.00E+00	0.00E+00
1218	GOT2	2	2	0.00E+00	0.00E+00	0.00E+00	0.00E+00	0.00E+00	0.00E+00	0.00E+00	0.00E+00	8.73E+06	9.20E+06	0.00E+00	0.00E+00
1219	PGK1	3	4	0.00E+00	0.00E+00	0.00E+00	0.00E+00	0.00E+00	0.00E+00	0.00E+00	0.00E+00	3.56E+07	5.64E+06	0.00E+00	0.00E+00
1220	TGFB1	1	1	0.00E+00	0.00E+00	0.00E+00	0.00E+00	0.00E+00	0.00E+00	0.00E+00	0.00E+00	0.00E+00	0.00E+00	0.00E+00	0.00E+00
1221	FGA	2	2	0.00E+00	0.00E+00	0.00E+00	0.00E+00	0.00E+00	0.00E+00	6.10E+06	0.00E+00	1.51E+07	0.00E+00	0.00E+00	0.00E+00
1222	FGG	2	7	0.00E+00	0.00E+00	6.61E+07	0.00E+00	0.00E+00	0.00E+00	1.33E+08	0.00E+00	9.12E+07	0.00E+00	6.13E+07	0.00E+00
1223	ALDOA	2	8	0.00E+00	0.00E+00	0.00E+00	0.00E+00	0.00E+00	0.00E+00	0.00E+00	0.00E+00	9.75E+07	8.57E+07	0.00E+00	0.00E+00
1224	KRT6B	1	33	0.00E+00	0.00E+00	0.00E+00	0.00E+00	0.00E+00	0.00E+00	1.45E+07	0.00E+00	0.00E+00	0.00E+00	0.00E+00	0.00E+00
1225	HSPB1	1	1	0.00E+00	0.00E+00	0.00E+00	0.00E+00	0.00E+00	0.00E+00	0.00E+00	0.00E+00	1.65E+07	0.00E+00	5.49E+06	0.00E+00
1226	ARG1	2	1	0.00E+00	0.00E+00	0.00E+00	0.00E+00	0.00E+00	0.00E+00	0.00E+00	0.00E+00	5.13E+06	0.00E+00	0.00E+00	0.00E+00
1227	ITGB1	5	2	0.00E+00	0.00E+00	0.00E+00	0.00E+00	2.66E+07	0.00E+00	0.00E+00	0.00E+00	0.00E+00	0.00E+00	0.00E+00	0.00E+00
1228	RHOA;RHO	2	1	0.00E+00	0.00E+00	0.00E+00	0.00E+00	2.31E+07	2.27E+07	0.00E+00	0.00E+00	0.00E+00	0.00E+00	0.00E+00	0.00E+00
1229	CNP	2	2	0.00E+00	0.00E+00	0.00E+00	0.00E+00	2.16E+06	0.00E+00	0.00E+00	0.00E+00	0.00E+00	0.00E+00	0.00E+00	0.00E+00
1230	DLD	3	1	0.00E+00	0.00E+00	0.00E+00	0.00E+00	0.00E+00	0.00E+00	0.00E+00	0.00E+00	2.54E+06	2.98E+06	0.00E+00	0.00E+00

MQ search SILAC data

hit number	Gene names	Number of proteins	Peptides	Intensity L 2%SDS_24hHU	Intensity H 2%SDS_24hHU	Intensity L 2%SDS_2hHU	Intensity H 2%SDS_2hHU	Intensity L 2%SDS_NT	Intensity H 2%SDS_NT	Intensity L el150_24hHU	Intensity H el150_24hHU	Intensity L el150_2hHU	Intensity H el150_2hHU	Intensity L el150_NT	Intensity H el150_NT
1231	UCHL1	1	3	0.00E+00	0.00E+00	0.00E+00	0.00E+00	0.00E+00	0.00E+00	0.00E+00	0.00E+00	1.92E+07	2.64E+06	0.00E+00	0.00E+00
1232	ZNF286A;Z	3	1	0.00E+00	0.00E+00	2.65E+06	3.61E+06	8.22E+06	7.83E+06	0.00E+00	0.00E+00	0.00E+00	0.00E+00	0.00E+00	0.00E+00
1233	TROVE2	5	1	0.00E+00	0.00E+00	0.00E+00	0.00E+00	0.00E+00	0.00E+00	0.00E+00	0.00E+00	0.00E+00	0.00E+00	0.00E+00	0.00E+00
1234	PTPRF	2	2	0.00E+00	0.00E+00	6.48E+07	1.46E+06	5.10E+09	1.67E+09	0.00E+00	0.00E+00	1.70E+07	3.32E+05	0.00E+00	0.00E+00
1235	PIP	1	1	0.00E+00	0.00E+00	0.00E+00	0.00E+00	0.00E+00	0.00E+00	0.00E+00	0.00E+00	3.32E+06	0.00E+00	4.39E+06	0.00E+00
1236	SKI	1	1	0.00E+00	0.00E+00	0.00E+00	0.00E+00	1.16E+07	0.00E+00	0.00E+00	0.00E+00	0.00E+00	0.00E+00	0.00E+00	0.00E+00
1237	PRKAR2A	2	1	0.00E+00	0.00E+00	0.00E+00	2.42E+06	0.00E+00	2.92E+06	0.00E+00	0.00E+00	0.00E+00	0.00E+00	0.00E+00	0.00E+00
1238	MIF	1	2	0.00E+00	0.00E+00	0.00E+00	0.00E+00	0.00E+00	0.00E+00	0.00E+00	0.00E+00	9.48E+06	9.56E+06	0.00E+00	0.00E+00
1239	TRIM27	2	2	0.00E+00	0.00E+00	0.00E+00	0.00E+00	9.23E+06	0.00E+00	0.00E+00	0.00E+00	0.00E+00	0.00E+00	0.00E+00	0.00E+00
1240	HSP90B1	1	8	0.00E+00	0.00E+00	0.00E+00	0.00E+00	0.00E+00	0.00E+00	0.00E+00	0.00E+00	3.19E+07	2.55E+07	0.00E+00	0.00E+00
1241	NME1	2	4	0.00E+00	0.00E+00	0.00E+00	0.00E+00	0.00E+00	0.00E+00	0.00E+00	0.00E+00	7.17E+06	0.00E+00	0.00E+00	0.00E+00
1242	POR	1	1	0.00E+00	0.00E+00	1.95E+06	1.71E+06	6.81E+06	4.02E+06	0.00E+00	0.00E+00	0.00E+00	0.00E+00	0.00E+00	0.00E+00
1243	JUND	1	2	0.00E+00	0.00E+00	0.00E+00	0.00E+00	1.33E+07	1.18E+07	0.00E+00	0.00E+00	0.00E+00	0.00E+00	0.00E+00	0.00E+00
1244	PTPN1	1	3	0.00E+00	0.00E+00	8.33E+06	0.00E+00	2.10E+07	0.00E+00	0.00E+00	0.00E+00	0.00E+00	0.00E+00	0.00E+00	0.00E+00
1245	COX5A	1	2	0.00E+00	0.00E+00	0.00E+00	0.00E+00	0.00E+00	0.00E+00	0.00E+00	0.00E+00	0.00E+00	0.00E+00	0.00E+00	0.00E+00
1246	UBA1	2	7	0.00E+00	0.00E+00	0.00E+00	0.00E+00	0.00E+00	0.00E+00	0.00E+00	0.00E+00	3.44E+07	1.03E+07	0.00E+00	0.00E+00
1247	UQCRC2	1	2	0.00E+00	0.00E+00	1.88E+07	2.31E+07	3.87E+07	1.59E+07	0.00E+00	0.00E+00	0.00E+00	0.00E+00	0.00E+00	0.00E+00
1248	KAL1	1	2	0.00E+00	0.00E+00	0.00E+00	0.00E+00	1.78E+07	2.42E+06	0.00E+00	0.00E+00	0.00E+00	0.00E+00	0.00E+00	0.00E+00
1249	NFYA	2	1	0.00E+00	0.00E+00	1.46E+07	0.00E+00	0.00E+00	0.00E+00	0.00E+00	0.00E+00	0.00E+00	0.00E+00	0.00E+00	0.00E+00
1250	AHCY	2	4	0.00E+00	0.00E+00	0.00E+00	0.00E+00	0.00E+00	0.00E+00	0.00E+00	0.00E+00	1.05E+07	7.92E+06	0.00E+00	0.00E+00
1251	CFL1;CFL2	3	3	0.00E+00	0.00E+00	0.00E+00	0.00E+00	0.00E+00	0.00E+00	0.00E+00	0.00E+00	3.27E+07	0.00E+00	2.52E+06	0.00E+00
1252	AZGP1	1	2	0.00E+00	0.00E+00	0.00E+00	0.00E+00	0.00E+00	0.00E+00	0.00E+00	0.00E+00	8.38E+06	0.00E+00	0.00E+00	0.00E+00
1253	LAMA1	1	1	0.00E+00	0.00E+00	0.00E+00	0.00E+00	0.00E+00	0.00E+00	0.00E+00	0.00E+00	0.00E+00	0.00E+00	0.00E+00	0.00E+00
1254	VARS	1	2	0.00E+00	0.00E+00	1.18E+07	0.00E+00	0.00E+00	0.00E+00	0.00E+00	0.00E+00	5.94E+06	2.29E+06	0.00E+00	0.00E+00
1255	DPP4	1	1	0.00E+00	0.00E+00	0.00E+00	0.00E+00	0.00E+00	0.00E+00	0.00E+00	0.00E+00	0.00E+00	0.00E+00	0.00E+00	0.00E+00
1256	CALR	1	2	0.00E+00	0.00E+00	0.00E+00	0.00E+00	0.00E+00	0.00E+00	0.00E+00	0.00E+00	1.35E+07	0.00E+00	0.00E+00	0.00E+00
1257	MPG	4	2	0.00E+00	0.00E+00	3.35E+06	2.45E+06	9.93E+06	0.00E+00	0.00E+00	0.00E+00	1.44E+06	1.00E+06	2.03E+06	0.00E+00
1258	TKT	2	4	0.00E+00	0.00E+00	0.00E+00	0.00E+00	0.00E+00	0.00E+00	0.00E+00	0.00E+00	2.51E+07	1.26E+07	0.00E+00	0.00E+00
1259	TYK2	1	2	0.00E+00	0.00E+00	0.00E+00	0.00E+00	1.43E+07	5.82E+06	0.00E+00	0.00E+00	0.00E+00	0.00E+00	0.00E+00	0.00E+00
1260	PRDX6	1	4	0.00E+00	0.00E+00	0.00E+00	0.00E+00	0.00E+00	0.00E+00	0.00E+00	0.00E+00	2.14E+07	3.20E+06	0.00E+00	0.00E+00
1261	PRDX3	2	1	0.00E+00	0.00E+00	0.00E+00	0.00E+00	0.00E+00	0.00E+00	0.00E+00	0.00E+00	5.60E+06	7.99E+06	0.00E+00	0.00E+00
1262	ATP5D	1	1	0.00E+00	0.00E+00	0.00E+00	0.00E+00	0.00E+00	3.08E+07	0.00E+00	0.00E+00	0.00E+00	0.00E+00	0.00E+00	0.00E+00
1263	PEBP1	1	1	0.00E+00	0.00E+00	0.00E+00	0.00E+00	0.00E+00	0.00E+00	0.00E+00	0.00E+00	6.11E+06	0.00E+00	0.00E+00	0.00E+00
1264	PDIA3	1	4	0.00E+00	0.00E+00	2.94E+06	3.89E+06	0.00E+00	0.00E+00	0.00E+00	0.00E+00	1.62E+07	3.96E+06	0.00E+00	0.00E+00
1265	HOXA9	1	2	0.00E+00	0.00E+00	1.22E+07	1.28E+07	0.00E+00	0.00E+00	0.00E+00	0.00E+00	2.80E+06	0.00E+00	5.28E+06	0.00E+00
1266	HNRNPH3	2	2	0.00E+00	0.00E+00	0.00E+00	0.00E+00	0.00E+00	0.00E+00	0.00E+00	0.00E+00	0.00E+00	0.00E+00	0.00E+00	0.00E+00
1267	YWHAB	2	4	0.00E+00	0.00E+00	0.00E+00	0.00E+00	5.63E+06	0.00E+00	0.00E+00	0.00E+00	3.67E+06	3.04E+06	0.00E+00	0.00E+00
1268	PRDX2	2	6	0.00E+00	0.00E+00	6.00E+06	0.00E+00	5.01E+06	0.00E+00	1.26E+07	0.00E+00	3.50E+07	3.77E+06	0.00E+00	0.00E+00
1269	SHMT2	3	4	0.00E+00	0.00E+00	0.00E+00	0.00E+00	0.00E+00	0.00E+00	0.00E+00	0.00E+00	5.02E+06	9.14E+06	0.00E+00	0.00E+00
1270	PFN2	2	1	0.00E+00	0.00E+00	0.00E+00	0.00E+00	0.00E+00	0.00E+00	0.00E+00	0.00E+00	0.00E+00	0.00E+00	0.00E+00	0.00E+00
1271	FDFT1	5	1	0.00E+00	0.00E+00	7.46E+06	9.97E+06	1.12E+07	1.73E+07	0.00E+00	0.00E+00	0.00E+00	0.00E+00	0.00E+00	0.00E+00
1272	SNCA	3	1	0.00E+00	0.00E+00	0.00E+00	0.00E+00	9.94E+06	0.00E+00	0.00E+00	0.00E+00	0.00E+00	0.00E+00	0.00E+00	0.00E+00
1273	COL18A1	3	1	0.00E+00	0.00E+00	0.00E+00	0.00E+00	8.21E+06	0.00E+00	0.00E+00	0.00E+00	0.00E+00	0.00E+00	0.00E+00	0.00E+00
1274	ANP32B;AI	3	2	0.00E+00	0.00E+00	0.00E+00	0.00E+00	0.00E+00	0.00E+00	0.00E+00	0.00E+00	9.72E+06	7.20E+06	0.00E+00	0.00E+00
1275	PBX1	6	6	0.00E+00	0.00E+00	0.00E+00	0.00E+00	0.00E+00	0.00E+00	1.10E+07	0.00E+00	9.12E+06	6.60E+06	1.01E+07	0.00E+00
1276	MDH1	2	1	0.00E+00	0.00E+00	0.00E+00	0.00E+00	0.00E+00	0.00E+00	0.00E+00	0.00E+00	1.15E+06	1.10E+06	0.00E+00	0.00E+00
1277	MDH2	2	3	0.00E+00	0.00E+00	0.00E+00	0.00E+00	0.00E+00	0.00E+00	0.00E+00	0.00E+00	1.43E+07	3.92E+06	0.00E+00	0.00E+00
1278	GRM5	3	1	0.00E+00	0.00E+00	0.00E+00	0.00E+00	0.00E+00	0.00E+00	0.00E+00	0.00E+00	0.00E+00	0.00E+00	0.00E+00	0.00E+00
1279	MLLT3	2	3	0.00E+00	0.00E+00	3.95E+06	0.00E+00	1.54E+07	5.09E+06	2.54E+06	0.00E+00	0.00E+00	0.00E+00	3.96E+06	2.85E+06
1280	RPL35	1	1	0.00E+00	0.00E+00	0.00E+00	0.00E+00	1.17E+07	0.00E+00	0.00E+00	0.00E+00	0.00E+00	0.00E+00	0.00E+00	0.00E+00
1281	SLC1A3	2	1	0.00E+00	0.00E+00	2.59E+06	2.89E+06	7.12E+06	7.39E+06	0.00E+00	0.00E+00	0.00E+00	0.00E+00	3.16E+06	1.42E+06
1282	GPD2	2	2	0.00E+00	0.00E+00	0.00E+00	0.00E+00	8.28E+06	0.00E+00	0.00E+00	0.00E+00	0.00E+00	0.00E+00	0.00E+00	0.00E+00
1283	RANGAP1	1	2	0.00E+00	0.00E+00	1.08E+07	0.00E+00	0.00E+00	0.00E+00	0.00E+00	0.00E+00	8.34E+06	0.00E+00	0.00E+00	0.00E+00
1284	BAG6	5	2	0.00E+00	0.00E+00	0.00E+00	6.36E+06	9.45E+06	3.72E+06	0.00E+00	0.00E+00	0.00E+00	0.00E+00	0.00E+00	0.00E+00
1285	CAPZB	2	2	0.00E+00	0.00E+00	1.98E+06	1.82E+06	0.00E+00	0.00E+00	0.00E+00	0.00E+00	5.65E+06	0.00E+00	0.00E+00	0.00E+00
1286	LGALS7	1	3	0.00E+00	0.00E+00	0.00E+00	0.00E+00	0.00E+00	0.00E+00	0.00E+00	0.00E+00	1.64E+07	0.00E+00	0.00E+00	0.00E+00
1287	ATP5O	1	2	0.00E+00	0.00E+00	0.00E+00	0.00E+00	0.00E+00	0.00E+00	0.00E+00	0.00E+00	0.00E+00	0.00E+00	0.00E+00	0.00E+00
1288	RPL34	1	2	0.00E+00	0.00E+00	2.75E+07	0.00E+00	1.68E+07	0.00E+00	0.00E+00	0.00E+00	0.00E+00	0.00E+00	0.00E+00	0.00E+00
1289	FNTB	2	1	0.00E+00	0.00E+00	3.69E+06	4.49E+06	0.00E+00	0.00E+00	0.00E+00	0.00E+00	1.23E+06	1.53E+06	0.00E+00	0.00E+00
1290	SRP9	2	1	0.00E+00	0.00E+00	0.00E+00	0.00E+00	1.40E+07	0.00E+00	0.00E+00	0.00E+00	0.00E+00	0.00E+00	0.00E+00	0.00E+00
1291	CSNK1E	1	8	0.00E+00	0.00E+00	0.00E+00	0.00E+00	3.23E+07	1.10E+07	0.00E+00	0.00E+00	2.10E+06	1.69E+06	0.00E+00	0.00E+00
1292	PSMB3	1	1	0.00E+00	0.00E+00	0.00E+00	0.00E+00	0.00E+00	0.00E+00	0.00E+00	0.00E+00	1.83E+06	1.30E+06	0.00E+00	0.00E+00
1293	MNX1	1	1	0.00E+00	0.00E+00	0.00E+00	0.00E+00	9.05E+06	5.14E+06	0.00E+00	0.00E+00	0.00E+00	0.00E+00	0.00E+00	0.00E+00
1294	GDI2	3	3	0.00E+00	0.00E+00	0.00E+00	0.00E+00	0.00E+00	0.00E+00	0.00E+00	0.00E+00	1.35E+07	0.00E+00	0.00E+00	0.00E+00
1295	SERPINH1	1	1	0.00E+00	0.00E+00	0.00E+00	0.00E+00	2.01E+07	0.00E+00	0.00E+00	0.00E+00	0.00E+00	0.00E+00	0.00E+00	0.00E+00
1296	DAP3	3	1	0.00E+00	0.00E+00	0.00E+00	0.00E+00	6.57E+06	4.48E+06	0.00E+00	0.00E+00	0.00E+00	0.00E+00	0.00E+00	0.00E+00
1297	AFF1	3	2	0.00E+00	0.00E+00	1.33E+07	0.00E+00	1.24E+07	0.00E+00	0.00E+00	0.00E+00	0.00E+00	0.00E+00	0.00E+00	0.00E+00
1298	PGD	2	1	0.00E+00	0.00E+00	0.00E+00	0.00E+00	0.00E+00	0.00E+00	0.00E+00	0.00E+00	4.01E+06	4.30E+06	0.00E+00	0.00E+00
1299	ARHGDIA	1	1	0.00E+00	0.00E+00	0.00E+00	0.00E+00	0.00E+00	0.00E+00	0.00E+00	0.00E+00	6.61E+06	0.00E+00	0.00E+00	0.00E+00
1300	SLC25A1	1	3	0.00E+00	0.00E+00	2.63E+07	5.86E+06	8.68E+06	7.39E+06	0.00E+00	0.00E+00	0.00E+00	0.00E+00	0.00E+00	0.00E+00
1301	BLM	1	1	0.00E+00	0.00E+00	0.00E+00	0.00E+00	1.34E+07	0.00E+00	0.00E+00	0.00E+00	0.00E+00	0.00E+00	0.00E+00	0.00E+00
1302	RARS	2	1	0.00E+00	0.00E+00	0.00E+00	0.00E+00	0.00E+00	7.35E+06	0.00E+00	0.00E+00	0.00E+00	0.00E+00	0.00E+00	0.00E+00
1303	NAPB;NAP/	4	1	0.00E+00	0.00E+00	1.58E+06	1.64E+06	3.59E+06	3.70E+06	0.00E+00	0.00E+00	0.00E+00	0.00E+00	0.00E+00	0.00E+00
1304	NPEPPS	2	2	0.00E+00	0.00E+00	0.00E+00	0.00E+00	0.00E+00	0.00E+00	0.00E+00	0.00E+00	0.00E+00	2.30E+06	0.00E+00	0.00E+00
1305	MAZ	1	16	0.00E+00	0.00E+00	0.00E+00	0.00E+00	1.25E+07	8.88E+06	0.00E+00	0.00E+00	0.00E+00	0.00E+00	0.00E+00	0.00E+00
1306	PRDM15	5	4	0.00E+00	0.00E+00	1.06E+07	0.00E+00	1.94E+07	0.00E+00	0.00E+00	0.00E+00	0.00E+00	0.00E+00	0.00E+00	0.00E+00
1307	TPI1	3	4	0.00E+00	0.00E+00	0.00E+00	0.00E+00	0.00E+00	0.00E+00	0.00E+00	0.00E+00	3.16E+07	1.61E+07	3.15E+06	0.00E+00
1308	PPP4C	1	1	0.00E+00	0.00E+00	0.00E+00	0.00E+00	0.00E+00	0.00E+00	3.38E+06	0.00E+00	4.53E+06	3.07E+06	6.71E+06	0.00E+00
1309	CDC42	1	1	0.00E+00	0.00E+00	0.00E+00	0.00E+00	7.57E+06	0.00E+00	0.00E+00	0.00E+00	1.77E+06	0.00E+00	0.00E+00	0.00E+00
1310	MAX	6	2	0.00E+00	0.00E+00	0.00E+00	0.00E+00	0.00E+00	0.00E+00	6.67E+06	5.37E+06	4.46E+06	6.49E+06	1.84E+07	1.02E+07
1311	MAGOH;M	2	2	0.00E+00	0.00E+00	0.00E+00	0.00E+00	2.98E+07	0.00E+00	0.00E+00	0.00E+00	1.96E+07	0.00E+00	0.00E+00	0.00E+00
1312	PSMC1	2	2	0.00E+00	0.00E+00	1.84E+06	1.69E+06	7.68E+06	2.83E+06	0.00E+00	0.00E+00	0.00E+00	0.00E+00	0.00E+00	0.00E+00

MQ search SILAC data

hit number	Gene names	Number of proteins	Peptides	Intensity L 2%SDS_24hHU	Intensity H 2%SDS_24hHU	Intensity L 2%SDS_2hHU	Intensity H 2%SDS_2hHU	Intensity L 2%SDS_NT	Intensity H 2%SDS_NT	Intensity L el150_24hHU	Intensity H el150_24hHU	Intensity L el150_2hHU	Intensity H el150_2hHU	Intensity L el150_NT	Intensity H el150_NT
1313	RPL23A	1	1	0.00E+00	0.00E+00	0.00E+00	0.00E+00	5.63E+07	0.00E+00	0.00E+00	0.00E+00	0.00E+00	0.00E+00	0.00E+00	0.00E+00
1314	SKP1	2	4	0.00E+00	0.00E+00	8.95E+07	3.10E+07	1.40E+08	5.42E+07	0.00E+00	0.00E+00	1.66E+07	1.00E+07	1.54E+07	7.33E+06
1315	ACTA1;ACT	4	9	0.00E+00	0.00E+00	7.30E+07	0.00E+00	8.12E+07	0.00E+00	2.57E+07	0.00E+00	5.59E+07	0.00E+00	4.54E+07	0.00E+00
1316	HBB;HBD	3	4	0.00E+00	0.00E+00	3.61E+07	0.00E+00	0.00E+00	0.00E+00	9.71E+06	0.00E+00	1.00E+08	9.79E+05	0.00E+00	0.00E+00
1317	HBA1	3	4	0.00E+00	0.00E+00	6.90E+06	0.00E+00	0.00E+00	0.00E+00	5.87E+06	0.00E+00	5.17E+07	0.00E+00	0.00E+00	0.00E+00
1318	DCD	2	3	0.00E+00	0.00E+00	0.00E+00	0.00E+00	0.00E+00	0.00E+00	1.62E+07	0.00E+00	6.85E+07	0.00E+00	8.51E+07	0.00E+00
1319	SET;SETSIP	5	4	0.00E+00	0.00E+00	1.08E+07	2.55E+06	0.00E+00	0.00E+00	9.09E+06	0.00E+00	3.37E+07	0.00E+00	6.61E+06	0.00E+00
1320	SRSF2	2	1	0.00E+00	0.00E+00	0.00E+00	0.00E+00	0.00E+00	0.00E+00	0.00E+00	0.00E+00	7.02E+06	5.51E+06	0.00E+00	0.00E+00
1321	FABP5	1	1	0.00E+00	0.00E+00	0.00E+00	0.00E+00	0.00E+00	0.00E+00	0.00E+00	0.00E+00	7.79E+06	1.11E+06	0.00E+00	0.00E+00
1322	SLC7A5	1	1	0.00E+00	0.00E+00	0.00E+00	0.00E+00	0.00E+00	1.13E+07	0.00E+00	0.00E+00	0.00E+00	0.00E+00	0.00E+00	0.00E+00
1323	DSG1	2	8	0.00E+00	0.00E+00	9.19E+06	0.00E+00	0.00E+00	0.00E+00	5.30E+06	0.00E+00	1.13E+08	0.00E+00	8.11E+06	0.00E+00
1324	FKBP4	1	3	0.00E+00	0.00E+00	0.00E+00	0.00E+00	0.00E+00	0.00E+00	0.00E+00	0.00E+00	1.45E+07	3.02E+06	0.00E+00	0.00E+00
1325	BAX	5	1	0.00E+00	0.00E+00	0.00E+00	0.00E+00	1.10E+07	0.00E+00	0.00E+00	0.00E+00	0.00E+00	0.00E+00	0.00E+00	0.00E+00
1326	SOS1	2	1	0.00E+00	0.00E+00	0.00E+00	0.00E+00	0.00E+00	0.00E+00	0.00E+00	0.00E+00	0.00E+00	0.00E+00	2.80E+06	3.66E+06
1327	CACNB2	22	11	0.00E+00	0.00E+00	0.00E+00	0.00E+00	0.00E+00	0.00E+00	2.31E+07	4.14E+06	1.07E+07	0.00E+00	4.96E+07	2.58E+07
1328	LGALS3BP	1	6	0.00E+00	0.00E+00	1.14E+07	0.00E+00	7.24E+07	3.99E+07	0.00E+00	0.00E+00	0.00E+00	0.00E+00	0.00E+00	0.00E+00
1329	PRDX4	1	5	0.00E+00	0.00E+00	8.72E+06	1.17E+07	0.00E+00	0.00E+00	0.00E+00	0.00E+00	2.07E+07	1.65E+07	0.00E+00	0.00E+00
1330	NNT	1	2	0.00E+00	0.00E+00	0.00E+00	0.00E+00	2.56E+07	0.00E+00	0.00E+00	0.00E+00	0.00E+00	0.00E+00	0.00E+00	0.00E+00
1331	TCOF1	8	2	0.00E+00	0.00E+00	0.00E+00	0.00E+00	0.00E+00	0.00E+00	4.13E+06	0.00E+00	2.91E+06	0.00E+00	3.09E+06	0.00E+00
1332	TUBB3	2	11	0.00E+00	0.00E+00	0.00E+00	0.00E+00	8.44E+06	1.04E+07	0.00E+00	0.00E+00	0.00E+00	0.00E+00	0.00E+00	0.00E+00
1333	SPTAN1	3	1	0.00E+00	0.00E+00	0.00E+00	0.00E+00	0.00E+00	0.00E+00	0.00E+00	0.00E+00	0.00E+00	0.00E+00	0.00E+00	0.00E+00
1334	PKP1	2	3	0.00E+00	0.00E+00	0.00E+00	0.00E+00	0.00E+00	0.00E+00	0.00E+00	0.00E+00	1.83E+07	0.00E+00	0.00E+00	0.00E+00
1335	HNRNPD	4	3	0.00E+00	0.00E+00	8.80E+06	0.00E+00	8.34E+06	0.00E+00	0.00E+00	0.00E+00	0.00E+00	0.00E+00	0.00E+00	0.00E+00
1336	MLEC	1	1	0.00E+00	0.00E+00	1.29E+07	1.11E+07	3.45E+07	1.94E+07	0.00E+00	0.00E+00	0.00E+00	0.00E+00	0.00E+00	0.00E+00
1337	DYNC1H1	1	3	0.00E+00	0.00E+00	0.00E+00	0.00E+00	3.50E+06	2.12E+06	0.00E+00	0.00E+00	0.00E+00	0.00E+00	1.48E+08	1.30E+08
1338	PSMD6	4	1	0.00E+00	0.00E+00	3.24E+06	3.25E+06	0.00E+00	0.00E+00	0.00E+00	0.00E+00	0.00E+00	0.00E+00	0.00E+00	0.00E+00
1339	SUZ12	1	4	0.00E+00	0.00E+00	2.69E+07	0.00E+00	5.57E+06	0.00E+00	0.00E+00	0.00E+00	1.10E+07	0.00E+00	0.00E+00	0.00E+00
1340	KARS	2	1	0.00E+00	0.00E+00	1.17E+06	1.59E+06	2.53E+06	2.53E+06	0.00E+00	0.00E+00	0.00E+00	0.00E+00	0.00E+00	0.00E+00
1341	ARHGEF6	2	6	0.00E+00	0.00E+00	0.00E+00	0.00E+00	0.00E+00	0.00E+00	0.00E+00	0.00E+00	3.25E+06	5.21E+06	1.55E+07	1.11E+07
1342	PPA1	1	2	0.00E+00	0.00E+00	0.00E+00	0.00E+00	0.00E+00	0.00E+00	0.00E+00	0.00E+00	7.15E+06	0.00E+00	0.00E+00	0.00E+00
1343	DHCR24	2	3	0.00E+00	0.00E+00	3.53E+07	3.09E+07	2.97E+07	2.93E+07	0.00E+00	0.00E+00	0.00E+00	0.00E+00	0.00E+00	0.00E+00
1344	CDSN	1	2	0.00E+00	0.00E+00	0.00E+00	0.00E+00	0.00E+00	0.00E+00	0.00E+00	0.00E+00	1.58E+07	0.00E+00	2.52E+06	0.00E+00
1345	TRAM1	2	2	0.00E+00	0.00E+00	5.51E+06	0.00E+00	9.41E+06	6.96E+06	0.00E+00	0.00E+00	0.00E+00	0.00E+00	0.00E+00	0.00E+00
1346	SF1	1	19	0.00E+00	0.00E+00	0.00E+00	0.00E+00	0.00E+00	0.00E+00	0.00E+00	0.00E+00	0.00E+00	0.00E+00	7.19E+06	0.00E+00
1347	JMJD1C	3	12	0.00E+00	0.00E+00	6.12E+07	0.00E+00	3.90E+07	0.00E+00	3.47E+07	3.54E+06	3.08E+07	1.98E+06	6.83E+07	0.00E+00
1348	SMAD1	1	11	0.00E+00	0.00E+00	9.37E+06	0.00E+00	1.47E+07	0.00E+00	0.00E+00	0.00E+00	0.00E+00	0.00E+00	0.00E+00	0.00E+00
1349	EZH2	3	1	0.00E+00	0.00E+00	6.89E+06	6.16E+06	1.96E+07	1.49E+07	0.00E+00	0.00E+00	0.00E+00	0.00E+00	0.00E+00	0.00E+00
1350	TAF9;TAF9I	2	2	0.00E+00	0.00E+00	0.00E+00	0.00E+00	1.21E+07	4.30E+06	0.00E+00	0.00E+00	0.00E+00	0.00E+00	1.12E+06	8.94E+05
1351	PDS5A	2	1	0.00E+00	0.00E+00	0.00E+00	0.00E+00	0.00E+00	0.00E+00	0.00E+00	0.00E+00	1.18E+06	1.08E+06	1.19E+06	1.31E+06
1352	TYSND1	2	2	0.00E+00	0.00E+00	5.50E+05	7.47E+05	1.09E+06	6.73E+05	1.47E+06	0.00E+00	0.00E+00	0.00E+00	0.00E+00	0.00E+00
1353	PCGF3	2	3	0.00E+00	0.00E+00	1.23E+07	0.00E+00	2.23E+07	0.00E+00	3.21E+06	0.00E+00	0.00E+00	0.00E+00	0.00E+00	0.00E+00
1354	CHD9	3	19	0.00E+00	0.00E+00	1.21E+07	0.00E+00	0.00E+00	0.00E+00	0.00E+00	0.00E+00	0.00E+00	0.00E+00	1.09E+07	2.51E+06
1355	ZNF260	5	5	0.00E+00	0.00E+00	0.00E+00	0.00E+00	6.28E+07	0.00E+00	0.00E+00	0.00E+00	0.00E+00	0.00E+00	0.00E+00	0.00E+00
1356	ARID4B	3	2	0.00E+00	0.00E+00	0.00E+00	0.00E+00	0.00E+00	0.00E+00	0.00E+00	0.00E+00	0.00E+00	0.00E+00	4.07E+06	0.00E+00
1357	C17orf85	2	1	0.00E+00	0.00E+00	4.42E+06	3.12E+06	0.00E+00	0.00E+00	0.00E+00	0.00E+00	0.00E+00	0.00E+00	0.00E+00	0.00E+00
1358	BRDT	5	2	0.00E+00	0.00E+00	0.00E+00	0.00E+00	0.00E+00	0.00E+00	0.00E+00	0.00E+00	0.00E+00	0.00E+00	0.00E+00	0.00E+00
1359	TOR1AIP1	2	1	0.00E+00	0.00E+00	0.00E+00	0.00E+00	5.73E+06	5.28E+06	0.00E+00	0.00E+00	0.00E+00	0.00E+00	0.00E+00	0.00E+00
1360	KPRP	1	2	0.00E+00	0.00E+00	0.00E+00	0.00E+00	0.00E+00	0.00E+00	0.00E+00	0.00E+00	2.39E+07	0.00E+00	6.40E+06	0.00E+00
1361	XP32	1	1	0.00E+00	0.00E+00	0.00E+00	0.00E+00	0.00E+00	0.00E+00	0.00E+00	0.00E+00	3.36E+06	0.00E+00	4.50E+06	0.00E+00
1362	CD276	3	1	0.00E+00	0.00E+00	0.00E+00	0.00E+00	4.88E+06	2.78E+06	0.00E+00	0.00E+00	0.00E+00	0.00E+00	0.00E+00	0.00E+00
1363	WDR25	2	1	0.00E+00	0.00E+00	0.00E+00	0.00E+00	1.48E+06	1.69E+06	0.00E+00	0.00E+00	0.00E+00	0.00E+00	0.00E+00	0.00E+00
1364	ARHGAP17	6	2	0.00E+00	0.00E+00	0.00E+00	0.00E+00	0.00E+00	0.00E+00	0.00E+00	0.00E+00	0.00E+00	0.00E+00	4.39E+06	6.19E+05
1365	ARMC6	2	2	0.00E+00	0.00E+00	0.00E+00	0.00E+00	7.48E+06	0.00E+00	0.00E+00	0.00E+00	0.00E+00	0.00E+00	0.00E+00	0.00E+00
1366	ZCCHC8	2	1	0.00E+00	0.00E+00	0.00E+00	0.00E+00	1.14E+07	0.00E+00	0.00E+00	0.00E+00	0.00E+00	0.00E+00	2.96E+06	0.00E+00
1367	FAM117B	2	2	0.00E+00	0.00E+00	0.00E+00	0.00E+00	0.00E+00	4.46E+06	4.80E+06	0.00E+00	0.00E+00	0.00E+00	0.00E+00	0.00E+00
1368	PRMT9	2	4	0.00E+00	0.00E+00	1.77E+06	0.00E+00	2.20E+06	0.00E+00	8.61E+06	1.50E+06	1.21E+06	0.00E+00	5.40E+06	0.00E+00
1369	INO80C	3	2	0.00E+00	0.00E+00	2.34E+06	0.00E+00	1.50E+07	1.87E+06	0.00E+00	0.00E+00	0.00E+00	0.00E+00	0.00E+00	0.00E+00
1370	TTC33	1	1	0.00E+00	0.00E+00	0.00E+00	0.00E+00	3.67E+06	4.04E+06	2.29E+06	1.73E+06	1.77E+06	2.18E+06	3.02E+06	3.56E+06
1371	PAPD4	2	1	0.00E+00	0.00E+00	0.00E+00	0.00E+00	5.77E+06	0.00E+00	0.00E+00	0.00E+00	0.00E+00	0.00E+00	0.00E+00	0.00E+00
1372	WDR59	4	3	0.00E+00	0.00E+00	0.00E+00	0.00E+00	3.82E+06	3.30E+06	0.00E+00	0.00E+00	0.00E+00	0.00E+00	2.07E+07	2.75E+06
1373	FIP1L1	1	18	0.00E+00	0.00E+00	0.00E+00	0.00E+00	0.00E+00	0.00E+00	0.00E+00	1.75E+07	0.00E+00	1.83E+07	0.00E+00	2.37E+07
1374	DPP8	6	1	0.00E+00	0.00E+00	0.00E+00	0.00E+00	0.00E+00	0.00E+00	0.00E+00	0.00E+00	1.38E+07	0.00E+00	0.00E+00	0.00E+00
1375	AEBP2	3	3	0.00E+00	0.00E+00	1.76E+06	0.00E+00	1.82E+07	1.07E+07	0.00E+00	0.00E+00	1.50E+06	4.46E+06	2.05E+07	1.20E+07
1376	TFAP2D	1	2	0.00E+00	0.00E+00	0.00E+00	0.00E+00	0.00E+00	4.61E+07	0.00E+00	0.00E+00	0.00E+00	0.00E+00	0.00E+00	0.00E+00
1377	SLFN11	1	2	0.00E+00	0.00E+00	0.00E+00	0.00E+00	1.22E+07	0.00E+00	0.00E+00	0.00E+00	0.00E+00	0.00E+00	4.68E+06	0.00E+00
1378	TRPT1	4	2	0.00E+00	0.00E+00	9.30E+06	8.25E+06	2.46E+07	1.58E+07	0.00E+00	0.00E+00	3.27E+06	3.29E+06	2.86E+06	0.00E+00
1379	MTDH	1	2	0.00E+00	0.00E+00	7.87E+06	7.51E+06	4.01E+07	1.80E+07	0.00E+00	0.00E+00	0.00E+00	0.00E+00	0.00E+00	0.00E+00
1380	CCDC50	2	1	0.00E+00	0.00E+00	0.00E+00	0.00E+00	0.00E+00	0.00E+00	0.00E+00	5.23E+06	0.00E+00	0.00E+00	0.00E+00	0.00E+00
1381	KIAA2013	2	1	0.00E+00	0.00E+00	2.39E+06	1.91E+06	0.00E+00	0.00E+00	0.00E+00	0.00E+00	0.00E+00	0.00E+00	0.00E+00	0.00E+00
1382	MICU2	1	1	0.00E+00	0.00E+00	0.00E+00	0.00E+00	1.05E+07	0.00E+00	0.00E+00	0.00E+00	0.00E+00	0.00E+00	0.00E+00	0.00E+00
1383	ZNF444	1	9	0.00E+00	0.00E+00	1.60E+07	0.00E+00	3.16E+07	0.00E+00	0.00E+00	0.00E+00	0.00E+00	0.00E+00	0.00E+00	0.00E+00
1384	ZNF655	2	3	0.00E+00	0.00E+00	0.00E+00	0.00E+00	2.18E+07	1.40E+07	0.00E+00	0.00E+00	2.50E+06	2.59E+06	0.00E+00	0.00E+00
1385	ABTB2	2	2	0.00E+00	0.00E+00	0.00E+00	0.00E+00	0.00E+00	0.00E+00	5.09E+06	2.69E+06	3.43E+06	2.91E+06	0.00E+00	0.00E+00
1386	KLHDC9	3	1	0.00E+00	0.00E+00	0.00E+00	0.00E+00	7.79E+06	6.58E+06	0.00E+00	0.00E+00	0.00E+00	0.00E+00	0.00E+00	0.00E+00
1387	SYNE1	6	1	0.00E+00	0.00E+00	0.00E+00	0.00E+00	0.00E+00	0.00E+00	0.00E+00	0.00E+00	0.00E+00	0.00E+00	0.00E+00	0.00E+00
1388	CASC5	4	1	0.00E+00	0.00E+00	0.00E+00	0.00E+00	0.00E+00	0.00E+00	0.00E+00	0.00E+00	0.00E+00	0.00E+00	0.00E+00	0.00E+00
1389	ADCK3	4	2	0.00E+00	0.00E+00	0.00E+00	0.00E+00	1.13E+07	9.23E+06	0.00E+00	0.00E+00	0.00E+00	0.00E+00	0.00E+00	0.00E+00
1390	WDR20	8	6	0.00E+00	0.00E+00	0.00E+00	0.00E+00	0.00E+00	0.00E+00	1.16E+07	0.00E+00	2.16E+06	3.36E+06	3.88E+07	2.26E+07
1391	RDH11	3	2	0.00E+00	0.00E+00	0.00E+00	0.00E+00	1.04E+07	2.93E+07	0.00E+00	0.00E+00	0.00E+00	0.00E+00	0.00E+00	0.00E+00
1392	HM13	2	1	0.00E+00	0.00E+00	0.00E+00	0.00E+00	2.84E+07	0.00E+00	0.00E+00	0.00E+00	0.00E+00	0.00E+00	0.00E+00	0.00E+00
1393	MIPOL1	2	1	0.00E+00	0.00E+00	0.00E+00	0.00E+00	0.00E+00	0.00E+00	0.00E+00	0.00E+00	0.00E+00	0.00E+00	0.00E+00	0.00E+00
1394	DYNLRB1;D	2	1	0.00E+00	0.00E+00	0.00E+00	0.00E+00	1.08E+07	6.56E+06	0.00E+00	0.00E+00	0.00E+00	0.00E+00	0.00E+00	0.00E+00

MQ search SILAC data

hit number	Gene names	Number of proteins	Peptides	Intensity L 2%SDS_24hHU	Intensity H 2%SDS_24hHU	Intensity L 2%SDS_2hHU	Intensity H 2%SDS_2hHU	Intensity L 2%SDS_NT	Intensity H 2%SDS_NT	Intensity L el150_24hHU	Intensity H el150_24hHU	Intensity L el150_2hHU	Intensity H el150_2hHU	Intensity L el150_NT	Intensity H el150_NT
1395	NSMCE1	1	3	0.00E+00	0.00E+00	1.66E+07	0.00E+00	6.49E+07	0.00E+00	4.87E+06	0.00E+00	0.00E+00	0.00E+00	1.85E+07	0.00E+00
1396	PHLDA1	1	1	0.00E+00	0.00E+00	0.00E+00	0.00E+00	9.57E+06	0.00E+00	1.71E+06	0.00E+00	0.00E+00	0.00E+00	0.00E+00	0.00E+00
1397	POF1B	3	3	0.00E+00	0.00E+00	0.00E+00	0.00E+00	0.00E+00	0.00E+00	1.68E+06	0.00E+00	1.24E+07	0.00E+00	0.00E+00	0.00E+00
1398	TCTEX1D2	1	1	0.00E+00	0.00E+00	0.00E+00	0.00E+00	2.93E+07	0.00E+00	0.00E+00	0.00E+00	0.00E+00	0.00E+00	0.00E+00	0.00E+00
1399	SRSF12	1	5	0.00E+00	0.00E+00	1.67E+06	1.35E+06	3.57E+07	5.19E+06	0.00E+00	0.00E+00	0.00E+00	0.00E+00	3.67E+06	2.87E+06
1400	BRI3BP	1	2	0.00E+00	0.00E+00	7.47E+06	1.56E+07	0.00E+00	0.00E+00	0.00E+00	0.00E+00	0.00E+00	0.00E+00	0.00E+00	0.00E+00
1401	THAP4	1	1	0.00E+00	0.00E+00	0.00E+00	3.73E+06	8.15E+06	0.00E+00	0.00E+00	0.00E+00	0.00E+00	0.00E+00	0.00E+00	0.00E+00
1402	FAM3C	1	2	0.00E+00	0.00E+00	9.06E+06	0.00E+00	4.35E+07	0.00E+00	0.00E+00	0.00E+00	0.00E+00	0.00E+00	0.00E+00	0.00E+00
1403	H1FX	1	2	0.00E+00	0.00E+00	0.00E+00	0.00E+00	6.55E+07	0.00E+00	0.00E+00	0.00E+00	0.00E+00	0.00E+00	0.00E+00	0.00E+00
1404	JARID2	3	3	0.00E+00	0.00E+00	1.07E+07	6.27E+06	8.93E+06	2.47E+06	0.00E+00	0.00E+00	9.20E+05	1.13E+06	2.33E+06	1.93E+06
1405	CELF1	6	1	0.00E+00	0.00E+00	0.00E+00	0.00E+00	0.00E+00	4.14E+06	0.00E+00	0.00E+00	0.00E+00	0.00E+00	0.00E+00	0.00E+00
1406	TOP1MT	2	6	0.00E+00	0.00E+00	8.29E+07	0.00E+00	0.00E+00	0.00E+00	0.00E+00	0.00E+00	0.00E+00	0.00E+00	0.00E+00	0.00E+00
1407	NCLN	2	1	0.00E+00	0.00E+00	0.00E+00	0.00E+00	0.00E+00	6.99E+06	0.00E+00	0.00E+00	0.00E+00	0.00E+00	0.00E+00	0.00E+00
1408	CCDC47	2	2	0.00E+00	0.00E+00	3.63E+06	0.00E+00	1.59E+07	0.00E+00	4.52E+06	0.00E+00	0.00E+00	0.00E+00	0.00E+00	0.00E+00
1409	EME1	2	3	0.00E+00	0.00E+00	0.00E+00	5.95E+06	0.00E+00	7.32E+06	0.00E+00	0.00E+00	0.00E+00	0.00E+00	0.00E+00	0.00E+00
1410	RPUSD4	2	3	0.00E+00	0.00E+00	1.83E+07	6.89E+06	3.04E+07	0.00E+00	0.00E+00	0.00E+00	0.00E+00	0.00E+00	0.00E+00	0.00E+00
1411	TUBGCP3	3	2	0.00E+00	0.00E+00	0.00E+00	0.00E+00	0.00E+00	0.00E+00	0.00E+00	0.00E+00	0.00E+00	0.00E+00	2.35E+06	0.00E+00
1412	NUS1	1	1	0.00E+00	0.00E+00	0.00E+00	0.00E+00	4.83E+06	2.77E+06	0.00E+00	0.00E+00	0.00E+00	0.00E+00	0.00E+00	0.00E+00
1413	EDC3	1	3	0.00E+00	0.00E+00	0.00E+00	0.00E+00	5.07E+06	2.03E+06	0.00E+00	0.00E+00	0.00E+00	0.00E+00	3.37E+06	0.00E+00
1414	TRMT2B	3	1	0.00E+00	0.00E+00	0.00E+00	0.00E+00	0.00E+00	1.63E+06	0.00E+00	0.00E+00	0.00E+00	0.00E+00	0.00E+00	0.00E+00
1415	THOC3	2	1	0.00E+00	0.00E+00	0.00E+00	9.47E+06	2.93E+07	1.64E+07	0.00E+00	0.00E+00	0.00E+00	0.00E+00	0.00E+00	0.00E+00
1416	ELMO2	2	1	0.00E+00	0.00E+00	0.00E+00	0.00E+00	4.57E+06	0.00E+00	0.00E+00	0.00E+00	0.00E+00	0.00E+00	0.00E+00	0.00E+00
1417	MARK4	2	2	0.00E+00	0.00E+00	0.00E+00	0.00E+00	4.01E+07	0.00E+00	0.00E+00	0.00E+00	0.00E+00	0.00E+00	0.00E+00	0.00E+00
1418	TCEANC2	1	1	0.00E+00	0.00E+00	0.00E+00	0.00E+00	4.63E+06	0.00E+00	0.00E+00	0.00E+00	0.00E+00	0.00E+00	0.00E+00	0.00E+00
1419	TSNARE1	2	1	0.00E+00	0.00E+00	0.00E+00	0.00E+00	1.23E+07	0.00E+00	0.00E+00	0.00E+00	0.00E+00	0.00E+00	0.00E+00	0.00E+00
1420	SERPINB12	2	2	0.00E+00	0.00E+00	0.00E+00	0.00E+00	0.00E+00	0.00E+00	8.99E+06	0.00E+00	3.05E+07	0.00E+00	6.86E+06	0.00E+00
1421	TUBGCP6	3	3	0.00E+00	0.00E+00	0.00E+00	0.00E+00	6.23E+06	0.00E+00	0.00E+00	0.00E+00	0.00E+00	0.00E+00	5.37E+06	1.50E+06
1422	CCNL2	5	3	0.00E+00	0.00E+00	0.00E+00	0.00E+00	2.68E+07	0.00E+00	0.00E+00	0.00E+00	0.00E+00	0.00E+00	6.20E+05	3.14E+06
1423	PSMD1	2	1	0.00E+00	0.00E+00	0.00E+00	0.00E+00	3.78E+06	3.28E+06	0.00E+00	0.00E+00	0.00E+00	0.00E+00	0.00E+00	0.00E+00
1424	MNT	1	6	0.00E+00	0.00E+00	1.71E+06	1.54E+06	0.00E+00	0.00E+00	1.78E+07	4.15E+06	0.00E+00	0.00E+00	3.11E+07	2.86E+06
1425	HSD17B10	2	2	0.00E+00	0.00E+00	0.00E+00	0.00E+00	0.00E+00	0.00E+00	0.00E+00	0.00E+00	5.92E+06	0.00E+00	0.00E+00	0.00E+00
1426	TM9SF2	1	5	0.00E+00	0.00E+00	7.60E+06	0.00E+00	5.24E+07	1.52E+07	0.00E+00	0.00E+00	0.00E+00	0.00E+00	0.00E+00	0.00E+00
1427	SLC29A1	2	1	0.00E+00	0.00E+00	0.00E+00	0.00E+00	6.44E+06	7.39E+06	0.00E+00	0.00E+00	0.00E+00	0.00E+00	0.00E+00	0.00E+00
1428	NIPSNAP1	1	1	0.00E+00	0.00E+00	0.00E+00	0.00E+00	1.65E+07	1.14E+07	0.00E+00	0.00E+00	0.00E+00	0.00E+00	0.00E+00	0.00E+00
1429	TUBA1C	1	19	0.00E+00	0.00E+00	2.10E+07	1.43E+07	0.00E+00	0.00E+00	0.00E+00	0.00E+00	0.00E+00	0.00E+00	0.00E+00	0.00E+00
1430	PIGQ	3	1	0.00E+00	0.00E+00	0.00E+00	0.00E+00	0.00E+00	0.00E+00	0.00E+00	0.00E+00	0.00E+00	0.00E+00	0.00E+00	0.00E+00
1431	NUDT22	2	1	0.00E+00	0.00E+00	0.00E+00	0.00E+00	0.00E+00	0.00E+00	0.00E+00	0.00E+00	0.00E+00	0.00E+00	0.00E+00	0.00E+00
1432	ERP44	1	1	0.00E+00	0.00E+00	0.00E+00	0.00E+00	0.00E+00	0.00E+00	3.98E+06	2.67E+06	3.65E+06	3.52E+06	0.00E+00	0.00E+00
1433	RIOK2	2	4	0.00E+00	0.00E+00	2.98E+07	0.00E+00	5.86E+07	0.00E+00	0.00E+00	0.00E+00	0.00E+00	0.00E+00	2.06E+06	0.00E+00
1434	KLF16	1	2	0.00E+00	0.00E+00	8.42E+06	0.00E+00	0.00E+00	0.00E+00	0.00E+00	0.00E+00	2.68E+06	0.00E+00	4.62E+06	0.00E+00
1435	WHSC1L1	5	3	0.00E+00	0.00E+00	0.00E+00	0.00E+00	2.46E+07	4.94E+06	0.00E+00	0.00E+00	0.00E+00	0.00E+00	0.00E+00	0.00E+00
1436	NUF2	1	1	0.00E+00	0.00E+00	0.00E+00	0.00E+00	0.00E+00	0.00E+00	0.00E+00	0.00E+00	0.00E+00	0.00E+00	0.00E+00	0.00E+00
1437	MRPL37	1	1	0.00E+00	0.00E+00	0.00E+00	0.00E+00	1.25E+07	7.34E+06	0.00E+00	0.00E+00	0.00E+00	0.00E+00	0.00E+00	0.00E+00
1438	OSBPL8	3	1	0.00E+00	0.00E+00	0.00E+00	0.00E+00	5.35E+06	3.69E+06	0.00E+00	0.00E+00	0.00E+00	0.00E+00	0.00E+00	0.00E+00
1439	CRNKL1	3	1	0.00E+00	0.00E+00	2.26E+06	1.71E+06	0.00E+00	0.00E+00	0.00E+00	0.00E+00	0.00E+00	0.00E+00	0.00E+00	0.00E+00
1440	TRIM4	3	1	0.00E+00	0.00E+00	1.87E+08	0.00E+00	0.00E+00	0.00E+00	0.00E+00	0.00E+00	4.11E+07	0.00E+00	3.06E+07	0.00E+00
1441	FAM117A	2	2	0.00E+00	0.00E+00	1.14E+06	7.00E+05	2.68E+06	2.00E+06	0.00E+00	0.00E+00	0.00E+00	0.00E+00	0.00E+00	0.00E+00
1442	ZCCHC2	2	4	0.00E+00	0.00E+00	1.34E+07	2.82E+06	0.00E+00	0.00E+00	0.00E+00	0.00E+00	6.51E+06	5.25E+06	9.78E+06	3.97E+06
1443	SENP6	2	1	0.00E+00	0.00E+00	3.28E+06	2.05E+06	7.59E+06	0.00E+00	0.00E+00	0.00E+00	0.00E+00	0.00E+00	3.91E+06	0.00E+00
1444	KATNBL1	1	2	0.00E+00	0.00E+00	0.00E+00	0.00E+00	5.79E+05	4.80E+05	0.00E+00	0.00E+00	0.00E+00	0.00E+00	0.00E+00	0.00E+00
1445	CCDC113	2	1	0.00E+00	0.00E+00	0.00E+00	0.00E+00	0.00E+00	0.00E+00	0.00E+00	0.00E+00	0.00E+00	0.00E+00	0.00E+00	0.00E+00
1446	KCTD10	9	8	0.00E+00	0.00E+00	3.33E+07	5.13E+06	0.00E+00	0.00E+00	1.38E+07	3.93E+06	2.70E+07	8.62E+06	5.42E+07	3.87E+06
1447	SENP3	1	1	0.00E+00	0.00E+00	2.66E+06	0.00E+00	0.00E+00	0.00E+00	0.00E+00	0.00E+00	0.00E+00	0.00E+00	0.00E+00	0.00E+00
1448	TMEM38A	1	1	0.00E+00	0.00E+00	2.72E+06	6.49E+06	0.00E+00	0.00E+00	0.00E+00	0.00E+00	0.00E+00	0.00E+00	0.00E+00	0.00E+00
1449	WDR26	2	2	0.00E+00	0.00E+00	3.21E+06	4.66E+06	0.00E+00	0.00E+00	1.85E+06	1.20E+06	1.79E+06	1.96E+06	2.44E+06	4.36E+06
1450	ZNF696	1	2	0.00E+00	0.00E+00	6.42E+06	0.00E+00	5.97E+06	4.12E+06	0.00E+00	0.00E+00	0.00E+00	0.00E+00	0.00E+00	0.00E+00
1451	ECT2	4	4	0.00E+00	0.00E+00	0.00E+00	0.00E+00	2.36E+07	0.00E+00	0.00E+00	0.00E+00	0.00E+00	0.00E+00	0.00E+00	0.00E+00
1452	TMEM165	2	1	0.00E+00	0.00E+00	0.00E+00	0.00E+00	2.30E+07	0.00E+00	0.00E+00	0.00E+00	0.00E+00	0.00E+00	0.00E+00	0.00E+00
1453	GPBP1L1	1	3	0.00E+00	0.00E+00	0.00E+00	0.00E+00	3.38E+07	2.88E+06	0.00E+00	0.00E+00	0.00E+00	0.00E+00	6.79E+06	4.33E+06
1454	RAVER2	2	2	0.00E+00	0.00E+00	0.00E+00	0.00E+00	1.10E+07	9.11E+06	2.14E+06	2.40E+06	0.00E+00	0.00E+00	6.01E+06	2.85E+06
1455	EPB41L5;EI	6	2	0.00E+00	0.00E+00	0.00E+00	0.00E+00	1.36E+07	0.00E+00	0.00E+00	0.00E+00	0.00E+00	0.00E+00	0.00E+00	0.00E+00
1456	BRMS1	1	1	0.00E+00	0.00E+00	0.00E+00	0.00E+00	0.00E+00	0.00E+00	0.00E+00	0.00E+00	0.00E+00	0.00E+00	3.80E+06	3.05E+06
1457	TM9SF3	1	2	0.00E+00	0.00E+00	0.00E+00	0.00E+00	2.54E+07	1.20E+07	1.52E+06	0.00E+00	0.00E+00	0.00E+00	0.00E+00	0.00E+00
1458	FAM60A	2	2	0.00E+00	0.00E+00	2.15E+06	0.00E+00	5.77E+06	0.00E+00	0.00E+00	0.00E+00	0.00E+00	0.00E+00	2.71E+06	1.41E+06
1459	FZD3	1	2	0.00E+00	0.00E+00	0.00E+00	0.00E+00	0.00E+00	1.47E+07	0.00E+00	0.00E+00	0.00E+00	0.00E+00	0.00E+00	0.00E+00
1460	LUC7L	3	2	0.00E+00	0.00E+00	0.00E+00	0.00E+00	0.00E+00	0.00E+00	0.00E+00	0.00E+00	0.00E+00	0.00E+00	0.00E+00	0.00E+00
1461	TCF7L2	38	3	0.00E+00	0.00E+00	6.63E+06	2.02E+07	2.13E+07	4.65E+07	0.00E+00	0.00E+00	0.00E+00	5.35E+06	4.16E+06	9.70E+06
1462	MRPL17	1	1	0.00E+00	0.00E+00	1.36E+07	1.93E+07	0.00E+00	0.00E+00	0.00E+00	0.00E+00	3.18E+06	8.30E+06	7.08E+06	1.30E+07
1463	DNAJB12	2	2	0.00E+00	0.00E+00	0.00E+00	0.00E+00	5.98E+06	3.45E+06	0.00E+00	0.00E+00	0.00E+00	0.00E+00	0.00E+00	0.00E+00
1464	TLR7	1	1	0.00E+00	0.00E+00	0.00E+00	0.00E+00	0.00E+00	0.00E+00	0.00E+00	0.00E+00	0.00E+00	0.00E+00	0.00E+00	0.00E+00
1465	HSPBP1	2	1	0.00E+00	0.00E+00	5.84E+06	4.20E+06	9.86E+06	7.92E+06	0.00E+00	0.00E+00	0.00E+00	0.00E+00	0.00E+00	0.00E+00
1466	CALML5	1	1	0.00E+00	0.00E+00	0.00E+00	0.00E+00	0.00E+00	0.00E+00	0.00E+00	0.00E+00	7.81E+06	0.00E+00	0.00E+00	0.00E+00
1467	FOXJ2	10	3	0.00E+00	0.00E+00	5.68E+06	3.52E+06	4.87E+06	3.02E+06	0.00E+00	0.00E+00	0.00E+00	0.00E+00	0.00E+00	0.00E+00
1468	MARK1;M/	10	2	0.00E+00	0.00E+00	0.00E+00	0.00E+00	2.20E+07	0.00E+00	0.00E+00	0.00E+00	0.00E+00	0.00E+00	0.00E+00	0.00E+00
1469	WRAP73	1	5	0.00E+00	0.00E+00	2.43E+07	2.83E+06	7.71E+06	3.49E+06	1.15E+06	8.45E+06	1.07E+07	1.67E+06	1.90E+07	2.83E+06
1470	SAE1	1	1	0.00E+00	0.00E+00	0.00E+00	0.00E+00	0.00E+00	0.00E+00	0.00E+00	0.00E+00	3.06E+06	2.17E+06	0.00E+00	0.00E+00
1471	DKK4	1	1	0.00E+00	0.00E+00	0.00E+00	0.00E+00	0.00E+00	0.00E+00	0.00E+00	0.00E+00	0.00E+00	0.00E+00	0.00E+00	0.00E+00
1472	FTSJ1	2	1	0.00E+00	0.00E+00	0.00E+00	0.00E+00	0.00E+00	2.99E+07	0.00E+00	0.00E+00	0.00E+00	0.00E+00	0.00E+00	0.00E+00
1473	SEC63	1	2	0.00E+00	0.00E+00	0.00E+00	0.00E+00	2.67E+07	1.26E+07	0.00E+00	0.00E+00	0.00E+00	0.00E+00	0.00E+00	0.00E+00
1474	SRP68	3	3	0.00E+00	0.00E+00	2.21E+07	3.64E+07	0.00E+00	0.00E+00	0.00E+00	0.00E+00	0.00E+00	0.00E+00	0.00E+00	0.00E+00
1475	PURG	2	1	0.00E+00	0.00E+00	0.00E+00	0.00E+00	2.79E+06	0.00E+00	0.00E+00	0.00E+00	0.00E+00	0.00E+00	0.00E+00	0.00E+00
1476	KMT2B	2	2	0.00E+00	0.00E+00	0.00E+00	0.00E+00	2.92E+07	0.00E+00	0.00E+00	0.00E+00	0.00E+00	0.00E+00	0.00E+00	1.75E+07

MQ search SILAC data

hit number	Gene names	Number of proteins	Peptides	Intensity L 2%SDS_24hHU	Intensity H 2%SDS_24hHU	Intensity L 2%SDS_2hHU	Intensity H 2%SDS_2hHU	Intensity L 2%SDS_NT	Intensity H 2%SDS_NT	Intensity L el150_24hHU	Intensity H el150_24hHU	Intensity L el150_2hHU	Intensity H el150_2hHU	Intensity L el150_NT	Intensity H el150_NT
1477	DIMT1	1	3	0.00E+00	0.00E+00	3.38E+06	5.69E+06	2.93E+07	2.34E+07	0.00E+00	0.00E+00	0.00E+00	0.00E+00	0.00E+00	0.00E+00
1478	COPS3	1	1	0.00E+00	0.00E+00	1.74E+06	1.56E+06	0.00E+00	0.00E+00	0.00E+00	0.00E+00	0.00E+00	0.00E+00	0.00E+00	0.00E+00
1479	BCS1L	1	2	0.00E+00	0.00E+00	5.81E+05	1.66E+06	7.85E+06	0.00E+00	0.00E+00	0.00E+00	0.00E+00	0.00E+00	0.00E+00	0.00E+00
1480	NISCH	3	1	0.00E+00	0.00E+00	0.00E+00	0.00E+00	0.00E+00	0.00E+00	0.00E+00	0.00E+00	0.00E+00	0.00E+00	0.00E+00	0.00E+00
1481	LEMD3	1	2	0.00E+00	0.00E+00	9.49E+06	4.57E+06	9.80E+06	8.53E+06	0.00E+00	0.00E+00	0.00E+00	0.00E+00	0.00E+00	0.00E+00
1482	ACOT9	4	1	0.00E+00	0.00E+00	0.00E+00	0.00E+00	5.65E+06	0.00E+00	0.00E+00	0.00E+00	0.00E+00	0.00E+00	0.00E+00	0.00E+00
1483	SH3GLB1	3	1	0.00E+00	0.00E+00	0.00E+00	0.00E+00	5.41E+06	3.41E+06	0.00E+00	0.00E+00	0.00E+00	0.00E+00	0.00E+00	0.00E+00
1484	TCAF1	2	2	0.00E+00	0.00E+00	0.00E+00	0.00E+00	4.18E+06	0.00E+00	0.00E+00	0.00E+00	0.00E+00	0.00E+00	2.08E+06	3.35E+05
1485	IRS2	1	8	0.00E+00	0.00E+00	0.00E+00	0.00E+00	6.27E+07	1.61E+07	0.00E+00	0.00E+00	0.00E+00	5.00E+06	9.69E+06	2.51E+06
1486	ZSCAN21	1	1	0.00E+00	0.00E+00	2.89E+06	2.20E+06	8.51E+06	5.22E+06	0.00E+00	0.00E+00	1.32E+06	1.12E+06	0.00E+00	0.00E+00
1487	CEPT1	1	1	0.00E+00	0.00E+00	0.00E+00	0.00E+00	6.23E+07	0.00E+00	5.00E+06	0.00E+00	0.00E+00	0.00E+00	1.66E+07	1.24E+07